NATIONAL TECHNICAL UNIVERSITY OF ATHENS
SCHOOL OF ELECTRICAL AND COMPUTER ENGINEERING
DIVISION OF INFORMATION TRANSMISSION AND MATERIAL TECHNOLOGY

Design and Implementation of Receivers and Measurement Equipment for Next-Generation Satellite Networks

Doctoral Thesis

Apostolos Zach. Papafragkakis

Three-member Advisory Committee:	A. D. Panagopoulos, Associate Professor, NTUA P. Cottis, Professor, NTUA G. Fikioris, Professor, NTUA

Athens, February 2021

ΕΘΝΙΚΟ ΜΕΤΣΟΒΙΟ ΠΟΛΥΤΕΧΝΕΙΟ
ΣΧΟΛΗ ΗΛΕΚΤΡΟΛΟΓΩΝ ΜΗΧΑΝΙΚΩΝ
ΚΑΙ ΜΗΧΑΝΙΚΩΝ ΥΠΟΛΟΓΙΣΤΩΝ
ΤΟΜΕΑΣ ΣΥΣΤΗΜΑΤΩΝ ΜΕΤΑΔΟΣΗΣ
ΠΛΗΡΟΦΟΡΙΑΣ ΚΑΙ ΤΕΧΝΟΛΟΓΙΑΣ ΥΛΙΚΩΝ

Σχεδίαση και Υλοποίηση Δεκτών και Μετρητικού Εξοπλισμού για Δορυφορικά Δίκτυα Νέας Γενιάς

ΔΙΔΑΚΤΟΡΙΚΗ ΔΙΑΤΡΙΒΗ

Απόστολος Ζαχ. Παπαφραγκάκης

Τριμελής	Αθ. Δ. Παναγόπουλος, Αναπλ. Καθηγητής Ε.Μ.Π.
Συμβουλευτική	Π. Κωττής, Καθηγητής Ε.Μ.Π.
Επιτροπή:	Γ. Φικιώρης, Καθηγητής Ε.Μ.Π.

Αθήνα, Φεβρουάριος 2021

ΕΘΝΙΚΟ ΜΕΤΣΟΒΙΟ ΠΟΛΥΤΕΧΝΕΙΟ
ΣΧΟΛΗ ΗΛΕΚΤΡΟΛΟΓΩΝ ΜΗΧΑΝΙΚΩΝ
ΚΑΙ ΜΗΧΑΝΙΚΩΝ ΥΠΟΛΟΓΙΣΤΩΝ
ΤΟΜΕΑΣ ΣΥΣΤΗΜΑΤΩΝ ΜΕΤΑΔΟΣΗΣ ΠΛΗΡΟΦΟΡΙΑΣ
ΚΑΙ ΤΕΧΝΟΛΟΓΙΑΣ ΥΛΙΚΩΝ

Σχεδίαση και Υλοποίηση Δεκτών και Μετρητικού Εξοπλισμού για Δορυφορικά Δίκτυα Νέας Γενιάς

ΔΙΔΑΚΤΟΡΙΚΗ ΔΙΑΤΡΙΒΗ

Απόστολος Ζαχ. Παπαφραγκάκης

Τριμελής	Αθ. Δ. Παναγόπουλος, Αναπλ. Καθηγητής Ε.Μ.Π.
Συμβουλευτική	Π. Κωττής, Καθηγητής Ε.Μ.Π.
Επιτροπή:	Γ. Φικιώρης, Καθηγητής Ε.Μ.Π.

Εγκρίθηκε από την επταμελή εξεταστική επιτροπή την 26/02/2021.
Η επιτροπή εξέτασης:

.....	.....	.....
Αθ. Παναγόπουλος Αναπλ. Καθηγητής Ε.Μ.Π.	Π. Κωττής Καθηγητής Ε.Μ.Π.	Γ. Φικιώρης Καθηγητής Ε.Μ.Π.
.....	.....	.....
Χ. Καψάλης Καθηγητής Ε.Μ.Π.	Ι. Γκόνος Αναπλ. Καθηγητής Ε.Μ.Π.	Αθ. Κανάτας Καθηγητής Παν. Πειραιώς

.....

Γ. Τσούλος
Καθηγητής Παν. Πελοποννήσου

Αθήνα, Φεβρουάριος 2021

.....
Απόστολος Ζαχ. Παπαφραγκάκης
Διδάκτωρ Ηλεκτρολόγος Μηχανικός και Μηχανικός Υπολογιστών Ε.Μ.Π.

Στην οικογένειά μου και
στη μνήμη του αγαπημένου μου παππού Απόστολου

Περίληψη

Οι ολοένα αυξανόμενες απαιτήσεις για υψηλότερους ρυθμούς μετάδοσης σε συνδυασμό με την εξάντληση του διαθεσίμου φάσματος για δορυφορικές επικοινωνίες επιβάλλουν τη μετάβαση των συστημάτων και υπηρεσιών σε ανώτερες φασματικές ζώνες όπως η Ka και οι Q/V. Η μετάβαση αυτή θα δώσει τη δυνατότητα για ανάπτυξη νέων δορυφορικών συστημάτων υψηλής ρυθμαπόδοσης (High Throughput Satellites, HTS), παρέχοντας αξιοσημείωτα μεγαλύτερη χωρητικότητα δικτύου και ρυθμούς μετάδοσης δεδομένων σε δορυφορικές ζεύξεις τροφοδοσίας (feeder links) τάξεως δεκάδων Tbps.

Ωστόσο, η διάδοση του σήματος στις ζώνες αυτές είναι πολύ πιο ευαίσθητη στα διάφορα ατμοσφαιρικά φαινόμενα και κυρίως στις ατμοσφαιρικές κατακρημνίσεις-βροχή (έντονη εξασθένηση - τάξεως δεκάδων dB) εγείροντας έτσι ζητήματα αξιοπιστίας και διαθεσιμότητας των ζεύξεων. Η χρήση ενός απλού περιθωρίου διαλείψεων (fade margin) ή ελέγχου ισχύος, τεχνικές που χρησιμοποιούνται με επιτυχία σε συστήματα με χαμηλότερες συχνότητες λειτουργίας, κρίνεται τόσο ασύμφορη όσο και ανεπαρκής στη συγκεκριμένη περίπτωση. Είναι επομένως απαραίτητη η χρήση εξειδικευμένων τεχνικών άμβλυνσης διαλείψεων (Fading Mitigation Techniques, FMTs) οι οποίες με τη σειρά τους προϋποθέτουν ακριβή μοντελοποίηση του καναλιού διάδοσης.

Τα τελευταία χρόνια, με πρωτοβουλία και υπό τον συντονισμό του Ευρωπαϊκού Οργανισμού Διαστήματος (European Space Agency, ESA) έγιναν διαθέσιμα σήματα-beacons για τη διεξαγωγή νέων μετρήσεων στις ζώνες Ka και Q (19.701 και 39.402 GHz) από τον δορυφόρο ALPHASAT (25.0^{o}E). Το γεγονός αυτό, σε συνδυασμό με την ωρίμανση της τεχνολογίας και τις νέες τεχνικές Software Defined Radio (SDR), αποτέλεσε το κίνητρο για την ανάπτυξη δεκτών για διεξαγωγή μετρήσεων σε αυτές τις φασματικές ζώνες, για πρώτη φορά σε ελληνικό έδαφος. Οι αναπτυχθέντες δέκτες αποτελούν πλέον μέρος του πανευρωπαϊκού δικτύου μετρήσεων του Alphasat Aldo Paraboni Propagation Experimenters (ASAPE) καθώς και του ερευνητικού προγράμματος της ESA «ASALASCA». Λίγο αργότερα, με σκοπό τη συλλογή περισσοτέρων δεδομένων προστέθηκαν άλλοι δύο δέκτες στις φασματικές ζώνες Ku (11.699 GHz) και Ka-band (19.680 GHz) χρησιμοποιώντας τους δορυφόρους Arabsat BADR-5 (26.0^{o}E) και Eutelsat KaSat (9.0^{o}E) αντίστοιχα.

Στην παρούσα εργασία παρουσιάζεται η αρχιτεκτονική των σχεδιασθέντων δεκτών και οι βασικές αρχές λειτουργίας τους. Δίνεται έμφαση στους παράγοντες που πρέπει να ληφθούν υπόψη σε μια τέτοια προσπάθεια, στις προκλήσεις που αντιμετωπίστηκαν πριν και κατά την εγκατάστασή των δεκτών αλλά και κατά τη διάρκεια της λειτουργίας τους καθώς και οι λύσεις που δόθηκαν. Μετά από εκτεταμένη στατιστική επεξεργασία των συλλεγέντων μετρητικών δεδομένων παρουσιάζονται τα στατιστικά πρώτης τάξης τόσο για την εξασθένηση όσο και για το ρυθμό βροχόπτωσης ανά περιοχή. Ακολούθως, παρουσιάζονται τα στατιστικά δεύτερης τάξης/δυναμική συμπεριφορά των φαινομένων απόσβεσης και πιο συγκεκριμένα ο ρυθμός μεταβολής της απόσβεσης, η διάρκεια διαλείψεων και το πλήθος αυτών ανά κατώφλι εξασθένησης καθώς και το μεσοδιάστημα μεταξύ διαλείψεων (inter-fade durations). Τέλος, χρησιμοποιώντας το σύνολο των χρονοσειρών απόσβεσης επιχειρείται εκτίμηση απόδοσης των διαφόρων σχημάτων FMTs (χωρικός διαφορισμός, χρονικός διαφορισμός, διαφορισμός τροχιάς), μελέτη της κλιμάκωσης

συχνότητας και των σπινθηρισμών αλλά και εξέταση ενός σεναρίου χωρικού διαφορισμού μεγάλης κλίμακας μεταξύ Μεγάλης Βρετανίας και Ελλάδας με εντυπωσιακά αποτελέσματα.

Η παρούσα εργασία συνιστά την πρώτη και πιο ολοκληρωμένη προσπάθεια συγκέντρωσης και ανάλυσης μετρητικών δεδομένων διάδοσης για τις δορυφορικές ζώνες συχνοτήτων Ku, Ka και Q στην Ελλάδα αλλά και στην ευρύτερη περιοχή της νοτίου Μεσογείου. Μέχρι πρότινος, η συντριπτική πλειοψηφία των διαθεσίμων μοντέλων στη βιβλιογραφία για την περιοχή αυτή βασιζόταν σε παραδοχές ή μετρήσεις άλλων, υποτιθέμενα παρόμοιων κλιματικών περιοχών. Στην πράξη, όπως άλλωστε αποδεικνύεται και από την ανάλυση των ληφθέντων μετρήσεων και την αντιπαραβολή τους με παρόμοιες προσπάθειες ανά την Ευρώπη, υπάρχουν σημαντικές αποκλίσεις.

Οι μετρήσεις αποδεικνύουν ότι εάν δε ληφθούν σημαντικά αντίμετρα, η διαθεσιμότητα συστημάτων με συχνότητες λειτουργίας στις ζώνες Ka ή Q θα είναι σημαντικά περιορισμένη. Από την άλλη, η εφαρμογή τεχνικών FMT και ειδικά σχημάτων χωρικού διαφορισμού φαίνεται εξαιρετικά αποδοτική (αν και κοστοβόρα) και θα μπορούσε να αυξήσει θεαματικά τη διαθεσιμότητα των συστημάτων.

Λέξεις Κλειδιά— δορυφόρος, διάδοση, μετρήσεις, Αττική, Ελλάδα, Ku-band, Ka-band, Q-band, Alphasat, KASAT, BADR5, beacon, θόρυβος, Software Defined Radio, SDR, Fast Fourier Transform, FFT, ατμοσφαιρικά φαινόμενα, εξασθένηση, υπερβάλλουσα εξασθένηση, πιθανότητα υπέρβασης, από κοινού κατανομή, ρυθμός μεταβολής εξασθένησης, πλήθος διαλείψεων, διάρκεια διαλείψεων, μεσοδιάστημα διαλείψεων, Τεχνικές Μετριασμού Διαλείψεων, FMTs, χωρικός διαφορισμός, διαφορισμός θέσης, χρονικός διαφορισμός, διαφορισμός τροχιάς, διαφορισμός συχνότητας, κλιμάκωση συχνότητας, σπινθηρισμοί.

Abstract

The ever-increasing demand for high data rate satellite services is necessitated by the vast number of new or planned services involving multimedia transmission or other data rate-intensive applications in the upcoming 5G era; the spectrum scarcity problem (congestion of the lower frequency bands such as the C and the Ku bands) naturally leads to the use of higher frequencies such as those at Ka- and Q-band. Signal propagation at Ka-band frequencies and above is, nevertheless, highly impaired by the various atmospheric phenomena, upping the ante on system design.

The end-user Quality of Service (QoS) is to great extent dictated by the system's resilience to the various propagation effects; such effects could - unless carefully addressed, jeopardize the throughput and/or the link availability potentially resulting into severe degradation of the overall system performance.

In the past, merely allocating a fade margin for earth-space systems operating in lower frequency bands such as e.g. C and Ku was the common practice in order to compensate for the signal fading due to the various atmospheric phenomena; nonetheless, when considering the signal propagation at higher frequency bands, the sole use of a conventional fade margin is generally an insufficient counter-measure since signal fading could be in excess of 20-30 dB for a non-negligible fraction of time. In order to compensate for the atmospheric attenuation, Propagation Impairment Mitigation Techniques (PIMTs) are employed, also commonly referred to as Fading Mitigation Techniques (FMTs); they are vital in order to meet the required Quality of Service - QoS) imposed by the services, keeping at same time the resource usage at an optimal level.

To enable the design of High Throughput Satellite (HTS) systems with FMTs, accurate propagation modelling is of utmost importance; compiling new propagation models is nevertheless a very challenging task, as it has to be supported by long-term experimental campaigns. Furthermore, the various parameters can vary across different geographic/climatic regions and hence the results cannot be easily generalized. Considering the imminent migration of satellite services to the Ka- and Q- bands, a payload dedicated to propagation measurements in these bands has become available from the Alphasat satellite under the coordination of the European Space Agency (ESA). This has strongly motivated the formation of many measurement campaigns across Europe in an effort to enhance the scientific databases with new, more reliable propagation data.

In the framework of the present thesis, an experimental propagation campaign has been initiated at the National Technical University of Athens (NTUA) in Greece. Six beacon receivers have been designed and installed, four of them targeting the Alphasat's Ka-band and Q-band beacons while one of them targets Arabsat's BADR5 Ku-band beacon and Eutelsat's KaSAT's beacon. The receivers make use of the relatively new Software Defined Radio (SDR) paradigm and besides the beacon measurements themselves, additional noise measurements are performed in order to supplement the campaign.

Apart from an elaborate description on the receiver's architecture, design choices and principles of operation, the whole obtained measurement dataset has been processed to allow for a comprehensive statistical evaluation. The thesis begins with a brief outline of the fundamental

propagation effects along with possible FMTs and measurement techniques; it continues with a detailed presentation on the design and deployment of new beacon receivers in Attica, Greece. An evaluation of the first order and second order (fade dynamics) statistics based on the obtained measurement dataset from all available receivers is conducted; after examining the performance of the various FMTs using the actual attenuation timeseries statistical evidence is provided for the efficiency of site, time and orbital diversity techniques; an investigation on the potential frequency scaling across Ku/Ka/Q bands is also considered. Finally, scintillation analysis is performed followed by an evaluation of a large-scale site diversity scenario across Greece and the UK using the actual, concurrent measurements at each location.

To the best of the author's knowledge, this work constitutes the most comprehensive work regarding actual satellite propagation measurements in Greece and the Southern Mediterranean area available to date, especially at so high frequency bands such as Ka- and Q-band. Up until now, any estimation regarding the propagation phenomena in this region relied almost exclusively on statistical/physical-mathematical models or time series synthesizers based on inference and extrapolation from measurements performed in other regions. It is now possible to test systems, techniques and models using actual measurement data.

Index Terms—satellite, propagation, measurements, campaign, Attica, Greece, Ku-band, Ka-band, Q-band, Alphasat, KASAT, BADR5, beacon, noise, Software Defined Radio, SDR, Fast Fourier Transform, FFT, atmospheric phenomena, attenuation, excess attenuation, exceedance probability, joint statistics, fade slope, fade count, fade duration, inter-fade duration, Fading Mitigation Techniques, FMTs, site diversity, time Diversity, orbital diversity, frequency scaling, Scintillation.

Ευχαριστίες

Φτάνοντας στο τέλος μιας πολυετούς πορείας εντός των ακαδημαϊκών αιθουσών αλλά και μιας επίπονης προσπάθειας, τα συναισθήματα είναι ποικίλα. Η χαρά, η ικανοποίηση και ίσως η ανακούφιση είναι πρόδηλες δεδομένου ότι ένας μεγαλεπήβολος στόχος, αυτός της εκπόνησης μιας διδακτορικής διατριβής σε ένα τόσο απαιτητικό αντικείμενο, επιτέλους επιτυγχάνεται. Το παρόν έργο είναι αποτέλεσμα αφοσίωσης και συστηματικής προσπάθειας πολλών ετών, πολλές φορές σε βάρος άλλων προσωπικών στιγμών και απολαύσεων. Δεν ήταν λίγες οι στιγμές που το άγχος έφτασε σε επίπεδα δύσκολα να διαχειριστεί κανείς, ωστόσο τελικά αποδεικνύεται ότι με υπομονή και καλή θέληση μπορεί κανείς να υπερνικήσει όλα τα εμπόδια.

Στο σύντομο αυτό κείμενο θα προσπαθήσω να εκφράσω τις ευχαριστίες μου απέναντι στα άτομα ο ρόλος των οποίων, άμεσα ή έμμεσα, ήταν σημαντικός για μένα σε όλη αυτήν την προσπάθεια και στην επιτυχή έκβασή της.

Πρωτίστως θα ήθελα να εκφράσω την απεριόριστη, εκ βάθους καρδίας ευχαριστία και ευγνωμοσύνη μου απέναντι στον επιβλέποντα καθηγητή μου, κ. Αθανάσιο Παναγόπουλο. Οι γραμμές αυτές ίσως δεν είναι αρκετές για να αποδώσουν επαρκώς όσα θα ήθελα να εκφράσω. Τον ευχαριστώ που μου εμπιστεύτηκε ένα τέτοιο δύσκολο εγχείρημα, κρίνοντας ότι είμαι άξιος να το φέρω εις πέρας. Με αντιμετώπισε εξ αρχής ως ισότιμο μέλος της ερευνητικής του ομάδας, με επιβράβευε σε κάθε μου προσπάθεια, επιτυχή ή μη και μου στάθηκε σε κάθε δύσκολη ακαδημαϊκή αλλά και προσωπική στιγμή ενθαρρύνοντάς με να συνεχίσω. Πραγματικά ήταν μεγάλη η τύχη μου να συνεργαστώ με έναν τόσο σπάνιο στις ημέρες μας άνθρωπο, τόσο σε επίπεδο επιστημονικής κατάρτισης και ευρύτητας πνεύματος, όσο και σε προσωπικό επίπεδο. Πάντα ένιωθα ότι μπορούσα να του εμπιστευθώ τις ανησυχίες και τα προβλήματά μου και πάντα κατάφερνε να με ενθαρρύνει και να μου δώσει λύση. Ο κ. Παναγόπουλος παρά την κατάρτισή του είναι ένας καθημερινός άνθρωπος, μακριά από κάθε υπεροψία ή εγωισμό, ένας άνθρωπος δίκαιος, ακέραιος και ανιδιοτελής. Τον ευχαριστώ για όλα.

Εξέχουσα θέση στις ευχαριστίες μου καταλαμβάνει η ερευνήτρια Δρ. Ροδούλα Μακρή, με την οποία όλα αυτά τα χρόνια είχαμε μια πολυδιάστατη, ευχάριστη και δημιουργική συνεργασία και την οποία ευχαριστώ εγκαρδίως για την εμπιστοσύνη της.

Μέρος της παρούσας εργασίας ανάγεται στα πλαίσια του έργου '*ASALASCA – LARGE SCALE ASSESSMENT KA/Q BAND ATMOSPHERIC CHANNEL USING THE ALPHASAT TDP 5 PROPAGATION BEACON (ESA)*'. Ευχαριστώ πολύ τον Ευρωπαϊκό Οργανισμό Διαστήματος (European Space Agency – ESA) καθώς και τον υπεύθυνο του έργου, Dr. Antonio Martellucci για την άψογη συνεργασία που είχαμε. Εγκάρδιες ευχαριστίες και στον project manager του έργου, Δρ. Σπ. Βεντούρα για την εποικοδομητική συνεργασία και την άριστη επικοινωνία που είχαμε όλα αυτά τα χρόνια.

Θα ήθελα να ευχαριστήσω τους πιο στενούς συνεργάτες, ερευνητές και υποψηφίους διδάκτορες και πλέον φίλους με τους οποίους συνεργάστηκα όλα αυτά τα χρόνια, και πιο συγκεκριμένα τους Δρ. Ν. Λύρα, Δρ. Χ. Κουρόγιωργα, Χρ. Εφραίμ, Θ. Καψή, Δρ. Γ. Πιτσιλαδή, Δρ. Μ. Πουλάκη, την Δρ. Στ. Βασσάκη, τους Δ. Παπανικολάου, Δρ. Ν. Μωραΐτη, την Δρ. Ι. Popescu, τους Δρ. Αθ. Μαρούση, Δρ. Αντ. Γκότση, Δρ. Κ. Μαλιάτσο, Δρ. Κ. Κακόγιαννη, Φ. Ρογάρη και Αλ. Ρογάρη. Ξεχωριστά θα

ήθελα να ευχαριστήσω τους φίλους και συνεργάτες Δρ. Στ. Σαγκριώτη, ο οποίος πέραν της ακαδημαϊκής μας συνεργασίας συνεισέφερε προσωπικό χρόνο και ιδρώτα κατά τη φάση εγκατάστασης των μετρητικών δεκτών και για τη βοήθεια του οποίου είμαι ευγνώμων, καθώς και τον Αν. Ρουμελιώτη, με τον οποίο περάσαμε ουκ ολίγα βράδια αλλά και Σαββατοκύριακα αλληλοενθαρρυνόμενοι ενώ εργαζόμασταν ο καθένας για το διδακτορικό του και στον οποίο εύχομαι καλή επιτυχία. Επιπλέον, θα ήθελα να ευχαριστήσω τους κυρίους Π. Κελέφα, Αθ. Γιδά και Ν. Μπούζη με τους οποίους είχα μια εξαιρετική συνεργασία.

Τέλος, θα ήθελα να ευχαριστήσω όλους τους καθηγητές, ερευνητές, συνεργάτες και λοιπό προσωπικό με τους οποίους συνεργάστηκα και ειδικότερα τους καθηγητές κ. Π. Κωττή, κ. Γ. Φικιώρη και κ. Χ. Καψάλη, η διδασκαλία των οποίων συνέβαλε καθοριστικά στην απόφασή μου να ασχοληθώ με το εν λόγω αντικείμενο και τομέα ευρύτερα. Ευχαριστώ πολύ και τα μέλη της επταμελούς επιτροπής εξέτασης για το χρόνο που αφιέρωσαν στην παρούσα εργασία.

Ευχαριστώ ακόμη όλους τους συγγενείς και φίλους που στάθηκαν κοντά μου σε όλη αυτή τη διαδρομή και ειδικότερα την Εμμ. Πεδιαδίτη, η οποία ελπίζω να με ανέχεται για πολλά ακόμη χρόνια.

Κλείνοντας, δε θα μπορούσα να παραλείψω τον σημαντικότερο συντελεστή στην περάτωση αυτής της εργασίας, την οικογένειά μου, τον πατέρα μου Ζαχ. Παπαφραγκάκη, τη μητέρα μου Σ. Γαλετάκη και την αδερφή μου Μ. Παπαφραγκάκη. Σας ευχαριστώ για όλα όσα μου έχετε προσφέρει, για την υπομονή σας απέναντί μου και την εμπιστοσύνη σας. Σας ευχαριστώ που θυσιάσατε τα πάντα για μας, τα παιδιά σας, και δώσατε τόση έμφαση στη μόρφωσή μας. Ελπίζω να είστε περήφανοι για εμάς και κάποια στιγμή να μπορέσουμε, έστω εν μέρει, να σας το ανταποδώσουμε.

Απόστολος Ζαχ. Παπαφραγκάκης
Αθήνα, Φεβρουάριος 2021

List of Publications

The following publications were accomplished within the scope of this thesis:

Journals:

S. Ventouras, A. Martellucci, A. Z. Papafragkakis, et al. "Assessment of spatial and temporal properties of Ka/Q band earth-space radio channel across Europe using Alphasat Aldo Paraboni payload", International Journal of Satellite Communications and Networking. 2019.

A. Z. Papafragkakis, C. I. Kourogiorgas and A. D. Panagopoulos, "Site-diversity Ka-band Satellite Propagation Campaign in Attica, Greece using ALPHASAT: First 2-years results" in IEEE Antennas and Wireless Propagation Letters, 2019.

A. Z. Papafragkakis, S. Ventouras, C. I. Kourogiorgas and A. D. Panagopoulos, "ALPHASAT site diversity experiments in Greece and the UK at Ka band: Comparison of 2-years' results" in ITU Journal: ICT Discoveries, Vol. 2, 1, Nov. 2019.

A. Z. Papafragkakis and A. D. Panagopoulos, "Site and Time Diversity Experimental Statistics at Ka and Q band in Attica Greece using ALPHASAT", URSI Radio Science Letters, Vol. 2, 2020.

Conferences:

A. Z. Papafragkakis, N. K. Lyras, C. I. Kourogiorgas and A. D. Panagopoulos, "Propagation measurements campaign in Athens with ALPHASAT at Ka-band using Software Defined Radio technologies," Electromagnetics in Advanced Applications (ICEAA), 2015 International Conference on, Turin, 2015, pp. 634-637.

A. Z. Papafragkakis, N. K. Lyras, C. I. Kourogiorgas and A. D. Panagopoulos, "Deploying a Ka-band SDR beacon receiver targeting ALPHASAT: challenges, implementation and propagation measurements", 21st Ka and Broadband Communications Conference – 33rd AIAA International Communications Satellite Systems Conference (ICSSC), Bologna, 2015.

A. Z. Papafragkakis et al., "Large Scale Assessment of Ka/Q band atmospheric channel across Europe with ALPHASAT TDP5: A new propagation campaign," 2016 10th European Conference on Antennas and Propagation (EuCAP), Davos, 2016, pp. 1-5.

A. Z. Papafragkakis, C. I. Kourogiorgas, A. D. Panagopoulos and S. Ventouras "Site Diversity Experimental Campaigns in Greece and UK Using ALPHASAT at Ka and Q Band", Loughborough Antennas and Propagation Conference LAPC 2016, Loughborough, 2016.

A. Z. Papafragkakis et al., "Large Scale Assessment of Ka/Q Band Atmospheric Channel Across Europe with ALPHASAT TDP5: The Augmented Network", 2017 11th European Conference on Antennas and Propagation (EuCAP), Paris, 2017.

A. Z. Papafragkakis, A. D. Panagopoulos and S. Ventouras, "Combined Beacon and Noise Satellite Propagation Measurements using Software Defined Radio", 2017 11th European Conference on Antennas and Propagation (EuCAP), Paris, 2017.

C. I. Kourogiorgas, A. Z. Papafragkakis, A. D. Panagopoulos and V. K. Sakarellos "Cooperative Diversity Performance of Hybrid Satellite and Terrestrial Millimeter Wave Backhaul 5G Networks", 2017 International Workshop on Antenna Technology: Small Antennas, Innovative Structures, and Applictions (iWAT), Athens, 2017.

A. Z. Papafragkakis, C. I. Kourogiorgas, A. D. Panagopoulos and S. Ventouras, "Investigation of long-term statistics and dynamics of in-excess attenuation at Q/V bands", 23rd Ka and Broadband Communications Conference – 35th AIAA International Communications Satellite Systems Conference (ICSSC), Trieste, 2017.

A. Z. Papafragkakis, C. I. Kourogiorgas, A. D. Panagopoulos and S. Ventouras, "Large- and short-scale diversity in Greece and UK for high throughput satellite systems", 23rd Ka and Broadband Communications Conference – 35th AIAA International Communications Satellite Systems Conference (ICSSC), Trieste, 2017.

A. Z. Papafragkakis, C. I. Kourogiorgas, A. D. Panagopoulos, S. Ventouras and P.-D. Arapoglou, "Large Scale Site Diversity Experimental Campaign Between Greece and UK Using ALPHASAT: First Results", Wireless and Satellite Systems. 9th International Conference, WiSATS 2017, Oxford, UK, September 14-15, 2017, Lecture Notes of the Institute for Computer Sciences, Social Informatics and Telecommunications Engineering, vol 231. pp 174-183, Springer, Cham.

C. I. Kourogiorgas, A. Z. Papafragkakis, A. D. Panagopoulos and S. Ventouras, "Long-Term and Short-Term Atmospheric Impairments Forecasting for High Throughput Satellite Communication Systems", 2018 12th European Conference on Antennas and Propagation (EuCAP), London, 2018, IET Conference Proceedings, pp. 260-265.

A. J. Roumeliotis, A. Z. Papafragkakis, C. I. Kourogiorgas and A. D. Panagopoulos, "Cellular networks backhauling through satellite: Performance evaluation using Alphasat site diversity experiment in Greece", 2018 12th European Conference on Antennas and Propagation (EuCAP), London, 2018, IET Conference Proceedings, pp. 807-811.

C. Kourogiorgas, A. Z. Papafragkakis, P. M. Arapoglou, A. D. Panagopoulos and S. Ventouras, "Total Atmospheric Attenuation Statistics for LEO Mega-Constellations Operating at Q/V Bands," 2019 13th European Conference on Antennas and Propagation (EuCAP), Krakow, Poland, 2019, pp. 1-5.

A. Z. Papafragkakis, C. I. Kourogiorgas and A. D. Panagopoulos, "Performance Evaluation of Ka- and Q-band Earth-Space Diversity Systems in Attica, Greece using the Synthetic Storm Technique," 2019 13th European Conference on Antennas and Propagation (EuCAP), Krakow, Poland, 2019, pp. 1-4.

A. Z. Papafragkakis, A. D. Panagopoulos and P. M. Arapoglou, "Performance of Site Diversity Reception Schemes in Next Generation Data Relay Systems," 8th ESA International Workshop on Tracking, Telemetry and Command Systems for Space (TTC 2019), Darmstadt, 24-27 Sept 2019.

A. Z. Papafragkakis, C. I. Kourogiorgas and A. D. Panagopoulos, "Triple Frequency Diversity and Frequency Scaling Experimental Campaign in Attica, Greece: Preliminary Results", URSI General Assembly and Scientific Symposium (GASS) 2020, Rome, Italy, 2020.

A. Z. Papafragkakis, C. I. Kourogiorgas, A. D. Panagopoulos and S. Ventouras, "Second Order Excess Attenuation Statistics in Athens, Greece at 19.701 GHz using ALPHASAT", 12th IEEE/IET International Symposium on Communication Systems, Networks and Digital Signal Processing - CSNDSP, held online, Portugal, 2020.

Book chapters:

C. I. Kourogiorgas, A. Z. Papafragkakis A. D. Panagopoulos and S. Ventouras, "Next-generation non-geostationary satellite communication systems: link characterization and system perspective", in Satellite Communications in the 5G Era, Chap. 6, pp. 151-179, 2018.

Table of Contents

List of Figures

List of Tables

List of Equations

Εκτεταμένη Περίληψη στα Ελληνικά

1.1 Εισαγωγή

Οι ολοένα αυξανόμενες απαιτήσεις για υψηλότερους ρυθμούς μετάδοσης σε συνδυασμό με την εξάντληση του διαθεσίμου φάσματος για δορυφορικές επικοινωνίες επιβάλλουν τη μετάβαση των συστημάτων και υπηρεσιών σε ανώτερες φασματικές ζώνες όπως η Ka και οι Q/V (Arapoglou et al. 2011). Η μετάβαση αυτή θα δώσει τη δυνατότητα για ανάπτυξη νέων δορυφορικών συστημάτων υψηλούς ρυθμαπόδοσης (High Throughput Satellites, HTS), παρέχοντας αξιοσημείωτα μεγαλύτερη χωρητικότητα δικτύου και ρυθμούς μετάδοσης δεδομένων σε δορυφορικές ζεύξεις τροφοδοσίας (feeder links) τάξεως δεκάδων Tbps (De Gaudenzi et al. 2012, Kyrgiazos et al. 2012). Ωστόσο, η διάδοση του σήματος στις ζώνες αυτές είναι πολύ πιο ευαίσθητη στα διάφορα ατμοσφαιρικά φαινόμενα και κυρίως στις ατμοσφαιρικές κατακρημνίσεις-βροχή (έντονη εξασθένηση - τάξεως δεκάδων dB) (Ippolito 2008), εγείροντας έτσι ζητήματα αξιοπιστίας και διαθεσιμότητας των ζεύξεων. Η χρήση ενός απλού περιθωρίου διαλείψεων (fade margin) ή ελέγχου ισχύος, τεχνικές που χρησιμοποιούνται με επιτυχία σε συστήματα με χαμηλότερες συχνότητες λειτουργίας, κρίνεται τόσο ασύμφορη όσο και ανεπαρκής στη συγκεκριμένη περίπτωση (Arapoglou et al. 2011, Gharanjik et al. 2015, De Gaudenzi 2012). Είναι επομένως απαραίτητη η χρήση εξειδικευμένων τεχνικών άμβλυνσης διαλείψεων (Fading Mitigation Techniques, FMTs) (Panagopoulos et al. 2004), οι οποίες με τη σειρά τους προϋποθέτουν ακριβή μοντελοποίηση του καναλιού διάδοσης.

Παρά το γεγονός ότι κατά το παρελθόν προτάθηκαν στη διεθνή βιβλιογραφία διάφορα μοντέλα για χρήση στις εν λόγω συχνότητες, τα μοντέλα αυτά είτε κρίνονται ελλιπή είτε μη καθολικά εφαρμόσιμα για χρήση σε οποιαδήποτε γεωγραφική περιοχή. Για την πρόταση ενός νέου μοντέλου διάδοσης είναι απαραίτητη η ύπαρξη πραγματικών μετρήσεων, η συλλογή και στατιστική ανάλυση των οποίων χρησιμοποιείται τόσο για την ανάπτυξή του όσο και για την εκτίμηση της ακρίβειάς του. Η συλλογή μετρήσεων όμως συνιστά πολύπλοκη διαδικασία, καθώς απαιτεί εξειδικευμένο, ακριβό εξοπλισμό και μακροχρόνια παρατήρηση σε παγκόσμια κλίμακα προκειμένου τα δεδομένα να είναι αντιπροσωπευτικά. Σε ευρωπαϊκό επίπεδο καταβλήθηκε την περασμένη δεκαετία μια πρώτη προσπάθεια συλλογής μετρήσεων διάδοσης στις συχνότητες αυτές χρησιμοποιώντας τους δορυφόρους ESA OLYMPUS και ITALSAT F1 (Paraboni et al. 2002, Ventouras et al. 2006), ωστόσο η χωρο-χρονική συσχέτιση των φαινομένων διάδοσης δεν μελετήθηκε σε βάθος.

Τα τελευταία χρόνια, με πρωτοβουλία και υπό τον συντονισμό του Ευρωπαϊκού Οργανισμού Διαστήματος (European Space Agency, ESA) έγιναν διαθέσιμα σήματα-beacons για τη διεξαγωγή νέων μετρήσεων στις ζώνες Ka και Q (19.701 και 39.402 GHz) από τον δορυφόρο ALPHASAT (25.0^{o}E). Το γεγονός αυτό, σε συνδυασμό με την ωρίμανση της τεχνολογίας και τις νέες τεχνικές Software Defined Radio (SDR), αποτέλεσε το κίνητρο για την ανάπτυξη δεκτών για διεξαγωγή μετρήσεων σε αυτές τις φασματικές ζώνες, για πρώτη φορά σε ελληνικό έδαφος. Οι αναπτυχθέντες δέκτες αποτελούν πλέον μέρος του πανευρωπαϊκού δικτύου μετρήσεων του Alphasat Aldo Paraboni Propagation Experimenters (ASAPE) καθώς και του ερευνητικού προγράμματος της ESA «ASALASCA» (Ventouras et al. 2017). Λίγο αργότερα, με σκοπό τη συλλογή

περισσοτέρων δεδομένων προστέθηκαν άλλοι δύο δέκτες στις φασματικές ζώνες Ku (11.699 GHz) και Ka-band (19.680 GHz) χρησιμοποιώντας τους δορυφόρους Arabsat BADR-5 (26.0^{o}E) και Eutelsat KaSat (9.0^{o}E) αντίστοιχα. Στα επόμενα παρουσιάζεται η αρχιτεκτονική των δεκτών, οι αρχές λειτουργίας τους καθώς και κάποια αποτελέσματα μετρήσεων και στατιστικής ανάλυσης.

1.2 Χρήση beacons για διεξαγωγή μετρήσεων διάδοσης

Η μεγάλη πλειοψηφία των δορυφόρων εκπέμπουν, εκτός των άλλων, σήματα τηλεμετρίας και beacons. Τα σήματα beacons, συνήθως αδιαμόρφωτα, σταθερής ισχύος σήματα Continuous Wave (CW), χρησιμοποιούνται κατά κύριο λόγο για τον εντοπισμό του δορυφόρου από επίγειους σταθμούς/προσανατολισμό κεραιών ή και ως σήματα πιλότοι για σκοπούς τηλεμετρίας. Η φύση των σημάτων αυτών (σταθερή ισχύς και μικρό φασματικό περιεχόμενο) τα καθιστούν κατάλληλα για τη διεξαγωγή μετρήσεων διάδοσης.

Ο δορυφόρος ALPHASAT στις 25.0^{o} E αν και προορισμένος για εμπορικούς σκοπούς (εμπορική ονομασία Inmarsat-4A F4) φέρει διάφορα τηλεπικοινωνιακά φορτία-payloads για τη διεξαγωγή πειραματικών δραστηριοτήτων υπό την αιγίδα του Ευρωπαϊκού Οργανισμού Διαστήματος (European Space Agency, ESA). Ένα εξ' αυτών είναι και το περιώνυμο Technology Demonstration Payload (TDP) #5, το οποίο αποτελείται από δύο beacons, στα 19.701 GHz (Ka-band) και 39.402 (Q-band) GHz αντίστοιχα. Αντίστοιχα σήματα beacons είναι διαθέσιμα και από τους δορυφόρους BADR5 και KaSAT στα 11.699 GHz (Ku-band) και 19.680 GHz (Ka-band).

Οι μετρητικοί δορυφορικοί δέκτες που παρουσιάζονται στην παρούσα εργασία λαμβάνουν τα εν λόγω beacons με κατάλληλα σχεδιασμένο και υλοποιημένο εξοπλισμό με σκοπό τη συλλογή μετρήσεων διάδοσης στις φασματικές ζώνες Ku, Ka και Q.

1.3 Αρχιτεκτονική των υλοποιηθέντων μετρητικών δορυφορικών δεκτών

Οι δέκτες που κατασκευάστηκαν για τον σκοπό του πειράματος αποτελούνται επιμέρους κατά το πλείστον από εξαρτήματα ήδη διαθέσιμα στην αγορά προκειμένου περί ελαχιστοποίησης τόσο του κόστους και του χρόνου υλοποίησης όσο και τη γρήγορη αντιμετώπιση και αποκατάσταση τυχόν βλαβών. Η βασική αρχιτεκτονική των δεκτών είναι κοινή για όλες τις συχνότητες και παρουσιάζεται στο παρακάτω απλοποιημένο μπλοκ διάγραμμα (Σχ. 1-1).

Για την περίπτωση της Ka-band χρησιμοποιείται δορυφορικό παραβολικό κάτοπτρο τύπου offset διαμέτρου 1.2 m ενώ για την περίπτωση της Q-band χρησιμοποιείται παραβολικό κάτοπτρο τύπου shrouded, διαμέτρου 0.6 m. Για την Ku-band χρησιμοποιείται επίσης παραβολικό κάτοπτρο offset 1.2 m, με το οποίο γίνεται και παράκεντρη λήψη του Ka-band beacon του KaSAT.

Το λαμβανόμενο σήμα κυματοδηγείται σε κατάλληλα Low Noise Blocks (LNBs) όπου το σήμα φιλτράρεται, ενισχύεται και υποβιβάζεται στη συχνότητα πριν μεταφερθεί στο επόμενο στάδιο. Μετά από δεύτερο φιλτράρισμα και ενίσχυση, το σήμα οδηγείται σε ένα Universal Software Radio Peripheral (USRP) B210 της Ettus, το οποίο και αναλαμβάνει το κομμάτι της δειγματοληψίας,

κβάντισης και ψηφιοποίησης του λαμβανόμενου σήματος. Τα ψηφιακά δείγματα μεταφέρονται τελικά σε έναν υπολογιστή ο οποίος εφοδιασμένος με λογισμικό που αναπτύχθηκε με βάση το δημοφιλές πλαίσιο ανάπτυξης GNU Radio εκτελεί το τελευταίο στάδιο επεξεργασίας και αποθήκευσης.

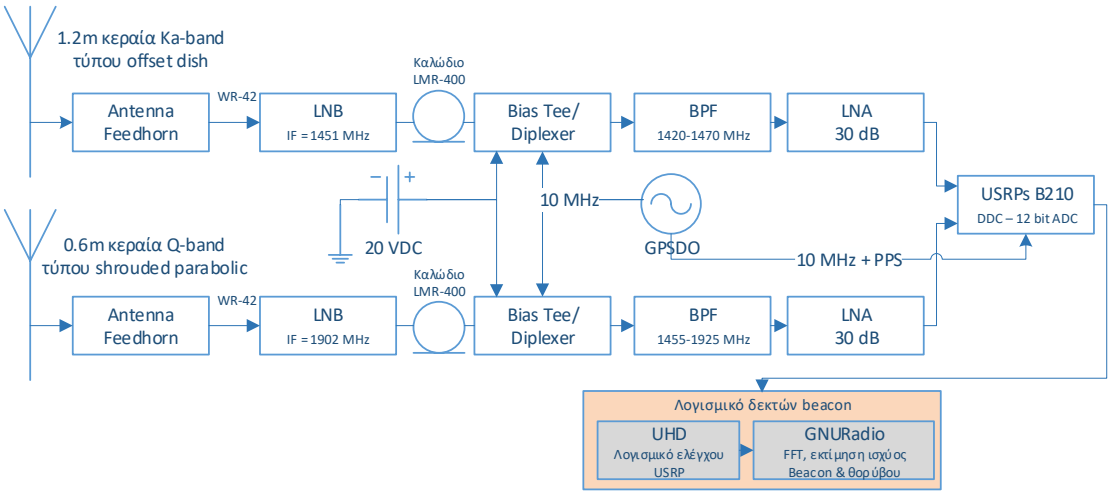

Σχήμα 1-1: Συνοπτικό μπλοκ διάγραμμα της αρχιτεκτονικής των δεκτών για τον ALPHASAT

Η μέτρηση της λαμβανόμενης ισχύος αλλά και του επιπέδου θορύβου γίνεται χρησιμοποιώντας τεχνικές εκτίμησης Fast Fourier Transform (FFT). Το επίπεδο θορύβου είναι ένα χρήσιμο μέγεθος, καθώς επηρεάζεται από τα διάφορα φαινόμενα διάδοσης και η γνώση της τιμής του μπορεί να βελτιώσει την ακρίβεια των μετρήσεων (Papafragkakis et al. 2017). Το δυναμικό εύρος (dynamic range) υπολογίζεται μεγαλύτερο των 40 dB για τους δέκτες Ka ενώ για τους δέκτες Q το δυναμικό εύρος αγγίζει τα 35 dB.

Τόσο η λαμβανόμενη ισχύς όσο και ο θόρυβος μετρώνται και αποθηκεύονται με ρυθμό δειγματοληψίας 10 Hz χρησιμοποιώντας χρονοσφραγίδες (timestamps) συγχρονισμένες μέσω GPS Disciplined Oscillator (GPSDO). Έτσι διασφαλίζεται πλήρως η ακρίβεια των μετρήσεων στο πεδίο του χρόνου. Επιπλέον, προκειμένου όλοι οι ταλαντωτές/ρολόγια να παραμείνουν σε πλήρη συγχρονισμό, επιστρατεύονται οι έξοδοι 10 MHz και Pulse Per Second (PPS) του GPSDO.

Παρά το γεγονός ότι ο ALPHASAT είναι γεωστατικός δορυφόρος η φαινόμενη θέση του από τη Γη μεταβάλλεται κατά τη διάρκεια της ημέρας λόγω μικρής κεκλιμένης τροχιάς. Η εν λόγω κεκλιμένη τροχιά συντηρείται σκοπίμως για οικονομία καυσίμων και προκειμένου να παραταθεί η διάρκεια ζωής του. Η μικρή απόκλιση στην τροχιά (εκτιμώμενη τιμή μικρότερη των 3 μοιρών κατά τη διάρκεια του πειράματος) εισάγει μια απόκλιση της τάξης των ±2 º στη γωνία ανύψωσης των κατόπτρων και μικρότερη των 0,2º στο αζιμούθιο. Η τελευταία μπορεί να αγνοηθεί καθώς είναι πολύ αργά μεταβαλλόμενη και δεν επηρεάζει ουσιαστικά τις μετρούμενες τιμές. Ωστόσο η μεταβολή στη φαινόμενη γωνία ανύψωσης χρήζει αντιμετώπισης μέσω κατάλληλου σχήματος παρακολούθησης του δορυφόρου (tracking system).

Για το σκοπό αυτό αναπτύχθηκε πλήρως αυτοματοποιημένο λογισμικό το οποίο σε συνδυασμό με ψηφιακά κλινόμετρα και γραμμικούς κινητήρες που έχουν εγκατασταθεί στα κάτοπτρα αλλά

και αρχεία Orbit Ephemeris Messages (OEM) που παρέχουν τη θέση του δορυφόρου κάθε στιγμή, είναι σε θέση να παρακολουθούν και να σκοπεύουν το κάτοπτρο στο δορυφόρο με ακρίβεια καλύτερη από 0.05º. Η βασική αρχιτεκτονική λειτουργίας του συστήματος παρακολούθησης του δορυφόρου παρατίθεται στο παρακάτω μπλοκ διάγραμμα (Σχ. 1-2).

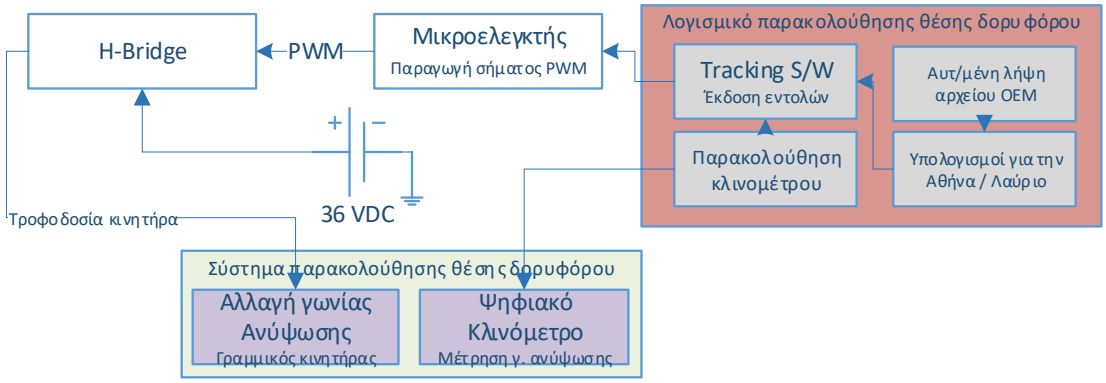

Σχήμα 1-2: Συνοπτικό μπλοκ διάγραμμα της αρχιτεκτονικής του συστήματος σκόπευσης δορυφόρου (tracking system)

1.4 Λεπτομέρειες πειράματος

Συνολικά σχεδιάστηκαν και υλοποιήθηκαν έξι δέκτες, ένας για τη ζώνη Ku, τρεις για τη ζώνη Ka και δύο για τη ζώνη Q. Η εγκατάστασή τους πραγματοποιήθηκε στο συγκρότημα της Πολυτεχνειούπολης Ζωγράφου (NTUA Campus) καθώς και στο Τεχνολογικό και Πολιτιστικό Πάρκο Λαυρίου (NTUA LTCP) και για την περίπτωση του ALPHASAT έγινε σε ζεύγη αποτελούμενα από έναν δέκτη Ka και έναν Q ανά τοποθεσία (Σχ. 1-3 και 1-4). Οι επιπλέον δέκτες Ku και Ka εγκαταστάθηκαν στην Πολυτεχνειούπολη Ζωγράφου.

Σχήμα 1-3: Τα κεραιοσυστήματα των δεκτών στην Πολυτεχνειούπολη (αριστερά) και στο Λαύριο (δεξιά)

Οι δύο τοποθεσίες απέχουν περί τα 36,5 km σε ευθεία γραμμή και διαφέρουν ως προς τις κλιματικές συνθήκες καθώς η μεν Πολυτεχνειούπολη βρίσκεται στους πρόποδες του Υμηττού, το δε Λαύριο βρίσκεται νοτιότερα, σε χαμηλό υψόμετρο και δίπλα στη θάλασσα. Η επιλογή των

θέσεων αυτών επιτρέπει την εξέταση σεναρίων διαφορισμού θέσης (site diversity) και την εκμετάλλευσή τους για την άμβλυνση διαλείψεων (Papafragkakis et al. 2016).

Σχήμα 1-4: Οι δέκτες στην Πολυτεχνειούπολη (αριστερά) και στο Λαύριο (δεξιά)

Οι δέκτες Ka βρίσκονται σε αδιάλειπτη λειτουργία από τον Ιούλιο του 2016 ενώ οι δέκτες Q εγκαταστάθηκαν και λειτουργούν από τον Ιούλιο του 2017. Οι επιπλέον δύο δέκτες Ku και Ka εγκαταστάθηκαν και λειτουργούν από τον Ιούλιο του 2017 και 2018 αντίστοιχα.

Παράλληλα με τους δέκτες λειτουργεί και εξοπλισμός για την υποστήριξη των μετρήσεων με μετεωρολογικά δεδομένα. Πιο συγκεκριμένα, μετρούνται μεγέθη όπως η θερμοκρασία, η υγρασία, η ατμοσφαιρική πίεση, η ταχύτητα και διεύθυνση του ανέμου, η ηλιακή ακτινοβολία και φυσικά η βροχόπτωση. Τα μετεωρολογικά δεδομένα είναι πλήρως συγχρονισμένα με τους δέκτες και αποθηκεύονται σε βάση δεδομένων προκειμένου να εξεταστεί η συσχέτισή τους με τα διάφορα φαινόμενα διάδοσης.

1.5 Αποτελέσματα

Όπως ήδη ειπώθηκε, οι μετρήσεις είναι ακόμα σε εξέλιξη. Στα παρακάτω σχήματα παρουσιάζεται ως παράδειγμα ένα κομμάτι των συλλεγέντων δεδομένων με τη μορφή χρονοσειρών συνοδευόμενο με τα αντίστοιχα δεδομένα βροχόπτωσης.

1.5.1 Παράδειγμα διαφορισμού θέσης (site diversity) στην Ka-band

Στο παρακάτω σχήμα (Σχ. 1-5) παρουσιάζονται δεδομένα για τρεις ημέρες, από 16/11/2017 έως και 18/11/2017 οπότε και μπορούν να γίνουν αξιόλογες παρατηρήσεις. Στο σχήμα γίνεται εμφανής η χρονική υστέρηση που παρουσιάζεται μεταξύ των φαινομένων μεταξύ Ζωγράφου και Λαυρίου, γεγονός που θα μπορούσε να αξιοποιηθεί για τη χρήση σχήματος διαφορισμού θέσης (site diversity).

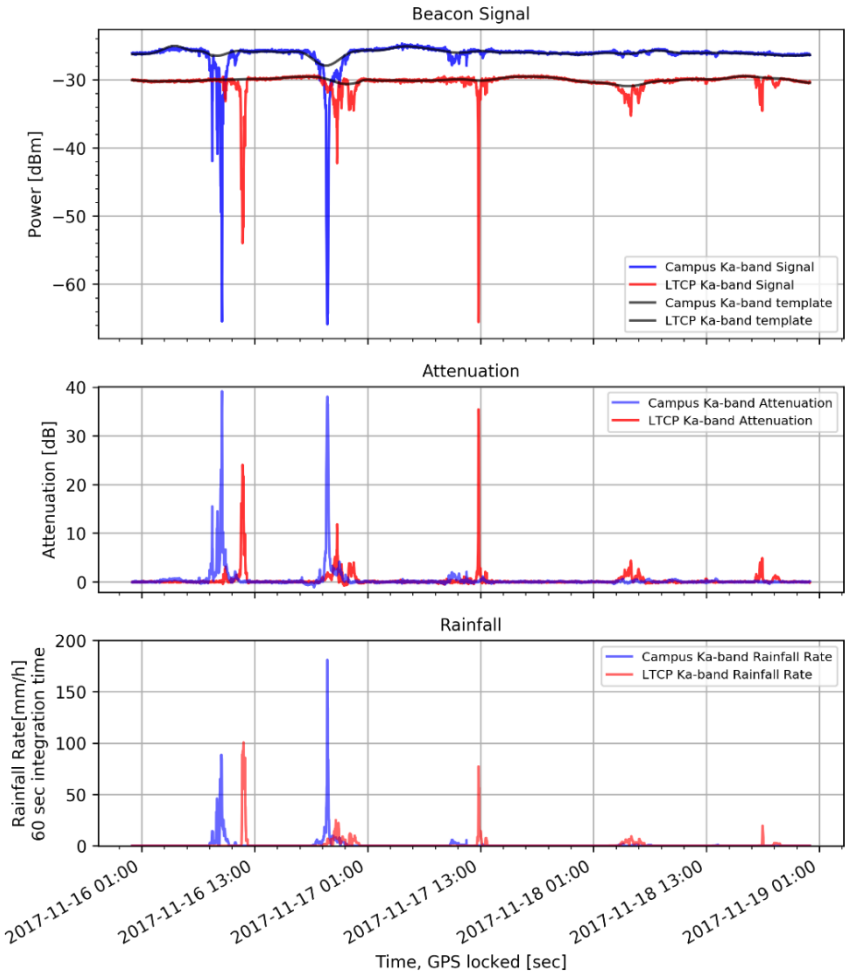

Σχήμα 1-5: Παράδειγμα site diversity - χρονοσειρές ζώνης Ka των δύο τοποθεσιών, από 16/11/2017, έως 18/11/2017

1.5.2 Παράδειγμα διαφορισμού συχνότητας (frequency diversity)

Προκειμένου να γίνει αντιληπτή η διαφορετική επίπτωση που έχουν τα ατμοσφαιρικά φαινόμενα στη διάδοση του σήματος στις ζώνες Ka και Q παρουσιάζονται στο παρακάτω σχήμα (Σχ. 1-6) δεδομένα διάρκειας μίας ημέρας (04/11/2017) για τους σταθμούς Ka και Q στην Πολυτεχνειούπολη Ζωγράφου. Παρά το μικρό ρυθμό βροχόπτωσης, η ζώνη Q αντιμετωπίζει μη αμελητέα εξασθένηση (τάξεως 3 dB) ενώ η ζώνη Ka λιγότερο από 1 dB και μάλιστα για αρκετά μικρότερο χρονικό διάστημα.

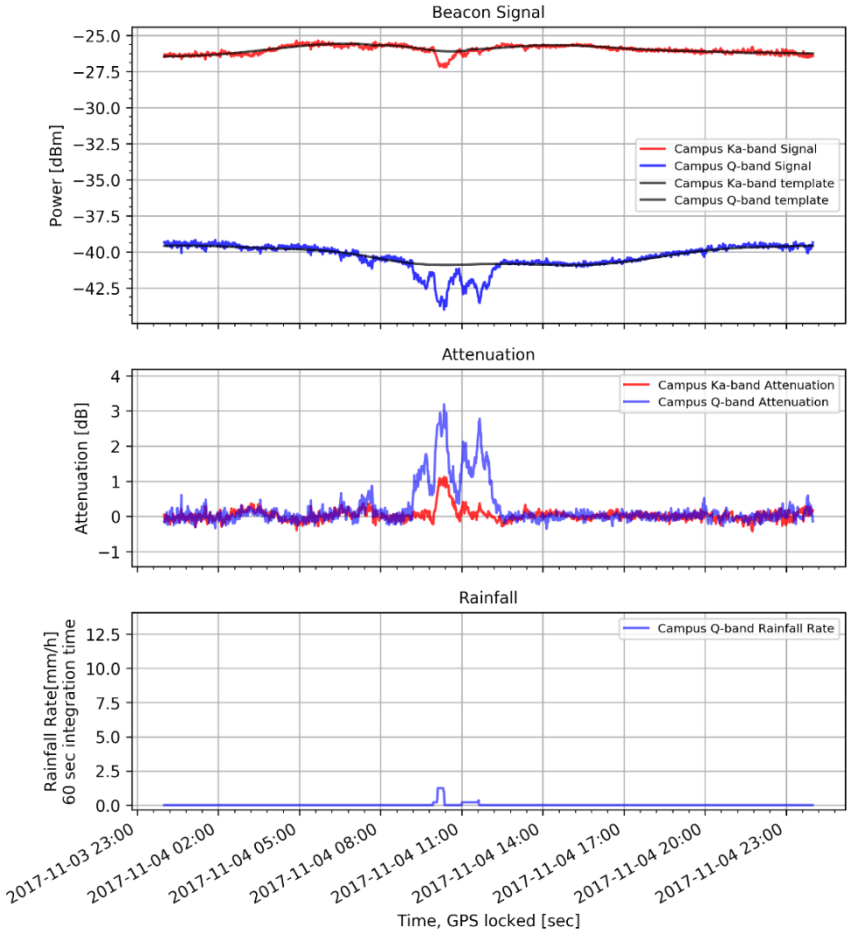

Σχήμα 1-6 Παράδειγμα frequency diversity – χρονοσειρές για την Πολυτεχνειούπολη Ζωγράφου την 04/11/2017

1.6 Στατιστικά πρώτης τάξης - αξιολόγηση

Τόσο κατά τη σχεδίαση των συστημάτων (διαστασιολόγηση ζεύξεων) όσο και κατά τη χρήση/έλεγχο μοντέλων διάδοσης, είναι αναγκαία η στατιστική περιγραφή των φαινομένων καθώς και η χωροχρονική συσχέτισή τους. Στα παρακάτω σχήματα (Σχ. 1-7 και Σχ. 1-8) παρουσιάζονται τα στατιστικά 1ης τάξεως και πιο συγκεκριμένα οι συμπληρωματικές αθροιστικές κατανομές πυκνότητας πιθανότητας (Complementary Cumulative Distribution Functions – CCDFs) τόσο για το ρυθμό βροχόπτωσης στις δύο περιοχές (mm/h, χρησιμοποιώντας μέθοδο ολοκληρωσης 1 min) όσο και για την υπερβάλλουσα εξασθένηση (excess attenuation).

Τα σχήματα αυτά αφορούν το πλήρες διάστημα των μετρήσεων ανά συχνότητα και περιοχή. Από αυτά γίνεται εύκολα αντιληπτό ότι η υπερβάλλουσα εξασθένηση (in-excess attenuation), δηλαδή η εξασθένηση που υφίσταται το σήμα λόγω συννέφων και ιδίως βροχής, λαμβάνει εξαιρετικά μεγάλες τιμές για μη αμελητέο ποσοστό του χρόνου σε όλες τις περιπτώσεις και ιδίως στην Q-band.

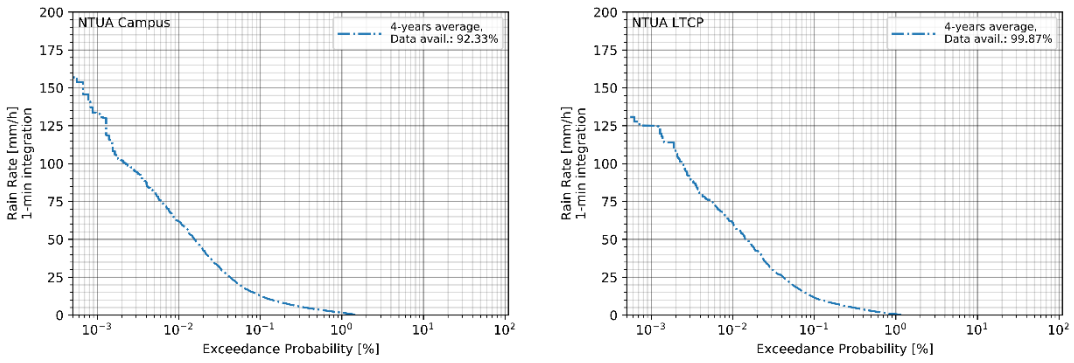

(a) **(b)**

Σχήμα 1-7: Κατανομές υπέρβασης βροχόπτωσης ως ποσοστό του χρόνου για τα 4 πλήρη έτη μετρήσεων στις δύο περιοχές (a) στην Πολυτεχνειούπολη Ζωγράφου και (b) στο Λαύριο

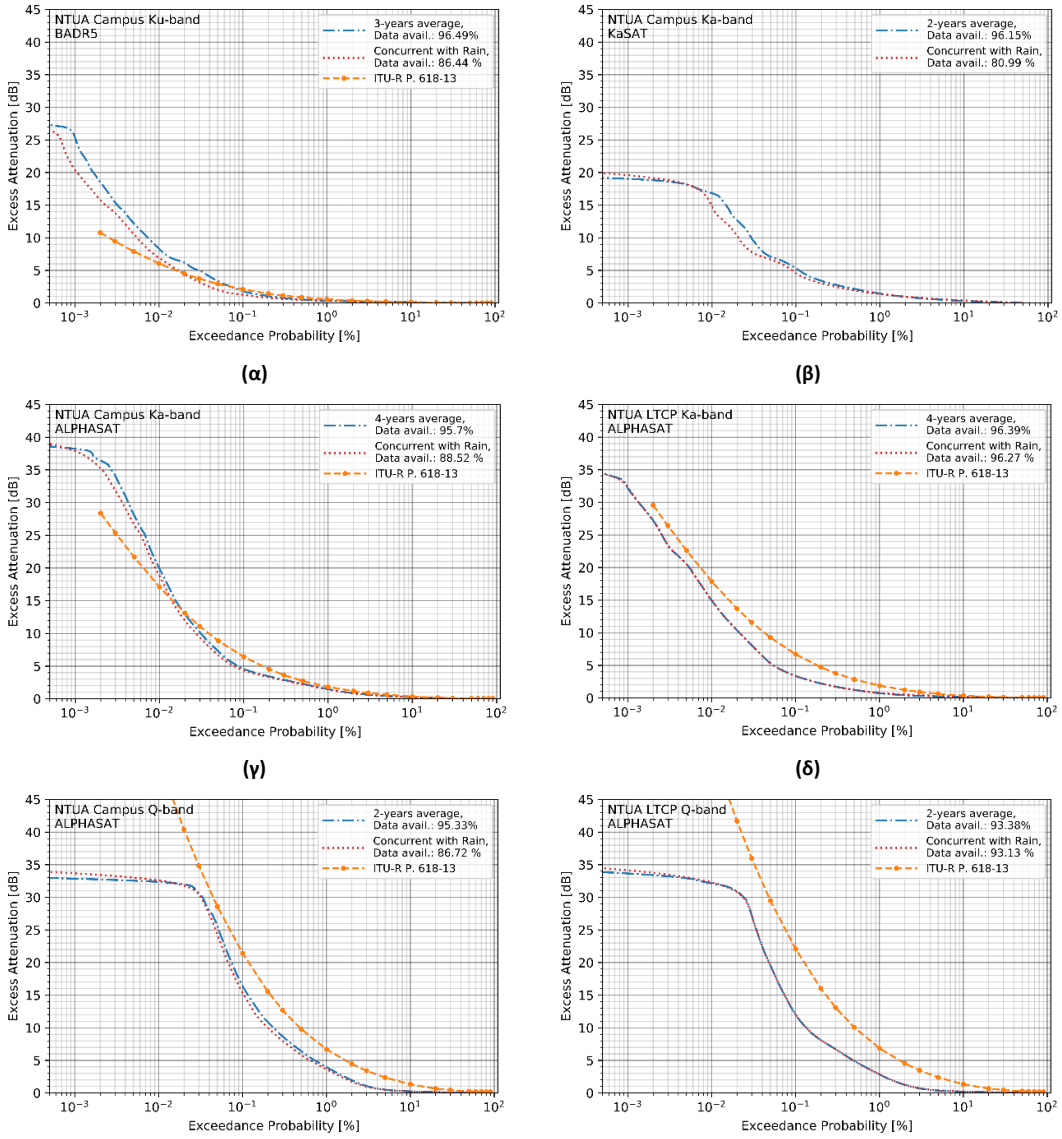

(α) **(β)**

(γ) **(δ)**

(ε) **(στ)**

Σχήμα 1-8: Κατανομές υπέρβασης εξασθένησης ως ποσοστό του χρόνου για όλες τις συχνότητες και στις δύο περιοχές (α) Ku-band BADR5 Campus, (β) Ka-band KaSAT Campus, (γ) Ka-band ALPHASAT Campus, (δ) Ka-band ALPHASAT LTCP, (ε) Q-band ALPHASAT Campus, (στ)Q-band ALPHASAT LTCP

Για την περίπτωση της Ka-band παρατηρούνται τιμές εξασθένησης περί τα 25 dB (Ζωγράφου) για σχεδόν 0.01% του χρόνου, καθιστώντας ένα απλό περιθώριο διαλείψεων ή τον έλεγχο ισχύος ανεπαρκή αντίμετρα για την επίτευξη υψηλούς διαθεσιμότητας.

Στην περίπτωση της Q-band παρατηρείται ακόμη μεγαλύτερη εξασθένηση για τα ίδια ποσοστά του χρόνου, καταδεικνύοντας πόσο σημαντικές είναι οι επιπτώσεις της διάδοσης σε αυτή τη φασματική ζώνη. Ενδεικτικά, για 0.01% του χρόνου παρατηρείται απόσβεση μεγαλύτερη των 35 dB και για τις δύο περιοχές.

Μόνο στη φασματική ζώνη Ku παρατηρούνται χαμηλότερες τιμές εξασθένησης, περί τα 10 dB στο 0.01% του χρόνου. Πράγματι έως τώρα, συμβατικές τεχνικές χρησιμοποιώντας κάποιο περιθώριο διαλείψεων μαζί με δυναμικό έλεγχο ισχύος είχαν αποδειχτεί αρκετές για την επίτευξη υψηλούς διαθεσιμότητας σε αυτή τη φασματική ζώνη, σε πλήρη αντίθεση όπως φαίνεται με τις ζώνες Ka και Q.

Θα πρέπει να σημειωθεί ότι η επιπέδωση των καμπύλων στα χαμηλά ποσοστά του χρόνου (δηλ. στις χαμηλές πιθανότητες) οφείλεται στην υπέρβαση του διαθεσίμου δυναμικού εύρους των δεκτών. Αντίστοιχα αποτελέσματα παρουσιάζονται στα (Papafragkakis et al. 2019) και (Papafragkakis et al. 2020).

1.7 Στατιστικά δεύτερης τάξης – δυναμική συμπεριφορά διαλείψεων

Ιδιαίτερο ενδιαφέρον παρουσιάζουν και τα στατιστικά δεύτερης τάξης τα οποία αφορούν τον ρυθμό μεταβολής της εξασθένησης (Fade slope, dB/sec), τη διάρκεια των διαλείψεων (fade durations) και το πλήθος αυτών ανά κατώφλι εξασθένησης καθώς και το μεσοδιάστημα μεταξύ διαλείψεων (inter-fade durations).

Στο παρακάτω σχήμα (Σχ. 1-9) παρουσιάζονται τα θηκογράμματα (boxplots) για τη διάρκεια των διαλείψεων ανά κατώφλι εξασθένησης.

Όπως διαπιστώνει κανείς μελετώντας τα παρακάτω θηκογράμματα, ανεξαρτήτως συχνότητας και τιμής εξασθένησης φαίνεται ότι η διάμεσος (median) των διαλείψεων είναι σχετικά σταθερή με τιμή από 2-6 sec, μια αξιοσημείωτη διαπίστωση. Αντίστοιχα, φαίνεται ότι το τρίτο τεταρτημόριο (quartile) των δεδομένων διάρκειας διαλείψεων ακολουθεί μια σχεδόν γκαουσιανού τύπου κατανομή .

Σε κάθε περίπτωση, τέτοια στατιστικά είναι πολύ σημαντικά στην υλοποίηση αποδοτικών τεχνικών FMTs καθώς μπορούν να εισαχθούν ως παράμετροι

- στο ρυθμό δειγματοληψίας των αλγορίθμων FMT
- στο κέρδος κλειστών βρόχων (closed loop gain)
- στον διάστημα υστέρησης μεταξύ εφαρμογής των FMTs

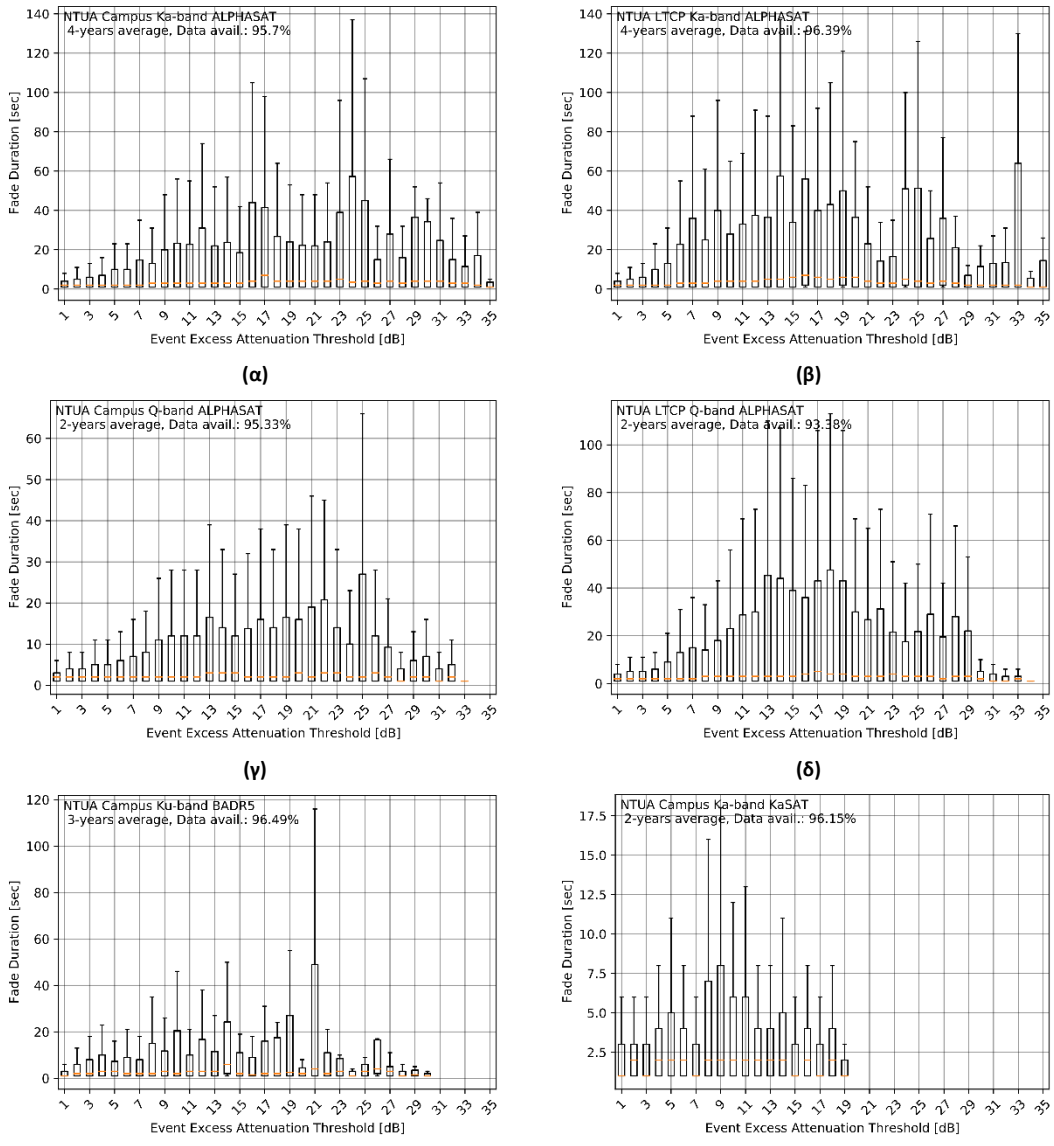

Σχήμα 1-9: Θηκογράμματα διάρκειας διαλείψεων για όλες τις συχνότητες και στις δύο περιοχές (α) Ku-band BADR5 Campus, (β) Ka-band KaSAT Campus, (γ) Ka-band ALPHASAT Campus, (δ) Ka-band ALPHASAT LTCP, (ε) Q-band ALPHASAT Campus, (στ)Q-band ALPHASAT LTCP

1.8 Στατιστικά χωρικού διαφορισμού/διαφορισμού θέσης

Από τα πλέον αποδοτικά σχήματα μετριασμού διαλείψεων θεωρείται η τεχνική χωρικού διαφορισμού (site diversity). Στα πλαίσια αυτής, το σήμα εκπέμπεται ή λαμβάνεται από πλέον της μιας γεωγραφικής περιοχής δίνοντας δυνατότητα αξιοποίησης της μη χωρικής κατανομής της βροχής. Γενικά, όσο μεγαλύτερη είναι η απόσταση μεταξύ των σταθμών (separation distance), τόσο μεγαλύτερο αναμένεται το κέρδος από τη χρήση του σχήματος αυτού. Επίσης, σε περιπτώσεις σωρειτόμορφης βροχής (convective precipitation), όπου η βροχή σχηματίζεται λόγω

ισχυρών ανοδικών κινήσεων, είναι μεγάλης έντασης αλλά μικρής διάρκειας και έκτασης, το κέρδος είναι συνήθως μεγαλύτερο έναντι περιπτώσεων στρατόμορφης βροχής (stratiform precipitation) η οποία είναι μικρής έντασης αλλά μεγάλης διάρκειας και γεωγραφικής έκτασης.

Στο παρακάτω σχήμα (Σχ. 1-10), απεικονίζεται η από κοινού πιθανότητα υπέρβασης εξασθένησης (joint exceedance probability) ανά συχνότητα χρησιμοποιώντας ταυτόχρονα δεδομένα από τις δύο περιοχές καθώς και ποιο θα ήταν το προκύπτον κέρδος (ανά συχνότητα), θεωρώντας κάποιον από τους δυο σταθμούς ως πρωτεύοντα.

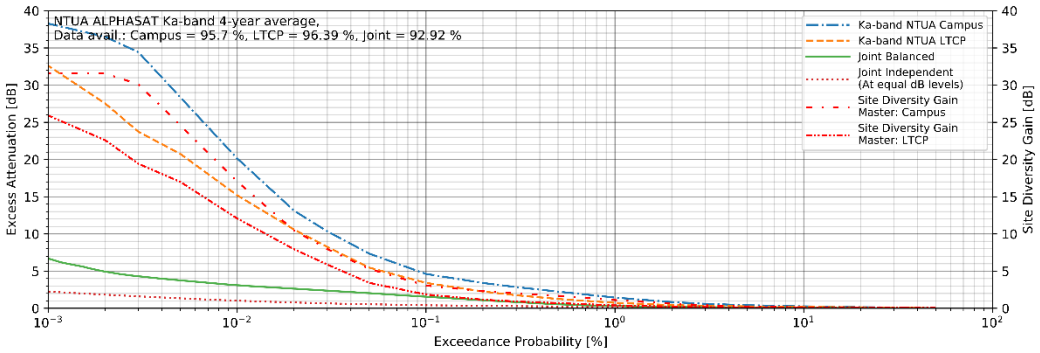

(α)

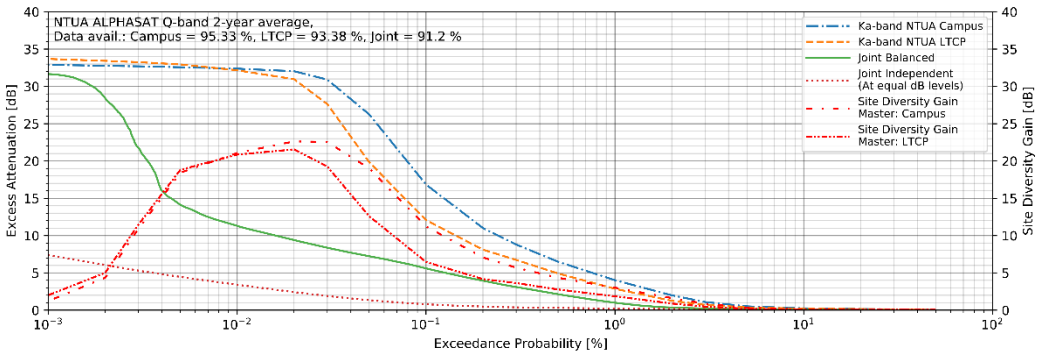

(β)

Σχήμα 1-10: Αποτελέσματα εφαρμογής χωρικού διαφορισμού χρησιμοποιώντας ταυτόχρονα δεδομένα για (α) την Ka-band, (β) την Q-band

Στο παραπάνω σχήμα, ουσιαστικά παρουσιάζεται η επίδοση ενός ιδεατού συστήματος διαφορισμού θέσης (selection combining site diversity), στο οποία θεωρείται δυνατή η στιγμιαία εναλλαγή μεταξύ των δεκτών. Είναι φανερό ότι ένα τέτοιο σύστημα όντως καταφέρνει να μετριάσει την επίπτωση των διαλείψεων. Παρά το γεγονός ότι ένα τέτοιο σύστημα ίσως δεν είναι πρακτικά υλοποιήσιμο, καθορίζει ωστόσο το ανώτατο όριο βελτίωσης που θα μπορούσε να επιτευχθεί χρησιμοποιώντας την εν λόγω τεχνική.

Ενδεικτικά, για 0.001% του χρόνου η προκύπτουσα απόσβεση είναι περί τα 6.7 dB στη ζώνη Ka (κέρδος διαφορισμού ~ 31 dB), παρουσιάζοντας μια σχετικά γραμμική συμπεριφορά κέρδους (σε dB) στο διάστημα μεταξύ 0.003% και 0.02%.

Για την περίπτωση της φασματικής ζώνης Q, η μελέτη περιορίζεται για πιθανότητες όχι μικρότερες του 0.03% λόγω πεπερασμένου δυναμικού εύρους των δεκτών και μεγάλης έντασης των φαινομένων. Στο ποσοστό αυτό του χρόνου (0.03%), το κέρδος διαφορισμού είναι περί τα 23

dB, απαιτώντας ένα επιπλέον περιθώριο 8.5 dB προκειμένου το σύστημα να φτάσει διαθεσιμότητα 99.97%).

Οι τιμές απόσβεσης που προκύπτουν μετά την εφαρμογή του χωρικού διαφορισμού είναι εν γένει δυνατό να αντισταθμιστούν με το περιθώριο διαλείψεων που συνήθως ούτως ή άλλως υιοθετείται, ειδικά αν το τελευταίο συνδυαστεί και με κάποιο σχήμα ελέγχου ισχύος. Έτσι, είναι δυνατόν να αυξηθεί σημαντικά το ποσοστό διαθεσιμότητας των συστημάτων ακόμη και στις φασματικές ζώνες Ka και Q.

1.9 Στατιστικά κλιμάκωσης συχνότητας

Χρησιμοποιώντας στατιστικά κλιμάκωσης συχνότητας (frequency scaling) ή ακόμη καλύτερα μοντέλα βασισμένα σε δεδομένα κλιμάκωσης συχνότητας μπορεί κανείς να αποκτήσει γνώση του τι συμβαίνει σε κάποια φασματική ζώνη χρησιμοποιώντας δεδομένα από κάποια άλλη, χαμηλότερη φασματική ζώνη. Ακόμη, συστήματα διαφορισμού συχνότητας μπορούν να υλοποιηθούν, αν και η ταυτόχρονη λειτουργία σε διαφορετικές ζώνες συνήθως είναι δύσκολη καθώς απαιτεί πολύ διαφορετικό εξοπλισμό και συνεπάγεται διαφορετικούς ρυθμούς μετάδοσης δεδομένων.

Έτσι σε κάποια περιοχή όπου μπορεί να μην υπάρχουν διαθέσιμα δεδομένα διάδοσης για τις συχνότητες ενδιαφέροντος, μπορεί ωστόσο να υπάρχουν σε κάποια χαμηλότερη, είναι δυνατή η χρήση των τελευταίων για την εξαγωγή συμπερασμάτων ή προβλέψεων. Αντίστοιχα, μοντέλα διάδοσης των οποίων η ακρίβεια έχει επαληθευτεί σε ένα εύρος συχνοτήτων μπορούν να επεκταθούν και σε άλλες υψηλότερες συχνότητες με κατάλληλες τροποποιήσεις.

Στο παρακάτω σχήμα (Σχ. 1-11) παρουσιάζεται η κλιμάκωση συχνότητας για την περίπτωση των ζωνών Ka και Q χρησιμοποιώντας μετρήσεις από τον ALPHASAT στις δύο περιοχές πειράματος. Χρησιμοποιώντας αφενός το σύνολο των δεδομένων και αφετέρου τις ενδιάμεσες τιμές ανά ζεύγος εξασθένησης Ka-Q πραγματοποιήθηκε απλή γραμμική παλινδρόμηση εξάγοντας πολύ καλά αποτελέσματα.

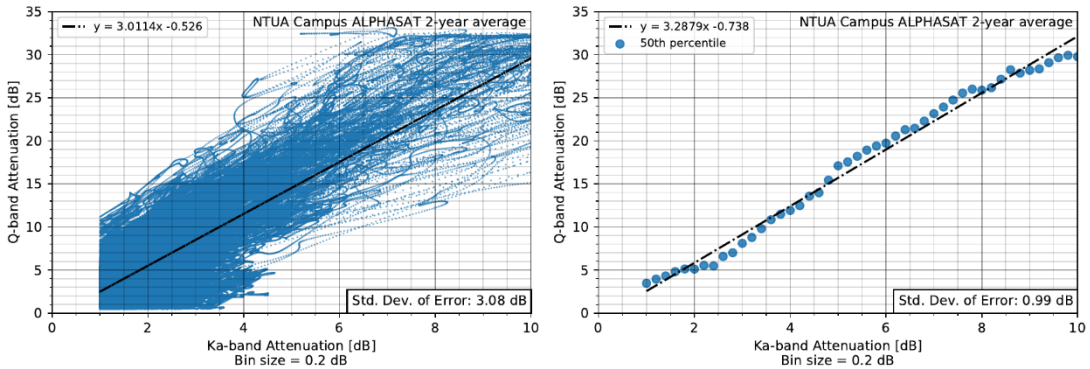

(α)

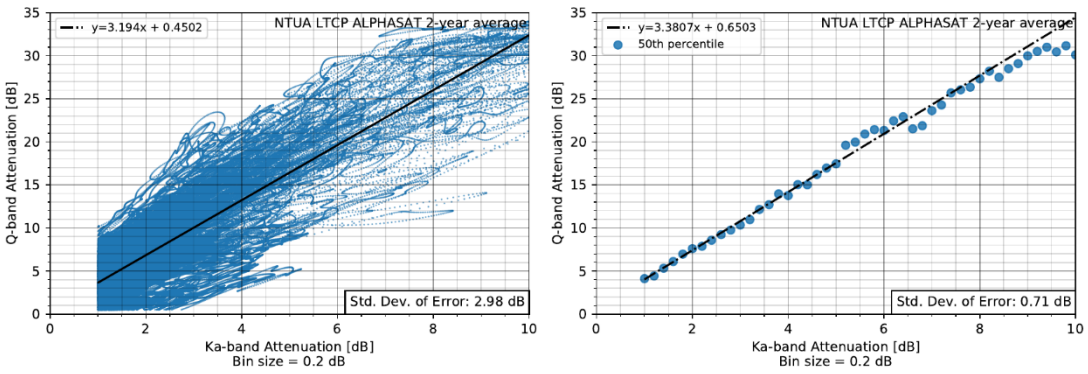

(β)

Σχήμα 1-11: Αποτελέσματα κλιμάκωσης συχνότητας χρησιμοποιώντας ταυτόχρονα δεδομένα για τις ζώνες Ka και Q (α) στην Πολυτεχνειούπολη (β) στο Λαύριο

1.10 Συμπεράσματα – Προεκτάσεις

Στην παρούσα εργασία παρουσιάζεται λεπτομερώς η σχεδίαση, ανάπτυξη, εγκατάσταση και λειτουργία δορυφορικών δεκτών για την εκτέλεση μετρήσεων διάδοσης στις φασματικές ζώνες Ku, Ka και Q. Παρουσιάζονται αναλυτικά οι παράγοντες που πρέπει να ληφθούν υπόψη σε μια τέτοια προσπάθεια, οι προκλήσεις που αντιμετωπίστηκαν καθώς και οι λύσεις που δόθηκαν.

Το σύνολο των ληφθέντων δεδομένων επεξεργάστηκε, δίνοντας τη δυνατότητα αξιολόγησης των στατιστικών πρώτης και δεύτερης τάξης, των διαφόρων σχημάτων FMTs (χωρικό διαφορισμό, χρονικό διαφορισμό, διαφορισμό τροχιάς) καθώς και μελέτης της κλιμάκωσης συχνότητας και των σπινθηρισμών.

Η παρούσα εργασία συνιστά την πρώτη και πιο ολοκληρωμένη προσπάθεια συγκέντρωσης και ανάλυσης μετρητικών δεδομένων διάδοσης για τις δορυφορικές ζώνες συχνοτήτων Ku, Ka και Q στην Ελλάδα αλλά και στην ευρύτερη περιοχή της νοτίου Μεσογείου. Μέχρι πρότινος, η συντριπτική πλειοψηφία των διαθεσίμων μοντέλων στη βιβλιογραφία βασιζόταν σε παραδοχές ή μετρήσεις άλλων, υποτιθέμενα παρόμοιων κλιματικών περιοχών. Στην πράξη, όπως άλλωστε αποδεικνύεται και από την ανάλυση των ληφθέντων μετρήσεων και την αντιπαραβολή τους με παρόμοιες προσπάθειες ανά την Ευρώπη, υπάρχουν σημαντικές αποκλίσεις.

Η Ελλάδα διαφέρει κατά πολύ από το ηπειρωτικό κλίμα της κεντρικής Ευρώπης (ακόμα και από αυτό της βόρειας-κεντρικής Ιταλίας) ή το τροπικό/υποτροπικό της Αφρικής. Ειδικά η Αττική όπου και λαμβάνουν χώρα οι μετρήσεις, ευρισκόμενη στο κέντρο της Ελλάδας, στο ηπειρωτικό της τμήμα αλλά δίπλα σε θάλασσα παρουσιάζει την πλέον χαρακτηριστική συμπεριφορά περιοχής της νοτίου Μεσογείου. Το καλοκαίρι χαρακτηρίζεται από μεγάλη διάρκεια, πολύ υψηλές θερμοκρασίες (>40^{o}C σε πολλές περιπτώσεις) και υγρασία ενώ ο χειμώνας είναι ήπιος, με θερμοκρασίες όχι συχνά χαμηλότερες των 10^{o}C. Κατά τους θερινούς μήνες οι βροχοπτώσεις δεν είναι ιδιαίτερα συχνές, είναι ωστόσο πολύ έντονες (σωρειτόμορφη βροχή), μικρής διάρκειας και έκτασης. Η εποχή με τις μεγαλύτερες συγκεντρώσεις υετού είναι διαχρονικά το φθινόπωρο.

Οι μετρήσεις αποδεικνύουν ότι εάν δε ληφθούν σημαντικά αντίμετρα, η διαθεσιμότητα συστημάτων με συχνότητες λειτουργίας στις ζώνες Ka ή Q θα είναι σημαντικά περιορισμένη. Από

την άλλη, η εφαρμογή τεχνικών FMT και ειδικά σχημάτων χωρικού διαφορισμού φαίνεται εξαιρετικά αποδοτική (αν και κοστοβόρα) και θα μπορούσε να αυξήσει θεαματικά τη διαθεσιμότητα των συστημάτων.

Η σύγκριση των δεδομένων με μοντέλα που υπάρχουν στη βιβλιογραφία καθώς και η βελτίωσή τους ή ανάπτυξη νέων θα μπορούσε να αποτελέσει μέρος μελλοντικής εργασίας. Ακόμη, οι χρονοσειρές θα μπορούσαν να χρησιμοποιηθούν για την προσομοίωση συστημάτων που βασίζονται στη συνέργεια με δορυφορικά συστήματα, όπως π.χ. στα πλαίσια του οικοσυστήματος των δικτύων 5G/6G.

1.11 Βιβλιογραφία

Arapoglou P.-D., Shankar M. R. B., Panagopoulos A. D, Ottersten B.: "Gateway diversity strategies in Q/V band feeder links", 17th Ka Broadband Communications Conference, 2011, Palermo, Italy

De Gaudenzi R., Re E., Angeletti P.: "Smart Gateways Concepts for High-Capacity Multi-beam Networks", 30th AIAA International Communications Satellite System Conference (ICSSC), International Communications Satellite Systems Conferences (ICSSC), 2012

Gharanjik A., Shankar M. R. B., Arapoglou P. D., Ottersten B.: "Multiple Gateway Transmit Diversity in Q/V Band Feeder Links", IEEE Transactions on Communications, vol. 63, no. 3, pp. 916-926, 2015

Ippolito L.J. "Satellite Communications Systems Engineering: Atmospheric Effects, Satellite Link Design and System Performance". 2008, Jon Wiley

Kyrgiazos A., Evans B., Thompson P., Jeannin N.: "Gateway diversity scheme for a future broadband satellite system", 2012 6th Advanced Satellite Multimedia Systems Conference (ASMS) and 12th Signal Processing for Space Communications Workshop (SPSC), pp. 363-370, 2012, Baiona

Panagopoulos A. D., Arapoglou P.-D. M., Cottis P. G.: "Satellite Communications at Ku, Ka and V Bands: Propagation Impairments and Mitigation Techniques", IEEE Communication Surveys and Tutorials, 2004

Papafragkakis A. Z., Kourogiorgas C. I., Panagopoulos A. D., S. Ventouras: "Site Diversity Experimental Campaigns in Greece and UK Using ALPHASAT at Ka and Q Band", Loughborough Antennas and Propagation Conference LAPC 2016, 2016, Loughborough

Papafragkakis, A. Z., Panagopoulos A. D., Ventouras S.: "Combined Beacon and Noise Satellite Propagation Measurements Using Software Defined Radio", 11th European Conference on Antennas and Propagation (EuCAP), 2017, Paris

Papafragkakis A. Z., Kourogiorgas C. I. and Panagopoulos A. D: "Site-diversity Ka-band Satellite Propagation Campaign in Attica, Greece using ALPHASAT: First 2-years results", IEEE Antennas and Wireless Propagation Letters, 2019.

Papafragkakis A. Z., Ventouras S., Kourogiorgas C. I. and. Panagopoulos A. D.: "ALPHASAT site diversity experiments in Greece and the UK at Ka band: Comparison of 2-years' results", ITU Journal: ICT Discoveries, Vol. 2, 1, Nov. 2019.

Papafragkakis A. Z. and Panagopoulos A. D.: “Site and Time Diversity Experimental Statistics at Ka and Q band in Attica Greece using ALPHASAT”, URSI Radio Science Letters, Vol 2,2020 (in press).

Paraboni A., Riva C., Valbonesiand L. and Mauri M.: “Eight years of ITALSAT copular attenuation statistics at Spino d’Adda”, Space Commun. Vol 18, pp.59-64, 2002

Ventouras S, Callaghan S.A, and Wrench C.L.: “Long-term statistics of tropospheric attenuation from the Ka/U band ITALSAT satellite experiment in the United Kingdom”, Radio Science, Vol. 41, 2006

Ventouras S. et al.: “Large Scale Assessment of Ka/Q Band Atmospheric Channel Across Europe with ALPHASAT TDP5: The Augmented Network”, 2017 11th European Conference on Antennas and Propagation (EuCAP), 2017, Paris.

Chapter 2

Introduction

The increasing demand for high data rate satellite services is necessitated by the vast number of new or planned services involving multimedia transmission or other data rate-intensive applications in the upcoming 5G era [1], [2]. Satellite communication will be key in the 5G vision [1], [3]-[5], by either providing backhaul services to the internet providers or extending the end-user internet connectivity in under-served, remote locations. Additionally, satellite links could serve as the prime solution for use cases such as emergency response, network backup and Internet of Things (IoT) applications.

2.1 Current Status – Open Issues

The spectrum scarcity problem [6]-[7], namely the congestion of the lower frequency bands such as the C and the Ku bands and the fact that system capacity increases with increasing the amount of available spectral bandwidth currently leads to the use of higher frequencies. Currently, fixed satellite services using GEO satellites commonly make use of the Ku (12/14GHz) and the Ka (20/30GHz) frequency bands [8]. These bands are used for both direct-to-the-user (DTU) and broadcasting applications as well as for feeder links and satellite backhaul networks [1], [9].

In order to increase the provided data rates in an efficient, cost-effective manner and taking into consideration the aforementioned spectrum scarcity problem, next generation satellite communication systems are migrating to the Ka and Q/V bands and are expected to make extensive use of link adaptation strategies combined with multi-beam satellites and/or other relevant techniques [10]-[15]. In particular, the Q/V-band or even the W-band and the optical range are investigated as solutions for the feeder links in order to release the whole Ka-band spectrum for the user links [16]-[18]. Operators and system designers have already started planning or even deploying High Throughput Satellite (HTS) systems [1], [19] operating at Ka and Q/V bands, enabling them to increase their offered bandwidth to up to 5 GHz for the Q/V band case [20]. The second generation of High Throughput Satellite (HTS) systems achieves capacities in the range from 10Gbps to 100Gbps by operating at Ka-band, where more bandwidth is available with less coordination issues (with respect to the over-utilized lower frequency bands). As an example, Eutelsat's KASAT offers a throughput of 90Gbps and the capability of supporting a million users [21], [22].

The migration to higher frequency bands combined with the sole use of Q/V bands for feeder links shall yield the following advantages (besides the larger available spectrum):

- Reduced risk of interference across feeder links and user links even when the gateways are deployed within the actual user service area; minimal spectrum coordination is thus required.

- Narrow/spot beams (multi-beam coverage) generation shall allow for even higher throughput, especially when accompanied by frequency and polarization reuse schemes.

Despite the abovementioned advantages, the system components and equipment operating at higher frequencies (although usually more compact) are more challenging in terms of design and manufacturing process rendering them more expensive and difficult to procure and to maintain; the cost of service/provision often denoted in terms of cost per Mbps is critical and has to be kept to a minimum. Such factors and constraints, especially when combined with the fact that signal propagation is more prone to the various atmospheric effects at these frequency bands, constitute a complex optimization problem involving both the satellite as well as the ground segment, where a compromise has to be made in order for the whole endeavor to achieve market success.

2.2 The role of atmospheric impairments

The end-user Quality of Service (QoS) is affected by the performance of each of the individual communication links involved in the overall data transmission chain; the throughput and the availability of each of the latter are, in turn, largely dictated by their resilience to the various propagation effects. Signal propagation at Ka-band frequencies and above is, nevertheless, highly impaired by the various atmospheric phenomena, upping the ante on system design.

The various atmospheric effects could - unless carefully addressed, jeopardize the throughput and/or the link availability [8], [23]-[25], potentially resulting into severe degradation of the overall system performance; more precisely, at Ka- and Q/V-band the atmospheric attenuation arising from precipitation, clouds and atmospheric gases (oxygen and water vapor) can cause signal fading in the order of tens of dB of magnitude for a non-negligible percentage of time with rain being the dominant fading mechanism [24]-[25] involving hydrometeor absorption and scattering. Additionally, tropospheric turbulence scintillates the signal (causes rapid fluctuation of its amplitude) posing further challenges in meeting the required system performance even when advanced mitigation techniques are used [8]. Such phenomena exhibit a stochastic behavior both temporally and spatially and thus differentiate themselves from other deterministic phenomena such as free space loss which can be accounted for in advance (i.e. during the system design/dimensioning phase). When considering feeder-links it is of utmost importance to understand the various limitations and to act proactively (i.e. during the design phase) in order devise mechanisms that counteract the various propagation losses; a feeder-link driven to outage could potentially impact millions of end-users served by this particular link.

In the past, merely allocating a fade margin for earth-space systems operating in lower frequency bands such as e.g. C and Ku was the common practice in order to compensate for the signal fading due to the various atmospheric effects. The fade margin was usually obtained via empirical calculations and modelling based on long-term statistics of signal attenuation for various climatic regions. Nonetheless, when considering the signal propagation at higher frequency bands, the sole use of a conventional fade margin is generally an insufficient counter-measure since signal fading could be in excess of 20-30 dB for a non-negligible fraction of time. The need for more advanced atmospheric attenuation mitigation techniques becomes even more evident, when one considers that for comparable size (effective area) antennas at e.g. Ku- and Ka-band, the latter already offers appreciably higher gain.

In order to compensate for the atmospheric attenuation, Propagation Impairment Mitigation Techniques (PIMTs) are employed [15], also commonly referred to as Fading Mitigation Techniques (FMTs); they are vital in order to meet the required Quality of Service - QoS) imposed by the services, keeping at same time the resource usage at an optimal level [26].

The core concept behind PIMTs is the on-the-fly reconfiguration of an earth-space link, enhancing overall link availability while at the same time maintaining an acceptable average throughput even during events of high path loss. Most PIMTs exploit the non-uniformity of the propagation impairments in time and in space by altering terms involved in the link budget or the baseband signal to compensate for the increased signal attenuation. The following could be considered as the main PIMTs widely proposed for use at Ka-band and above:

- Rate Adaptation, supplemented by ACM and/or VCM
- Power control
- Reconfigurable antennas
- Frequency diversity
- Orbital diversity
- Site diversity
- Time diversity

2.3 Experimental Propagation Campaigns

To enable the design of HTS systems with FMTs, accurate propagation modelling is of utmost importance; compiling new propagation models is nevertheless a very challenging task, as it has to be supported by long-term experimental campaigns. Furthermore, the various parameters can vary across different geographic/climatic regions and hence the results cannot be easily generalized. Regarding the Ka-, Q- and V-bands, experimental data have been relatively limited, despite the major effort the research community put during the propagation experiments using ESA OLYMPUS and ITALSAT F1 in the past. Most importantly, the spatio-temporal correlation characteristics of signal propagation at these bands were not comprehensively studied in the aforementioned campaigns.

Although there has been an effort to conduct propagation measurement campaigns around the globe in the past, it is the first time such a campaign takes place at a south-Mediterranean country like Greece. Greece has a distinct geophysical morphology, consisting of tall mountains and a vast coastline; also, its close proximity to Africa has to be taken into consideration as it influences the climate. It is characterized by long-lasting, hot summers with significant diurnal temperature variations (very high temperatures during the day that drastically drop at night). During the summer season the rain precipitation is sparse and mostly convective (very intense rainfall taking place at irregular intervals), while winter is mostly mild with moderate temperatures and less intense rainfall events.

With the advent Software Defined Radio (SDR) technologies, the execution of propagation measurement campaigns has fortunately become less painstaking and of far lower cost than before. This fact, along with the availability of experimental beacons in the Ka- and Q-band from

ALPHASAT satellite has led many experimenter groups around Europe to initiate new propagation campaigns. Other similar experimental campaigns are ongoing around the globe [27]-[37].

2.4 Structure of the Thesis

In Chapter 3 of this thesis the fundamental propagation effects are briefly outlined along with possible FMTs and measurement techniques; in Chapter 4 the design and deployment of new beacon receivers in Attica, Greece are presented in detail. Chapter 5 provides an evaluation of the first order statistics based on the obtained measurement dataset from all available receivers. The second order statistics (fade dynamics) are investigated in Chapter 6. Chapters 7 to 9 provide statistical evidence for the efficiency of site, time and orbital diversity techniques while in Chapter 10 the frequency scaling across Ku/Ka/Q bands is considered. Scintillation analysis is performed in Chapter 11 followed by an evaluation of a large-scale site diversity scenario across Greece and the UK using the actual, concurrent measurements at each location in Chapter 12. The thesis concludes with Chapter 13 where the main conclusions are drawn and possible future work is outlined. The statistics presented in this thesis can be found in tabular format in the Appendix.

2.5 Chapter References

[1] S. K. Sharma, S. Chatzinotas and P.-D. Arapoglou, (ed.), Satellite Communications in the 5G Era (Telecommunications, 2018) DOI: IET Digital Library, https://digital-library.theiet.org/content/books/te/pbte079e

[2] F. Völk, K. Liolis, M. Corici, J. Cahill, R.T. Schwarz, T. Schlichter, E. Troudt and A. Knopp, "Satellite Integration into 5G: Accent on First Over-The-Air Tests of an Edge Node Concept with Integrated Satellite Backhaul", Future Internet, vol. 11, no. 193, 2019.

[3] A. Gupta and R.K. Jha, A Survey of 5G Network: "Architecture and Emerging Technologies", IEEE Access 2015, vol. 3, pp. 1206–1232. doi:10.1109/ACCESS.2015.2461602.

[4] B.G. Evans, "The role of satellites in 5G", 2014 7th Advanced Satellite Multimedia Systems Conference and the 13th Signal Processing for Space Communications Workshop (ASMS/SPSC), 2014, pp. 197–202, doi:10.1109/ASMS-SPSC.2014.6934544.

[5] K. Liolis, et al. "Use cases and scenarios of 5G integrated satellite-terrestrial networks for enhanced mobile broadband: The SaT5G approach", Int J Satell Commun Network. 2018, pp. 1–22.

[6] S. Shi, K. An, G. Li, Z. Li, H. Zhu and G. Zheng "Optimal Power Control in Cognitive Satellite Terrestrial Networks With Imperfect Channel State Information", IEEE Wireless Communications Letters, vol. 7, 2018, pp. 34–37, doi:10.1109/LWC.2017.2752160.

[7] C. Wang, D. Bian, S. Shi, J. Xu, G. Zhang, "A Novel Cognitive Satellite Network With GEO and LEO Broadband Systems in the Downlink Case". IEEE Access 2018, 6, pp. 25987–26000. doi:10.1109/ACCESS.2018.2831218.

[8] A. D. Panagopoulos, P.-D. M. Arapoglou, P. G. Cottis, "Satellite Communications at Ku, Ka and V Bands: Propagation Impairments and Mitigation Techniques", IEEE Communication Surveys and Tutorials, 2004.

[9] A. D. Panagopoulos, “Propagation Phenomena and Fade Mitigation Techniques for Fixed Satellite Systems”, Book Chapter in the Book Radio Wave Propagation and Channel Modeling for Earth-Space Systems, Taylor and Francis CRC Press, May 2016.

[10] C. Morel, P.-D.Arapoglou, M. Angelone and A. Ginesi, “Link adaptation strategies for next generation satellite video broadcasting: A system approach”, IEEE Transactions on Broadcasting, vol. 61, 2015, pp. 603–614.

[11] S. Nakazawa, M. Nagasaka, S. Tanaka, K. Shogen, “A method to control phased array antenna for rain fading mitigation of 21-GHz band broadcasting satellite”, Proceedings of the Fourth European Conference on Antennas and Propagation (EuCAP),IEEE, 2010, pp. 1–5.

[12] J. Lei and M.Á. Vázquez-Castro, “Multibeam satellite frequency/time duality study and capacity optimization”, Journal of Communications and Networks, vol 13, 2011, pp. 472–480.

[13] Y. Vasavada, R. Gopal, C. Ravishankar, G. Zakaria and N. BenAmmar, ”Architectures for next generation high throughput satellite systems”, International Journal of satellite communications and networking, vol. 34, 2016, pp. 523–546.

[14] Z. Katona, F. Clazzer, K. Shortt, S. Watts, H.P Lexow and R. Winduratna, “Performance, cost analysis, and ground segment design of ultra high throughput multi-spot beam satellite networks applying different capacity enhancing techniques”, International Journal of Satellite Communications and Networking, vol. 34, 2016, pp. 547–573.

[15] A. J. Roumeliotis, C. I Kourogiorgas, A. D. Panagopoulos, “Dynamic Capacity Allocation in Smart Gateway High Throughput Satellite Systems Using Matching Theory”, IEEE Systems Journal, vol. 13, 2019, pp. 2001–2009.

[16] M. Aloisio et al.: “Exploitation of Q/V-band for Future Braodband Telecommunication Satellites”, IVEC 2012, 2012, pp. 351-352.

[17] A. Mengali et al., “Optical Feeder Links Study towards Future Generation MEO VHTS Systems”, 35th AIAA International Communications Satellite Systems Conference, International Communications Satellite Systems Conferences (ICSSC).

[18] S. Ventouras, P. Crawford, and Charilaos Kourogiorgas, “Propagation Elements for the Link Budget of Broadband Satellite Systems in Ka and Q/V Band”, WISATS, Springer, 2018.

[19] N. Jeannin, L. Castanet, J. Radzik, M. Bousquet, B. Evans, and P. Thompson, “Smart gateways for terabit/s satellite”, International Journal of Satellite Communications and Networking, vol. 32, no. 2, 2014, pp. 93–106.

[20] A. Kyrgiazos, B. Evans, P. Thompson, N. Jeannin,”Gateway diversity scheme for a futurebroadband satellite system” in 2012 6th Advanced Satellite Multimedia Systems Conference (ASMS) and 12th Signal Processing for Space Communications Workshop (SPSC), Baiona, 2012, pp. 363–370.

[21] “Eutelsat’s KA-SAT goes live”, ITU News Magazine, 2011, vol. 5, p.46.

[22] H. Fenech, A. Tomatis, S. Amos, V. Soumpholphakdy and J. L. Serrano Merino, “Eutelsat HTS systems”, International Journal of Satellite Communications and Networking, vol. 34, no. 4, 2016, pp. 503– 521, doi: 10.1002/sat.1171.

[23] L. J. Ippolito, Satellite Communications Systems Engineering: Atmospheric Effects, Satellite Link Design and System Performance, John Wiley, 2008.

[24] R.K. Crane, Propagation handbook for wireless communication system design; CRC press, 2003.

[25] A. Kanatas and A. D. Panagopoulos, Radio Wave Propagation and Channel Modeling for Earth–Space Systems; CRC Press: Boca Raton, 2016; chapter 2.

[26] P.-D. M. Arapoglou, E. T. Michailidis, A. D. Panagopoulos, A. G. Kanatas and R. Prieto Cerdeira, “The Land Mobile Earth-Space Channel: SISO to MIMO Modeling from L to Ka-Bands”, IEEE

Vehicular Technology Magazine, June 2011.

[27] J. M. Riera, P. García-del-Pino, G. A. Siles and A. Benarroch, "Propagation experiment in Madrid using the Alphasat Q-Band beacon", Proc. 8th Eur. Conf. Antennas Propag., 2014, pp. 1035-1039.

[28] A. Vilhar, A. Kelmendi, A. Hrovat and G. Kandus, "First year analysis of Alphasat Ka- and Q-band beacon measurements in Ljubljana Slovenia", Proc. 22nd Ka Broadband Conf., Oct. 17–20, 2016.

[29] F. Machado, F. P. Fontán, V. Pastoriza and P. Mariño, "The Ka- and Q-band Alphasat ground station in Vigo", Proc. 9th Eur. Conf. Antennas Propag., 2015, pp. 1-4.

[30] V. Pek and O. Fiser, "Atmospheric attenuation analysis using Aldo-Alphasat beacon signal in Prague", Proc. Microw. Radio Electronics Week Conf., 2017.

[31] J. Nessel, G. Gousetis, M. Zemba and J. Houts, "Design and preliminary results from Edinburgh UK Alphasat Q-band propagation terminal", Proc. 22nd Ka Broadband Commun. Conf., Oct. 2016.

[32] Vilhar, A. Kelmendi and A. Hrovat, "Satellite propagation experiment in Ljubljana: Beacon measurements at Ka and Q-band", Proc. 11th Eur. Conf. Antennas Propag., pp. 3300-3304, Mar. 2017.

[33] S. Ventouras et al., "Large scale assessment of Ka/Q band atmospheric channel across Europe with ALPHASAT TDP5: The augmented network", Proc. 11th Eur. Conf. Antennas Propag., pp. 1471-1475, Mar. 2017.

[34] Rocha, S. Mota and F. Jorge, "Propagation campaign at Q-band and Ka-band using the Alphasat and Ka-Sat satellites", Proc. 12th Eur. Conf. Antennas Propag., pp. 904-909, 2018.

[35] Pastrav, T. Palade, P. Dolea, R. Simedroni, C. Codau and E. Puschita, "The Alphasat experiment at Cluj-Napoca – Preliminary results", Proc. Int. Symp. Electron. Telecommun., pp. 1-4, 2018.

[36] X. Boulanger and L. Castanet, "Ka and Q band propagation experiments in Toulouse using ASTRA 3B and ALPHASAT satellites", Int. J. Satell. Commun. Netw, vol. 37, no. 5, pp. 1-11, 2019.

[37] M. Rytir, M. Cheffena, P. A. Grotthing, L. E. Bråten and T. Tjelta, "Three-site diversity at Ka-B and satellite links in Norway: Gain fade duration and the impact of switching schemes", IEEE Transactions on Antennas and Propagation, vol. 65, no. 11, Nov. 2017, pp. 5992-6001.

Chapter 3

Propagation Effects, Mitigation Techniques & Measurements

3.1 Introduction

In this chapter the main signal propagation phenomena affecting earth-space links at frequencies above 10 GHz are outlined together with the possible countermeasures to minimize their impact on system performance and availability. The chapter ends with a brief discussion on the design and execution of propagation measurements using conventional as well as Software Defined Radio (SDR) techniques.

3.2 Propagation Phenomena

Apart from the free space losses present in any wireless system, satellite communication systems (and earth-space links in general) suffer from effects induced by the earth's atmosphere. Such effects are usually divided in two subcategories, namely in *ionospheric* effects affecting systems operating below 3 GHz and *tropospheric* effects regarding systems operating above 3 GHz [1], [2]. The latter can be very significant especially for operating frequency bands above 10 GHz, where the signal deterioration can lead to significant outage times and overall performance degradation. A brief summary of the tropospheric effects follows in this section.

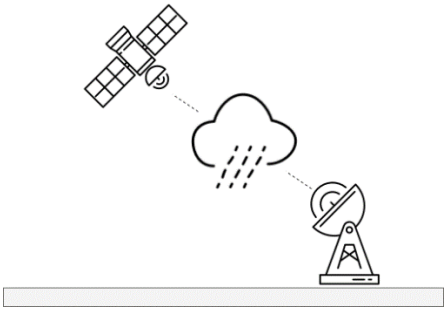

Figure 3-1: A satellite link slant path impaired by atmospheric effects

3.2.1 Precipitation-induced attenuation

Precipitation-induced attenuation, and more particularly rain attenuation constitutes a strong limiting factor in satellite communication system's performance and availability. It is the major

factor of signal degradation and can affect links operating at all frequency bands above 3 GHz, although its role becomes very significant for frequencies above 10 GHz [3].

Precipitation-induced attenuation apart from rain also involves snow and hail, although rain has the most dominating effect on the signal. Rain drops present in the signal's slant path can both absorb and scatter energy and the strength of their effect depends on the signal frequency, rain rate, rain drop size distribution as well as their shape/oblateness. Two main types of rain structure can be distinguished, namely stratiform and convective rain.

Stratiform rain has a large horizontal extent reaching hundreds of kilometers with a vertical height from 4 to 6 km [4] resulting in a rather uniform spatial rainfall rate distribution; it is associated with low to medium rainfall rates, typically less than 25 mm/h which, however, can have large durations throughout the day.

Convective rain usually spans across a smaller horizontal extent (in the order of a few kilometers [4]), nonetheless, it has greater vertical height and can yield rainfall rates in excess of 100 mm/h, albeit for a small duration (in the order of a few minutes); such events are often accompanied by thunderstorms and are more often in tropical and subtropical climatic regions, easily driving the satellite link to outage unless proper countermeasures are taken.

The rain attenuation A_R in dB of a signal propagating through a rain medium along a path L is [1]-[4]:

$$A_R = \int_0^L \gamma_R(x)dx \qquad [3\text{-}1]$$

where

$$\gamma_R = kR^\alpha \qquad [3\text{-}2]$$

the rain specific attenuation expressed in dB/km, with k and α functions of frequency, drop-size distribution, temperature, assuming uniform medium and R the rainfall rate in mm/h. Using the effective path length parameter, often a function of rainfall rate, $L(R)$ (km), A_R in dB can be calculated from:

$$A_R = kR^\alpha L(R) \qquad [3\text{-}3]$$

3.2.2 Cloud - Fog Attenuation

Apart from the precipitation-induced attenuation mentioned above, clouds as well as fog interact with the signal causing further attenuation. The clouds are formed by condensed water droplets rather than water vapor; the relative humidity inside the cloud is typically in the vicinity of 100%. Higher altitude clouds could also include/constitute of ice crystals; the latter, although do not play an important role in attenuating the signal, could cause strong depolarization as explained later in this section.

The diameter of the water droplets in the clouds are typically less than 0.1 mm [5] (rain droplets being in the range 0.1 to 10 mm), allowing for the application of Rayleigh scattering theory to determine the cloud specific attenuation (in dB/km) as a function of its average liquid water

content. Statistics of the total columnar content of liquid water can be obtained from e.g., radiometric measurements or using radiosonde sounding techniques. Depending on the type of clouds, a vastly different value of liquid water content could be present; in any case, the cloud attenuation generally increases with frequency and with decreasing elevation angle. The cloud attenuation is much smaller in magnitude when compared to precipitation-induced attenuation, however, clouds are more common than e.g., rain and at higher frequencies can still play a decisive role as far as link availability is concerned.

Attenuation due to fog is very low for signals operating at frequencies below 100 GHz even at low elevation angles and considering the small path length through fog (in the order of a few hundred meters), it can be safely neglected.

3.2.3 Gaseous Attenuation

Gaseous attenuation is caused due to absorption taking place upon interaction of the propagating electromagnetic wave with oxygen (paramagnetic molecule) and water vapor (polar molecule) in the atmosphere [1]; when absorbed, RF energy is converted into heat. The magnitude of attenuation depends on the frequency as well as on the climatic conditions (air temperature, pressure and humidity). The contribution of gaseous attenuation to the total attenuation is considered small compared to other effects, however, at higher frequencies and/or low elevation angles can still be of significant importance.

Oxygen absorption is considered relatively constant among different climatic conditions (oxygen partial pressure is nearly constant around the world). On the other hand, absorption due to water vapor greatly varies depending on the temperature and humidity, parameters showing spatial (location, altitude) and temporal (season and time of the day) variability. The zenith attenuation due to gases can be obtained in dB as [6]:

$$A_{g,zenith} = \gamma_o \, h_o + \gamma_w \, h_w \qquad [3\text{-}4]$$

where γ_O the specific attenuation due to oxygen in dB/km, γ_W the specific attenuation due to water vapor in dB/km, h_O and h_W the equivalent heights attributable to the oxygen and water vapor component correspondingly. Then, to derive the gaseous attenuation in the slant path [6]:

$$A_{g,slant} = \frac{A_o + A_w}{\sin\theta} = \frac{A_{g,zenith}}{\sin\theta} \qquad [3\text{-}5]$$

where θ the elevation angle in degrees (applicable from 5° to 90°).

In general water vapor absorption is the main contributor to gaseous attenuation, exhibiting maximums at 22.5, 183 and 320 GHz; oxygen absorption dominates at frequencies around 60 and 119 GHz as shown in the figure below [6]:

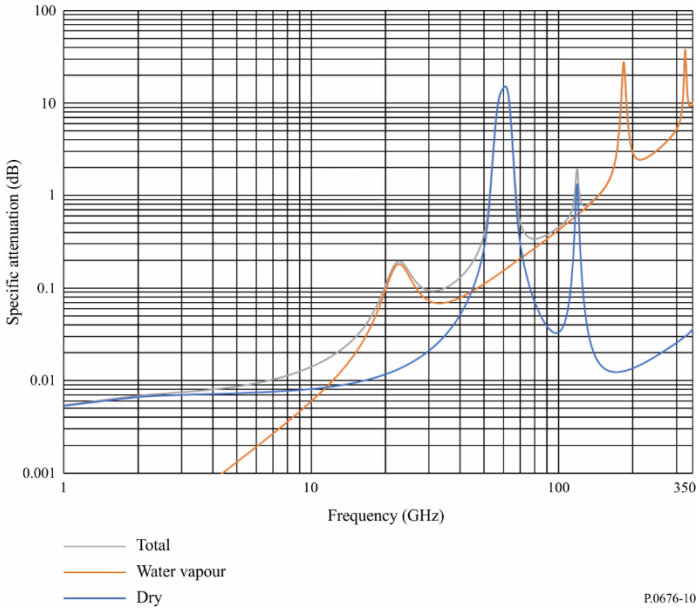

Figure 3-2: Specific attenuation due to atmospheric gases [6]
(Pressure = 1 013.25 hPa; Temperature = 15°C; Water Vapour Density = 7.5 g/m³)

3.2.4 Tropospheric Scintillation & Ray Bending

Tropospheric scintillation refers to the rapid fluctuations of the received signal's amplitude and phase caused due to short-term variations/irregularities of the refractive index in the troposphere along the slant path. Such rapid variations of the refractive index are attributed to atmospheric turbulence; two mechanisms can be distinguished [1]:

- In the lower part of the atmosphere/near the Earth's surface, where wind/turbulence mixes vertical layers of air
- In clouds, where turbulence is a result of the outer edge of the cloud mixing with dry air outside of it causing severe scintillation

Tropospheric scintillation effects greatly depend on the season and the daily weather conditions; they increase with frequency and slant path length and decrease with antenna beamwidth; therefore, at lower the elevation angles where the path length is significantly increased, higher tropospheric scintillation is to be expected [7].

Besides the short-term variations of the refractive index, additional longer-term variations can be observed based on the meteorological conditions; such variations cause the apparent elevation angle from a ground station towards the satellite to be higher than the actual (non-refracted) one (ray bending); such affects are normally neglected except for cases involving very low elevation angles (<10°) and very narrow-beam-width antennas.

3.2.5 Signal Depolarization

Apart from the previous effects, depolarization occurs when a signal propagates through non-spherical scatterers, commonly hydrometeors (raindrops, ice crystals) that are anisotropic and introduce a differential attenuation and/or differential phase shift to each polarization

component; part of the transmitted energy from the incident polarization is transferred/coupled to the orthogonal polarization resulting in polarization crosstalk/interference. Normally, as the raindrop's size increases its shape tends to deform from the spherical one, forming oblate spheroids, often randomly inclined due to wind.

Such a phenomenon is of particular significance in the context of frequency reuse systems employing two independent orthogonal polarization channels to optimize spectrum utilization and increase capacity. In this case, signal depolarization can severely impair system performance as a result of cross-channel interference, limiting its operational availability [8].

Depolarization due to rain involves both differential attenuation and phase shift while depolarization due to ice merely involves a differential phase shift in the polarization components [9].

A metric commonly used to describe the performance of systems is the cross-polarization discrimination XPD defined for linear polarized waves as the ratio [1]:

$$XPD = 20\log\left|\frac{E_{11}}{E_{12}}\right| \qquad [3\text{-}6]$$

where E_{11} the received electric field in the desired (transmitted) polarization (co-polarized field) and E_{12} the electric field received in the orthogonal (undesired) polarization; for this measurement a single-polarized signal is transmitted and received at both polarizations.

An equivalent metric taking into account the performance of the receiving antenna is the cross-polarization isolation or XPI for linear polarized waves, defined as [1]:

$$XPI = 20\log\left|\frac{E_{11}}{E_{21}}\right| \qquad [3\text{-}7]$$

where similarly E_{11} is the received electric field in the desired polarization and E_{21} the electric field received in the desired polarization but originally transmitted at the orthogonal polarization; for this measurement two orthogonally polarized signals are transmitted and received at one polarization.

3.2.6 Sky Noise Increase

Atmospheric attenuation (gaseous and precipitation-induced) is always accompanied by an increase in sky (brightness) temperature; this can be attributed to the energy absorbed by the molecules in the atmosphere being radiated back as thermal noise. The latter is added to the receiver system noise reducing the dynamic range (effective carrier to noise ratio) of systems even further. More precisely, the sky noise temperature T_s (neglecting cosmic noise) in K can be calculated from [1], [3], [7]:

$$T_s \simeq T_m(1-10^{-A/10}) \qquad [3\text{-}8]$$

where T_m is the equivalent medium temperature of the atmosphere (typically around 260-280K).

3.2.7 Other effects

3.2.7.1 Melting Layer Attenuation

Signal can deteriorate as it propagates through the melting layer [10], i.e. above the effective rain height, where snow and ice particles are converted into precipitation; such effects are more pronounced during light rain for systems operating at low elevation angles.

3.2.7.2 Inter-system interference

Inter-system interference can be present at clear-sky, between either satellite systems or terrestrial and satellite systems and is attributed mainly to the antenna side lobes 'leaking' energy towards unwanted directions. Such effects can be further deteriorated by differential rain attenuation, i.e., when the desired signal suffers from higher attenuation than the unwanted, interfering one [11], [12].

3.2.7.3 Antenna Gain effects

Potential amplitude and/or phase fluctuations of the propagating signal can lead to a deviation of the apparent antenna gain, which of course on its own does not change as it only depends on the structural characteristics of the antenna. More precisely, the effective angle of arrival of the incident signal can deviate from the antenna maximum gain direction, possibly accompanied by phase dispersion of the signals reflected from the surface of the antenna reflector resulting in summation of rays that are no longer in-phase [4], [13]. Such effects are more prominent in large and very large antennas, particularly the ones pointing at very low elevation angles.

3.3 Fade Mitigation Techniques

As already mentioned in the introductory chapter of this thesis, due to the magnitude of the attenuation experienced at frequency bands such as Ka-band and above as well as the fraction of time it occurs, the use of only a fade margin is insufficient. In order to combat the aforementioned effects on signal propagation, the following schemes, usually termed Fading Mitigation Techniques (FMTs) or Propagation Impairment Mitigation Techniques (PIMTs) have been devised by the system designers [14], ; each of them can either be used on its own or combined with other(s), depending on the severity of the expected signal degradation and the resources available.

3.3.1 Power Control Schemes

Power control schemes involve the alteration of the transmitted power [15], [16] either at the earth station (Up-link power control, UPLC) or at the satellite (Down-link power control, DLPC). Under normal conditions, the High-Power Amplifier (HPA) at the ground station or the Travelling Wave Tube Amplifier (TWTA) at the satellite have a particular output back-off, i.e., there is a margin between the amplifier's operational point and its saturation point).

During a fade event, the output back-off can be reduced, effectively increasing the transmitted power and therefore compensating (at least partially) for the attenuation effects. In order for this

technique to function, constant monitoring of the channel conditions is required; channel information can be acquired either by:

- in-situ measurements of the received power at a pilot frequency or from the information signal (*open-loop power control*) providing an estimate of the propagation conditions or
- by receiving feedback from the receiver on the other end of the link (*closed-loop power control*)

The latter is expected to provide more accurate efficient management of the power control scheme; however, it is more difficult to implement and can introduce significant round trip delays.

The fundamental limitations of the power control technique are the following:

- Higher transmitted power can result into adjacent satellite interference [17] (ULPC case) or terrestrial network interference (DLPC case), potentially violating regulations on maximum power flux density as imposed by the corresponding spectral masks
- intermodulation interference [17] due to the non-linear amplification of multiple carriers
- limited margin for satellite DLPC due to the tighter output back-off and the limited resources available on-board the satellite

3.3.2 Spot-beam shaping – adaptive antennas

This technique involves the reshaping of the transmitted satellite beam by means of active antennas in order to focus the transmitted power to smaller geographical areas (spot beams) effectively increasing the EIRP at the coverage area of interest or higher priority while removing coverage from other areas. The inherent complexity of such systems (i.e. the very sophisticated algorithms, antennas) as well as the reduction of global coverage are the main downsides of this FMT.

3.3.3 Link Adaptation Techniques

Link adaptation techniques include *Hierarchical Coding* (HC), *Hierarchical Modulation* (HM) and *Data Rate Reduction* (DRR). The common denominator across these techniques is that they act on the signal to be transmitted itself rather than altering the system's link budget parameters. They function by providing higher error correction capabilities (HC technique), lower required E_b/N for the same C/N to maintain a certain Bit Error Rate (BER) (HM technique) or by decreasing the required C/N itself (DRR technique).

3.3.4 Diversity Schemes

Diversity schemes are usually employed on top of the two aforementioned techniques and exploit either the spatial inhomogeneity of the rainfall medium (site & orbital diversity), the temporal dependence of rainfall (time diversity) or its frequency-spectral dependence (frequency diversity).

Two metrics are often used to quantify the performance of a diversity technique, the *diversity gain G* and the *diversity improvement*. Diversity gain is defined as the difference between single attenuation and joint-attenuation statistics in dB for the same exceedance probability level; Diversity improvement is defined as the ratio of the single exceedance probability to the joint one for the same attenuation value [18].

3.3.4.1 Site Diversity

Site diversity schemes exploit the spatial inhomogeneity of (mainly) convective rain; convective rain cells usually span across a few km and are responsible for very high rainfall rates which in turn result in deep signal fades. The goal is to create spatially uncorrelated slant-paths by strategically placing multiple earth stations (two for double site diversity, three for triple site diversity etc) at a separation distance *D* greater than the typical horizontal extent of a convective rain cell. Then, the (joint) probability that the received signals simultaneously experience a deep fade across all slant paths can be significantly lowered compared to the case of a single slant path. Naturally larger separation distances and/or higher number of earth stations can yield higher performance in terms of diversity gain, although appreciable gain can be observed even for very small distances (pico-scale diversity scenarios) [19].

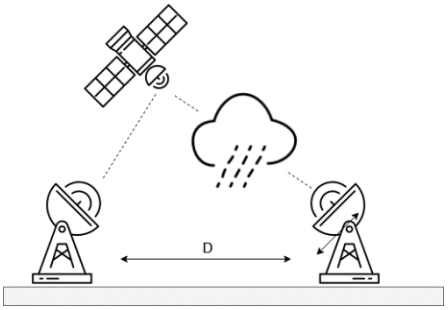

Figure 3-3: Example of a double site diversity scheme, separation distance D

The earth stations are interconnected (usually by means of optical fiber lines) and are managed by a central controller/system broker. The received signals can be further processed using:

- *Switching Combining*, where at any given moment the received signal from a single station is used, switching to another one only after an attenuation threshold is exceeded
- *Selection Combining* where at any given moment the received signal from the station with the best C/N ratio is used
- *Maximal Ratio Combining* where all signals are synthesized using appropriate weighting to produce the final signal

Site diversity can also be used for the uplink by appropriately designing the system controller and monitoring the channel state.

Although a properly designed site diversity system can offer gain in excess of 30 dB for Ka-band and higher frequencies [20], the costs associated with deploying and maintaining multiple earth stations as well as the infrastructure for their operation and control constitute a substantial drawback.

3.3.4.2 Orbital Diversity

Similar to the side diversity technique, orbital diversity tries to exploit the spatial variability of the rain medium, only this time, by pointing the earth-station antenna to different, back-up satellites in order to change the slant path; either another antenna can be used or the same if equipped with a fast-acquisition tracking system. Needless to mention that the back-up satellite(s) should be in LOS with the earth station and be able to convey the information from/to the other end,

either by inter-satellite connection with the master satellite, or multiple antennas/tracking system at the other earth station to adjust pointing to the back-up satellite(s).

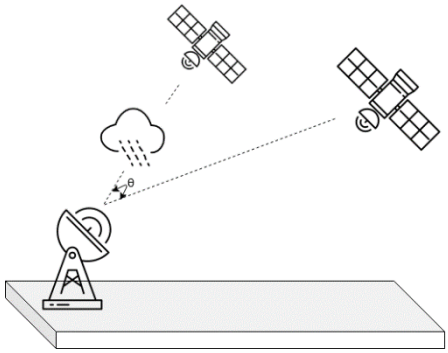

Figure 3-4: Example of a double orbital diversity scheme, separation angle ϑ

Such a technique is expected to yield less gain over site diversity as the alternate slant paths are not significantly uncorrelated. Naturally, the higher the separation angle θ between the satellites, the greater the gain is expected to be, generally in the range of 10 dB for Ka-band and above [20]. It is a more economically viable solution, as only a single earth station needs to be maintained, nonetheless, it still requires a system controller and can result in delay upon satellite switching / traffic rerouting if a single antenna is used.

3.3.4.3 Time Diversity

Time Diversity is a technique that exploits the temporal correlation of rainfall; a particular duration of transmission suffering from a deep fade can be retransmitted at a later time, when the magnitude of the rainfall rate will allow for higher C/N. In this context, the inter-fade intervals play an important role since they are the ones to determine the time delay after which the data will be retransmitted. For such a scheme to function, continuous monitoring of the propagation phenomena is required accompanied by an estimate of their duration.

This technique can be very effective for non-real time applications such as data transfer, video on demand, etc., however, cannot be used e.g. for voice or live streaming services. Also, for rainfall events of very high duration, although the data will eventually be successfully transmitted to the other end, from a user's point of view the long delay could appear similar as a system outage.

3.3.4.4 Frequency Diversity

As satcom systems move towards higher frequency bands, the atmospheric impairments become stronger both in magnitude and probability of exceedance. A possible countermeasure could then be the use of high frequency bands (Ka, Q/V) for regular operation (no to minimum rainfall conditions), while switching to lower frequency bands (Ku or even C) in the case of a strong rainfall event.

Such a scheme, however, requires the presence of spare lower frequency transponders onboard the satellite and multiple antennas/RF chains on the earth stations. Moreover, the switching to a lower frequency band offers less capacity, possibly raising issues on channel allocation and excluding or downgrading bandwidth-intensive services. In any case, an appreciable gain could be achieved, estimated in the order of 30 dB for the Ka-Ku band case [20].

3.4 ITU Models

In the following table, the ITU-R Recommendation per propagation effect mentioned in this chapter is presented:

Table 3-1: ITU-R Recommendation per propagation effect

Propagation effect	ITU-R Recommendation
Gaseous Attenuation	P. 676-12
Cloud Attenuation	P. 840-8
Rain Attenuation	P. 618-13
Scintillation	P. 618-13
Depolarization	P. 618-13

3.5 Propagation Measurements

3.5.5 Radiometric Measurements

Radiometric techniques utilize sky noise temperature measurements to provide an absolute estimation of the attenuation in the slant path [21]; using this technique attenuation only due to absorption is considered. They typically comprise of very specialized equipment requiring very stable temperature control, have a relatively low dynamic range and are prone to errors arising from thermal emissions outside the slant path; they are rarely used on their own but rather in conjunction with beacon measurements [22].

3.5.6 Beacon Measurements

Most of the experimental satellite propagation campaigns are based on the reception of beacon signals; satellite beacons are commonly available to the ground stations:

- to enable monitoring of the satellite's position
- as pilots to receive telemetry data or
- for antenna pointing purposes

In most cases beacon signals are merely CW signals of constant power and frequency and can therefore be exploited to measure the spatiotemporal changes in the propagation conditions.

The measurements obtained using beacons are in essence differential measurements: the signal power measured during clear sky conditions is considered the reference signal; during a fade event the received signal power is subtracted from the reference signal to yield the so-called excess attenuation (values relative to the reference signal power). They can provide a very high dynamic range (in the order of a few tens of dB) and are not susceptible to effects around the slant path as they lock on the particular beacon signal; furthermore, measurement set-ups can be easily designed using readily available (common off-the-shelf, COTS) satcom or commercial stand-alone hardware. The drawback of this technique is that using beacon measurements alone it is virtually

impossible to distinguish and measure the bulk effects of the atmosphere such as gaseous attenuation.

Apart from the antenna(s), conventional beacon receivers consist of an RF front-end including Low Noise Amplifiers (LNAs), filters, Intermediate Frequency (IF) conversion stages, Phase Locked Loops (PLLs) and/or Frequency Locked Loops (FLLs), external stable oscillators and RMS power detector(s). Part of the RX chain can be implemented using either analog or digital electronics depending on cost and design choices. The measurements are then digitized using an Analog to Digital Converter (ADC) connected using appropriate interface to a computer for further data processing and storage.

With the advent of Software Defined Radio (SDR) techniques and supporting hardware, many of the RX chain stages have been migrated from hardware to software. In practice not all of the RF chain stages can be implemented in software, especially taking into account the high cost of wide-band ADCs, however, the remaining hardware blocks can often easily be parametrized in software.

The *advantages* of using the SDR paradigm in the framework of beacon measurements are:

- Quicker prototyping
- Lower provision and maintenance costs
- Less bulky equipment
- Straightforward adaptation and reuse of already developed software to accommodate required changes in the configuration or future needs
- Interoperability with different types of equipment
- Possibly higher accuracy and dynamic range depending on the processing techniques used (e.g. substitution of PLL/FLL and power detectors by Fast Fourier Transform estimation)

Possible *disadvantages* of using SDR techniques within the scope of beacon measurements are:

- Software complexity/overhead requiring significant processing power for real-time power estimation
- Potential bugs in the developed code requiring further investigation/debugging which unless addressed could lead to inconclusive data or reduce the data availability

A more in-depth analysis of the receivers' design within the scope of this thesis follows in the next chapter.

3.6 Chapter References

[1] L. J. Ippolito, Satellite Communications Systems Engineering: Atmospheric Effects, Satellite Link Design and System Performance, John Wiley, 2008.

[2] R. K. Crane, Propagation handbook for wireless communication system design; CRC press, 2003.

[3] D. V. Rogers, "Propagation Considerations for Satellite Broadcasting at Frequencies Above 10 GHz", *IEEE Journal on Selected Areas in Communications*, vol. 3, 1, 1985, pp. 100-110.

[4] L. J. Ippolito, "Radio propagation for space communications systems" in *Proceedings of the IEEE*, vol. 69, no. 6, June 1981, pp. 697-727.

[5] S. D. Slobin, "Microwave noise temperature and attenuation of clouds: Statistics of these effects at various sites in the United States, Alaska, and Hawaii," in *Radio Science*, vol. 17, no.

06, Nov.-Dec. 1982, pp. 1443-1454.

[6] ITU-R P. 676-12, "Attenuation by atmospheric gases and related effects", Geneva, 2020.

[7] ITU-R P. 618-13, "Propagation data and prediction methods required for the design of Earth-space telecommunication systems", Geneva, 2017.

[8] J. D.Kanellopoulos and R. H. Clarke, "A study of the joint statistics of rain depolarization and attenuation applied to the prediction of radio link performance", *Radio Science*, vol. 16, no 2, 1981, pp. 203– 211.

[9] C. W. Bostian and J. E. Allnutt, "Ice-crystal depolarisation on satellite-earth microwave radio paths", *Institution of Electrical Engineers Proceedings*, vol. 126, 1979, pp. 951–960.

[10] W. Zhang, S. I. Karhu and E. T. Salonen, "Predictions of radiowave attenuations due to a melting layer of precipitation" in *IEEE Transactions on Antennas and Propagation*, vol. 42, no. 4, April 1994, pp. 492-500.

[11] R. L. Olsen, D. V. Rogers, R. A. Hulays and M. M. Z. Kharadly, "Interference due to hydrometeor scatter on satellite communication links", in *Proceedings of the IEEE*, vol. 81, no. 6, June 1993, pp. 914-922.

[12] S.N. Livieratos, G. Ginis and P.G. Cottis "Availability and Performance of satellite links suffering from interference by an adjacent satellite and rain fades", *IEE Proc. – Commun*., vol. 146, no 1, Feb. 1999, pp. 61-67.

[13] Theobold, David McClead, Gain degradation and amplitude scintillation due to tropospheric turbulence, PhD diss., The Ohio State University, 1978.

[14] A. D. Panagopoulos, P. M. Arapoglou and P. G. Cottis, "Satellite communications at KU, KA, and V bands: Propagation impairments and mitigation techniques" in *IEEE Communications Surveys & Tutorials*, vol. 6, no. 3, Third Quarter 2004, pp. 2-14, doi: 10.1109/COMST.2004.5342290.

[15] P. M. Bakken and T. Maseng, "Adaptive-Control of Satellite EIRP to Reduce Outage Caused by Fading", *IEEE Trans. Commun*., vol. 31, no. 5, 1983, pp. 726-734.

[16] D. G. Sweeney and C. W. Bostian, "Implementing Adaptive Power Control as a 30/20-GHz Fade Countermeasure", *IEEE Transactions on Antennas and Propagation*, vol. 47, no. 1, 1999, pp. 40-46.

[17] R. N. Ghose, Interference Mitigation Theory and Application, IEEE Press, 1996.

[18] D. B. Hodge, "An Improved Model for Diversity Gain on Earth-Space Propagation Paths", *Radio Science*, vol. 17, no. 6, 1982, pp. 1393-1399.

[19] C. Kourogiorgas, A. D. Panagopoulos, S. N. Livieratos, G. E. Chatzarakis "Pico-scale Dynamic Diversity Gain Evaluation" in *Broadband Satellite Communication Systems. Proc. 18th Ka and broadband communication, navigation and earth observation conf*., 2012.

[20] COST Action 255: Radiowave Propagation Modelling for SatCom Services at Ku-Band and Above - Final Report, ESA Publications Division, The Netherlands, 2002.

[21] A. Dissanayake, J. Allnutt and F. Haidara, "A prediction model that combines rain attenuation and other propagation impairments along Earth-satellite paths" in *IEEE Transactions on Antennas and Propagation*, vol. 45, no. 10, Oct. 1997, pp. 1546-1558.

[22] W.L. Stutzman, F. Haidara, P.W.Remaklus, "Correction of satellite beacon propagation data using radiometer measurements", *IEE Proceedings - Microwaves, Antennas and Propagation*, vol. 141, no. 1, 1994, pp. 62-64.

Chapter 4

Receivers' Design and Deployment

In this chapter, the implementation of Software Defined Radio (SDR) beacon receivers targeting the Alphasat's beacon at the Ka- and Q-band is presented; the experimental campaign was later augmented by the deployment of another two receivers, one targeting Arabsat's BADR5 Ku-band beacon and another one targeting Eutelsat's KaSAT Ka-band beacon.

4.1 Receiver Locations

As part of this thesis, satellite beacon receivers were designed, deployed and are still maintained across two locations in Attica, Greece, approximately 36.5 km apart as depicted in Figure 4-1. The first one is located within the NTUA Campus in Athens (NTUA Campus), while the other one at the NTUA Lavrion Technological and Cultural Park (NTUA LTCP) near the town of Lavrion. This configuration allows for the study of frequency diversity as well as site diversity schemes in small- and large-scale distances; (Table 4-1). As per common practice, the measurements are carried out using beacon signals, i.e. Continuous Wave (CW) signals of constant power and frequency. At each site, one Ka-band and one Q-band receiver targeting the ALPHASAT satellite is installed.

Figure 4-1: The two experimental locations in Attica, Greece.

Table 4-1: Summary of the experimental campaign geometry.

Location	Coordinates	Height amsl*	Azimuth	Elevation
Zografou NTUA Campus	37.98º N, 23.79º E	210 m	178.03º	45.97º
Lavrion NTUA LTCP	37.72º N, 24.05º E	20 m	178.44º	46.26º

The **NTUA Campus** station (37.98 °N, 23.79° E) consists of fully-outdoor receivers (antennas and equipment) placed on one of the buildings' rooftop, above offices and laboratories as shown in Figure 4-2; the selected building faces to the south and is the tallest in the campus, ensuring unobstructed line-of-site with the Alphasat satellite. Access to the area is restricted by means of a permanently locked steel door; hence, the equipment is easily accessible by the campaign staff for inspection and maintenance on a daily basis, while at the same time secure from unauthorized persons.

Figure 4-2: The deployment site at the NTUA Campus location.

The **NTUA LTCP** station (37.72°N, 24.05°E) consists of outdoor receivers placed on top of the campus reception/data-room as depicted in Figure 4-3, while the rest of the equipment is installed indoors in a rack. The location of the building allows full view to the south, ensuring unobstructed line of site with the satellite at all times. Access to the room inside which the rest of the receiver equipment is installed is restricted by means of a security door lock. The status of this station is monitored remotely, while maintenance visits are regularly scheduled.

Figure 4-3: The deployment site at the NTUA LTCP location.

4.2 Details on ALPHASAT satellite

The receivers used throughout this thesis make use of the ALPHASAT satellite located at 25.0º E. ALPHASAT, despite being a commercial geostationary communications satellite (official name: Inmarsat-4A F4) bears payloads for research purposes under the coordination of the European Space Agency (ESA). One of them is the so-called Technology Demonstration Payload (TDP) #5, also referred to as the Aldo Paraboni payload, named after the Italian scientist and professor who inspired it. This payload makes available two fully coherent unmodulated Continuous Wave (CW) beacon signals, appropriate for the conduction of propagation experiments. One beacon is transmitted at 19.701 GHz (Ka-band) while the other one at double that frequency, namely at 39.402 GHz (Q-band) [1]-[2]. By measuring the received beacon power at the ground and considering that the beacons are transmitted at constant power, one can derive the excess attenuation induced by the atmospheric propagation; in essence a differential measurement is performed in order to obtain the atmospheric attenuation.

Table 4-2: Overview of the available beacons from ALPHASAT

PARAMETER	REQUIREMENT
Beacons	1 at Ka Band 1 at Q Band
Carrier modulation	Un-modulated CW
Ka Band Frequency	19.701 GHz
Q Band Frequency	39.402 GHz
Ka/Q Beacon Frequency	Coherent
Coverage	Q Band: boresight pointed to [45°24' N; 9°29' E] (Spino D'Adda)  Ka Band: boresight pointed to [32.5°N; 20°E] 
Ka Band Polarization	Linear V
Q Band Polarization	Liner tilted by 45°
Ka Band EIRP	19,5 dBW
Q Band EIRP	26,5 dBW

4.3 Detailed Receivers' Description

4.3.1 General Architecture

As already mentioned in Section Receiver Locations4.1 of this chapter, two identical Ka-band beacon receivers and two identical Q-band receivers (i.e. 4 receivers in total, covering two frequency bands per location) have been designed and built in-house using primarily common, off-the-shelf components (COTS); they receive and measure the power of the ALPHASAT's CW Ka-band beacon at 19.701 GHz (vertical polarization) and 39.402 GHz (45º tilted linear polarization); for each frequency band, the receiver architecture, configuration and components used are identical across the two locations.

The receivers have been designed around the Software Defined Radio (SDR) paradigm, offering vast reconfiguration options while keeping the costs at reasonable levels. Beacon power estimation is accomplished by means of Fast Fourier Transform (FFT) techniques using tools from the popular SDR framework GNU Radio along with custom software developed in-house.

Regarding the Ka-band, the receivers' front-end consists of 1.2 m offset glass fiber parabolic antennas and commercially available Low Noise Blocks (LNBs); for the Q-band case, 0.6 m glass fiber parabolic shrouded antennas are used, along with custom-developed Low Noise Converters (LNCs) as described in the next sections.

A simplified block-diagram of the receivers is presented in Figure 4-4.

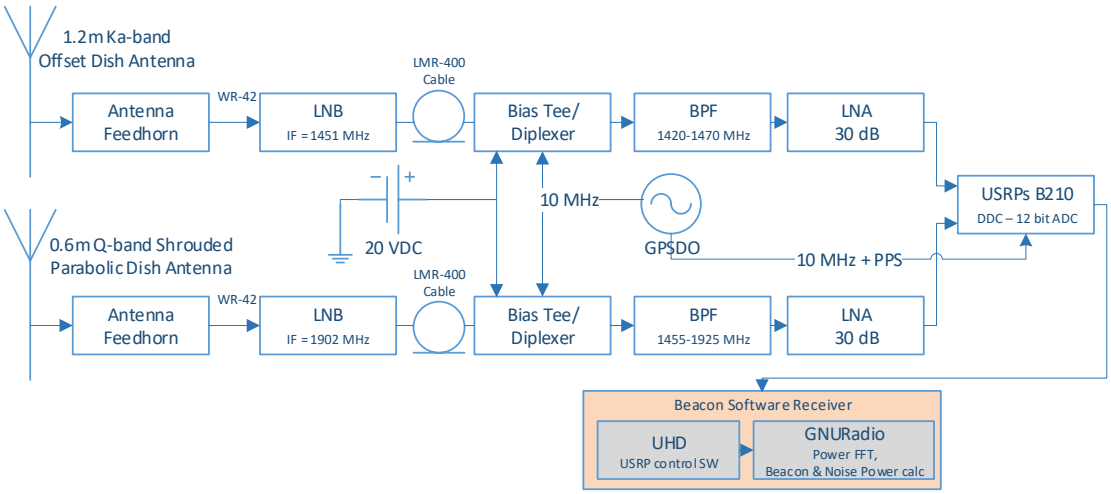

Figure 4-4:Simplified block diagram of the beacon receivers deployed at each location.

After receiving each signal at the antenna feed, it goes through the LNB/LNC in order to filter it, amplify it and down-convert it to a lower Intermediate Frequency (IF). After further filtering and amplification, the main signal acquisition (sampling, quantization, digitization) is then accomplished at an SDR device, namely at ETTUS USRP B210 units connected to an onboard computer running the required software. The estimation is based on the Fast Fourier Transform (FFT) technique using libraries from the very popular GNU Radio framework; using similar techniques, the signal noise floor is also estimated and recorded. The data are recorded and stored using time stamps and all the relevant meta-data to allow for further processing and analysis. In

order to establish fully coherent measurements, all oscillators are locked to a common GPS Disciplined Oscillator (GPSDO) installed at each location, including the computer, whose real time clock (RTC) is constantly adjusted using Pulse Per Second signals from the GPS. This ensures minimal frequency drift/jitter and phase noise in the measurements.

The output measurement sampling rate is 10 Hz and the achieved dynamic range is in excess of 40 dB for Ka-band and 35 dB for Q-band.

4.3.2 RF Front End

4.3.2.1 Antennas

As already mentioned, 1.2 m offset parabolic antennas are used for Ka-band while 0.6 m parabolic shrouded ones for Q-band. Their main specifications are the following:

Table 4-3: Antennas' Specifications (Manufacturer's nominal values)

	Ka-band	**Q-band**
Manufacturer/Model	General Dynamics Satcom Model 3122-990	Radio Frequency Systems (RFS) Model SC2-380BB
Size [m]	1.2	0.6
Operating Frequency [GHz]	18.20 – 21.20	37.0 – 40.0
Gain at midband [dBi] (±0.5dB)	46.10	45.4 (45.8 at Alphasat freq.)
VSWR	1.5:1	1.29:1
Beamwidth – 3 dB – 15 dB	 0.84º 1.88º	0.8º
Cross Polar Isolation On Axis Within 1.0dB Beamwidth	 30.0 26.0	30
Output Waveguide Flange	WR42 using XMW FD9000L as matched antenna feed	WR28, UG599/U
Reflector Material	Glass Fiber Reinforced Polyester SMC	Glass Fiber
Wind loading tolerance [km/h]	80 (operational) 201 (survival)	140 (operational) 252 (survival)
Temperature tolerance [ºC]	-40 to 60	-
Rain ["/hr]	½ (operational)	-
Solar radiation [BTU/h/ft2]	360	-

Figure 4-5: The antennas used: 1.2m Ka-band (on the left), 0.6m Q-band (on the right)

4.3.2.2 Low Noise Blocks (LNBs) / Low Noise Converters (LNCs)

The specifications for the Low Noise Blocks/Converters are listed in the following table:

Table 4-4: LNBs/LNCs specifications

	Ka-band	Q-band
Manufacturer/Model	Norsat 9000XBN-2	LC Technologies Custom Prototype
Noise Figure [dB]	1.3	3.5
L.O. stability	Phase locked to external reference	Phase locked to external reference
Phase noise (SSB) [dBc/Hz]	-65 (100 Hz) -75 (1 kHz) -80 (10 kHz) -100 (100 kHz)	-
Input VSWR	2.0:1	-
Output VSWR	2.0:1	-
Gain flatness over 1000 MHz [dB p-p]	4.0	-
Max gain variation over temperature [dB]	5	0.012 dB / ºC
Input frequency [GHz]	19.20 to 20.20	39.402
L.O frequency [GHz]	18.25	
Output frequency [MHz]	950 to 1950	1902
Conversion gain [dB]	55	43.6
Output P1dB [dBm]	3	-35.1
Power requirements [V] (supplied through center conductor of IF cable)	15-24	22.0
Current drain [mA]	160	56

Figure 4-6: Low Noise Block/Converter for Ka-band (on the left) and Q-band (on the right)

4.3.2.3 10 MHz external reference oscillator /GPS Disciplined Oscillator (GPSDO)

The 10 MHz external reference frequency is generated using a Trimble Thunderbolt GPS Disciplined Oscillator (GPSDO), model 48050-61 which has the following specifications:

Table 4-5: The Trimble Thunderbolt GPSDO specifications

	Value
General	L1 frequency, CA/code (SPS), 8-channel continuous tracking receiver

Update Rate [Hz]	1
1 PPS accuracy	GPS or UTC 20 ns (one sigma)
Max harmonic Level [dBc]	-40
Max spurious [dBc]	-70
Phase Noise [dBc/Hz]	-120 (10 Hz) -135 (100 Hz) -135 (1 kHz) -145 (10 kHz) -145 (100 kHz)
Interfaces	1 PPS: BNC Connector, TTL levels into 50 ohm 10 ms-wide pulse with the leading edge sync to GPS or UTC within 20 ns (one sigma) in static, time-only mode (rising time < 20 ns, pulse shape affected by capacitance of interface cable/circuit) 10 MHz: BNC Connector, sinusoidal wave, +12.5 dBm, ±2.5 dB into 50 ohms Serial Interface: RS-232 through DB-9 connector
Power requirements	+24 V DC (19-34 V), 15 W cold, 10 W steady-state

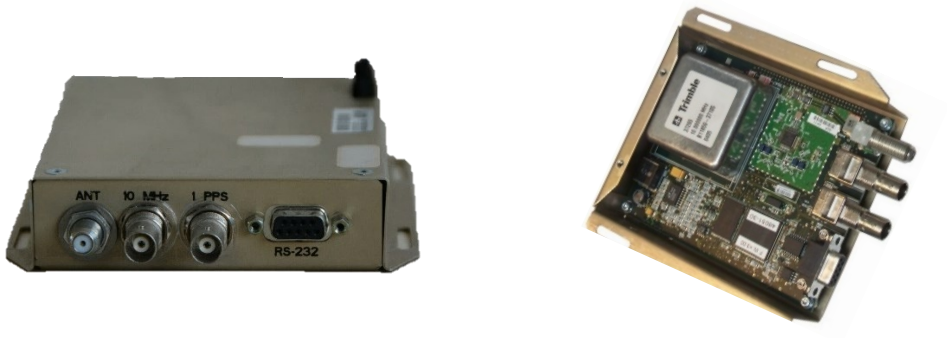

Figure 4-7:The Trimble Thunderbolt GPSDO used at each campaign location.

4.4 Link-budget calculation

Considering the nominal values of the individual components in the RF chain as well as the information provided for the ALPHASAT beacons, the calculated link-budget for Ka- and Q-band is provided below:

The basic link-budget parameters for the NTUA receivers are listed in the following table:

Table 4-6: NTUA Campus receiver link-budget summary

	Ka-band	Q-band
Frequency	19.701 GHz	39.402 GHz
Polarization	Linear V	Linear 45º tilted
EIRP	19.5 dBW	26.5 dBW
Antenna Size and type	1.2m offset	0.6 m prime focus
Antenna Gain (G_{ant})	46.1 dBi	45.8 dBi

Half power beamwidth (HPBW)	0.84º	0.8º
Free Space Loss (FSL)	209 dB	216 dB
Atmospheric Loss	0.3 dB	0.7dB
Pointing Loss	0.5dB	0.5dB
Waveguide Loss	0.5dB	1.0 dB
LNB Gain (G_{LNB})	55 dB	43.6 dB
LNB Noise Figure (NF_{LNB})	1.3 dB	3.5 dB
Reference Temperature	290 K	290 K
T_{sys} Clear Sky	234.93 K	648.33 K
G/T	22.39 dB/K	17.68 dB/K
C/N_0 Clear Sky	60.69 dB-Hz	55.58 dB-Hz
Receiver Bandwidth	112.7 Hz	112.7 Hz
Sampling Rate	10 Hz	10 Hz
C/N Clear Sky (nominal)	40.17 dB	35.06 dB

In order to enhance the campaign with even more measurement data, another 1.2m satellite antenna was deployed at the Campus site in July 2017 targeting the Ku-band at 11.699 GHz (vertical polarization) using Arabsat's BADR5 satellite located at 26.0ºE. The practically negligible angular separation of BADR5 with ALPHASAT allows for the evaluation of frequency scaling effects as well the investigation of frequency diversity schemes.

In July 2018, the experiment was further augmented by installing an offset feed/LNB to the Ku-band antenna, in order to provide measurements from Eutelsat's KASAT at 9.0ºE operating at Ka-band (19.680 GHz, horizontal polarization). Although placing a feed outside the antennas main focal point reduces its effective gain, it still constitutes a viable option for the evaluation of orbital diversity scenarios.

The following table summarizes the augmented summarizes the extra equipment installed for the BADR5 and KASAT reception.

Table 4-7: Ku-band antenna specifications (also used for Ka-band KASAT reception)

	Ku-band
Manufacturer/Model	Gibertini OP125L
Size [m]	1.245 x 1.335
Operating Frequency [GHz]	10.00-13.00
Gain at 11.70 GHz [dBi]	41.90
Beamwidth at 11.70 GHz – 3 dB	1.32º
Cross Polar Isolation On Axis [dBc] at 10.95 GHz	28 26.0
Output Waveguide Flange	C120 using Gibertini C120 as matched antenna feed, adapted to WR 75 for Ku-band

	WR42 using XMW FD9000L as matched antenna feed for KASAT
Reflector Material	Aluminium Alloy
Wind loading tolerance [km/h]	80 (operational) 201 (survival)
Temperature tolerance [ºC]	-30 to 70

The extra LNBs used are:

Table 4-8: LNBs/LNCs specifications for the augmented Campus receivers

	Ku-band	**Ka-band (KASAT)**
Manufacturer/Model	Norsat 1208HCN	XMW R9015XBN
Noise Figure [dB]	0.8	1.5
L.O. stability	25 kHz	Phase locked to external reference
Phase noise (SSB) [dBc/Hz]	-75 (1 kHz) -80 (10 kHz) -95 (100 kHz)	-60 (100 Hz) -70 (1 kHz) -80 (10 kHz)
Input VSWR	2.5:1	2.2:1
Output VSWR	2.2:1	2.0:1
Gain flatness [dB p-p]	4	2.0
Input frequency [GHz]	10.95-11.70	19.20 to 20.20
L.O frequency [GHz]	10.0	18.25
Output frequency [MHz]	950-1700	950 to 1950
Conversion gain [dB]	60 (min 55, max 65)	58
Output P1db [dBm]	5	5
Power requirements [V] (supplied through center conductor of IF cable)	15-24	12-24
Current drain [mA]	300	300

The estimated clear sky C/N (at 112.7 Hz bandwidth) for the Ku-band BADR5 and Ka-band KASAT reception is 41.5 dB and 20 dB respectively.

4.5 Antenna Pointing – Tracking system

Although a geostationary satellite, ALPHASAT orbits the earth at an inclined plane (variation in the range of ±3º, probably in order to prolong its lifespan). Therefore, a tracking system is essential to account for small deviations in its apparent position as observed from the ground stations. For the case of Attica, Greece, this movement is particularly pronounced at the elevation plane, with a diurnal peak-to-peak elevation angle change of 5º at the time of writing this; on the other hand, the diurnal peak-to-peak change observed in the azimuth plane is slow and in the order of 0.2º, rendering it practically negligible.

To account for the diurnal discrepancies in the elevation angle, a custom, fully automated tracking systems based on linear actuators and feedback from digital MEMS inclinometers have been developed in-house for each antenna (at each frequency band). There are many techniques commonly applied in satellite tracking [3]; this particular implementation operates based on position information contained in Orbit Ephemeris Messages (OEM) files. These files are usually available by the satellite maintenance provider/contractor and include information about the satellite's current and future position in the sky; this information can then be algebraically manipulated to deterministically calculate the exact azimuth and elevation angle for a particular location on the ground.

The developed tracking system downloads the available OEM files at regular intervals (once per week), calculates the position of the satellite for each of the two locations using the OEM information and adjusts each antenna's elevation angle accordingly every two minutes; the OEM files are provided by the Politecnico di Milano University, which coordinates the file distribution to the researchers. Finally, to mitigate effects from wind loading, a push-pull gas spring configuration has been employed at each antenna mount. Regarding the Ka-band antennas, the mounts provided by the manufacturer have been used after extensive modification to accommodate the tracking system; the Q-band antennas make use of fully custom mounts, designed and manufactured in house.

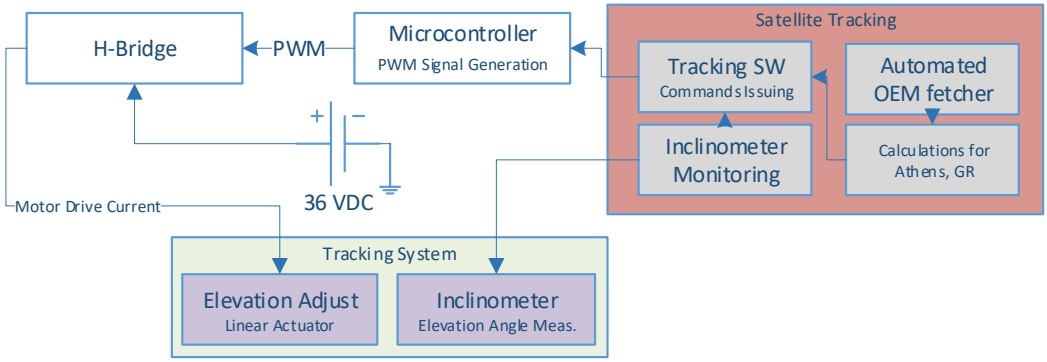

Figure 4-8: Simplified block diagram of the tracking system for each antenna.

Figure 4-9: The LMD18200T H-bridge driver used to drive the linear actuators.

Figure 4-10: The MEMS digital inclinometer used to generate tracking feedback.

The tracking system's principle of operation is as follows:

- Alphasat Orbit Ephemeris Messages (OEM) files are automatically downloaded by the collocated computer at regular intervals (once per week) and processed to calculate the

future satellite positions in terms of elevation and azimuth angles, as observed by each NTUA campaign location. In order to account for the lower time resolution in the OEM file data, a linear interpolation is performed, resulting in a final dataset consisting of 2-min intervals. The elevation angles along with their (future) timestamp are then stored in a scheduler.

- Every two minutes, the scheduler issues a tracking command, sending a message to a USB-connected microcontroller.
- The tracking microcontroller, after receiving the tracking message from the computer generates a control signal (PWM) which is fed to an H-Bridge driver; the H-bridge driver used is based on the LMD18200T to drive a linear actuator;
- While the actuator is energized, the antenna's movement is monitored in the elevation plane by means of a MEMS digital inclinometer providing an accuracy in the order of 0.05º (feedback signals from the actuator's reed sensors are also available, however not used in this configuration).
- After the target elevation angle is reached the system enters standby mode waiting for the next adjustment.

Significant effort has been placed to ensure that the tracking system's error will be kept in the range of ±0.05°. This has been achieved through an elaborate calibration phase before any actual measurement data was recorded.

4.6 Data acquisition, beacon amplitude detection and raw data management

4.6.3 Conventional PLL vs SDR measurement techniques

Past measurement campaigns almost exclusively relied on conventional Phase Locked Loop (PLL) envelope detection techniques in the receiver front-end. Although PLLs are a mature technology with a wide area of application, ranging from FM receivers to state-of-the-art digital transceivers, they clearly pose some limitations. Such systems have to be carefully designed beforehand as their realization is usually non-trivial and their reconfiguration is limited, if not virtually impossible. Moreover, they can monitor a narrow bandwidth and are characterized by relatively low dynamic range and response times (especially in cases of loss-of-lock, i.e. when the signal is lost due to very high attenuation).

In contrast to the above, more-and-more experimenters [4]-[9] nowadays make use of SDR techniques to deploy low-cost, highly reconfigurable receivers that are reliable and overcome many of the drawbacks the conventional receivers used to have. Although it is possible to design a SDR receiver that simulates a PLL in software, most experiment designers build their receivers upon Fast Fourier Transform (FFT)-based techniques, as is the case of the receivers designed in the context of this thesis.

After down conversion from the LNB, the signal is fed to a Universal Software Radio Peripheral (USRP) model B210 by Ettus Research which digitizes it, samples it and serves as an interface to a single-board computer which measures the signal's magnitude using an FFT-based real-time

processing algorithm. The processing application is based on modification of available code from the popular GNU-Radio platform, while results are stored in a database for future use.

The supported specifications of the USRP B210 are the following (when used in receive-mode):

Table 4-9: The Ettus USRP B210 SDR board specifications

Parameter	Value
SSB / LO suppression [dBc]	-35 / 50
Receive Noise Figure [dB]	< 8
IIP3 (at typical NF) [dBm]	-20
Max supported ADC Sample Rate [MS/s]	61.44
ADC Resolution [bits]	12
ADC Wideband SFDR [dBc]	78
Host Sample Rate (16b) [MS/s]	61.44
Frequency Accuracy [ppm]	±2 (±75 ppb w/ GPS unlocked TCXO Reference) (< 1 ppb w/ GPS locked TCXO Reference)
Power requirements	6V DC / 3A

Figure 4-11: The Ettus USRP B210 SDR device used

The algorithm's principle of operation is as follows:

- On every X chunk of received samples an FFT function is called to calculate the signal's power spectrum
- Another function then looks for the FFT's bin of maximum magnitude and considers it the center of the beacon lobe. To account for any phase noise introduced, another Y number of bins around the maximum are summed together to estimate the received beacon power; according to the former interpretation, the beacon's bandwidth shall be equal to B = (Y+1) Hz/bin
- Finally, the corresponding Noise Spectral Density (NSD) or preferably, the noise power in the beacon bandwidth can be estimated. The algorithm averages the magnitude of Q number of bins away from both sides of the beacon lobe and multiplies it by (Y+1) to yield the equivalent noise power.
- The aforementioned average is calculated a few bins to the left and right of the beacon lobe (in the order of a few Hz), in order to minimize its variance.

At this point it is worth mentioning that the selection of parameters (sample rate, FFT size etc.) can significantly affect the accuracy of the measurements; in particular a longer FFT usually improves the consistency of the resulting dataset by lowering the variance of the measured signals. Nonetheless, it also lowers the time resolution of the data since more samples have to be accumulated before the algorithm can operate on them.

During the first year of the experiment, the single board computer used for processing the received signal was an ARM-based 8-core unit from Hardkernel co. Ltd, model ODROID-XU3 Lite with the following specifications:

Table 4-10: Single board computer specifications -NTUA

Parameter	Value
CPUs	Samsung Exynos 5422 Cortex-A15 2.0 GHz quad core and Cortex A7 quad core (8 cores in total)
GPU	Mali-T628 MP6 (OpenGL ES3.0/2.0/1.1 and OpenCL 1.1 Full profile)
RAM	2GB LPDDR3 at 933 MHz (14.9GB/s memory bandwidth) PoP stacked
Storage	eMMC5.0 HS400 Flash Storage (Toshiba eMMC)
Interfaces	USB 3.0 Host x1, USB 3.0 OTG x1, USB 2.0 Host x4 Ethernet RJ-45 1/100 LAN HDMI 1.4a 30 GPIO/IRQ/SPI/ADC header pins
Miscellaneous	Integrated power consumption monitoring tool Integrated PWM controlled cooler
Power requirements	5V / 4A

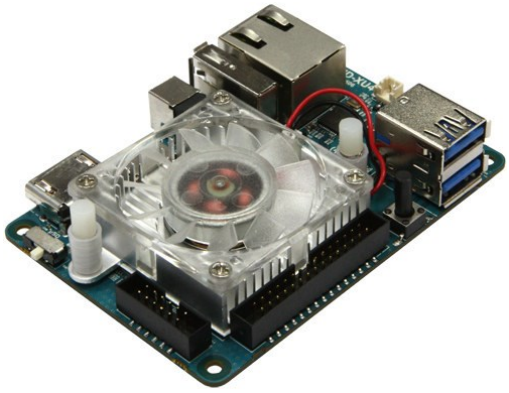

Figure 4-12: The single-board computer used at each location during the first year of measurements

In order to facilitate the processing of further beacon signals, i.e. at Q-band with possible extension to even more, it was decided to upgrade to another computer. Thus, the ODROID units mentioned before were swapped for Intel NUC NUC6i3SYH mini computers; the latter are equipped with an Intel i3-6100U processor, 16 GB of DDR4 Ram and 500GB SSD for storage.

Figure 4-13: The Intel NUC mini-computer currently used at each location.

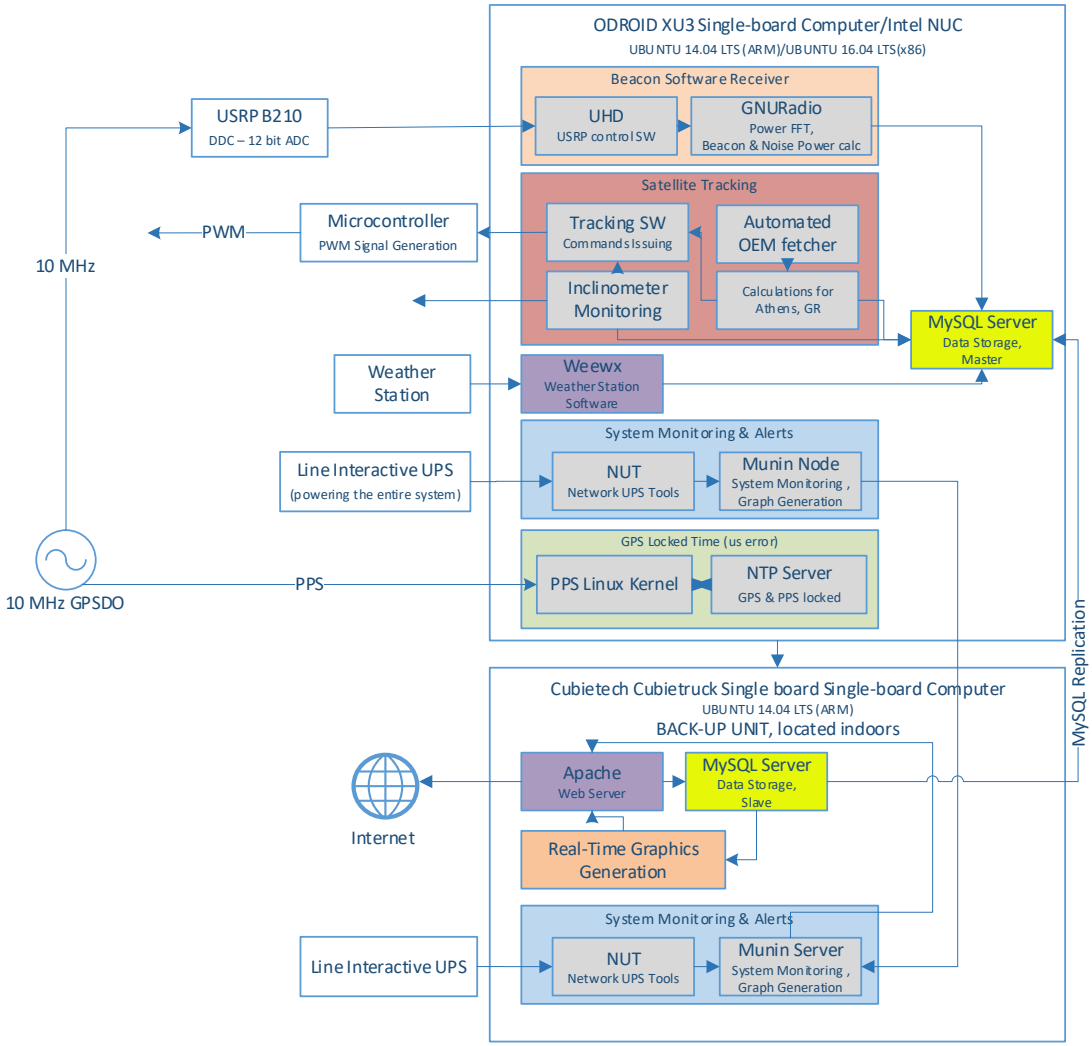

Figure 4-14: Functional Block diagram of the receiver onboard computer

The software used to do the processing has been implemented using the open-source GNU-Radio platform; one file is output per day and its contents have the following format per line:

time_stamp, power_measurement

where:

$$timestamp = current\_hour*60*60*100 + current\_minute*60*100 + current\_second*100 + round(current\_microsecond/10000)$$

This is to avoid the use of floating-point numbers during logging (and therefore improve accuracy). The power measurement is extracted by squaring and adding together a sufficient number of bins around the beacon lobe of the FFT signal spectrum as described in the previous section.

One output file per day is generated and is later decomposed by a python script to insert its contents to a MySQL database for storage, inspection and further manipulation. The MySQL database is stored in a secure server in our offices and is backed up on a daily basis.

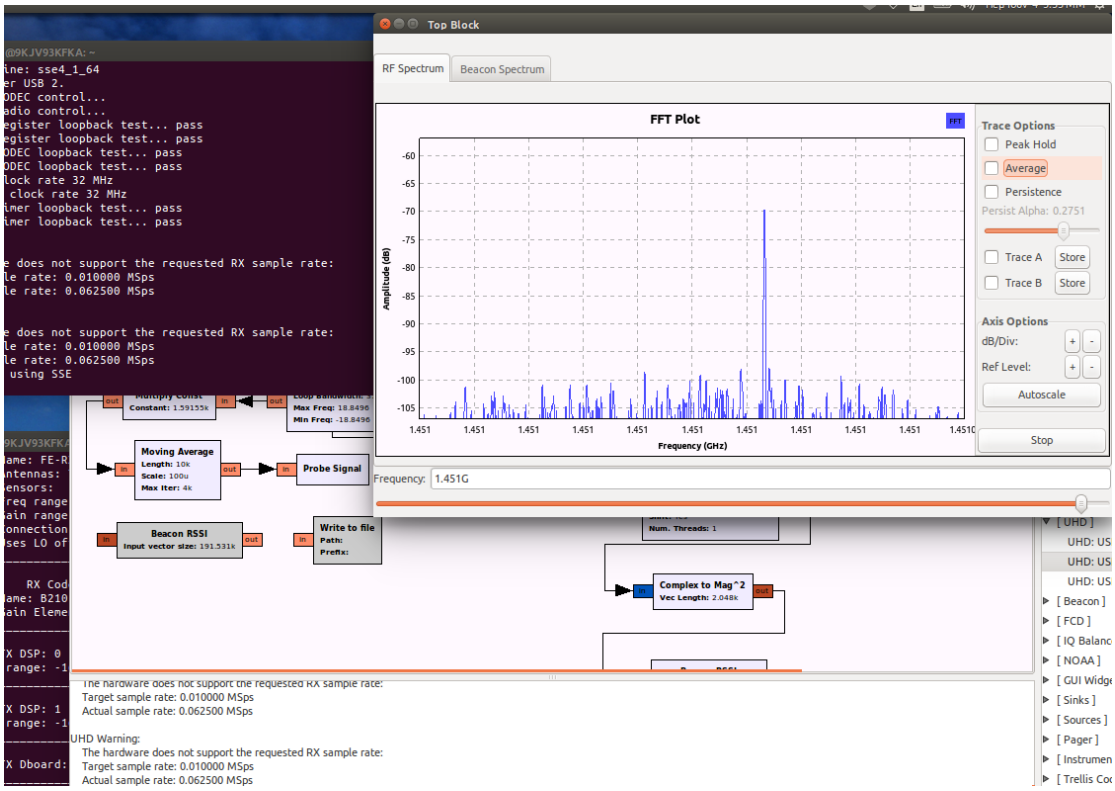

Figure 4-15: Snapshot of the acquisition software during testing.

4.6.4 Data Pre-processing

Before proceeding with the statistical analysis, the obtained signal data undergo both an automatic as well as a manual pre-processing and inspection. In absence of a radiometer, the receivers are capable of measuring in-excess attenuation, i.e. neglecting gaseous effects (arising from oxygen and water vapor), which in any case are slowly varying and can be considered reasonably constant.

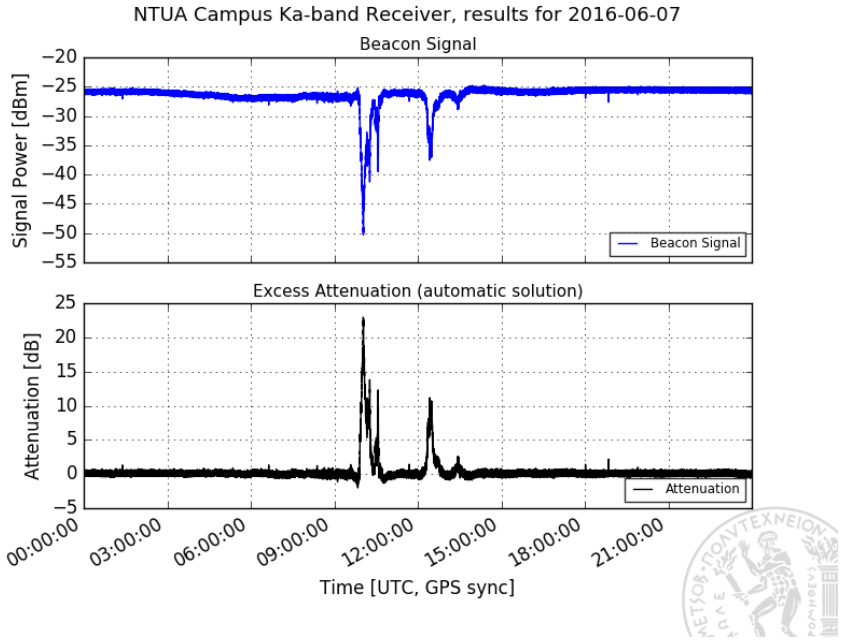

Figure 4-16: Sample preliminary results from NTUA campus receiver for a single day [9], © 2017 IEEE

To remove any signal fluctuation arising from non-propagation related causes (e.g. temperature variation or tracking inconsistencies), the well-established RAL method [10] has been applied to identify the clear-sky signal level and used to pre-process the obtained time series. This particular methodology is based on Fourier Series fitting and allows for both automatic and manual data pre-processing. The resulting pre-processed time series have been visually inspected on a per-day basis to assess the resulting dataset and ensure that no inconsistencies are present (e.g. due to excessive wind loading effects, random software hiccups and any other non-propagation related variations in signal power level).

4.6.5 Concurrent Noise Measurements

4.6.5.1 General Properties of Noise in Beacon Measurements

Noise has always been regarded a barrier to high-capacity communication systems. It is most commonly considered Additive White Gaussian Noise (AWGN), i.e. a random process of uniform power across all frequency bands, Gaussian distributed in the time domain that is superimposed to the signal of interest (in this case the CW beacon signal).

Although its effects on the received signal are largely undesirable as it constitutes a major bottleneck in system performance, it can be manipulated by a SDR beacon receiver to assist in the measurement procedure as will be explained below. Its main properties/advantages when measured along with a beacon signal could be outlined as:

- It is Gaussian white distributed, retaining a constant mean value (under clear sky conditions)
- It is s not affected by spectral leakage during FFT
- It can be averaged as required in order to minimize uncertainty/variance
- It is not affecting the beacon signal itself, the beacon signal can be considered overlaid to the noise

- Atmospheric events cause an increase in measured sky noise temperature ⇒ Radiometer's principle of operation; Recorded noise by the beacon receiver also increases during atmospheric events
- Is less sensitive to changes in the atmosphere (compared to beacon signal fluctuations)

4.6.5.2 Practical Usage Scenarios

4.6.5.2.1 Low-cost Integrated Radiometer

Although in most cases the beacon receiver constitutes the core of a satellite propagation experiment, it is often necessary to supplement the measurements with ones from a radiometer. The latter gives the experimenter the capability to capture slower, lower attenuation propagation effects, namely gas and cloud attenuation; nevertheless, the cost of such equipment is in most cases prohibitive.

FFT based solutions and especially the SDR based ones provide a unique opportunity to operate a beacon receiver and radiometer using the same system setup [11]-[12]. Apart from being a low-cost solution compared to operating a separate radiometer, another advantage is that the slant path is exactly the same for both modes (beacon receiver and radiometer) as they share the same antenna.

The simplest form of a radiometer, the total-power radiometer merely measures the time-averaged power delivered by the antenna to the receiver. The output of such a receiver shall be:

$$P_{out} = \left(T_a + T_r\right) kBG \qquad [4\text{-}1]$$

where T_a is the temperature seen at the output of the antenna, T_r is the total receiver temperature, k the Boltzmann's constant, B the measured bandwidth and G the total receiver gain. More specifically,

$$T_a = T_b + T_g \qquad [4\text{-}2]$$

where T_b is the sky noise temperature (also referred to as brightness temperature) and T_g the noise temperature resulting from the reception of unwanted signals mainly via the antenna side lobes [13]-[14]. Considering all parameters but T_b practically fixed, one could calculate T_a and then using ITU-R Recommendation P.1322 [15] convert it into path attenuation (dB) using the following equation:

$$A = 10 \log_{10} \frac{T_{mr} - T_0}{T_{mr} - T_b} \qquad [4\text{-}3]$$

where T_{mr} the atmospheric effective or mean radiating temperature and T_0 the cosmic background temperature. T_{mr} generally depends on frequency, however for the 20 GHz band it can be estimated by multiplying the surface temperature by 0.95; T_0 is usually chosen as 2.7K [15].

As expected, a temperature stabilized environment is essential to obtain accurate measurements, as any temperature variation can change both the level of noise introduced to the system as well as the gain of the various components. To compensate for such variations, it is suggested that a calibrated reference noise source at the band of interest is periodically coupled between the antenna and the LNB to allow for accurate recalibration and calculation of the system parameters e.g. using the well-known Y-factor method of others [16]-[17].

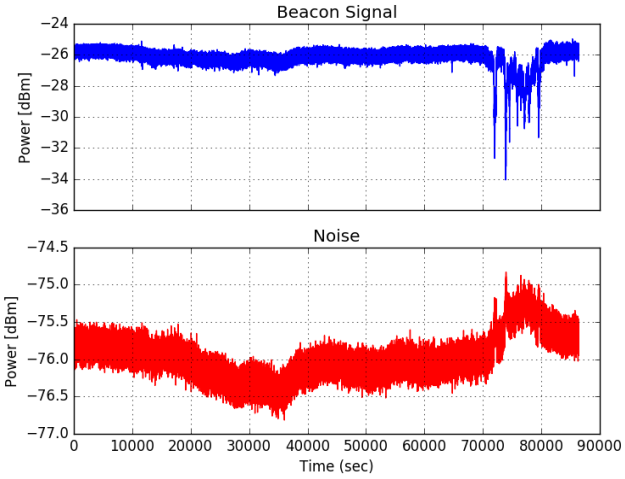

Figure 4-17: Actual beacon and noise power time series for a day involving a light rain event (13/06/2016) [9], © 2017 IEEE

4.6.5.2.2 Antenna Pointing Monitoring

As a result of the inclination of Alphasat's orbital plane, its apparent position as observed from the ground varies over time; although its azimuth variation is insignificant in Greece (< ±0.15º), its variation with regard to the elevation plane cannot be neglected as it is in excess of ±1.5º. Therefore, an in-house elevation tracking solution was designed and installed in both receivers, with an accuracy in the order of 0.05º; this way practically zero pointing losses are introduced in the measurements.

During the system's operation it became apparent that once the installed elevation tracking system was halted –either due to malfunction or scheduled maintenance- causing a pointing error, the measured noise power was reduced in the order of a few dB as in Figure 4-18. This is an interesting observation, as it could be exploited by the campaign designer to generate flags indicating pointing error; the corresponding measurement data could then be either manually revised before final processing, or be automatically excluded from the final data set.

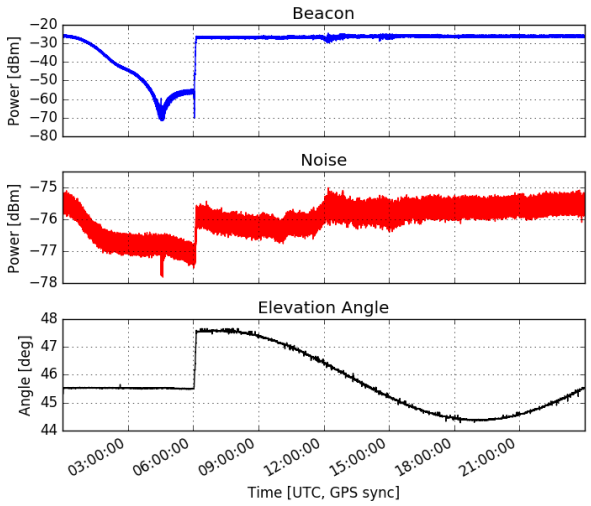

Figure 4-18: Apparent reduction in noise power due to pointing error (antenna tracking system halted from 00:00 until 06:00) [9], © 2017 IEEE

4.6.5.2.3 Assisted Preprocessing – Events Identification

Preprocessing is one of the most crucial tasks in any propagation measurement campaign. Ultimately the chosen preprocessing procedure should:

- Yield accurate and consistent results
- Be mathematically rigorous
- Require minimal human intervention
- Be compatible with most experimental set-ups
- Require no radiometer or previous events identification

At NTUA the chosen method for pre-processing the collected data is the Fourier series as proposed in [10], since it meets all the aforementioned criteria. The method is based on the extraction of a template by successively calculating a Fourier series fitting while progressively removing any non-clear sky points. The initial data are then subtracted from the calculated template yielding the excess attenuation results.

This method requires setting the clear sky thresholds during its execution, rendering it considerably labor-consuming; in an effort to automate the whole process, after various attempts it was observed that it could be enhanced by using the recorded noise measurements. According to the proposed procedure:

- Apply the Fourier series method to the noise samples
- By setting appropriate thresholds, spikes in noise should be easily identified
- Spikes in noise ⇒ Atmospheric events with extremely high confidence
- Because of 1:1 correspondence between beacon and noise samples:
    - Mark the above identified beacon samples for exclusion from fitting
    - Finally run the Fourier Series method on the remaining beacon signal samples
- The final excess attenuation values are calculated

The advantages of this enhanced version could be summarized below:

- No need for daily flags or specialized meteorological equipment
- Small calibration period required for each receiver (to define the necessary thresholds)
- If thresholds set appropriately, the whole procedure can be automated
- Time series are not altered by any means (no padding whatsoever)
- Method mathematically rigorous
- Fast execution, sampling rate of 1 Hz is required for the fitting

Figure 4-19 presents an example plot of time-series resulting from the application of this method to the raw data on a day with light rain.

4.6.5.2.4 Mitigation of Temperature Variation Effects

As already mentioned in a previous section, variations of the ambient temperature can significantly impact the gain of the various components. During our testing and actual operation of the receivers the LNB –being outdoors- was proven to be the most susceptible component to such variations. Its daily variation can reach up to a few dB, despite being thoroughly covered with thermally isolating material. Fortunately, the above preprocessing method taking into account noise can successfully mitigate this issue.

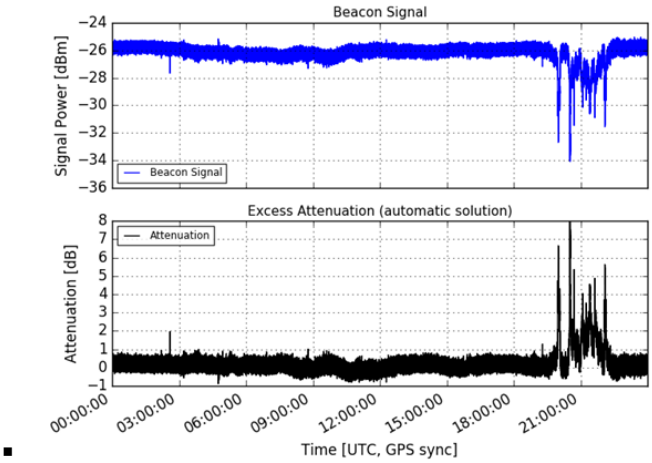

Figure 4-19: Recorded beacon power and automatically preprocessed excess attenuation result using the proposed methodology (13/06/2016) [9], © 2017 IEEE

4.6.5.2.5 Narrowband Interference Discovery

In a different context, instead of using noise as an enhancement to the preprocessing procedure it can be used on its own to indicate any possible interference close the beacon frequency. This method assumes therefore that one runs the Fourier series preprocessing method on the noise measurements to calculate a template. Then, merely subtracting the initial noise data from the template should return a time series in which any spikes could indicate interference. The disadvantages of this method are that it is accurate only for clear-sky conditions along with the relatively small observation bandwidth it offers (a larger bandwidth could severely affect the available dynamic range of the beacon measurements)

4.7 Ka Receiver deployment, management and maintenance

The official start of the measurements preceded an extensive laboratory testing of the RF chains, along with any necessary calibration of the USRP and the developed software. The experimental campaign officially commenced at both NTUA locations on the 1st of July 2016 with two Ka-band receivers (one at each campaign location). On the 1st of July 2017, after a successful year of operation, the experiment was augmented with another two receivers at Q-band.

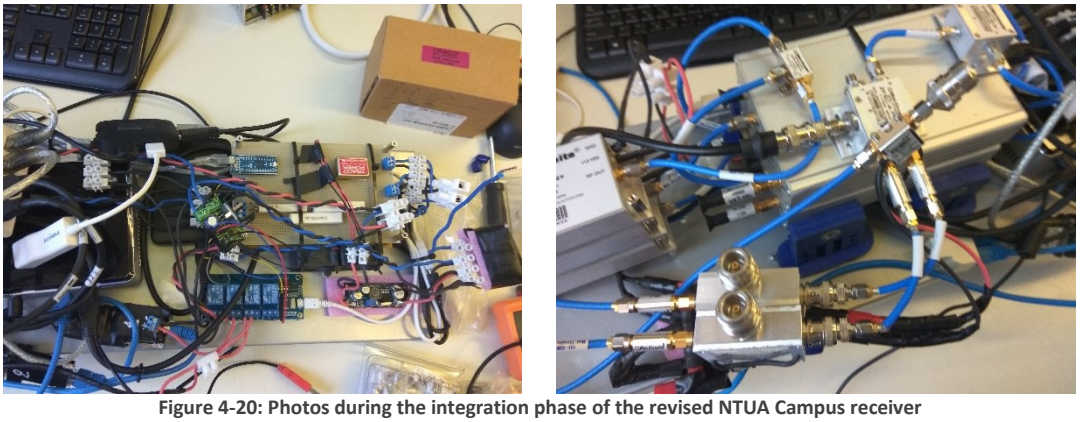

Figure 4-20: Photos during the integration phase of the revised NTUA Campus receiver

Taking advantage of the first year of operation and the lessons learned, the configuration was revised, along with many components which were swapped for better-performing ones such as the linear actuators, the onboard computers, power supplies, enclosures, custom-fabricated PCBs, extra fans for cooling; even the placement of the equipment on the rack/cabinet shelves changed to accommodate the larger number of components.

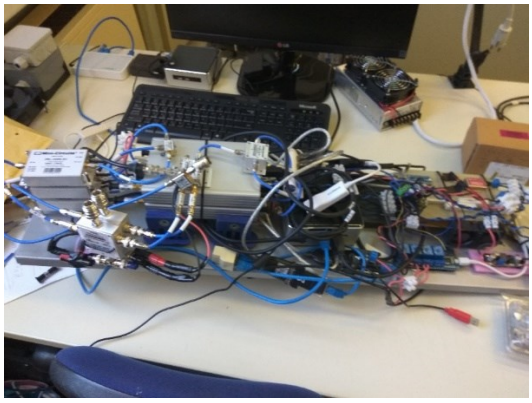

Figure 4-21: Testing of the 2nd revision of the NTUA Campus receiver

Regarding the Q-band tracking system and its mounts, custom ones were fabricated starting from plain steel plates as shown in Figure 4-22. The particular design was selected based on the demand for highly stable movement on the elevation plain and the requirements posed by the type of antennas used (particularly the fact that they are rear fed). In the following photos, the deployment process is being presented.

Figure 4-22: The construction of fully custom antenna mounts with integrated tracking functionality for Q-band

Figure 4-23: The finished Q-band antenna mounts

Figure 4-24: Overview of the Q-band front-end installed at NTUA Campus (on the left) and NTUA LTCP (on the right)

Figure 4-25: Overview of the RF front- and back-end along with all electronic equipment (outdoor enclosure), located at NTUA Campus.

Figure 4-26: Overview of the RF front- and back-end along with all electronic equipment, located at NTUA LTCP.

To ensure availability and integrity of the measurements, the following precautions have been taken:

- Data are backed up and uploaded to the NTUA cloud at regular intervals (daily).
- A UPS of appropriate rating is employed to keep the whole system powered in the event of mains power outage/failure combined with software for automated event logging and e-mail notifications.
- The antenna masts are grounded for lightening protection.
- The antennas have been made resilient to severe wind loading by installing gas springs in a push-pull configuration; this way, it they are fully operational for winds up to 80 km/h with minimal effect on the received beacon power (<0.5 dB).
  In case of extreme phenomena their condition is assessed and if necessary they are manually repositioned.
- The antenna feeder has an integrated plastic cap which protects it from rain.
- To establish a more weather-proof antenna profile (in terms of rain, snow as well as solar radiation), the LNBs have been wrapped inside "Thermawrap" insulating material; also, a piece of acrylic sheet wrapped on the outside with aluminum tape has been installed on top of each LNB. This is expected to minimize both the effects of heat during summer (by limiting the exposure to direct sunlight) as well as the effects of rain drops on the LNB feeder. No significant change in the antenna radiation pattern was observed after the installation of the acrylic sheet.
- All outdoor cable connections have been sealed and waterproofed using a layer of vinyl electrical tape on top of a layer of rubber splicing tape.
- Weekly inspection of the installed receivers takes place.
- Regarding the NTUA Campus receiver, the acquisition, processing and logging equipment along with components from the RF chain (e.g. the Bias Tee/Diplexers, GPSDO) have been placed inside an IP67 enclosure to avoid possible issues caused by water ingress or humidity. The enclosure temperature is maintained at the desired level by installing PWM controlled fans. The enclosure has been placed in a highly secure and tamper-proof environment.
- Regarding the NTUA LTCP receiver, all receiver hardware is placed indoors.

4.8 Ancillary Equipment

Water precipitation measurements and more particularly extracting the rainfall rate is key to understanding the impact that the former has on signal propagation; it allows the correlation of with the actual recorded signal attenuation enabling the validation and development of accurate signal propagation models. As already mentioned in previous sections of this thesis, the experimental propagation campaigns conducted at NTUA locations included the colocation of ancillary meteorological instrumentation, i.e. an advanced wireless weather stations and highly accurate tipping bucket rain gauges.

The weather stations are made by Pro Funk (Germany), model WH 3080 (this is eq. to Fine Offset/Ambient Temperature/Maplin/Tycon/Watson WH 3080 models) and are capable of recording ambient temperature, atmospheric pressure, relative humidity, wind speed and direction as well as solar radiation; although each station includes a sensor for rain measurements too, a separate advanced tipping bucket solution is preferable for extra accuracy.

Figure 4-27: View of the professional weather station deployed outdoors.

Table 4-11: Pro Funk WH 3080 weather station specifications

Parameter	Value
Ambient Air temperature	Range: -40 ºC- 65 ºC Accuracy: ±0.1 ºC Update interval: 48 sec
Relative Air Humidity	Range: 1% - 99%
Wind speed	Range: 0-180 km/h w/speed direction sensor
Miscellaneous	UV sensor included, 60 sec update intervals

The weather station comprises of two units: an outdoor unit where all the sensors are mounted (except for the atmospheric pressure sensor) and an indoor one utilizing an LCD screen to display real-time data; the two units connect with each other wirelessly over the 433 MHZ ISM band using FSK modulation. The indoor unit interfaces with the single-board computer via USB and a custom software has been developed in python for real-time monitoring, logging and graphing. The software makes use of existing libraries from the popular *weewx* meteorological software.

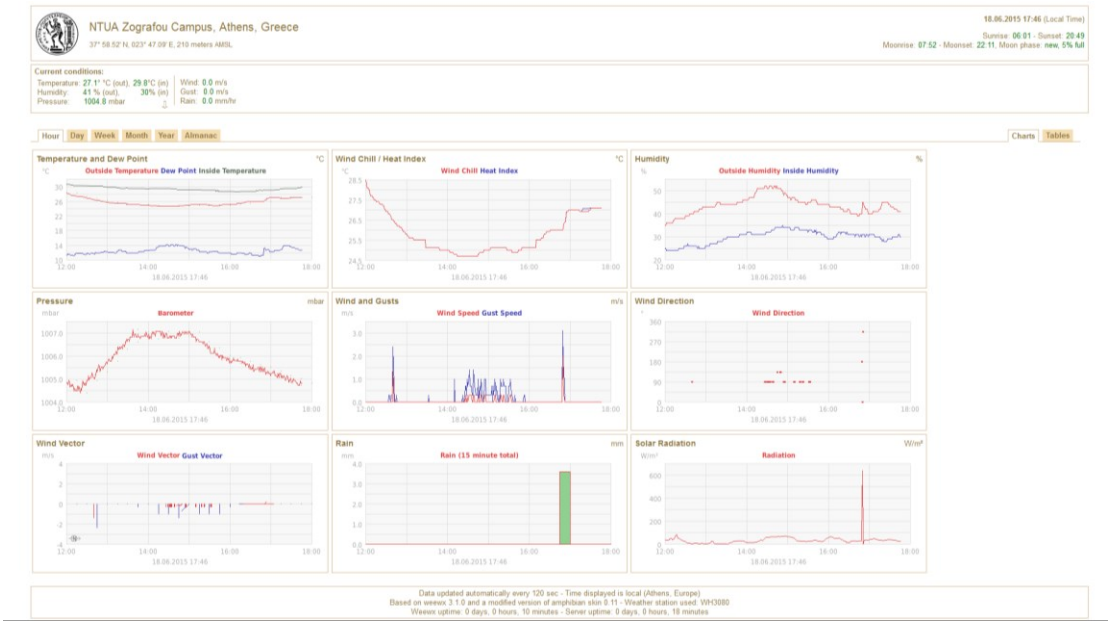

Figure 4-28: Overview of the developed weather station's monitoring application.

Apart from the aforementioned weather station, a professional precipitation sensor (rain gauge) from Environmental Measurements (EML) Ltd., model ARG100 has been employed. It is a tipping bucket type sensor and its specifications are:

Table 4-12: EML Arg100 rain gauge specifications. NTUA

Parameter	Value
Funnel Diameter [mm]	254
Funnel Rim Height [mm]	340
Tip sensitivity	0.20 mm of rain per tip
Output	Contact closure (reed switch)

The rain gauge is paired with a data logger from Onset Computer Corporation, model HOBO Pendant® Event Data Logger UA-003-64, allowing for logging up to 3200 mm of rain at 0.2 mm resolution at a maximum sampling frequency of 1 Hz. The data logger operates using a single CR2032 coin-size lithium battery; it includes a real-time clock (RTC) for accurate time keeping and a 64KB EEPROM for logging/data storage. Using the software provided, it has been configured to log 0.2 mm rain events (each tip of the rain gauge spoon) along with the corresponding timestamp; the data can then be downloaded to a PC for further (offline) manipulation and processing.

Figure 4-29: The EML ARG100 tipping bucket rain gauge used at each location

A preliminary analysis revealed that the weather phenomena were expected to be mild during all seasons; both locations exhibit similar weather conditions. In Figure 4-30 to Figure 4-33 the time series from the Hydrological Observatory of Athens (hoa.ntua.gr), Zografou Station (about 1 km away from the NTUA Campus receiver) are presented.

Timeseries Details

ID	916
Related Station	Zografou (NTUA)
Name	Mean Daily Temp
Variable	Temperature
Unit Of Measurement	deg C
Precision	2
Time Zone	EET (UTC+0200)
Remarks	Generated with auto aggregation from ten-minute values, may contain errors. Each daily mean value could contain up to 10 missing (ten-minute) values.
Instrument	Air temperature sensor
Start Date	Aug. 7, 2005, midnight
End Date	May 12, 2015, midnight
Time stamps properties	
Time scale	Daily - 1 day(s)
Time stamps regularity	Time step is strict
Time stamps nominal offset	0 minutes, 0 months
Time stamps reference	Interval, Average value
Actual offset of reference	0 minutes, 0 months

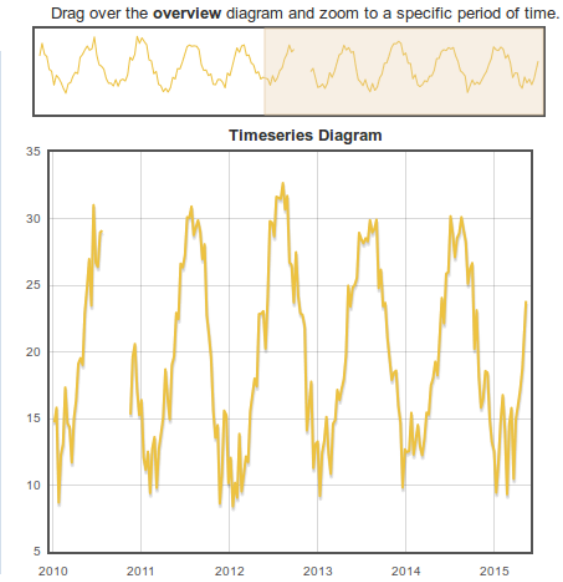

Figure 4-30: Mean Daily Temperature graph for NTUA Campus, source: hoa.ntua.gr

Timeseries Details

ID	1017
Related Station	Zografou (NTUA)
Name	Daily Precipitation
Variable	Rainfall
Unit Of Measurement	mm
Precision	2
Time Zone	EET (UTC+0200)
Remarks	Generated with auto aggregation from ten-minute values, may contain errors. Each daily value could contain up to 10 missing (ten-minute) values.
Instrument	None
Start Date	Aug. 7, 2005, midnight
End Date	May 12, 2015, midnight
Time stamps properties	
Time scale	Daily - 1 day(s)
Time stamps regularity	Time step is strict
Time stamps nominal offset	0 minutes, 0 months
Time stamps reference	Interval, Sum
Actual offset of reference	0 minutes, 0 months

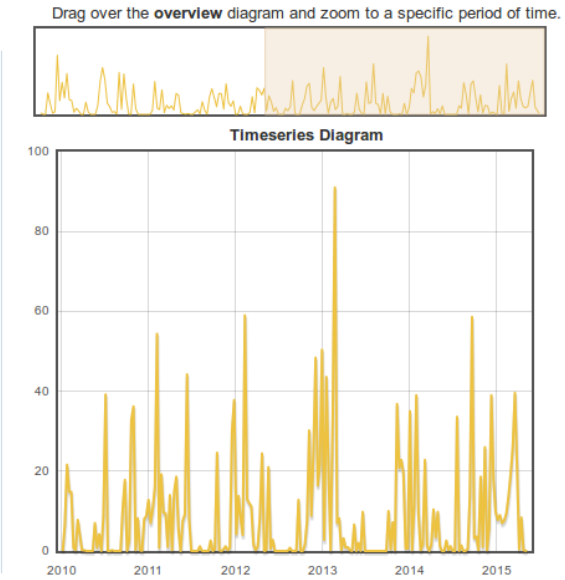

Figure 4-31: Daily Precipitation graph for NTUA Campus, source: hoa.ntua.gr

Timeseries Details

ID	568
Related Station	Zografou (NTUA)
Name	ntua_windvelsecond_irr
Variable	Wind speed
Unit Of Measurement	m/s
Precision	None
Time Zone	EET (UTC+0200)
Remarks	
Instrument	Wind velocity-direction 2
Start Date	Aug. 5, 2005, 11:30 a.m.
End Date	May 12, 2015, 2:40 p.m.
Time stamps properties	
Time scale	10-minute - 10 minute(s)
Time stamps regularity	Time step is not strict
Time stamps reference	Instantaneous values
Actual offset of reference	0 minutes, 0 months

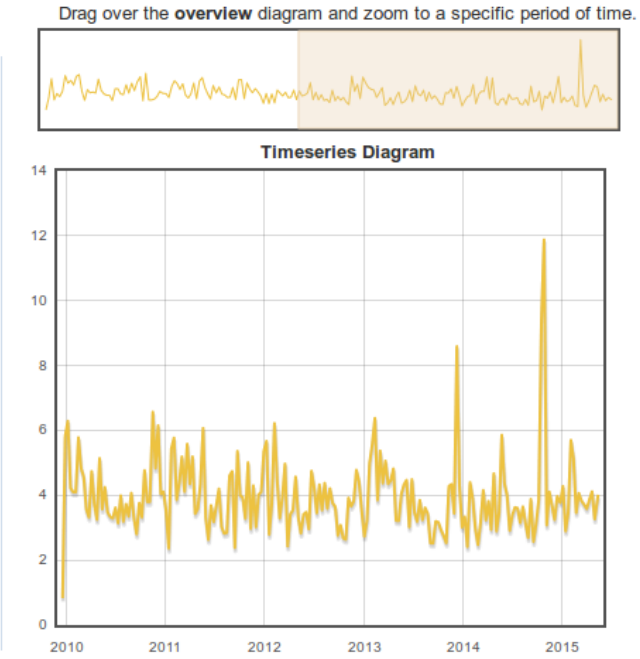

Figure 4-32: Wind speed graph for NTUA Campus, source: hoa.ntua.gr

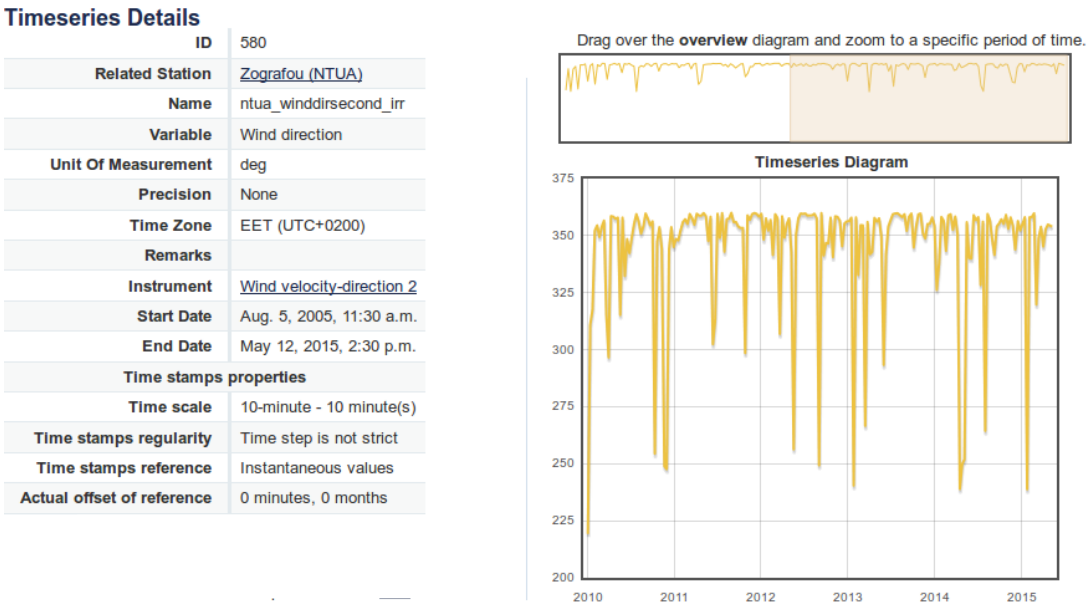

Figure 4-33: Wind direction graph for NTUA Campus, source: hoa.ntua.gr

4.8.6 Selection of tipping bucket rain gauge/errors

The errors arising from the use of tipping bucket rain gauges (TBRs) can be categorized in two main groups, namely the instrumental and environmental errors [18]-[21].

4.8.6.1 Instrumental errors/counting errors

Instrumental errors (also referred to as counting errors) are related to the ability of the instrument to correctly estimate the amount of water actually collected; such errors are systematic mechanical errors at different rainfall intensities, low repeatability of the tipping bucket mechanism operation, gauge blockage, electronic and data logging errors (i.e. depleted logger battery or power failure, memory corruption). Such errors can be random and apply for both catching and non-catching type rain gauges; due to their nature, it is virtually impossible to quantify or simulate in laboratory conditions. To help prevent or at least mitigate them, quality equipment has to be used and be maintained regularly; also, to the extent possible, laboratory calibration could be done prior to installation or at regular intervals (e.g. annually) to estimate the performance of the instrument.

4.8.6.2 Environmental/catching errors

Environmental errors (also commonly referred to as catching errors) account for the incapability of the instrument to collect the volume of water corresponding to the definition of precipitation at the ground (i.e. the amount of water falling through the horizontal projection of the collector area). Such errors could be attributed to evaporation of rainfall inside the instrument not yet accounted for (i.e. in the funnel or in the tipping bucket mechanism), splashing (in/out) of rain drops as well as wetting/adhesion effects. Finally, a common source of error is the so-called wind-induced under-catch, arising from the wind commonly inherent in rainfall measurement.

Using a pit gauge is the ideal solution for measuring rainfall in situ and therefore measurements obtained using pit gauges serve as a reference. Nevertheless, mounting a rain gauge in a pit is very impractical in real terms and is usually implemented only by NMHSs (e.g. the UK Met office etc).

Common good practice suggests that in order to maximize the quantity of information obtained from the TBRs, the time of bucket tip is recorded; this allows for later selection of interpolation technique to be implemented on the recorded data.

4.9 Experiment Verification

The following section outlines the procedures and the results of the hardware and software verification tests conducted at the NTUA Campus station. All procedures and tests comply with standard tests conducted on similar experimental propagation campaigns.

4.9.1 Ka-band Hardware verification

In order to conduct the hardware verification, the actual Alphasat beacon is used; the theoretical results are compared with the measurements to assess the performance of the system. For reference, the block diagram of the receiver is presented in Figure 4-4.

4.9.1.1 Antenna Radiation Pattern

Leaving the system running without engaging the tracking system resulted into significant fluctuation of the received signal throughout the day as shown in Figure 4-34; this can be attributed to the very narrow beamwidth of the antenna.

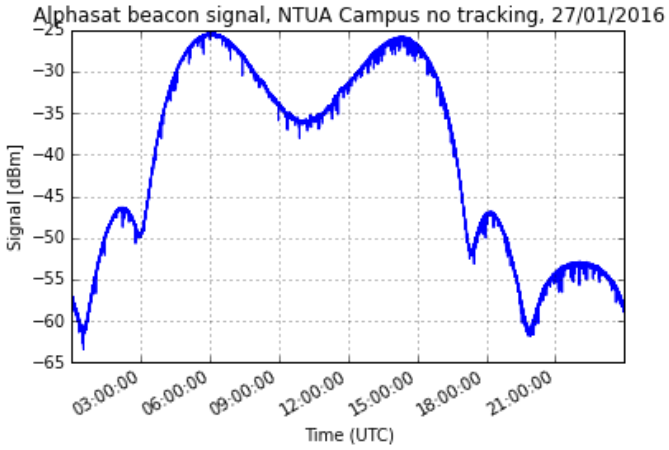

Figure 4-34: Received signal fluctuation without tracking

This fluctuation was in fact exploited to measure the radiation pattern of the antenna; the antenna is fixed in the azimuth and elevation having values that fall inside the satellite's range of motion (the antenna shall be pointed to the median value of the azimuth range to ensure minimum drift throughout the day). First the range of variation in azimuth and elevation was calculated using the Orbit Ephemeris Messages (OEM) files for this particular day (i.e. on 27th January 2016). Considering the azimuth variation to be negligibly small (±0.07º) and very slow throughout the day, any variation in the received signal power could be attributed to the pointing error due to the satellite's movement in the elevation plane (±1.3º). The latter exhibits a sinusoidal-like pattern; the satellite crosses each elevation value within the range [44.678º - 47.283º] twice per day (except for the extreme values which are reached once per day) as presented in Figure 4-35.

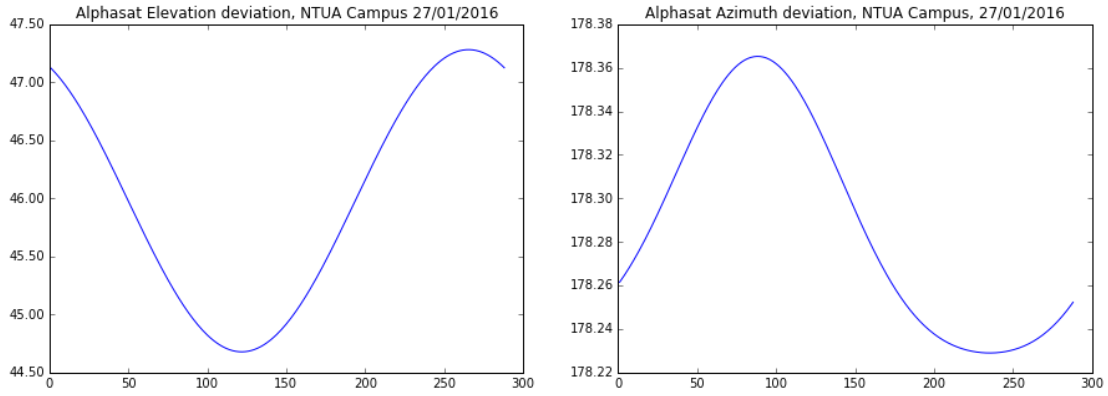

Figure 4-35: Alphasat's variation in elevation (left) and azimuth angles as observed from NTUA Campus

The following steps were necessary to calculate the exact radiation pattern:

- After recording the beacon's signal power for this day, the data samples are aligned to the elevation values calculated from the OEM file. As for each signal power value throughout the day, the maximum signal power value should correspond to an elevation value (Figure 4-36). This shall be the elevation angle of the antenna with very high precision as no measurement error is involved here (the antenna is perfectly aligned to the satellite at this time instant); this can then be considered the zero-reference angle of the antenna (0.0º).
- Subtracting this elevation value from all other elevation values throughout the day should yield the antenna's relative motion with respect to the perfect pointing to the satellite.
- Similarly, subtracting the corresponding power value in dB (i.e. the maximum value as stated earlier) from all other power values results into the normalized gain of the antenna.
- Combining both the relative angles and the normalized gain, the normalized radiation pattern of the antenna in the elevation plane is finally obtained as depicted below in Figure 4-37. **The -3 dB BW of the antenna has been calculated at 0.751º and the -10 dB BW at 1.324º.** These values are in good accordance to the ones provided by the manufacturer, i.e.0.84 dB half power beam width (HPBW).

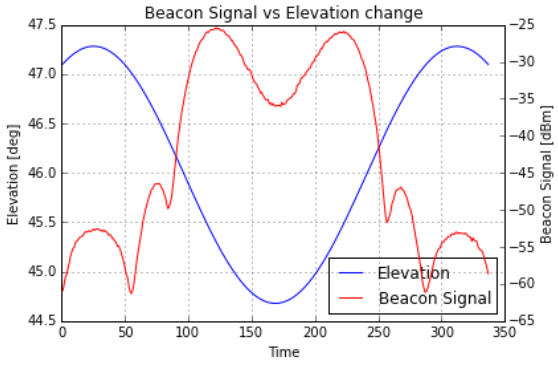

Figure 4-36: Aligning power data with elevation angles

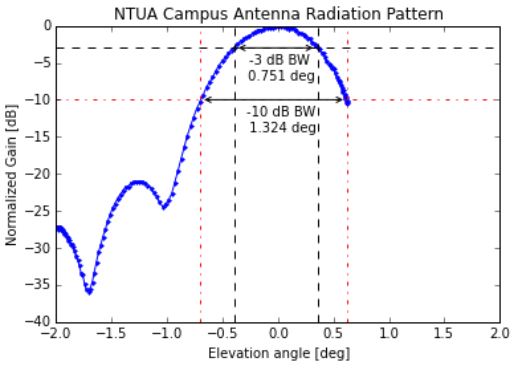

Figure 4-37: The normalized Ka-band antenna radiation pattern

4.9.1.2 Antenna Offset

Although the antenna specifications provide a nominal value of 17.35º offset in the elevation plane, the measurements suggested that the **actual offset shall be 18.289º**. This value was measured by means of a digital very high precision MEMS inclinometer with 0.001º resolution and 0.05º accuracy (DDK Sensors HDA516V) and has been confirmed over a long time period by sweeping the elevation angle up- and down using this value.

4.9.1.3 Outdoor Installation

4.9.1.3.1 Wind loading mitigation

During the testing period extreme wind gusts (in excess of 19 m/s or 64.8 km/h) were repeatedly recorded by the meteorological sensors located in the vicinity of the beacon receiver at NTUA Campus; gusts of such magnitude seemed to cause temporary misalignment of the antenna which in turn translated into deep signal fades appearing at the beacon receiver (in the order of tenths of dB). After investigating the aforementioned incidents in more detail, it was concluded that there had been an inherent shortcoming in the construction of the antenna mount and tracking system. More particularly, up until then the antenna was retained at the required elevation angle only by the linear actuator itself and not any other supporting mechanism (such as a steel cable, hinge or rod). Although the actuator did not have to bear the full weight of the antenna, substantial backlash was noticed should torque have been exerted on the dish. Although this should normally not be of particular concern under mild wind, after carefully examining the weather data, it was apparent that wind gusts above 12 m/s systematically caused instability which had to be addressed to ensure accurate and consistent measurements.

To this end, it was decided that the mount be reinforced by thicker steel plates (10 mm galvanized steel) at the sensitive areas; moreover, a set of push (compression) – pull (tension) gas springs was considered necessary to support the antenna at the elevation plane thus relieving this duty from the linear actuator (Figure 4-38).

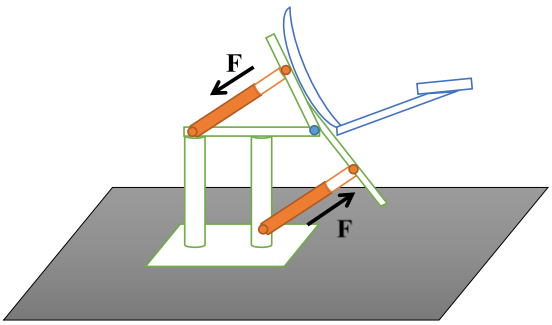

Figure 4-38: The push-pull gas spring architecture supporting the antenna

This way, zero backlash shall be expected even for wind gusts exerting forces in the order of 1000 Newtons during both antenna movement and idle periods. One gas spring (tension-type) is located at the back of the antenna pulling the latter towards its maximum elevation position, while the other gas spring (compression type) is placed at the bottom of the antenna pushing it towards the maximum elevation position; the two springs therefore form a force couple producing enough torque to keep the antenna stable at all times. In this configuration the linear actuator only serves as a mechanical stop to adjust the desired elevation angle. By using such a mechanism, the

movement of the antenna shall also be smoother maximizing pointing accuracy. Indeed, during a very windy day (wind gust speed > 15 m/s) the receiver exhibited a very stable operation with some small signal fades in the range of 0-1 dB at the maximum.

4.9.1.3.2 Temperature effects mitigation

Since both the antenna and the receiver are deployed outdoors it was necessary to verify that all equipment and connections are waterproof. All equipment used is IP67 rated and has sustained numerous rain events during its installation without any particular issues.

As the LNB exhibits a gain variation in the range of (± 3 dB with temperature), it was decided to insulate it using a highly reflective aluminium bubble wrap (Thermawrap). This has mitigated the problem to great extent.

To establish a more weather-proof antenna profile (in terms of rain, snow as well as solar radiation), apart from the "Thermawrap" insulating material, a piece of acrylic sheet wrapped on the outside with aluminium tape has been installed on top of the LNB (Figure 4-39 - Figure 4-40). This is expected to minimize both the effects of heat during summer (by limiting the exposure to direct sunlight) as well as the effects of rain drops or snow on the LNB feeder. No significant change in the antenna radiation pattern was observed after the installation of the acrylic sheet.

Figure 4-39: Front view of the antenna with the acrylic sheet installed around the LNB and feeder

Figure 4-40: Back view of the antenna with the acrylic sheet installed around the LNB and feeder

4.9.1.3.3 Antenna Wetting

To verify the impact of rain on the antenna, the dish was spilled with 10L of water; although this is an experimental exaggeration (as under no circumstances can 10L of water fall on the dish at once), it has been observed that the measurements return to their former values after no more than one (1) minute (Figure 4-41 and Figure 4-42). The time required to fully dry the dish and the whole antenna structure has been timed to approximately four (4) minutes at 23ºC ambient temperature.

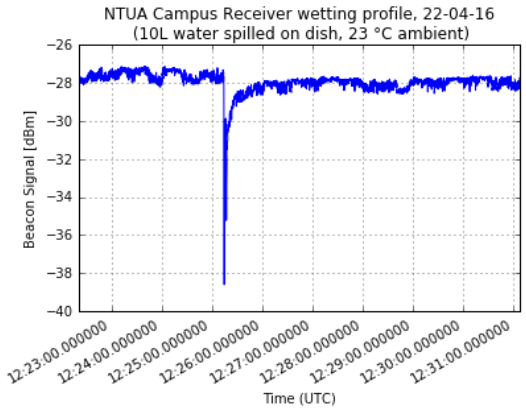

Figure 4-41: NTUA Ka-band antenna wetting profile

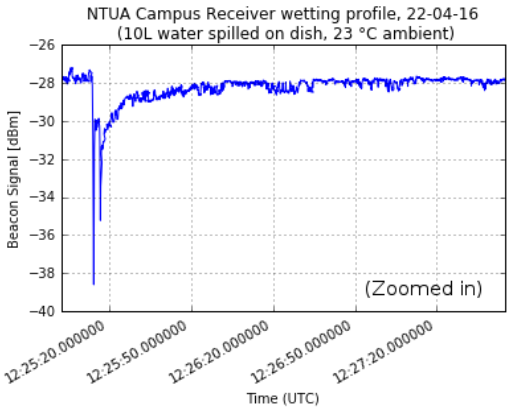

Figure 4-42: NTUA antenna wetting profile (zoomed in)

4.9.1.4 Power outage protection & recovery

The whole system is equipped with an 2200VA/1200W UPS. During normal operation, the UPS load is about 5-10% of its nominal capacity, or 60-120W; this equates to a maximum of 0.5A at 230V or 10A at 12V. Since its batteries are rated at 12V and 18Ah, its maximum runtime considering 90% efficiency shall be about 0.9*18Ah/10A = **1.62 hours**. The status of the UPS is monitored through special software (Network UPS Tools, NUT) and the system can be automatically shut down when battery depletion is reached and re-powered up when mains power is back online.

4.9.1.5 Deep fade recovery

As the receiver is FFT-based, with a rate of 9.85 FFTs/sec, the maximum recovery time after a deep fade is 0.1 sec. This has been verified by introducing a piece of thick paper in front of the LNB to attenuate the signal.

4.9.2 Performance Verification

4.9.2.1 RF front-end: intermediate frequency CNR measurements

On a sunny, non-cloudy day a spectrum analyzer was used to conduct measurements at the output signal of the receiving chain, just before the USRP. The spectrum analyzer was configured as follows:

- Center Frequency: 1.451 GHz for Ka-band, 1.902 GHz for Q-band
- Frequency Span: 10 kHz
- Resolution Bandwidth: 100 Hz
- Averages: 100

Table 4-13: IF measurements

	Ka-band	Q-band
First intermediate frequency (IF_1)	1.451 GHz	1.902 GHz
Received power at USRP (C_1)	–25.2 dBm	-39.2 dBm
CNR (100 Hz BW)	44 dB	37.6 dB
C/N_0 Clear Sky	64 dB - Hz	57.6 dB - Hz

4.9.2.2 Beacon receivers

The most important part of the beacon receiver is the USRP B210, located at the end of the receiving chain. It down-converts the signal once again, filters it and feeds it to the Analog to Digital Converters (ADCs). Finally, the recorded samples are passed to the computer (via USB 3.0) for further processing and calculation of the actual beacon and noise power.

4.9.2.2.1 Second Down-conversion

As stated above, the USRP B210 at the end of the receiving chain undertakes the role of direct down conversion (Zero-IF). Since an integrated LNA is connected before the USRP'SADC, the latter's gain has been set to 0 dB as this setting seems to perform the best. The signal bandwidth passed through to the ADC is 28 MHz (default USRP B210 setting).

4.9.2.2.2 Analog to digital conversion (ADC noise and range)

The Zero-IF down-converted signal is passed on a dual 12-bit ADC (Analog Devices AD9361) running at a sampling rate of 640 kSps. According to the manufacturer, the full-scale input power (0 dBFs) is 8.93 dBm and the ADC is expected to achieve a signal-to-noise ratio (SNR) of about 60 dB over the Nyquist bandwidth, dc to fs/2. This total *SNR* considers the A/D quantization, thermal, differential non-linearity (DNL) and jitter noise contributions. It should be noted that the manufacturer suggests no more than 2.5 dBm at the input of the ADC to avoid possible damage.

It is necessary to investigate whether signal input to the ADC is below its maximum accepted level:

The wanted signal at the Ka-band ADC input, C_1, is at -25.2 dBm.

Since C/N_0 is equal to 64 dB-Hz, the signal noise level at the Ka-band ADC input, N_1, considering a bandwidth of 28 MHz, is

$$N_1 = C_1 - C/N_0 + 10\log(BW) = -14.73 \text{ dBm} \quad [4\text{-}4]$$

The next step is to calculate the effective input noise of the ADC from its *SNR*. Considering the total *SNR* of the ADC, SNR_{ADC} = 60 dBFS (dB full-scale), and the full-scale range, FS=8.93 dBm, the effective input noise is

$$N_{ADC} = FS - SNR_{ADC} = 8.93 - 60 = -51.07 \text{ dBm} \quad [4\text{-}5]$$

It is therefore observed that the total noise power at the ADC input is dominated by the noise level from the previous stages, N_1, thus, the CNR is practically not degraded by the ADC noise:

$$CNR = C_1 - N_1 = -10.47\text{dBm} \quad [4\text{-}6]$$

and the total power at the input of the ADC:

$$P_{ADC} = -14.36\text{dBm} \quad [4\text{-}7]$$

which is well below the maximum allowed ADC input level. According to the above, the full dynamic range of the ADCs is expected to be used.

4.9.2.3 Signal processing

The USRP B210 samples the beacon signal at a rate of 640 kS/s. The received I-Q samples stream is converted to a 62464 samples vector on which a Blackman-Harris window is applied. A Fast Fourier Transform is calculated on the vectorized samples and its result is squared to yield the power spectrum. The resulting FFT frequency resolution is 10.2459 Hz. A peak-search function locates the bin of maximum power and power-sums it with another 10 bins (5 on either side) to capture part of the beacon signal's spectral lobe. The total processed bandwidth is therefore 11x10.2459 = 112.7 Hz.

This results in a 43.48 dB available dynamic range for Ka-band and 37.08 dB for Q-band, not considering the increase in noise floor due to the atmospheric effects.

4.9.2.4 Receiver Linearity

To check the receiver linearity a CW was generated using a signal generator and injected to the LNB input port (using a SMA to WR-42 adapter). The power of the generated signal was varied in steps of 1 dB and the results suggest that the receiver is reacting as expected, exhibiting a highly linear performance in the entire calculated dynamic range.

4.9.2.5 Pointing System

The antenna is mounted on a base capable of moving on the elevation plane. Movement is achieved by means of a heavy duty 12" linear actuator. The actuator is controlled by special software developed in-house; an open-loop tracking system based on OEM files has been installed to adjust the elevation angle accordingly by means of a linear actuator (Jaeger SuperJack HARL 3612+), capable of handling up to 250 kg dynamically at a rated speed of 5.6 mm/sec; actual position feedback is achieved by means of a high-performance MEMS inclinometer with 0.001º resolution and 0.05º accuracy (DDK Sensors HDA516V) measuring the elevation angle in real-time.

Significant effort has been placed to ensure that the tracking system's error will be kept in the range of ±0.05º which indeed appears to be the case, with the measurements indicating no particular signal power variation due to mis-pointing errors.

4.9.3 Software verification

The software developed had undergone meticulous debugging for more than two months before officially commencing the collection of data. All precautions have been taken, such as error logging/reporting and auto-recover in case of error. All data seem to be consistent without any gaps or crashes.

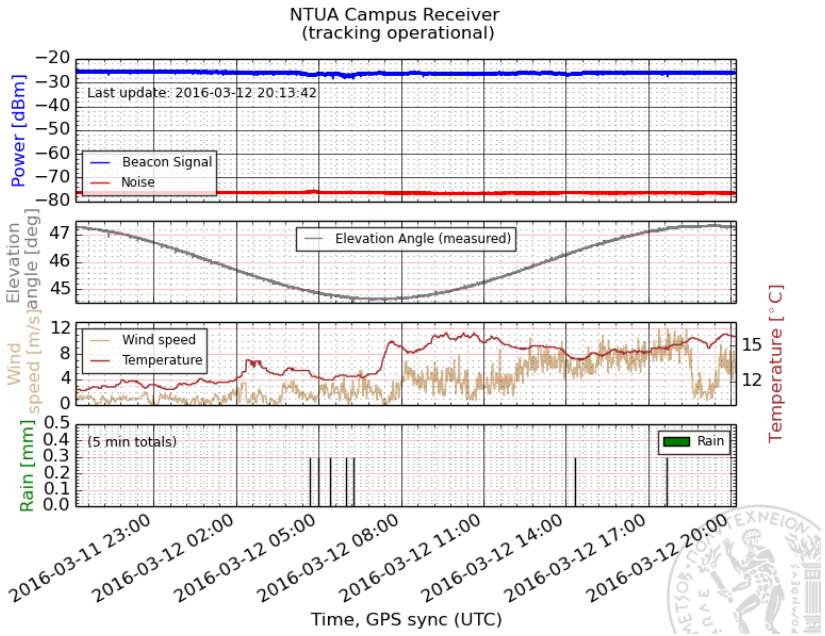

Figure 4-43: Screenshot from the automatic generated plots at the receiver

The OEM files are automatically fetched every week, downloaded locally and after running the necessary calculations for NTUA Campus, the results are stored in a MySQL database. A scheduler is responsible for fetching the elevation values and launching an instance of the tracking class shall it be required.

Figure 4-44: Screenshot from the Munin monitoring software

All measurement data (beacon signal, noise, elevation angle and meteorological data) are stored in a MySQL database; for purposes of extra redundancy, a MySQL replication has been set-up at a slave MySQL server.

The receiver computer does not directly access internet; instead it is located behind a firewall and NAT to protect it from malicious attacks. Access to it is possible through SSH connection.

To assist in the monitoring of system status, the system is monitored using the Munin software; also, real-time data from the receiver are plotted and uploaded to a web-server for internal access.

4.10 Chapter References

[1] ALPHASAT Overview, http://www.esa.int/Our_Activities/Telecommunications_Integrated_Applications/Alphasat/Overview, retrieved on 03/10/3016.

[2] Alphasat - eoPortal Directory - Satellite Missions, https://directory.eoportal.org/web/eoportal/satellite-missions/a/alphasat, retrieved on 03/10/2016.

[3] W. D. Deike, Airborne protected military satellitecommunications: analysis of open-loop pointing andclosed-loop tracking with noisy platform attitude infor-mation.Master's thesis, Massachusetts Institute of Technology. Department of Aeronautics and Astronautics, 2010.

[4] A.Z. Papafragkakis et al., "Site Diversity Experimental Campaigns in Greece and UK Using ALPHASAT at Ka and Q Band", Loughborough Antennas and Propagation Conference LAPC 2016, Loughborough, 2016.

[5] S.Ventouras et al., "Large Scale Assessment of Ka/Q Band Atmospheric Channel Across Europe with ALPHASAT TDP5: The Augmented Network", 11th European Conference on Antennas and Propagation (EuCAP), Paris, 2017.

[6] S.Ventouras et al., "Large Scale Assessment of Ka/Q Band Atmospheric Channel Across Europe with ALPHASAT TDP5: A New Propagation Campaign", 10th European Conference on Antennas and Propagation (EuCAP), Davos, 2016, pp. 1-5.

[7] A. Vilhar, A. Kelmendi, A. Hrovat, G. Kandus, "First year analysis of Alphasat Ka- and Q-band beacon measurements in Ljubljana, Slovenia", Proc. 22nd Ka and Broadband Conf., Cleveland (USA), October 17-20, 2016.

[8] X. Boulanger, B. Gabard, L. Casadebaig and L. Castanet, "Four Years of Total Attenuation Statistics of Earth-Space Propagation Experiments at Ka-Band in Toulouse", in IEEE Transactions on Antennas and Propagation, vol. 63, no. 5, May 2015, pp. 2203-2214.

[9] A.Z. Papafragkakis et al., "Combined Beacon and Noise Satellite Propagation Measurements using Software Defined Radio", 2017 11th European Conference on Antennas and Propagation (EuCAP), Paris, 2017.

[10] S. Ventouras, S. Callagha and C. Wrench, "Long-term statistics of tropospheric attenuation from the Ka/V band ITALSAT satellite experiment in the United Kingdom", Radio Science, April 2006.

[11] J.M. Riera, A. Benarroch, P. Garcia-del-Pino and J.M. Garcia-Rubia, "Simultaneous Beacon and Radiometer Propagation Measurements in the Ka-Band", Proceedings of the 5th European Conference on Antennas and Propagation (EUCAP), Rome, 2011, pp. 3958-3962.

[12] J. Kikkert and O. P. Kenny, "A digital signal processing based Ka band Satellite Beacon Receiver / Radiometer", 2nd International Conference on Signal Processing and Communication Systems, 2008 - ICSPCS 2008., Gold Coast, 2008, pp. 1-8.

[13] R. E. Sheriff and Y. F. Hu, Mobile Satellite Communication Networks, John Wiley & Sons, Ltd, 2002.

[14] G. Brussaard and P.A. Watson, Atmospheric Modelling and Millimetre Wave Propagation, Springer Netherlands, 1994.

[15] ITU-R Recommendation P.1322, "Radiometric estimation of atmospheric attenuation", International Telecommunication Union, Tech. Rep, Geneva, Switzerland, 1997.

[16] M. Celep, S. Yaran, Y. Gulmez Y and A. Dolma, "Characterization of a total power radiometer", Turk J Electr Eng Co 2012.

[17] A. Thompson, R. L. Rogers and J. H. Davis, "Temperature compensation of total power radiometers," in IEEE Transactions on Microwave Theory and Techniques, vol. 51, no. 10, Oct. 2003, pp. 2073-2078.

[18] L. G. Lanza, M. Stagnaro, A. Cauteruccio, "Accuracy of precipitation measurements, instrument calibration and techniques for data correction and interpretation", JMA/WMO Workshop on Quality Management of Surface Observations RA II WIGOS Project, Tokyo, Japan, 19-23 March 2018.

[19] M. D. Pollock G. O'Donnell P. Quinn M. Dutton A. Black M. E. Wilkinson et al., "Quantifying and mitigating wind-induced undercatch in rainfall measurements", Water Resources Research, 54, 2018, pp. 3863– 3875.

[20] L. G. Lanza, E. Vuerich and I. Gnecco, "Analysis of highly accurate rain intensity measurements from a field test site", Advances in Geosciences, vol. 25, 2010, pp.37–44.

[21] Q. Sun, C. Miao, Q. Duan, H. Ashouri, S. Sorooshian, S and K.-L. Hsu, "A review of global precipitation data sets: Data sources, estimation, and intercomparisons", Reviews of Geophysics, vol. 56, 2018, pp. 79– 107.

Chapter 5

First-Order Statistics

In the following, the results for the four years of the propagation measurement campaign conducted at the two NTUA locations in the region of Attica, Greece are presented. The chapter begins with the evaluation of the rainfall rate statistics obtained throughout the entire duration of the experimental campaign; it continues with the presentation of the attenuation first-order statistics (overall, seasonal, monthly and diurnal) for the two locations at all measured frequency bands.

5.1 Evaluation parameters

The first-order statistics for both rain and attenuation have been evaluated.

5.1.1 Rainfall Rate Statistics

For the case of rainfall rate statistics, the rainfall data collected from the rain gauges [1] have been converted to rainfall rate timeseries with one-minute integration window according to [2], [3].

The rainfall rate exceedance probability (CCDF) is calculated as:

$$P[R(t) > r] \quad [5\text{-}1]$$

where $R(t)$ the obtained rainfall rate in mm/h at time instant t.

The time resolution for the rainfall rate is 1 minute (1-minute integration time is used to convert rainfall height in mm to rainfall rate in mm/h).

5.1.2 Attenuation Statistics

The signal attenuation exceedance probability (CCDF) is calculated as:

$$P[A(t) > a] \quad [5\text{-}2]$$

where $A(t)$ the obtained attenuation in dB time instant t.

Regarding the attenuation statistics, these can be distinguished in two categories:

5.1.2.1 Excess Attenuation Statistics

In absence of a radiometer, the received beacon power is preprocessed as already explained in Chapters 3 and 4 in order to yield the clear-sky level, after which the excess attenuation is extracted.

5.1.2.2 Gaseous Attenuation Statistics

In order to enhance the provided measurement results the methodology included in the Annex 2 of the ITU-R Rec. P. 676 [4] is used to derive an approximate estimation of the gaseous attenuation (due to oxygen & water vapor) from meteorological data. The meteorological data required i.e., mean ground temperature (°C), atmospheric pressure (hPa) integrated water vapour content (kg/m^2) have been obtained from the ERA5-Copernicus product "ERA5 monthly averaged data on single levels from 1979 to present" [5] for the campaign locations and duration and were used as input to emulate gaseous attenuation timeseries for the campaign observation period. Data only from ERA5 have been chosen over the local data for extra consistency; more particularly, the variables derived were {*2m_temperature*, *surface_pressure*, *total_column_water*_vapour}.

5.1.3 Structure of the presented results

The following statistics for the rainfall rate and the excess attenuation are provided:

- Long-term (overall) CCDF:
  - using the whole valid dataset
  - period duration is considered the whole duration of the experiment where samples are valid
- Yearly CCDF
  - only full calendar years are considered
  - the valid dataset is grouped per year (from July to June of the next calendar year)
  - period duration equals the total duration of samples grouped in each year
- Seasonal CCDF
  - the valid dataset is grouped per season (four seasons per year, each season represented n times, where n the number of full calendar years)
  - period duration equals the total duration of samples grouped in each season, i.e. n *(single season duration),* considering a 100% data availability case
- Monthly CCDF
  - the valid dataset is grouped per calendar month (12 months per year, each month represented n times, where n the number of full calendar years)
  - period duration equals the total duration of samples grouped in each month, i.e. n *(single month duration),* considering a 100% data availability case
- Diurnal CCDF
  - the valid dataset is grouped in 4-hour intervals (six 4-hour intervals per day)
  - period duration equals the total duration of samples grouped in each 4-hour interval, i.e. (*overall duration)/4,* considering a 100% data availability case

The following table summarizes the measurement results period for each receiver:

Table 5-1: Summary of the measurement periods for which results are presented

Receiver:	Start Date	End Date	Total Duration
Campus & LTCP ALPHASAT Ka-band	July 2016	June 2020	4 years
Campus & LTCP ALPHASAT Q-band	July 2017	June 2019	2 years
Campus BADR5 Ku-band	July 2017	June 2020	3 years
Campus KaSAT Ka-Band	July 2018	June 2020	2 years

5.2 Rainfall Rate Statistics

5.2.4 Overall rainfall rate

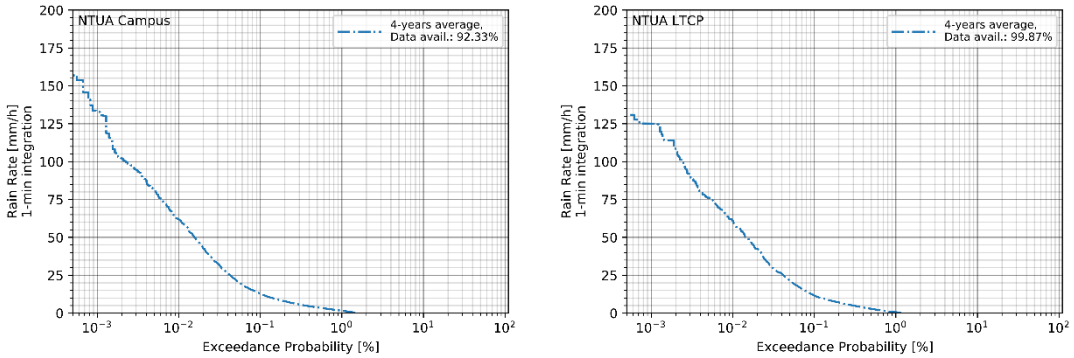

Figure 5-1: Long-term (4-year) rainfall rate exceedance probability (CCDF) for Campus (left) and LTCP (right)

5.2.5 Yearly rainfall rate

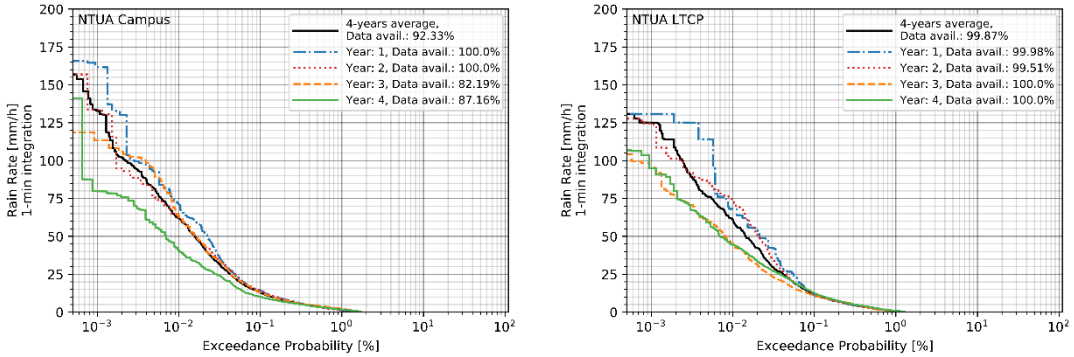

Figure 5-2: Yearly rainfall rate exceedance probability (CCDF) for Campus (left) and LTCP (right)

5.2.6 Seasonal rainfall rate

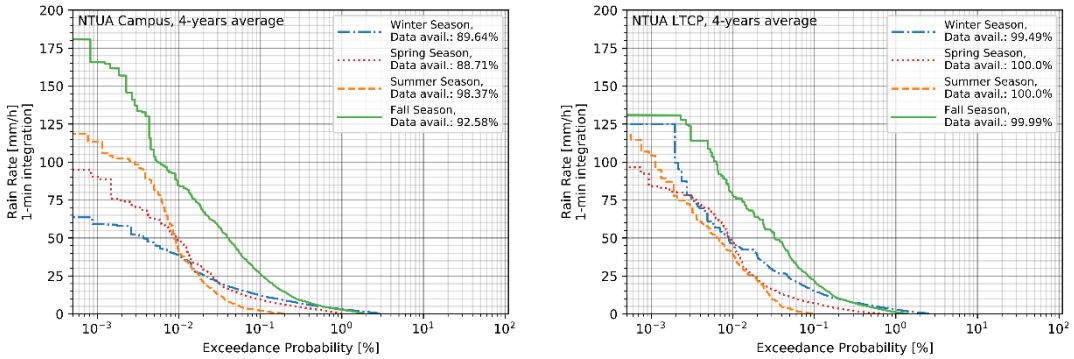

Figure 5-3: Seasonal rainfall rate exceedance probability (CCDF) for Campus (left) and LTCP (right), 4-year average

5.2.7 Monthly rainfall rate

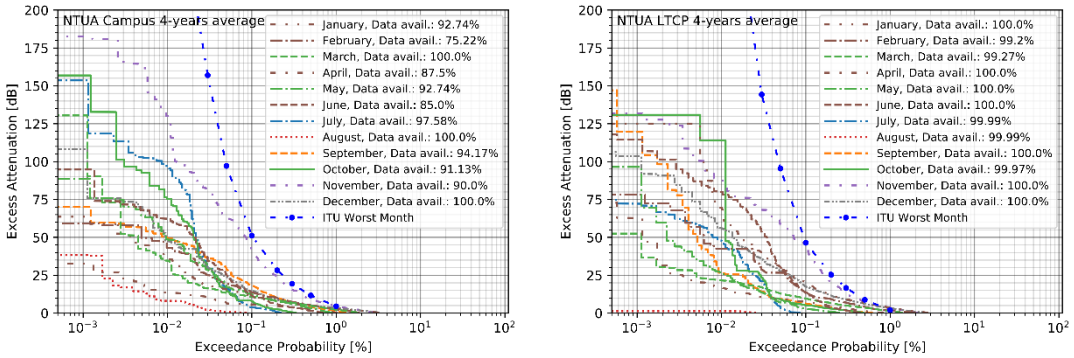

Figure 5-4: Monthly rainfall rate exceedance probability (CCDF) for Campus (left) and LTCP (right) 4-year average

5.2.8 Diurnal rainfall rate

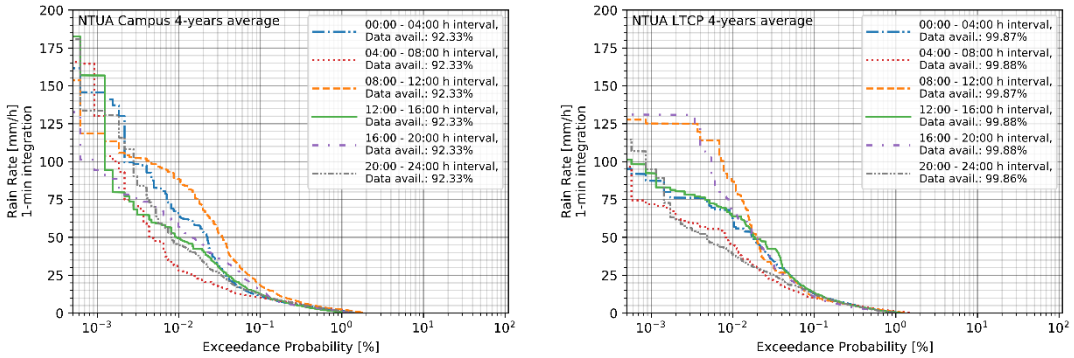

Figure 5-5: Diurnal rainfall rate exceedance probability (CCDF) for Campus (left) and LTCP (right) 4-year average

5.3 Attenuation statistics

5.3.9 Overall Attenuation

5.3.9.1 Campus Ka-band ALPHASAT

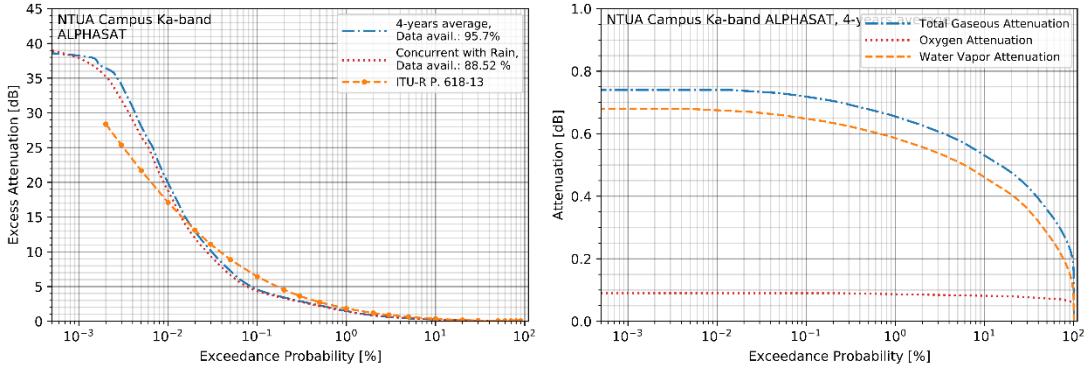

Figure 5-6: Long-term (4-year) attenuation probability (CCDF) for Campus Ka-band ALPHASAT, Left: Excess Attenuation, Right: Gaseous Attenuation

5.3.9.2 LTCP Ka-band ALPHASAT

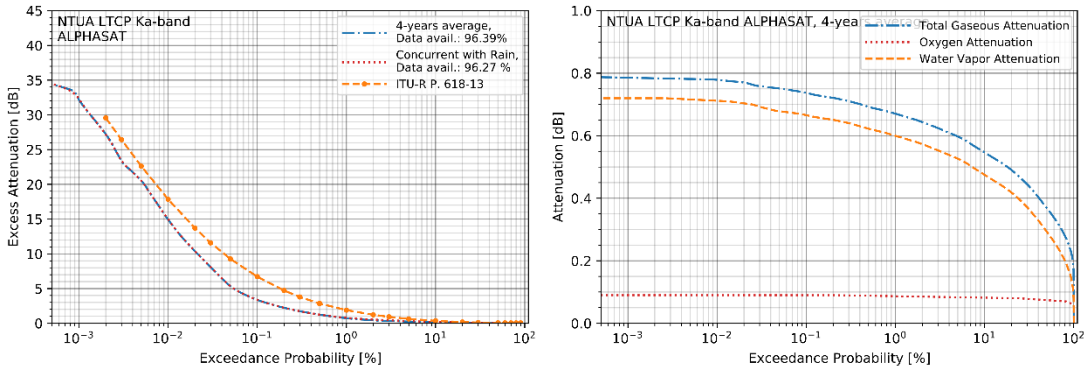

Figure 5-7: Long-term (4-year) attenuation probability (CCDF) for LTCP Ka-band ALPHASAT, Left: Excess Attenuation, Right: Gaseous Attenuation

5.3.9.3 Campus Q-band ALPHASAT

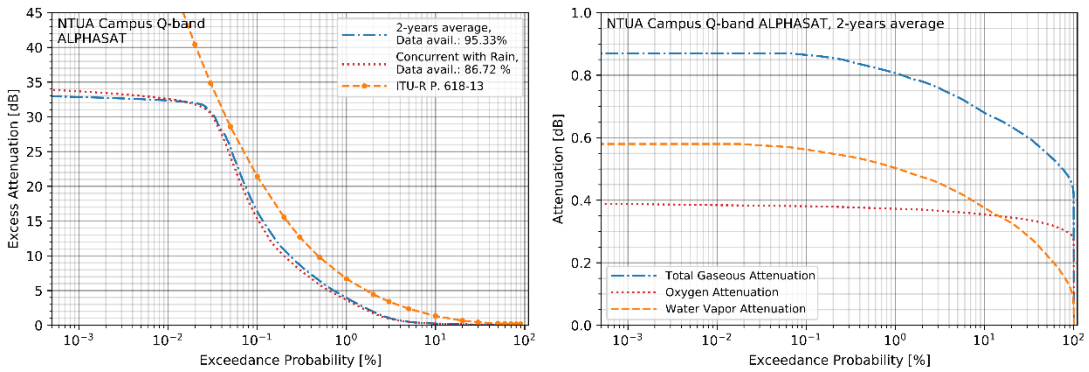

Figure 5-8: Long-term (2-year) attenuation probability (CCDF) for Campus Q-band ALPHASAT, Left: Excess Attenuation, Right: Gaseous Attenuation

5.3.9.4 LTCP Q-band ALPHASAT

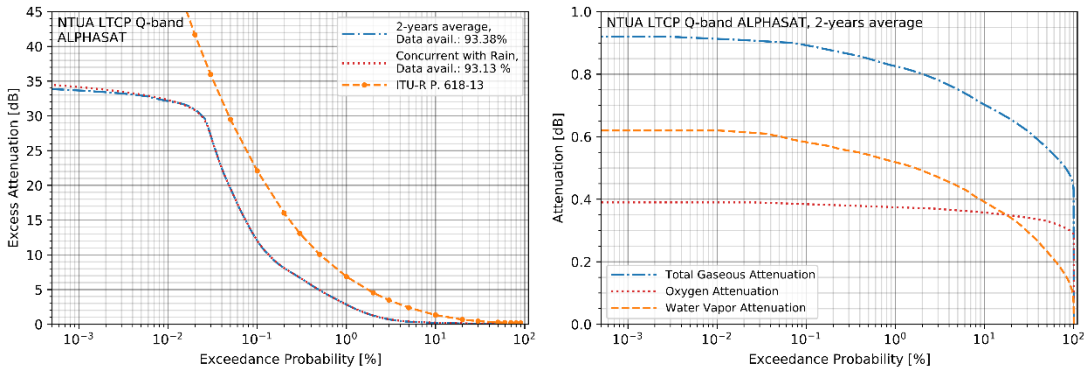

Figure 5-9: Long-term (2-year) attenuation probability (CCDF) for LTCP Q-band ALPHASAT, Left: Excess Attenuation, Right: Gaseous Attenuation

5.3.9.5 Campus Ku-band BADR5

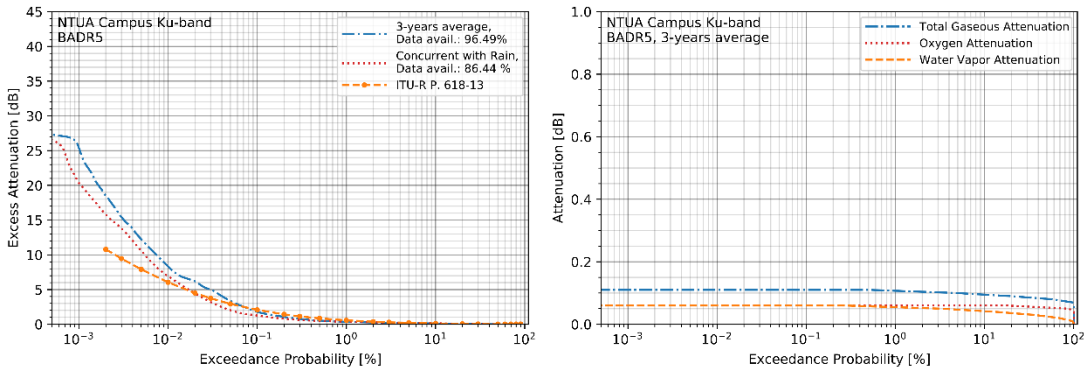

Figure 5-10: Long-term (3-year) attenuation probability (CCDF) for Campus Ku-band BADR5, Left: Excess Attenuation, Right: Gaseous Attenuation

5.3.9.6 Campus Ka-band KaSAT[1]

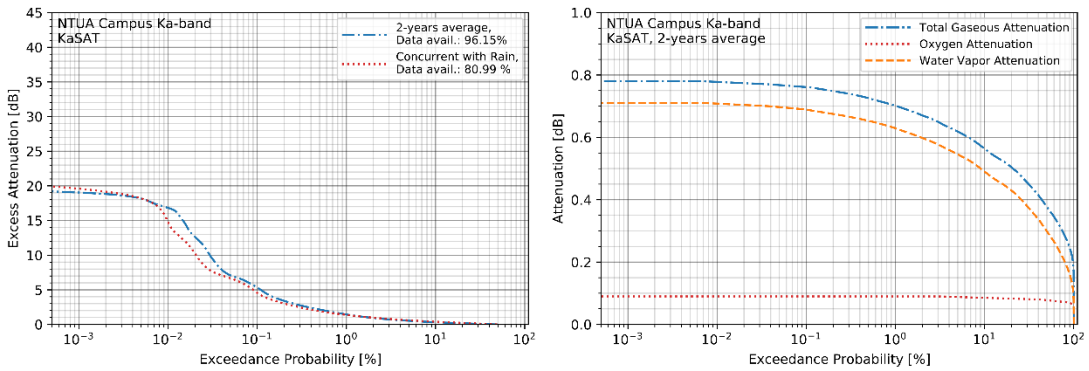

Figure 5-11: Long-term (2-year) attenuation probability (CCDF) for Campus Ka-band KaSAT, Left: Excess Attenuation, Right: Gaseous Attenuation

[1] The dynamic range of the Campus Ka-band KaSAT receiver is about 16 dB.

5.3.10 Yearly Attenuation

5.3.10.1 Campus Ka-band ALPHASAT

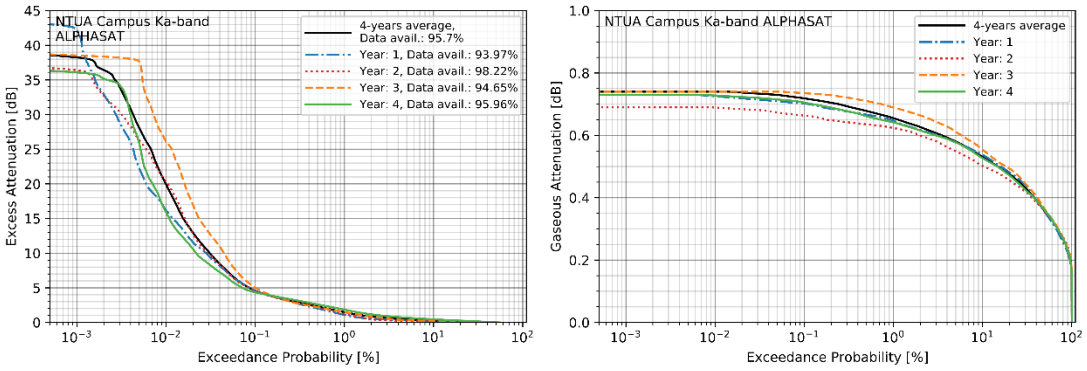

Figure 5-12: Yearly attenuation probability (CCDF) for Campus Ka-band ALPHASAT, Left: Excess Attenuation, Right: Gaseous Attenuation

5.3.10.2 LTCP Ka-band ALPHASAT

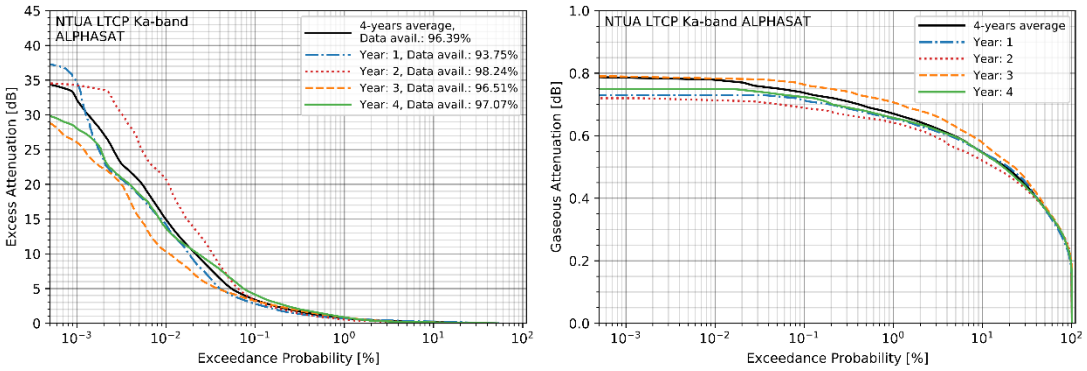

Figure 5-13: Yearly attenuation probability (CCDF) for LTCP Ka-band ALPHASAT, Left: Excess Attenuation, Right: Gaseous Attenuation

5.3.10.3 Campus Q-band ALPHASAT

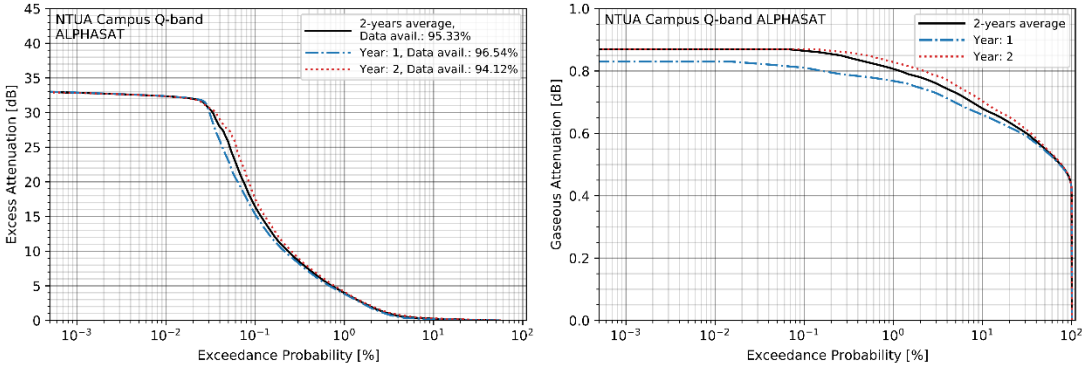

Figure 5-14: Yearly attenuation probability (CCDF) for Campus Q-band ALPHASAT, Left: Excess Attenuation, Right: Gaseous Attenuation

5.3.10.4 LTCP Q-band ALPHASAT

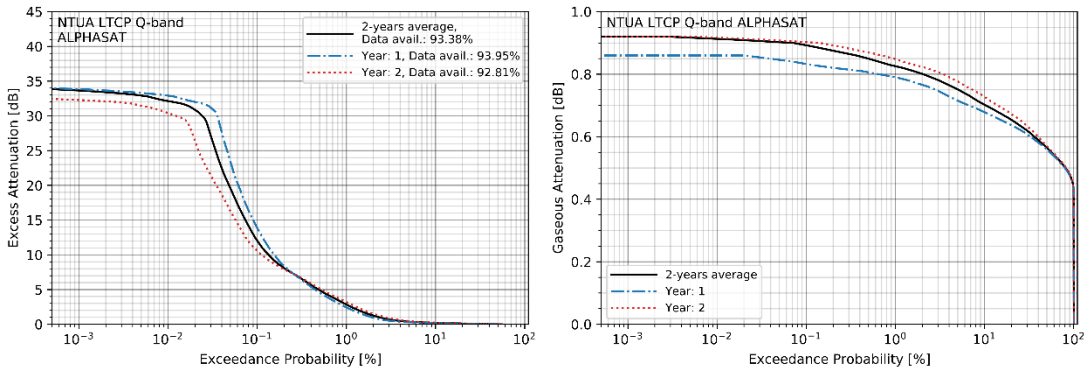

Figure 5-15: Yearly attenuation probability (CCDF) for LTCP Q-band ALPHASAT, Left: Excess Attenuation, Right: Gaseous Attenuation

5.3.10.5 Campus Ku-band BADR5

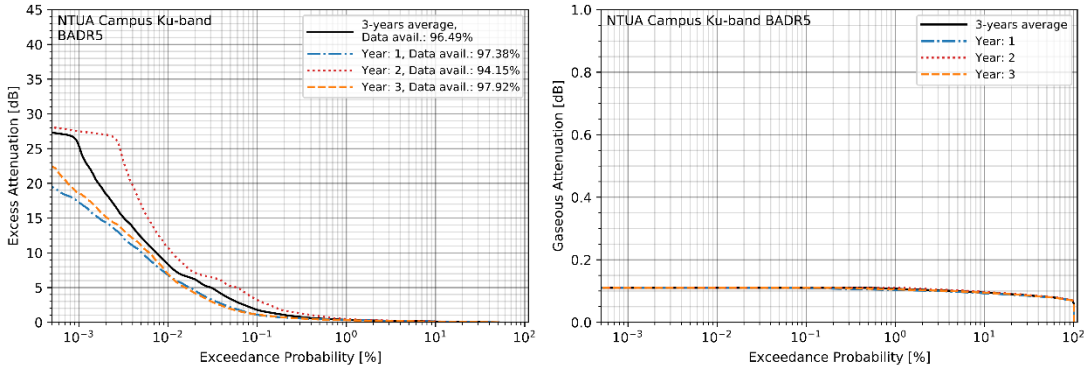

Figure 5-16: Yearly attenuation probability (CCDF) for Campus Ku-band BADR5, Left: Excess Attenuation, Right: Gaseous Attenuation

5.3.10.6 Campus Ka-band KaSAT

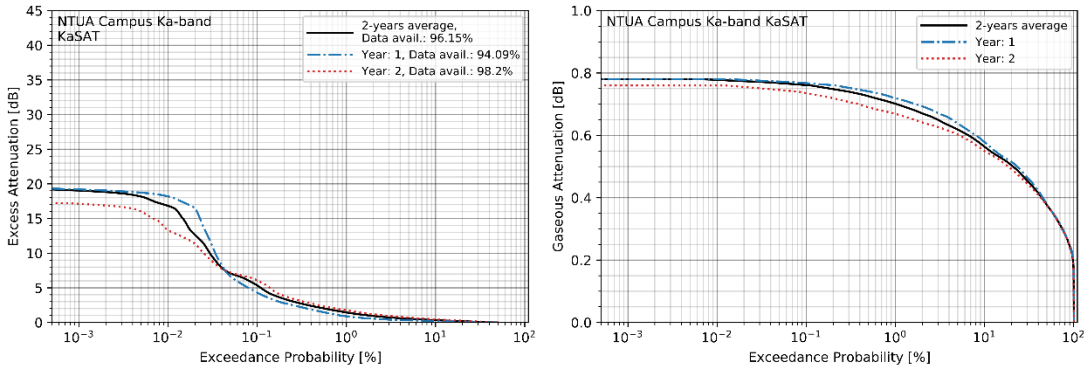

Figure 5-17: Yearly attenuation probability (CCDF) for Campus Ka-band KaSAT, Left: Excess Attenuation, Right: Gaseous Attenuation

5.3.11 Seasonal Attenuation

5.3.11.1 Campus Ka-band ALPHASAT

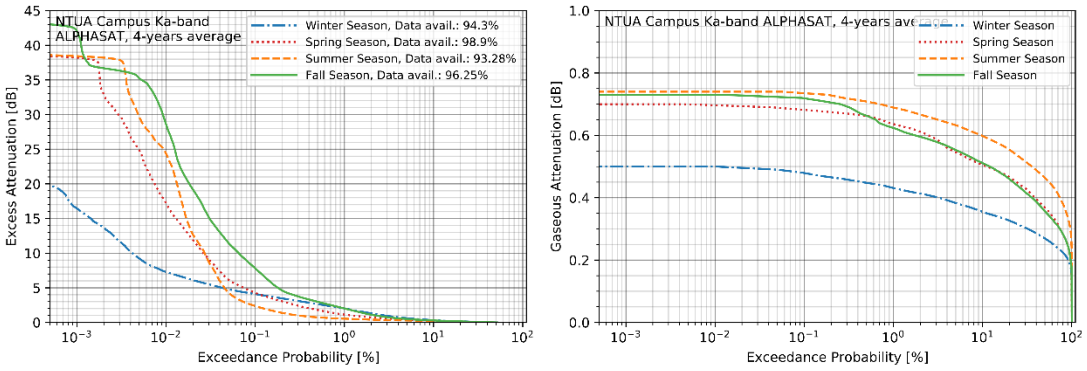

Figure 5-18: Seasonal attenuation probability (CCDF) for Campus Ka-band ALPHASAT, Left: Excess Attenuation, Right: Gaseous Attenuation

5.3.11.2 LTCP Ka-band ALPHASAT

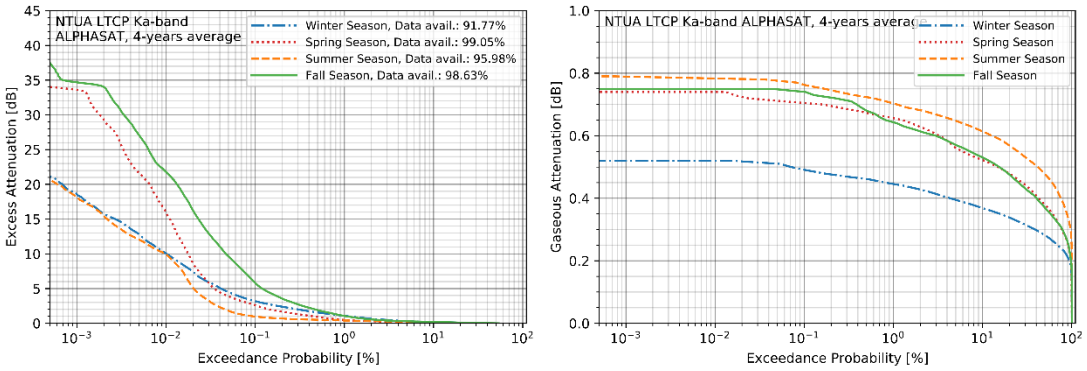

Figure 5-19: Seasonal attenuation probability (CCDF) for LTCP Ka-band ALPHASAT, Left: Excess Attenuation, Right: Gaseous Attenuation

5.3.11.3 Campus Q-band ALPHASAT

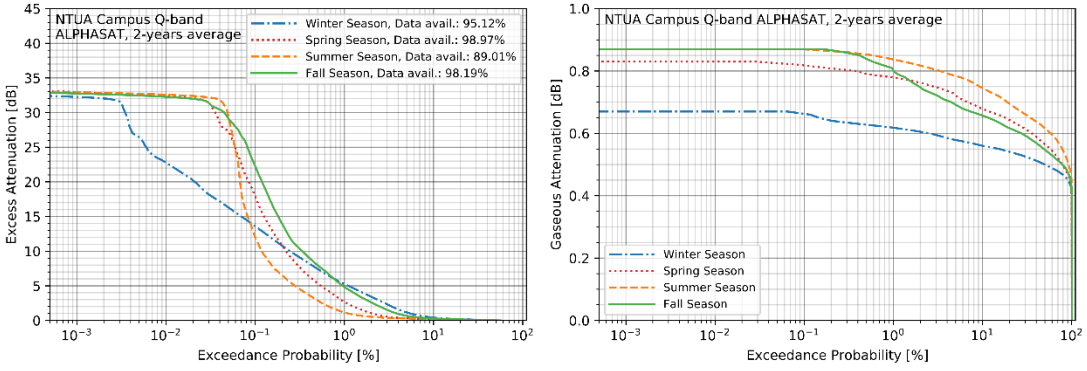

Figure 5-20: Seasonal attenuation probability (CCDF) for Campus Q-band ALPHASAT, Left: Excess Attenuation, Right: Gaseous Attenuation

5.3.11.4 LTCP Q-band ALPHASAT

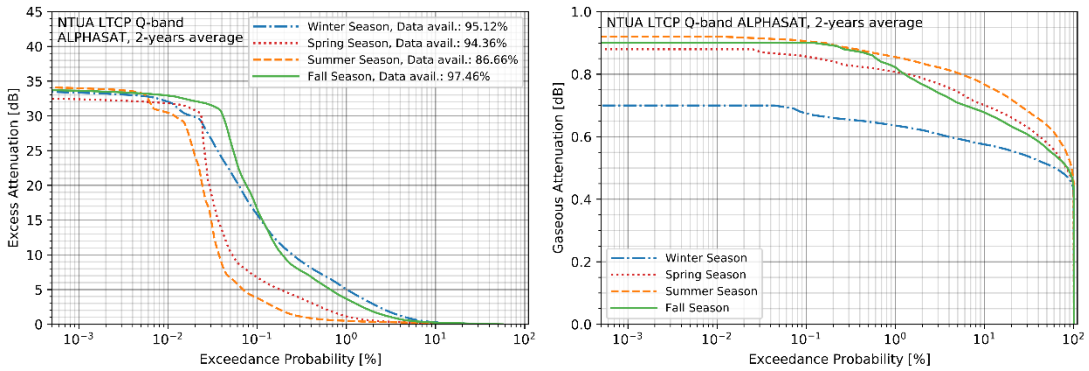

Figure 5-21: Seasonal attenuation probability (CCDF) for LTCP Q-band ALPHASAT, Left: Excess Attenuation, Right: Gaseous Attenuation

5.3.11.5 Campus Ku-band BADR5

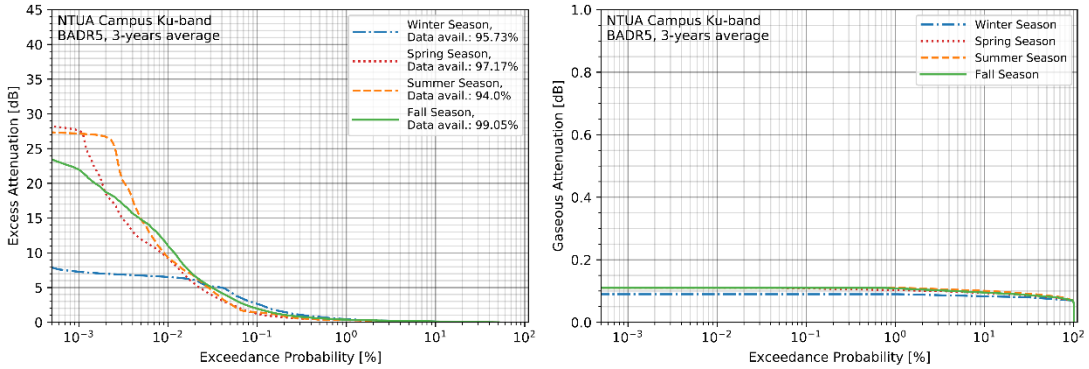

Figure 5-22: Seasonal attenuation probability (CCDF) for Campus Ku-band BADR5, Left: Excess Attenuation, Right: Gaseous Attenuation

5.3.11.6 Campus Ka-band KaSAT

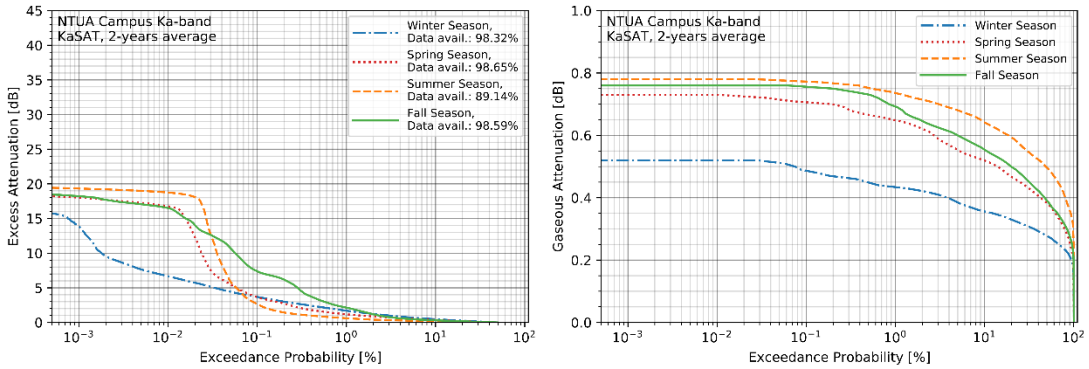

Figure 5-23: Seasonal attenuation probability (CCDF) for Campus Ka-band KaSAT, Left: Excess Attenuation, Right: Gaseous Attenuation

5.3.12 Monthly Attenuation

5.3.12.1 Campus Ka-band ALPHASAT

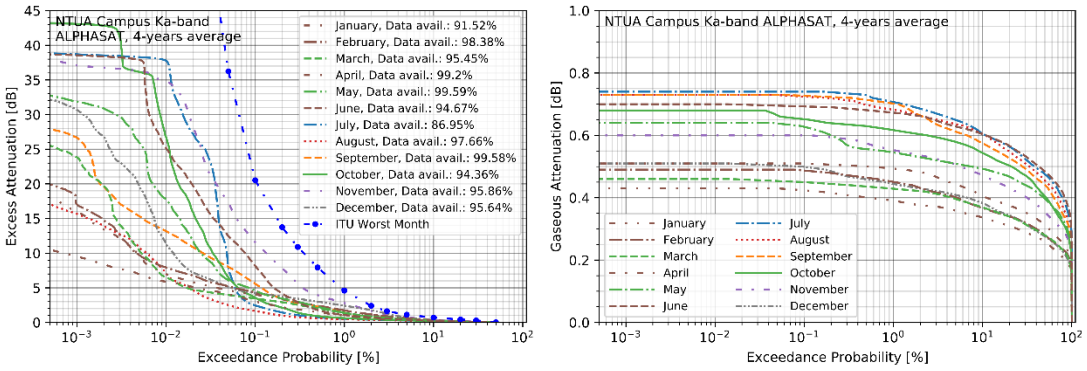

Figure 5-24: Monthly attenuation probability (CCDF) for Campus Ka-band ALPHASAT, Left: Excess Attenuation, Right: Gaseous Attenuation

5.3.12.2 LTCP Ka-band ALPHASAT

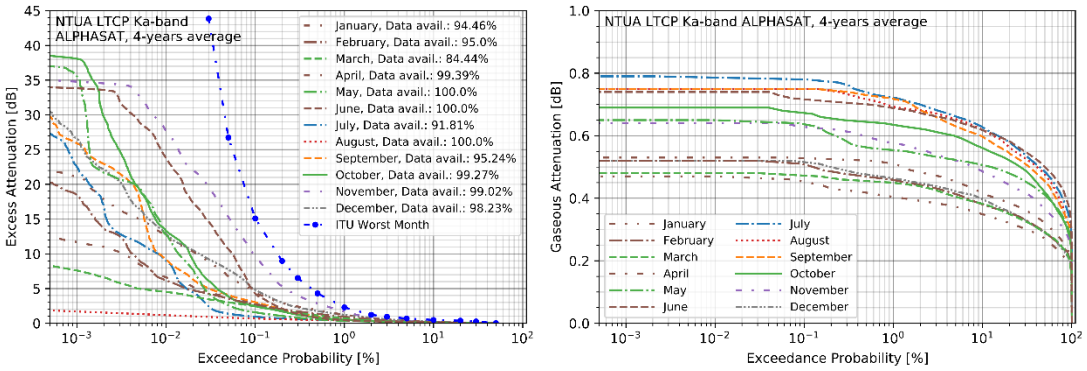

Figure 5-25: Monthly attenuation probability (CCDF) for LTCP Ka-band ALPHASAT, Left: Excess Attenuation, Right: Gaseous Attenuation

5.3.12.3 Campus Q-band ALPHASAT

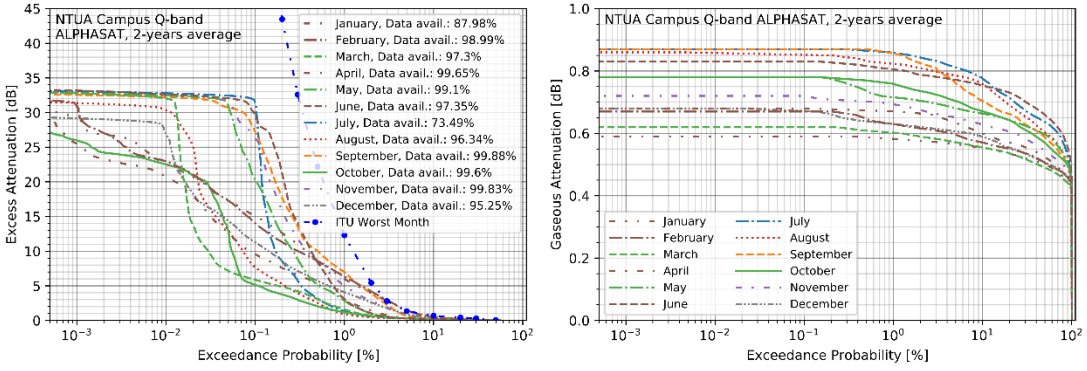

Figure 5-26: Monthly attenuation probability (CCDF) for Campus Q-band ALPHASAT, Left: Excess Attenuation, Right: Gaseous Attenuation

5.3.12.4 LTCP Q-band ALPHASAT

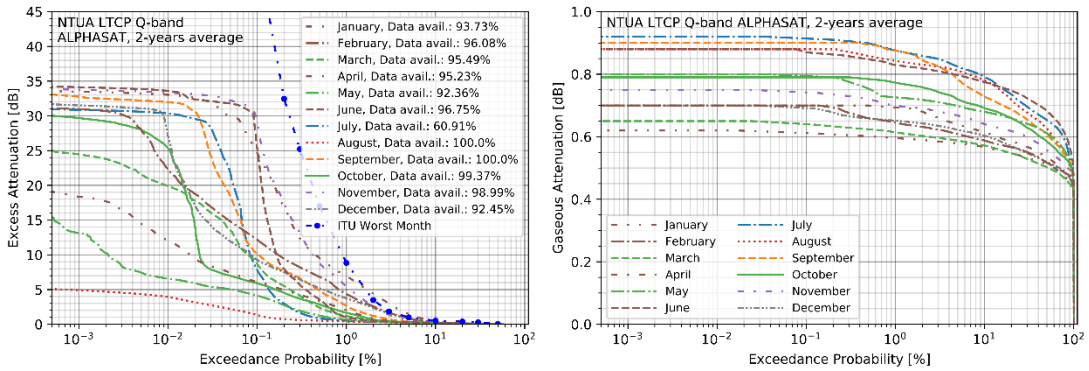

Figure 5-27: Monthly attenuation probability (CCDF) for LTCP Q-band ALPHASAT, Left: Excess Attenuation, Right: Gaseous Attenuation

5.3.12.5 Campus Ku-band BADR5

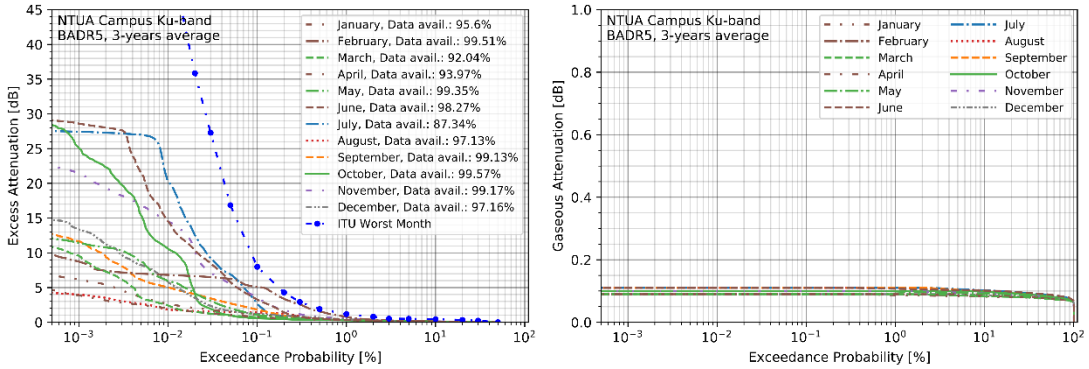

Figure 5-28: Monthly attenuation probability (CCDF) for Campus Ku-band BADR5, Left: Excess Attenuation, Right: Gaseous Attenuation

5.3.12.6 Campus Ka-band KaSAT

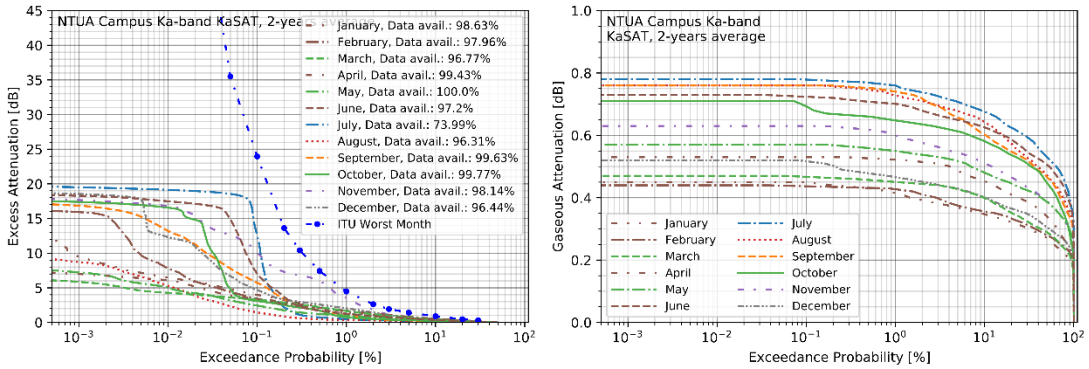

Figure 5-29: Monthly attenuation probability (CCDF) for Campus Ka-band KaSAT, Left: Excess Attenuation, Right: Gaseous Attenuation

5.3.13 Diurnal Attenuation

5.3.13.1 Campus Ka-band ALPHASAT

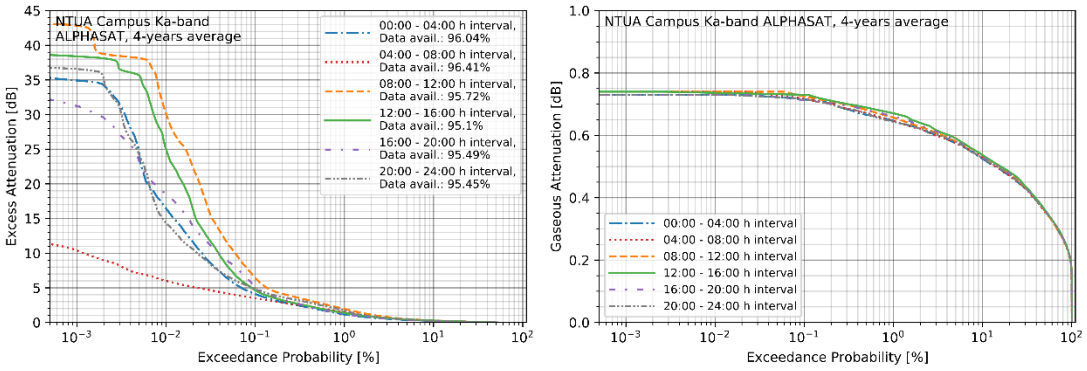

Figure 5-30: Diurnal attenuation probability (CCDF) for Campus Ka-band ALPHASAT, Left: Excess Attenuation, Right: Gaseous Attenuation

5.3.13.2 LTCP Ka-band ALPHASAT

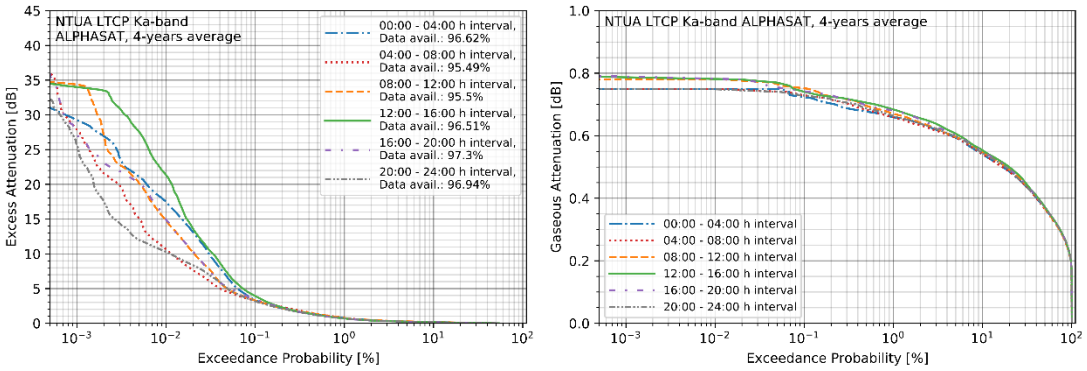

Figure 5-31: Diurnal attenuation probability (CCDF) for LTCP Ka-band ALPHASAT, Left: Excess Attenuation, Right: Gaseous Attenuation

5.3.13.3 Campus Q-band ALPHASAT

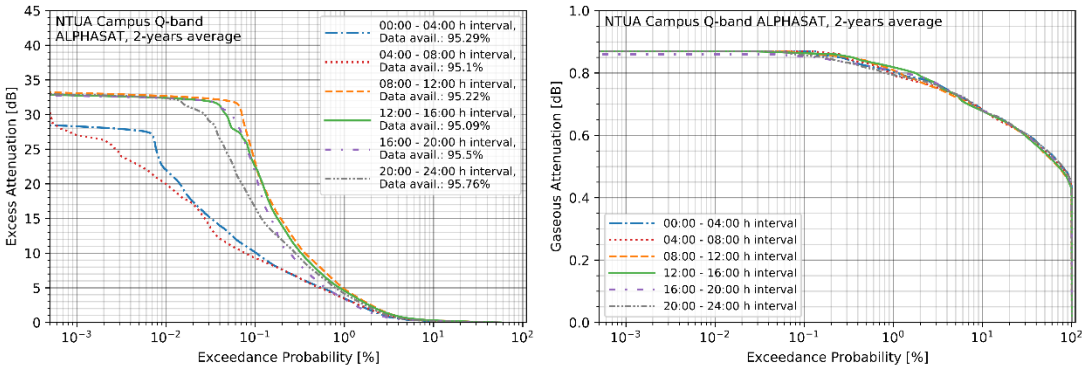

Figure 5-32: Diurnal attenuation probability (CCDF) for Campus Q-band ALPHASAT, Left: Excess Attenuation, Right: Gaseous Attenuation

5.3.13.4 LTCP Q-band ALPHASAT

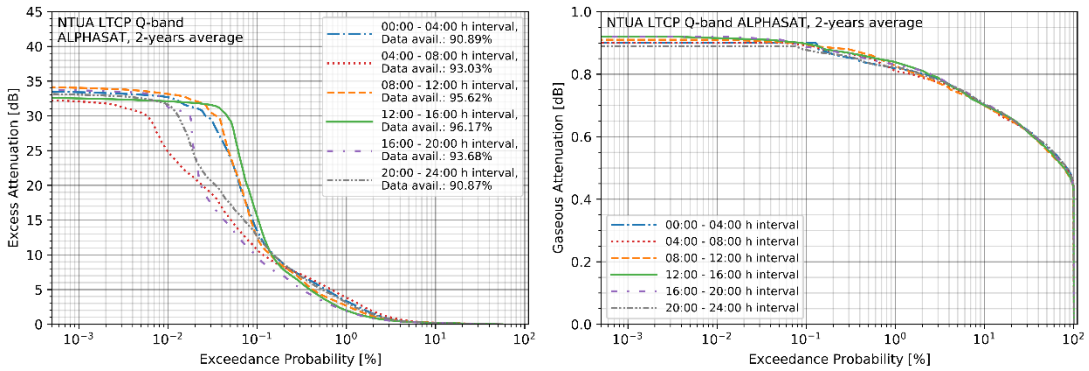

Figure 5-33 Diurnal attenuation probability (CCDF) for LTCP Q-band ALPHASAT, Left: Excess Attenuation, Right: Gaseous Attenuation

5.3.13.5 Campus Ku-band BADR5

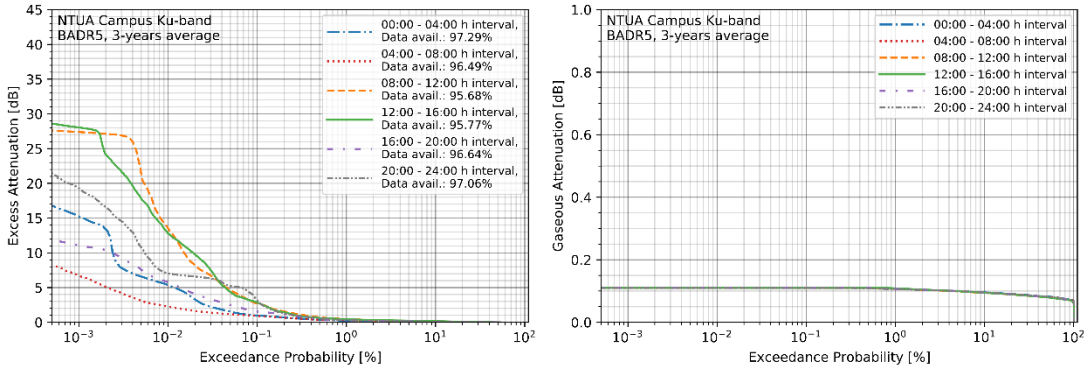

Figure 5-34: Diurnal attenuation probability (CCDF) for Campus Ku-band BADR5, Left: Excess Attenuation, Right: Gaseous Attenuation

5.3.13.6 Campus Ka-band KaSAT

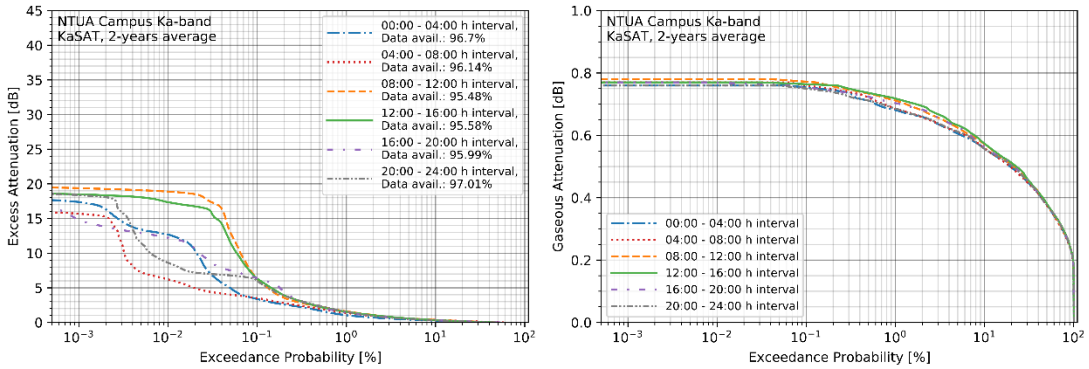

Figure 5-35: Diurnal attenuation probability (CCDF) for Campus Ka-band KaSAT, Left: Excess Attenuation, Right: Gaseous Attenuation

5.4 Discussion

Examining the rainfall rate statistics, it is evident that the Attica region exhibits a typical South-Mediterranean climate; there is a significant rainfall rate discrepancy between the four seasons, with Fall consistently being the season with the most rain events. The rainfall rate for this season ranges from a few mm/h up to more than 125 mm across both campaign locations. It can therefore be deduced that during this season, both convective- and stratiform-type rain occurs; the month with the highest rainfall rate is November, reaching values in excess of 100 m/h and 80 mm/h for up to 0.01 % of the season's time for Campus and LTCP respectively.

During Winter and Spring more stratiform-type events tend to dominate yielding rain events of much lower intensity, while in Summer, although it being almost dry for up to 99.97% of the season's duration (0.03% exceedance probability), some extreme rainfall events have been recorded reaching rates higher than 100 mm/h for up to 0.01% of the season's duration. Such events can be attributed almost exclusively to convective rain cells, they are sparse and with very limited duration (typically in the order of a few minutes). It should be noted that the seasonal differences are more exaggerated at the Campus location than the LTCP one; the Ymmitos mountain range as well as other tall mountain ranges surrounding the Campus site definitely play a key role in this behavior, contrary to the Lavrion site which is by the sea in absence of any tall nearby mountains. In any case, each site's 4-year average rainfall rate seems to very tightly follow the yearly averages for up to 0.1% exceedance probability while still maintaining good accordance for even lower exceedance probabilities. It should be stressed that the latter is the very reason for conducting long-term measurements, as only then any temporal biases can be minimized.

Finally, comparing the two location's statistics, both on a yearly basis as well as overall, it seems that there is no significant discrepancy as the exceedance probabilities almost coincide for values higher than 0.001% of the total time; this result is expected because of their close proximity (about 36.5 km).

Carefully evaluating the attenuation statistics for different frequency bands, remarkable results are obtained regarding the potential system availability of Ka and Q band systems.

For the Ka-band case, a 5 dB total attenuation level is exceeded for up to 0.1% and 0.07% of the total time for Campus and LTCP respectively, while a 15 dB level for up to 0.015% and 0.01% of the time respectively; in practical terms, for a typical satellite link requiring availability at least 99.999% (i.e., approx. 5.26 min of yearly outage allowed) more than 38 dB of fade margin would be required.

Regarding Q-band, the exceedance probability lines appear to be shifted to the right compared to the Ka-band ones, meaning that the same total attenuation thresholds are exceeded for far greater time than at Ka-band. The 5 dB total attenuation level is exceeded for up to 0.9% and 0.6% for Campus and LTCP, while the 15 dB level for up to almost 0.1% of the time for Campus and 0.07 % for LTCP. To meet a 99.9% availability requirement (8.76 hours of outage allowed), more than about 17 and 13 dB of margin are required for Campus and LTCP respectively; the margin required to reach 99.999% availability cannot even be estimated since it is higher than the dynamic range of the receivers (greater than 33-34 dB).

Even in the case of Ku-band, in order to meet a 99.999% availability more than 25 dB of margin have to be considered; for this frequency band, however, a conventional link-budget fade margin

combined with power control techniques should be capable of sustaining a relatively high availability target (a 10 dB effective margin could compensate for up to 99.993% of the time, resulting in approx. 39.42 minutes of yearly outage).

In practical terms, employing not only a conventional fade margin alone, but even combined with uplink/downlink power control will probably not have the capacity to compensate for the induced signal attenuation. It is therefore apparent that other, more sophisticated fading mitigation techniques are essential to maintain the high Quality of Service (QoS) as prescribed in the operator's SLAs. In the following table, a quick comparison between the fade margins required to meet various availability targets based on the obtained measurements can be found:

Table 5-2: Fade margins required to meet availability target based on measurement data (approximate values)

Availability Target [%]	Yearly Outage Duration	Approximate margin Required [dB]		
		Ku-band	Ka-band	Q-band
99	87.6 hours	0.5	2	4.5
99.9	8.76 hours	2	5	13-17.5
99.99	52.56 minutes	8.5	16-21	34
99.999	5.256 minutes	25	33-39	>35 (out of DR)

Another interesting observation is the massive diurnal variability of the excess attenuation across all frequency bands; the period from 04:00-08:00 h (UTC) consistently appears to exhibit much lower attenuation values, in some cases up to e.g. 40 dB lower than for the 08:00-12:00 h interval at 0.01% of time at Campus Ka-band; massive differences can be seen for all frequency bands though. The interval with the highest excess attenuation is 08:00-16:00 h, i.e., during daytime. Such a finding further suggests that statically allocating transmission power is totally inefficient, as not only seasonal variations exist but also diurnal ones, e.g. during most of the night-time (when usually less system utilization occurs anyway) much of the transmitted energy would be wasted.

Comparing the obtained results with the ITU-R Rec. P.618-13 [6] prediction (derived using the locally measured rain rate at 0.01% exceedance probability):

- For *Ku-band*, the ITU model is in good accordance with the measurement results for exceedance probabilities up to about 0.04% while under-estimating excess attenuation for lower probabilities.
- For *Ka-band* the ITU model seems to greatly over-estimate excess attenuation for exceedance probabilities between 0.01% to 1% of the time, while for lower probabilities it either considerably under-estimates it (Campus Ka-band) or mildly over-estimate it (LTCP Ka-band).
- For *Q-band* the ITU model seriously over-estimates excess attenuation across all exceedance probabilities, reaching errors in the order of 10 dB for probabilities around 0.1%.

The ITU worst month estimation according to ITU-R Rec. P. 841-6 [7] obtained using the values for "Europe/Mediterannean" region for excess attenuation and "Tropical, subtropical and temperate climate regions with frequent rain" for the rain rate:

- Seems to be in good accordance for the rain rate for exceedance probabilities higher than 0.1% while significantly over-estimating rain rate for lower probabilities

- Appears to over-estimate excess attenuation for all frequency bands and campaign locations for exceedance probabilities lower than 1-2%.

5.5 Chapter References

[1] ARG100 Rain Gauge User Manual, EML Environmental Measurements Limited, 2017, ver. 2.

[2] E. Matricciani and C. Riva, "The search for the most reliable long-term rain attenuation CDF of a slant path and the impact on prediction models," IEEE Transactions on Antennas and Propagation, vol. 53, no. 9, 2005, pp. 3075–3079.

[3] ITU-R Study Group 3 Fascicle 3M/FAS/8, The processing of tipping bucket rain gauge data for Study Group 3 experimental database, https://www.itu.int/en/ITU-R/study-groups/rsg3/Pages/fascicles.aspx

[4] ITU-R Recommendation P. 676-12, "Attenuation by atmospheric gases and related effects", International Telecommunication Union, Tech. Rep, Geneva, 2020.

[5] H. Hersbach, B. Bell, P. Berrisford, G. Biavati, A. Horányi, J. Muñoz Sabater, J. Nicolas, C. Peubey, R. Radu, I. Rozum, D. Schepers, A. Simmons, C. Soci, D. Dee and J-N. Thépaut, ERA5 monthly averaged data on single levels from 1979 to present, Copernicus Climate Change Service (C3S) Climate Data Store (CDS), 2019, 10.24381/cds.f17050d7, doi: https://doi.org/10.24381/cds.f17050d7

[6] ITU-R Recommendation P. 618-13, "Propagation data and prediction methods required for the design of Earth-space telecommunication systems", International Telecommunication Union, Tech. Rep, Geneva, 2017.

[7] ITU-R Recommendation P P.841-6, "Conversion of annual statistics to worst-month statistics", International Telecommunication Union, Tech. Rep, Geneva, 2019.

Chapter 6

Second Order Statistics

6.1 Evaluation parameters

The first order statistics analysis presented in the previous chapter provides useful insight regarding the long-term system performance; nevertheless, for more accurate system design and channel modeling the second order statistics are often essential, especially for the development and testing of efficient FMTs.

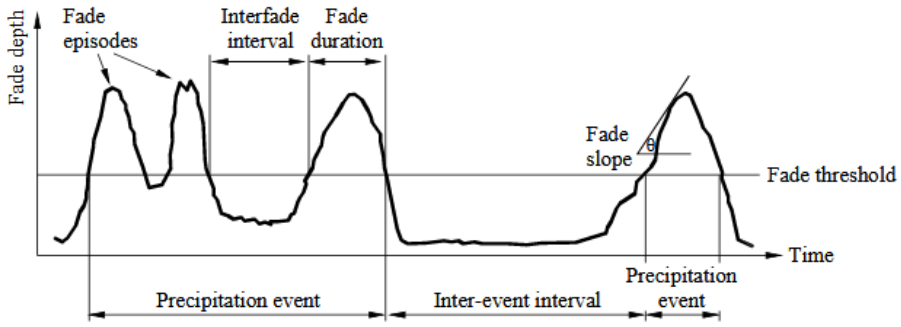

Figure 6-1: Graphical Representation of fade dynamics [1]

In this chapter, the following statistics have been evaluated and are presented:

6.1.1 Fade slope statistics

In order to evaluate the excess attenuation fade slope statistics:

- The data have been harmonized to 1 sec time resolution
- They have been low-pass filtered with a Butterworth filter of 10th order with a cut-off frequency of 0.02 Hz as per [1] to remove rapid fluctuations of the signal due to scintillation.
- The fade slope calculation interval Δt is 60 sec using the definition [1]:

$$\zeta(t) = \frac{A(t+\frac{1}{2}\Delta t) - A(t-\frac{1}{2}\Delta t)}{\Delta t} \quad [6\text{-}1]$$

The following fade slope analysis is performed:

6.1.1.1 Calculation of the PDF of fade slope

The normalized probability density function $P[a \le Z \le b \mid A > a]$ in percent (%), where Z the fade slope values (or equivalently the number of occurrences) for fade events with excess attenuation $A > a$. The fade slope values are classified into bins of 0.05 [dB/sec]:

<-0.5, [-0.5,-0.45], [-0.45,-0.40],…, [-0.05,0],[0,0.05], [0.05,0.1],…, [0.45,0.50], >0.50.

6.1.1.2 Calculation of the CCDF of absolute fade slope

The normalized probability of occurrence $P[|Z| > z \mid A > a]$ in percent (%), where $|Z|$ is the absolute value of the fade slope for fade events with excess attenuation $A > a$. The values of absolute fade slope x considered for the calculation are 0.001, 0.002, 0.003, 0.005, 0.01, 0.02, 0.03, 0.05, 0.1,0.2,0.3, 0.5, 1, 2, 3 and 5 |dB/sec| and the attenuation levels a : 1,3, 5, 10,15, 20 and 25dB.

6.1.1.3 Calculation of the CCDF of absolute fade slope at given attenuation exceedance probabilities

The normalized probability of occurrence $P[|Z| > z \mid A > \tilde{a}]$ in percent (%), where $|Z|$ is the absolute value of the fade slope for fade events with excess attenuation $A > \tilde{a}$. The attenuation threshold $\tilde{a}$ is defined by the long-term exceedance probability $P[A > \tilde{a}] = \tilde{p}$. The values of absolute fade slope x considered for the calculation are 0.001, 0.002, 0.003, 0.005, 0.01, 0.02, 0.03, 0.05, 0.1,0.2,0.3, 0.5, 1, 2, 3 and 5 |dB/sec| and the attenuation levels $\tilde{a}$ corresponding to excess attenuation exceedance probability values $\tilde{p}$ (%): 0.001, 0.002, 0.003, 0.005, 0.01, 0.02, 0.03, 0.05, 0.1,0.2,0.3, 0.5, 1.

6.1.2 Fade duration statistics

In order to evaluate the excess attenuation fade duration statistics, the data have been harmonized to 1 sec time resolution

The following fade duration analysis is performed:

6.1.2.1 Calculation of the CCDF of fade duration

The normalized probability of occurrence $P[D > d \mid A > a]$ in percent (%) of fade events with duration $D > d$ and excess attenuation $A > a$. The values of fade duration d considered for the calculation are 1,10, 30, 60, 120, 180, 300, 600, 900, 1200, 1500, 1800, 2400, 3600 sec and the attenuation levels a : 1,3, 5, 10,15, 20 and 25dB.

6.1.2.2 Calculation of the CCDF of fade duration at given attenuation exceedance probabilities

The normalized probability of occurrence $P[D > d \mid A > \tilde{a}]$ in percent (%) of fade events with duration $D > d$ and excess attenuation $A > \tilde{a}$. The attenuation threshold $\tilde{a}$ is defined by the long-term exceedance probability $P[A > \tilde{a}] = \tilde{p}$. The values of fade duration d considered for the calculation are 1,10, 30, 60, 120, 180, 300, 600, 900, 1200, 1500, 1800, 2400, 3600 sec and the

attenuation levels $\tilde{a}$ corresponding to excess attenuation exceedance probability values $\tilde{p}$ (%): 0.001, 0.002, 0.003, 0.005, 0.01, 0.02, 0.03, 0.05, 0.1,0.2,0.3, 0.5 and 1.

6.1.2.3 Calculation of the CCDF of accumulate fade duration

The normalized cumulative exceedance probability $F[D > d \mid A > a]$ in percent (%), or equivalently the fraction of total fade time due to fades of with duration d longer than D, corresponding to fade events with excess attenuation $A > a$. The values of fade duration d considered for the calculation are 1,10, 30, 60, 120, 180, 300, 600, 900, 1200, 1500, 1800, 2400, 3600 sec and the attenuation levels a : 1,3, 5, 10,15, 20 and 25dB.

6.1.2.4 Calculation of the CCDF of accumulate fade duration at given attenuation exceedance probabilities

The normalized cumulative exceedance probability $F[D > d \mid A > \tilde{a}]$ in percent (%), or equivalently the fraction of total fade time due to fades with duration d longer than D, corresponding to fade events with excess attenuation $A > \tilde{a}$. The values of fade duration d considered for the calculation are 1,10, 30, 60, 120, 180, 300, 600, 900, 1200, 1500, 1800, 2400, 3600 sec and the attenuation levels $\tilde{a}$ corresponding to excess attenuation exceedance probability values $\tilde{p}$ (%): 0.001, 0.002, 0.003, 0.005, 0.01, 0.02, 0.03, 0.05, 0.1,0.2,0.3, 0.5 and 1.

6.1.3 Inter-fade duration statistics

In order to evaluate the excess attenuation inter-fade duration statistics, the data have been harmonized to 1 sec time resolution

The following inter-fade duration analysis is performed:

6.1.3.1 Calculation of the CCDF of inter-fade duration

The normalized probability of occurrence $P[D > d \mid A \le a]$ in percent (%) of inter-fade intervals with duration $D > d$ and excess attenuation $A \le a$. The values of inter- fade duration d considered for the calculation are 1, 2, 3, 5, 10, 20, 30, 50, 100, 200, 300, 500, 1000, 2000, 3000, 5000, 10^4, $2*10^4$, $3*10^4$, $5*10^4$, 10^5, $2*10^5$, $3*10^5$, $5*10^5$, 10^6, $2*10^6$, $3*10^6$, $5*10^6$, 10^7 sec and the attenuation levels a : 1,3, 5, 10,15, 20 and 25dB.

6.1.3.2 Calculation of the CCDF of inter-fade duration at given attenuation exceedance probabilities

The normalized probability of occurrence $P[D > d \mid A > \tilde{a}]$ in percent (%) of inter-fade intervals with duration $D > d$ and excess attenuation $A \le \tilde{a}$. The attenuation threshold $\tilde{a}$ is defined by the long-term exceedance probability $P[A > \tilde{a}] = \tilde{p}$. The values of fade duration d considered for the calculation are 1, 2, 3, 5, 10, 20, 30, 50, 100, 200, 300, 500, 1000, 2000, 3000, 5000, 10^4, $2*10^4$, $3*10^4$, $5*10^4$, 10^5, $2*10^5$, $3*10^5$, $5*10^5$, 10^6, $2*10^6$, $3*10^6$, $5*10^6$, 10^7 sec and the attenuation levels $\tilde{a}$ corresponding to excess attenuation exceedance probability values $\tilde{p}$ (%): 0.001, 0.002, 0.003, 0.005, 0.01, 0.02, 0.03, 0.05, 0.1,0.2,0.3, 0.5 and 1.

6.2 Results

6.2.4 Fade Slope Results

6.2.4.1 Campus Ka-band ALPHASAT fade slope analysis

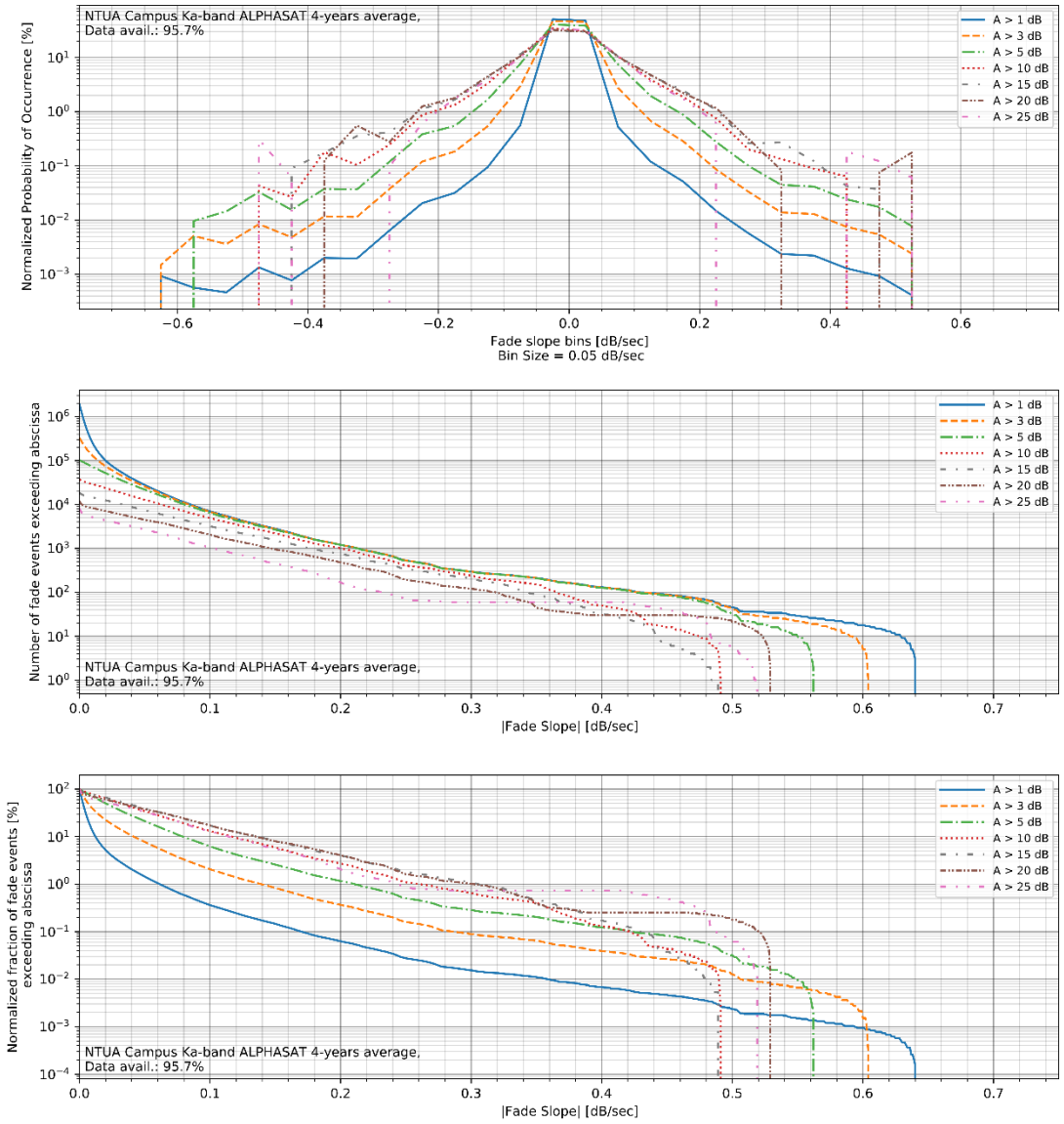

Figure 6-2: Fade slope statistics, Campus Ka-band ALPHASAT (4-year average)
Top: Fade slope normalized probability of occurrence
Middle: Number of events whose absolute fade slopes exceed abscissa
Bottom: Normalized fraction of events whose absolute fade slopes exceed abscissa

6.2.4.2 LTCP Ka-band ALPHASAT fade slope analysis

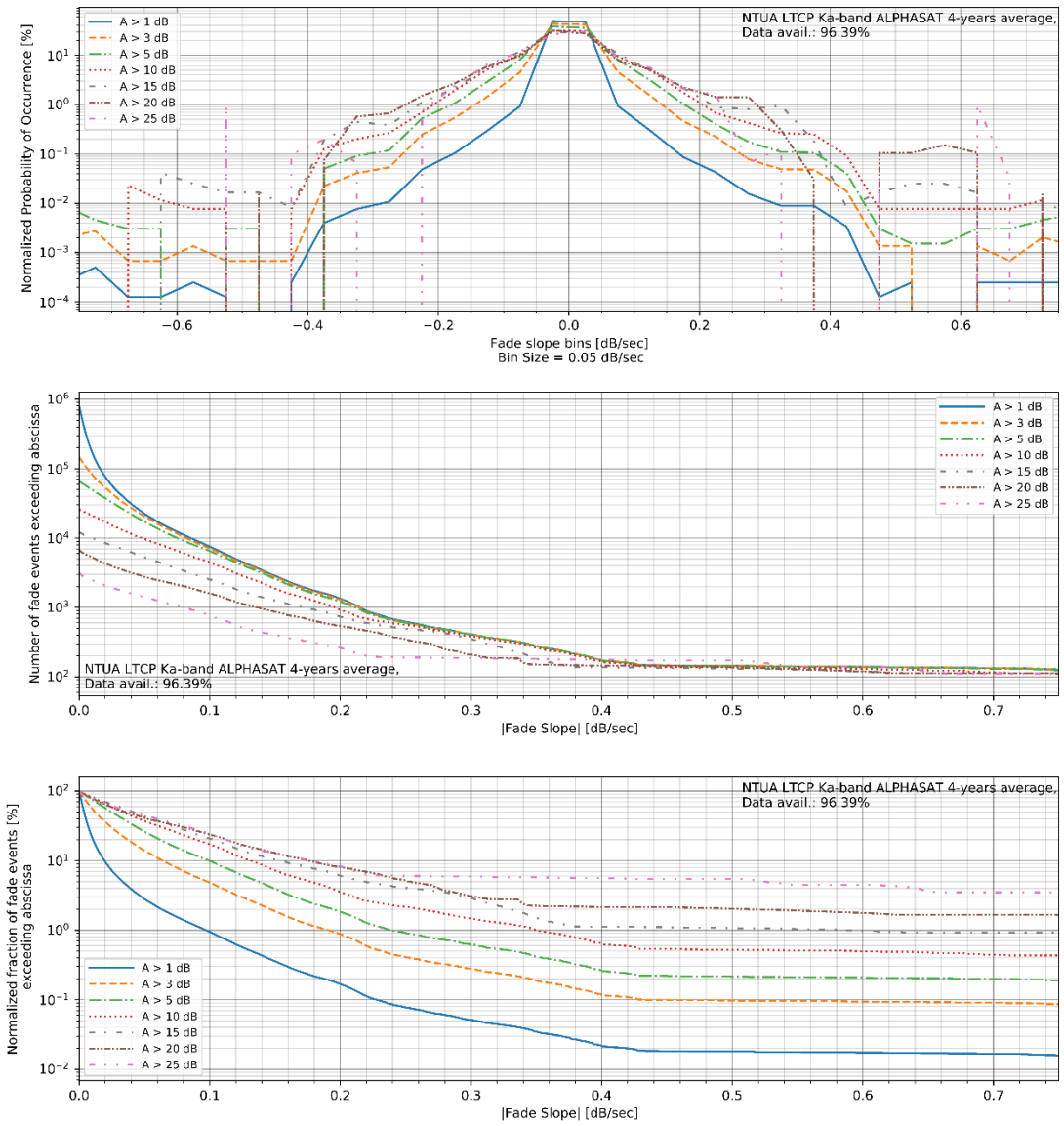

Figure 6-3: Fade slope statistics, LTCP Ka-band ALPHASAT (4-year average)
Top: Fade slope normalized probability of occurrence
Middle: Number of events whose absolute fade slopes exceed abscissa
Bottom: Normalized fraction of events whose absolute fade slopes exceed abscissa

6.2.4.3 Campus Q-band ALPHASAT fade slope analysis

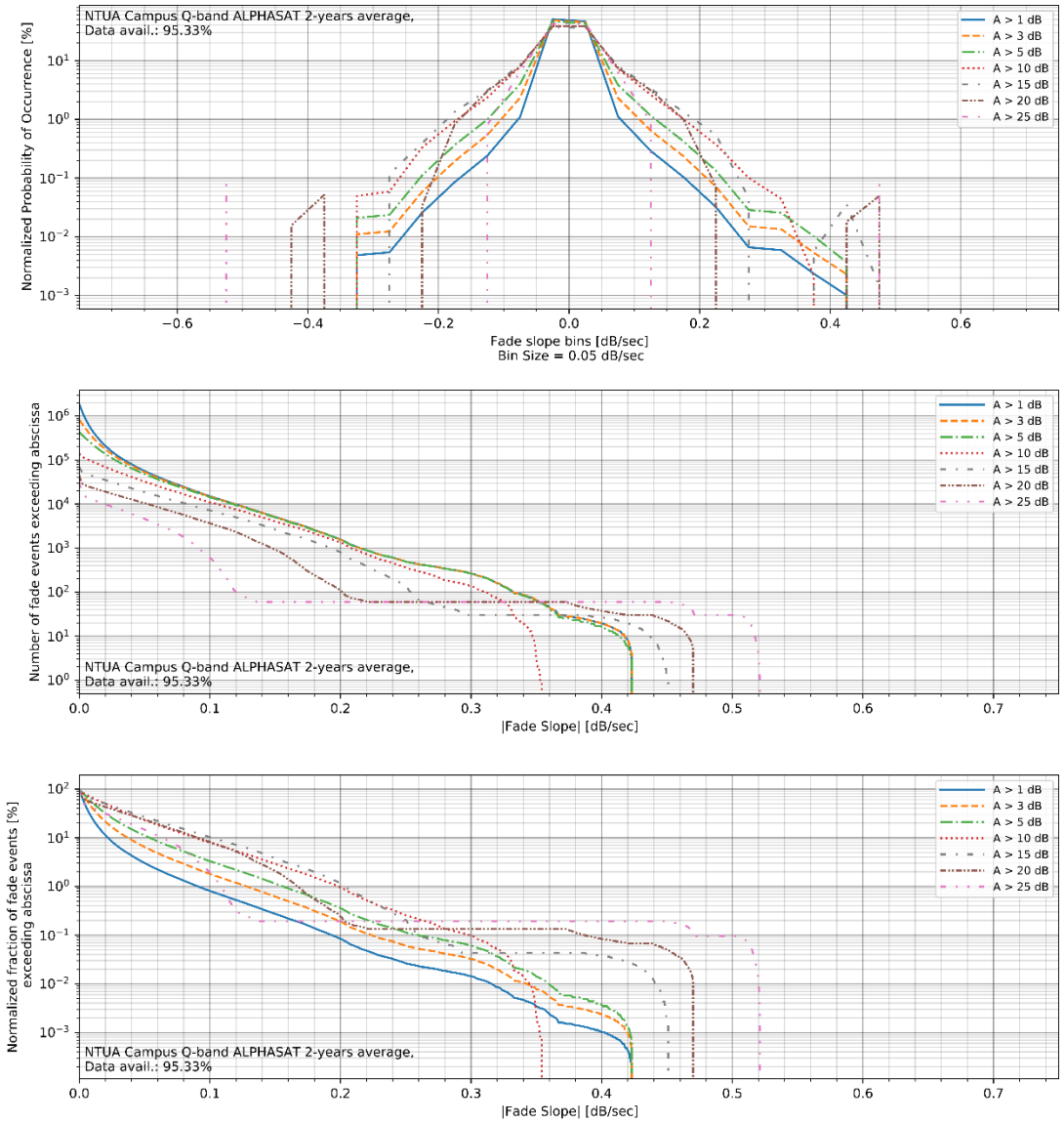

Figure 6-4: Fade slope statistics, Campus Q-band ALPHASAT (2-year average)
Top: Fade slope normalized probability of occurrence
Middle: Number of events whose absolute fade slopes exceed abscissa
Bottom: Normalized fraction of events whose absolute fade slopes exceed abscissa

6.2.4.4 LTCP Q-band ALPHASAT fade slope analysis

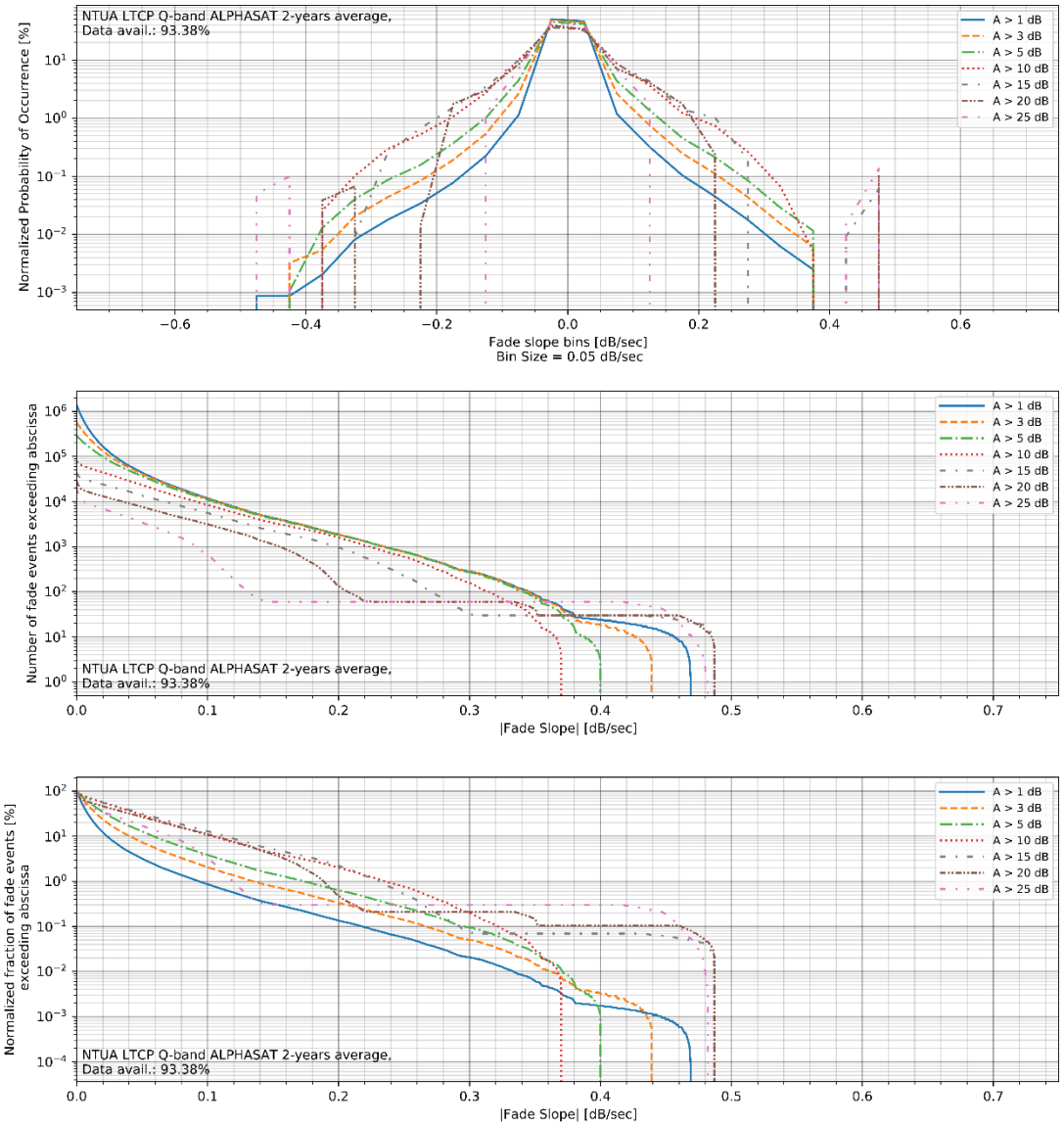

Figure 6-5: Fade slope statistics, LTCP Q-band ALPHASAT (2-year average)
Top: Fade slope normalized probability of occurrence
Middle: Number of events whose absolute fade slopes exceed abscissa
Bottom: Normalized fraction of events whose absolute fade slopes exceed abscissa

6.2.4.5 Campus Ku-band BADR5 fade slope analysis

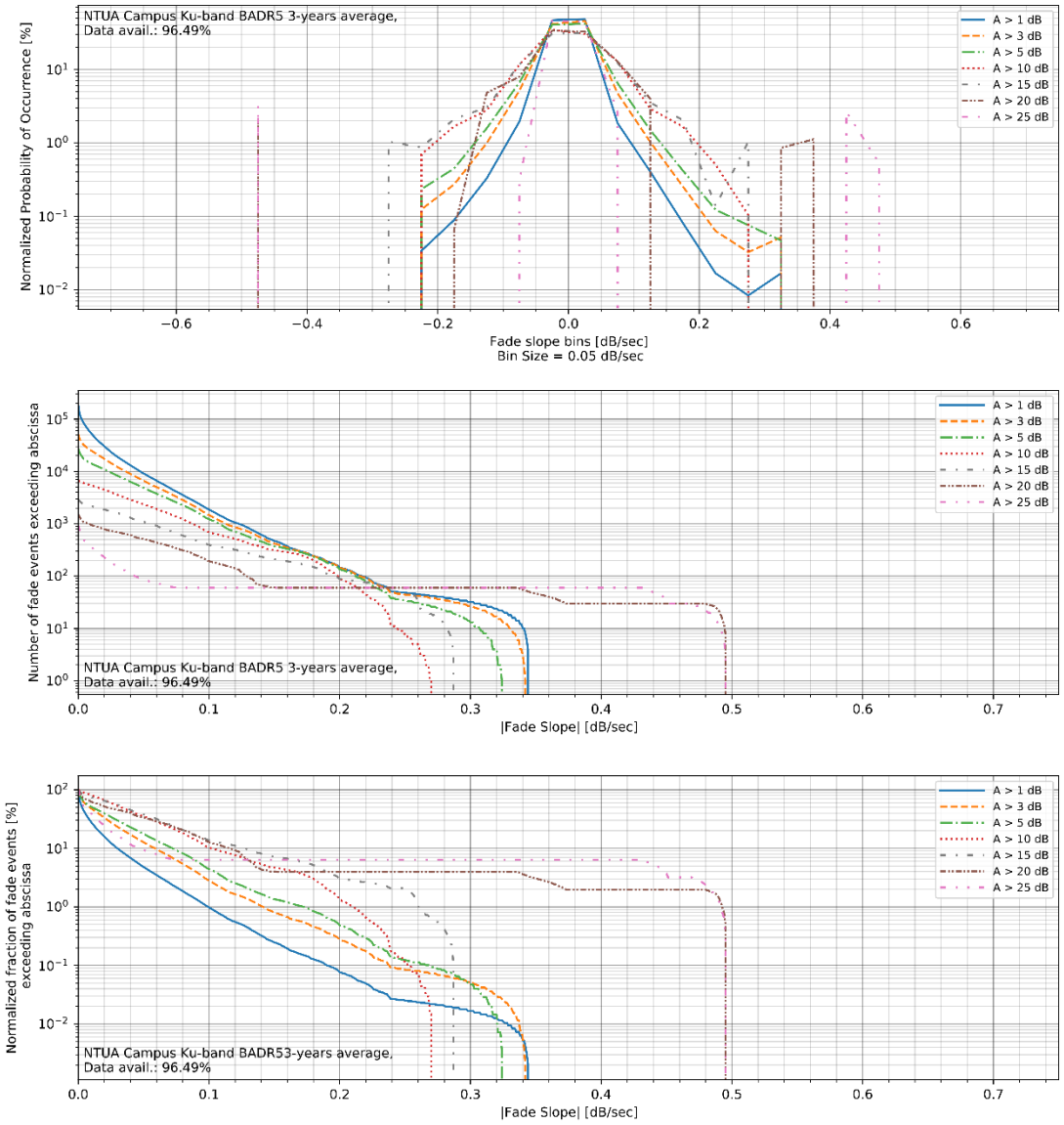

Figure 6-6: Fade slope statistics, Campus Ku-band BADR5 (3-year average)
Top: Fade slope normalized probability of occurrence
Middle: Number of events whose absolute fade slopes exceed abscissa
Bottom: Normalized fraction of events whose absolute fade slopes exceed abscissa

6.2.4.6 Campus Ka-band KaSAT fade slope analysis

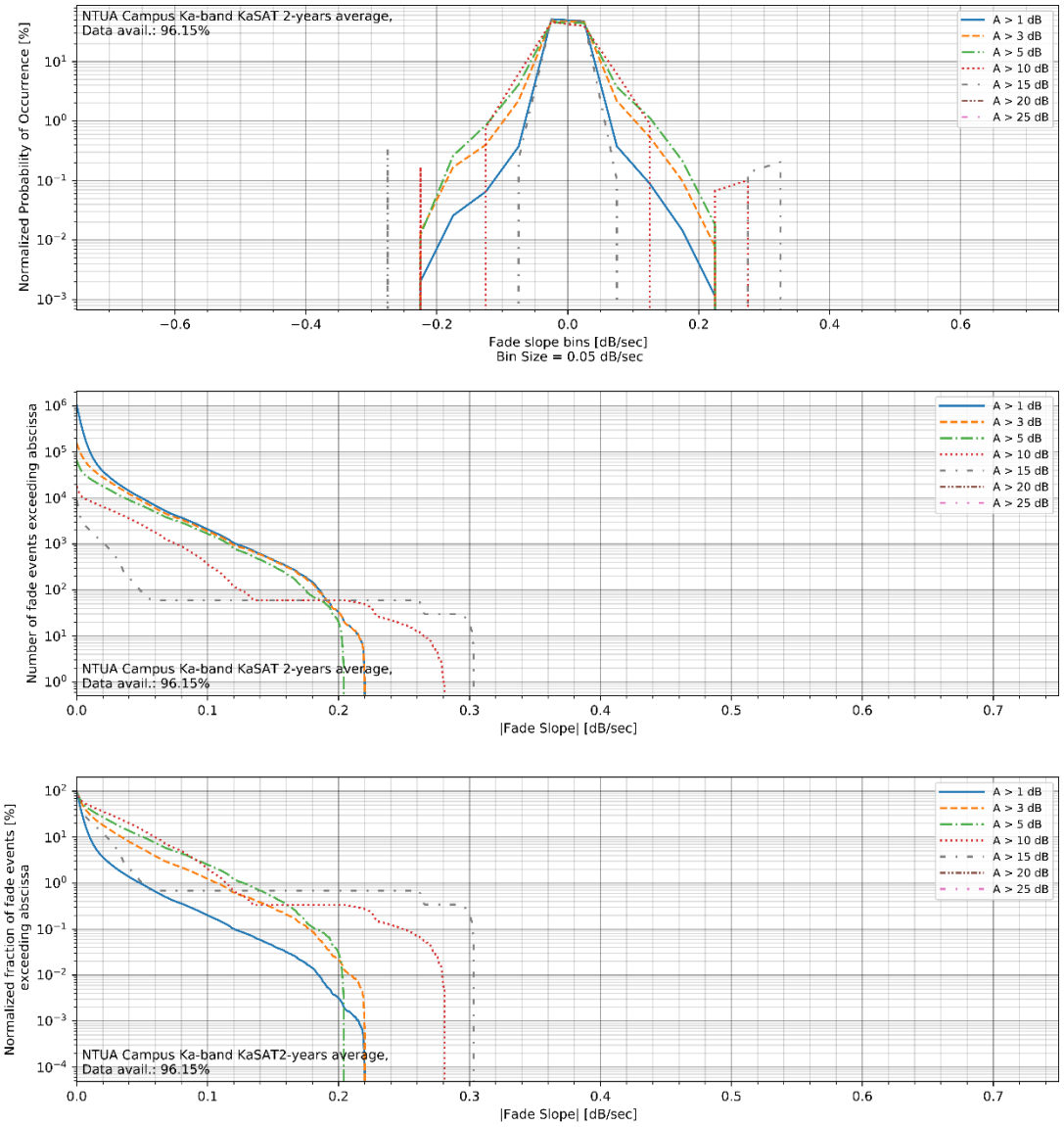

Figure 6-7: Fade slope statistics, Campus Ka-band KaSAT (2-year average)
Top: Fade slope normalized probability of occurrence
Middle: Number of events whose absolute fade slopes exceed abscissa
Bottom: Normalized fraction of events whose absolute fade slopes exceed abscissa

6.2.5 Fade Duration Results

6.2.5.1 Yearly Event Statistics

6.2.5.1.1 Campus Ka-band ALPHASAT yearly event counts & duration per dB

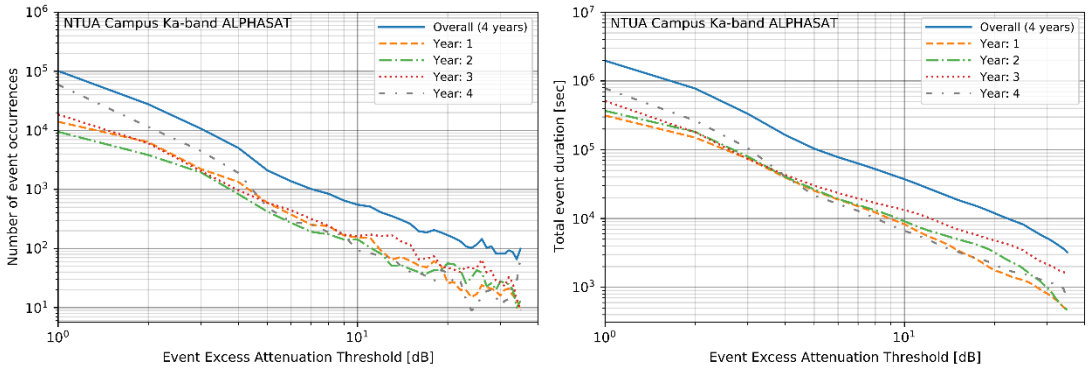

Figure 6-8: NTUA Campus Ka-band ALPHASAT
left: total number of fade events exceeding attenuation threshold
right: total event duration exceeding attenuation threshold

6.2.5.1.2 LTCP Ka-band ALPHASAT yearly event counts & duration per dB

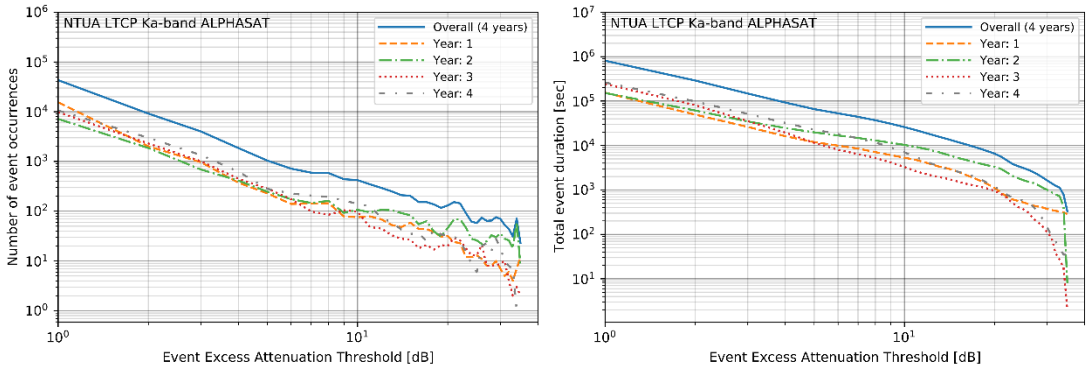

Figure 6-9: NTUA LTCP Ka-band ALPHASAT
left: total number of fade events exceeding attenuation threshold
right: total event duration exceeding attenuation threshold

6.2.5.1.3 Campus Q-band ALPHASAT yearly event counts & duration per dB

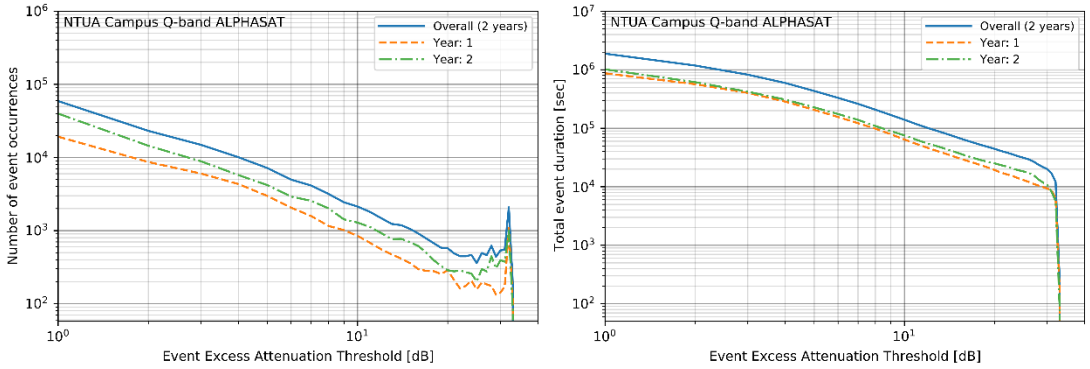

Figure 6-10: NTUA Campus Q-band ALPHASAT
left: total number of fade events exceeding attenuation threshold
right: total event duration exceeding attenuation threshold

6.2.5.1.4 LTCP Q-band ALPHASAT yearly event counts & duration per dB

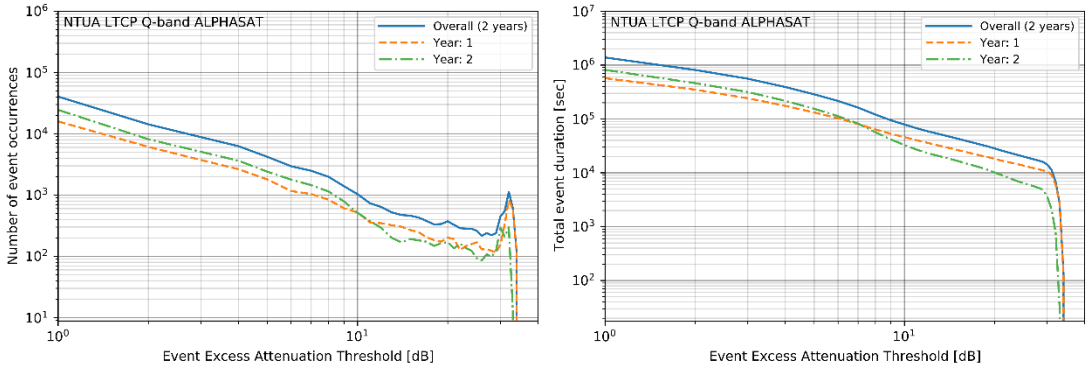

Figure 6-11: NTUA LTCP Q-band ALPHASAT
left: total number of fade events exceeding attenuation threshold
right: total event duration exceeding attenuation threshold

6.2.5.1.5 Campus Ku-band BADR5 yearly event counts & duration per dB

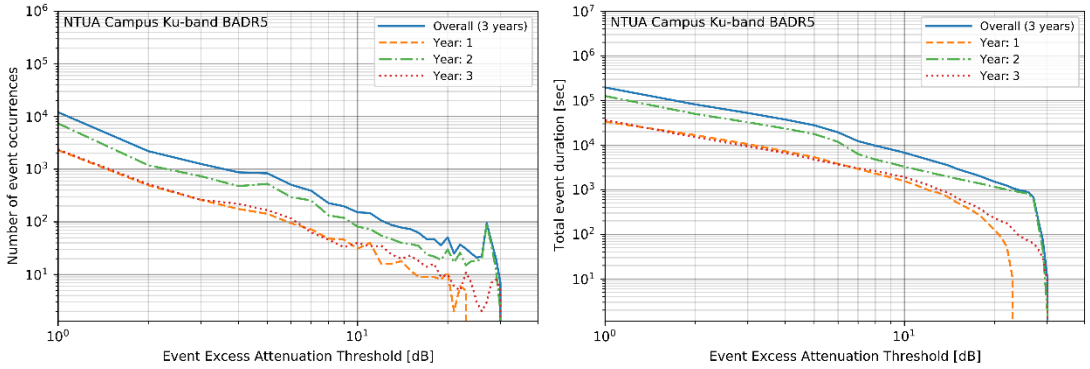

Figure 6-12: NTUA Campus Ku-band BADR5
left: total number of fade events exceeding attenuation threshold
right: total event duration exceeding attenuation threshold

6.2.5.1.6 Campus Ka-band KaSAT yearly event counts & duration per dB

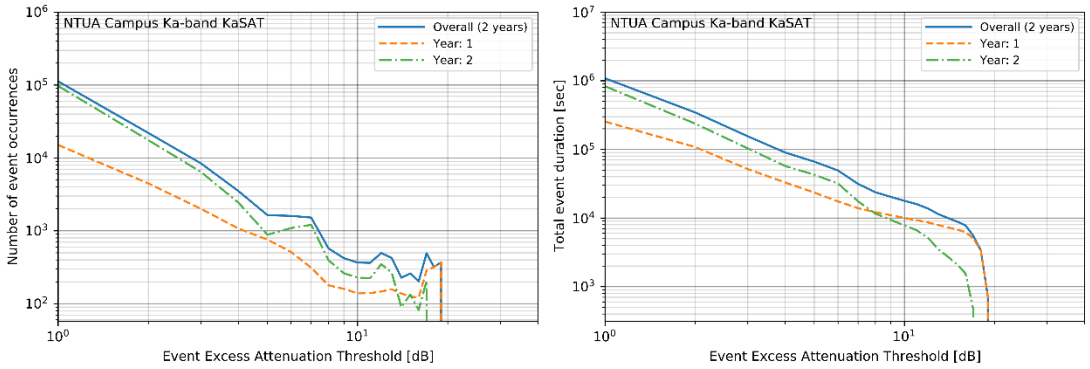

Figure 6-13: NTUA Campus Ka-band KaSAT
left: total number of fade events exceeding attenuation threshold
right: total event duration exceeding attenuation threshold

6.2.5.2 Mean & Median Event Duration Statistics

6.2.5.2.1 Campus Ka-band ALPHASAT mean & media event duration per dB

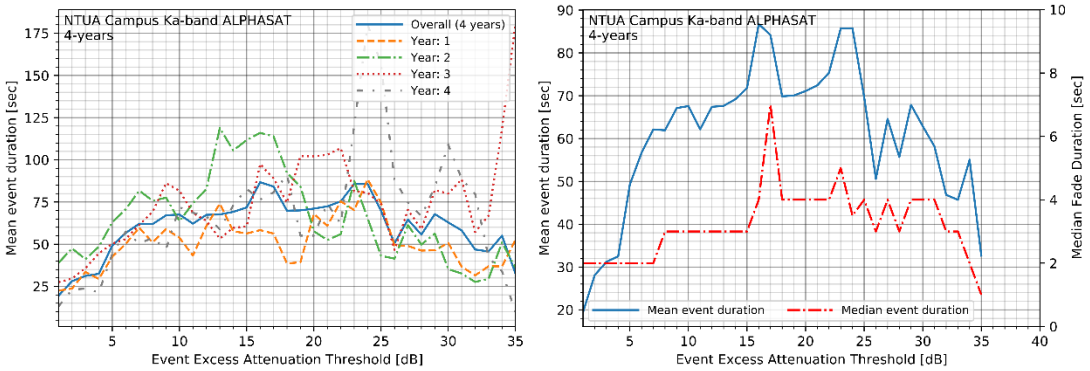

Figure 6-14: NTUA Campus Ka-band ALPHASAT
left: mean duration of fade events exceeding attenuation threshold
right: mean & median event duration exceeding attenuation threshold averaged over 4-years

6.2.5.2.2 LTCP Ka-band ALPHASAT mean & media event duration per dB

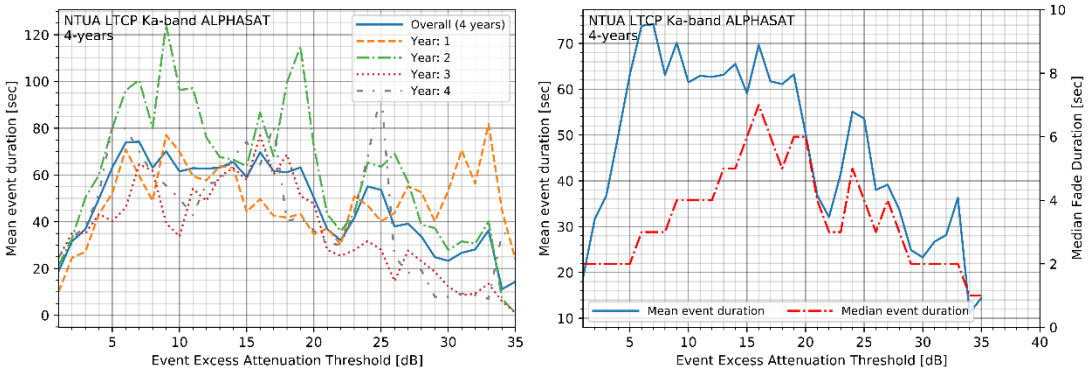

Figure 6-15: NTUA LTCP Ka-band ALPHASAT
left: mean duration of fade events exceeding attenuation threshold
right: mean & median event duration exceeding attenuation threshold averaged over 4-years

6.2.5.2.3 Campus Q-band ALPHASAT mean & media event duration per dB

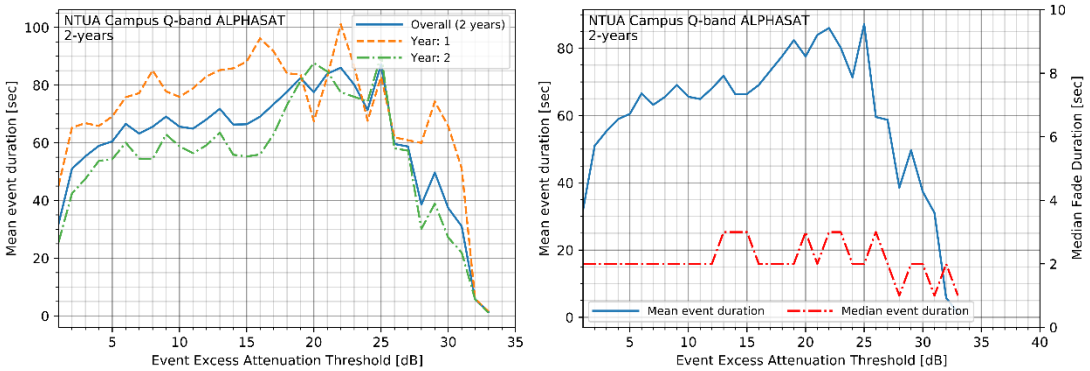

Figure 6-16: NTUA Campus Q-band ALPHASAT
left: mean duration of fade events exceeding attenuation threshold
right: mean & median event duration exceeding attenuation threshold averaged over 2-years

6.2.5.2.4 LTCP Q-band ALPHASAT mean & media event duration per dB

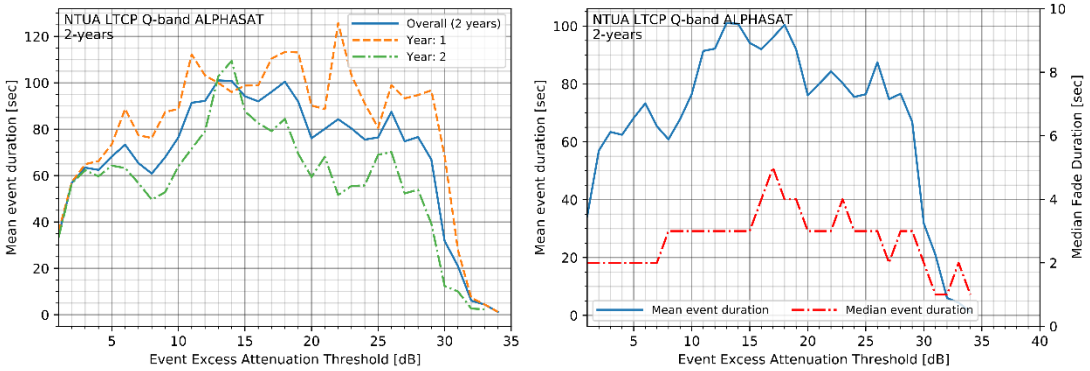

Figure 6-17: NTUA LTCP Q-band ALPHASAT
left: mean duration of fade events exceeding attenuation threshold
right: mean & median event duration exceeding attenuation threshold averaged over 2-years

6.2.5.2.5 Campus Ku-band BADR5 mean & media event duration per dB

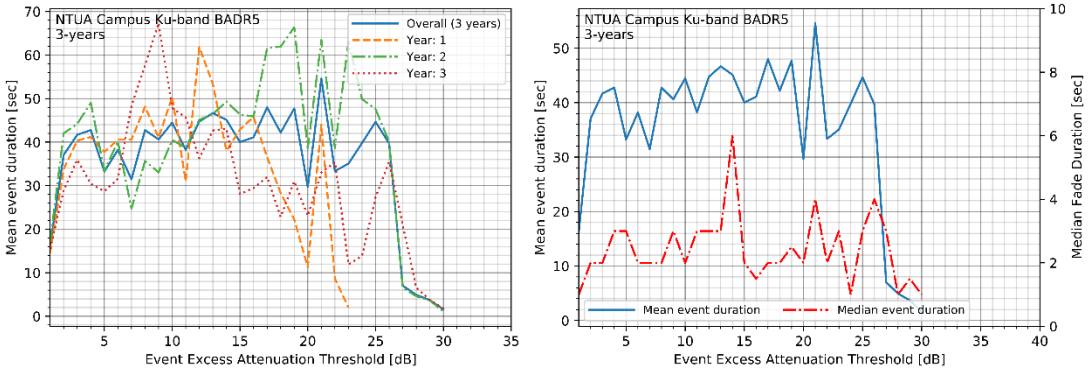

Figure 6-18: NTUA Campus Ku-band BADR5
left: mean duration of fade events exceeding attenuation threshold
right: mean & median event duration exceeding attenuation threshold averaged over 3-years

6.2.5.2.6 Campus Ka-band KaSAT mean & media event duration per dB

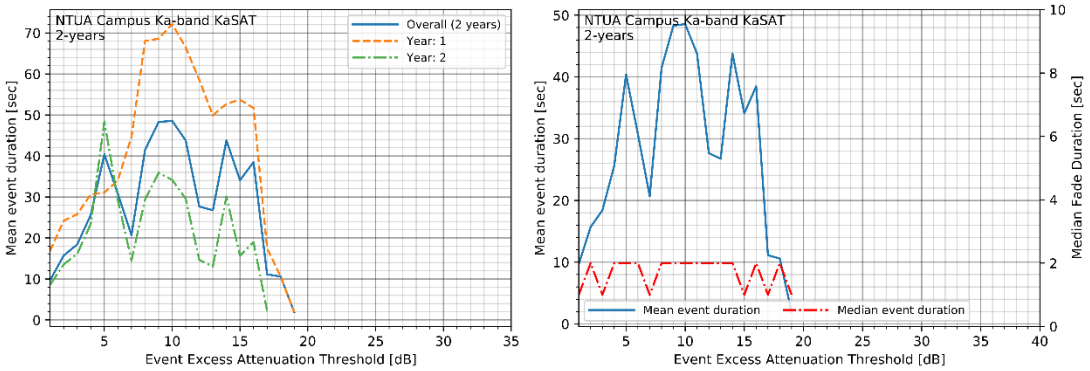

Figure 6-19: NTUA Campus Ka-band KaSAT
left: mean duration of fade events exceeding attenuation threshold
right: mean & median event duration exceeding attenuation threshold averaged over 2-years

6.2.5.3 Fade Duration CCDF

6.2.5.3.1 Campus Ka-band ALPHASAT fade duration CCDF

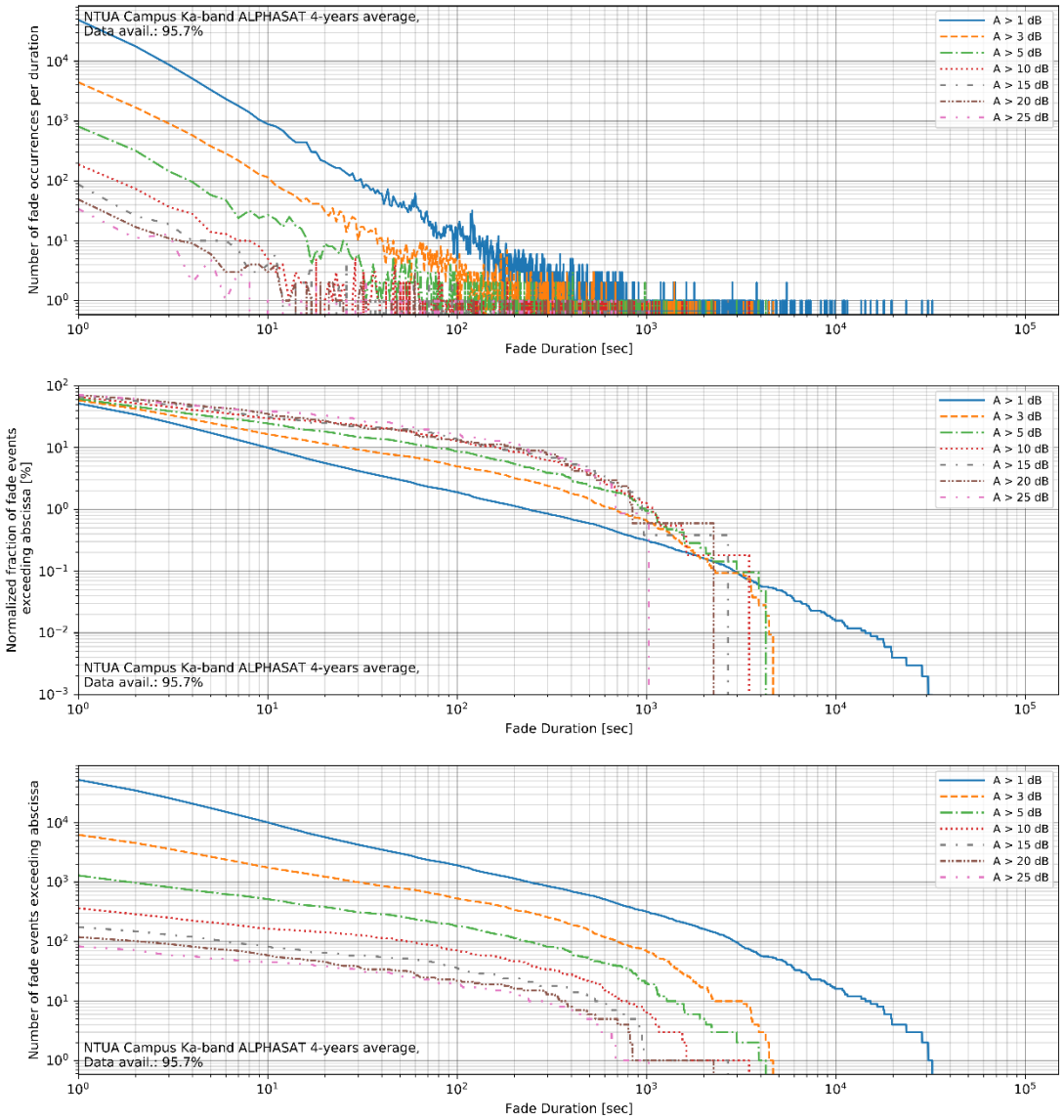

Figure 6-20: Fade duration statistics, Campus Ka-band ALPHASAT (4-year average)
Top: Total number of occurrences per fade duration
Middle: Normalized fraction of events whose fade duration exceed abscissa
Bottom: Number of events whose fade duration exceed abscissa

6.2.5.3.2 LTCP Ka-band ALPHASAT fade duration CCDF

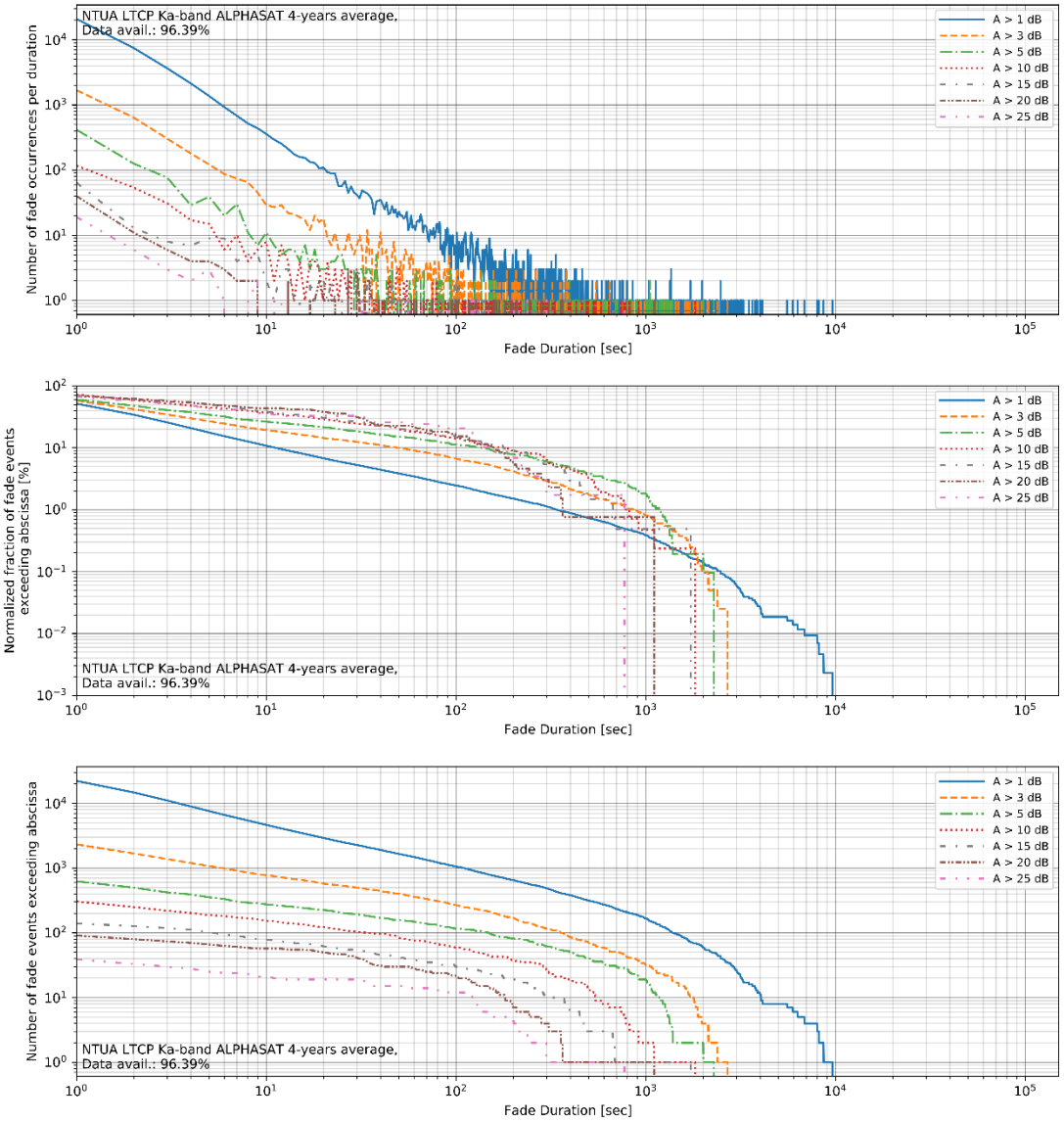

Figure 6-21: Fade duration statistics, LTCP Ka-band ALPHASAT (4-year average)
Top: Total number of occurrences per fade duration
Middle: Normalized fraction of events whose fade duration exceed abscissa
Bottom: Number of events whose fade duration exceed abscissa

6.2.5.3.3 Campus Q-band ALPHASAT fade duration CCDF

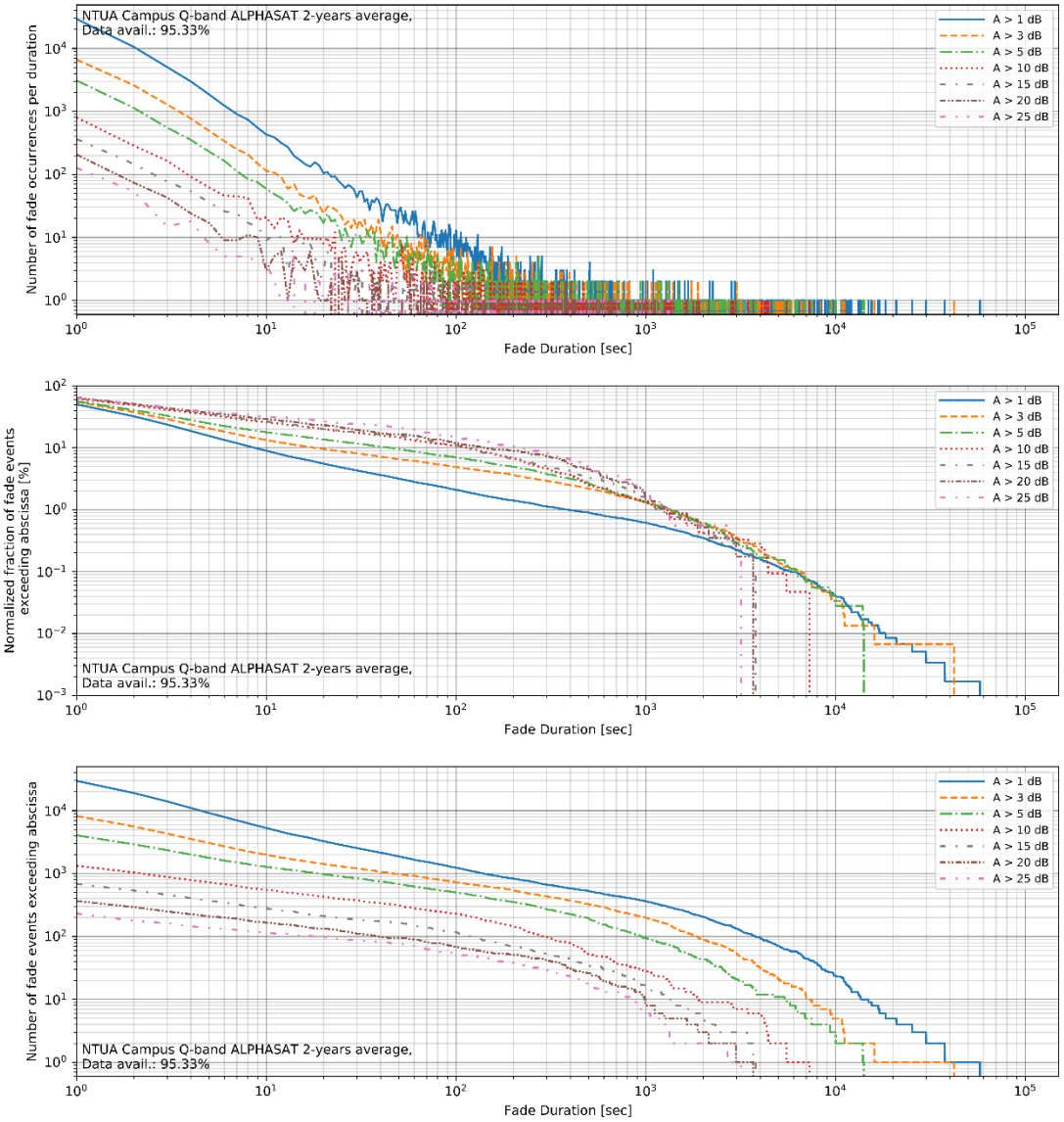

Figure 6-22: Fade duration statistics, Campus Q-band ALPHASAT (2-year average)
Top: Total number of occurrences per fade duration
Middle: Normalized fraction of events whose fade duration exceed abscissa
Bottom: Number of events whose fade duration exceed abscissa

6.2.5.3.4 LTCP Q-band ALPHASAT fade duration CCDF

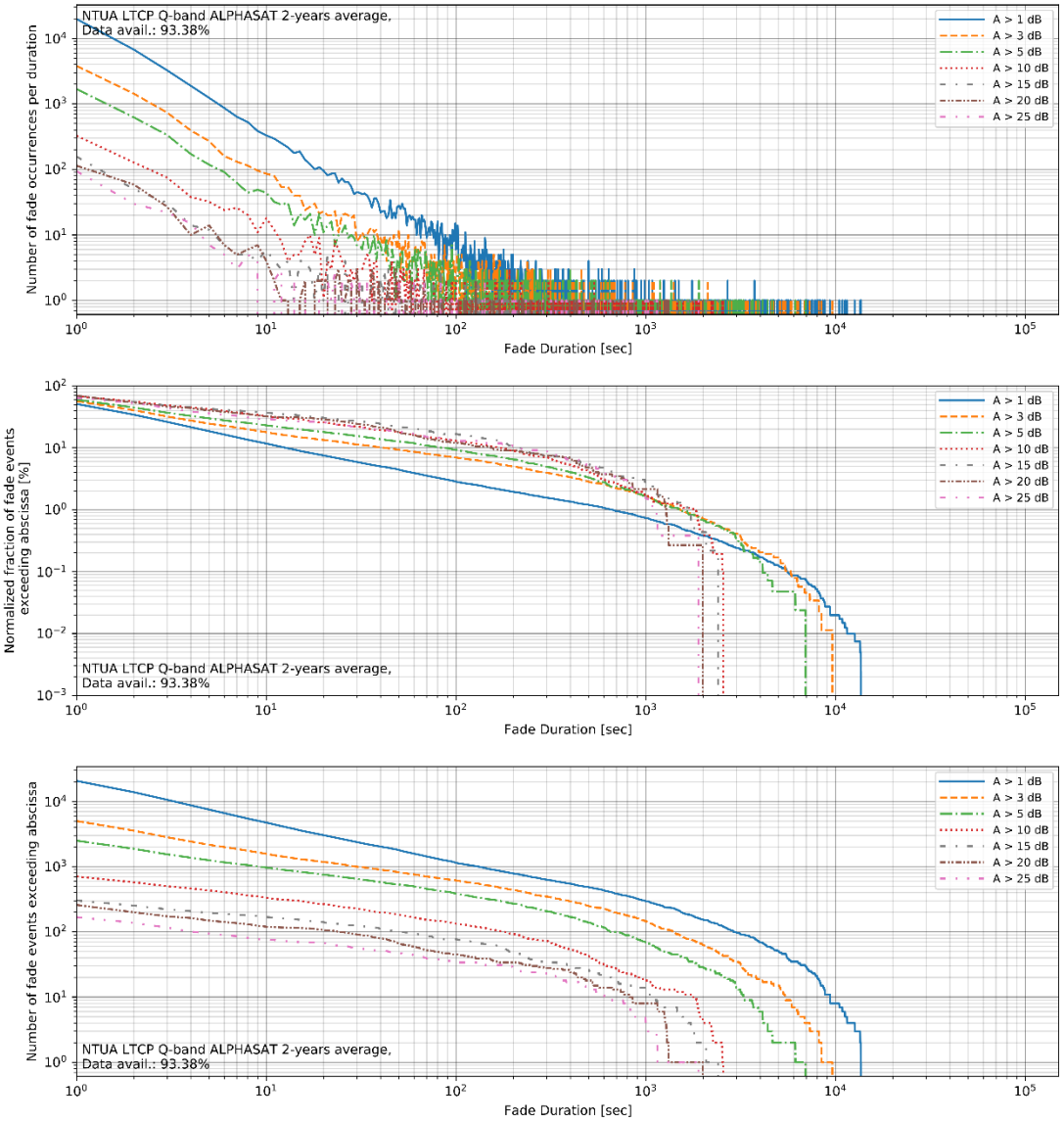

Figure 6-23: Fade duration statistics, LTCP Q-band ALPHASAT (2-year average)
Top: Total number of occurrences per fade duration
Middle: Normalized fraction of events whose fade duration exceed abscissa
Bottom: Number of events whose fade duration exceed abscissa

6.2.5.3.5 Campus Ku-band BADR5 fade duration CCDF

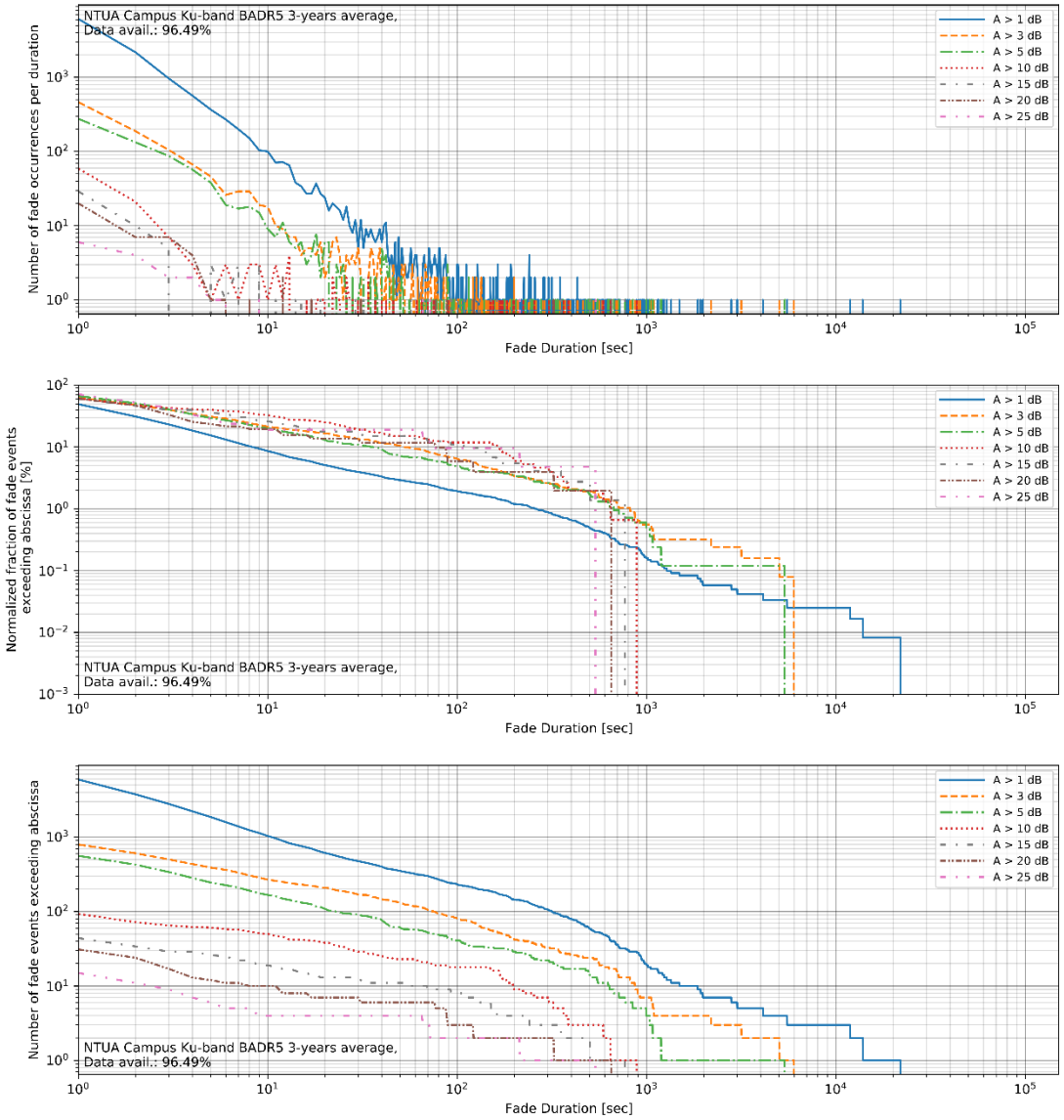

Figure 6-24: Fade duration statistics, Campus Ku-band BADR5 (3-year average)
Top: Total number of occurrences per fade duration
Middle: Normalized fraction of events whose fade duration exceed abscissa
Bottom: Number of events whose fade duration exceed abscissa

6.2.5.3.6 Campus Ka-band KaSAT fade duration CCDF

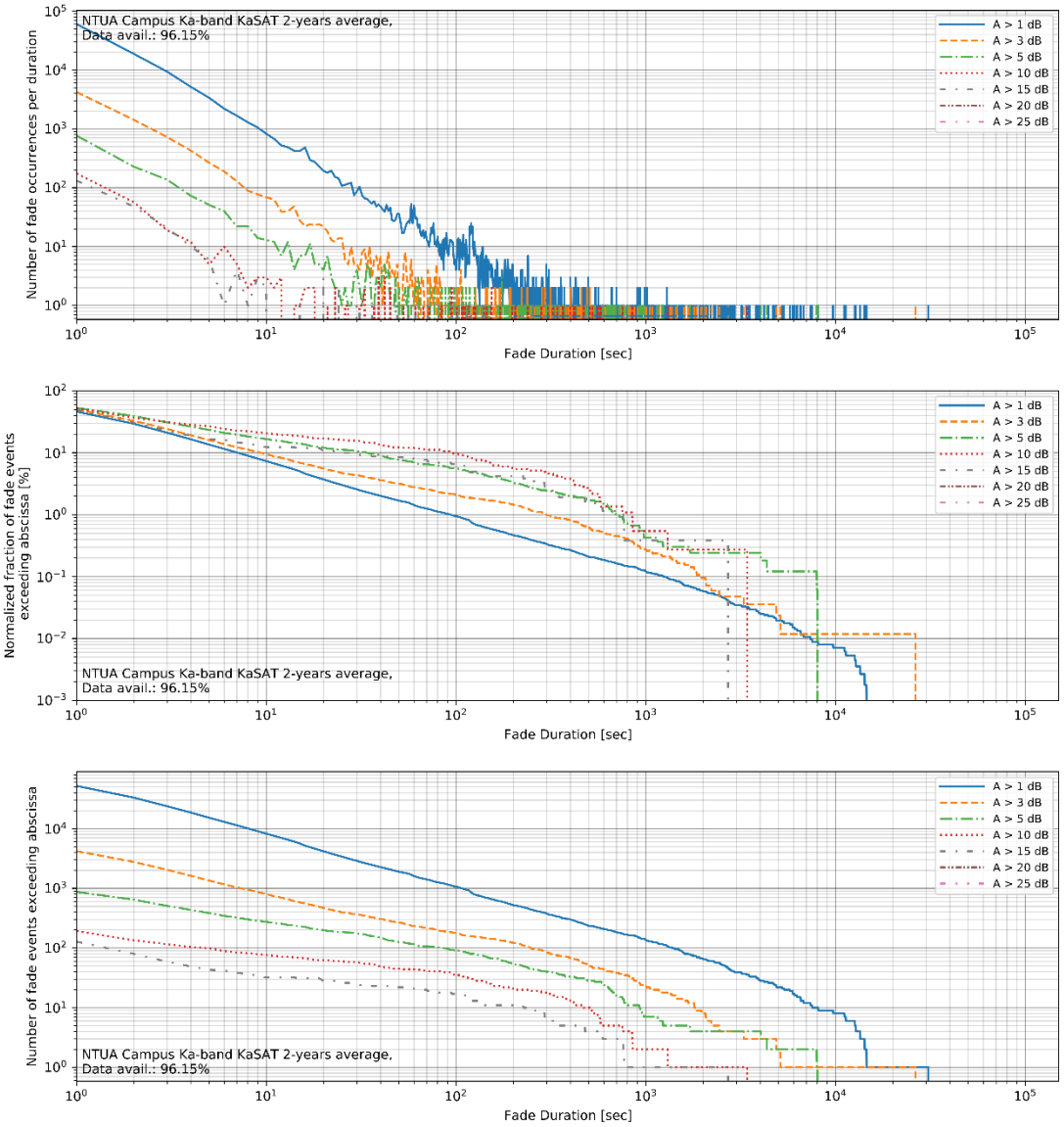

Figure 6-25: Fade duration statistics, Campus Ka-band KaSAT (2-year average)
Top: Total number of occurrences per fade duration
Middle: Normalized fraction of events whose fade duration exceed abscissa
Bottom: Number of events whose fade duration exceed abscissa

6.2.5.4 Fade Duration Box-plots

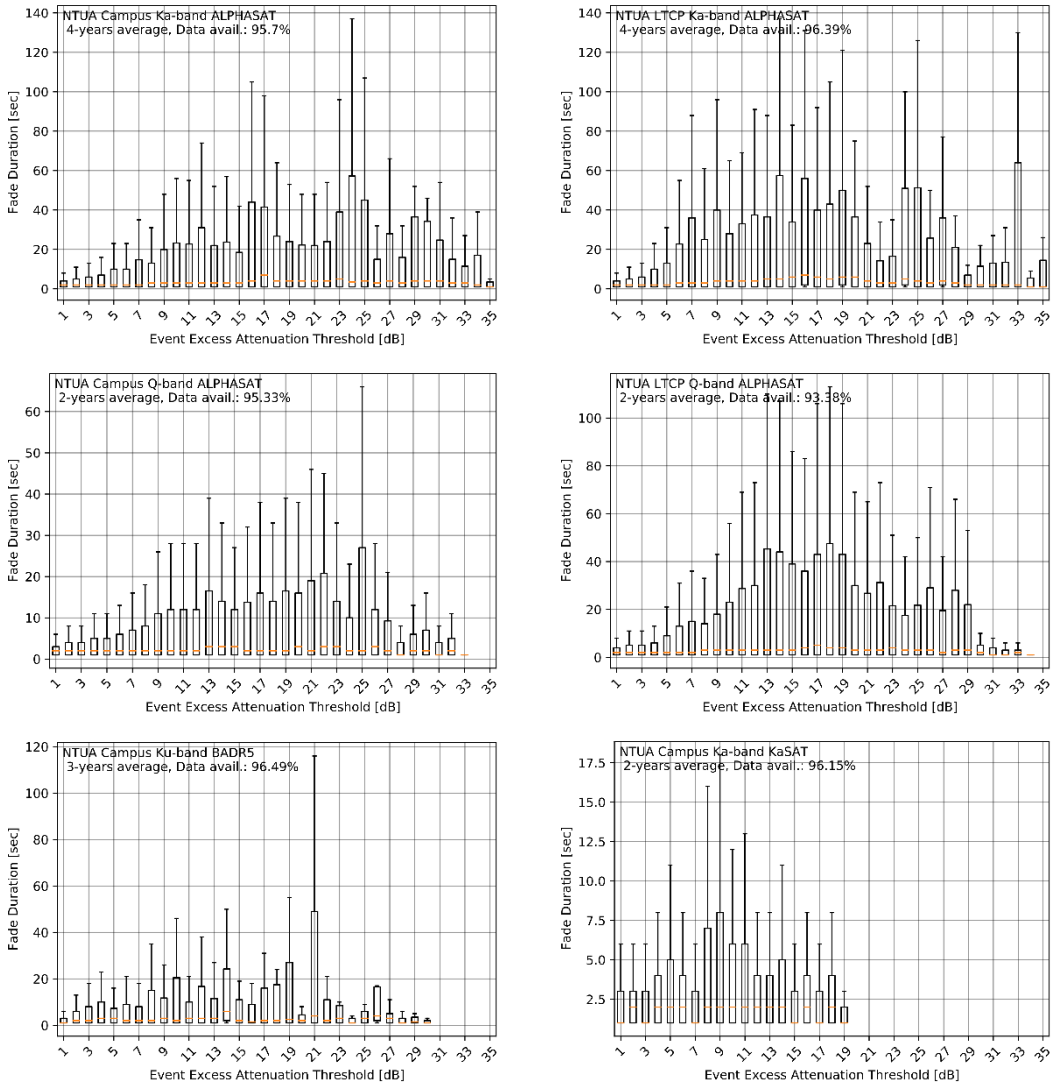

Figure 6-26: Fade Durations Box-plot analysis
First Row: ALPHASAT Ka-band Campus (left) & LTCP (right)
Second Row: ALPHASAT Q-band Campus (left) & LTCP (right)
Third Row: BADR5 Ku-band Campus (left) & KaSAT Ka-band Campus (right)

6.2.5.5 Accumulate Fade Duration CCDF

6.2.5.5.1 Campus Ka-band ALPHASAT accumulate fade duration analysis

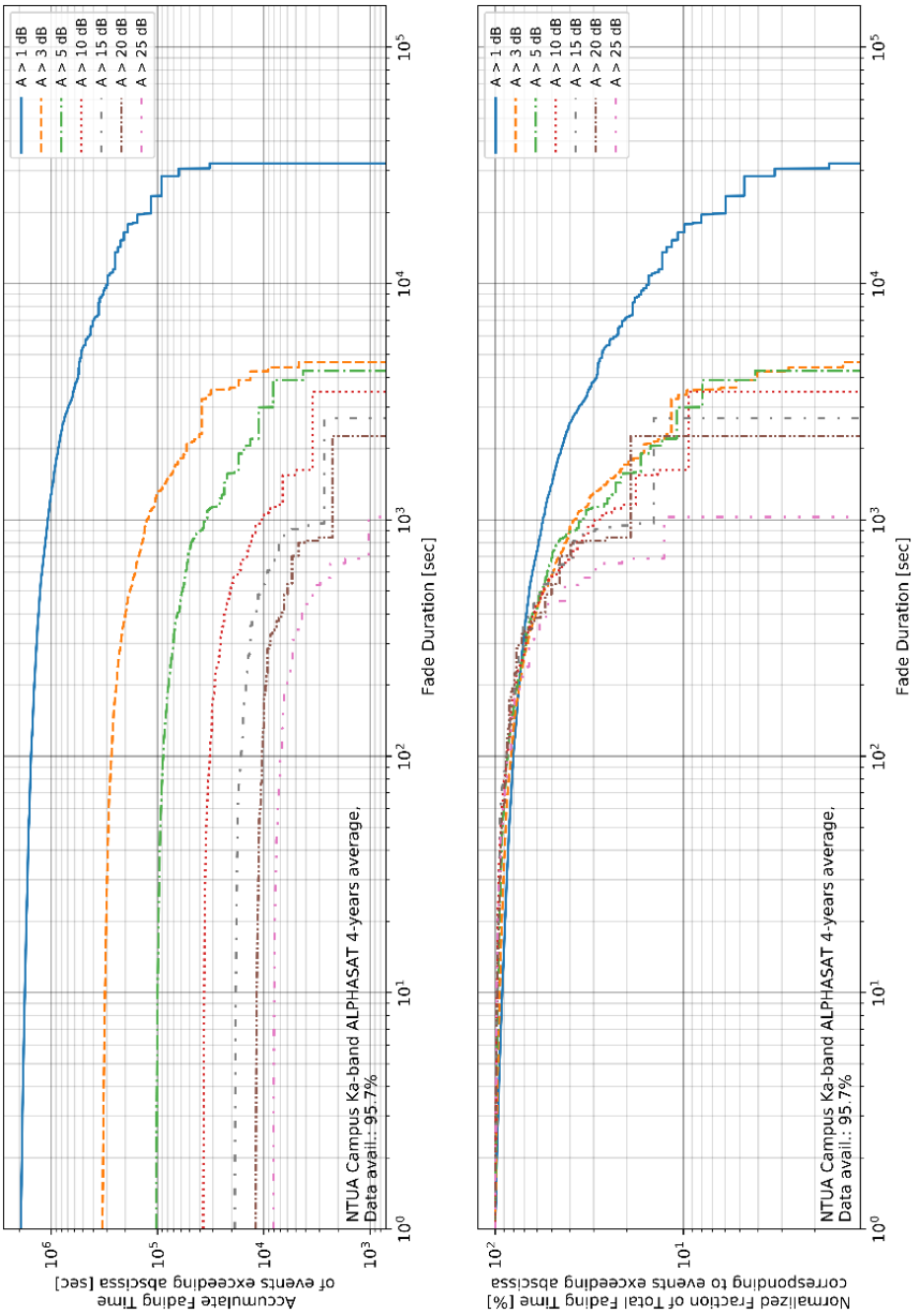

Figure 6-27: Accumulate fade duration statistics, Campus Ka-band ALPHASAT (4-year average)
Top: Total (accumulate) fading time of events whose duration exceed abscissa
Middle: Normalized fraction of total fading time of events whose duration exceed abscissa

6.2.5.5.2 LTCP Ka-band ALPHASAT accumulate fade duration analysis

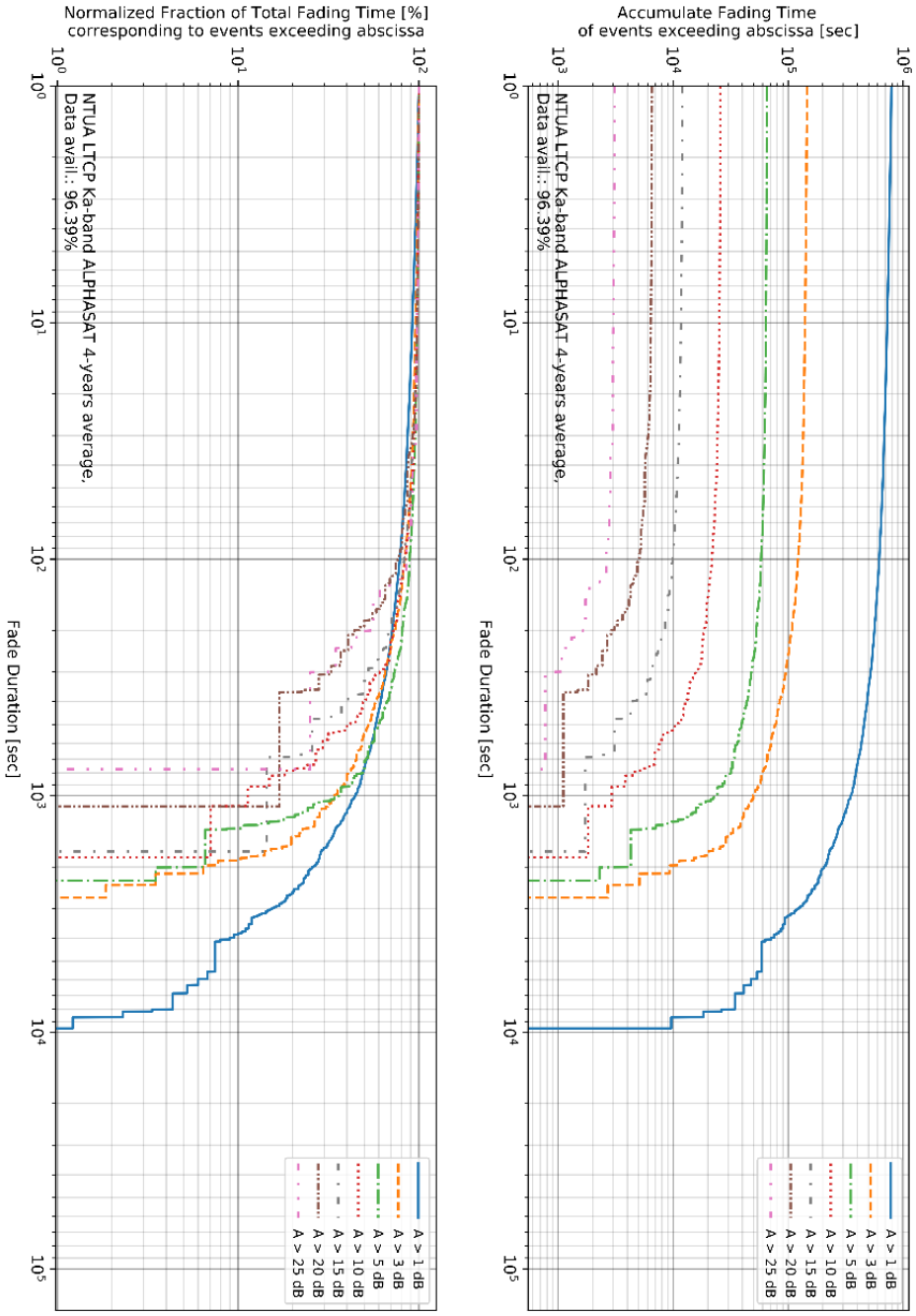

Figure 6-28: Accumulate fade duration statistics, LTCP Ka-band ALPHASAT (4-year average)
Top: Total (accumulate) fading time of events whose duration exceed abscissa
Middle: Normalized fraction of total fading time of events whose duration exceed abscissa

6.2.5.5.3 Campus Q-band ALPHASAT accumulate fade duration analysis

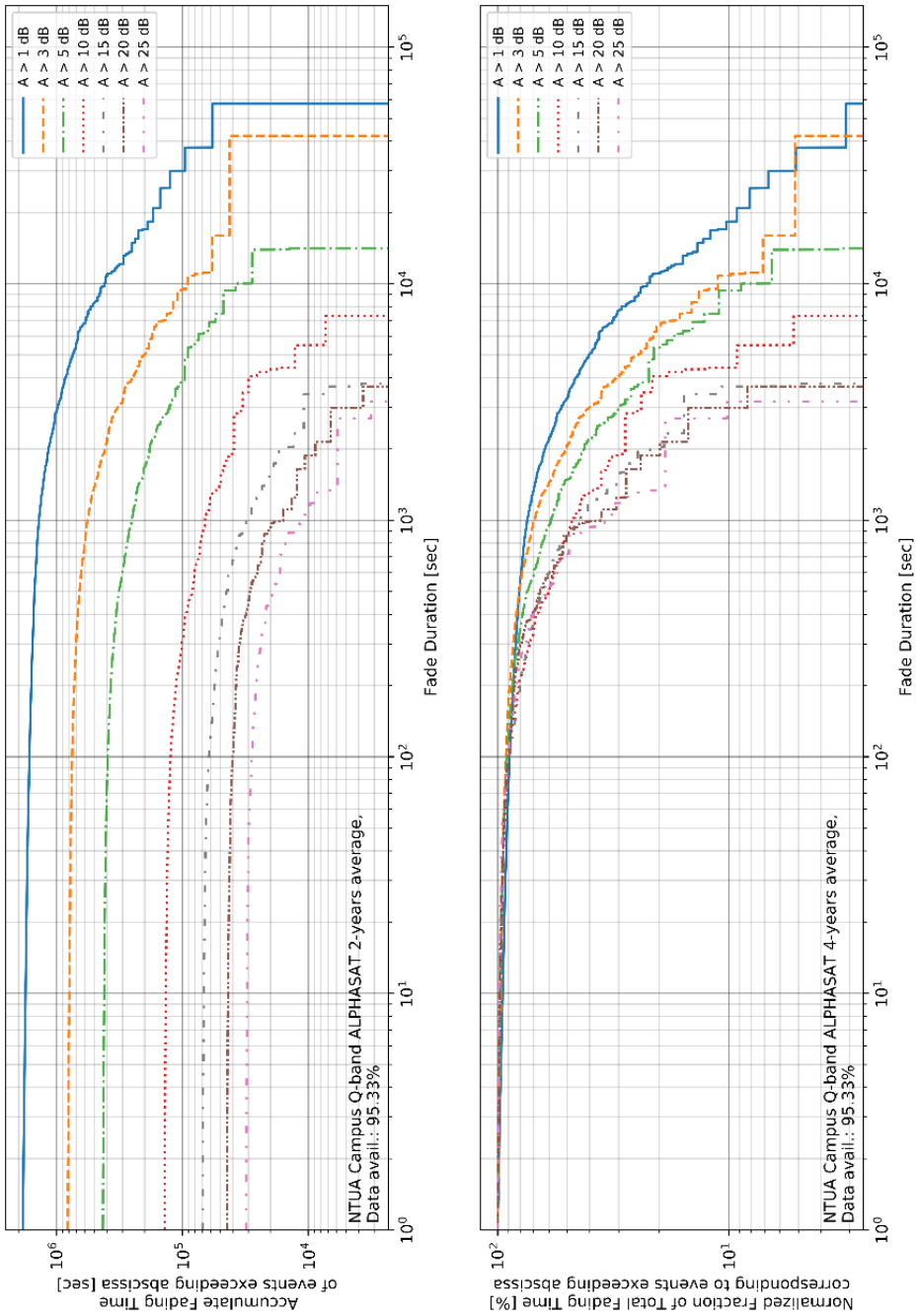

Figure 6-29: Accumulate fade duration statistics, Campus Q-band ALPHASAT (2-year average)
Top: Total (accumulate) fading time of events whose duration exceed abscissa
Middle: Normalized fraction of total fading time of events whose duration exceed abscissa

6.2.5.5.4 LTCP Q-band ALPHASAT accumulate fade duration analysis

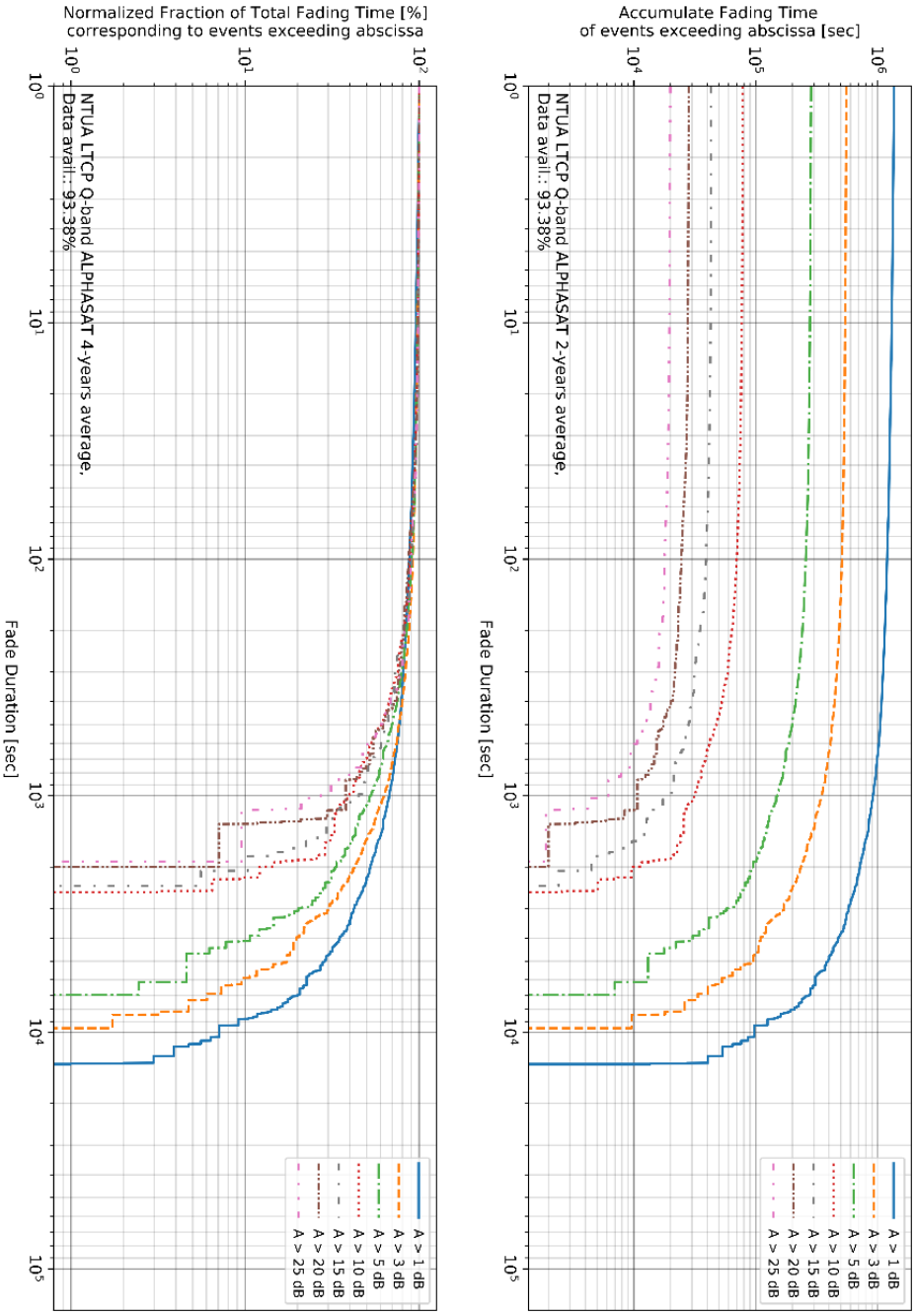

Figure 6-30: Accumulate fade duration statistics, LTCP Q-band ALPHASAT (2-year average)
Top: Total (accumulate) fading time of events whose duration exceed abscissa
Middle: Normalized fraction of total fading time of events whose duration exceed abscissa

6.2.5.5.5 Campus Ku-band BADR5 accumulate fade duration analysis

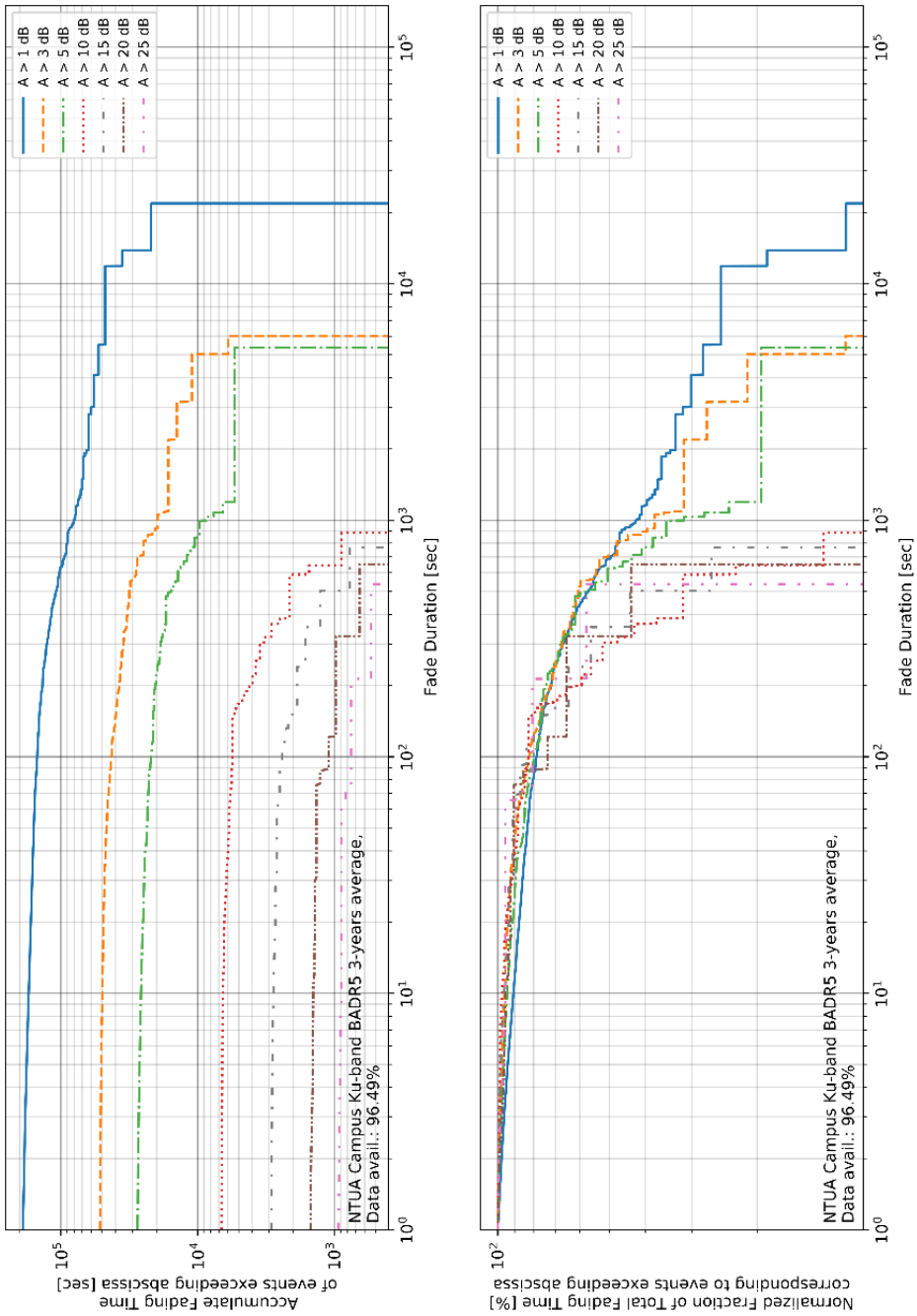

Figure 6-31: Accumulate fade duration statistics, Campus Ku-band BADR5 (3-year average)
Top: Total (accumulate) fading time of events whose duration exceed abscissa
Middle: Normalized fraction of total fading time of events whose duration exceed abscissa

6.2.5.5.6 Campus Ka-band KaSAT accumulate fade duration analysis

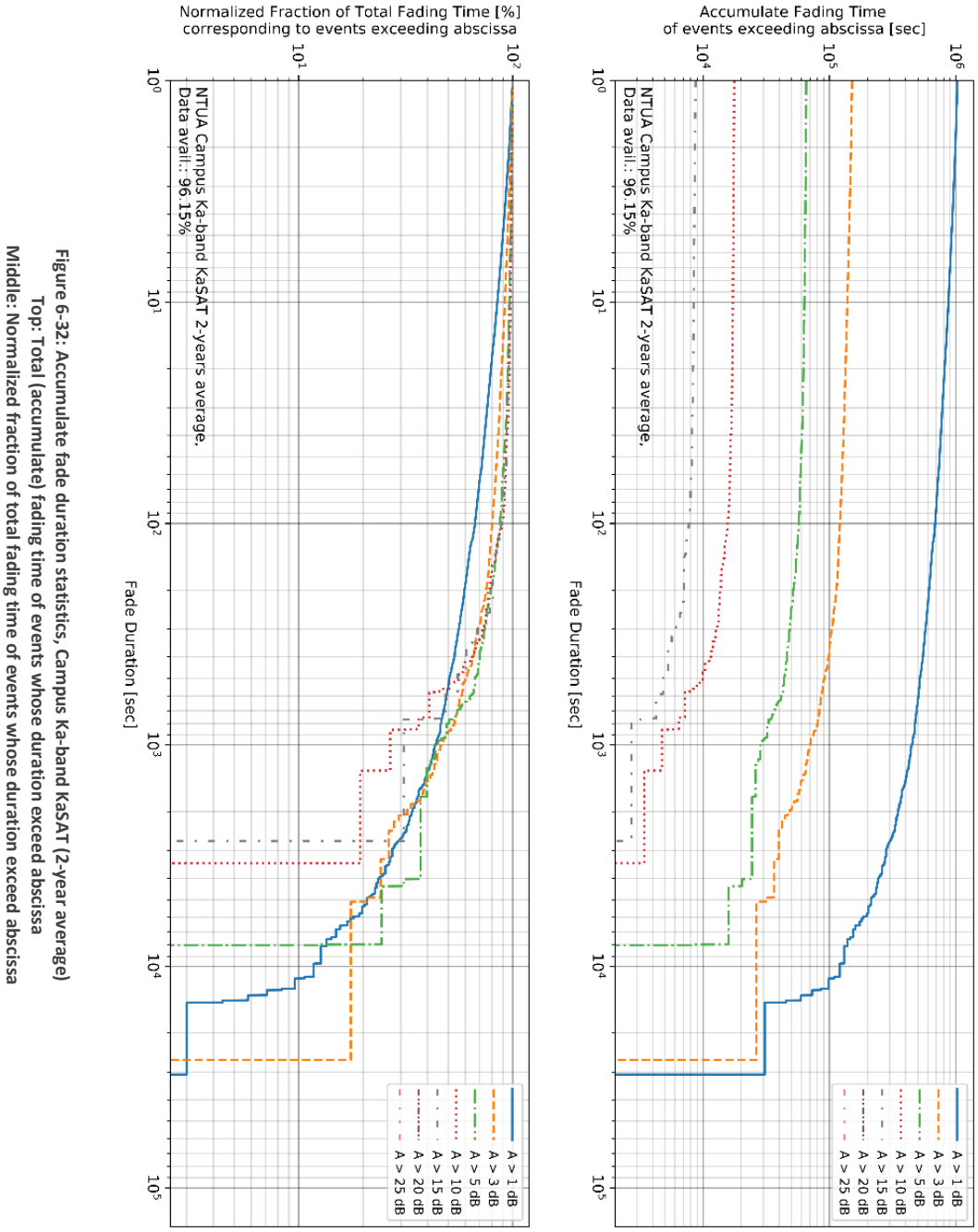

Figure 6-32: Accumulate fade duration statistics, Campus Ka-band KaSAT (2-year average)
Top: Total (accumulate) fading time of events whose duration exceed abscissa
Middle: Normalized fraction of total fading time of events whose duration exceed abscissa

6.2.6 Inter-fade Duration Results

6.2.6.1 Campus Ka-band ALPHASAT inter-fade duration analysis

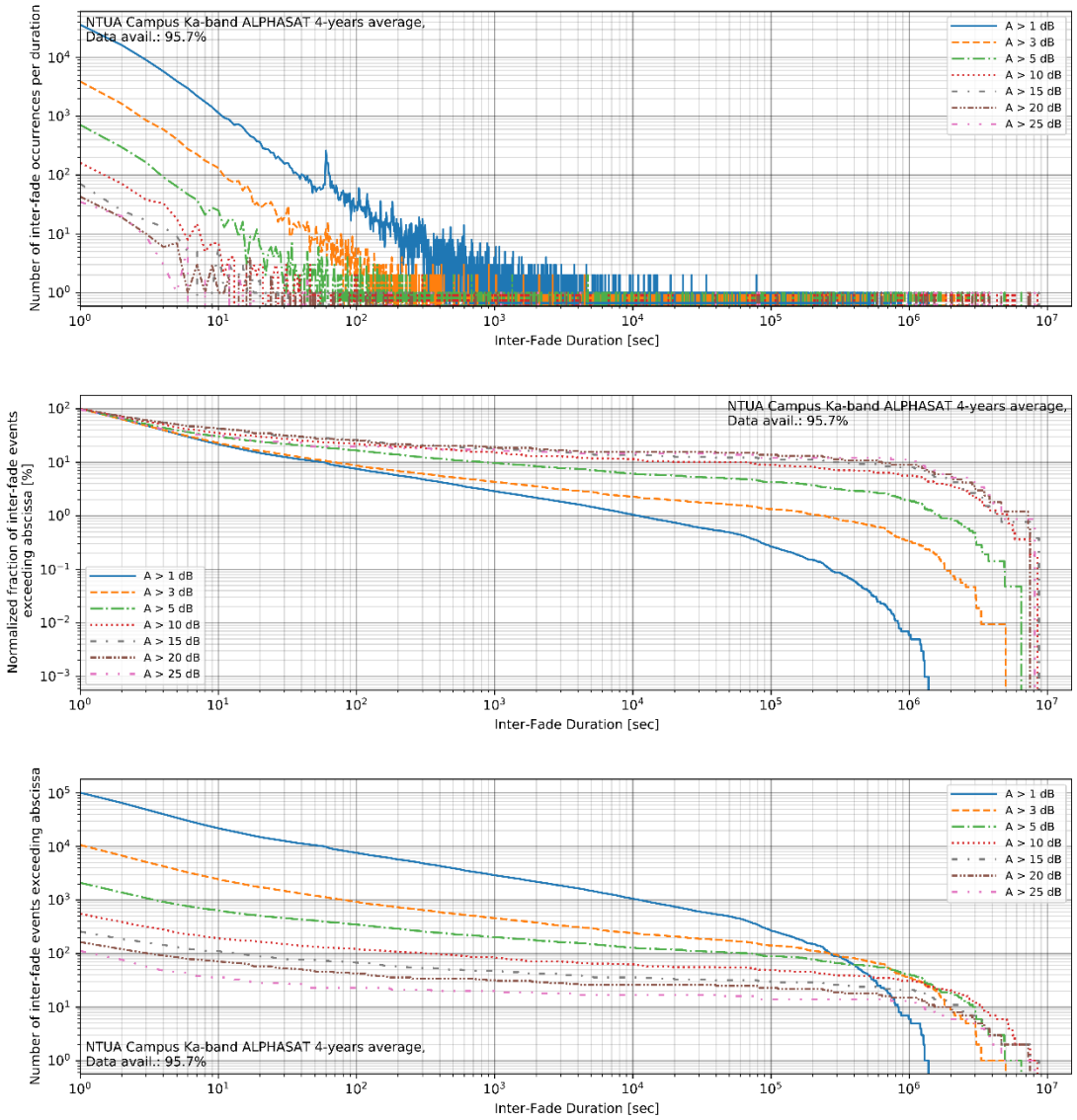

Figure 6-33: Inter-fade duration statistics, Campus Ka-band ALPHASAT (4-year average)
Top: Total number of occurrences per inter-fade duration
Middle: Normalized fraction of events whose inter-fade duration exceed abscissa
Bottom: Number of events whose inter-fade duration exceed abscissa

6.2.6.2 LTCP Ka-band ALPHASAT inter-fade duration analysis

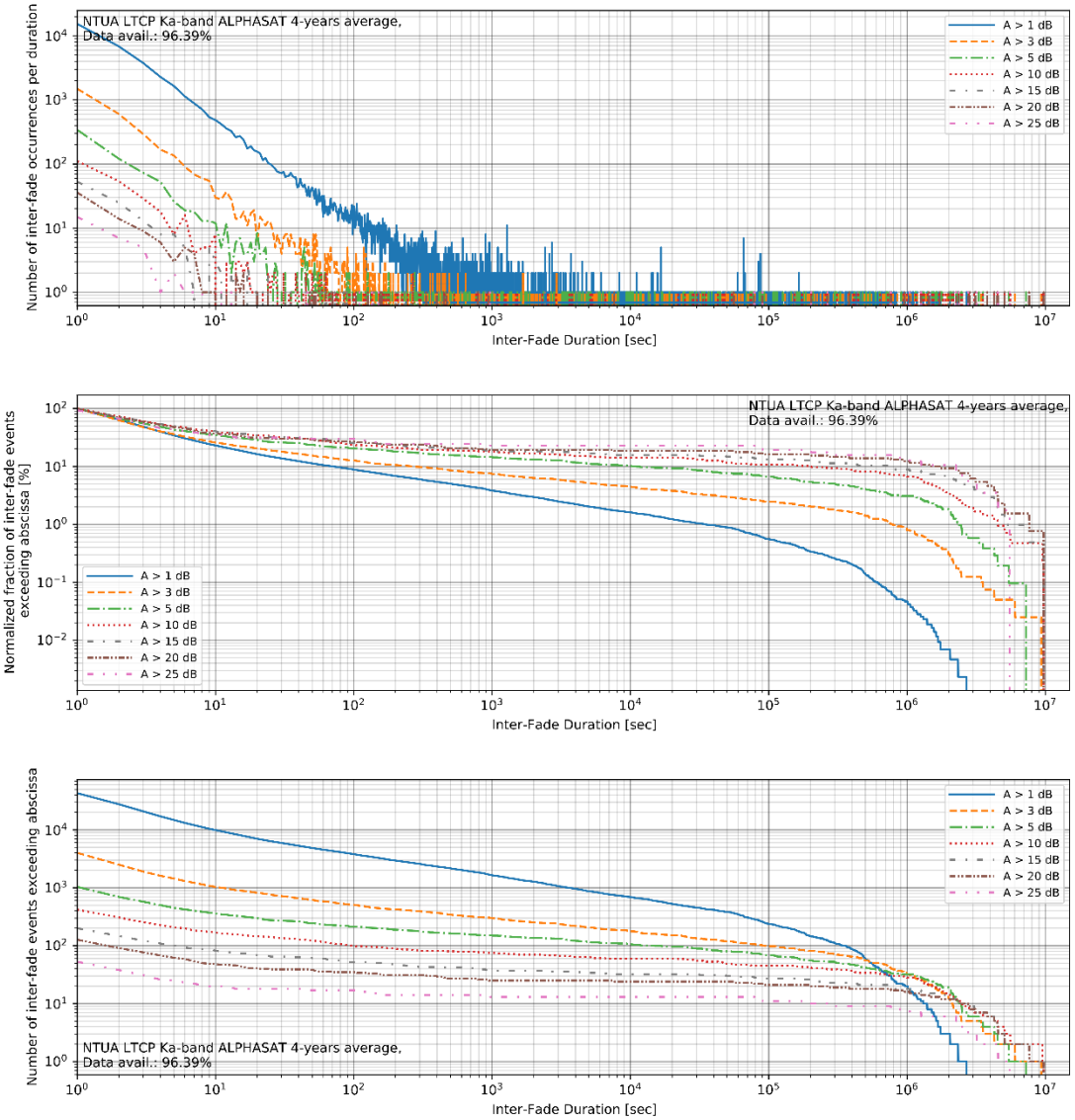

Figure 6-34: Inter-fade duration statistics, LTCP Ka-band ALPHASAT (4-year average)
Top: Total number of occurrences per inter-fade duration
Middle: Normalized fraction of events whose inter-fade duration exceed abscissa
Bottom: Number of events whose inter-fade duration exceed abscissa

6.2.6.3 Campus Q-band ALPHASAT inter-fade duration analysis

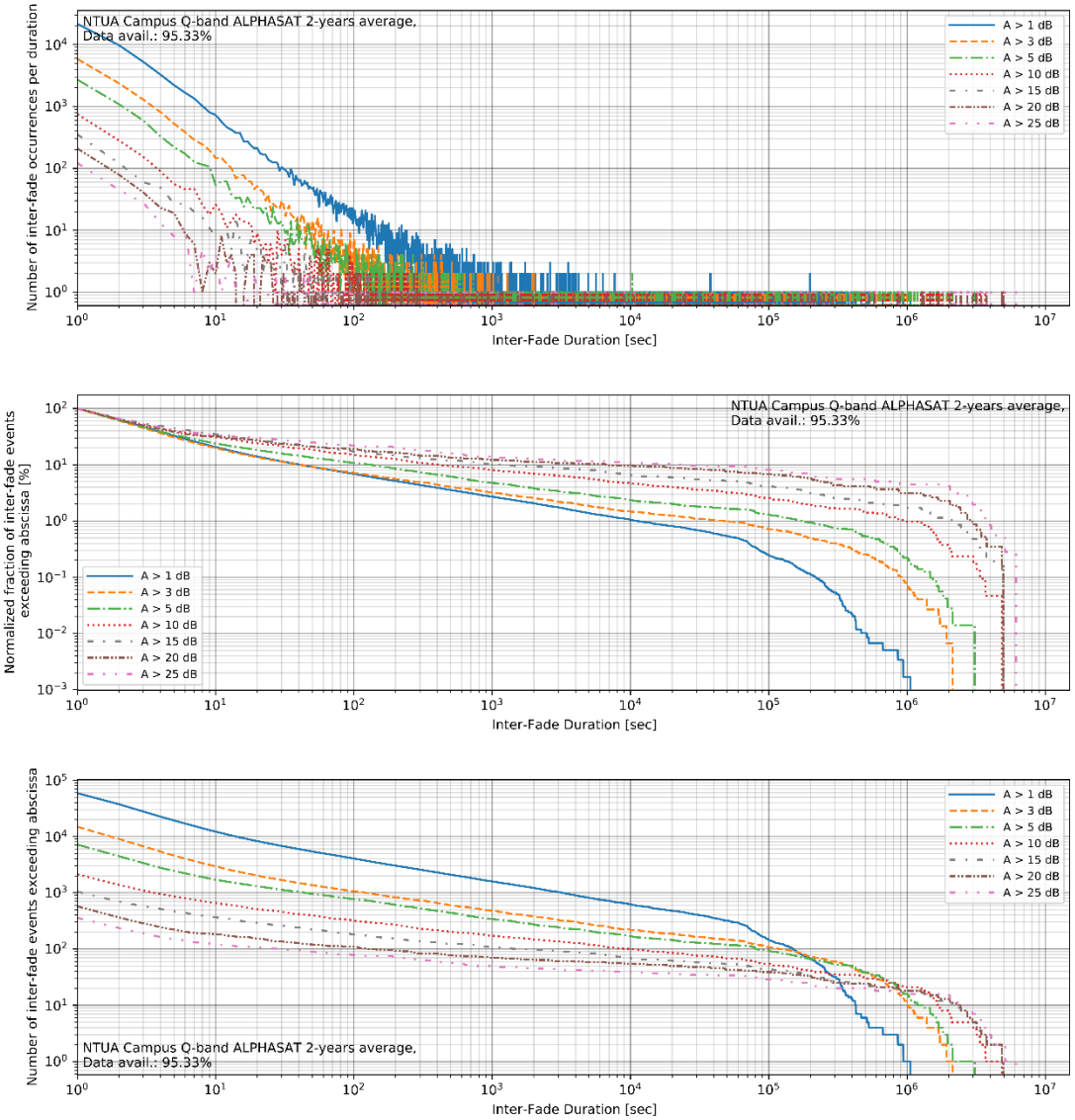

Figure 6-35: Inter-fade duration statistics, Campus Q-band ALPHASAT (2-year average)
Top: Total number of occurrences per inter-fade duration
Middle: Normalized fraction of events whose inter-fade duration exceed abscissa
Bottom: Number of events whose inter-fade duration exceed abscissa

6.2.6.4 LTCP Q-band ALPHASAT inter-fade duration analysis

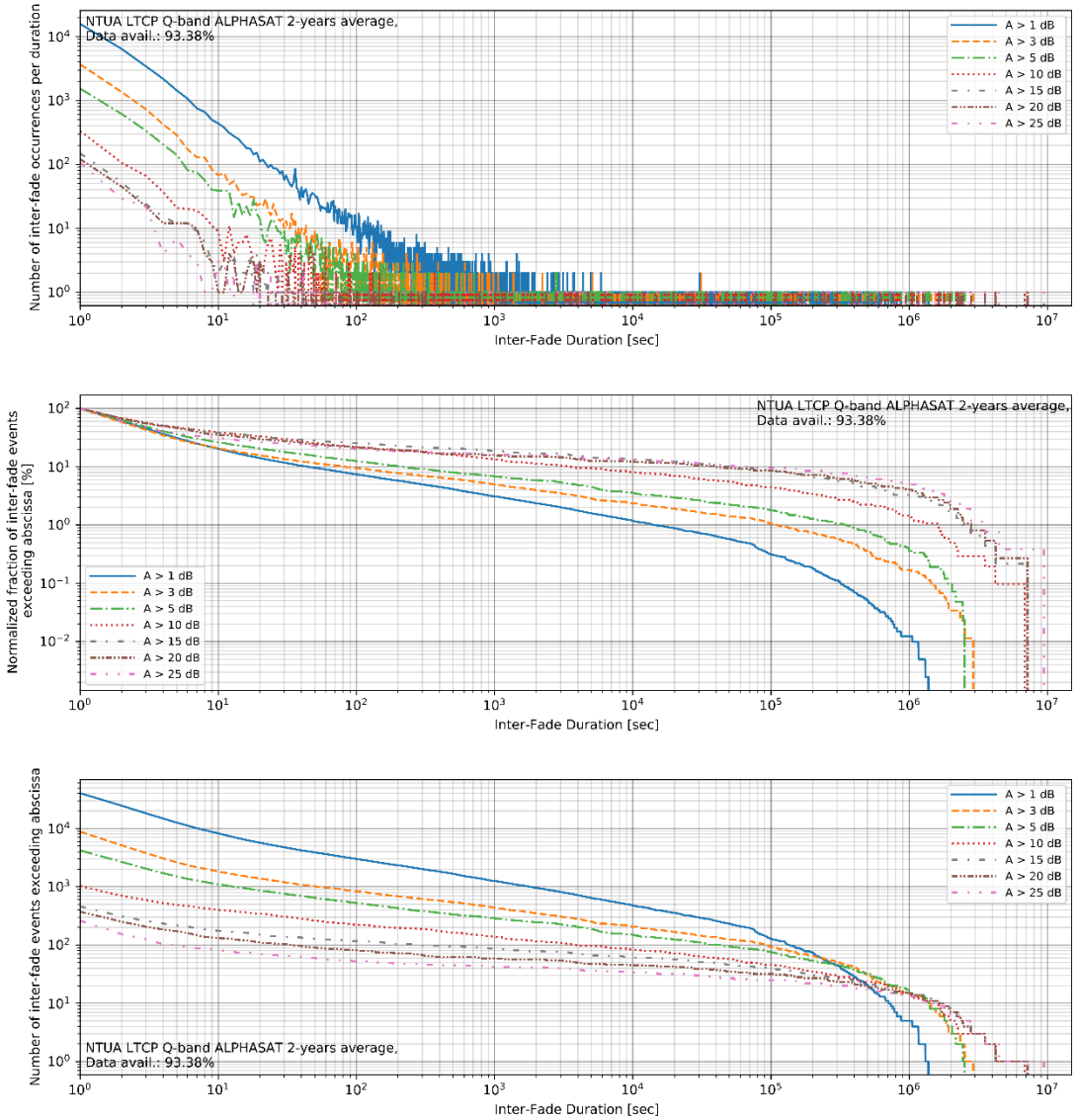

Figure 6-36: Inter-fade duration statistics, LTCP Q-band ALPHASAT (2-year average)
Top: Total number of occurrences per inter-fade duration
Middle: Normalized fraction of events whose inter-fade duration exceed abscissa
Bottom: Number of events whose inter-fade duration exceed abscissa

6.2.6.5 Campus Ku-band BADR5 inter-fade duration analysis

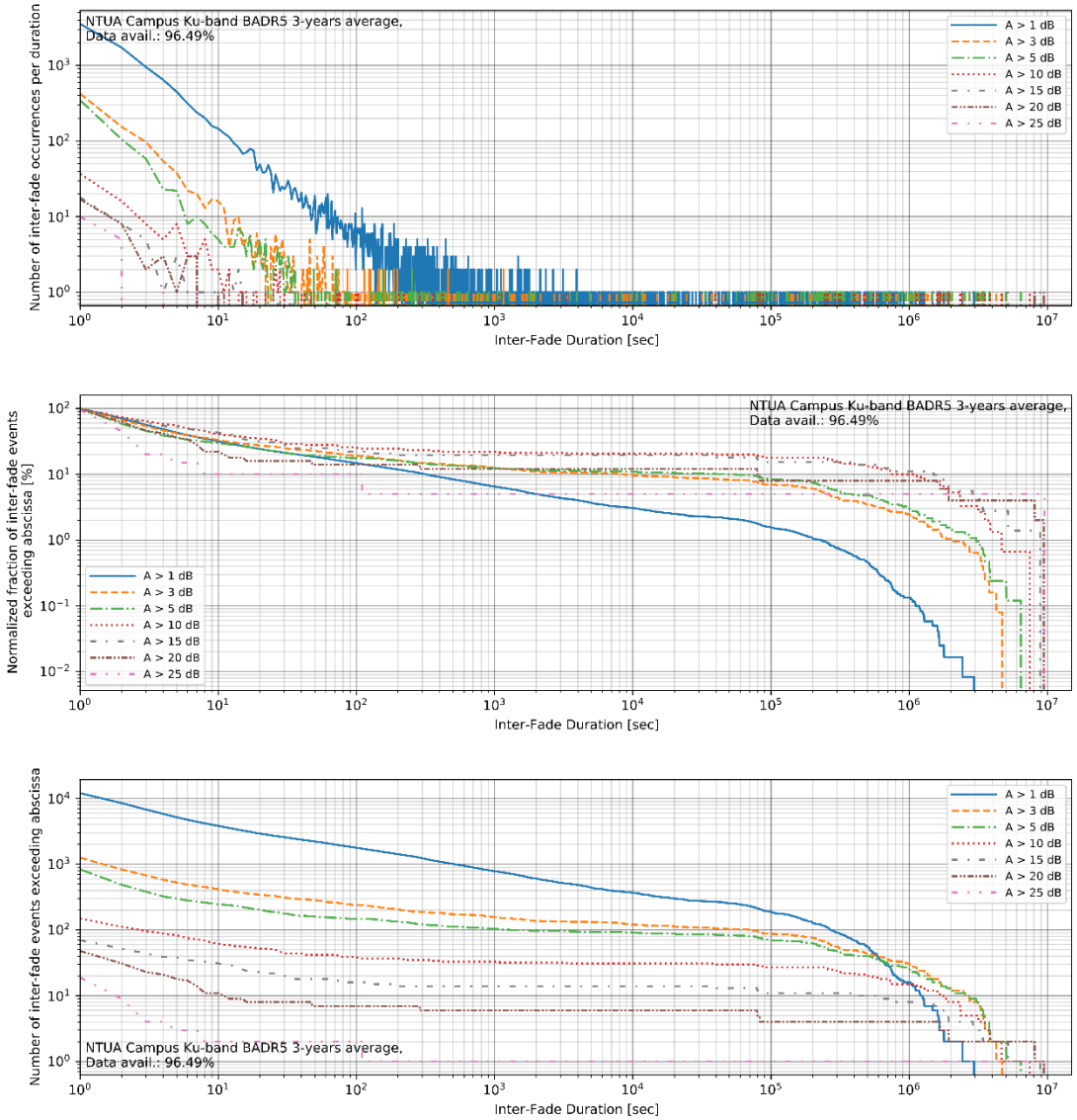

Figure 6-37: Inter-fade duration statistics, Campus Ku-band BADR5 (3-year average)
Top: Total number of occurrences per inter-fade duration
Middle: Normalized fraction of events whose inter-fade duration exceed abscissa
Bottom: Number of events whose inter-fade duration exceed abscissa

6.2.6.6 Campus Ka-band KaSAT inter-fade duration analysis

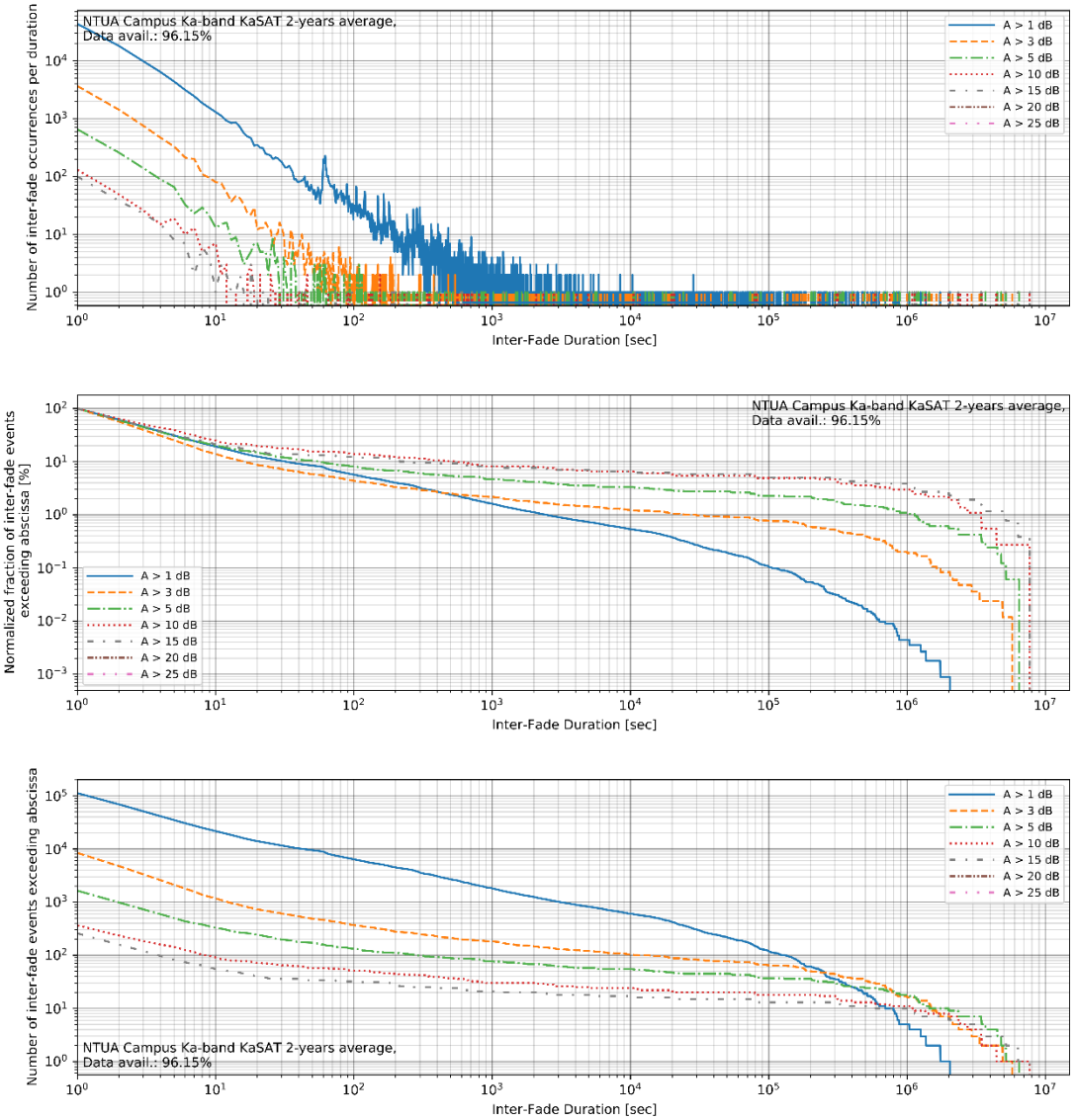

Figure 6-38: Inter-fade duration statistics, Campus Ka-band KaSAT (2-year average)
Top: Total number of occurrences per inter-fade duration
Middle: Normalized fraction of events whose inter-fade duration exceed abscissa
Bottom: Number of events whose inter-fade duration exceed abscissa

6.3 Discussion

In this chapter the second order statistics have been presented; such results can usually be utilized in the framework of an FMT to adjust the sampling rate of the monitoring algorithm, hysteresis thresholds or Automatic Gain Control (AGC) loops.

Examining the fade slope statistics, it appears that their PDF is almost symmetrical around 0 dB/sec, closely resembling a gaussian-type distribution. As was anticipated, for higher attenuation thresholds higher absolute fade slope values are obtained more frequently. Interestingly enough, lower attenuation events at Ka-band seem to reach higher absolute fade slope values, an effect not present at Ku- or Q-band. It should be noted that for LTCP Ka-band some artifacts appear after ±0.55 dB/sec probably due to spurious filtering effects.

From the yearly statistics of the fade duration results, it appears that on average, both the number of event occurrences as well as the total event duration tend to follow an almost loglinear relationship with excess attenuation threshold levels. This appears to hold true for all frequency bands; any peaks at the tail of the distributions should be ignored as they are a result of the finite dynamic range available for the measurements.

According to the normalized fade duration exceedance probabilities it is evident that the number of fades with duration longer than 1000 sec drastically decrease as the attenuation threshold increases; this effect is more pronounced at Ku- and Ka-band. For Q-band, this phenomenon occurs at one order of magnitude higher fade duration, i.e., after 10^4 sec.

From the accumulate fade duration statistics it is suggested that:

- for Ku- and Ka-band 80% of the total fading time corresponding to each attenuation threshold comprises of event lasting up to circa 80-100 seconds
- for Q-band almost 80 % of the total fading time comprises of events with up to 300 seconds duration (5 minutes) time

Additionally, from the mean and median event duration statistics one can deduce that although the mean event duration can significantly deviate for different values of excess attenuation, the median event duration is relatively constant, ranging from 2 to 6 seconds for all frequency bands; from the box-plot analysis it appears that the 3rd quartiles of fade durations are almost normally distributed. The mean duration appears to rapidly increase after 3-4 dB reaching a plateau at about 20-25 dB for Ka-band gradually decreasing after that; for Q-band a slow increase appears after 2-3 dB reaching a plateau again around 20-25 accompanied by a drastic drop after about 27 dB. Finally, at Ku-band the fade duration mean value appears to be stable after about 2 up to 26 dB where a sudden decrease occurs.

Regarding inter-fade events, the larger the attenuation threshold, the lower the number of inter-fade events as expected; this is also reflected in the normalized probability of inter-fade events exceeding a particular duration, with higher attenuation events involving much higher inter-fade durations (i.e. they are less frequent). It is interesting though, that above 15 dB, the normalized inter-fade event durations occurrence curves seem to flatten and coincide with one another around 10% exceedance probability; this implies that given an attenuation threshold above 15 dB, their temporal distribution is equiproportional. One exception is Ku-band where this phenomenon is not so pronounced.

6.4 Chapter References

[1] ITU-R Recommendation P.1623, "Prediction method of fade dynamics on Earth-space paths", International Telecommunication Union, Tech. Rep, Geneva, 2003.

Chapter 7

Site Diversity Evaluation

7.1 Evaluation parameters

As already explained in the introduction of this thesis, in order to meet the required performance in terms of availability and QoS special techniques have to be employed to compensate for the high magnitude of attenuation induced in the signals. Such techniques are commonly referred to as Fading Mitigation Techniques (FMTs), with site diversity being the most prominent one.

The site diversity statistics for two sites s_1, s_2 are derived from the measured excess attenuation timeseries based on the following definition:

$$P_{s_1,s_2}[A_{s_1}(t) > a, A_{s_2}(t) > a] \quad [7\text{-}1]$$

where $P[.]$ is the joint (bi-variate) probability (CCDF) that attenuation values A_{s_1} and A_{s_2} at the time instant t exceed the attenuation threshold a.

The ideal minimum attenuation experienced at time instant t would be:

$$A_{SD}(t) = \min\{A_{s_1}(t), A_{s_2}(t)\} \quad [7\text{-}2]$$

In Figure 7-1 two example realizations of the site-diversity technique are presented using the NTUA ALPHASAT Ka-band and Q-band timeseries across Campus and LTCP locations as obtained on the 16th of November 2017.

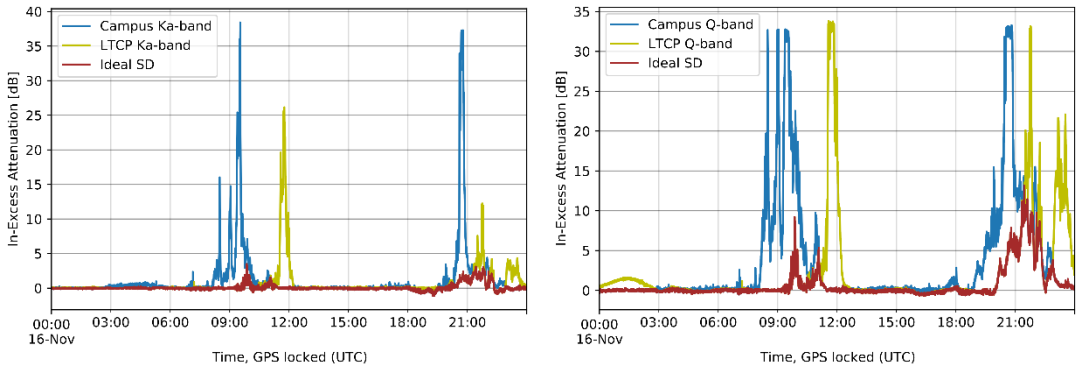

Figure 7-1: Example of the idealized site diversity technique for Ka- and Q-band across the NTUA campaign locations on a rainy day

The joint independent CCDF would be:

$$P_{join,ind} = P[A_{s_1}(t) > a] \cdot P[A_{s_2}(t) > a] \quad [7\text{-}3]$$

where $P[A_{s_1}(t) > a]$ and $P[A_{s_2}(t) > a]$ the single exceedance probabilities

The instantaneous site diversity gain in dB referred to site s_1 is therefore expressed as:

$$G_{SD_1}(t) = A_{s_1}(t) - A_{SD}(t) \quad [7\text{-}4]$$

or equivalently, if referred to s_2:

$$G_{SD_2}(t) = A_{s_2}(t) - A_{SD}(t) \quad [7\text{-}5]$$

Another metric of interest is the equiprobable site diversity gain, i.e:

$$G_{SD}(p_{\%}) = A_s(p_{\%}) - A_{SD}(p_{\%}) \quad [7\text{-}6]$$

where p% the probability of the respective exceedance probability distributions.

The site diversity statistics presented below are obtained after harmonizing all the data to 1 sec time resolution, including only data concurrent at both campaign locations (hence the lower data availability when compared to the single site statistics of Chapter 4). In the following figures the concurrent single site attenuation CCDF and the resulting joint attenuation complementary cumulative distribution function (CCDF) are presented, along with the joint independent CCDF and the site diversity gain referred to each location.

7.2 Results

7.2.1 Ka-band ALPHASAT Site Diversity

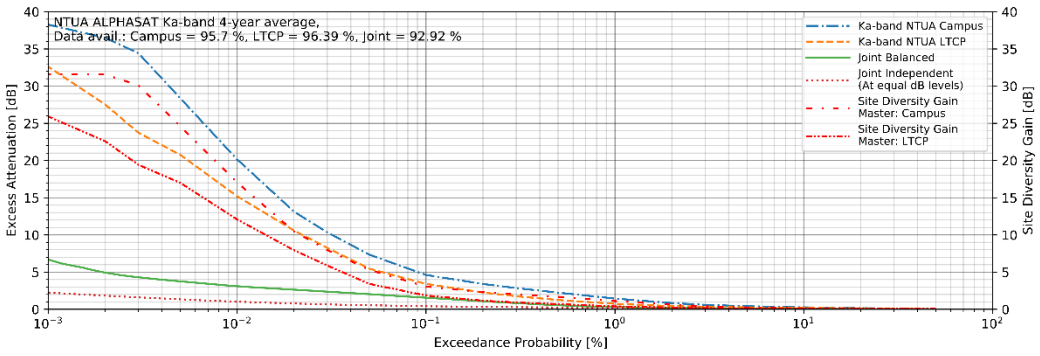

Figure 7-2: Site diversity evaluation for Ka-band ALHASAT across the NTUA campaign locations

7.2.2 Q-band ALPHASAT Site Diversity

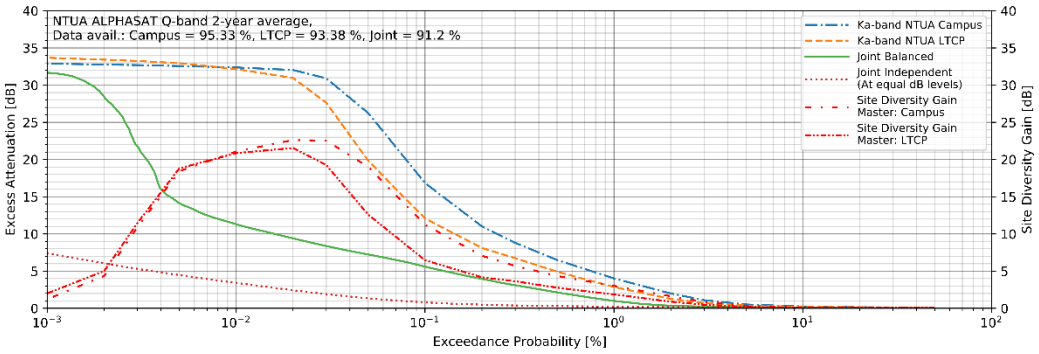

Figure 7-3: Site diversity evaluation for Q-band ALPHASAT across the NTUA campaign locations

7.3 Discussion

The evaluation of the Site Diversity technique has proven that even for small distances such as the one between Campus and Lavrion (approx. 36.5 km), significant gain can be obtained both at Ka-band and Q-band.

For Ka-band, using a hypothetical Selection Combining scheme, i.e., selecting the samples from the receiver with the higher C/N at each time instant, gain in excess of 31 dB can be obtained at 0.001% of the time, resulting in an approx. 6.7 dB extra fade margin required to fully compensate for excess attenuation and maintain 99.999% availability. The gain (in dB) follows an almost linear relationship with exceedance probabilities for values from 0.003% up to 0.02%, reaching a plateau below 0.003%

For the Q-band case, due to the lower dynamic range offered by the receivers combined with the higher attenuation rain magnitude, an evaluation below 0.03% of the total time is not possible. However, at this exceedance probability a gain of nearly 23 dB can be accomplished, considerably relaxing the extra margin required to maintain 99.97% availability to about 8.5 dB.

Comparing the joint balanced (bi-variate) curves with the joint independent ones as defined in the introduction of this chapter, it is obvious that they exhibit very high discrepancy across all exceedance probabilities. Should the single CCDFs be independent from one another, according to probability theory their joint independent distribution should be the same as their joint bi-variate which is clearly not the case meaning that they are clearly not independent.

7.4 Site Diversity Scenarios

It is evident from the above that should the system be able to use the two receivers interchangeably (at each frequency band), being able to instantaneously switch from one station to another would yield a massive performance gain. Such a scenario is ideal and hence not practically realizable; three more cases are examined in the following, namely switching with an

attenuation threshold, switching with an attenuation threshold and spatial hysteresis and switching with an attenuation threshold with both spatial and temporal hysteresis as explained in the following subsections. For this study the measurements from the first two years of the experiment at Ka-band are used.

The impact of the various switching schemes has also been investigated in [1]. In all scenarios it is assumed that the receivers are interconnected, fully synchronized and constantly measure attenuation levels from effects occurring in their slant path. It should be noted that data loss during ground stations' hand-over can be prevented using an appropriate higher-level protocol (e.g. UDP/TCP, or even DVB frame retransmission) depending on the application of interest (i.e. real/non-real time) and its specific requirements.

7.4.3 Switching with threshold

In this scenario, NTUA Campus is considered the master receiver serving the system under normal conditions (active selection); upon exceedance of an attenuation threshold the system's switching broker selects the NTUA LTCP receiver (slave, otherwise inactive), provided that the latter experiences less attenuation. When the master receiver's attenuation falls below the threshold, the system switches back to it.

7.4.4 Switching with threshold and spatial hysteresis

The difference between this and the first scenario is that upon switching to the second receiver, the system does not revert back to the original/master one up until the slave's attenuation exceeds the threshold and the first one experiences less attenuation. Such a scheme could be considered as a dual-master with spatial hysteresis and can significantly reduce the total number of switches by more than an order of 10.

7.4.5 Switching with threshold, spatial and temporal hysteresis

This is an extension to the second scenario, adding time hysteresis to the play; more particularly, after registering a threshold exceedance, the broker waits for *x* seconds (10 sec in this study) before switching to the next one. If and only if during this sliding window the attenuation continues to fall above the threshold then the broker selects the other receiver. As expected, this results into even less switches as shown in Table 7-1, making such a system configuration less complex and hence realizable.

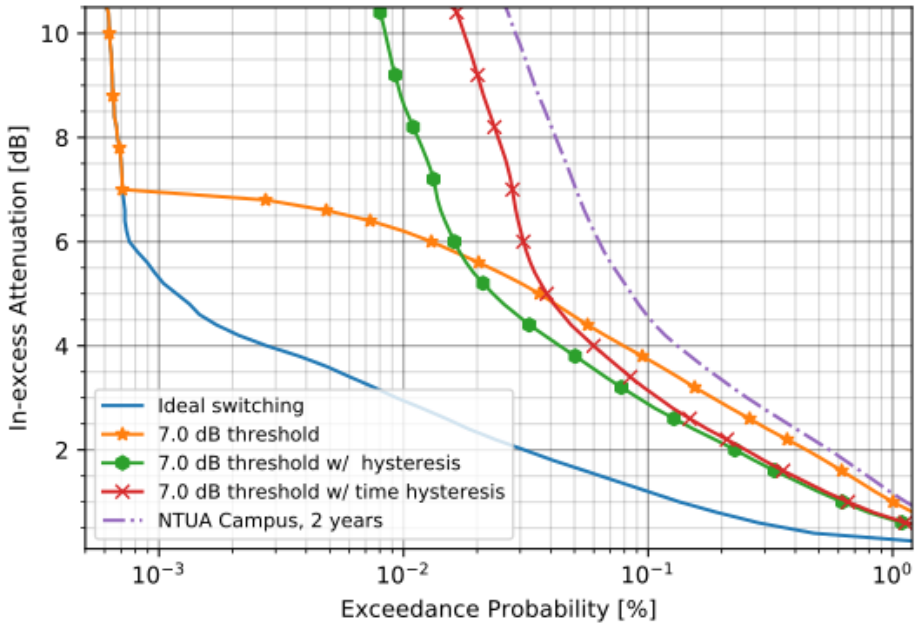

Figure 7-4: Switching techniques performance comparison with 7.0 dB threshold using 2 years of Ka-band ALPHASAT attenuation data

All the above scenarios have been compared against each other in terms of attenuation performance and number of switches required; there is a clear trade-off between these two factors that the designer has to consider when setting the corresponding thresholds.

Table 7-1: Ground Station Switches Required for different Attenuation Thresholds with Hysteresis (2-year Ka-band ALPHASAT attenuation data used)

Switching Threshold [dB]	Number of switches		
	Threshold	*Threshold with spatial hysteresis*	*Threshold with spatial and time hysteresis*
0.0 (ideal switching)	13463613		
1.0	44964	3936	686
2.5	10294	764	318
4.0	3820	330	244
5.5	1742	258	216
7.0	878	226	178

7.5 Chapter References

[1] M. Rytir, M. Cheffena, P. A. Grotthing, L. E. Bråten and T. Tjelta, "Three-Site Diversity at Ka-Band Satellite Links in Norway: Gain, Fade Duration, and the Impact of Switching Schemes," *in IEEE Transactions on Antennas and Propagation*, vol. 65, no. 11, Nov. 2017, pp. 5992-6001.

Chapter 8

Time Diversity Evaluation

8.1 Evaluation parameters

Another proposed FMT is the time diversity technique: a link affected by a propagation impairment leading to outage merely retransmits the signal after a scheduled time delay; this technique is therefore suitable for time-delay tolerant applications and services (i.e., non-real-time) such as data transfer. A noteworthy advantage of time diversity over other FMTs is that it makes use of only one single link, i.e., the very same propagation channel but delayed in time [1]-[3].

The time diversity statistics for a time delay *TD* are derived from the measured excess attenuation timeseries based on the following definition:

$$P[A(t) > a, A(t+TD) > a] \quad [8\text{-}1]$$

where $P[.]$ is the joint (bi-variate) probability (CCDF) that both attenuation values $A(t)$ and $A(t+TD)$ at the instant t and $t+TD$ accordingly exceed the attenuation threshold a.

The attenuation experienced at time instant t would be:

$$A_{TD}(t) = \min\{A(t), A(t+TD)\} \quad [8\text{-}2]$$

In Figure 8-1 example realizations of the time-diversity technique are presented using the NTUA Campus Ka-band and Q-band timeseries obtained on the 14th of November 2017.

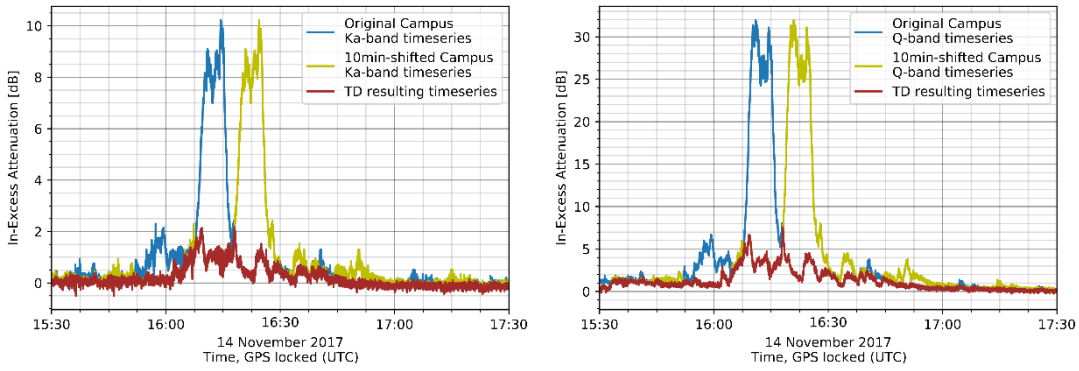

Figure 8-1: Example of the idealized time diversity technique for Ka- and Q-band at the NTUA Campus location on a rainy day using a 10-min delay

The instantaneous time diversity gain in dB is therefore expressed as:

$$G_{TD}(t) = A(t) - A_{TD}(t) \quad [8\text{-}3]$$

Another metric of interest is the equiprobable time diversity gain, i.e:

$$G_{TD}(p_{\%}) = A(p_{\%}) - A_{TD}(p_{\%}) \quad [8\text{-}4]$$

where p% the probability of the respective exceedance probability distributions.

The time diversity statistics presented below are obtained after harmonizing all the data to 1 sec time resolution. The time delay TD values used are: **1 s**, **5 s**, **10 s**, **1 min**, **3 min**, **5 min**, **10 min**, **30 min**, **1 h**, **3 h**, **6 h**, **12 h** and **18 h**.

In the following figures the resulting joint attenuation complementary cumulative distribution function (CCDF) is provided for all frequency bands at both campaign locations, along with the equiprobable time diversity gain at **1%**, **0.1%**, **0.01%** and **0.001%** of the overall time.

8.2 Results

8.2.1 Campus Ku-band BADR5 Time Diversity

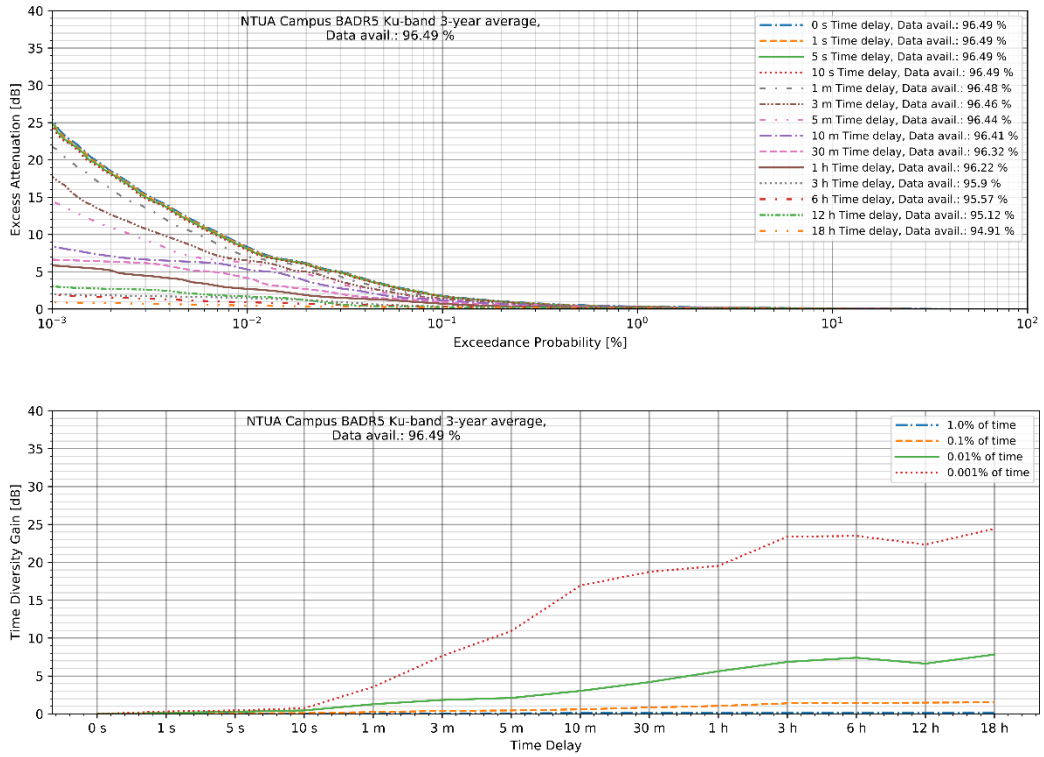

Figure 8-2: Time diversity evaluation for Ku-band BADR5 at NTUA Campus for different time delays

8.2.2 Campus Ka-band ALPHASAT Time Diversity

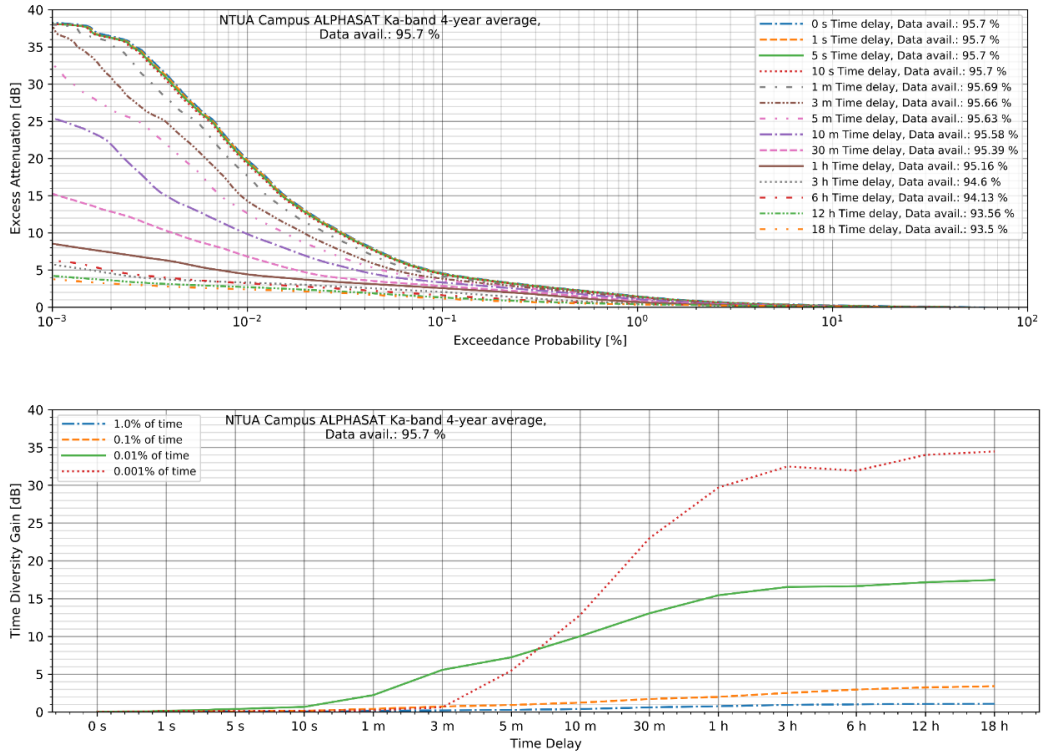

Figure 8-3: Time diversity evaluation for Ka-band ALPHASAT at NTUA Campus for different time delays

8.2.3 LTCP Ka-band ALPHASAT Time Diversity

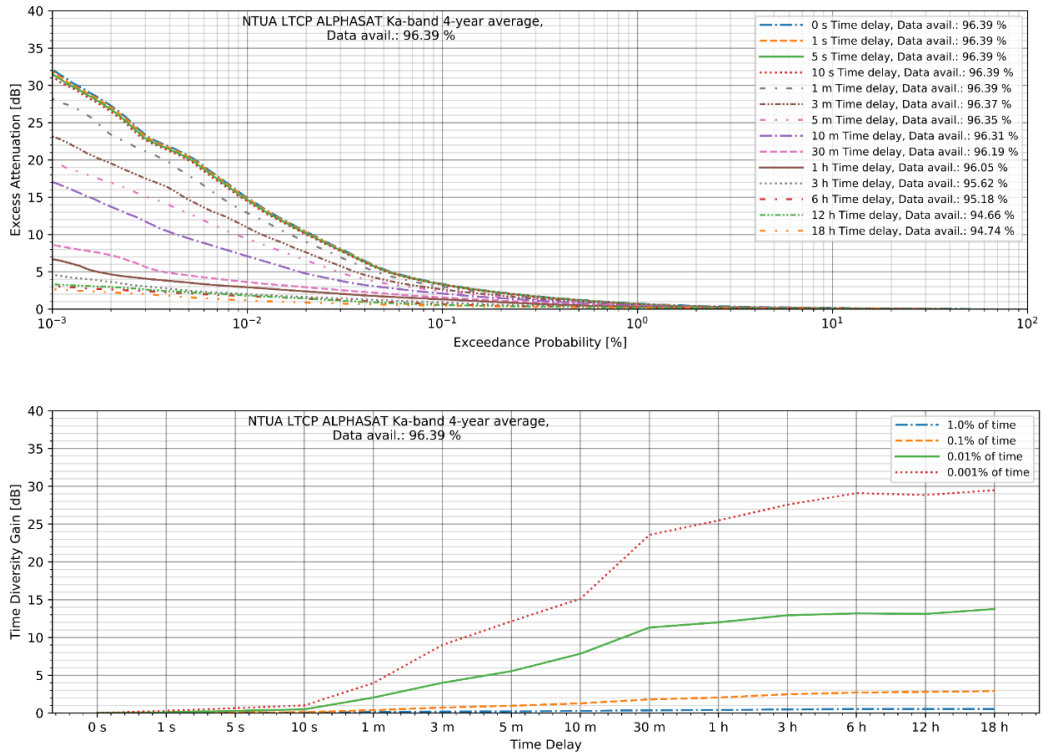

Figure 8-4: Time diversity evaluation for Ka-band ALPHASAT at NTUA LTCP for different time delays

8.2.4 Campus Q-band ALPHASAT Time Diversity

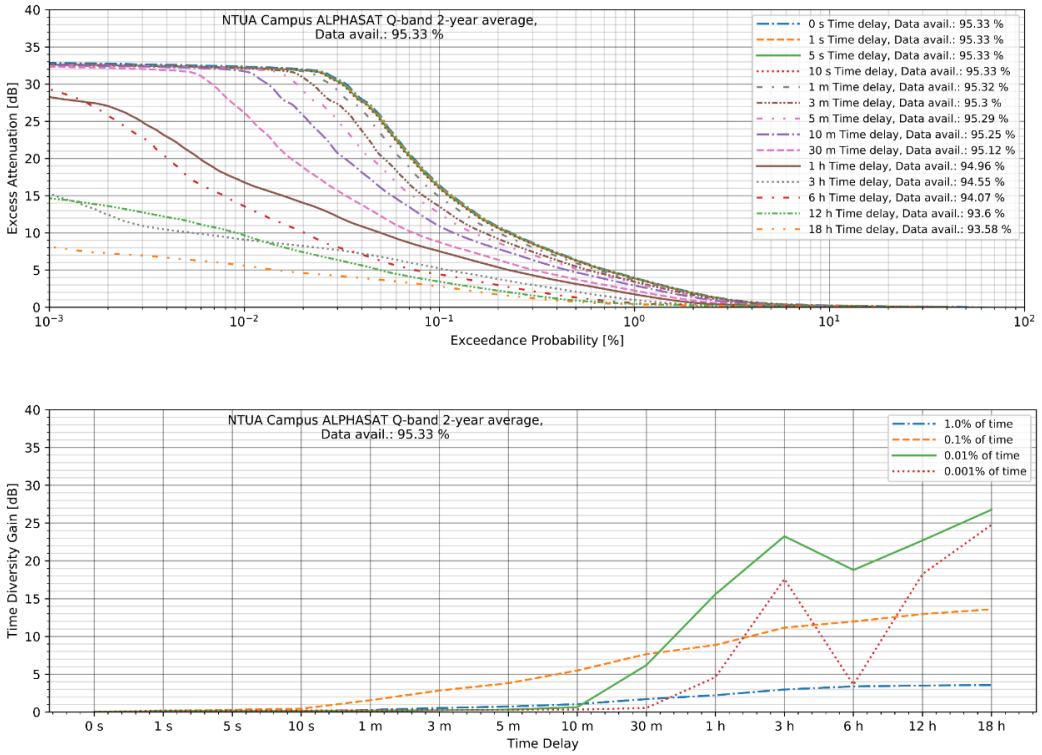

Figure 8-5: Time diversity evaluation for Q-band ALPHASAT at NTUA Campus for different time delays

8.2.5 LTCP Q-band ALPHASAT Time Diversity

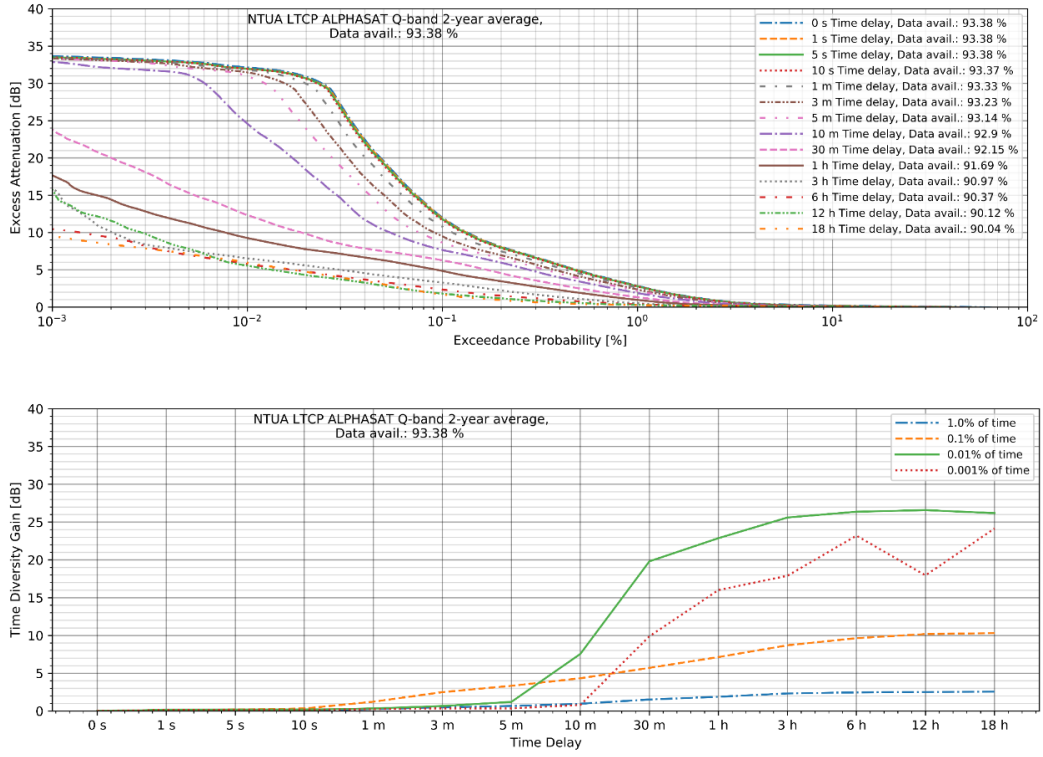

Figure 8-6: Time diversity evaluation for Q-band ALPHASAT at NTUA LTCP for different time delays

8.2.6 Campus Ka-band KaSAT Time Diversity

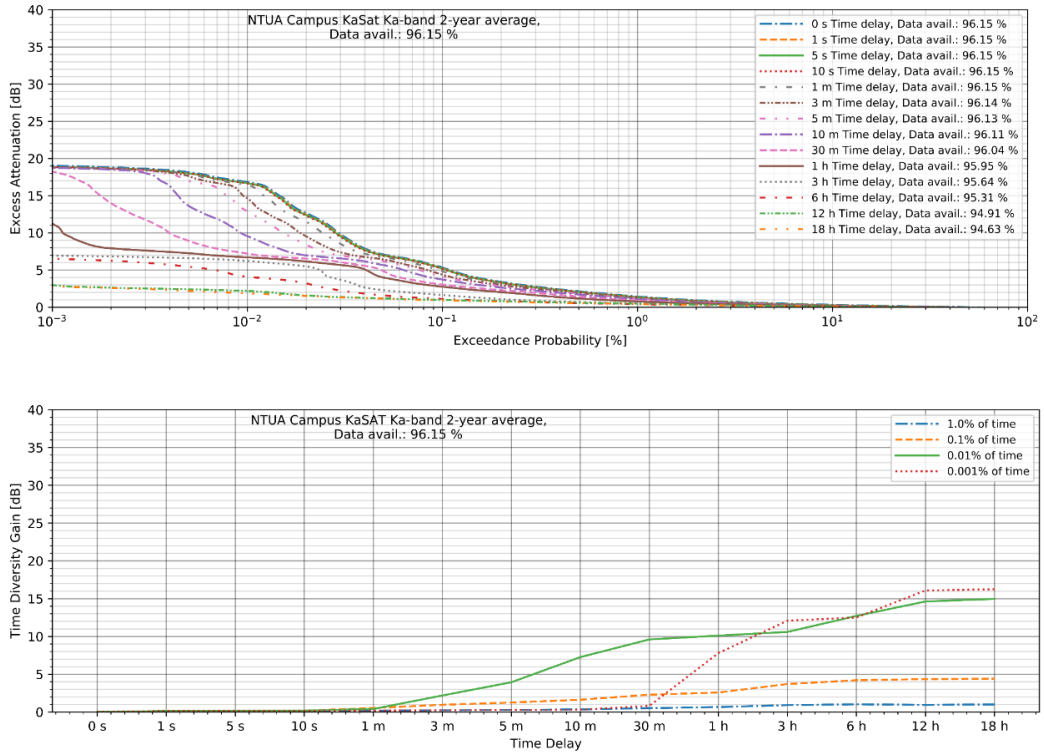

Figure 8-7: Time diversity evaluation for Ka-band KaSAT at NTUA Campus for different time delays

8.3 Discussion

In this chapter the results derived after applying this idealized time diversity technique are presented for each frequency band available at each site. It is obvious from the analysis that a relatively short time delay (i.e., in the order of a few seconds) offers minimal gain in the long-run irrespective of operating frequency band; nevertheless, the application of a time delay in the order of a few minutes (reasonable for some types of non-real time applications and services) could yield considerable improvement.

As an example, the use of a 5 min delay can reduce the obtained long-term excess attenuation value from 20 dB to about 12.5 dB for 0.01% of the total time for Ka-band Campus and 9.5 dB for LTCP. The gain appears to be vast also at Q-band, where at 0.03% of the total time, the attenuation can be minimized from over 30 dB to just about 16 dB using a 5 min delay.

The use of longer time delays naturally leads to a higher performance gain, however, a long delay would most probably appear similar to an outage from an end-user's point of view, since it would also be resulting in (temporal) service disruption.

The relation of the performance of time and site diversity has been studied in [4]-[5].

8.4 Chapter References

[1] V. Fabbro, L. Castanet, S. Croce and C. Riva, "Characterization and modelling of time diversity statistics for satellite communications from 12 to 50 GHz," International. Journal of Satellite Communications and Networking, 27, 2, January 2009 pp. 87-101.

[2] H. Fukuchi and T. Nakayama, "Quantitative evaluation of time diversity as a novel attenuation mitigation technology for future high speed satellite communication," IEICE Transactions on Communications, 87, 8, 2004, pp. 2119–2123.

[3] P. D. Arapoglou, A. D. Panagopoulos, and P. G. Cottis, "An analytical prediction model of time diversity performance for earth-space fade mitigation," International Journal of Antennas and Propagation, March 2008.

[4] C. Capsoni, M. D'Amico and R. Nebuloni, "Time and site diversity gain: A close relationship," International Workshop on Satellite and Space Communications, Tuscany, Italy, September 2009, pp. 166-170.

[5] C. Capsoni, M. D'Amico, R. Nebuloni, C. Riva, "Performance of site diversity technique estimated from time diversity," Proceedings of the 5th European Conference on Antennas and Propagation (EUCAP), Rome, Italy, April 2011, pp. 1463-1466.

Chapter 9

Orbital Diversity Evaluation

9.1 Evaluation parameters

Besides the techniques presented in the previous chapters, another promising FMT involves the communication of a single-site receiver with multiple satellites, each orbiting the earth at different orbital positions. This technique utilizes the fact that the signal propagating from/and to the satellite follows a different slant path, experiencing uncorrelated (or low-correlated) atmospheric impairments. It is therefore to be expected that the greater the separation angle across the satellites, the greater the gain would be.

The orbital diversity statistics for satellites at two orbital locations o_1 , o_2 are derived from the measured excess attenuation timeseries based on the following definition:

$$P_{o_1,o_2}[A_{o_1}(t) > a, A_{o_2}(t) > a] \quad [9\text{-}1]$$

where $P[.]$ is the joint (bi-variate) probability (CCDF) that attenuation values A_{o_1} and A_{o_2} at the time instant t exceed the attenuation threshold a .

The ideal minimum attenuation experienced at time instant t would be:

$$A_{OD}(t) = \min\{A_{o_1}(t), A_{o_2}(t)\} \quad [9\text{-}2]$$

In Figure 9-1 example realizations of the orbital-diversity technique are presented using the NTUA Campus Ka-band ALPHASAT and KaSAT timeseries obtained on the 31st July 2018 and 28th August 2018 respectively.

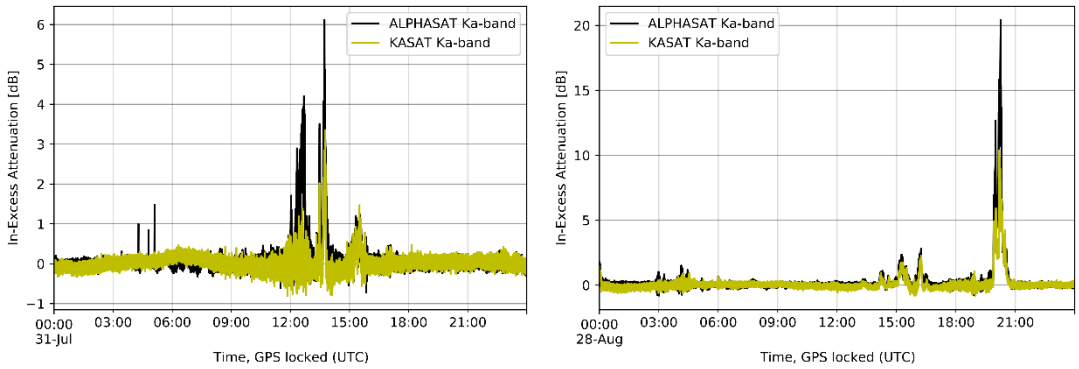

Figure 9-1: Example of the potential idealized orbital diversity technique for Ka-band at the NTUA Campus location during two rainy days

The joint independent CCDF would be:

$$P_{join,ind} = P[A_{o_1}(t) > a] \cdot P[A_{o_2}(t) > a] \quad [9\text{-}3]$$

where: $P[A_{o_1}(t) > a]$ and $P[A_{o_2}(t) > a]$ the single exceedance probabilities

The instantaneous orbital diversity gain in dB referred to satellite in orbit o_1 is therefore expressed as:

$$G_{OD_1}(t) = A_{o_1}(t) - A_{OD}(t) \quad [9\text{-}4]$$

or equivalently, if referred to orbit o_2 :

$$G_{OD_2}(t) = A_{o_2}(t) - A_{OD}(t) \quad [9\text{-}5]$$

Another metric of interest is the equiprobable orbital diversity gain, i.e:

$$G_{OD}(p_{\%}) = A_o(p_{\%}) - A_{OD}(p_{\%}) \quad [9\text{-}6]$$

where p% the probability of the respective exceedance probability distributions.

The orbital diversity statistics presented below are obtained after harmonizing all the data to 1 sec time resolution, including only Ka-band attenuation data concurrent for both ALPHASAT at 25°E and KaSAT at 9°E measured at the Campus location (hence the lower data availability when compared to the single frequency/satellite statistics of Chapter 5). It should be noted again that there is a slight frequency discrepancy between the two transmitted beacons, namely ALPHASAT transmits at 19.701 GHz vertical polarization, while KaSAT at 19.680 GHz horizontal polarization. Nevertheless, one can still obtain a good indication of the performance gain using orbital diversity as a possible FMT.

In the following figures the concurrent single-orbit attenuation CCDF and the resulting joint attenuation complementary cumulative distribution function (CCDF) are presented, along with the joint independent CCDF and the orbital diversity gain referred to each satellite.

9.2 Results

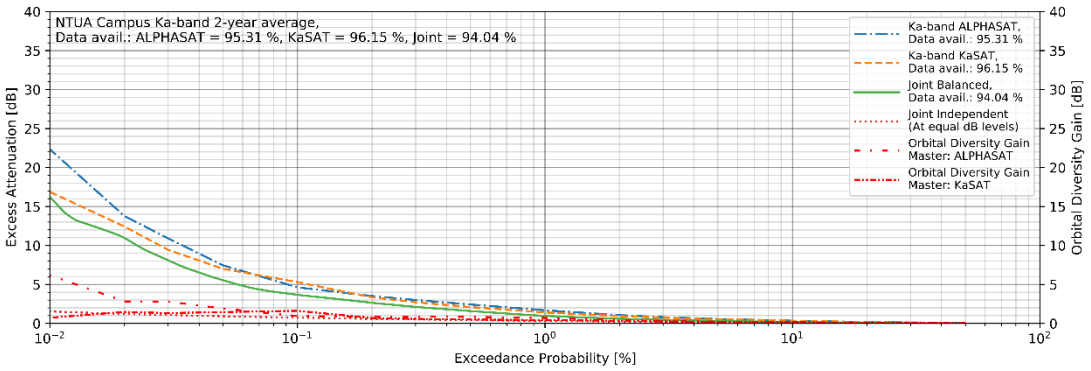

Figure 9-2: Orbital diversity evaluation for Ka-band at NTUA Campus

9.3 Discussion

The results of the orbital diversity evaluation at Ka-band indicate that there is an appreciable gain in the order of 6 dB at 0.01% of the time, lowering the required margin from about 22 to 16 dB. Nevertheless, for higher exceedance probabilities (i.e., greater than 0.1%) the gain is minimal at this separation angle, namely 16^{o}.

Another set of measurements at a greater separation angle would probably provide a better insight on the effectiveness of this technique as suggested by [1]. Also, the fact that the KaSAT Ka-band receiver provides a lower measurement dynamic range limits the extent of this evaluation to exceedance probabilities only higher than 0.01%, while it is expected that at lower probabilities the gain could be significantly higher.

9.4 Chapter References

[1] E. Matricciani and M. Mauri, “Italsat-Olympus 20-GHz orbital diversity experiment at Spino d'Adda” in *IEEE Transactions on Antennas and Propagation*, vol. 43, no. 1, Jan. 1995, pp. 105-108.

Chapter 10

Frequency Scaling Evaluation

10.1 Evaluation parameters

Frequency scaling of excess attenuation involves the prediction of attenuation at a desired frequency based on attenuation values obtained at another frequency. Such a prediction is particularly valuable in the design of new systems as well as regarding the use of FMTs. An example realization of frequency scaling is depicted in Figure 10-1.

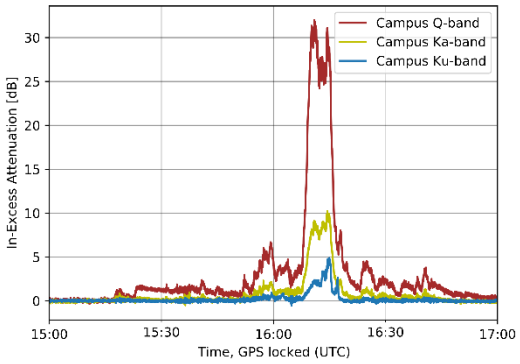

Figure 10-1: Example of frequency scaling for Ku, Ka and Q bands at NTUA Campus for a rain event

After time aligning the attenuation data for each of the frequency pairs (only concurrent data are used), the scintillation effects are removed using a low-pass Butterworth filter of 10th order with a cut-off frequency of 0.02 Hz (similarly to the one to calculate fade slopes in Chapter 6).

In this chapter, according to a methodology similar to [1], the following statistics are evaluated:

10.1.1 Excess attenuation at frequency 1 vs Excess attenuation at frequency 2 at different occurrence levels (percentiles)

- After binning the excess attenuation at base frequency f_1 in 0.2 dB increments, the corresponding values of excess attenuation at frequency f_2 are identified for each bin.
- For each bin corresponding to an attenuation level at frequency 1: the mean and the standard deviation of the excess attenuation values at frequency 2 are calculated, along with the excess attenuation values occurring at the 1st, 10th, 20th, 30th, 40th, 50th (median value), 60th, 70th, 80th, 90th and 99th percentile.

10.1.2 Instantaneous Frequency Scaling Factor (IFSF) for a pair of frequencies at different occurrence levels (percentiles)

- After binning the excess attenuation at frequency f_1 in 0.2 dB increments, for each bin the binned Instantaneous Frequency Scaling Factor (IFSF) ratios are calculated as:

$$IFSF(bin) = \frac{A_{f_2}(t, bin)}{A_{f_1}(t, bin)} \quad [10\text{-}1]$$

  where $A_{f_1}(t, bin)$ and $A_{f_2}(t, bin)$ the corresponding excess attenuation values in dB for frequency 1 and frequency 2 at time instant t corresponding to the same bin.
- For each bin corresponding to an attenuation level at frequency f_1: the mean and the standard deviation of the IFSF are calculated, along with the IFSF values occurring at the 1st, 10th, 20th, 30th, 40th, 50th (median value), 60th, 70th, 80th, 90th and 99th percentile.

10.1.3 IFSF Exceedance Probability (CCDF) for a pair of frequencies

This time, without binning the attenuation values, the IFSF is calculated for the entire available dataset as:

$$IFSF(t) = \frac{A_{f_2}(t)}{A_{f_1}(t)} \quad [10\text{-}2]$$

The probability of exceedance (CCDF) $P[IFSF(t) > k]$, i.e., the fraction of total time that $IFSF(t) > k$ is obtained.

10.1.4 Equiprobable (Statistical) Frequency Scaling Factor (EFSF) for a pair of frequencies

Using the attenuation exceedance probabilities (%) for each frequency, the Equiprobable Frequency Scaling Factor (EFSF) can be obtained as:

$$EFSF(p_{\%}) = \frac{A_{f_1}(p_{\%})}{A_{f_2}(p_{\%})} \quad [10\text{-}3]$$

where $A_{f_1}(p_{\%})$ and $A_{f_2}(p_{\%})$ are the excess attenuation probabilities for the two frequencies at the same exceedance probability $p_{\%}$.

10.1.5 Linear Regression Fitting of excess attenuation for a pair of frequencies

- After binning the excess attenuation at frequency f_1 in 0.2 dB increments, the corresponding values of excess attenuation at frequency f_2 are identified for each bin.
  - The whole set of values $A_{f_1}(t, bin)$ and $A_{f_2}(t, bin)$ are used to perform linear regression fitting.

- The values $A_{f_1}(t, bin, 50^{th}\, p)$ and $A_{f_2}(t, bin, 50^{th}\, p)$ are used to perform another linear regression, this time using only the values at 50th percentile for each bin.

Based on the data available, all the possible combinations have been considered for the evaluation of the frequency scaling statistics. More particularly, the statistics shown below correspond to the following pairs:

- Campus ALPHASAT Ka-band vs ALPHASAT Q-band
- LTCP ALPHASAT Ka-band vs ALPHASAT Q-band
- Campus BADR5 Ku-band vs ALPHASAT Ka-band
- Campus BADR5 Ku-band vs ALPHASAT Q-band

It should be noted that in order to produce the above results the base attenuation for the frequency was considered greater than 1.0 dB; this is to done in order to remove any odd ratios that would arise due to dividing numbers less than 1.0. When using Ku-band (BADR5) as the base frequency, since the satellite's slant path is slightly different than the one for the Ka and Q bands (ALPHASAT), namely 1° difference in orbital position, in order to make sure the events are truly concurrent another constraint is imposed, namely that attenuation at Ku-band (base frequency) is also lower than its counterpart frequency (Ka- or Q-band).

10.2 Results

10.2.6 Campus Ka-band ALPHASAT vs Campus Q-band ALPHASAT frequency scaling

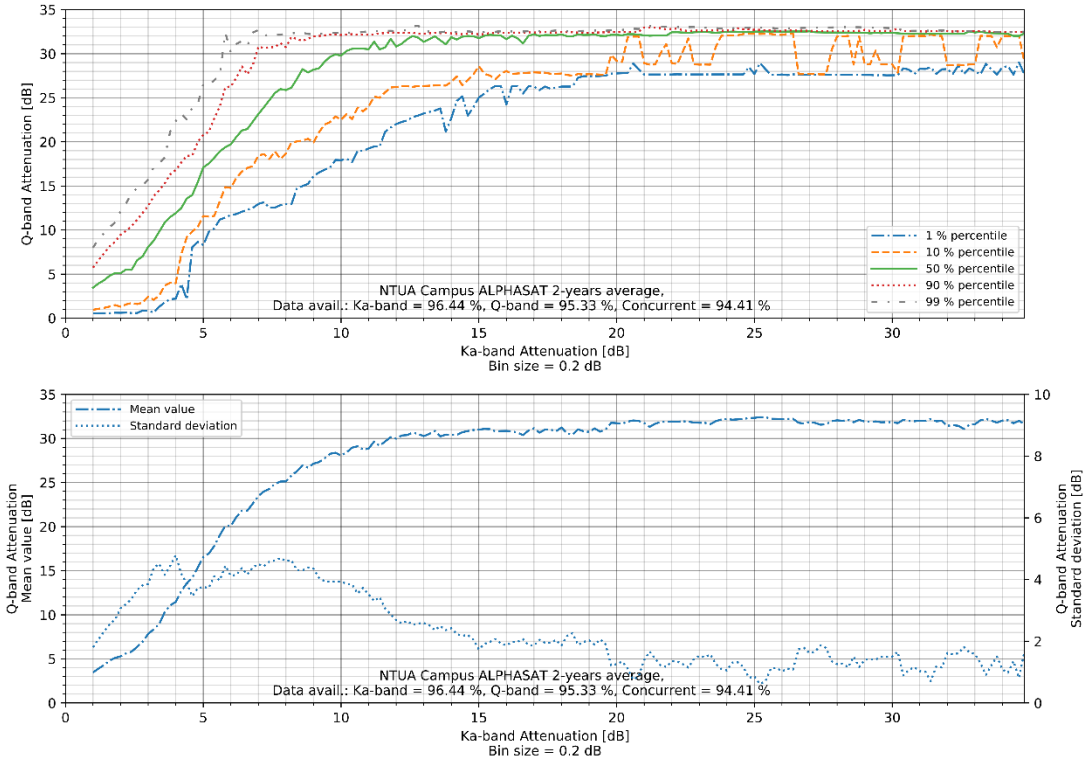

Figure 10-2: Campus Ka-band ALPHASAT vs Q-band ALPHASAT excess attenuation

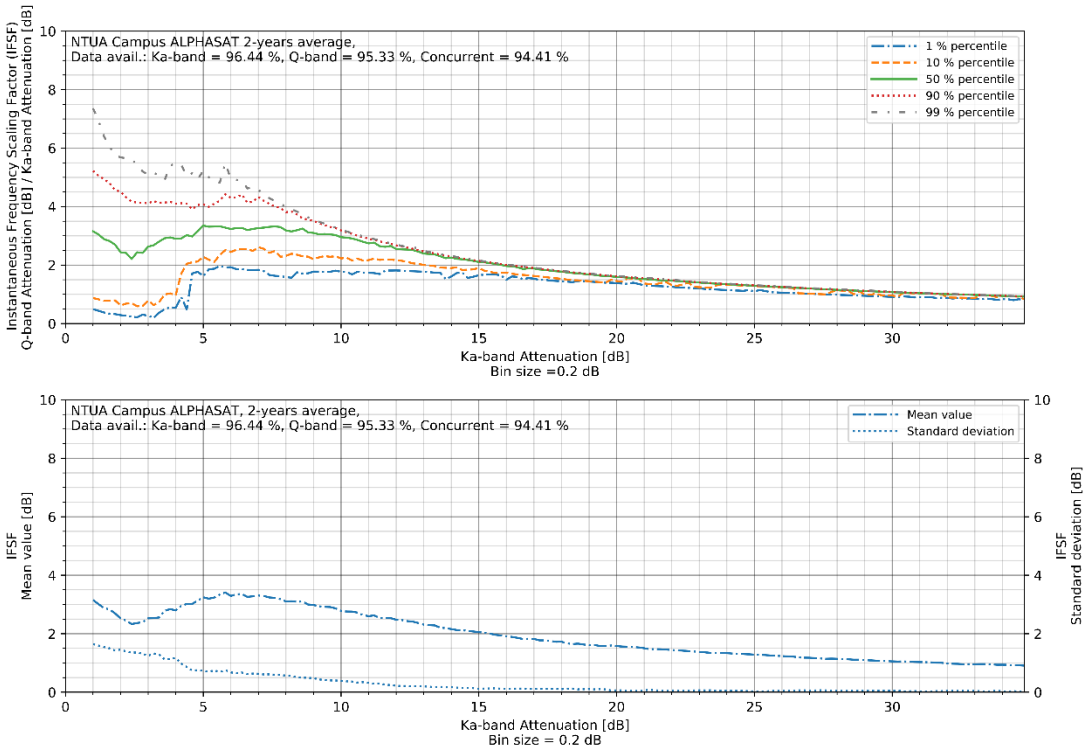

Figure 10-3: Instantaneous Frequency Scaling Factor (IFSF), Campus Ka-band ALPHASAT vs Q-band ALPHASAT

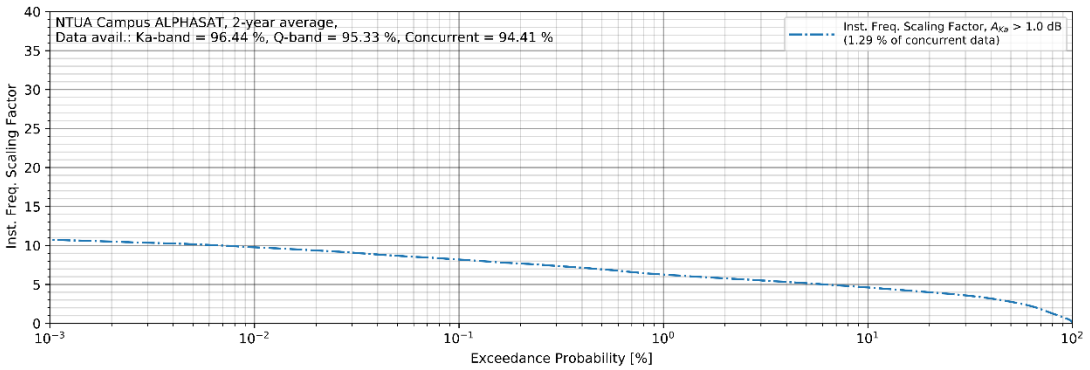

Figure 10-4: IFSF Exceedance Probability, Campus Ka-band ALPHASAT vs Q-band ALPHASAT

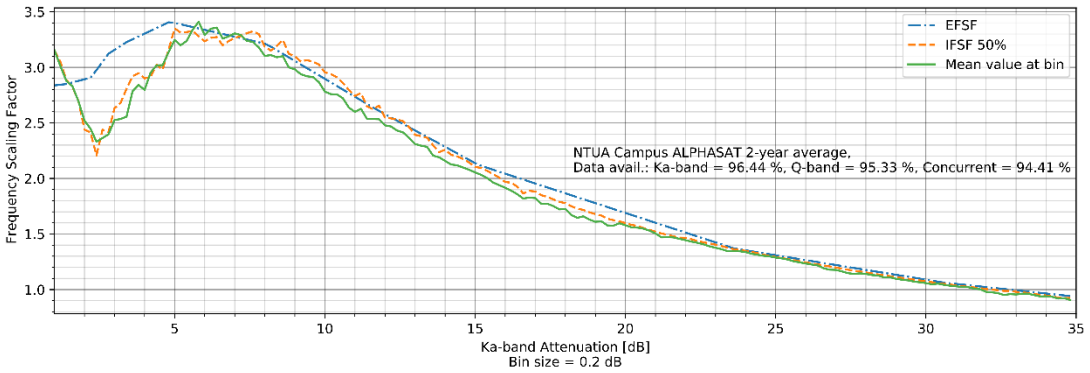

Figure 10-5: Comparison between EFSF, IFSF at 50th percentile and IFSF mean value, Campus Ka-band ALPHASAT vs Q-band ALPHASAT

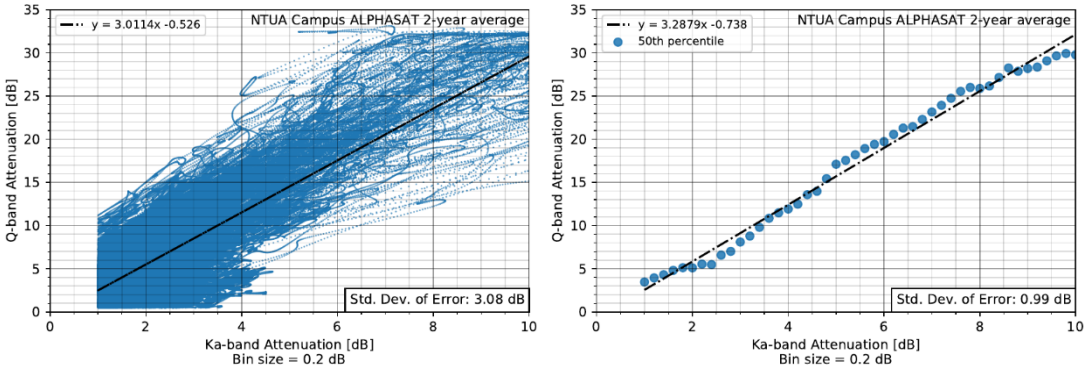

Figure 10-6: Scatter plot Excess Attenuation Campus Ka-band ALPHASAT vs Q-band ALPHASAT with linear regression fitting (left: all data, right: data at 50th percentile)

10.2.7 LTCP Ka-band ALPHASAT vs LTCP Q-band ALPHASAT frequency scaling

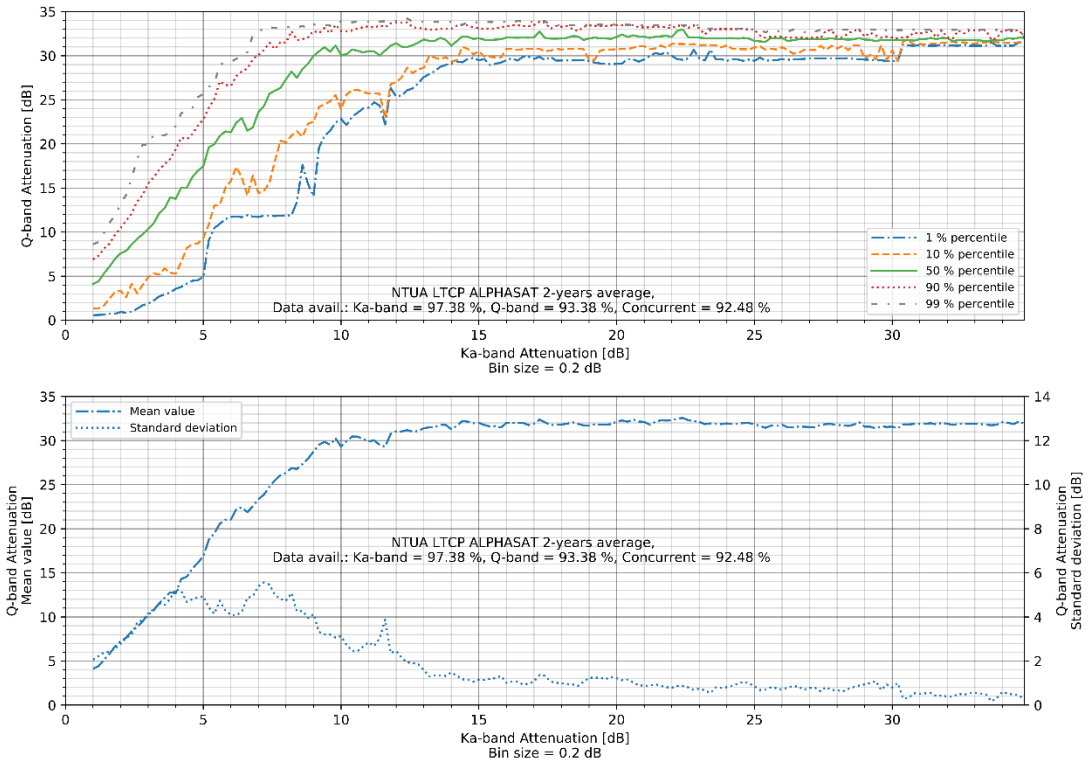

Figure 10-7: LTCP Ka-band ALPHASAT vs Q-band ALPHASAT excess attenuation

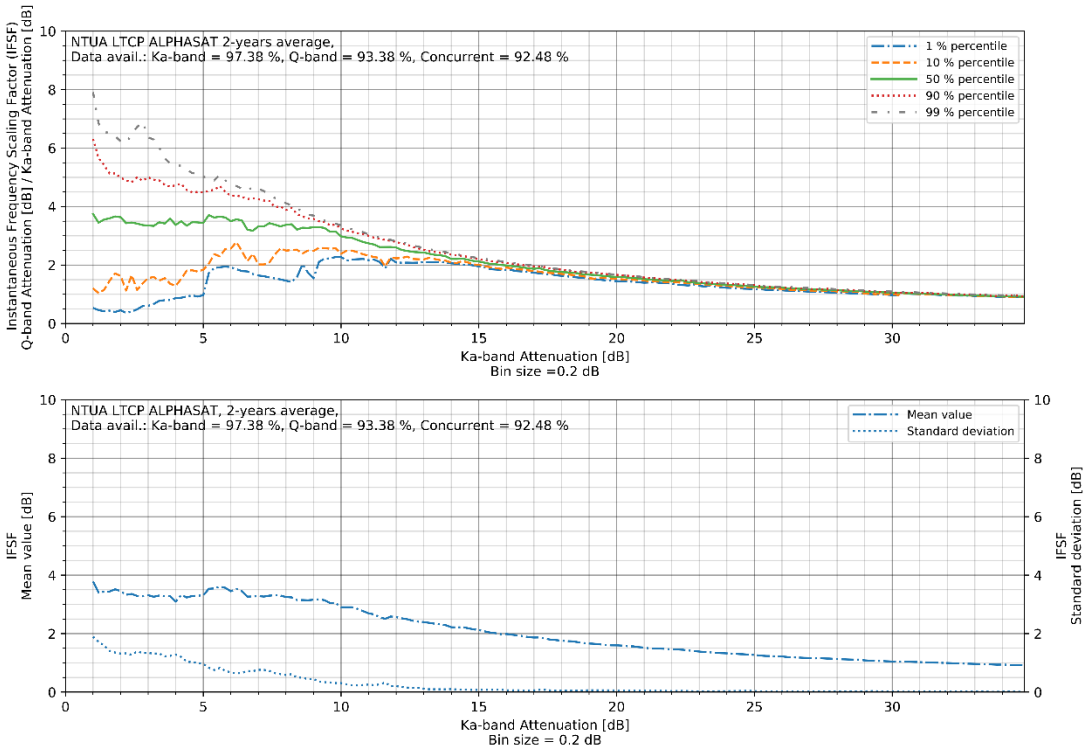

Figure 10-8: Instantaneous Frequency Scaling Factor (IFSF), LTCP Ka-band ALPHASAT vs Q-band ALPHASAT

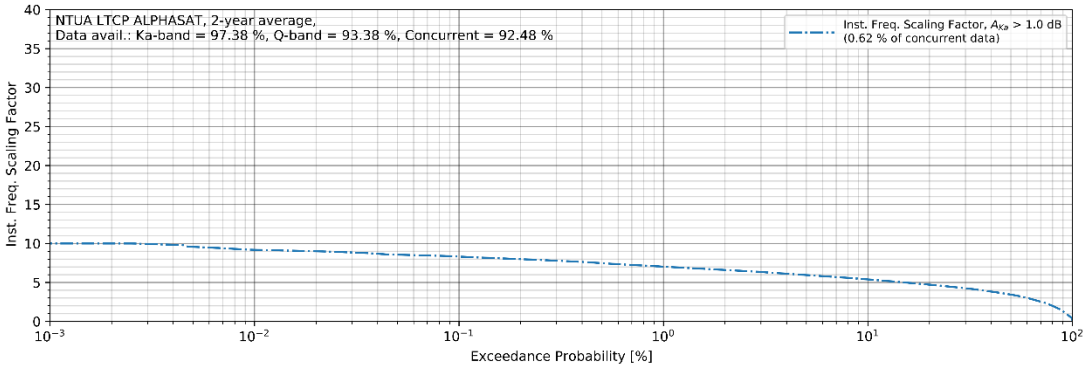

Figure 10-9: IFSF Exceedance Probability, LTCP Ka-band ALPHASAT vs Q-band ALPHASAT

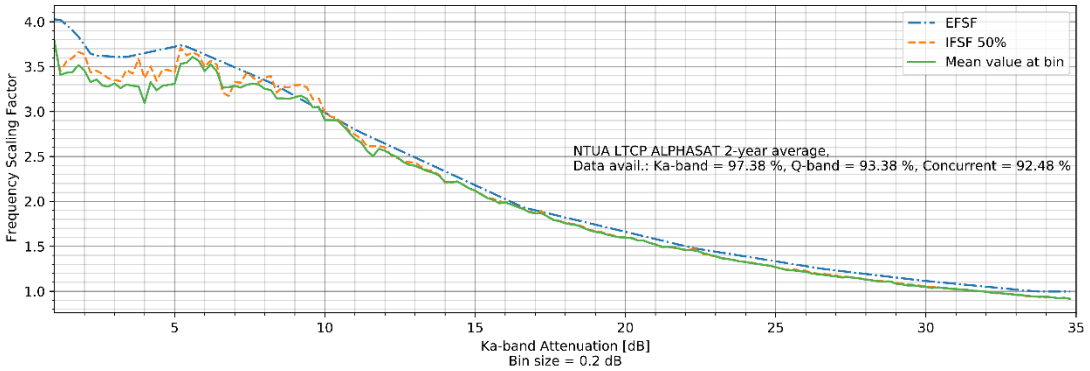

Figure 10-10: Comparison between EFSF, IFSF at 50th percentile and IFSF mean value, LTCP Ka-band ALPHASAT vs Q-band ALPHASAT

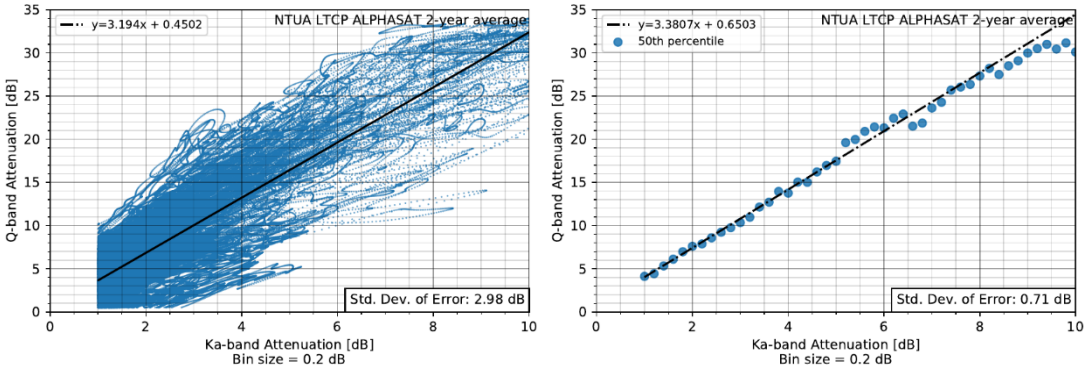

Figure 10-11: Scatter plot Excess Attenuation LTCP Ka-band ALPHASAT vs Q-band ALPHASAT with linear regression fitting (left: all data, right: data at 50th percentile)

10.2.8 Campus Ku-band BADR5 vs Campus Ka-band ALPHASAT frequency scaling

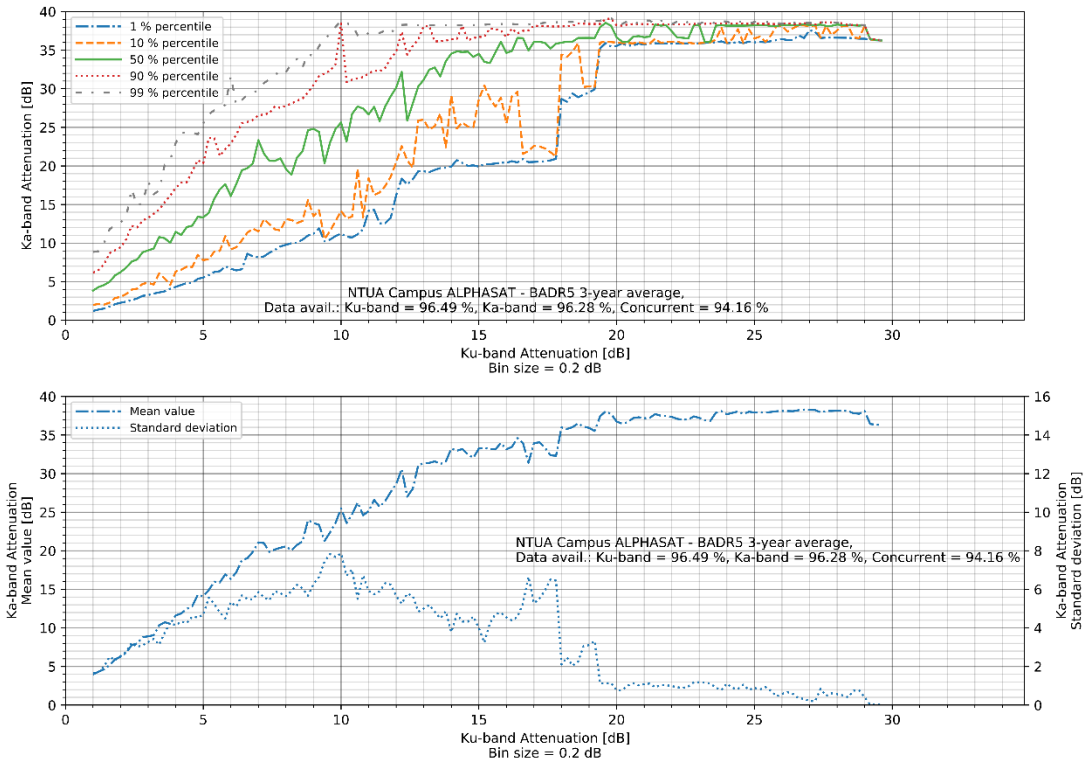

Figure 10-12: Campus Ku-band BADR5 vs Ka-band ALPHASAT excess attenuation

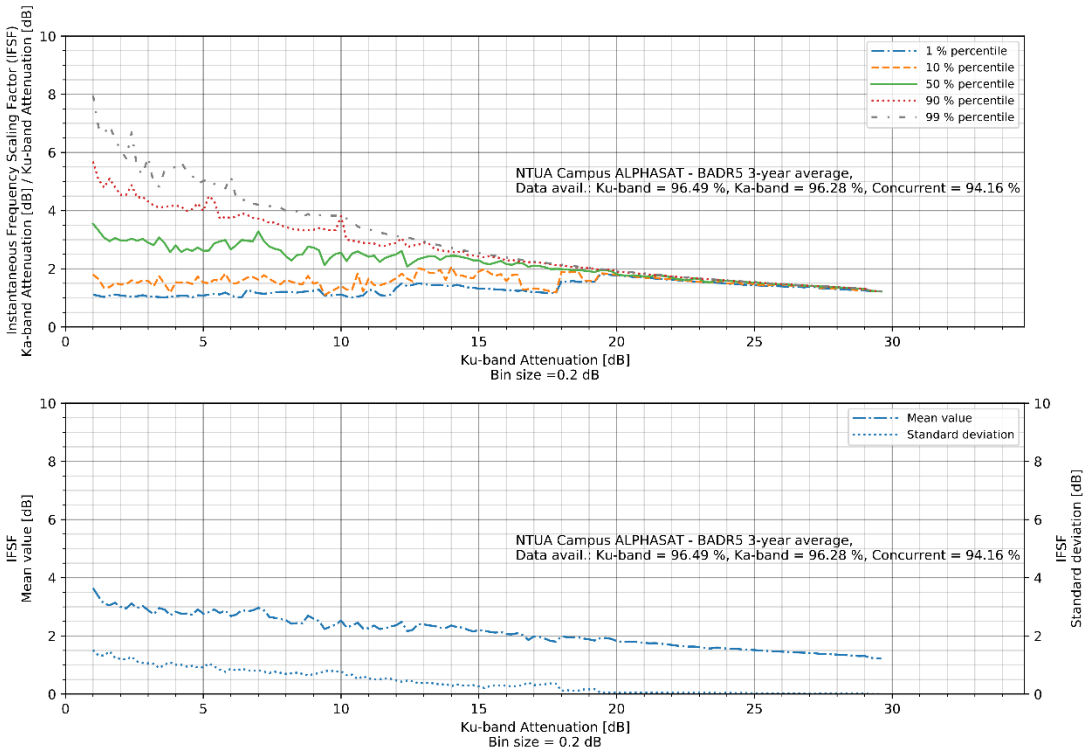

Figure 10-13: Instantaneous Frequency Scaling Factor (IFSF), Campus Ku-band BADR5 vs Ka-band ALPHASAT

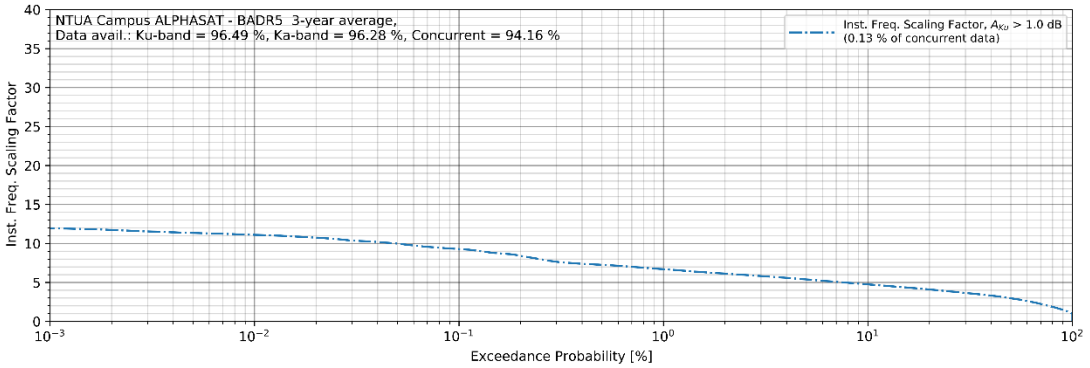

Figure 10-14: IFSF Exceedance Probability, Campus Ku-band BADR5 vs Ka-band ALPHASAT

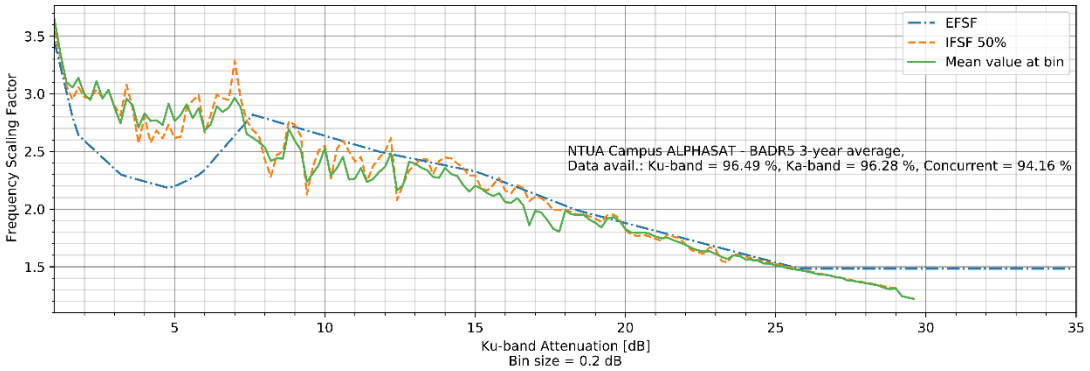

Figure 10-15: Comparison between EFSF, IFSF at 50th percentile and IFSF mean value, Campus Ku-band BADR5 vs Ka-band ALPHASAT

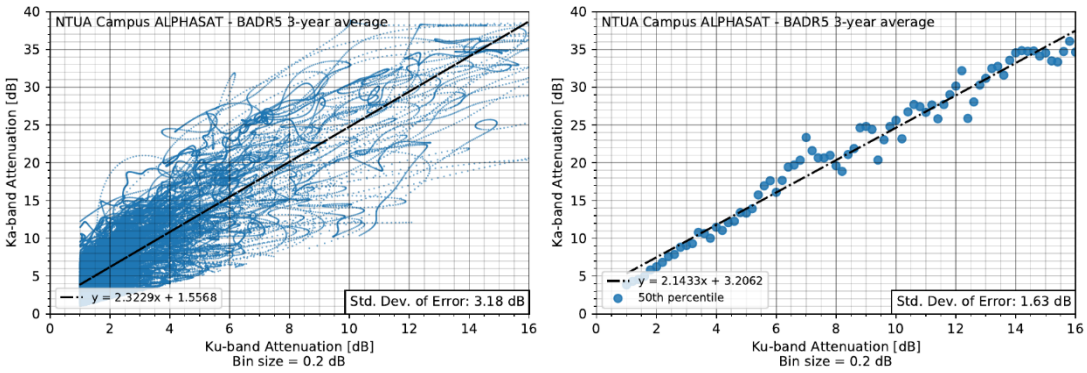

Figure 10-16: Scatter plot Excess Attenuation Campus Ku-band BADR5 vs Ka-band ALPHASAT with linear regression fitting (left: all data, right: data at 50th percentile)

10.2.9 Campus Ku-band BADR5 vs Campus Q-band ALPHASAT frequency scaling

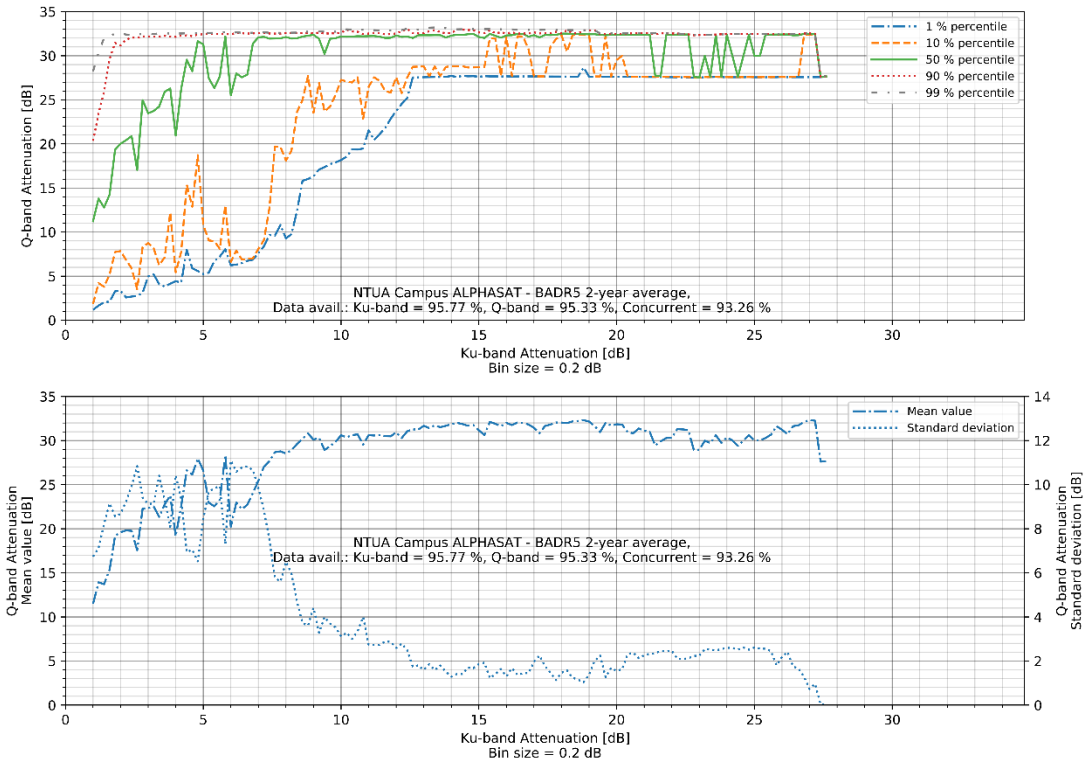

Figure 10-17: Campus Ku-band BADR5 vs Q-band ALPHASAT excess attenuation

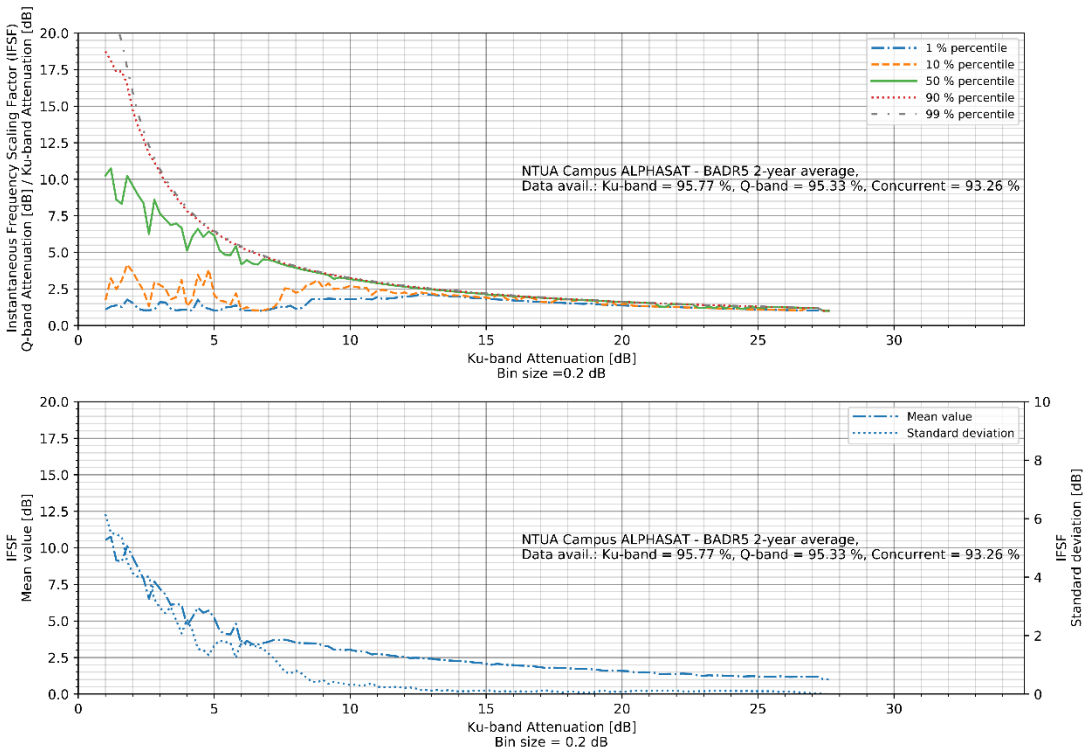

Figure 10-18: Instantaneous Frequency Scaling Factor (IFSF), Campus Ku-band BADR5 vs Q-band ALPHASAT

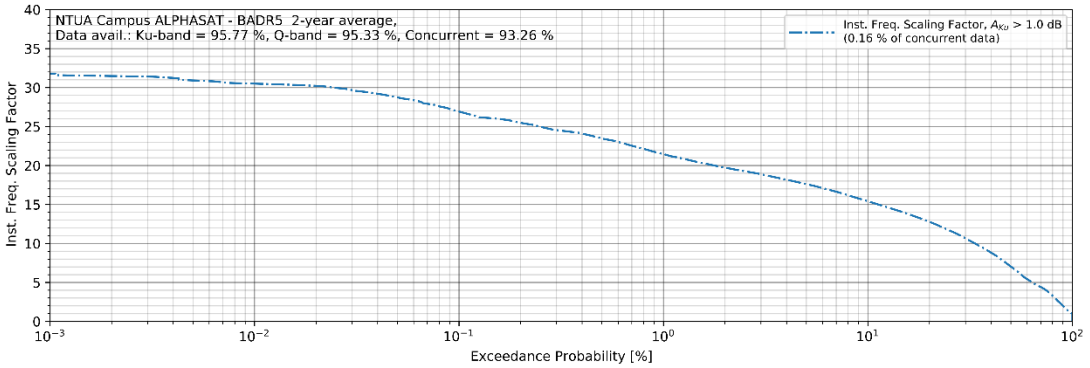

Figure 10-19: IFSF Exceedance Probability, Campus Ku-band BADR5 vs Q-band ALPHASAT

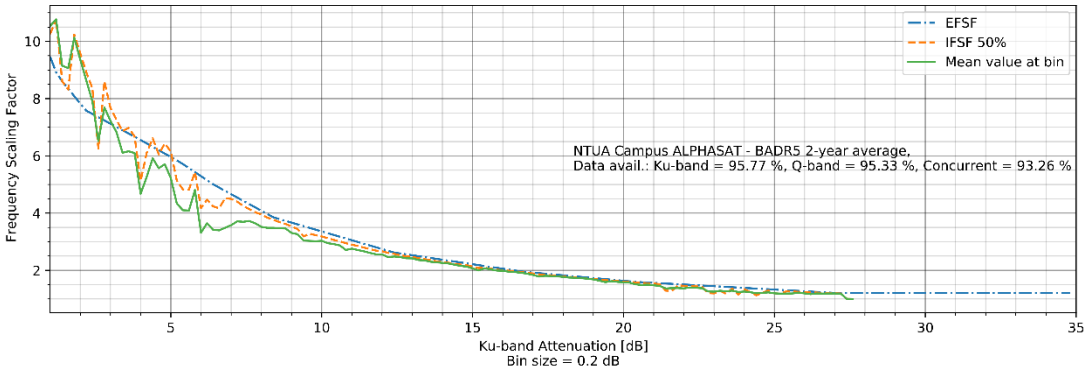

Figure 10-20: Comparison between EFSF, IFSF at 50th percentile and IFSF mean value, Campus Ku-band BADR5 vs Q-band ALPHASAT

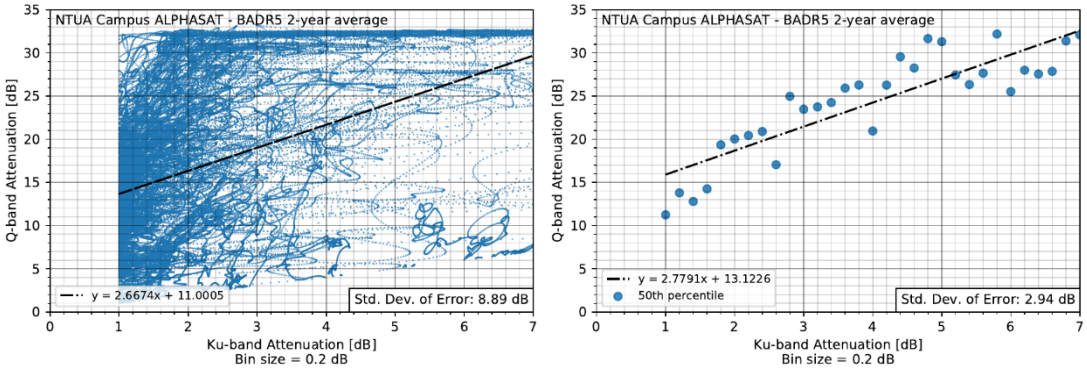

Figure 10-21: Scatter plot Excess Attenuation Campus Ku-band BADR5 vs Q-band ALPHASAT with linear regression fitting (left: all data, right: data at 50th percentile)

10.3 Discussion

The results obtained suggest the following values for the Instantaneous Frequency Scaling Factor at the 50th percentile ($IFSF_{50\%}$) for the frequency groups:

- IFSF Ka vs Q-band:
  - around 2.5 to 3 (slight deviations) estimated using Campus data
  - around 3.5 (very stable) estimated using LTCP data
- IFSF Ku vs Ka:
  - Around 2.0 to 3 (linearly decreasing with higher attenuation values) estimated using Campus data
- IFSF Ku vs Q:
  - 11 to 7 (exponentially decreasing with higher attenuation values) estimated using Campus data

An interesting observation is that the EFSF, $IFSF_{50\%}$ and mean IFSF (per attenuation bin) values are in very good accordance for attenuation values higher than 5 dB for the Ka-Q case, 10 dB for the Ku-Ka case; for the Ku-Q case there is no appreciable correspondence.

Trying a plain linear regression fit on the attenuation values at the 50th percentile of each bin, great results were obtained for the Ka-Q bands case resulting in an RMS error of 0.71 and 0.99 dB for LTCP and Campus respectively. For the Ku-Ka bands couple, the resulting regression line still provides a good fit with an RMS error of 1.63 dB, while for the Ku-Q bands case, the error grows significantly to 2.94 dB. When fitting the whole dataset, again acceptable results are obtained for the Ka-Q bands case with an RMS error of 3.08 dB for Campus and 2.98 dB for LTCP; for the Ku-Ka case the rms error is 3.18 while for Ku-Q it is 8.89 dB. The simple regression formulas obtained from this evaluation could therefore be employed in the context of frequency scaling predictions with substantial ease and without any major errors (except for the Ku-Q case).

10.4 Chapter References

[1] J. D. Laster and W. L. Stutzman, "Frequency scaling of rain attenuation for satellite Communications links", *IEEE Transaction on Antennas and Propagation*, Vol. 43, No. 11, Nov. 1995, pp 1207-1215.

Chapter 11

Scintillation Analysis

In this chapter the effects of scintillation, i.e., the rapid fluctuation of the received signal level due to changes in the refractive index of the atmosphere are investigated based on the collected measurements. The analysis is performed similar to [1], [2] while the relevant mathematical background can be found in [3].

In the following figures, two examples of scintillation effects encountered at the Campus location are shown for a dry day during the summer (04/08/2017) and a rainy day during the spring season (05/05/2018); both figures have been obtained after high-pass filtering the obtained attenuation timeseries using a Butterworth filter of 5th order at a 3-dB cut-off frequency of 0.025 Hz [3].

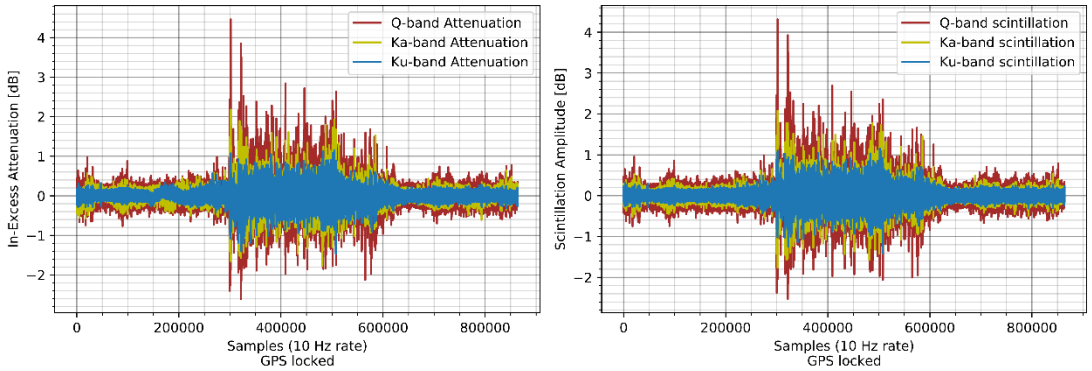

Figure 11-1: Example of scintillation effects at the Campus site for a dry summer day

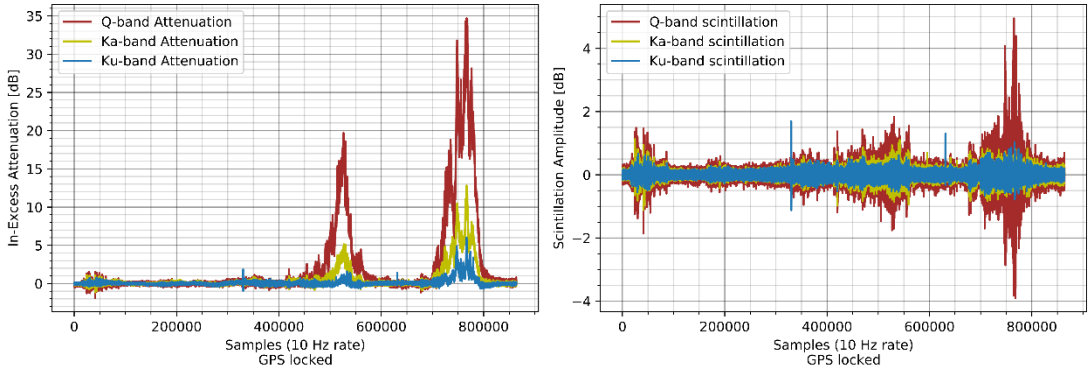

Figure 11-2: Example of scintillation effects at the Campus site for a rainy day during the spring

11.1 Evaluation parameters

For this study, the data collected at the full available sampling rate (10 Hz) are used to allow for better insight of the underlying phenomena. The following parameters are evaluated for all frequency bands at both campaign locations:

- Signal spectral analysis
  - overall, wet
  - yearly, monthly, daily

  In order to calculate the signal power spectrum, the power spectral density (PSD, units dB^2 /Hz), of each signal was computed on blocks of 18000 samples accounting for 30 minutes of duration per block (zero-padded if required). Each block has been split into half-overlapping chunks of 6000 samples upon which Fast Fourier Transform is performed, after having removed the mean from each chunk and multiplied it by a Hanning window $w(n) = 0.5 - 0.5\cos\left(\frac{2\pi n}{M-1}\right), 0 \le n \le M-1$, where M the number of points (6000 in this case) and finally averaging the resulting periodograms (essentially the geometric mean is obtained). The resulting PSD is further smoothed using 3rd order median filtering.

  The identification of rain events (for wet scintillation spectral analysis) is performed using the rainfall data obtained using the collocated tipping bucket rain gauges at each site. To ensure the rain events are fully captured, each event is considered to begin 30 minutes before the first tip and to complete 15 minutes after the last tip, the minimum interval before a new event can be considered is set to 10 minutes.

- Scintillation amplitude analysis
  - Overall, yearly, seasonal
- Diurnal scintillation analysis (1-min intervals)
  - Mean diurnal scintillation intensities,
  - Mean diurnal peak-to-peak scintillation amplitude
  - Scintillation intensities normality test
- Wet scintillation analysis (1-min intervals)
  - Mean scintillation intensity vs mean excess attenuation
  - Mean scintillation intensity vs mean rain rate
  - Mean scintillation intensity vs mean peak-to-peak scintillation amplitude
  - Mean peak-to-peak scintillation amplitude exceedance probability
  - Mean scintillation amplitude exceedance probability

In order to obtain scintillation amplitude timeseries, the 10 Hz attenuation timeseries are high-pass filtered using a Butterworth filter of 5th order at a 3-dB cutoff frequency of 0.025 Hz. These values are compliant with [3] and have been selected upon further own experimentation.

11.2 Results

11.2.1 Scintillation Spectral Analysis

In order to maintain a reasonable thesis length only the yearly spectra are provided, both considering all the data (dry & wet) as well as considering only wet conditions (rain events) during each year.

11.2.1.1 July 2016-June 2017

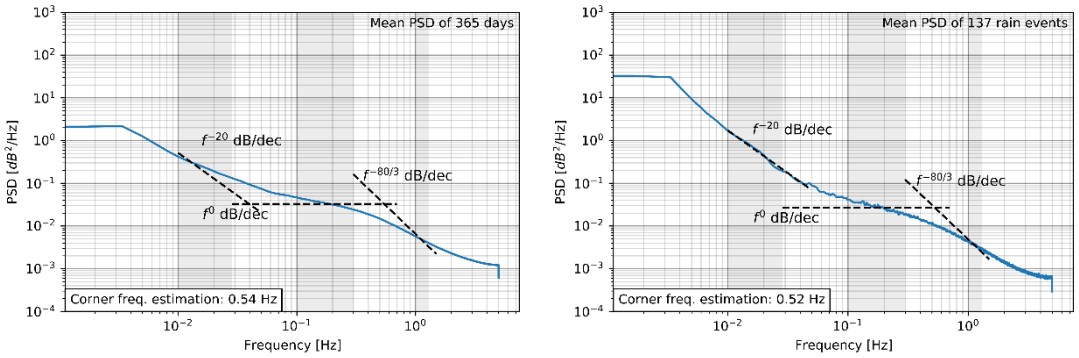

Figure 11-3: Yearly spectra for Campus Ka-band ALPHASAT, 2016-2017

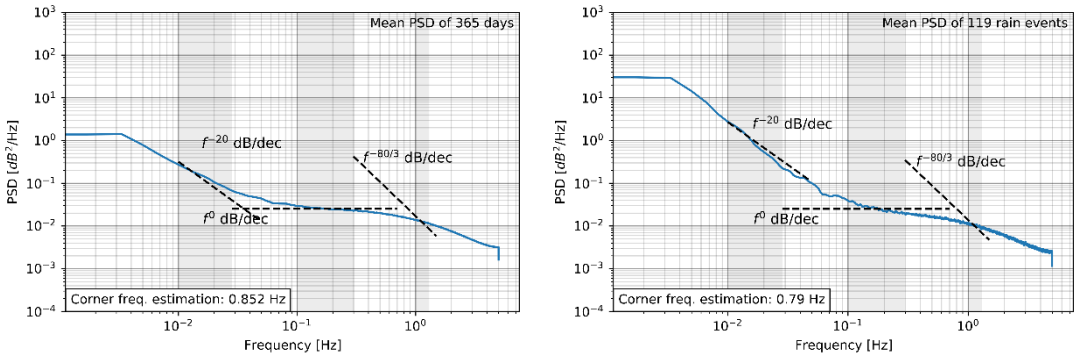

Figure 11-4: Yearly spectra for LTCP Ka-band ALPHASAT, 2016-2017

11.2.1.2 July 2017-June 2018

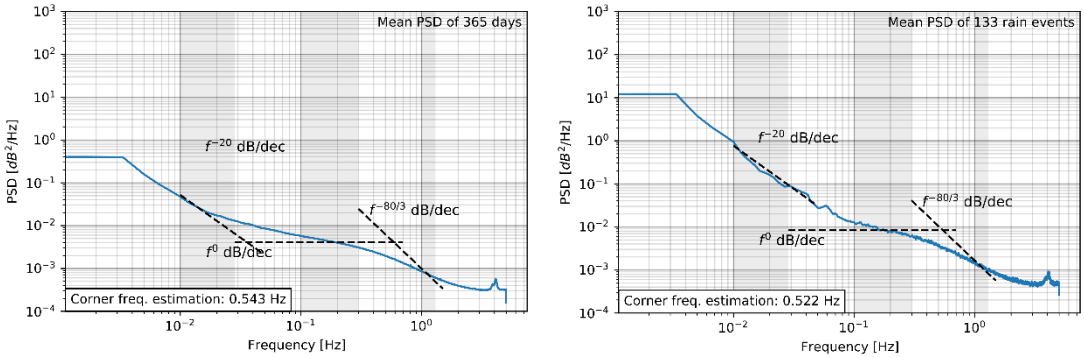

Figure 11-5: Yearly spectra for Campus Ku-band BADR5, 2017-2018

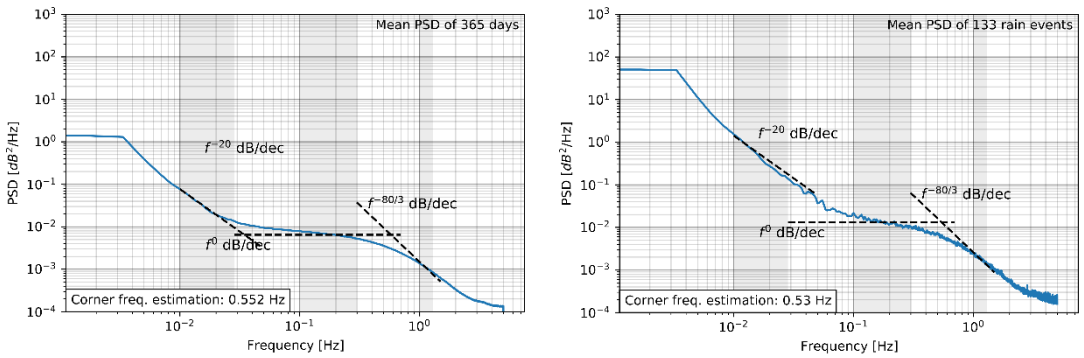

Figure 11-6: Yearly spectra for Campus Ka-band ALPHASAT, 2017-2018

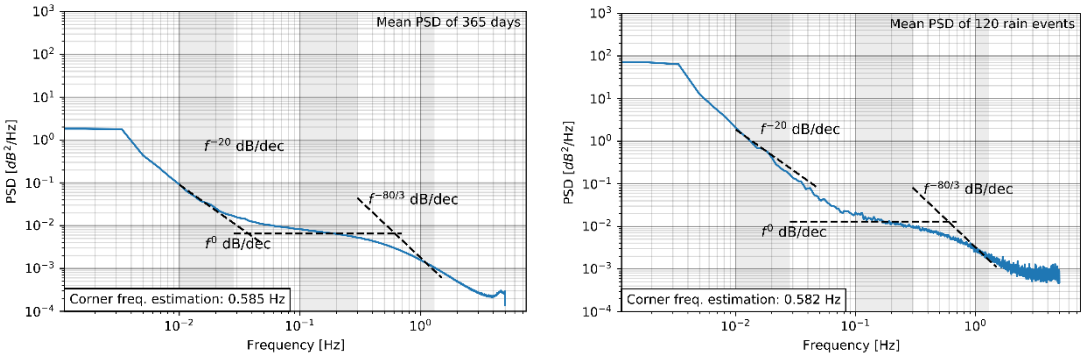

Figure 11-7: Yearly spectra for LTCP Ka-band ALPHASAT, 2017-2018

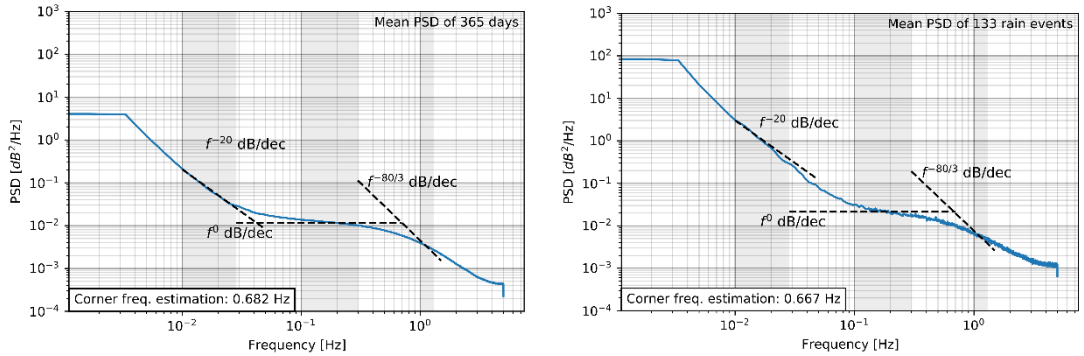

Figure 11-8: Yearly spectra for Campus Q-band ALPHASAT, 2017-2018

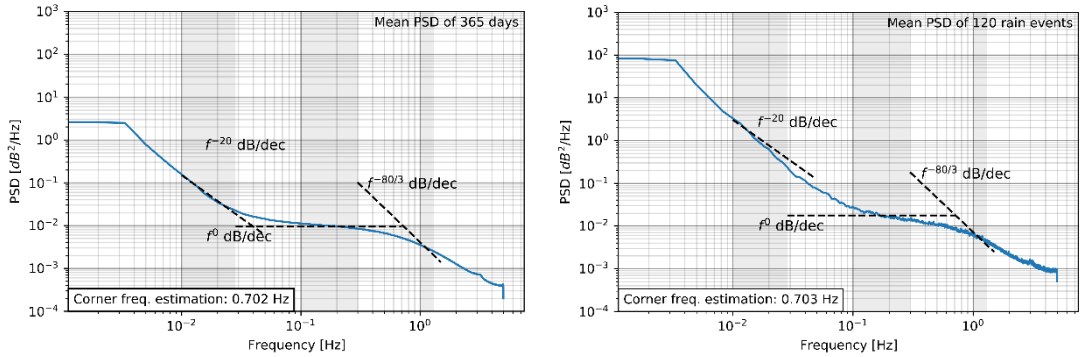

Figure 11-9: Yearly spectra for LTCP Q-band ALPHASAT, 2017-2018

11.2.1.3 July 2018-June 2019

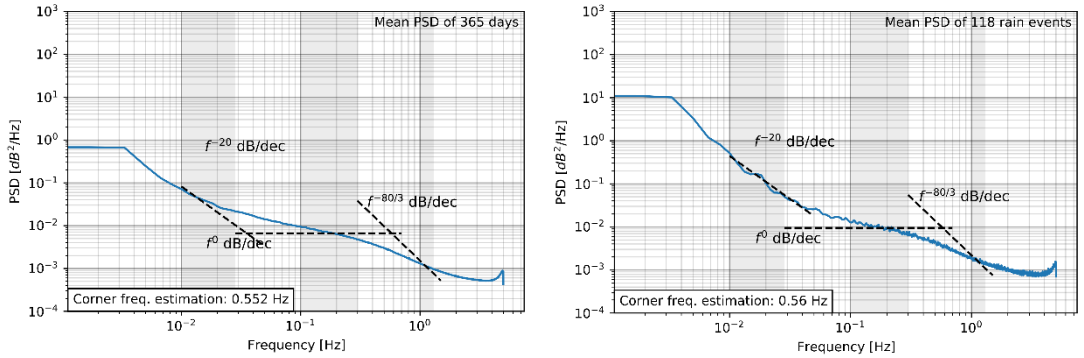

Figure 11-10: Yearly spectra for Campus Ku-band BADR5, 2018-2019

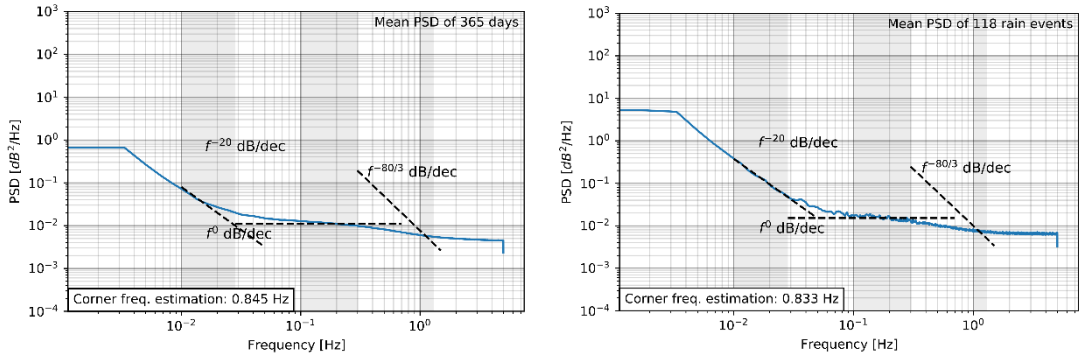

Figure 11-11: Yearly spectra for Campus Ka-band KaSAT, 2018-2019

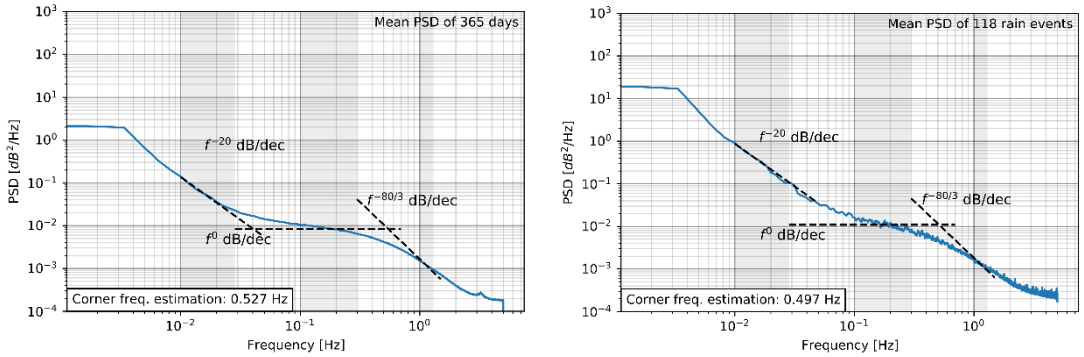

Figure 11-12: Yearly spectra for Campus Ka-band ALPHASAT, 2018-2019

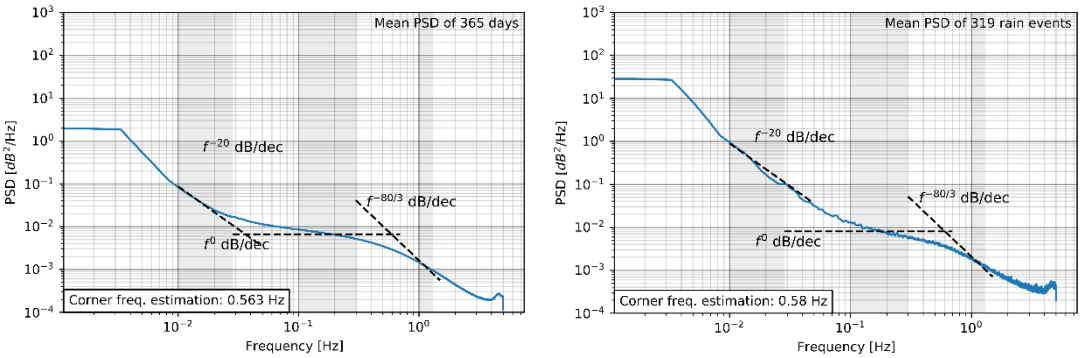

Figure 11-13: Yearly spectra for LTCP Ka-band ALPHASAT, 2018-2019

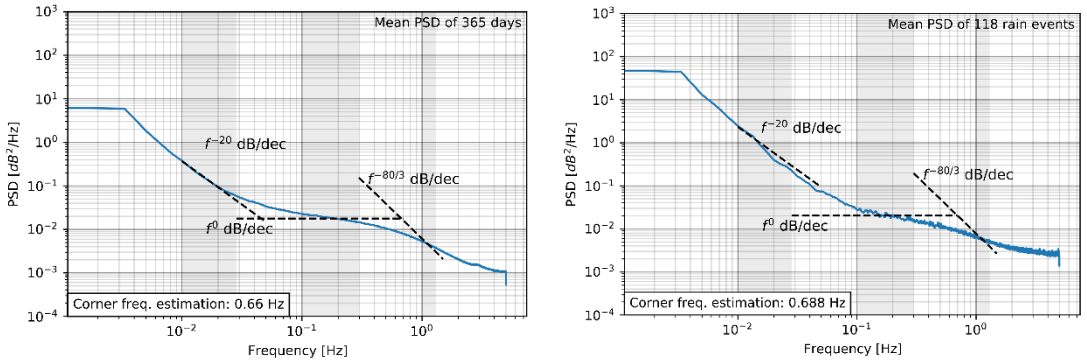

Figure 11-14: Yearly spectra for Campus Q-band ALPHASAT, 2018-2019

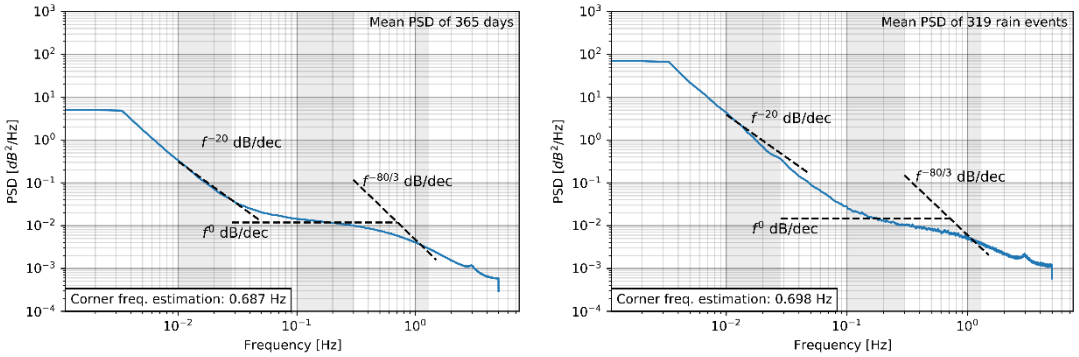

Figure 11-15: Yearly spectra for LTCP Q-band ALPHASAT, 2018-2019

11.2.1.4 July 2019-June 2020

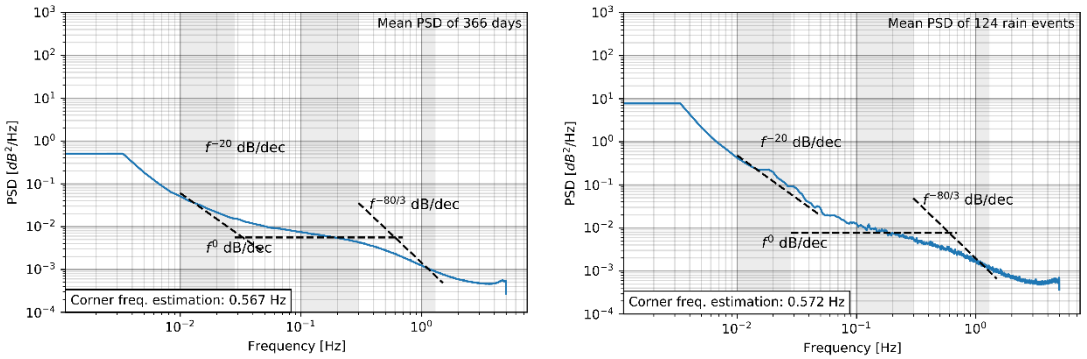

Figure 11-16: Yearly spectra for Campus Ku-band BADR5, 2019-2020

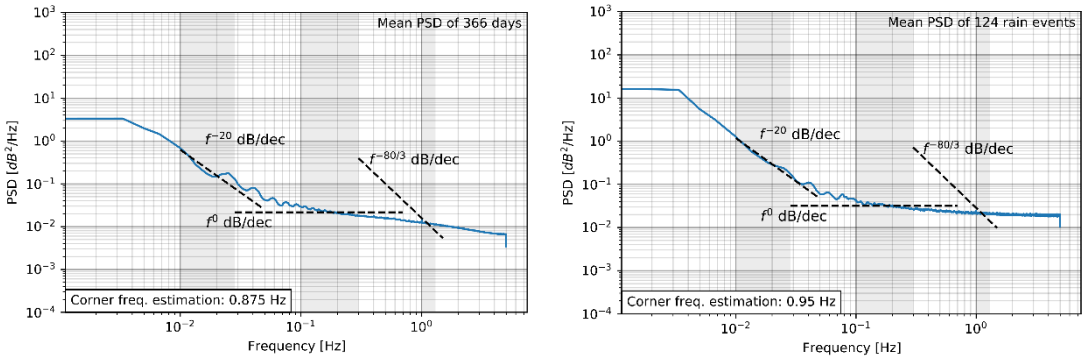

Figure 11-17: Yearly spectra for Campus Ka-band KaSAT, 2019-2020

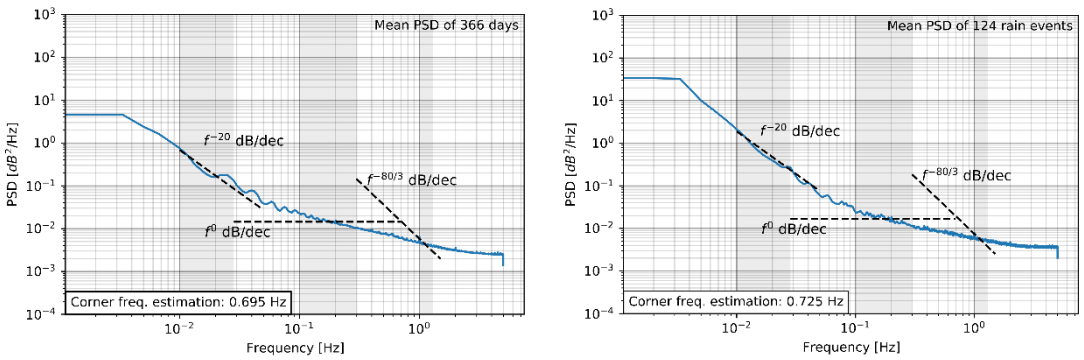

Figure 11-18: Yearly spectra for Campus Ka-band ALPHASAT, 2019-2020

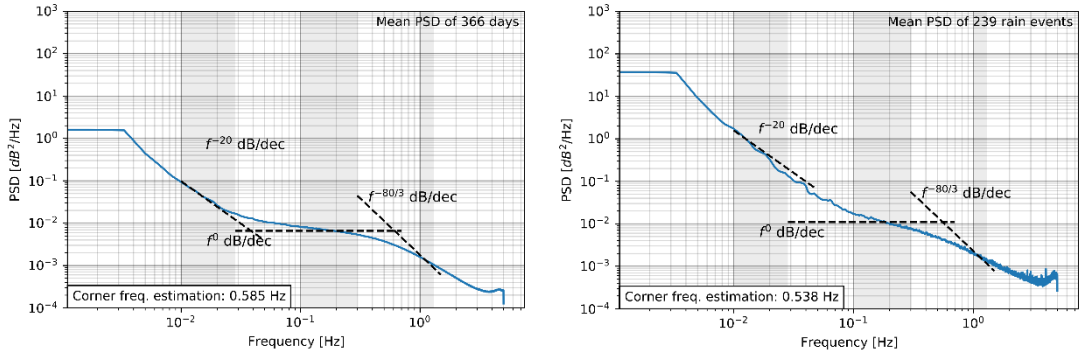

Figure 11-19: Yearly spectra for LTCP Ka-band ALPHASAT, 2019-2020

11.2.2 Scintillation Amplitude Evaluation

To attain a reasonable thesis length, only the overall/yearly, seasonal and diurnal results are presented.

11.2.2.1 Overall/Yearly results

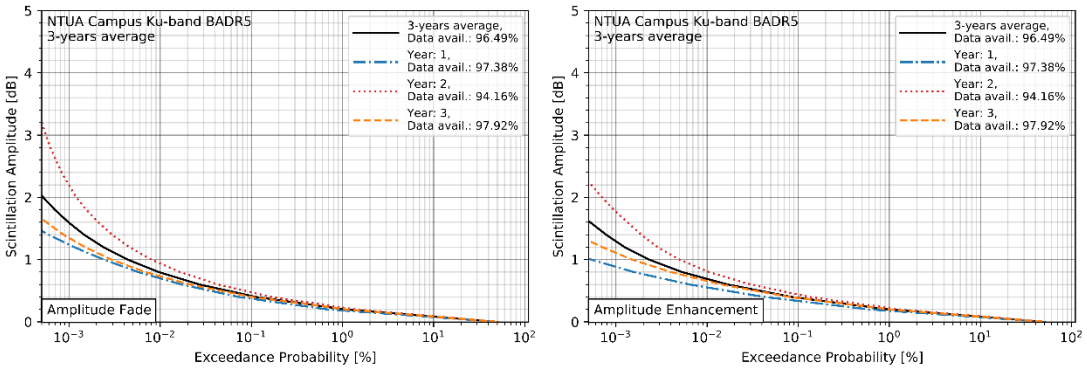

Figure 11-20: Overall and yearly scintillation amplitude fade & enhancement for Campus Ku-band BADR5

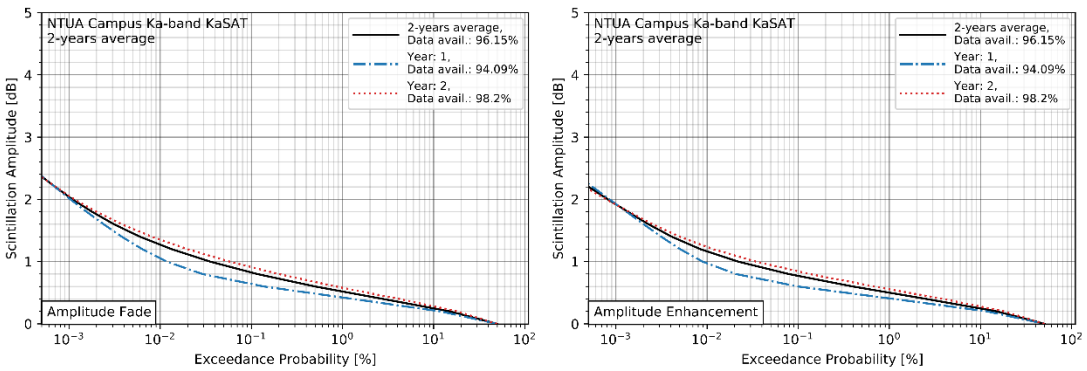

Figure 11-21: Overall and yearly scintillation amplitude fade & enhancement for Campus Ka-band KaSAT

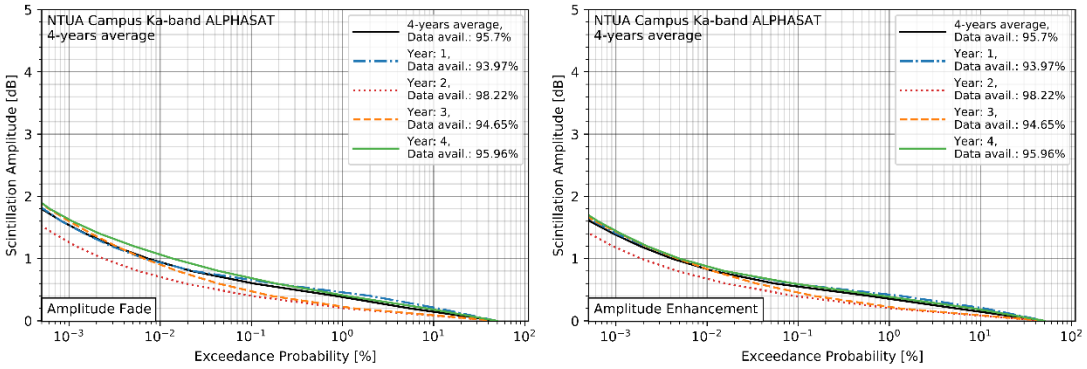

Figure 11-22: Overall and yearly scintillation amplitude fade & enhancement for Campus Ka-band ALPHASAT

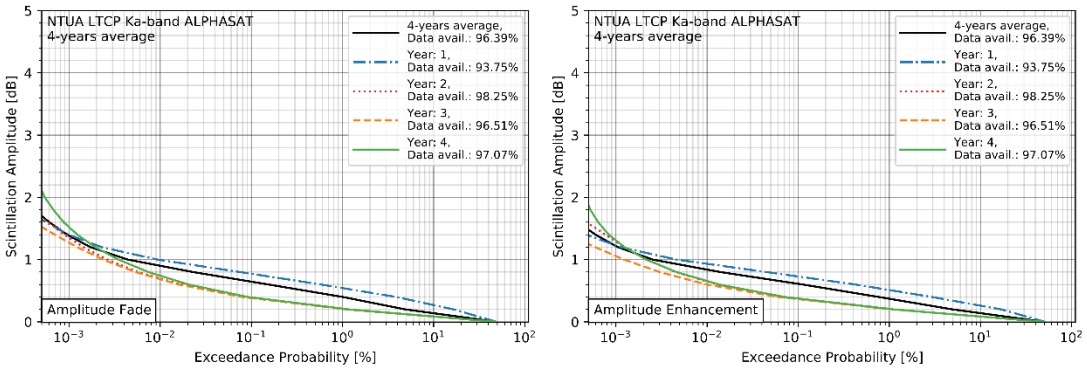

Figure 11-23: Overall and yearly scintillation amplitude fade & enhancement for LTCP Ka-band ALPHASAT

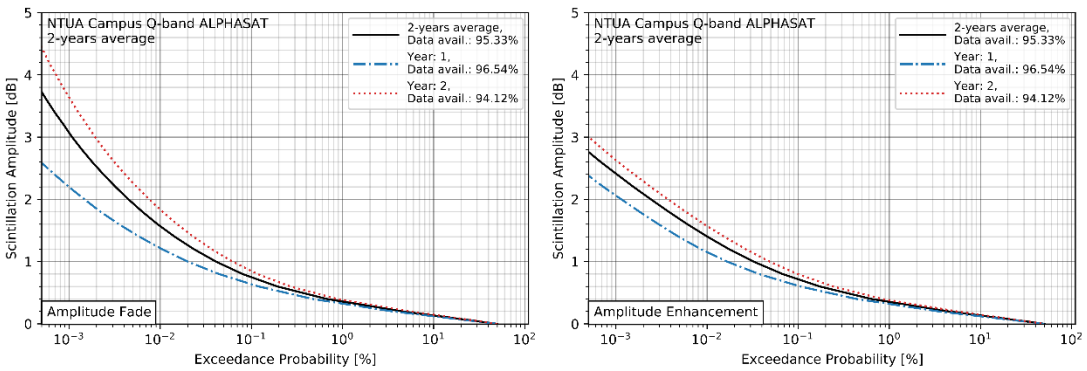

Figure 11-24: Overall and yearly scintillation amplitude fade & enhancement for Campus Q-band ALPHASAT

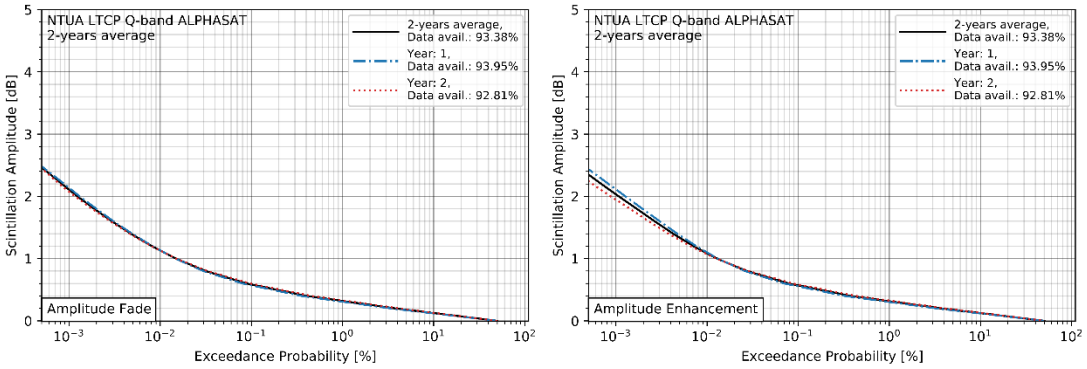

Figure 11-25: Overall and yearly scintillation amplitude fade & enhancement for LTCP Q-band ALPHASAT

11.2.2.2 Seasonal results

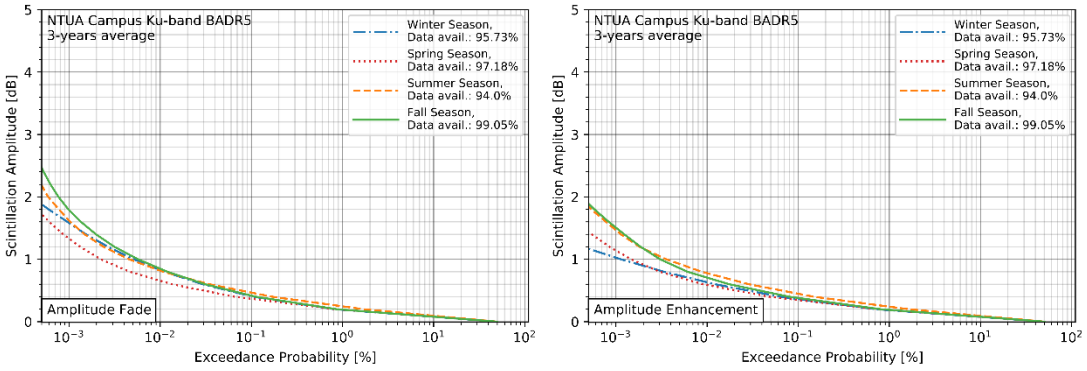

Figure 11-26: Seasonal scintillation amplitude fade & enhancement for Campus Ku-band BADR5

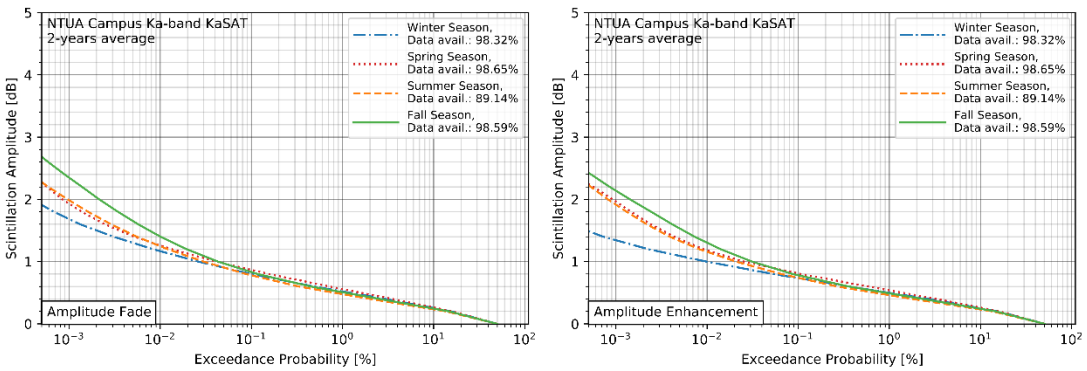

Figure 11-27: Seasonal scintillation amplitude fade & enhancement for Campus Ka-band KaSAT

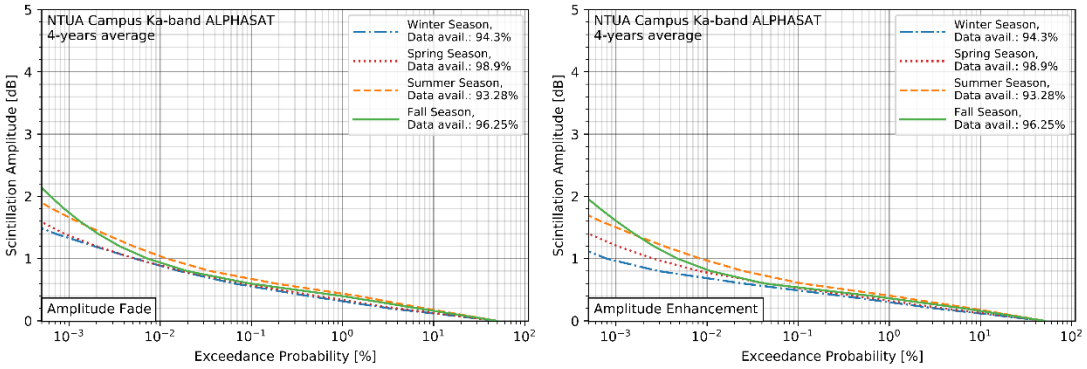

Figure 11-28: Seasonal scintillation amplitude fade & enhancement for Campus Ka-band ALPHASAT

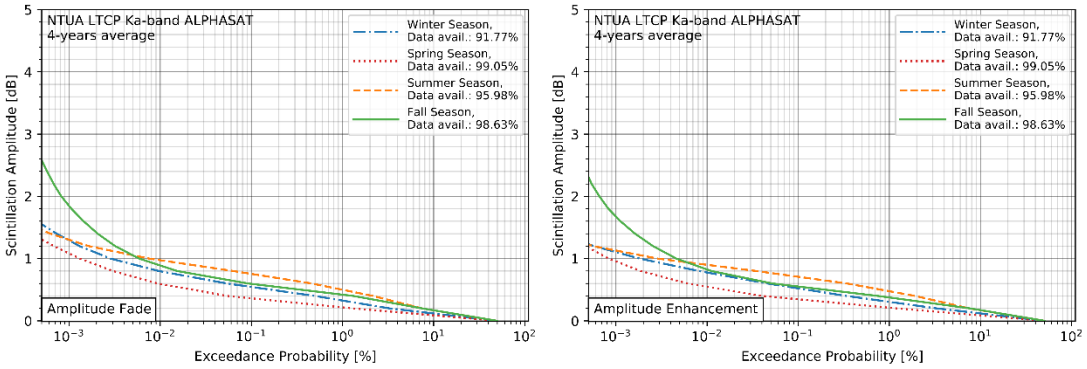

Figure 11-29: Seasonal scintillation amplitude fade & enhancement for LTCP Ka-band ALPHASAT

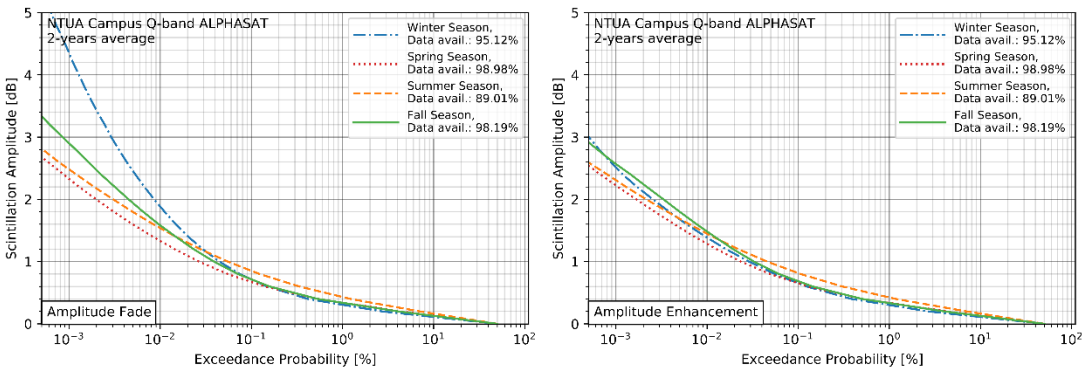

Figure 11-30: Seasonal scintillation amplitude fade & enhancement for Campus Q-band ALPHASAT

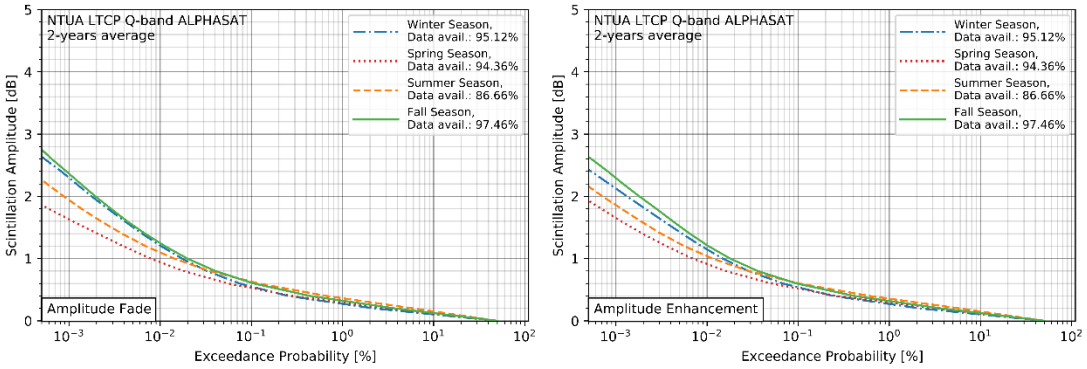

Figure 11-31: Seasonal scintillation amplitude fade & enhancement for LTCP Q-band ALPHASAT

11.2.2.3 Diurnal Scintillation intensities, diurnal peak-to-peak scintillation amplitude analysis, scintillation intensities normality test

11.2.2.3.1 Campus Ku-band BADR5

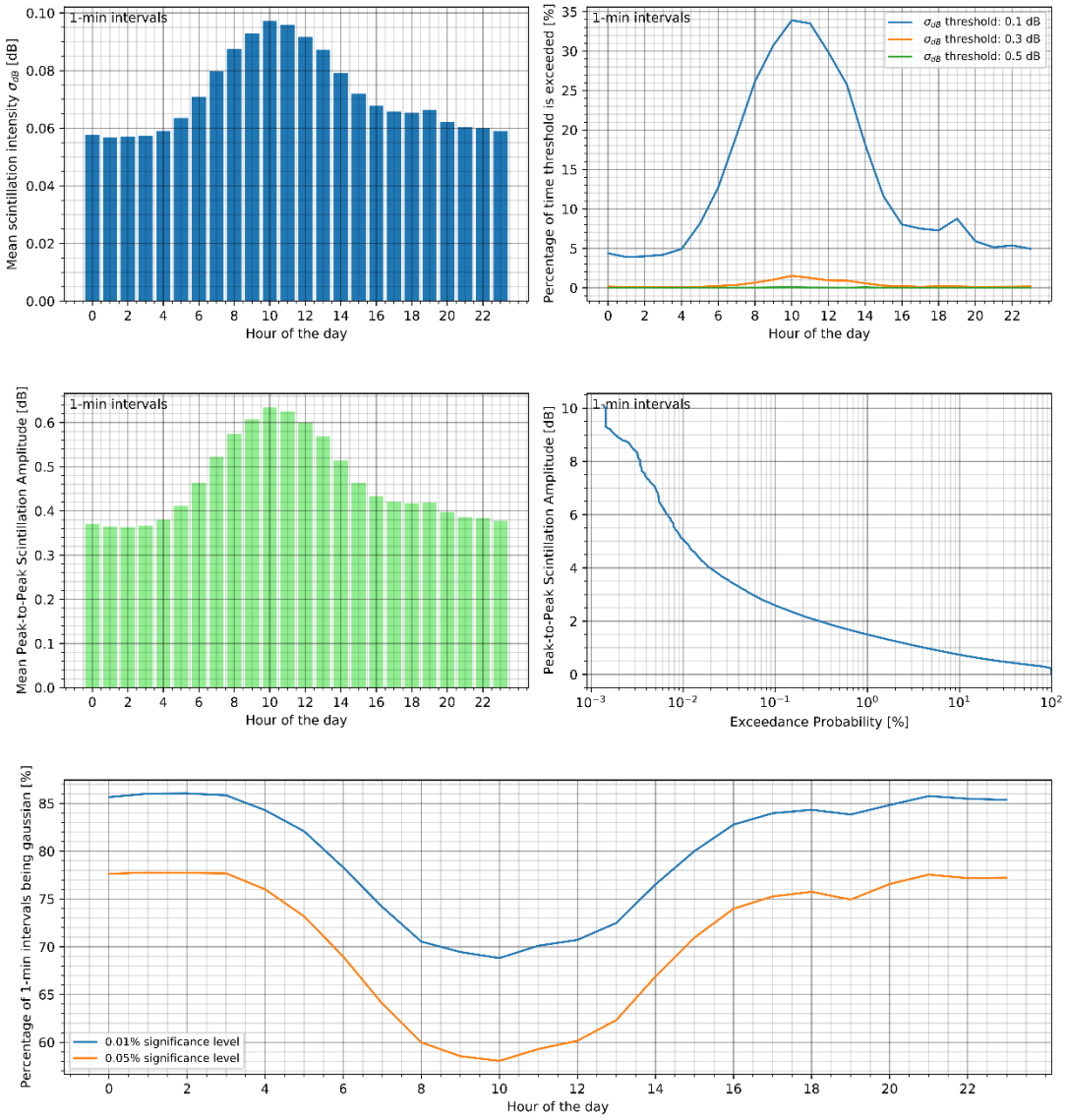

Figure 11-32: Diurnal scintillation analysis Campus Ku-band BADR5

11.2.2.3.2 Campus Ka-band KASAT

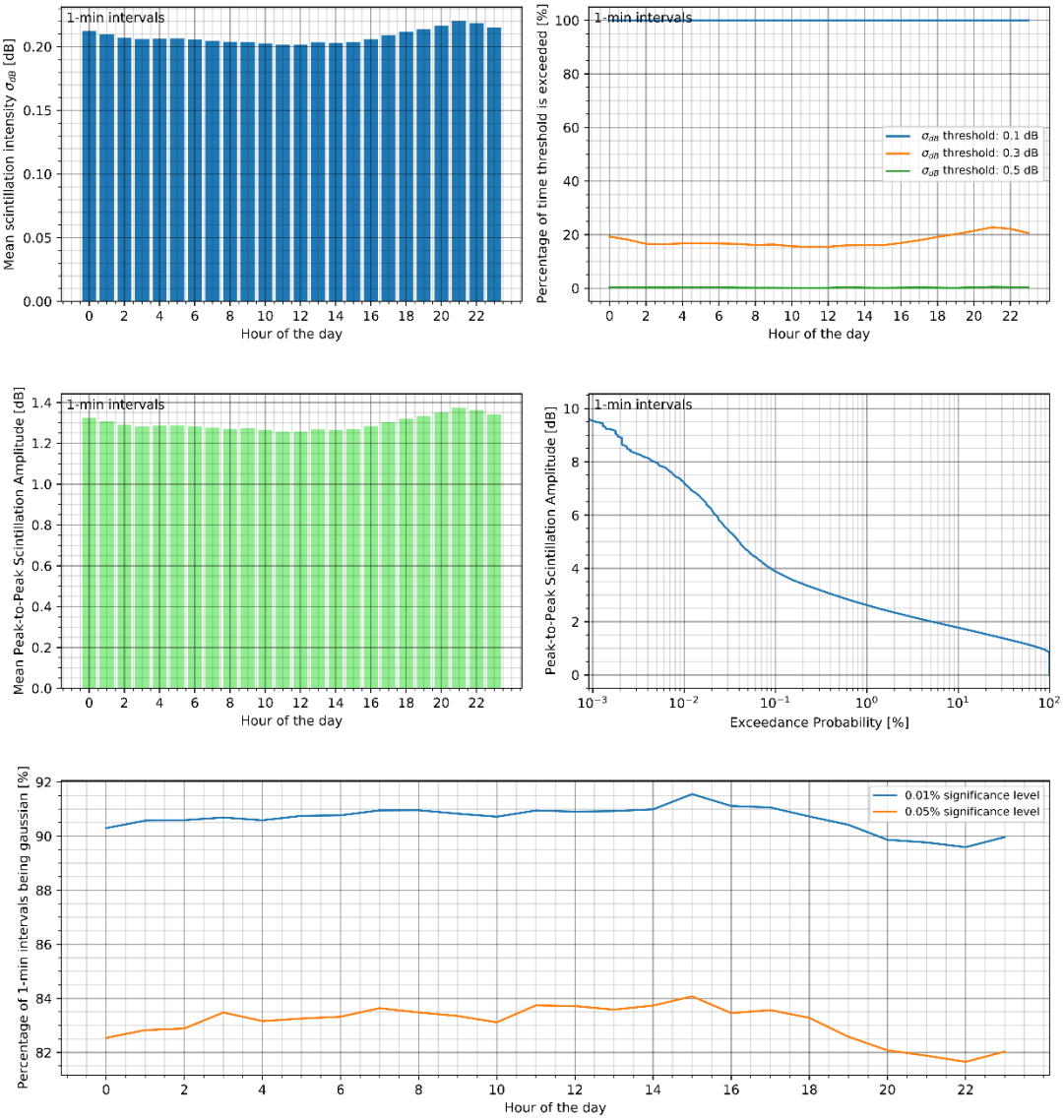

Figure 11-33: Diurnal scintillation analysis Campus Ka-band KaSAT

11.2.2.3.3 Campus Ka-band ALPHASAT

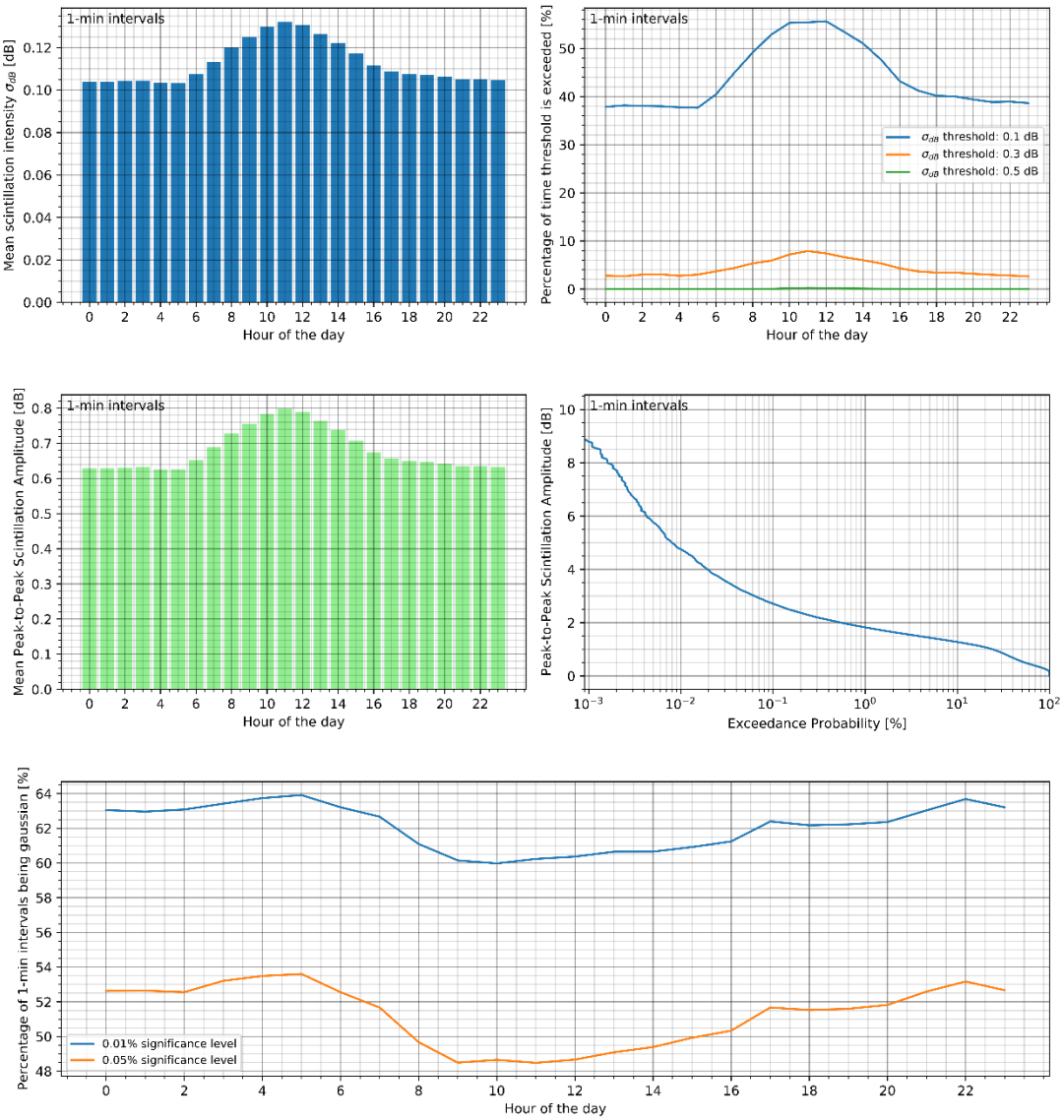

Figure 11-34: Diurnal scintillation analysis Campus Ka-band ALPHASAT

11.2.2.3.4 LTCP Ka-band ALPHASAT

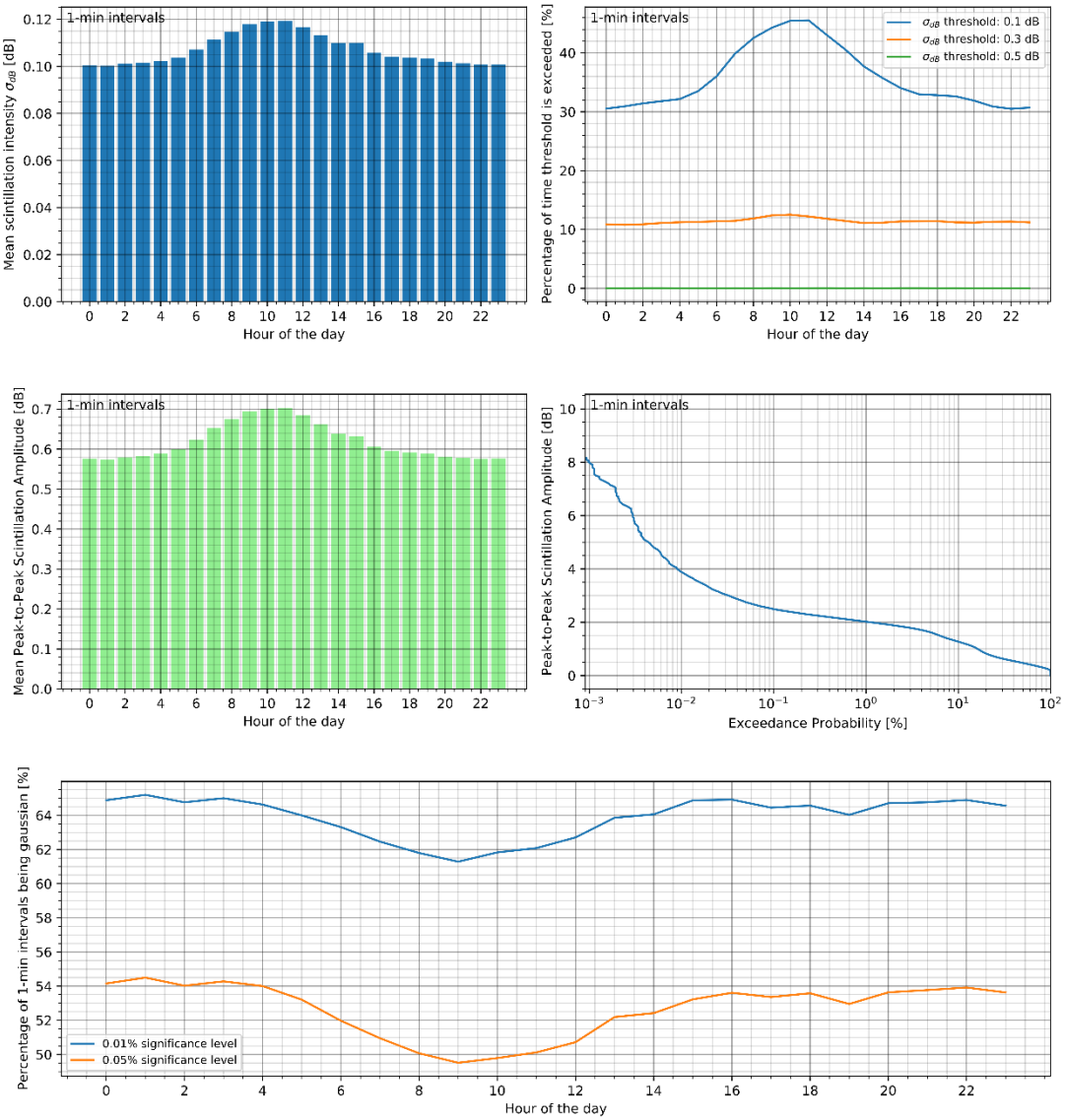

Figure 11-35: Diurnal scintillation analysis LTCP Ka-band ALPHASAT

11.2.2.3.5 Campus Q-band ALPHASAT

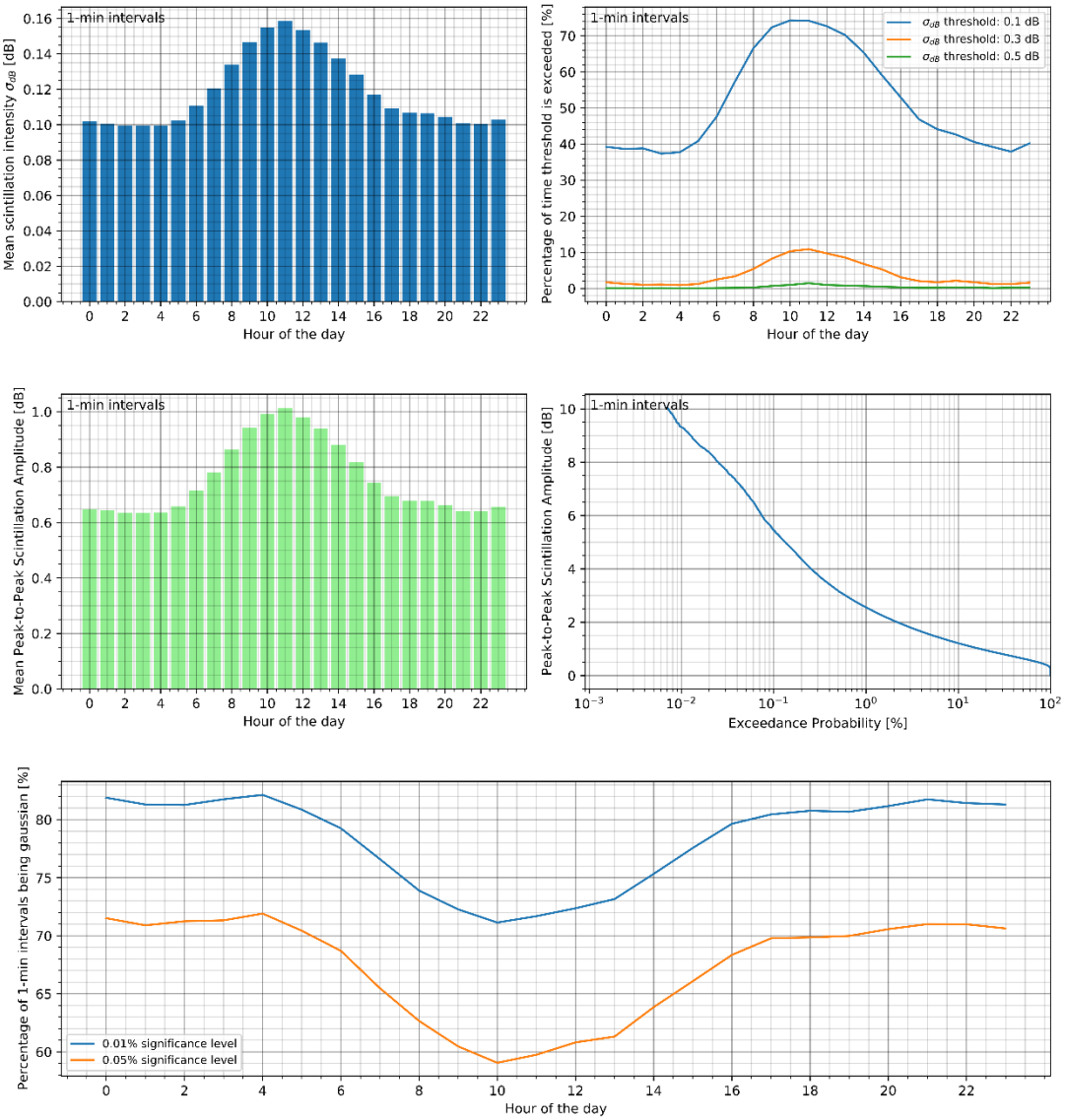

Figure 11-36: Diurnal scintillation analysis Campus Q-band ALPHASAT

11.2.2.3.6 LTCP Q-band ALPHASAT

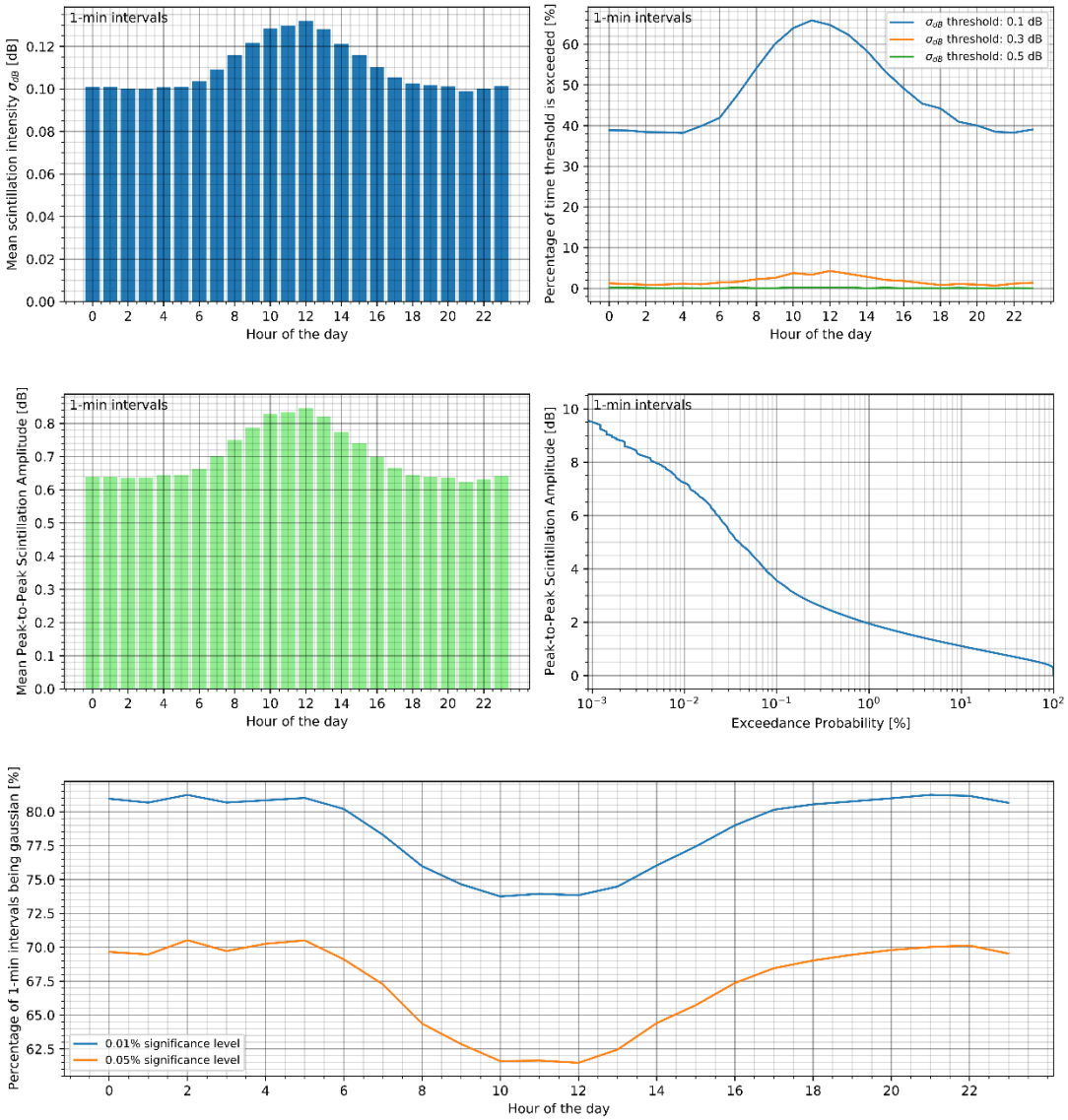

Figure 11-37: Diurnal scintillation analysis LTCP Q-band ALPHASAT

11.2.3 Wet scintillation analysis (1-min intervals)

11.2.3.1 Campus Ku-band BADR5

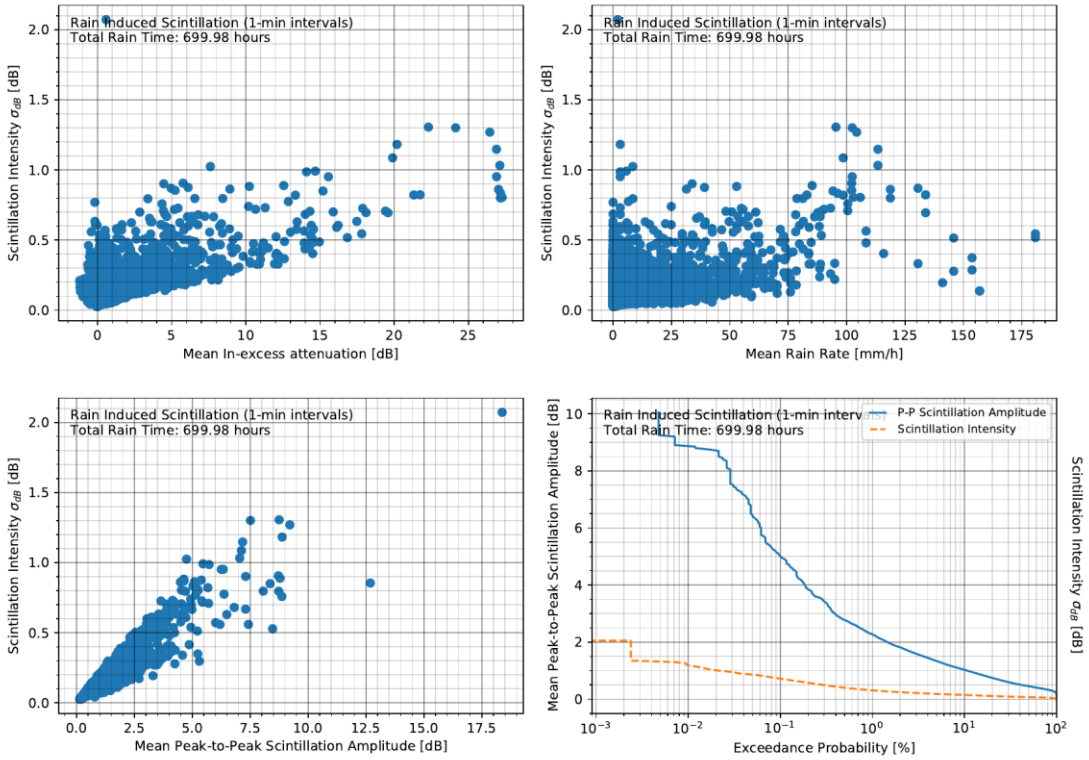

Figure 11-38: Wet scintillation analysis for Campus Ku-band BADR5

11.2.3.2 Campus Ka-band KaSAT

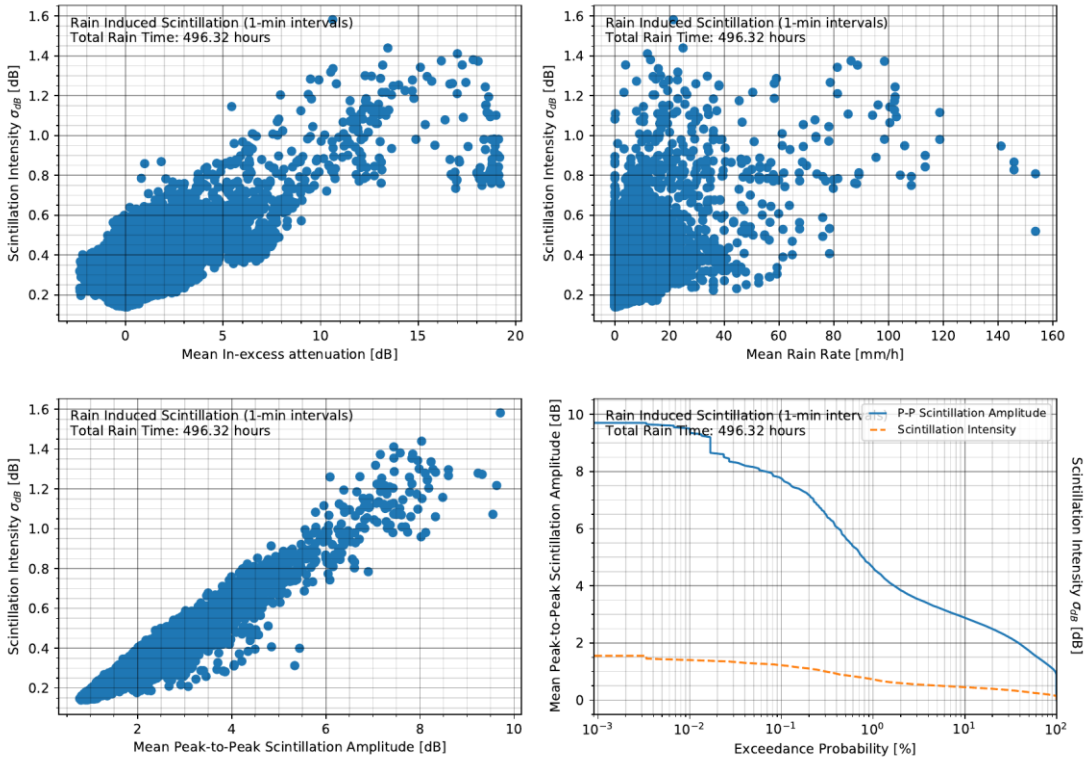

Figure 11-39: Wet scintillation analysis for Campus Ka-band KaSAT

11.2.3.3 Campus Ka-band ALPHASAT

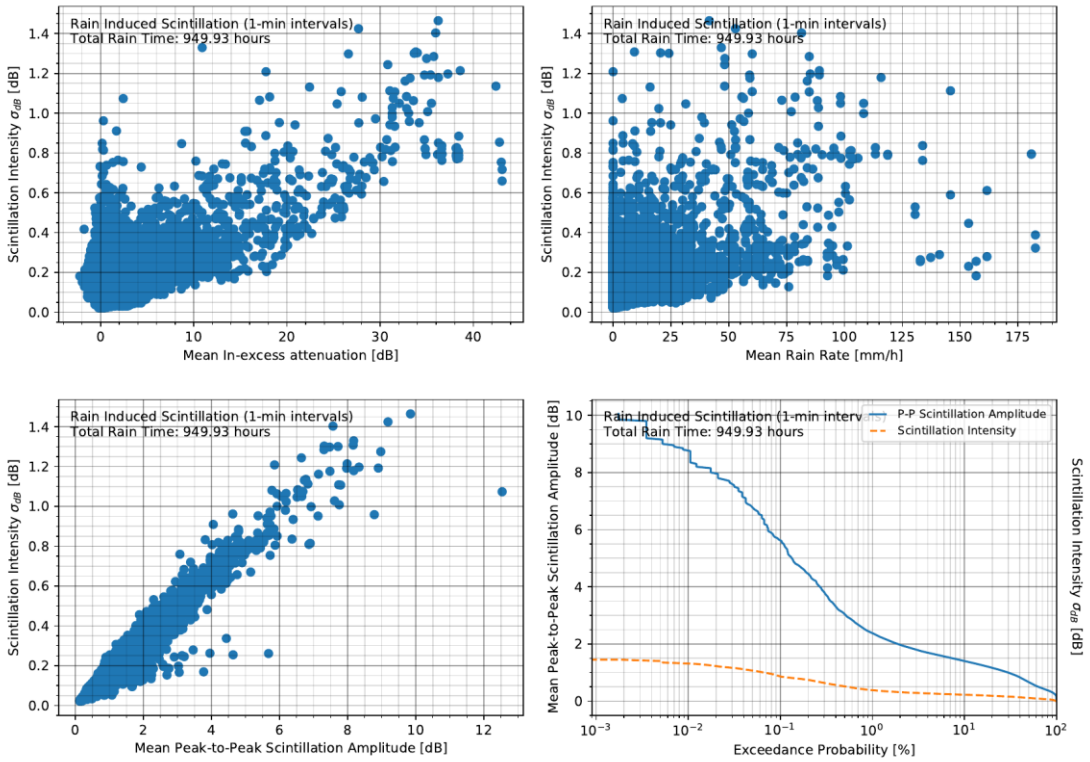

Figure 11-40: Wet scintillation analysis for Campus Ka-band ALPHASAT

11.2.3.4 LTCP Ka-band ALPHASAT

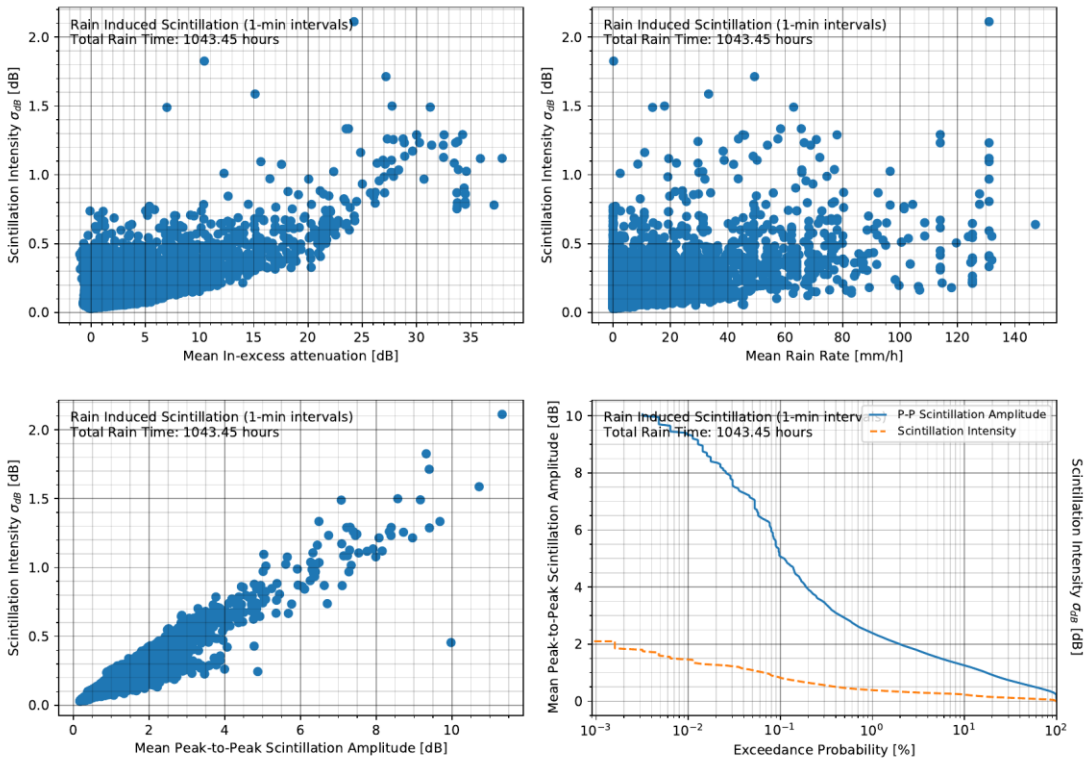

Figure 11-41: Wet scintillation analysis for LTCP Ka-band ALPHASAT

11.2.3.5 Campus Q-band ALPHASAT

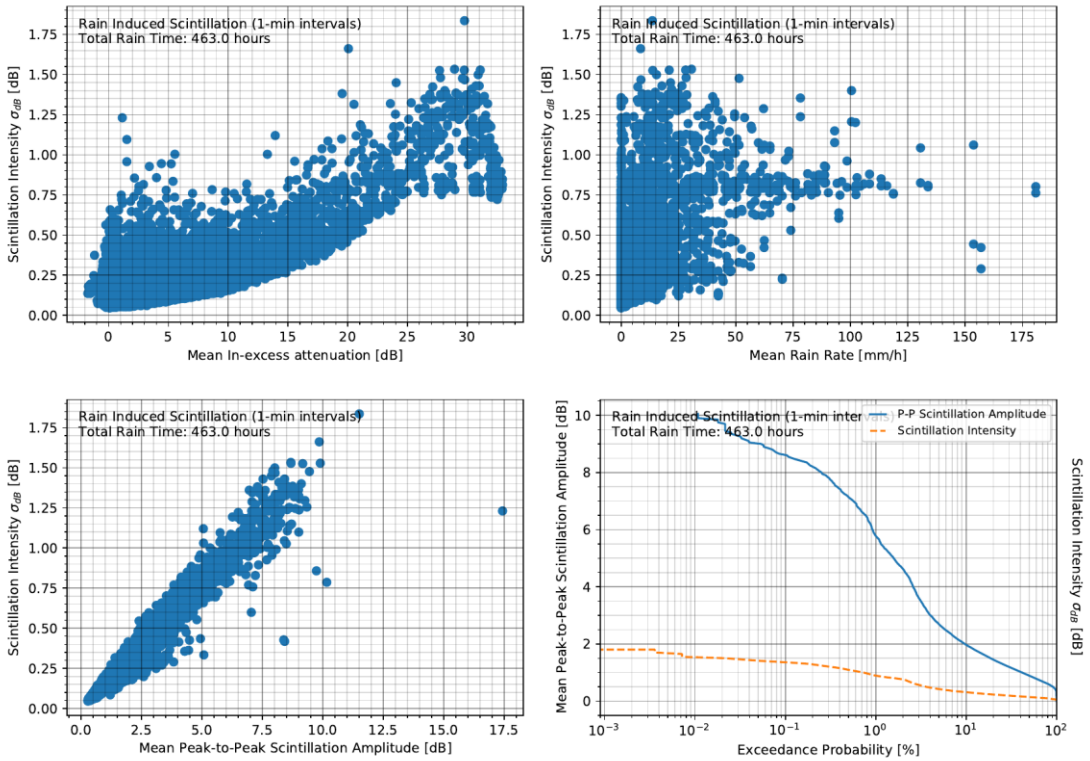

Figure 11-42: Wet scintillation analysis for Campus Q-band ALPHASAT

11.2.3.6 LTCP Q-band ALPHASAT

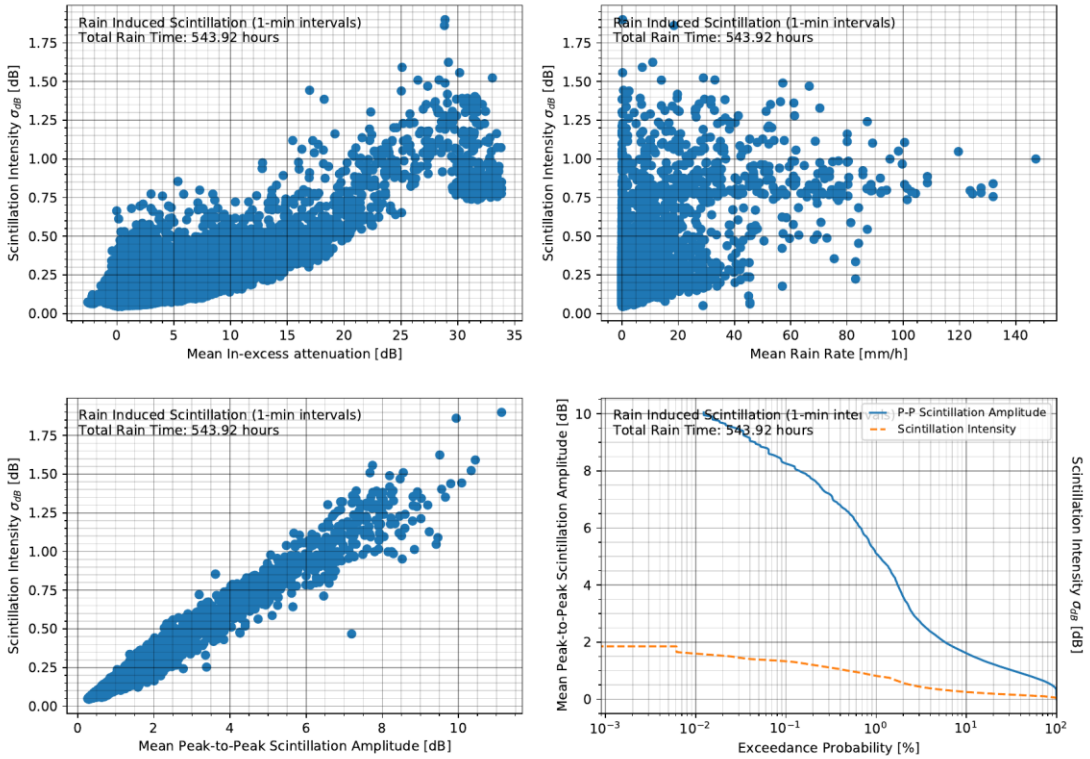

Figure 11-43: Wet scintillation analysis for LTCP Q-band ALPHASAT

11.3 Discussion

Scintillation is an effect that can play an important role in the performance of an earth-space link as not all signal fluctuations can be compensated for using an Automatic Gain Control (AGC) loop on the receiving end of a link; more particularly, systems operating at Q-band can show significant power excursions around the median signal value. In any case, as shown in the above analysis, due to the relatively high elevation angles used throughout these measurements, scintillation does not appear to be a major bottleneck, especially during dry conditions.

Regarding the spectral analysis, the derived results seem to be in good accordance to the theoretical ones. It is difficult to fully isolate scintillation from other effects, especially using an outdoor experimental setup since wind gusts can affect the pointing accuracy of the antennas and induce signal fluctuations. Also, when averaging multiple spectra (as is the case in the yearly spectra presented), high noise levels that could have randomly occurred for a short period of time can negatively influence the results. In any case, using the above methodology as well as thanks to the wind-loading countermeasures taken at the antenna mounts and tracking systems, such effects have hopefully been minimized. An exception might be the results obtained for the Ka-band using KASAT, where the presence of noise is quite evident in the calculated spectra, probably disqualifying them from further practical consideration.

For approximately equal elevation angles, it has been shown that although a difference in scintillation amplitude exists across Ku and Ka band, it is not substantial; on the contrary, Q-band seems to exhibit almost double scintillation amplitude values, especially during rainy conditions. It is worth noting that the “total rain time” mentioned in the wet scintillation analysis figures refers to the total duration of events the way they processed (as explained in the introduction of this chapter) and not to the actual accumulate rainfall time.

Regarding the seasonality of the scintillation effects, it seems that the summer season seems to be associated with higher scintillation for high exceedance probabilities (namely higher than 0.05% of the time) while fall is linked with higher scintillation amplitudes for lower exceedance probabilities. It is also worth pointing out that according to the diurnal analysis, the interval between 6:00 am to 16:00 pm (UTC) consistently seems to yield higher values of scintillation intensity (in dB), which can be attributed to the higher gaseous concentration in the atmosphere, higher probability of rain, as well as in higher wind speeds occurring during daytime.

11.4 Chapter References

[1] I. E. Otung, M. O. Al-Nuaimi and B. G. Evans, "Extracting scintillations from satellite beacon propagation data," in *IEEE Transactions on Antennas and Propagation*, vol. 46, no. 10, Oct. 1998, pp. 1580-1581.

[2] I.E. Otung, Amplitude scintillation of Ka-band satellite signals, PhD Thesis, University of Surrey, 1995

[3] E. Matricciani, M. Mauri, C. Riva, "Relationship between scintillation and rain attenuation at 19.77 GHz", *Radio Science*, vol. 31, no. 2, 1996, pp. 273– 279.

Chapter 12

Large Scale Site Diversity: Greece – UK

The research novelty presented in this chapter is that it evaluates and compares the statistical performance of the site diversity technique based on 2-year measurements at two vastly different climatic regions within Europe: Greece (Southern Mediterranean climate) and Southern England (North Atlantic climate).

Greece is well-known for its Mediterranean climate with irregular whilst intense rainfalls (convective precipitation) as well as for its long and hot summers; in particular Greece has been known to suffer from heavy storms and rain commonly originating from the west because of its unique location and terrain morphology.

On the other hand, the United Kingdom is characterized by frequent showers throughout the entire year (stratiform precipitation) with small temperature fluctuations between different seasons. For both regions the measurement data were acquired using the Alphasat SCIEX Ka-band beacon signal in the framework of the European Space Agency (ESA) ASALASCA propagation experiment [1]. RAL Space, who led the ASALASCA consortium, is responsible for the site diversity experiment in England while the Radio and Satellite Communications Group at the National Technical University of Athens (NTUA), also member of the ASALASCA consortium, is responsible for the experimental campaign in Greece.

Figure 12-1: View of the experimental locations in Greece and the UK along with the traces of the slant paths to Alphasat

Table 12-1: Experimental Campaign Receivers' Sites

Locations	Longitude, Latitude	Altitude a.m.s.l.*	Azimuth Angle	Elev. Angle
Greece, Athens NTUA Campus	37.98° N 23.79° E	0.21 km	178.03°	45.97°
Greece, Lavrion NTUA LTCP	37.72° N 24.05° E	0.02 km	178.44°	46.26°
UK, Chilbolton	51.15° N 1.43° W	0.1 km	147.45°	26.40°
UK, Chilton	51.57° N 1.29° W	0,1 km	147.77°	26.07°

*above mean sea level

12.1 Receivers' Details

The ongoing experimental campaign described in this paper takes place at four sites in total, two in Greece (Athens and Lavrion, about 36.5 km apart) and two in the UK (Chilbolton and Chilton, 47.8 km apart); such a configuration enables the study of site diversity schemes in small- and large-scale distances. The Ka-band beacon signal transmitted by ALPHASAT is a constant power Continuous Wave (CW) (unmodulated signal) at 19.701 GHz. The ground terminals receive and measure the beacon power to extract the signal attenuation induced by its propagation through the atmosphere.

12.1.1 Receivers in Greece

More details on the Greek receivers can be found in **Chapter 4** of this thesis.

12.1.2 Receivers in the UK

RAL Space has installed four receivers targeting both Ka- and Q- bands; the receivers are located at Chilbolton and Chilton (47.8 km apart) and have been successfully used again in past propagation measurement campaigns.

They use 50 cm lens horn antennas and 50 cm Cassegrain-type antennas for the Ka- and Q-band receivers respectively; they employ a single down-conversion scheme to a 70 MHz IF and are based on conventional techniques, i.e., Phase Locked Loop (PLL) envelope detection using a Novella SatComs B150 70 MHz PLL tracking receiver. The latter is configured with a noise bandwidth of 300 Hz and a tracking range of 100 kHz. Its output is fed to an Analog to Digital Converter (ADC) backend, responsible for feeding the digitized signals to the processing computers. The local oscillators are DROs phase locked to an internal crystal reference and the LO frequency is multiplied by 3 to drive the mixer. The dynamic range for the receivers is 19 dB for the Ka- and 22 for the Q-band ones, both at 10 Hz sampling rate (all measuring only the co-polar component).

An antenna tracking system has been procured to obtain the highest link budget available. The receivers (and the antennas) are located inside a specially adapted Portakabin (similarly to that used in the ITALSAT campaign) and point towards the satellite through radomes of woven PTFE windows.

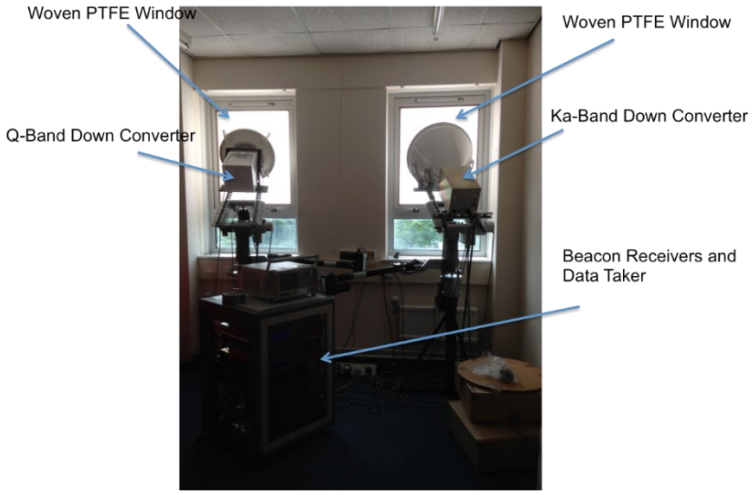

Figure 12-2: Overview of the receivers' configuration at Chilton, UK

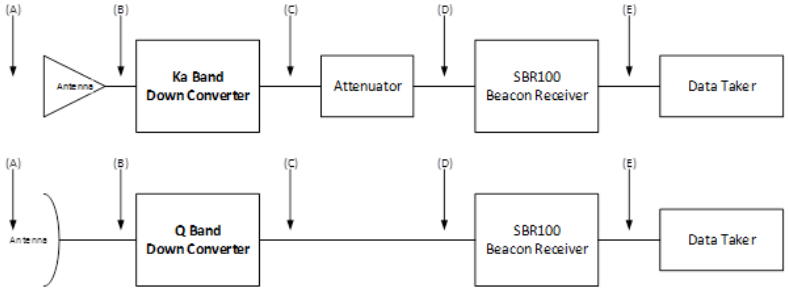

Figure 12-3: Simplified block diagram for the ALPHASAT beacon receivers in the UK

12.1.3 Ancillary Equipment

Since the beginning of the campaign, collocated ancillary equipment has been deployed at all campaign locations allowing for in-situ meteorological measurements. All measurements are synchronized to the receivers and archived with the necessary meta-tags for later processing. The use of collocated meteorological instrumentation should allow for further study of the correlation between the fading statistics and the observed meteorological events.

12.1.3.1 Ancillary Equipment installed at NTUA locations in Greece

The ancillary equipment installed at the two NTUA campaign locations in Attica, Greece is described in detail in **Chapter 4** of this thesis.

12.1.3.2 Ancillary Equipment installed at RAL Space locations in the UK

To measure rainfall, high resolution drop-counting, tipping bucket rain gauges and impact disdrometers are used; the drop-counting gauges have a 10-sec integration time at 0.0033mm resolution. Other measurements include air temperature, humidity, air pressure, wind speed and direction. Available are also an operational radiosonde, approximately 28 km from Chilbolton, a radiometer (channels in the 20-30GHz interval for water vapor), a GPS receiver and Ceilometer Zenith-pointing cloud radars (35GHz and 94GHz) providing continuous cloud profiles over Chilbolton. Should it be required, a 3GHz rain radar is available for event-based studies (i.e., not in continuous operation) as well as access to data from Met Office C-band radar network.

12.1.4 Data Processing

NTUA and RAL Space monitor the data collection and visually inspect the obtained time series on a daily basis to ensure data consistency and integrity. Additionally, data preprocessing is performed using the well-established RAL method based on Fourier Series [2]. Data preprocessing is critical in any propagation experiment campaign and involves the following tasks:

- Removal of the effect the ground equipment has on the received signal
- Identification of valid data
- Data merge from beacon receivers and ancillary instruments
- Raw and processed measurements archiving

All measurements have timestamps synchronized to GPS time and are stored using a common format (netCDF) for further processing and evaluation. Apart from the actual propagation measurements, ancillary data are recorded to support the experiment with essential metadata (e.g. meteorological events).

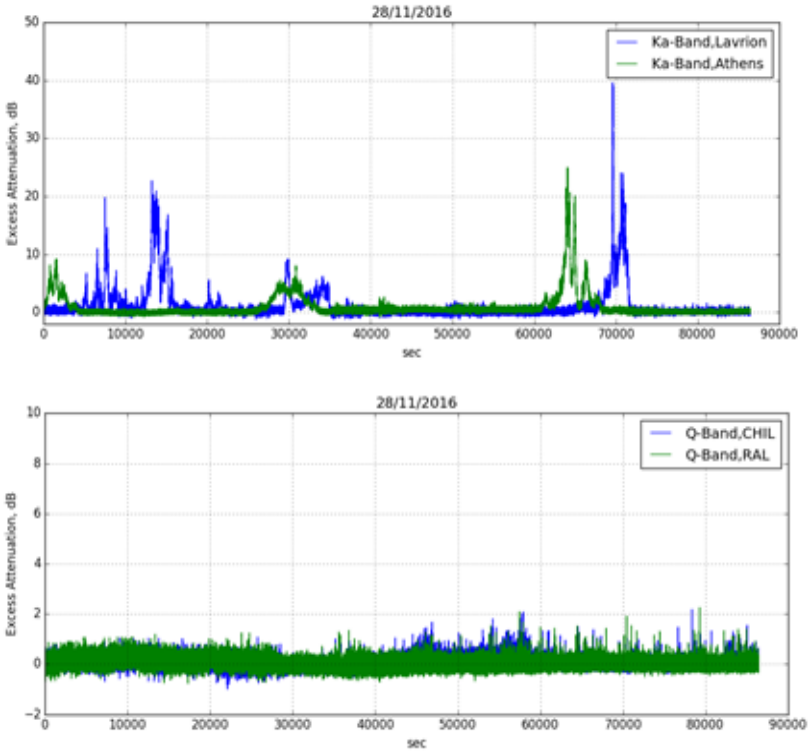

Figure 12-4: Example time series for one day in 2016 in Greece at Ka-band (upper figure) and the UK at Q-band (lower figure)

12.2 Experimental Results

In the following, the results obtained from the first two years of the campaign are analyzed and presented. The processed beacon data availability for the Greek campaign has been 96.11% for Athens and 95.99% for Lavrion; for the UK campaign the processed data availability has been 98.33% for Chilton and 97.82% for Chilbolton. Regarding the processed rainfall data, NTUA has

100.00% availability for both locations while RAL Space has 98.93% availability for Chilton and 98.81% availability for Chilbolton.

12.2.5 Single Site Statistics

Table 12-2 summarizes the annual measured rain characteristics across the four locations in Greece and the UK. Rainfall data in mm have been converted to rainfall rate in mm/h using a 60 sec integration window according to the methodology in [3]. The annual probability of (detectable) rain, i.e. the probability that the rain rate is greater than 0.25 mm/h, is higher in England than in Greece. As an example, there is detectable rain in Attica, Greece for about 365x24x0.01=87.6 hours/year in average whereas in the UK 365x24x0.04=350.4 hours/year. However, the rain rate used in the ITU-R Predictions Model (ITU-R Rec. P.618-13) [4] - i.e. at 0.01% of the year or 52.56 minutes/year- is much higher in Greece. This is reflected into the attenuation statistics depicted in Figure 12-5 and Figure 12-6.

Table 12-2: Rainfall Rate Data

Location	Exceedance time (%) of 0.25 mm/hr	Rain Rate at 0.01% (mm/hr)
Athens, GR	1.23	64.98
Lavrion, GR	1.06	70.27
Chilton, UK	3.99	19.67
Chilbolton, UK	4.70	20.82

The attenuation exceedance probabilities suggest that systems operating at Ka-band require a larger fade margin in Greece than in Southern England for a given availability. As an example, for an annual availability of (100-0.01) % = 99.99 % the required fade margin in Attica, Greece must attain at least 18 dB whereas in Southern England 12 dB; the fade margin values merely serve as a baseline as they refer to the received ALPHASAT unmodulated CW signals. In addition, the exceeded attenuation levels at the lower exceedance probability values experience a significant annual variability in both countries.

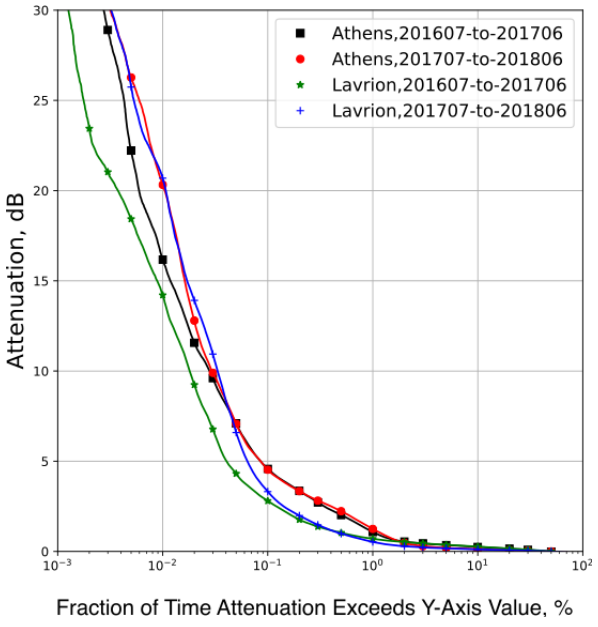

Figure 12-5: Measured annual complementary cumulative distribution of excess attenuation in Greece

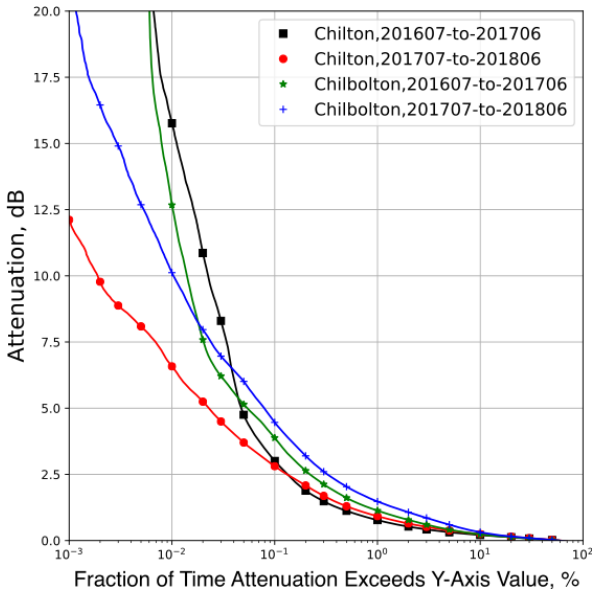

Figure 12-6: Measured annual complementary cumulative distribution of excess attenuation in the UK

Figure 12-7 and Figure 12-8 show the comparison of the average annual statistics with the ITU-R P.618-13 [4] model in the two regions, i.e. in Greece and the UK respectively. As can be seen in Figure 12-7 and Figure 12-8, the ITU-R Model [4] for the prediction of the excess attenuation, i.e. the combination of all the propagation impairments except for the gaseous attenuation, overestimates the actually measured values. This is more evident at the English sites where the elevation angles are lower compared to the Greek sites and therefore the former experience more cloud attenuation. In Figure 12-7 and Figure 12-8 a modified methodology proposed in [1] for the calculation of in-excess attenuation using the ITU-R model is also shown. As can be observed it yields better results for all the campaign locations.

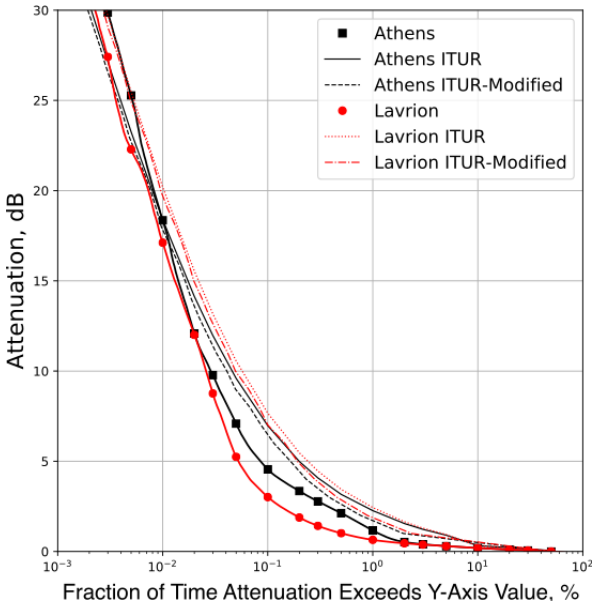

Figure 12-7: Average annual complementary cumulative distribution of excess attenuation in Greece in comparison with the ITU-R P.618-13 predictions

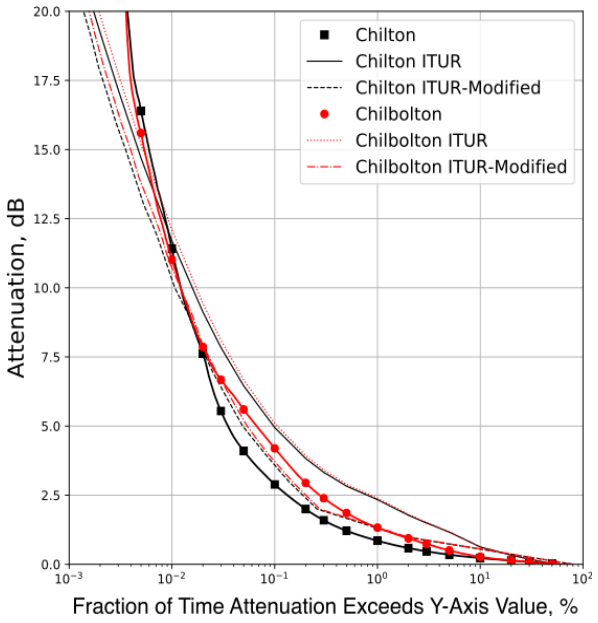

Figure 12-8: Average annual complementary cumulative distribution of excess attenuation in the UK in comparison with the ITU-R P.618-13 predictions

12.2.6 Joint Site Diversity Statistics

In Figure 12-9 and Figure 12-10, the performance of the site diversity FMT [5], [6] in Greece and the UK is evaluated against the ITU-R P.618-13 [4] predictions. The attenuation statistics are the average annual over the observation period of two years. A very significant observation not yet mentioned anywhere in the literature is that for an annual availability of (100-0.01) % = 99.99 % the required Fade Margin using Site Diversity, despite the different radio propagation characteristics in England and Greece, for both countries is very similar and around 2.8 dB as shown in Figure 12-9, Figure 12-10 and Figure 12-11. This suggests that the diversity gain in Greece is much higher since the corresponding single link excess attenuation experienced at 0.01% of the time is also much greater than in the UK.

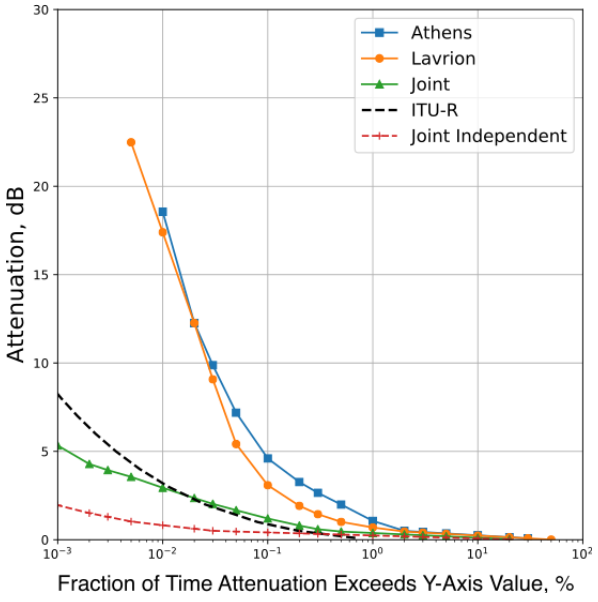

Figure 12-9: Average annual complementary cumulative distribution of excess attenuation in Greece in comparison with the ITU-R predictions

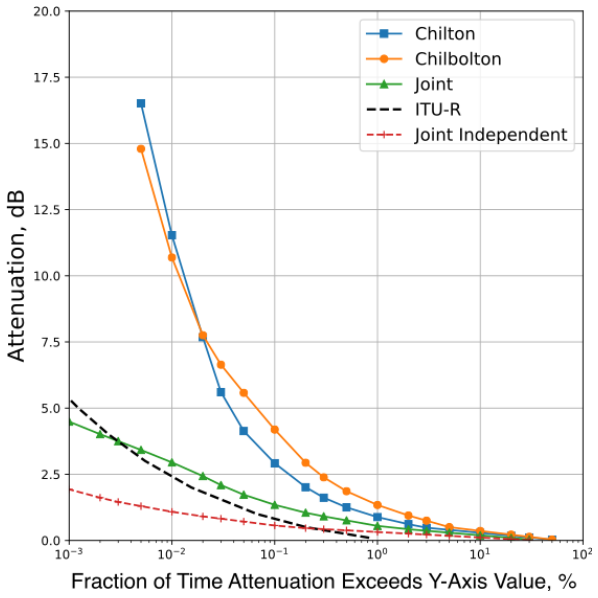

Figure 12-10: Average annual complementary cumulative distribution of excess attenuation in the UK in comparison with the ITU-R predictions

The independent joint attenuation cumulative attenuation statistics [7], i.e. the product of the single attenuation statistics, clearly shows that even for site separations of 36.5 km and 48 km – as is the case for the campaigns in Greece and the UK respectively, there is a significant dependence between the propagation effects at the two sites (Chilton-Chilbolton and Athens-Lavrion).

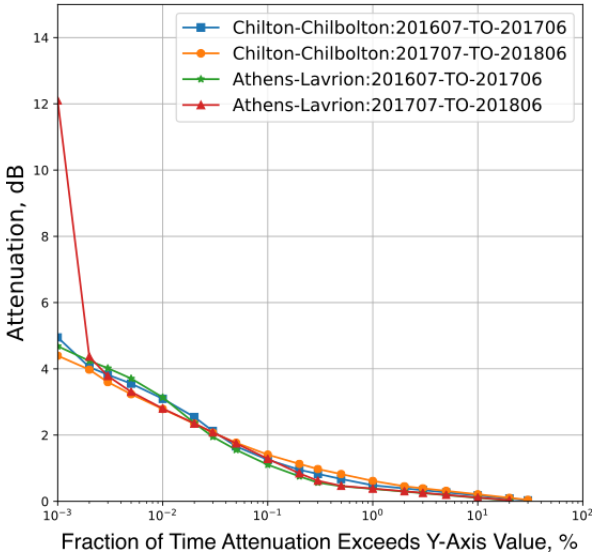

Figure 12-11: Measured annual joint complementary distribution of excess attenuation for Greece and the UK

A significant observation can be made in Figure 12-11; it is apparent that the measured annual joint complementary distribution of excess attenuation for both experiments in Greece and the UK share a very similar behavior and their lines almost overlap; this is an outstanding result that - despite potentially being a random effect, has to be noted. Finally, in Figure 12-12 the results for the measured annual joint complementary distribution of excess attenuation between Greece and

UK are presented; these results are presented considering the application of the smart gateway diversity concept in feeder links [8].

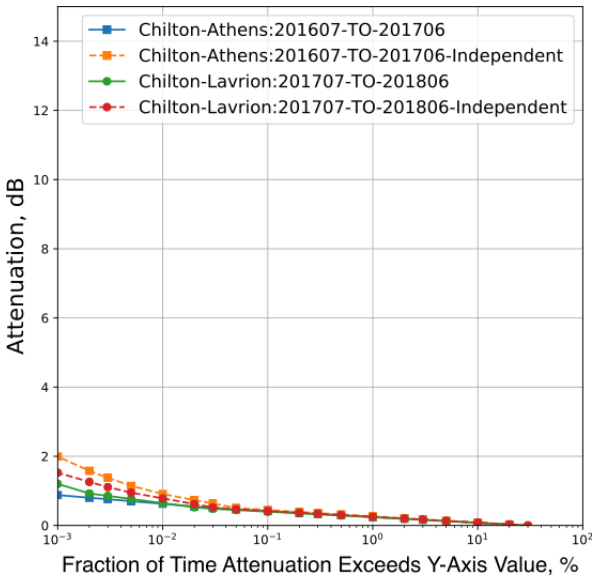

Figure 12-12: Measured annual joint complementary distribution of excess attenuation between Greece and the UK in comparison with the independent joint distributions

There is a notable discrepancy in elevation angles across the two regions potentially influencing the derived results to some extent; the UK receivers operate at an elevation angle of approximately 26º while the Greek ones around 46º. However, precisely quantifying the impact such a difference has is a non-trivial task, especially considering the substantially dissimilar meteorological conditions between Greece (more convective rain) and the UK (more stratiform rain). More details regarding the impact of the stratiform and convective type of precipitation on the site diversity gain can be found in [9] - [11].

In order to better explain the impact that the elevation angle has on the site diversity gain considering also the type of precipitation more experimental data in various climatic regions and in different separation distances are required [5], [12]- [14]. In [15] an investigation of the factors that affect the site diversity gain has been conducted and it has shown that the dependence of the elevation angle on the diversity gain should in any case not be particularly pronounced.

As can be observed in Figure 12-7 to Figure 12-12, the effectiveness and practical value of a site diversity scheme becomes apparent at time exceedance probabilities less than <0.1%; above that value a dual antenna scheme could provide a solid 3 dB gain as mentioned in [10].

12.3 Discussion

In this chapter the results from the first two years of the ALPHASAT Ka-band site-diversity experiment in Greece and the UK are presented side-to-side yielding interesting observations regarding both the small and the large-scale site diversity scenarios (as can be seen in Figure

12-12). The deployment of receivers at two sites per region enables the study and development of new site diversity techniques, based on the temporal and the spatial distribution of statistics.

12.4 Chapter References

[1] S. Ventouras, A. Martellucci, R. Reeves, et al., "Assessment of spatial and temporal properties of Ka/Q band earth-space radio channel across Europe using Alphasat Aldo Paraboni payload", Int J Satell Commun Network, 2019, pp. 1-25.

[2] S. Ventouras, S.A Callaghan, and C.L. Wrench, "Long-term statistics of tropospheric attenuation from the Ka/U band ITALSAT satellite experiment in the United Kingdom", Radio Science, vol. 41, 2006.

[3] E. Matricciani and C. Riva, "The search for the most reliable long-term rain attenuation CDF of a slant path and the impact on prediction models", IEEE Transactions on Antennas and Propagation, vol. 53, no. 9, 2005, pp. 3075–3079.

[4] ITU-R Recommendation P. 618-13, "Propagation data and prediction methods required for the design of Earth-space telecommunication systems", International Telecommunication Union, Tech. Rep, Geneva, 2017.

[5] A. D. Panagopoulos, P.-D. M. Arapoglou and P. G. Cottis, "Satellite Communications at Ku, Ka and V Bands: Propagation Impairments and Mitigation Techniques", IEEE Communication Surveys and Tutorials, 2004.

[6] A. D. Panagopoulos, "Propagation Phenomena and Fade Mitigation Techniques for Fixed Satellite Systems", Book Chapter in the Book "Radio Wave Propagation and Channel Modeling for Earth-Space Systems", Taylor and Francis CRC Press, May 2016.

[7] A. Papoulis, Athanasios; Pillai, S. Unnikrishna, Probability, Random Variables and Stochastic Processes (4th ed.). Boston: McGraw Hill, 2002, ISBN 0-07-366011-6.A.

[8] A. Gharanjik, B. Shankar M. R., P. Arapoglou and B. Ottersten, "Multiple Gateway Transmit Diversity in Q/V Band Feeder Links" , IEEE Transactions on Communications, vol. 63, no. 3, March 2015, pp. 916-926.

[9] J. Goldhirsh, B. H. Musiani, A. W. Dissanayake and Kuan-Ting Lin, "Three-site space-diversity experiment at 20 GHz using ACTS in the Eastern United States" in Proceedings of the IEEE, vol. 85, no. 6, June 1997, pp. 970-980.

[10] R. K. Crane, Propagation Handbook for Wireless Communication System Design. Boca Raton, FL, USA: CRC Press, 2003.

[11] E. Matricciani, "Prediction of site diversity performance in satellite communications systems affected by rain attenuation: Extension of the two-layer rain model", European Transactions on Telecommunications, vol. 5, no. 3, 1994, pp. 327-336.

[12] G. A. Karagiannis, A. D. Panagopoulos and J. D. Kanellopoulos, "Multidimensional Rain Attenuation Stochastic Dynamic Modeling: Application to Earth–Space Diversity Systems" in IEEE Transactions on Antennas and Propagation, vol. 60, no. 11, Nov. 2012, pp. 5400-5411.

[13] C. I. Kourogiorgas, A. D. Panagopoulos and J. D. Kanellopoulos, "On the Earth-Space Site Diversity Modeling: A Novel Physical-Mathematical Outage Prediction Model", IEEE Transactions on Antennas and Propagation, vol. 60, no. 9, Sept. 2012, pp. 4391-4397.

[14] E. Matricciani, "Micro scale site diversity in satellite and tropospheric communication systems affected by rain attenuation", Space Communications, vol. 19, April 2003, pp. 83-90.

[15] A. D. Panagopoulos, P. -. M. Arapoglou, J. D. Kanellopoulos and P. G. Cottis, "Long-term rain attenuation probability and site diversity gain prediction formulas", IEEE Transactions on Antennas and Propagation, vol. 53, no. 7, July 2005, pp. 2307-2313.

Chapter 13

Thesis Summary & Future Work

In this thesis, the design, deployment and operation of satellite beacon receivers is presented along with a broad statistical analysis of the observed phenomena. To the best of the author's knowledge, this work constitutes the most comprehensive work regarding actual satellite propagation measurements in the Southern Mediterranean area available to date.

The design of the receivers was based on mostly Common, Off-The-Shelf (COTS) parts, keeping the budget to reasonable levels, while at the same time ensuring that the quality of the data is not compromised. The availability of the parts makes the receivers easier to replicate in order to conduct further measurements at other locations of interest, while also making maintenance fairly straightforward. The main challenges involved in the receivers' design and operation as well as on the statistical analysis of the obtained data are summarized in the following section.

13.1 Challenges

13.1.1 Equipment/Hardware related challenges

The **main challenges** involved in such a campaign from a **receiver's perspective** as well as the proposed solutions are the following:

- Outdoor receivers are **vulnerable to all kinds of meteorological phenomena and subsequent effects** such as:
    - Antenna wind loading
        - Dangerous for the installation
        - Unless carefully addressed it can lead to inconsistent measurements
    - Water precipitation/Humidity
        - Antenna wetting effects, particularly pronounced for prime focus antennas without radomes (not the case in this thesis).
        - Water ingress across all junction boxes, equipment cases, connections. All equipment and accessories should either be IP6X rated, or be placed inside sealed enclosures.
        - Metal parts either have to be hot-dip galvanized, be painted using high-build epoxy primer or at the very least be covered using a thin oil film to minimize rust.
        - Moving parts and joints should employ high quality bushings/bearings and be lubed on a regular basis using water-resistant grease based on lithium, PTFE, graphite or a combination of the above.
    - Solar/heat contamination

        - The excessive heat radiated by the sun can cause diurnal variation of the active components' temperature, consequently altering their gain values; especially affected are the LNAs which are placed directly under sun-light. This phenomenon although more pronounced during spring, is largely present throughout the year.
        - Usually inclinometer/position sensors based on MEMS are also sensitive to temperature changes, requiring some form of internal temperature compensation circuitry to maintain accurate readings across a wide operational temperature range.
        - Frequency sources/crystal oscillators have to be GPS locked and/or OCXOs in order to provide a reliable, stable frequency reference with minimum drift and phase noise.
        - UV protection must be applied to sensitive plastics and rubber parts to avoid cracking; cables must be rated for outdoor application and bear a UV protective layer.
    - Lightning protection
        - The equipment and/or the facility where it is placed must incorporate lightning protection and proper grounding.

- Outdoor receivers are also **vulnerable** in terms of **physical security and nearby effects**:
    - Their location must not be publicly accessible while at the same time be spacious, have unobstructed line of site to the satellite(s), have access to stable electricity and offer high speed internet; generally, it is rather difficult to simultaneously meet all these criteria.
    - The receivers have to be resilient to interference that can occur from nearby works.
    - Even birds or other animals or rodents can play a significant role and have to be kept far from the installation to avoid equipment or measurement degradation.

For all the above reasons, it is strongly advisable to use indoor receivers where possible.

It should also be noted, that upon installation of the receiver, despite any prior lab testing, close monitoring is always required. It is not uncommon for equipment to fail partially or completely upon installation or to operate drifting outside of its nominal values. Usually any bugs, defects or even design mistakes can be found within the first 1-2 months of full operation.

13.1.2 Software related challenges

- Regarding the actual **software operation**, the **following measures** have to be taken:
    - The software should be able to either run an equipment self-test at scheduled intervals or (preferably) to monitor the health of the equipment in real-time.
    - The system has to sustain random crashes or power outages. It should be able to notify of the erroneous condition and unless fully automated recovery is possible, at least maintain data integrity by means of redundancy/back-up solutions.
    - The system should ideally be isolated from the outside internet to avoid any form of malicious attack that could compromise it or exhaust resources thereby stopping the measurements. At the same time, remote management is required especially for remotely located campaign sites.

- The receivers must maintain a stable time reference using GPS time utilizing pulse per second (PPS) output combined with NTP to ensure correct data time-stamping.
- As the equipment ages (regarding both the ground stations and the satellite), operational parameters (such as thresholds, bandwidths, sampling rates etc.) might need to be adjusted to account for any discrepancies.

The above are considered the bare minimum required to maintain stable receiver operation in terms of software.

13.1.3 Data preprocessing challenges

Another very **significant challenge** is the **preprocessing of the raw data**. The measurements, at their initial form might include:

- spikes or artifacts as a result of software glitches, nearby interference, local maintenance works etc.
- gaps due to permanent or intermittent equipment hardware failure, power outage or maintenance
- intervals without functional antenna tracking or erroneous antenna pointing (e.g., due to unavailable OEM file, equipment failure), resulting in significant loss of power which should either be accounted for or else such data be discarded
- intervals where diurnal temperature variations cause variation of the received power
- solar eclipse outage intervals, when the satellite and the sun are aligned; this phenomenon happens twice a year during fall and spring for a few days and lasts for a few minutes per day, causing significant signal degradation; such events have to be removed or else they would appear as outage due to propagation
- satellite out-of-orbit situations or on-board malfunctions, causing problems on the actual satellite; such cases are not rare and the corresponding intervals have to be discarded
- The Fourier series method chosen is based on a solid mathematical background and if applied correctly can lead to very accurate measurements. It can be automated to some extent, however, in order for the data to be qualified for further use, manual visual inspection (and in most cases intervention) is required. This process is tremendously time consuming and requires extreme dedication especially when processing of data from many receivers is involved.

13.1.4 Statistical analysis challenges

The **statistical analysis** also posed quite a few **challenges**, a few of which are:

- The analysis is conducted on a massive dataset (in the order of hundreds of GBs of data per receiver's frequency band). In order to analyze all this data, big data practices have to be employed in order to maintain an efficient resource management. Also, despite the efforts to use the optimal practices in terms of algorithm design e.g., using as much vectorized operations as possible, the resources required are still massive especially in cases where very high sampling rate must be maintained (e.g. for scintillation analysis where 10 Hz sampling rate is used- for this particular analysis, the instantaneous RAM required reached values in excess of 145 GB!)

- Any software bug, logical error or change of parameters requires the re-execution of the analysis on this massive dataset, requiring very significant processing time (in the order of a few hours at the very least)

13.2 Observations

The frequency bands under, examination, namely the Ku-band, Ka-band and Q-band provide significant evidence that different strategies should be employed in order to meet the required availabilities.

From the statistical analysis conducted on the gathered data, the following conclusions can be drawn:

Regarding the **Ka-band**, significantly high levels of atmospheric attenuation can be observed in comparison to e.g. Ku-band. The methods and techniques commonly used to compensate for fades in Ku-band seem to be insufficient for the most part. However, FMTs such as site diversity (and to lesser extent orbital and time diversity) can almost completely compensate for such effects, at the expense of more complex, less cost-effective system implementations.

Regarding the **Q-band** case, the atmospheric attenuation experienced is so significant that unless a rather large network of gateways/feeder-links configured in a site diversity scheme is considered, the resulting availability and therefore QoS to the end-users can reach intolerable values. The system design should therefore be done very carefully, selecting teleport sites that are expected to face the least rainfall rates possible and also reside at locations as spatially uncorrelated as possible. The target availabilities could be reached only by means of a very effective combination of almost all FMTs available, possibly combined with advanced weather prediction/nowcasting techniques.

A **strong seasonal** as well as **diurnal dependence** has been measured across all frequency bands; Fall consistently appeared to be the season most affected by atmospheric attenuation, closely followed by the summer where sparse yet very intense convective rainfall events take place. Also, the time window from 08:00 to 16:00 (UTC) exhibited significantly higher attenuation levels for a large fraction of the total time, proving that the use of a single static fade margin not only is insufficient for a great part of the time, but also could lead to system over-dimensioning or waste of energy.

The **second order statistics**/fade dynamic analysis presented can be useful in the parametrization of the various FMT schemes, and more particularly regarding the measurement sampling rates, the closed-loop gains and the switching hysteresis intervals. It has been shown, that despite the large deviation of fade durations, they tend to exhibit a stable median value and a gaussian-like distributed 3rd quartile.

Site diversity techniques have shown their strength, providing significant gains even when relatively small separation distances are considered. They are undoubtedly expensive solutions but seem to effectively cancel out the limiting effects of propagation at higher frequency bands. Other forms of site diversity which involve more efficient traffic routing and switching, also termed as smart gateway diversity are expected to provide even better results.

Orbital diversity surely offers a considerable gain as proven using KaSAT and ALPHASAT at Ka-band, however, very large satellite separation angles seem to be required in order to obtain a very significant gain; in this context, it should also be considered that this might not be an option when a particular coverage area is required.

Time diversity has shown its strength when high delays are used (i.e., greater than 5 min), however, its applicability is questioned as it targets only delay-tolerant, non-real-time applications, it would require massive buffers and from a user's point of view would appear similar to a system outage (despite the fact that eventually the data will be successfully transmitted, yet after a particular delay).

It has been shown, that given the attenuation values at Ka-band, one can obtain the corresponding value at Q-band through **frequency scaling** factors. It was concluded, that even a plain linear regression can give surprisingly accurate results at 50% of the time and also good approximations for 100% of the time.

Scintillation does not appear to be significantly strong at these elevation angles; it surely is considerable especially during the Summer and the Fall, however, apart from proper AGC/power control parameter setting it should not be a limiting factor even at Q-band.

13.3 Universality of the results

It could be questioned whether the obtained measurement results are to some extent bound to the region as well as the timeframe they were conducted; while inarguably the short-term effects can exhibit a considerably varying spatial distribution, in the long-run they generally tend to converge to stable average values as indicated by the two measurement sets at Campus and Lavrion. In order to remove any temporal or spatial biases the conduction of **multi-site**, **long-term** (multi-year) propagation campaigns is required; the obtained results can then be generalized for the climatic region of interest under the assumption that no extreme regional peculiarities could lead to false conclusions.

The campaign locations offer a rather representative Southern Mediterranean climate with long lasting summers reaching extremely high temperatures (>40^{o}C), often greatly varying throughout the day; infrequent, very intensive rainfall events lasting a few minutes are typical during the summer months. Winter is relatively dry and mild (temperatures rarely drop below 5-10^{o}C), while Fall is usually characterized by the higher accumulated rainfall, a combination of both stratiform- as well as convective-type rain cells. Attica is in the middle between the northern continental part (whose climate shares a lot of similarities with central European countries) and the southern islandic part (whose climate shares a lot of similarities with the subtropical countries of northern Africa [1].

In any case it is the very first time a campaign of such a magnitude is conducted, especially at so high frequency bands such as Ka- and Q-band; up to now, any estimation regarding the propagation phenomena in the surrounding region relied almost exclusively on statistical/physical-mathematical models or time series synthesizers based on inference and extrapolation from measurements performed in other regions. It is now possible to test systems, techniques and models using actual measurement data.

13.4 Future Work

Due to the finite timeframe within which a doctoral dissertation should be completed, the present work includes the design and deployment of the beacon receivers, the acquisition and preprocessing of the measurement data as well a first statistical analysis and the investigation of some FMT techniques.

Having this work as a base, a broad horizon of future work opens, such as:

- The validation and improvement of the existing physical-mathematical propagation models using real data
- The development of new, very accurate long-term propagation models and new time series synthesizers
- The development of simplified models based on the correlation between long-term distributions and rainfall rates, also expandable for use within the framework of MEO or LEO satellites, or even cubesats/nano-satellites and UAV links
- The parametrization and testing of existing and new FMTs e.g., the conceptual validation and derivation of new performance models for Smart Gateway Diversity High Throughput Satellite Systems [2]-[4], possibly incorporating the measured data with meteorological predictions (nowcasting) and or Machine Learning (ML) techniques [5]
- The development and the performance evaluation of hybrid RF/FSO (Free Space Optics) satellite feeder links potentially exploiting diversity techniques
- The performance evaluation of Cognitive Hybrid Satellite Systems operating above 10GHz
- The proposition of new synergies/integration/coexistence possibilities within the scope of the 5G and 6G mobile network systems exploiting the advantages of satellite communications [6]
- The further evolution and standardization of the receivers to a final product, available to easily conduct measurements around the world either for the propagation community or the satellite operators

The aforementioned list is by no means exhaustive, as there are countless areas where either the receivers themselves or the measurements could play a significant role in the advance of the scientific knowledge.

13.5 Chapter References

[1] M. Kottek, J. Grieser, C. Beck, B. Rudolf and and F. Rubel, "World Map of the Köppen-Geiger Climate Classification Updated" in *Meteorologische Zeitschrift*, vol. 15, 2006, pp. 259-263.

[2] T. Rossi, M. De Sanctis, F. Maggio, M. Ruggieri, C. Hibberd and C. Togni, "Smart Gateway Diversity Optimization for EHF Satellite Networks", in *IEEE Transactions on Aerospace and Electronic Systems*, vol. 56, no. 1, pp. 130-141, Feb. 2020.

[3] T. Delamotte and A. Knopp, "Smart Diversity Through MIMO Satellite Q/V-Band Feeder Links", in *IEEE Transactions on Aerospace and Electronic Systems*, vol. 56, no. 1, Feb. 2020, pp. 285-300.

[4] S. Ventouras and P. -D. Arapoglou, “Assessment of Practical Smart Gateway Diversity Based on Multi-Site Measurements in Q/V band”, in *IEEE Transactions on Antennas and Propagation*, doi: 10.1109/TAP.2020.3044370.

[5] L. Bai, C. Wang, Q. Xu, S. Ventouras and G. Goussetis, “Prediction of Channel Excess Attenuation for Satellite Communication Systems at Q-Band Using Artificial Neural Network”, in *IEEE Antennas and Wireless Propagation Letters*, vol. 18, no. 11, Nov. 2019, pp. 2235-2239.

[6] O. Kodheli et al., “Satellite Communications in the New Space Era: A Survey and Future Challenges”, in *IEEE Communications Surveys & Tutorials*, doi: 10.1109/COMST.2020.3028247.

Appendix

Statistics in tabular format

In the following, the results graphically presented throughout this thesis are appended in tabular format. The format of the tables is in accordance to the one specified by the ITU-R SG3 regarding the submission of experimental data.

The tables included in this appendix are organized as per the following structure:

a. Data Availability Matrix
b. First-Order Statistics
c. Second-Order Statistics
d. Site Diversity Statistics
e. Time Diversity Statistics
f. Orbital Diversity Statistics
g. Frequency Scaling Statistics

Appendix - 1
Data Availability Matrix

Overall Data Availability per site and frequency:

	NTUA Campus				NTUA LTCP	
	Ka-band ALPHASAT	**Q-band ALPHASAT**	**Ku-band BADR5**	**Ka-band KASAT**	**Ka-band ALPHASAT**	**Q-band ALPHASAT**
	Data Availability [%]					
Total Duration	95.70 (4 years)	95.33 (2 years)	96.49 (3 years)	96.15 (2 years)	96.39 (4 years)	93.38 (2 years)

Yearly Data Availability per site and frequency:

	NTUA Campus				NTUA LTCP	
	Ka-band ALPHASAT	**Q-band ALPHASAT**	**Ku-band BADR5**	**Ka-band KASAT**	**Ka-band ALPHASAT**	**Q-band ALPHASAT**
Year	**Data Availability [%]**					
07/2016 - 06/2017	93.97	-	-	-	93.75	-
07/2017 - 06/2018	98.22	96.54	97.38	-	98.25	93.95
07/2018 - 06/2019	94.65	94.12	94.16	94.09	96.51	92.81
07/2019 - 06/2020	95.96	-	97.92	98.20	97.07	-

Monthly Data Availability per site and frequency

	NTUA Campus				NTUA LTCP	
	Ka-band ALPHASAT	**Q-band ALPHASAT**	**Ku-band BADR5**	**Ka-band KASAT**	**Ka-band ALPHASAT**	**Q-band ALPHASAT**
Month	**Data Availability [%]**					
Jul-16	95.95	-	-	-	100.00	-
Aug-16	98.28	-	-	-	100.00	-
Sep-16	98.87	-	-	-	84.57	-

Oct-16	88.96	-	-	-	98.10	-
Nov-16	99.18	-	-	-	99.21	-
Dec-16	90.80	-	-	-	99.98	-
Jan-17	80.46	-	-	-	82.24	-
Feb-17	96.30	-	-	-	88.23	-
Mar-17	87.75	-	-	-	72.45	-
Apr-17	99.34	-	-	-	99.94	-
May-17	100.00	-	-	-	100.00	-
Jun-17	92.40	-	-	-	100.00	-
Jul-17	86.85	70.08	71.70	-	89.56	44.49
Aug-17	99.84	99.84	98.52	-	100.00	100.00
Sep-17	99.95	99.75	99.95	-	100.00	100.00
Oct-17	99.56	99.60	99.53	-	99.71	100.00
Nov-17	98.72	99.91	99.90	-	99.24	99.81
Dec-17	99.86	94.64	100.00	-	92.93	91.39
Jan-18	98.17	100.00	99.84	-	98.83	96.61
Feb-18	99.28	99.13	100.00	-	99.85	100.00
Mar-18	98.43	96.87	99.75	-	99.18	97.25
Apr-18	99.17	100.00	100.00	-	100.00	100.00
May-18	99.75	99.78	99.96	-	100.00	99.63
Jun-18	99.37	99.52	99.99	-	100.00	99.52
Jul-18	75.31	76.90	98.29	57.90	77.68	77.34
Aug-18	92.67	92.84	92.88	92.63	100.00	100.00
Sep-18	99.84	100.00	100.00	99.95	96.40	100.00
Oct-18	99.04	99.61	99.53	99.69	99.77	98.74
Nov-18	99.26	99.75	99.97	98.67	97.63	98.17
Dec-18	95.23	95.86	95.32	95.80	100.00	93.52
Jan-19	93.92	75.97	91.50	99.99	100.00	90.85
Feb-19	98.37	98.85	99.66	95.84	91.96	92.15
Mar-19	97.62	97.73	77.95	95.31	94.52	93.73

Apr-19	98.31	99.30	81.92	98.86	100.00	90.46
May-19	99.84	98.43	98.35	100.00	100.00	85.09
Jun-19	86.92	95.19	95.03	95.14	100.00	93.97
Jul-19	89.69	-	92.05	90.08	100.00	-
Aug-19	99.83	-	100.00	100.00	100.00	-
Sep-19	99.65	-	97.46	99.31	100.00	-
Oct-19	89.88	-	99.65	99.84	99.52	-
Nov-19	86.26	-	97.64	97.62	100.00	-
Dec-19	96.67	-	96.16	97.08	100.00	-
Jan-20	93.52	-	95.45	97.26	96.77	-
Feb-20	99.55	-	98.88	100.00	99.81	-
Mar-20	98.02	-	98.42	98.22	71.60	-
Apr-20	100.00	-	100.00	100.00	97.63	-
May-20	98.78	-	99.74	100.00	100.00	-
Jun-20	100.00	-	99.78	99.25	100.00	-

Appendix - 2
First-Order Statistics

NTUA Campus ALPHASAT Ka-band 4-year average				
Start Date			1st July 2016	
End Date			30th June 2020	
Location			NTUA Campus	
Attenuation Data Availability [%]			95.70	
Rain Data Availability [%]			92.33	
Concurrent Attenuation & Rain Data Availability [%]			88.52	
Exceedance Probability [%]	**Excess Attenuation [dB] (Full Dataset)**	**Rain Rate [mm/h] (Full Dataset)**	**Excess Attenuation [dB] (Concurrent Dataset)**	**Rain Rate [mm/h] (Concurrent Dataset)**
50	0.006	0.000	0.005	0.000
30	0.083	0.000	0.081	0.000
20	0.144	0.000	0.141	0.000
10	0.281	0.000	0.274	0.000
5	0.463	0.000	0.447	0.000
3	0.654	0.000	0.627	0.000
2	0.881	0.000	0.835	0.000
1	1.489	1.601	1.407	1.627
0.5	2.294	3.735	2.212	3.841
0.3	2.900	5.730	2.807	5.863
0.2	3.433	7.886	3.315	7.978
0.1	4.587	12.856	4.334	13.087
0.05	7.239	21.974	6.642	22.469
0.03	10.197	32.906	9.376	33.244
0.02	12.957	42.649	11.953	42.978
0.01	19.879	61.958	18.752	61.738
0.005	28.053	81.487	26.617	79.794
0.003	34.025	94.572	31.870	93.006
0.002	36.515	102.157	35.239	99.488
0.001	38.259	132.779	37.872	130.569

NTUA LTCP ALPHASAT Ka-band 4-year average				
Start Date			1st July 2016	
End Date			30th June 2020	
Location			NTUA LTCP	
Attenuation Data Availability [%]			96.39	
Rain Data Availability [%]			99.87	
Concurrent Attenuation & Rain Data Availability [%]			96.27	
Exceedance Probability [%]	**Excess Attenuation [dB] (Full Dataset)**	**Rain Rate [mm/h] (Full Dataset)**	**Excess Attenuation [dB] (Concurrent Dataset)**	**Rain Rate [mm/h] (Concurrent Dataset)**
50	0.005	0.000	0.005	0.000
30	0.063	0.000	0.063	0.000
20	0.103	0.000	0.103	0.000
10	0.191	0.000	0.191	0.000
5	0.321	0.000	0.321	0.000
3	0.435	0.000	0.435	0.000
2	0.537	0.000	0.537	0.000
1	0.785	0.691	0.784	0.624
0.5	1.252	2.818	1.252	2.729
0.3	1.739	4.937	1.739	4.863
0.2	2.238	7.065	2.240	6.978
0.1	3.370	11.648	3.373	11.605
0.05	5.341	21.590	5.346	21.205
0.03	8.078	30.241	8.085	29.772
0.02	10.382	42.320	10.389	41.923
0.01	14.934	60.944	14.944	61.323
0.005	20.517	76.169	20.525	76.337
0.003	23.419	90.748	23.430	92.012
0.002	27.179	106.898	27.190	108.575
0.001	32.310	125.140	32.321	125.147

NTUA Campus ALPHASAT Q-band 2-year average				
Start Date			1st July 2017	
End Date			30th June 2019	
Location			NTUA Campus	
Attenuation Data Availability [%]			95.33	
Rain Data Availability [%]			91.1	
Concurrent Attenuation & Rain Data Availability [%]			86.72	
Exceedance Probability [%]	**Excess Attenuation [dB] (Full Dataset)**	**Rain Rate [mm/h] (Full Dataset)**	**Excess Attenuation [dB] (Concurrent Dataset)**	**Rain Rate [mm/h] (Concurrent Dataset)**
50	0.016	0.000	0.016	0.000
30	0.093	0.000	0.091	0.000
20	0.151	0.000	0.147	0.000
10	0.278	0.000	0.264	0.000
5	0.537	0.000	0.488	0.000
3	1.091	0.000	0.954	0.000
2	1.960	0.000	1.732	0.000
1	3.965	1.667	3.627	1.757
0.5	6.408	3.979	5.835	4.113
0.3	8.678	5.847	7.993	5.991
0.2	10.844	8.135	10.003	8.344
0.1	16.409	13.806	15.343	14.074
0.05	25.565	23.344	24.255	24.240
0.03	30.606	34.786	30.484	35.950
0.02	31.807	44.648	31.799	46.084
0.01	32.569	62.462	32.578	63.984
0.005	33.010	84.706	33.023	85.242
0.003	33.257	96.127	33.271	98.433
0.002	33.423	102.885	33.438	104.277
0.001	33.669	130.521	33.684	130.544

NTUA LTCP ALPHASAT Q-band 2-year average				
Start Date			1st July 2017	
End Date			30th June 2019	
Location			NTUA LTCP	
Attenuation Data Availability [%]			93.38	
Rain Data Availability [%]			99.75	
Concurrent Attenuation & Rain Data Availability [%]			93.13	
Exceedance Probability [%]	**Excess Attenuation [dB] (Full Dataset)**	**Rain Rate [mm/h] (Full Dataset)**	**Excess Attenuation [dB] (Concurrent Dataset)**	**Rain Rate [mm/h] (Concurrent Dataset)**
50	0.014	0.000	0.014	0.000
30	0.085	0.000	0.084	0.000
20	0.136	0.000	0.136	0.000
10	0.239	0.000	0.239	0.000
5	0.415	0.000	0.414	0.000
3	0.727	0.000	0.725	0.000
2	1.264	0.000	1.261	0.000
1	2.851	0.443	2.853	0.564
0.5	4.910	2.534	4.918	2.700
0.3	6.709	4.984	6.719	5.263
0.2	8.096	6.981	8.106	7.175
0.1	11.996	11.344	12.018	11.662
0.05	19.554	19.545	19.586	20.075
0.03	27.134	28.842	27.183	29.515
0.02	30.792	40.528	30.802	41.907
0.01	32.296	61.007	32.299	61.805
0.005	33.075	77.128	33.077	78.026
0.003	33.492	87.027	33.494	87.231
0.002	33.764	92.303	33.765	94.042
0.001	34.156	104.351	34.157	108.510

NTUA Campus BADR5 Ku-band 3-year average				
Start Date			1st July 2017	
End Date			30th June 2020	
Location			NTUA Campus	
Attenuation Data Availability [%]			96.49	
Rain Data Availability [%]			89.78	
Concurrent Attenuation & Rain Data Availability [%]			86.44	
Exceedance Probability [%]	**Excess Attenuation [dB] (Full Dataset)**	**Rain Rate [mm/h] (Full Dataset)**	**Excess Attenuation [dB] (Concurrent Dataset)**	**Rain Rate [mm/h] (Concurrent Dataset)**
50	0.002	0.000	0.002	0.000
30	0.047	0.000	0.046	0.000
20	0.080	0.000	0.080	0.000
10	0.131	0.000	0.130	0.000
5	0.187	0.000	0.184	0.000
3	0.235	0.000	0.229	0.000
2	0.280	0.000	0.270	0.000
1	0.382	1.710	0.355	1.638
0.5	0.555	3.809	0.482	3.766
0.3	0.795	5.643	0.628	5.742
0.2	1.079	7.605	0.801	7.808
0.1	1.798	12.422	1.279	12.687
0.05	3.370	21.126	2.024	21.898
0.03	5.006	31.438	3.203	32.188
0.02	6.158	39.180	4.458	39.986
0.01	8.349	57.865	6.927	58.292
0.005	12.246	75.972	10.607	76.090
0.003	15.463	88.725	13.812	89.104
0.002	18.522	100.433	15.817	100.486
0.001	25.172	118.642	20.349	118.668

NTUA Campus KaSAT Ka-band 2-year average				
Start Date			1st July 2018	
End Date			30th June 2020	
Location			NTUA Campus	
Attenuation Data Availability [%]			96.15	
Rain Data Availability [%]			84.68	
Concurrent Attenuation & Rain Data Availability [%]			80.99	
Exceedance Probability [%]	**Excess Attenuation [dB] (Full Dataset)**	**Rain Rate [mm/h] (Full Dataset)**	**Excess Attenuation [dB] (Concurrent Dataset)**	**Rain Rate [mm/h] (Concurrent Dataset)**
50	0.000	0.000	-0.001	0.000
30	0.139	0.000	0.136	0.000
20	0.234	0.000	0.229	0.000
10	0.400	0.000	0.392	0.000
5	0.610	0.000	0.598	0.000
3	0.811	0.000	0.792	0.000
2	1.012	0.000	0.975	0.000
1	1.495	1.979	1.375	2.060
0.5	2.183	3.888	1.929	3.978
0.3	2.811	5.519	2.472	5.623
0.2	3.456	7.184	3.011	7.400
0.1	5.335	11.410	4.556	11.497
0.05	7.190	19.977	6.662	20.522
0.03	9.846	28.380	7.757	29.512
0.02	12.722	35.981	10.240	36.525
0.01	16.800	53.086	14.738	54.787
0.005	18.136	75.948	18.201	77.037
0.003	18.728	89.113	18.836	89.171
0.002	19.072	102.109	19.173	102.147
0.001	19.515	113.304	19.597	113.324

Appendix - 3
Second-Order Statistics

NTUA Campus Ka-band 4-year average, Data Availability: 95.70 %																	
Start Date								1st July 2016									
End Date								30th June 2020									
Attenuation threshold [dB]	Absolute Fade Slope [dB/sec]																Number of fade slope samples
	0.001	0.002	0.003	0.005	0.01	0.02	0.03	0.05	0.1	0.2	0.3	0.5	1	2	3	5	
	Probability of exceedance [%]																
1	76.860	59.324	46.364	29.857	13.118	5.202	3.083	1.439	0.360	0.063	0.015	0.002	0.000	0.000	0.000	0.000	1933452
3	88.453	78.865	70.644	57.909	38.921	22.464	14.911	7.706	2.044	0.367	0.089	0.013	0.000	0.000	0.000	0.000	331432
5	95.807	92.226	88.988	83.075	69.769	50.222	36.836	21.164	6.191	1.163	0.283	0.032	0.000	0.000	0.000	0.000	103232
10	95.581	92.394	90.037	86.136	78.066	63.875	52.196	34.415	13.064	2.714	0.642	0.000	0.000	0.000	0.000	0.000	37248
15	93.415	89.262	86.613	83.118	77.091	66.231	56.035	38.840	16.951	3.999	1.094	0.000	0.000	0.000	0.000	0.000	18831
20	90.055	84.163	80.573	76.143	69.973	60.214	51.564	37.912	17.216	4.027	1.017	0.177	0.000	0.000	0.000	0.000	11896
25	86.307	78.610	73.923	68.833	62.261	53.806	45.717	33.186	12.910	2.068	0.734	0.061	0.000	0.000	0.000	0.000	8172

Prob. of exceedance [%]	Corr. Attenuation A [dB]	Absolute Fade Slope [dB/sec]																Number of fade slope samples
		0.001	0.002	0.003	0.005	0.01	0.02	0.03	0.05	0.1	0.2	0.3	0.5	1	2	3	5	
		Probability of exceedance [%]																
0.001	38.26	67.730	55.319	46.099	34.752	19.592	14.096	11.525	7.801	5.319	5.319	5.319	5.319	0.000	0.000	0.000	0.000	1128
0.002	36.51	63.530	44.463	35.803	28.310	20.899	14.779	7.993	4.455	2.540	2.498	2.498	2.498	0.000	0.000	0.000	0.000	2402
0.003	34.03	70.658	54.932	46.000	37.233	28.274	22.000	15.507	8.658	2.137	1.644	1.644	1.644	0.000	0.000	0.000	0.000	3650
0.005	28.05	82.248	72.418	66.788	61.109	54.151	46.612	39.738	28.446	11.259	1.677	0.996	0.299	0.000	0.000	0.000	0.000	6022
0.01	19.88	90.273	84.515	80.970	76.519	70.228	60.301	51.672	37.918	17.266	4.069	1.057	0.175	0.000	0.000	0.000	0.000	12018
0.02	12.96	94.342	90.596	88.082	84.485	77.873	66.568	55.787	39.513	16.469	3.717	0.755	0.000	0.000	0.000	0.000	0.000	24106
0.03	10.20	95.391	92.095	89.696	85.781	77.931	64.157	52.295	34.757	13.313	2.791	0.660	0.000	0.000	0.000	0.000	0.000	36191
0.05	7.24	96.298	93.363	90.923	86.304	76.263	59.480	47.224	29.388	9.370	1.891	0.461	0.028	0.000	0.000	0.000	0.000	60340
0.1	4.59	95.281	91.178	87.402	80.764	66.498	46.436	33.696	18.980	5.405	1.007	0.245	0.029	0.000	0.000	0.000	0.000	119591
0.2	3.43	90.833	82.896	75.949	64.599	46.714	28.807	19.588	10.349	2.795	0.506	0.123	0.017	0.000	0.000	0.000	0.000	239870
0.3	2.90	88.052	78.204	69.619	56.441	37.293	21.198	13.959	7.178	1.898	0.339	0.082	0.012	0.000	0.000	0.000	0.000	357959
0.5	2.29	84.205	71.624	61.376	46.599	27.567	14.208	9.038	4.437	1.148	0.203	0.049	0.007	0.000	0.000	0.000	0.000	598560
1	1.49	80.789	65.461	53.549	37.255	18.340	8.000	4.902	2.322	0.586	0.103	0.025	0.004	0.000	0.000	0.000	0.000	1183027

NTUA Campus Ka-band 4-year average, Data Availability: 95.70 %												
Start Date	1st July 2016											
End Date	30th June 2020											
Attenuation threshold [dB]	Fade Slope [dB/sec]											
	< 0.5	-0.5 to -0.45	-0.45 to -0.4	-0.4 to -0.35	-0.35 to -0.3	-0.3 to -0.25	-0.25 to -0.2	-0.2 to -0.15	-0.15 to -0.1	-0.1 to -0.05	-0.05 to 0.0
	Probability of exceedance [%]										
1	0.002	0.001	0.001	0.002	0.002	0.006	0.021	0.032	0.094	0.555	50.842
3	0.010	0.008	0.005	0.012	0.011	0.038	0.120	0.185	0.536	2.910	46.758
5	0.024	0.033	0.015	0.038	0.037	0.120	0.383	0.547	1.659	7.586	40.412
10	0.000	0.043	0.027	0.180	0.105	0.247	0.870	1.334	3.286	10.830	34.415
15	0.000	0.000	0.090	0.175	0.356	0.420	1.136	1.662	4.243	11.423	31.459
20	0.000	0.000	0.000	0.126	0.555	0.277	1.253	1.782	4.447	10.466	32.070
25	0.000	0.306	0.061	0.000	0.000	0.098	0.612	1.750	3.781	9.765	35.095

Attenuation threshold [dB]	Fade Slope [dB/sec]										
	0.0 to 0.05	0.05 to 0.1	0.1 to 0.15	0.15 to 0.2	0.2 to 0.25	0.25 to 0.3	0.3 to 0.35	0.35 to 0.4	0.4 to 0.45	0.45 to 0.5	> 0.5
	Probability of exceedance [%]										
1	47.720	0.524	0.120	0.051	0.015	0.006	0.002	0.002	0.001	0.001	0.000
3	45.536	2.751	0.673	0.284	0.087	0.033	0.014	0.013	0.008	0.005	0.002
5	38.424	7.387	1.943	0.878	0.278	0.100	0.045	0.042	0.024	0.017	0.008
10	31.169	10.521	3.858	1.871	0.754	0.201	0.134	0.089	0.064	0.000	0.000
15	29.701	10.467	4.615	2.432	1.089	0.260	0.271	0.122	0.042	0.037	0.000
20	30.018	10.230	4.766	2.194	1.168	0.311	0.084	0.000	0.000	0.076	0.177
25	31.718	10.512	3.585	1.725	0.624	0.000	0.000	0.000	0.184	0.122	0.061

NTUA Campus Ka-band 4-year average, Data Availability: 95.70 %														
Start Date									1st July 2016					
End Date									30th June 2020					
Attenuation threshold [dB]	Fade Duration [sec]													
	1	10	30	60	120	180	300	600	900	1200	1500	1800	2400	3600
	Normalized Probability of exceedance [%]													
1	100.000	19.236	8.114	5.032	3.109	2.366	1.646	0.977	0.659	0.518	0.412	0.349	0.257	0.133
3	100.000	28.257	16.014	11.842	7.702	6.162	4.108	1.909	1.252	0.818	0.497	0.337	0.160	0.080
5	100.000	40.015	24.149	18.421	12.848	9.675	6.347	3.406	1.858	0.929	0.697	0.464	0.232	0.155
10	100.000	45.330	35.165	26.648	17.033	14.286	9.341	4.121	2.198	0.824	0.824	0.275	0.275	0.000
15	100.000	47.429	33.143	28.000	17.714	13.714	10.286	5.143	2.286	0.571	0.571	0.571	0.571	0.000
20	100.000	49.580	31.933	22.689	17.647	15.126	10.924	4.202	0.840	0.840	0.840	0.840	0.000	0.000
25	100.000	54.217	40.964	30.120	20.482	18.072	12.048	3.614	1.205	0.000	0.000	0.000	0.000	0.000

Probability of exceedance [%]	Corresponding Attenuation A [dB]	Fade Duration [sec]													
		1	10	30	60	120	180	300	600	900	1200	1500	1800	2400	3600
		Normalized Probability of exceedance [%]													
0.001	38.26	100.000	4.046	1.734	0.578	0.578	0.578	0.578	0.000	0.000	0.000	0.000	0.000	0.000	0.000
0.002	36.51	100.000	10.465	4.651	4.651	3.488	3.488	3.488	1.163	1.163	0.000	0.000	0.000	0.000	0.000
0.003	34.03	100.000	46.341	34.146	24.390	21.951	14.634	9.756	2.439	2.439	0.000	0.000	0.000	0.000	0.000
0.005	28.05	100.000	52.174	34.783	26.087	18.841	14.493	11.594	2.899	1.449	0.000	0.000	0.000	0.000	0.000
0.01	19.88	100.000	46.875	28.906	22.656	16.406	14.063	10.938	3.906	0.781	0.781	0.781	0.781	0.000	0.000
0.02	12.96	100.000	46.388	28.517	23.574	17.490	13.688	7.605	3.802	1.901	0.380	0.380	0.380	0.380	0.000
0.03	10.20	100.000	47.863	36.467	26.496	17.664	14.245	9.687	4.274	2.279	0.855	0.570	0.285	0.285	0.000
0.05	7.24	100.000	46.942	31.570	23.636	18.347	13.554	9.587	3.967	2.149	1.157	0.661	0.661	0.331	0.165
0.1	4.59	100.000	33.043	20.924	15.000	10.054	7.609	5.163	2.500	1.902	0.815	0.543	0.326	0.217	0.109
0.2	3.43	100.000	30.506	17.981	12.525	8.129	6.097	4.285	1.701	1.171	0.707	0.420	0.243	0.155	0.088
0.3	2.90	100.000	28.144	15.715	11.542	7.547	5.815	3.936	1.894	1.154	0.799	0.518	0.355	0.207	0.089
0.5	2.29	100.000	25.419	13.543	9.183	6.122	4.608	3.198	1.676	1.154	0.829	0.607	0.479	0.325	0.154
1	1.49	100.000	22.146	10.878	7.372	5.027	3.874	2.769	1.608	1.101	0.793	0.650	0.516	0.364	0.225

NTUA Campus Ka-band 4-year average, Data Availability: 95.70 %							
Start Date				1st July 2016			
End Date				30th June 2020			
Attenuation threshold [dB]	**Total number of fades > 1.0 sec**	**Total number of fades > 10.0 sec**	**Total fading time > 1.0 sec (ITU Total Outage time)**	**Total fading time > 10.0 sec (ITU Total unavailable time)**	**Mean Duration of fade events > 1.0 sec**	**Mean Duration of fade events > 10.0 sec**	**Unavailable to Outage Time Ratio[%]**
1	52489	10097	1924928	1770111	36.673	175.311	91.957
3	6232	1761	328682	311492	52.741	176.884	94.770
5	1292	517	102766	99817	79.540	193.070	97.130
10	364	165	37118	36327	101.973	220.164	97.869
15	175	83	18721	18322	106.977	220.747	97.869
20	119	59	11894	11624	99.950	197.017	97.730
25	83	45	8120	7973	97.831	177.178	98.190

Probability of exceedance [%]	**Corresponding Attenuation A [dB]**	**Total number of fades > 1.0 sec**	**Total number of fades > 10.0 sec**	**Total fading time > 1.0 sec (ITU Total Outage time)**	**Total fading time > 10.0 sec (ITU Total unavailable time)**	**Mean Duration of fade events > 1.0 sec**	**Mean Duration of fade events > 10.0 sec**	**Unavailable to Outage Time Ratio[%]**
0.001	38.26	173	7	1020	456	5.896	65.143	44.706
0.002	36.51	86	9	2267	1978	26.360	219.778	87.252
0.003	34.03	41	19	3602	3524	87.854	185.474	97.835
0.005	28.05	69	36	6001	5866	86.971	162.944	97.750
0.01	19.88	128	60	12044	11747	94.094	195.783	97.534
0.02	12.96	263	122	24031	23534	91.373	192.902	97.932
0.03	10.2	351	168	36083	35349	102.801	210.411	97.966
0.05	7.24	605	284	60022	58816	99.210	207.099	97.991
0.1	4.59	1840	608	119018	114223	64.684	187.867	95.971
0.2	3.43	4527	1381	237342	225651	52.428	163.397	95.074
0.3	2.9	6758	1902	355072	336862	52.541	177.109	94.871
0.5	2.29	11696	2973	592793	559931	50.683	188.339	94.456
1	1.49	23074	5110	1172831	1106481	50.829	216.532	94.343

NTUA Campus Ka-band 4-year average, Data Availability: 95.70 %														
Start Date								1st July 2016						
End Date								30th June 2020						
Attenuation threshold [dB]	**Accumulate Fading Time [sec]**													
	1	**10**	**30**	**60**	**120**	**180**	**300**	**600**	**900**	**1200**	**1500**	**1800**	**2400**	**3600**
	Normalized Probability of exceedance [%]													
1	100.000	91.957	86.821	83.195	78.652	75.718	71.211	63.415	57.129	53.135	49.250	46.423	41.263	31.405
3	100.000	94.770	90.624	87.298	80.665	76.294	67.310	49.373	40.398	31.784	23.495	18.481	11.599	6.339
5	100.000	97.130	93.550	90.237	84.210	78.363	68.634	52.896	37.666	25.297	21.457	16.855	10.859	7.945
10	100.000	97.869	95.945	92.257	84.164	80.085	68.907	45.765	32.154	17.897	17.897	9.365	9.365	0.000
15	100.000	97.869	95.572	93.312	84.707	78.885	70.942	48.998	29.454	14.358	14.358	14.358	14.358	0.000
20	100.000	97.730	94.602	90.281	86.186	82.554	72.507	45.594	19.010	19.010	19.010	19.010	0.000	0.000
25	100.000	98.190	95.567	90.899	82.586	79.039	66.108	29.175	12.672	0.000	0.000	0.000	0.000	0.000

Probability of exceedance [%]	**Corresponding Attenuation A [dB]**	**Accumulate Fading Time [sec]**												
		1	**10**	**30**	**60**	**120**	**180**	**300**	**600**	**900**	**1200**	**1500**	**1800**	**2400**	**3600**
		Normalized Probability of exceedance [%]													
0.001	38.26	100.000	44.706	38.137	31.863	31.863	31.863	31.863	0.000	0.000	0.000	0.000	0.000	0.000	0.000
0.002	36.51	100.000	87.252	83.150	83.150	79.180	79.180	79.180	39.921	39.921	0.000	0.000	0.000	0.000	0.000
0.003	34.03	100.000	97.835	95.253	90.228	87.146	74.903	62.299	25.541	25.541	0.000	0.000	0.000	0.000	0.000
0.005	28.05	100.000	97.750	94.518	89.618	81.703	73.554	65.972	26.679	16.381	0.000	0.000	0.000	0.000	0.000
0.01	19.88	100.000	97.534	93.922	91.041	86.026	82.365	74.892	45.068	18.773	18.773	18.773	18.773	0.000	0.000
0.02	12.96	100.000	97.932	94.490	92.135	86.139	79.789	64.080	43.881	28.147	11.352	11.352	11.352	11.352	0.000
0.03	10.20	100.000	97.966	95.959	91.708	84.247	79.076	68.736	45.642	31.915	17.377	13.328	8.860	8.860	0.000
0.05	7.24	100.000	97.991	95.130	91.691	87.358	80.137	70.897	46.856	33.641	23.326	16.701	16.701	10.541	6.028
0.1	4.59	100.000	95.971	92.753	88.940	82.517	76.856	67.801	50.190	43.310	26.104	20.639	15.204	11.834	7.104
0.2	3.43	100.000	95.074	90.768	86.341	79.032	73.301	65.269	44.237	36.902	27.499	20.190	14.482	10.966	7.061
0.3	2.90	100.000	94.871	90.727	87.334	80.836	75.967	67.715	50.669	40.278	33.133	25.937	20.792	14.724	7.622
0.5	2.29	100.000	94.456	90.380	86.623	81.417	77.003	70.434	57.527	49.670	42.909	36.892	32.726	26.475	16.813
1	1.49	100.000	94.343	90.525	87.581	83.644	80.309	75.192	65.558	58.272	52.002	48.178	43.912	37.788	30.033

NTUA Campus Ka-band 4-year average, Data Availability: 95.70 %																		
Start Date														1st July 2016				
End Date														30th June 2020				
Attenuation threshold [dB]	Inter-Fade Duration [sec]																	
	1	2	3	5	10	20	30	50	100	200	300	500	1000	2000				
	Normalized Probability of exceedance [%]																	
1	100.000	64.515	48.517	33.873	21.676	14.890	12.488	10.440	7.543	5.645	4.807	3.856	2.879	2.171				
3	100.000	63.463	48.173	34.617	22.990	16.376	13.912	11.345	8.675	6.867	6.118	5.237	4.310	3.551				
5	100.000	66.016	51.880	39.695	30.271	24.084	21.942	19.752	16.611	13.993	12.565	11.042	9.710	8.377				
10	100.000	70.599	57.713	44.828	35.209	30.309	27.586	24.319	21.960	19.419	18.693	17.241	15.426	13.067				
15	100.000	72.481	62.791	51.163	43.411	34.496	31.395	29.457	26.357	22.481	20.930	19.380	18.605	16.279				
20	100.000	73.780	62.195	52.439	43.293	35.366	32.317	28.659	26.220	21.951	20.732	20.732	19.512	17.683				
25	100.000	68.750	50.893	40.179	32.143	25.000	25.000	20.536	20.536	18.750	18.750	17.857	17.857	16.964				

Attenuation threshold [dB]	Inter-Fade Duration [sec]																	
	3000	5000	10000	20000	30000	50000	100000	200000	300000	500000	1000000	2000000	3000000	5000000	10000000			
	Normalized Probability of exceedance [%]																	
1	1.840	1.474	1.053	0.744	0.606	0.490	0.265	0.150	0.088	0.040	0.006	0.000	0.000	0.000	0.000			
3	3.129	2.792	2.277	1.958	1.789	1.621	1.330	1.059	0.881	0.675	0.347	0.084	0.047	0.009	0.000			
5	7.806	7.092	6.092	5.616	5.283	4.950	4.284	3.713	3.141	2.808	1.951	0.857	0.476	0.048	0.000			
10	12.886	11.797	11.434	10.163	10.163	9.982	8.893	8.348	7.260	6.897	5.626	3.630	2.359	1.089	0.000			
15	16.279	14.341	13.953	12.791	12.791	12.403	11.628	11.240	10.078	9.302	8.140	5.039	2.713	0.775	0.000			
20	17.073	15.854	15.854	15.854	15.854	15.244	14.024	13.415	11.585	10.976	9.146	6.098	3.659	1.220	0.000			
25	16.071	15.179	15.179	15.179	15.179	14.286	12.500	12.500	12.500	12.500	10.714	6.250	4.464	0.893	0.000			

NTUA Campus Ka-band 4-year average, Data Availability: 95.70 %															
Start Date		1st July 2016													
End Date		30th June 2020													
Probability of exceedance [%]	Corresponding Attenuation A [dB]	Inter-Fade Duration [sec]													
		1	2	3	5	10	20	30	50	100	200	300	500	1000	2000
		Normalized Probability of exceedance [%]													
0.001	38.26	100.000	52.439	29.573	9.146	2.439	1.220	0.915	0.915	0.915	0.915	0.915	0.915	0.915	0.915
0.002	36.51	100.000	52.318	30.464	18.543	11.258	8.609	6.623	5.960	5.960	5.298	4.636	4.636	4.636	4.636
0.003	34.03	100.000	64.407	54.237	47.458	33.898	22.034	20.339	20.339	18.644	18.644	18.644	18.644	18.644	16.949
0.005	28.05	100.000	77.885	61.538	42.308	34.615	27.885	23.077	22.115	21.154	20.192	17.308	16.346	16.346	15.385
0.01	19.88	100.000	71.779	60.736	49.693	44.172	36.810	33.129	28.221	25.767	22.086	20.859	20.859	19.632	17.791
0.02	12.96	100.000	72.652	58.840	48.066	38.950	32.597	29.834	27.072	21.547	18.508	17.403	16.298	14.641	12.707
0.03	10.20	100.000	67.203	55.734	48.692	38.833	33.602	30.584	26.761	23.944	21.529	20.322	18.511	16.499	13.883
0.05	7.24	100.000	65.835	53.688	44.794	33.731	29.067	26.139	23.427	20.390	17.570	16.377	14.534	12.798	11.714
0.1	4.59	100.000	64.386	50.911	38.948	29.082	22.723	20.385	17.635	14.163	11.894	10.760	9.694	8.422	7.150
0.2	3.43	100.000	64.210	48.765	35.022	23.301	16.468	14.319	11.887	9.226	7.370	6.590	5.797	4.747	3.967
0.3	2.90	100.000	63.924	48.379	34.081	22.354	16.104	13.679	11.254	8.598	6.723	5.872	5.021	4.118	3.310
0.5	2.29	100.000	63.011	47.107	32.618	20.685	14.206	11.904	9.333	6.840	5.215	4.459	3.766	3.039	2.493
1	1.49	100.000	62.772	46.062	31.203	19.278	13.076	10.769	8.804	6.511	4.994	4.353	3.689	2.960	2.433

Probability of exceedance [%]	Corresponding Attenuation A [dB]	Inter-Fade Duration [sec]														
		3000	5000	10000	20000	30000	50000	100000	200000	300000	500000	1000000	2000000	3000000	5000000	10000000
		Normalized Probability of exceedance [%]														
0.001	38.26	0.915	0.915	0.915	0.915	0.915	0.915	0.610	0.610	0.610	0.610	0.610	0.000	0.000	0.000	0.000
0.002	36.51	4.636	4.636	4.636	4.636	4.636	3.974	2.649	2.649	2.649	2.649	2.649	1.325	1.325	0.662	0.000
0.003	34.03	15.254	15.254	15.254	15.254	15.254	13.559	10.169	10.169	10.169	10.169	8.475	5.085	3.390	3.390	0.000
0.005	28.05	14.423	14.423	14.423	14.423	14.423	13.462	11.538	11.538	11.538	11.538	9.615	4.808	2.885	0.962	0.000
0.01	19.88	17.178	15.951	15.951	15.951	15.951	15.337	14.110	13.497	11.656	11.043	9.202	6.135	3.681	1.227	0.000
0.02	12.96	12.707	11.326	11.326	10.221	9.945	9.669	8.564	8.287	7.182	6.906	6.077	3.867	2.210	0.552	0.000
0.03	10.20	13.682	12.676	12.475	11.268	11.066	10.865	9.658	9.054	7.847	7.445	6.237	4.225	2.616	1.207	0.000
0.05	7.24	10.954	10.304	9.328	8.677	8.351	7.918	7.050	6.508	5.423	4.989	3.905	2.386	1.410	0.434	0.000
0.1	4.59	6.531	5.947	5.122	4.572	4.297	3.988	3.438	2.853	2.406	2.200	1.375	0.584	0.275	0.034	0.000
0.2	3.43	3.583	3.173	2.623	2.278	2.099	1.945	1.612	1.280	1.062	0.857	0.486	0.154	0.090	0.013	0.000
0.3	2.90	2.975	2.674	2.175	1.883	1.728	1.556	1.238	0.989	0.808	0.602	0.301	0.077	0.043	0.009	0.000
0.5	2.29	2.225	2.005	1.644	1.366	1.210	1.083	0.859	0.649	0.502	0.356	0.161	0.044	0.005	0.005	0.000
1	1.49	2.124	1.811	1.472	1.161	1.016	0.857	0.589	0.387	0.287	0.154	0.050	0.002	0.000	0.000	0.000

NTUA Campus Ka-band 4-year average, Data Availability: 95.70 %			
Start Date		1st July 2016	
End Date		30th June 2020	
Attenuation threshold [dB]	Total number of inter-fades	Total duration of inter-fades [sec]	
1	101365	118602335	
3	10674	114752958	
5	2101	11928723	
10	551	103175856	
15	258	101167512	
20	164	99871138	
25	112	99874860	

Probability of exceedance [%]	Corresponding Attenuation A [dB]	Total number of inter-fades	Total duration of inter-fades [sec]
0.001	38.26	328	79538764
0.002	36.51	151	92429330
0.003	34.03	59	92428242
0.005	28.05	104	95254943
0.01	19.88	163	99870998
0.02	12.96	362	101162231
0.03	10.20	497	103176919
0.05	7.24	922	111333587
0.1	4.59	2909	114622928
0.2	3.43	7815	114845444
0.3	2.90	11631	114726137
0.5	2.29	20498	119435654
1	1.49	42130	119377398

NTUA LTCP Ka-band 4-year average, Data Availability: 96.39 %																	
Start Date								1st July 2016									
End Date								30th June 2020									
Attenuation threshold [dB]	Absolute Fade Slope [dB/sec]																Number of fade slope samples
	0.001	0.002	0.003	0.005	0.01	0.02	0.03	0.05	0.1	0.2	0.3	0.5	1	2	3	5	
	Probability of exceedance [%]																
1	82.765	68.513	57.082	40.736	21.278	9.584	5.719	2.805	0.947	0.168	0.051	0.018	0.014	0.013	0.012	0.011	799041
3	93.561	87.718	82.399	73.113	55.502	35.984	24.996	13.943	4.826	0.879	0.278	0.098	0.076	0.071	0.066	0.058	147374
5	97.151	94.480	91.769	86.675	75.414	57.064	43.505	26.073	9.900	1.838	0.620	0.216	0.170	0.158	0.149	0.131	65815
10	97.584	95.206	93.224	89.460	81.159	65.971	53.257	37.048	17.204	3.526	1.471	0.526	0.426	0.396	0.369	0.330	26034
15	97.519	94.758	92.877	89.418	82.542	69.717	60.081	43.411	20.785	6.038	2.875	1.076	0.912	0.846	0.789	0.698	12172
20	96.936	93.099	90.869	86.808	78.361	64.218	54.253	41.136	23.780	8.046	3.108	2.023	1.621	1.502	1.413	1.264	6724
25	96.616	91.556	88.963	84.029	77.767	66.034	57.147	44.592	24.288	8.286	5.946	5.440	3.416	3.194	3.004	2.657	3162

Prob. of exceedance [%]	Corr. Attenuation A [dB]	Absolute Fade Slope [dB/sec]																Number of fade slope samples
		0.001	0.002	0.003	0.005	0.01	0.02	0.03	0.05	0.1	0.2	0.3	0.5	1	2	3	5	
		Probability of exceedance [%]																
0.001	32.31	91.901	80.192	74.419	64.635	51.564	36.728	26.945	18.524	13.392	12.831	12.510	11.949	8.821	8.180	7.698	6.816	1247
0.002	27.18	95.731	89.447	86.166	80.949	73.834	59.684	51.344	36.759	17.984	7.787	7.470	6.798	4.269	4.032	3.755	3.320	2530
0.003	23.42	96.974	92.572	90.371	86.520	79.945	68.253	60.055	47.758	25.530	8.308	5.117	4.732	2.971	2.779	2.613	2.311	3635
0.005	20.52	97.313	93.762	91.699	87.924	79.607	65.083	55.998	42.674	24.760	8.381	3.039	2.239	1.743	1.615	1.520	1.360	6252
0.01	14.93	97.601	94.828	92.869	89.267	82.306	69.556	60.042	43.479	20.792	6.017	2.838	1.065	0.903	0.838	0.781	0.691	12298
0.02	10.38	97.640	95.211	93.233	89.703	81.885	66.742	54.586	38.134	17.643	3.636	1.576	0.562	0.456	0.423	0.394	0.349	24367
0.03	8.08	97.527	95.155	93.011	88.789	79.903	64.077	50.787	33.199	14.785	2.872	1.107	0.377	0.303	0.281	0.262	0.235	36598
0.05	5.34	97.233	94.659	92.254	87.363	76.981	58.985	45.140	27.123	10.561	1.972	0.670	0.233	0.184	0.171	0.161	0.141	60893
0.1	3.37	94.676	89.727	85.093	76.749	60.463	40.679	29.138	16.469	5.814	1.060	0.339	0.118	0.093	0.086	0.081	0.071	121076
0.2	2.24	91.144	83.447	76.490	64.560	44.256	25.537	16.842	8.878	3.023	0.543	0.169	0.060	0.046	0.043	0.040	0.036	241510
0.3	1.74	89.096	79.489	70.873	57.042	35.719	18.823	12.007	6.119	2.072	0.368	0.115	0.040	0.031	0.029	0.027	0.024	357931
0.5	1.25	85.142	72.486	62.053	46.428	26.009	12.450	7.585	3.768	1.273	0.225	0.069	0.024	0.019	0.018	0.017	0.015	592139
1	0.78	79.852	63.824	51.509	34.925	17.074	7.265	4.269	2.071	0.698	0.124	0.038	0.013	0.010	0.010	0.009	0.008	1085642

NTUA LTCP Ka-band 4-year average, Data Availability: 96.39 %											
Start Date	1st July 2016										
End Date	30th June 2020										
Attenuation threshold [dB]	Fade Slope [dB/sec]										
	< 0.5	-0.5 to -0.45	-0.45 to -0.4	-0.4 to -0.35	-0.35 to -0.3	-0.3 to -0.25	-0.25 to -0.2	-0.2 to -0.15	-0.15 to -0.1	-0.1 to -0.05	-0.05 to 0.0
	Probability of exceedance [%]										
1	0.002	0.000	0.000	0.004	0.008	0.011	0.048	0.103	0.296	0.923	49.335
3	0.011	0.001	0.001	0.022	0.041	0.054	0.246	0.538	1.450	4.544	44.003
5	0.023	0.003	0.000	0.050	0.091	0.119	0.528	1.059	2.912	8.105	38.176
10	0.050	0.000	0.008	0.127	0.201	0.266	0.698	1.929	5.154	10.458	31.690
15	0.083	0.017	0.008	0.191	0.448	0.381	1.111	2.147	5.713	11.914	30.138
20	0.030	0.015	0.000	0.076	0.574	0.665	1.512	2.691	5.941	9.675	31.731
25	1.048	0.000	0.098	0.196	0.065	0.000	0.753	2.390	6.549	11.886	26.654

Attenuation threshold [dB]	Fade Slope [dB/sec]										
	0.0 to 0.05	0.05 to 0.1	0.1 to 0.15	0.15 to 0.2	0.2 to 0.25	0.25 to 0.3	0.3 to 0.35	0.35 to 0.4	0.4 to 0.45	0.45 to 0.5	> 0.5
	Probability of exceedance [%]										
1	47.873	0.936	0.293	0.086	0.042	0.016	0.009	0.009	0.003	0.000	0.002
3	42.119	4.580	1.501	0.460	0.223	0.078	0.049	0.048	0.018	0.001	0.011
5	35.877	8.096	3.071	1.033	0.399	0.175	0.110	0.107	0.041	0.003	0.023
10	31.532	9.470	4.895	1.759	0.675	0.424	0.262	0.251	0.093	0.008	0.050
15	26.971	10.919	4.842	2.181	0.887	0.813	0.945	0.182	0.008	0.017	0.083
20	28.103	7.967	5.125	2.237	1.421	1.421	0.302	0.030	0.000	0.106	0.378
25	30.714	9.136	5.534	2.096	1.604	0.065	0.131	0.000	0.000	0.033	1.048

NTUA LTCP Ka-band 4-year average, Data Availability: 96.39 %														
Start Date									1st July 2016					
End Date									30th June 2020					
Attenuation threshold [dB]	Fade Duration [sec]													
	1	10	30	60	120	180	300	600	900	1200	1500	1800	2400	3600
	Normalized Probability of exceedance [%]													
1	100.000	20.896	10.248	6.676	4.193	3.163	2.191	1.237	0.850	0.571	0.414	0.310	0.198	0.072
3	100.000	33.405	21.524	15.540	10.331	7.749	4.994	2.540	1.679	1.033	0.646	0.387	0.043	0.000
5	100.000	44.000	31.040	24.000	17.760	13.760	9.920	5.440	3.520	1.440	0.320	0.320	0.000	0.000
10	100.000	50.492	34.098	24.918	17.377	14.098	8.852	2.623	0.984	0.328	0.328	0.328	0.000	0.000
15	100.000	55.714	37.857	27.857	20.000	14.286	7.857	2.143	0.714	0.714	0.714	0.000	0.000	0.000
20	100.000	62.637	45.055	30.769	19.780	12.088	4.396	1.099	1.099	0.000	0.000	0.000	0.000	0.000
25	100.000	53.846	48.718	35.897	28.205	12.821	2.564	2.564	0.000	0.000	0.000	0.000	0.000	0.000

Probability of exceedance [%]	Corresponding Attenuation A [dB]	Fade Duration [sec]												
		1	10	30	60	120	180	300	600	900	1200	1500	1800	2400	3600
		Normalized Probability of exceedance [%]													
0.001	32.31	100.000	50.000	40.909	31.818	18.182	9.091	0.000	0.000	0.000	0.000	0.000	0.000	0.000	0.000
0.002	27.18	100.000	44.444	33.333	24.074	9.259	5.556	1.852	0.000	0.000	0.000	0.000	0.000	0.000	0.000
0.003	23.42	100.000	45.455	36.364	27.273	21.818	10.909	3.636	1.818	0.000	0.000	0.000	0.000	0.000	0.000
0.005	20.52	100.000	53.000	31.000	26.000	15.000	8.000	4.000	1.000	1.000	0.000	0.000	0.000	0.000	0.000
0.01	14.93	100.000	54.967	35.762	25.828	18.543	13.245	7.285	1.987	0.662	0.662	0.662	0.000	0.000	0.000
0.02	10.38	100.000	53.506	38.745	26.937	17.712	14.760	8.487	2.583	1.107	0.369	0.369	0.369	0.000	0.000
0.03	8.08	100.000	55.457	38.938	28.319	22.419	16.224	11.504	4.720	2.065	0.590	0.295	0.295	0.000	0.000
0.05	5.34	100.000	44.328	31.763	25.480	17.976	14.834	10.820	5.410	2.967	1.222	0.349	0.349	0.000	0.000
0.1	3.37	100.000	35.063	23.183	16.378	11.707	8.708	5.825	2.653	1.961	1.096	0.692	0.346	0.058	0.000
0.2	2.24	100.000	30.173	18.081	12.879	9.110	6.775	4.347	2.104	1.225	0.809	0.555	0.324	0.162	0.046
0.3	1.74	100.000	26.415	14.745	10.279	7.036	5.673	3.932	1.798	1.123	0.730	0.506	0.407	0.169	0.056
0.5	1.25	100.000	23.255	12.246	8.048	5.413	4.247	2.932	1.590	0.975	0.636	0.438	0.332	0.155	0.042
1	0.78	100.000	19.067	8.848	5.511	3.421	2.552	1.736	0.971	0.632	0.470	0.334	0.255	0.170	0.054

NTUA LTCP Ka-band 4-year average, Data Availability: 96.39 %							
Start Date				1st July 2016			
End Date				30th June 2020			
Attenuation threshold [dB]	**Total number of fades > 1.0 sec**	**Total number of fades > 10.0 sec**	**Total fading time > 1.0 sec (ITU Total Outage time)**	**Total fading time > 10.0 sec (ITU Total unavailable time)**	**Mean Duration of fade events > 1.0 sec**	**Mean Duration of fade events > 10.0 sec**	**Unavailable to Outage Time Ratio[%]**
1	22229	4645	790724	727324	35.572	156.582	91.982
3	2323	776	146023	140243	62.860	180.726	96.042
5	625	275	65416	64031	104.666	232.840	97.883
10	305	154	25842	25226	84.728	163.805	97.616
15	140	78	11992	11682	85.657	149.769	97.415
20	91	57	6546	6404	71.934	112.351	97.831
25	39	21	3091	3015	79.256	143.571	97.541

Probability of exceedance [%]	**Corresponding Attenuation A [dB]**	**Total number of fades > 1.0 sec**	**Total number of fades > 10.0 sec**	**Total fading time > 1.0 sec (ITU Total Outage time)**	**Total fading time > 10.0 sec (ITU Total unavailable time)**	**Mean Duration of fade events > 1.0 sec**	**Mean Duration of fade events > 10.0 sec**	**Unavailable to Outage Time Ratio[%]**
0.001	32.31	22	11	1184	1138	53.818	103.455	96.115
0.002	27.18	54	24	2436	2329	45.111	97.042	95.608
0.003	23.42	55	25	3614	3499	65.709	139.960	96.818
0.005	20.52	100	53	6056	5857	60.560	110.509	96.714
0.01	14.93	151	83	12114	11811	80.225	142.301	97.499
0.02	10.38	271	145	24182	23715	89.232	163.552	98.069
0.03	8.08	339	188	36222	35605	106.850	189.388	98.297
0.05	5.34	573	254	60477	59264	105.545	233.323	97.994
0.1	3.37	1734	608	120236	116030	69.340	190.839	96.502
0.2	2.24	4325	1305	238973	227598	55.254	174.405	95.240
0.3	1.74	7121	1881	354794	335366	49.824	178.291	94.524
0.5	1.25	14152	3291	586316	546968	41.430	166.201	93.289
1	0.78	35308	6732	1075824	974155	30.470	144.705	90.550

NTUA LTCP Ka-band 4-year average, Data Availability: 96.39 %														
Start Date								1st July 2016						
End Date								30th June 2020						
Attenuation threshold [dB]	Accumulate Fading Time [sec]													
	1	10	30	60	120	180	300	600	900	1200	1500	1800	2400	3600
	Normalized Probability of exceedance [%]													
1	100.000	91.982	86.797	82.515	76.575	72.361	66.018	54.929	47.068	38.889	32.974	28.218	21.596	11.420
3	100.000	96.042	92.683	88.511	81.376	75.155	64.936	48.618	38.708	28.192	19.724	12.812	1.848	0.000
5	100.000	97.883	95.573	92.798	87.865	82.189	73.289	55.071	41.317	20.590	6.558	6.558	0.000	0.000
10	100.000	97.616	94.010	89.006	81.062	75.729	60.885	29.367	14.867	7.051	7.051	7.051	0.000	0.000
15	100.000	97.415	93.487	88.534	80.921	70.881	52.702	25.667	14.360	14.360	14.360	0.000	0.000	0.000
20	100.000	97.831	92.392	84.647	70.975	55.469	32.676	16.942	16.942	0.000	0.000	0.000	0.000	0.000
25	100.000	97.541	96.797	90.456	81.139	55.840	25.008	25.008	0.000	0.000	0.000	0.000	0.000	0.000

Probability of exceedance [%]	Corresponding Attenuation A [dB]	Accumulate Fading Time [sec]												
		1	10	30	60	120	180	300	600	900	1200	1500	1800	2400	3600
		Normalized Probability of exceedance [%]													
0.001	32.31	100.000	96.115	92.736	85.389	64.105	41.976	0.000	0.000	0.000	0.000	0.000	0.000	0.000	0.000
0.002	27.18	100.000	95.608	91.585	83.169	52.709	40.599	22.003	0.000	0.000	0.000	0.000	0.000	0.000	0.000
0.003	23.42	100.000	96.818	94.106	87.908	80.354	57.111	31.682	23.132	0.000	0.000	0.000	0.000	0.000	0.000
0.005	20.52	100.000	96.714	89.069	85.816	68.659	50.248	34.957	18.230	18.230	0.000	0.000	0.000	0.000	0.000
0.01	14.93	100.000	97.499	93.124	87.857	80.287	70.291	52.254	25.433	14.215	14.215	14.215	0.000	0.000	0.000
0.02	10.38	100.000	98.069	95.033	89.240	79.679	74.948	57.927	28.558	15.859	7.522	7.522	7.522	0.000	0.000
0.03	8.08	100.000	98.297	95.309	90.862	85.964	77.370	66.509	40.003	22.580	8.467	5.129	5.129	0.000	0.000
0.05	5.34	100.000	97.994	95.752	93.168	87.177	82.919	73.924	51.848	34.706	17.666	7.013	7.013	0.000	0.000
0.1	3.37	100.000	96.502	93.345	88.938	82.954	76.522	66.539	47.321	39.999	27.088	19.110	10.591	2.182	0.000
0.2	2.24	100.000	95.240	91.320	87.267	81.332	75.077	64.947	47.622	35.987	28.286	22.243	15.326	9.749	4.242
0.3	1.74	100.000	94.524	90.437	86.584	80.942	76.950	68.743	50.036	40.302	32.050	25.954	22.676	13.196	6.765
0.5	1.25	100.000	93.289	88.571	84.169	78.858	74.661	67.150	53.293	42.547	34.140	27.772	23.637	14.465	6.500
1	0.78	100.000	90.550	84.696	80.038	74.271	70.073	63.869	53.172	44.906	39.269	33.246	29.008	23.157	11.888

NTUA LTCP Ka-band 4-year average, Data Availability: 96.39 %																			
Start Date																		1st July 2016	
End Date																		30th June 2020	
Attenuation threshold [dB]	Inter-Fade Duration [sec]																		
	1	2	3	5	10	20	30	50	100	200	300	500	1000	2000	3000	5000	10000	20000	30000
	Normalized Probability of exceedance [%]																		
1	100.000	64.322	48.447	34.413	22.988	16.285	13.800	11.298	8.826	6.846	5.997	5.039	3.822	2.954	2.483	2.031	1.611	1.228	1.051
3	100.000	62.681	47.604	36.071	25.811	20.419	17.973	15.402	12.681	10.559	9.760	8.562	7.439	6.291	5.941	5.167	4.468	3.769	3.345
5	100.000	67.052	55.395	43.256	34.682	28.805	26.012	23.603	20.424	18.208	17.052	15.800	14.451	13.102	12.717	11.175	10.212	9.249	8.574
10	100.000	73.508	60.621	49.403	40.334	34.606	32.220	29.594	23.866	21.480	19.570	19.093	17.900	16.706	15.990	15.274	14.320	14.320	13.365
15	100.000	73.500	61.000	50.500	41.000	34.500	32.500	30.500	26.000	24.000	21.500	21.000	19.000	18.500	18.000	17.000	16.000	16.000	16.000
20	100.000	71.654	60.630	48.819	37.795	32.283	30.709	29.921	27.559	24.409	24.409	21.260	19.685	19.685	19.685	19.685	18.898	18.898	18.898
25	100.000	71.698	58.491	47.170	37.736	33.962	33.962	32.075	32.075	26.415	26.415	24.528	24.528	24.528	24.528	24.528	24.528	24.528	24.528

Attenuation threshold [dB]	Inter-Fade Duration [sec]																		
	3000	5000	10000	20000	30000	50000	100000	200000	300000	500000	1000000	2000000	3000000	5000000	10000000				
	Normalized Probability of exceedance [%]																		
1	2.483	2.031	1.611	1.228	1.051	0.887	0.552	0.339	0.258	0.137	0.046	0.007	0.000	0.000	0.000				
3	5.941	5.167	4.468	3.769	3.345	2.971	2.446	2.022	1.797	1.398	0.799	0.300	0.125	0.050	0.000				
5	12.717	11.175	10.212	9.249	8.574	7.707	6.647	5.395	5.010	4.046	3.083	1.734	0.578	0.193	0.000				
10	15.990	15.274	14.320	14.320	13.365	11.695	10.740	10.263	9.308	8.115	6.683	3.341	1.909	0.955	0.000				
15	18.000	17.000	16.000	16.000	16.000	15.000	13.500	13.000	11.500	10.500	9.000	6.500	4.500	1.500	0.000				
20	19.685	19.685	18.898	18.898	18.898	18.898	16.535	16.535	14.961	14.173	12.598	9.449	6.299	2.362	0.000				
25	24.528	24.528	24.528	24.528	24.528	24.528	20.755	20.755	16.981	16.981	15.094	11.321	5.660	1.887	0.000				

NTUA LTCP Ka-band 4-year average, Data Availability: 96.39 %															
Start Date		1st July 2016													
End Date		30th June 2020													
Probability of exceedance [%]	Corresponding Attenuation A [dB]	Inter-Fade Duration [sec]													
		1	2	3	5	10	20	30	50	100	200	300	500	1000	2000
		Normalized Probability of exceedance [%]													
0.001	32.31	100.000	78.125	53.125	28.125	25.000	15.625	15.625	15.625	15.625	15.625	15.625	15.625	15.625	15.625
0.002	27.18	100.000	73.846	55.385	44.615	29.231	23.077	21.538	20.000	20.000	18.462	18.462	18.462	18.462	18.462
0.003	23.42	100.000	78.125	64.063	59.375	54.688	45.313	42.188	32.813	28.125	28.125	28.125	28.125	26.563	26.563
0.005	20.52	100.000	69.014	56.338	42.958	38.028	29.577	26.056	25.352	22.535	19.718	19.718	17.606	16.197	16.197
0.01	14.93	100.000	73.367	58.291	48.744	40.201	34.171	32.161	30.653	26.131	24.121	21.608	21.106	19.095	18.593
0.02	10.38	100.000	70.617	60.000	50.370	40.494	33.827	32.593	28.395	23.457	20.988	19.506	18.272	17.284	16.296
0.03	8.08	100.000	71.298	57.952	48.263	38.940	32.541	29.433	24.863	21.389	19.013	17.916	16.636	15.539	14.260
0.05	5.34	100.000	67.154	52.193	40.495	31.946	27.109	24.634	23.510	21.260	19.573	18.110	16.985	15.411	13.948
0.1	3.37	100.000	63.795	48.832	36.310	27.381	22.009	19.986	18.103	14.370	12.313	11.371	10.150	8.999	7.499
0.2	2.24	100.000	61.939	46.187	32.675	23.100	17.832	15.369	13.368	11.208	9.324	8.376	7.099	5.940	4.912
0.3	1.74	100.000	63.231	47.993	35.660	24.752	18.412	15.746	13.096	10.500	8.459	7.565	6.425	5.077	4.083
0.5	1.25	100.000	64.515	48.605	34.605	23.170	16.529	14.167	11.741	9.282	7.266	6.305	5.328	4.158	3.238
1	0.78	100.000	65.766	50.558	36.480	24.663	17.938	15.414	12.878	10.217	8.263	7.134	5.835	4.324	3.062

Probability of exceedance [%]	Corresponding Attenuation A [dB]	Inter-Fade Duration [sec]														
		3000	5000	10000	20000	30000	50000	100000	200000	300000	500000	1000000	2000000	3000000	5000000	10000000
		Normalized Probability of exceedance [%]														
0.001	32.31	15.625	15.625	15.625	15.625	15.625	15.625	15.625	15.625	12.500	9.375	9.375	6.250	6.250	0.000	0.000
0.002	27.18	18.462	18.462	18.462	18.462	18.462	18.462	16.923	16.923	15.385	13.846	12.308	9.231	4.615	1.538	0.000
0.003	23.42	26.563	26.563	25.000	25.000	25.000	25.000	21.875	21.875	18.750	17.188	15.625	10.938	6.250	1.563	0.000
0.005	20.52	16.197	16.197	15.493	15.493	15.493	15.493	13.380	13.380	11.972	11.268	9.859	7.042	4.225	1.408	0.000
0.01	14.93	18.090	17.085	16.080	16.080	16.080	15.075	13.568	13.065	11.558	10.553	9.045	6.533	4.523	1.508	0.000
0.02	10.38	15.556	14.815	13.827	13.827	12.840	11.111	10.123	9.630	8.642	7.407	6.173	2.716	1.728	0.494	0.000
0.03	8.08	14.077	13.346	12.249	11.700	10.969	9.506	8.592	8.044	7.495	6.581	5.302	2.742	1.280	0.548	0.000
0.05	5.34	13.498	11.924	11.136	10.011	9.336	8.211	6.974	5.962	5.737	4.612	3.487	2.025	0.787	0.225	0.000
0.1	3.37	7.185	6.139	5.476	4.779	4.220	3.802	3.104	2.546	2.302	1.814	1.151	0.419	0.140	0.035	0.000
0.2	2.24	4.570	3.951	3.227	2.726	2.357	2.081	1.673	1.330	1.093	0.869	0.461	0.198	0.053	0.026	0.000
0.3	1.74	3.698	3.120	2.527	2.165	1.941	1.679	1.317	1.009	0.801	0.601	0.270	0.077	0.015	0.008	0.000
0.5	1.25	2.772	2.299	1.837	1.449	1.274	1.081	0.805	0.596	0.429	0.268	0.093	0.022	0.000	0.000	0.000
1	0.78	2.544	1.951	1.428	1.037	0.830	0.605	0.350	0.207	0.146	0.072	0.013	0.000	0.000	0.000	0.000

NTUA LTCP Ka-band 4-year average, Data Availability: 96.39 %		
Start Date	1st July 2016	
End Date	30th June 2020	
Attenuation threshold [dB]	**Total number of inter-fades**	**Total duration of inter-fades [sec]**
1	43088	120044447
3	4006	115320470
5	1038	115401922
10	419	115440106
15	200	112844803
20	127	110650863
25	53	95548169

Probability of exceedance [%]	Corresponding Attenuation A [dB]	Total number of inter-fades	Total duration of inter-fades [sec]
0.001	32.31	32	95550020
0.002	27.18	65	95548808
0.003	23.42	64	96987093
0.005	20.52	142	110651344
0.01	14.93	199	112844693
0.02	10.38	405	115441743
0.03	8.08	547	115429805
0.05	5.34	889	115406952
0.1	3.37	2867	115346685
0.2	2.24	7593	115227008
0.3	1.74	12981	120414277
0.5	1.25	26837	120187441
1	0.78	71908	120196939

NTUA Campus Q-band 2-year average, Data Availability: 95.33 %																	
Start Date								1st July 2017									
End Date								30th June 2019									
Attenuation threshold [dB]	**Absolute Fade Slope [dB/sec]**																**Number of fade slope samples**
	0.001	**0.002**	**0.003**	**0.005**	**0.01**	**0.02**	**0.03**	**0.05**	**0.1**	**0.2**	**0.3**	**0.5**	**1**	**2**	**3**	**5**	
	Probability of exceedance [%]																
1	83.478	69.833	59.249	44.332	24.803	11.258	6.483	3.016	0.806	0.084	0.014	0.000	0.000	0.000	0.000	0.000	1868269
3	90.409	81.835	74.436	62.025	40.777	21.370	13.177	6.444	1.807	0.189	0.032	0.000	0.000	0.000	0.000	0.000	822216
5	92.498	86.105	80.844	71.471	52.957	31.689	20.993	11.124	3.302	0.358	0.061	0.000	0.000	0.000	0.000	0.000	432115
10	91.592	85.878	82.385	77.122	65.847	49.500	37.916	22.985	7.869	0.961	0.096	0.000	0.000	0.000	0.000	0.000	139918
15	86.348	78.127	74.384	70.270	62.677	50.455	40.751	26.821	10.283	1.148	0.043	0.000	0.000	0.000	0.000	0.000	69520
20	79.910	68.168	63.376	59.146	52.582	42.920	34.966	23.579	8.204	0.240	0.135	0.000	0.000	0.000	0.000	0.000	44515
25	72.712	57.256	51.244	46.562	40.221	31.393	24.667	14.732	1.907	0.191	0.191	0.096	0.000	0.000	0.000	0.000	31354

Prob. of exceedance [%]	**Corr. Attenuation A [dB]**	**Absolute Fade Slope [dB/sec]**																**Number of fade slope samples**
		0.001	**0.002**	**0.003**	**0.005**	**0.01**	**0.02**	**0.03**	**0.05**	**0.1**	**0.2**	**0.3**	**0.5**	**1**	**2**	**3**	**5**	
		Probability of exceedance [%]																
0.001	33.67	nan	nan	nan	nan	nan	nan	nan	nan	nan	nan	nan	nan	nan	nan	nan	nan	0
0.002	33.42	nan	nan	nan	nan	nan	nan	nan	nan	nan	nan	nan	nan	nan	nan	nan	nan	0
0.003	33.26	nan	nan	nan	nan	nan	nan	nan	nan	nan	nan	nan	nan	nan	nan	nan	nan	0
0.005	33.01	95.455	92.424	90.909	90.909	90.909	90.909	90.909	90.909	90.909	90.909	90.909	90.909	0.000	0.000	0.000	0.000	66
0.01	32.57	48.759	25.975	18.262	12.323	5.496	5.319	5.319	5.319	5.319	5.319	5.319	5.319	0.000	0.000	0.000	0.000	1128
0.02	31.81	50.343	24.306	14.566	7.487	2.165	0.441	0.407	0.407	0.407	0.407	0.407	0.407	0.000	0.000	0.000	0.000	14733
0.03	30.61	58.764	36.837	28.654	22.081	14.380	4.764	0.658	0.332	0.332	0.332	0.332	0.332	0.000	0.000	0.000	0.000	18074
0.05	25.56	71.770	55.773	49.573	44.818	38.485	29.662	23.115	13.219	1.294	0.198	0.198	0.099	0.000	0.000	0.000	0.000	30305
0.1	16.41	84.582	75.330	71.297	67.118	59.824	48.549	39.670	27.028	10.307	1.015	0.100	0.000	0.000	0.000	0.000	0.000	60008
0.2	10.84	90.714	84.555	81.084	76.275	66.157	51.020	39.828	24.451	8.589	1.038	0.093	0.000	0.000	0.000	0.000	0.000	119917
0.3	8.68	92.320	86.784	83.186	77.222	64.634	46.480	34.687	20.304	6.657	0.788	0.091	0.000	0.000	0.000	0.000	0.000	180038
0.5	6.41	92.803	87.031	82.499	74.452	58.258	37.885	26.447	14.733	4.531	0.491	0.076	0.000	0.000	0.000	0.000	0.000	300548
1	3.97	91.552	84.148	77.835	66.853	46.893	26.277	16.667	8.464	2.446	0.259	0.044	0.000	0.000	0.000	0.000	0.000	598434

NTUA Campus Q-band 2-year average, Data Availability: 95.33 %												
Start Date	1st July 2017											
End Date	30th June 2019											
Attenuation threshold [dB]	Fade Slope [dB/sec]											
	< 0.5	-0.5 to -0.45	-0.45 to -0.4	-0.4 to -0.35	-0.35 to -0.3	-0.3 to -0.25	-0.25 to -0.2	-0.2 to -0.15	-0.15 to -0.1	-0.1 to -0.05	-0.05 to 0.0
	Probability of exceedance [%]										
1	0.000	0.000	0.000	0.000	0.005	0.005	0.026	0.086	0.241	1.095	50.678
3	0.000	0.000	0.000	0.000	0.011	0.012	0.059	0.194	0.544	2.326	48.501
5	0.000	0.000	0.000	0.000	0.021	0.024	0.111	0.366	0.998	3.986	46.070
10	0.000	0.000	0.000	0.000	0.049	0.059	0.332	0.928	2.357	7.902	38.808
15	0.000	0.000	0.000	0.000	0.000	0.118	0.394	1.341	3.119	8.497	36.633
20	0.000	0.000	0.016	0.052	0.000	0.000	0.034	0.829	3.001	7.887	38.082
25	0.096	0.000	0.000	0.000	0.000	0.000	0.000	0.000	0.804	6.513	42.247

Attenuation threshold [dB]	Fade Slope [dB/sec]										
	0.0 to 0.05	0.05 to 0.1	0.1 to 0.15	0.15 to 0.2	0.2 to 0.25	0.25 to 0.3	0.3 to 0.35	0.35 to 0.4	0.4 to 0.45	0.45 to 0.5	> 0.5
	Probability of exceedance [%]										
1	46.306	1.115	0.291	0.105	0.032	0.007	0.006	0.002	0.001	0.000	0.000
3	45.055	2.311	0.644	0.236	0.071	0.015	0.014	0.005	0.002	0.000	0.000
5	42.805	3.836	1.156	0.424	0.134	0.029	0.026	0.010	0.004	0.000	0.000
10	38.207	7.214	2.609	1.014	0.372	0.101	0.044	0.002	0.000	0.000	0.000
15	36.546	8.041	3.341	1.335	0.547	0.046	0.000	0.006	0.036	0.001	0.000
20	38.340	7.487	3.127	1.006	0.072	0.000	0.000	0.000	0.018	0.049	0.000
25	43.022	6.312	0.912	0.000	0.000	0.000	0.000	0.000	0.000	0.096	0.000

NTUA Campus Q-band 2-year average, Data Availability: 95.33 %														
Start Date									1st July 2017					
End Date									30th June 2019					
Attenuation threshold [dB]	Fade Duration [sec]													
	1	10	30	60	120	180	300	600	900	1200	1500	1800	2400	3600
	Normalized Probability of exceedance [%]													
1	100.000	17.857	8.566	5.615	3.702	2.921	2.233	1.587	1.300	1.061	0.899	0.755	0.559	0.364
3	100.000	24.236	14.754	11.187	8.156	7.012	5.307	3.579	2.617	2.057	1.534	1.254	0.913	0.511
5	100.000	31.524	20.770	15.392	11.322	9.225	6.660	3.799	2.639	1.973	1.455	1.159	0.839	0.395
10	100.000	41.385	28.141	21.144	15.576	11.663	7.374	3.612	2.333	1.731	1.129	0.903	0.677	0.451
15	100.000	40.876	27.299	21.460	14.453	10.803	7.883	4.380	2.774	1.898	1.168	0.876	0.438	0.292
20	100.000	45.504	30.245	24.523	17.166	14.714	11.444	5.177	3.542	1.635	1.362	1.090	0.545	0.272
25	100.000	49.138	37.500	30.603	21.121	17.241	12.500	5.603	3.448	1.724	0.862	0.862	0.862	0.000

Probability of exceedance [%]	Corresponding Attenuation A [dB]	Fade Duration [sec]												
		1	10	30	60	120	180	300	600	900	1200	1500	1800	2400	3600
		Normalized Probability of exceedance [%]													
0.001	33.67	nan	nan	nan	nan	nan	nan	nan	nan	nan	nan	nan	nan	nan	nan
0.002	33.42	nan	nan	nan	nan	nan	nan	nan	nan	nan	nan	nan	nan	nan	nan
0.003	33.26	100.000	0.000	0.000	0.000	0.000	0.000	0.000	0.000	0.000	0.000	0.000	0.000	0.000	0.000
0.005	33.01	100.000	0.000	0.000	0.000	0.000	0.000	0.000	0.000	0.000	0.000	0.000	0.000	0.000	0.000
0.01	32.57	100.000	2.617	0.000	0.000	0.000	0.000	0.000	0.000	0.000	0.000	0.000	0.000	0.000	0.000
0.02	31.81	100.000	27.273	7.856	4.153	1.908	1.122	0.673	0.224	0.224	0.000	0.000	0.000	0.000	0.000
0.03	30.61	100.000	20.930	12.920	9.561	7.494	6.460	3.876	1.809	1.034	0.517	0.517	0.258	0.258	0.000
0.05	25.56	100.000	48.077	35.385	25.769	18.077	15.000	10.385	4.615	3.077	1.538	0.769	0.769	0.769	0.000
0.1	16.41	100.000	45.402	30.460	21.456	15.709	12.261	8.812	4.981	3.257	2.107	1.341	0.958	0.575	0.383
0.2	10.84	100.000	41.312	28.705	20.443	14.395	10.988	7.070	3.663	2.385	1.874	1.193	1.022	0.596	0.426
0.3	8.68	100.000	38.717	25.714	20.117	14.111	11.837	7.755	3.848	2.566	1.574	1.050	0.758	0.525	0.408
0.5	6.41	100.000	36.255	24.431	18.090	12.682	10.183	7.646	4.140	2.835	2.238	1.641	1.119	0.746	0.410
1	3.97	100.000	28.617	18.207	13.744	10.374	8.345	6.440	3.811	2.717	1.923	1.517	1.164	0.865	0.406

NTUA Campus Q-band 2-year average, Data Availability: 95.33 %							
Start Date				1st July 2017			
End Date				30th June 2019			
Attenuation threshold [dB]	**Total number of fades > 1.0 sec**	**Total number of fades > 10.0 sec**	**Total fading time > 1.0 sec (ITU Total Outage time)**	**Total fading time > 10.0 sec (ITU Total unavailable time)**	**Mean Duration of fade events > 1.0 sec**	**Mean Duration of fade events > 10.0 sec**	**Unavailable to Outage Time Ratio[%]**
1	29686	5301	1855116	1768530	62.491	333.622	95.333
3	8215	1991	816880	794312	99.438	398.951	97.237
5	4054	1278	430104	419874	106.094	328.540	97.622
10	1329	550	139050	135995	104.628	247.264	97.803
15	685	280	69398	67792	101.311	242.114	97.686
20	367	167	44319	43536	120.760	260.695	98.233
25	232	114	31173	30727	134.366	269.535	98.569

Probability of exceedance [%]	**Corresponding Attenuation A [dB]**	**Total number of fades > 1.0 sec**	**Total number of fades > 10.0 sec**	**Total fading time > 1.0 sec (ITU Total Outage time)**	**Total fading time > 10.0 sec (ITU Total unavailable time)**	**Mean Duration of fade events > 1.0 sec**	**Mean Duration of fade events > 10.0 sec**	**Unavailable to Outage Time Ratio[%]**
0.001	33.67	0	0	0	0			
0.002	33.42	0	0	0	0			
0.003	33.26	3	0	6	0	2.000		0.000
0.005	33.01	30	0	84	0	2.800		0.000
0.01	32.57	535	14	1644	230	3.073	16.429	13.990
0.02	31.81	891	243	13799	11020	15.487	45.350	79.861
0.03	30.61	387	81	17910	16848	46.279	208.000	94.070
0.05	25.56	260	125	30181	29611	116.081	236.888	98.111
0.1	16.41	522	237	59711	58661	114.389	247.515	98.242
0.2	10.84	1174	485	119515	116842	101.802	240.911	97.763
0.3	8.68	1715	664	179082	175090	104.421	263.690	97.771
0.5	6.41	2681	972	298462	292128	111.325	300.543	97.878
1	3.97	5668	1622	594983	580185	104.972	357.697	97.513

NTUA Campus Q-band 2-year average, Data Availability: 95.33 %														
Start Date								1st July 2017						
End Date								30th June 2019						
Attenuation threshold [dB]	Accumulate Fading Time [sec]													
	1	10	30	60	120	180	300	600	900	1200	1500	1800	2400	3600
	Normalized Probability of exceedance [%]													
1	100.000	95.333	92.783	90.750	88.113	86.278	83.658	79.135	75.730	71.704	68.216	64.379	57.804	48.627
3	100.000	97.237	95.594	94.082	91.479	89.789	85.860	78.481	71.539	65.666	58.552	53.907	46.915	35.261
5	100.000	97.622	95.814	93.598	90.313	87.432	81.667	69.725	61.764	55.357	48.591	43.920	37.548	25.724
10	100.000	97.803	95.531	92.552	87.885	82.397	72.844	57.977	49.279	43.313	35.709	32.108	28.058	21.455
15	100.000	97.686	95.370	92.677	86.475	81.216	74.491	59.796	47.839	39.020	29.561	24.756	15.658	10.748
20	100.000	98.233	95.830	93.847	88.709	85.916	79.494	56.937	46.630	30.610	27.794	24.080	15.021	8.294
25	100.000	98.569	96.956	94.620	88.958	84.737	76.383	53.726	40.609	27.306	18.824	18.824	18.824	0.000

Probability of exceedance [%]	Corresponding Attenuation A [dB]	Accumulate Fading Time [sec]												
		1	10	30	60	120	180	300	600	900	1200	1500	1800	2400	3600
		Normalized Probability of exceedance [%]													
0.001	33.67	nan	nan	nan	nan	nan	nan	nan	nan	nan	nan	nan	nan	nan	nan
0.002	33.42	nan	nan	nan	nan	nan	nan	nan	nan	nan	nan	nan	nan	nan	nan
0.003	33.26	100.000	0.000	0.000	0.000	0.000	0.000	0.000	0.000	0.000	0.000	0.000	0.000	0.000	0.000
0.005	33.01	100.000	0.000	0.000	0.000	0.000	0.000	0.000	0.000	0.000	0.000	0.000	0.000	0.000	0.000
0.01	32.57	100.000	13.990	0.000	0.000	0.000	0.000	0.000	0.000	0.000	0.000	0.000	0.000	0.000	0.000
0.02	31.81	100.000	79.861	59.359	49.322	37.387	30.502	23.821	13.494	13.494	0.000	0.000	0.000	0.000	0.000
0.03	30.61	100.000	94.070	91.066	87.973	84.428	81.200	68.135	50.592	37.644	25.907	25.907	16.750	16.750	0.000
0.05	25.56	100.000	98.111	96.279	92.694	87.548	83.834	74.017	52.354	41.665	28.064	19.353	19.353	19.353	0.000
0.1	16.41	100.000	98.242	95.672	92.229	87.990	83.608	76.289	61.046	49.795	39.254	30.457	24.875	17.742	12.361
0.2	10.84	100.000	97.763	95.572	92.064	86.838	81.991	73.145	59.245	50.313	45.003	36.334	33.510	25.287	20.710
0.3	8.68	100.000	97.771	95.503	93.213	88.207	84.939	75.753	59.723	50.626	40.831	33.930	29.256	24.613	21.000
0.5	6.41	100.000	97.878	95.931	93.406	89.279	85.893	80.467	66.577	57.721	52.166	45.100	37.633	30.894	22.688
1	3.97	100.000	97.513	95.738	93.941	91.246	88.371	84.074	73.190	65.463	57.396	52.319	46.826	40.819	28.376

NTUA Campus Q-band 2-year average, Data Availability: 95.33 %																		
Start Date														1st July 2017				
End Date														30th June 2019				
Attenuation threshold [dB]	Inter-Fade Duration [sec]																	
	1	2	3	5	10	20	30	50	100	200	300	500	1000	2000				
	Normalized Probability of exceedance [%]																	
1	100.000	63.471	46.972	32.590	20.632	13.987	11.526	9.167	6.868	5.164	4.339	3.552	2.698	2.066				
3	100.000	60.719	44.839	30.733	19.677	13.575	11.391	9.234	7.157	5.578	4.899	4.032	3.206	2.554				
5	100.000	62.160	46.976	34.125	23.746	18.299	15.784	13.312	10.812	8.521	7.347	6.160	4.735	3.799				
10	100.000	64.758	51.525	40.122	31.065	24.073	21.445	18.583	14.969	12.670	10.840	9.526	8.071	6.945				
15	100.000	66.349	54.814	44.423	34.795	27.836	24.595	21.068	17.255	14.395	13.155	11.821	10.391	9.247				
20	100.000	63.525	49.738	38.569	31.937	26.527	23.735	20.942	19.197	16.230	14.660	13.438	12.216	11.169				
25	100.000	65.922	53.352	41.899	34.358	29.888	27.374	24.860	22.067	20.112	18.436	15.922	13.687	12.849				

Attenuation threshold [dB]	Inter-Fade Duration [sec]																	
	3000	5000	10000	20000	30000	50000	100000	200000	300000	500000	1000000	2000000	3000000	5000000	10000000			
	Normalized Probability of exceedance [%]																	
1	1.748	1.382	1.060	0.811	0.694	0.542	0.244	0.112	0.054	0.010	0.002	0.000	0.000	0.000	0.000			
3	2.198	1.868	1.472	1.250	1.095	0.995	0.712	0.491	0.403	0.255	0.074	0.007	0.000	0.000	0.000			
5	3.408	2.919	2.361	2.011	1.816	1.676	1.299	0.936	0.740	0.531	0.223	0.028	0.014	0.000	0.000			
10	6.382	5.631	4.693	3.989	3.566	3.191	2.581	1.924	1.689	1.408	0.985	0.328	0.235	0.000	0.000			
15	8.675	8.103	6.578	6.006	5.529	5.148	4.194	3.146	2.574	2.097	1.716	1.144	0.477	0.000	0.000			
20	10.646	10.297	9.599	8.726	8.377	7.504	6.806	5.759	4.363	4.188	3.141	2.269	0.873	0.000	0.000			
25	11.732	11.453	10.894	10.056	9.777	9.497	8.101	6.704	5.587	5.587	4.469	4.190	1.955	0.559	0.000			

NTUA Campus Q-band 2-year average, Data Availability: 95.33 %																							
Start Date																			1st July 2017				
End Date																			30th June 2019				
Probability of exceedance [%]	Corresponding Attenuation A [dB]	Inter-Fade Duration [sec]																					
		1	2	3	5	10	20	30	50	100	200	300	500	1000	2000								
		Normalized Probability of exceedance [%]																					
0.001	33.67	nan	nan	nan	nan	nan	nan	nan	nan	nan	nan	nan	nan	nan	nan								
0.002	33.42	100.000	100.000	100.000	100.000	77.778	66.667	33.333	22.222	0.000	0.000	0.000	0.000	0.000	0.000								
0.003	33.26	100.000	92.593	92.593	81.481	44.444	22.222	18.519	7.407	7.407	3.704	3.704	3.704	3.704	3.704								
0.005	33.01	100.000	86.782	75.287	59.770	48.851	38.506	32.759	20.115	12.069	7.471	5.172	3.448	3.448	3.448								
0.01	32.57	100.000	67.818	47.899	28.785	14.105	6.966	4.721	3.166	2.073	1.439	1.209	1.151	0.979	0.748								
0.02	31.81	100.000	31.076	16.972	9.960	5.976	4.861	4.382	3.825	2.709	2.311	2.151	2.072	1.833	1.514								
0.03	30.61	100.000	56.017	38.451	23.928	15.214	11.618	9.820	8.437	7.469	5.947	5.809	5.256	4.564	3.596								
0.05	25.56	100.000	60.250	46.500	36.500	29.500	24.500	22.500	20.250	18.250	16.500	14.750	13.250	12.250	10.750								
0.1	16.41	100.000	68.632	56.014	46.462	36.910	29.245	26.769	23.349	19.811	15.330	14.033	12.500	10.967	10.024								
0.2	10.84	100.000	65.955	51.868	40.235	31.644	25.027	21.985	19.210	15.635	12.860	11.740	10.352	8.645	7.204								
0.3	8.68	100.000	64.813	50.359	39.096	28.336	21.521	18.831	16.320	13.307	11.119	10.115	8.895	7.389	6.313								
0.5	6.41	100.000	62.147	47.416	35.424	25.375	20.119	17.668	14.996	12.478	10.137	9.055	7.951	6.073	5.146								
1	3.97	100.000	60.991	46.120	32.618	22.336	16.358	13.857	11.523	9.041	6.864	5.978	4.944	3.890	3.122								

Probability of exceedance [%]	Corresponding Attenuation A [dB]	Inter-Fade Duration [sec]																					
		3000	5000	10000	20000	30000	50000	100000	200000	300000	500000	1000000	2000000	3000000	5000000	10000000							
		Normalized Probability of exceedance [%]																					
0.001	33.67	nan	nan	nan	nan	nan	nan	nan	nan	nan	nan	nan	nan	nan	nan	nan							
0.002	33.42	0.000	0.000	0.000	0.000	0.000	0.000	0.000	0.000	0.000	0.000	0.000	0.000	0.000	0.000	0.000							
0.003	33.26	3.704	3.704	3.704	3.704	3.704	3.704	3.704	3.704	3.704	3.704	3.704	3.704	3.704	3.704	3.704							
0.005	33.01	3.448	3.448	3.448	3.448	3.448	2.874	2.874	2.299	2.299	1.724	1.724	1.724	1.149	0.000	0.000							
0.01	32.57	0.748	0.748	0.748	0.748	0.691	0.518	0.518	0.288	0.288	0.230	0.230	0.230	0.173	0.058	0.000							
0.02	31.81	1.434	1.434	1.355	1.355	1.275	1.036	0.876	0.637	0.637	0.558	0.478	0.478	0.398	0.239	0.000							
0.03	30.61	3.320	3.320	3.181	3.043	3.043	2.905	2.490	2.213	1.798	1.798	1.521	1.383	0.968	0.692	0.000							
0.05	25.56	9.750	9.500	9.000	8.250	8.000	7.750	6.500	5.750	4.750	4.750	3.750	3.500	2.000	0.500	0.000							
0.1	16.41	9.434	8.844	7.665	7.075	6.486	6.014	5.189	3.892	3.184	2.712	2.123	1.415	0.590	0.000	0.000							
0.2	10.84	6.617	5.816	4.749	4.269	3.895	3.469	2.828	2.134	1.868	1.601	1.121	0.427	0.267	0.000	0.000							
0.3	8.68	5.488	5.022	4.125	3.479	3.049	2.726	2.188	1.578	1.435	1.112	0.789	0.251	0.108	0.000	0.000							
0.5	6.41	4.483	3.931	3.180	2.672	2.341	2.164	1.678	1.259	1.060	0.817	0.420	0.066	0.044	0.000	0.000							
1	3.97	2.728	2.265	1.743	1.546	1.339	1.251	0.926	0.680	0.522	0.364	0.148	0.020	0.010	0.000	0.000							

NTUA Campus Q-band 2-year average, Data Availability: 95.33 %			
Start Date		1st July 2017	
End Date		30th June 2019	
Attenuation threshold [dB]	Total number of inter-fades	Total duration of inter-fades [sec]	
1	59040	57944805	
3	14880	57919070	
5	7159	58309061	
10	2131	58517196	
15	1049	55521341	
20	573	55465062	
25	358	55478220	

Probability of exceedance [%]	Corresponding Attenuation A [dB]	Total number of inter-fades	Total duration of inter-fades [sec]
0.001	33.67	0	0
0.002	33.42	9	293
0.003	33.26	27	21113043
0.005	33.01	174	47994012
0.01	32.57	1737	48292450
0.02	31.81	1255	55495192
0.03	30.61	723	55491147
0.05	25.56	400	55479196
0.1	16.41	848	55450670
0.2	10.84	1874	58536805
0.3	8.68	2788	58476935
0.5	6.41	4528	58356877
1	3.97	10154	58143067

NTUA LTCP Q-band 2-year average, Data Availability: 93.38 %																	
Start Date								1st July 2017									
End Date								30th June 2019									
Attenuation threshold [dB]	**Absolute Fade Slope [dB/sec]**																**Number of fade slope samples**
	0.001	**0.002**	**0.003**	**0.005**	**0.01**	**0.02**	**0.03**	**0.05**	**0.1**	**0.2**	**0.3**	**0.5**	**1**	**2**	**3**	**5**	
	Probability of exceedance [%]																
1	84.296	71.893	61.938	47.145	26.972	12.190	6.971	3.185	0.861	0.135	0.021	0.000	0.000	0.000	0.000	0.000	1376579
3	91.261	83.452	76.472	64.491	43.849	23.679	14.805	7.339	2.061	0.332	0.050	0.000	0.000	0.000	0.000	0.000	558049
5	93.154	87.309	82.099	72.818	55.409	34.409	23.380	12.686	3.839	0.635	0.095	0.000	0.000	0.000	0.000	0.000	285962
10	92.412	87.136	83.690	78.897	69.998	56.659	45.612	29.493	10.667	2.018	0.198	0.000	0.000	0.000	0.000	0.000	78694
15	88.742	81.505	77.675	73.693	66.604	55.678	46.542	31.299	12.898	2.211	0.079	0.000	0.000	0.000	0.000	0.000	43292
20	83.498	73.188	68.030	63.202	56.092	46.239	38.419	26.576	11.069	0.464	0.211	0.000	0.000	0.000	0.000	0.000	28439
25	77.249	63.203	56.587	50.987	43.822	34.354	27.294	17.117	3.256	0.299	0.299	0.000	0.000	0.000	0.000	0.000	20056

Prob. of exceedance [%]	**Corr. Attenuation A [dB]**	**Absolute Fade Slope [dB/sec]**																**Number of fade slope samples**
		0.001	**0.002**	**0.003**	**0.005**	**0.01**	**0.02**	**0.03**	**0.05**	**0.1**	**0.2**	**0.3**	**0.5**	**1**	**2**	**3**	**5**	
		Probability of exceedance [%]																
0.001	34.16	nan	nan	nan	nan	nan	nan	nan	nan	nan	nan	nan	nan	nan	nan	nan	nan	0
0.002	33.76	61.905	33.333	24.812	19.549	15.038	15.038	15.038	15.038	15.038	15.038	15.038	15.038	0.000	0.000	0.000	0.000	399
0.003	33.49	75.441	58.073	42.198	21.438	8.141	8.141	8.141	8.141	8.141	8.141	8.141	8.141	0.000	0.000	0.000	0.000	737
0.005	33.07	60.268	38.031	27.114	18.613	5.861	2.685	2.685	2.685	2.685	2.685	2.685	2.685	0.000	0.000	0.000	0.000	2235
0.01	32.30	68.133	49.820	39.851	29.319	13.960	3.608	1.353	1.353	1.353	1.353	1.353	1.353	0.000	0.000	0.000	0.000	4434
0.02	30.79	68.610	49.858	41.291	33.400	21.847	9.351	4.304	0.559	0.501	0.501	0.501	0.501	0.000	0.000	0.000	0.000	11988
0.03	27.13	74.082	58.249	50.625	44.200	36.092	25.591	18.226	8.429	0.619	0.338	0.338	0.000	0.000	0.000	0.000	0.000	17760
0.05	19.55	84.127	74.170	69.147	64.436	57.394	46.946	38.771	26.990	11.175	0.673	0.203	0.000	0.000	0.000	0.000	0.000	29566
0.1	12.00	91.131	85.206	81.797	77.675	70.307	58.454	48.178	32.082	11.984	2.235	0.170	0.000	0.000	0.000	0.000	0.000	58836
0.2	8.10	93.479	88.492	84.906	79.017	67.347	50.483	38.701	23.656	8.233	1.400	0.187	0.000	0.000	0.000	0.000	0.000	117215
0.3	6.71	93.347	87.946	83.536	75.788	61.021	41.777	30.577	17.741	5.865	0.984	0.144	0.000	0.000	0.000	0.000	0.000	176606
0.5	4.91	93.173	87.171	81.898	72.555	54.910	33.971	22.978	12.409	3.738	0.617	0.092	0.000	0.000	0.000	0.000	0.000	294258
1	2.85	90.977	82.851	75.766	63.605	42.869	22.905	14.213	7.004	1.960	0.316	0.048	0.000	0.000	0.000	0.000	0.000	588412

NTUA LTCP Q-band 2-year average, Data Availability: 93.38 %												
Start Date	1st July 2017											
End Date	30th June 2019											
Attenuation threshold [dB]	Fade Slope [dB/sec]											
	< 0.5	-0.5 to -0.45	-0.45 to -0.4	-0.4 to -0.35	-0.35 to -0.3	-0.3 to -0.25	-0.25 to -0.2	-0.2 to -0.15	-0.15 to -0.1	-0.1 to -0.05	-0.05 to 0.0
	Probability of exceedance [%]											
1	0.000	0.001	0.001	0.002	0.008	0.018	0.034	0.078	0.225	1.133	50.426
3	0.000	0.000	0.003	0.005	0.020	0.044	0.084	0.191	0.540	2.636	48.157
5	0.000	0.000	0.001	0.013	0.041	0.086	0.156	0.369	1.015	4.494	45.226
10	0.000	0.000	0.000	0.025	0.102	0.295	0.525	1.070	2.730	10.091	36.525
15	0.000	0.000	0.000	0.000	0.009	0.256	0.668	1.529	3.453	9.905	36.282
20	0.000	0.000	0.000	0.039	0.067	0.000	0.014	1.755	3.017	8.453	39.485
25	0.000	0.050	0.100	0.000	0.000	0.000	0.000	0.000	1.197	7.040	44.082

Attenuation threshold [dB]	Fade Slope [dB/sec]										
	0.0 to 0.05	0.05 to 0.1	0.1 to 0.15	0.15 to 0.2	0.2 to 0.25	0.25 to 0.3	0.3 to 0.35	0.35 to 0.4	0.4 to 0.45	0.45 to 0.5	> 0.5
	Probability of exceedance [%]										
1	46.388	1.191	0.320	0.104	0.045	0.018	0.006	0.002	0.000	0.000	0.000
3	44.504	2.642	0.750	0.248	0.111	0.044	0.015	0.006	0.000	0.000	0.000
5	42.087	4.354	1.365	0.456	0.213	0.085	0.029	0.012	0.000	0.000	0.000
10	33.982	8.735	3.623	1.226	0.736	0.264	0.066	0.005	0.000	0.000	0.000
15	32.419	8.496	4.287	1.418	1.014	0.194	0.000	0.000	0.009	0.060	0.000
20	33.939	7.054	4.072	1.762	0.239	0.000	0.000	0.000	0.000	0.105	0.000
25	38.801	6.821	1.760	0.000	0.000	0.000	0.000	0.000	0.015	0.135	0.000

NTUA LTCP Q-band 2-year average, Data Availability: 93.38 %														
Start Date								1st July 2017						
End Date								30th June 2019						
Attenuation threshold [dB]	Fade Duration [sec]													
	1	10	30	60	120	180	300	600	900	1200	1500	1800	2400	3600
	Normalized Probability of exceedance [%]													
1	100.000	22.939	11.528	7.672	5.058	4.045	3.075	2.095	1.566	1.227	1.023	0.834	0.635	0.403
3	100.000	31.486	20.004	15.263	11.322	9.262	6.961	4.541	3.221	2.280	1.820	1.480	0.980	0.420
5	100.000	38.498	25.958	19.888	13.978	11.542	8.267	4.673	3.075	2.037	1.677	1.358	0.919	0.359
10	100.000	47.234	32.340	23.546	17.447	14.184	10.355	4.539	2.837	1.844	1.702	1.418	0.284	0.000
15	100.000	55.776	40.924	31.023	23.432	18.152	11.221	7.261	4.620	2.640	1.980	0.660	0.330	0.000
20	100.000	46.332	35.135	23.166	15.830	13.127	10.811	5.405	3.089	2.317	0.386	0.386	0.000	0.000
25	100.000	45.833	33.929	25.595	20.238	17.857	13.690	6.548	2.976	0.595	0.595	0.595	0.000	0.000

Probability of exceedance [%]	Corresponding Attenuation A [dB]	Fade Duration [sec]													
		1	10	30	60	120	180	300	600	900	1200	1500	1800	2400	3600
		Normalized Probability of exceedance [%]													
0.001	34.16	100.000	0.000	0.000	0.000	0.000	0.000	0.000	0.000	0.000	0.000	0.000	0.000	0.000	0.000
0.002	33.76	100.000	1.099	0.000	0.000	0.000	0.000	0.000	0.000	0.000	0.000	0.000	0.000	0.000	0.000
0.003	33.49	100.000	13.014	0.000	0.000	0.000	0.000	0.000	0.000	0.000	0.000	0.000	0.000	0.000	0.000
0.005	33.07	100.000	10.855	2.632	0.987	0.987	0.658	0.000	0.000	0.000	0.000	0.000	0.000	0.000	0.000
0.01	32.30	100.000	16.204	11.111	6.944	3.704	2.778	1.389	0.463	0.000	0.000	0.000	0.000	0.000	0.000
0.02	30.79	100.000	25.574	15.410	10.820	7.869	5.902	3.279	1.311	0.328	0.328	0.328	0.328	0.000	0.000
0.03	27.13	100.000	50.365	38.686	29.197	22.628	19.708	14.599	6.569	2.920	0.730	0.730	0.730	0.000	0.000
0.05	19.55	100.000	49.794	39.506	27.160	18.519	15.226	11.523	6.173	3.292	2.469	0.412	0.412	0.000	0.000
0.1	12.00	100.000	56.338	37.324	30.047	22.066	15.728	10.798	6.103	3.756	2.582	2.582	2.113	0.469	0.000
0.2	8.10	100.000	43.550	28.924	20.871	15.201	11.997	7.642	4.108	2.383	1.397	1.233	1.150	0.411	0.082
0.3	6.71	100.000	43.436	29.583	22.384	15.910	12.886	9.074	4.719	2.904	1.512	1.270	0.968	0.544	0.060
0.5	4.91	100.000	38.527	25.415	19.668	13.961	11.570	8.330	4.666	3.047	2.083	1.658	1.311	0.887	0.347
1	2.85	100.000	32.674	20.524	15.108	11.731	9.632	7.194	4.696	3.497	2.498	1.938	1.559	1.019	0.460

NTUA LTCP Q-band 2-year average, Data Availability: 93.38 %							
Start Date				1st July 2017			
End Date				30th June 2019			
Attenuation threshold [dB]	**Total number of fades > 1.0 sec**	**Total number of fades > 10.0 sec**	**Total fading time > 1.0 sec (ITU Total Outage time)**	**Total fading time > 10.0 sec (ITU Total unavailable time)**	**Mean Duration of fade events > 1.0 sec**	**Mean Duration of fade events > 10.0 sec**	**Unavailable to Outage Time Ratio[%]**
1	20620	4730	1365203	1307552	66.208	276.438	95.777
3	4999	1574	554547	542025	110.932	344.361	97.742
5	2504	964	284536	278790	113.633	289.201	97.981
10	705	333	78577	77019	111.457	231.288	98.017
15	303	169	43170	42648	142.475	252.355	98.791
20	259	120	28266	27729	109.135	231.075	98.100
25	168	77	19936	19588	118.667	254.390	98.254

Probability of exceedance [%]	**Corresponding Attenuation A [dB]**	**Total number of fades > 1.0 sec**	**Total number of fades > 10.0 sec**	**Total fading time > 1.0 sec (ITU Total Outage time)**	**Total fading time > 10.0 sec (ITU Total unavailable time)**	**Mean Duration of fade events > 1.0 sec**	**Mean Duration of fade events > 10.0 sec**	**Unavailable to Outage Time Ratio[%]**
0.001	34.16	3	0	6	0	2.000		0.000
0.002	33.76	91	1	295	13	3.242	13.000	4.407
0.003	33.49	146	19	753	342	5.158	18.000	45.418
0.005	33.07	304	33	2094	1230	6.888	37.273	58.739
0.01	32.30	216	35	4520	4032	20.926	115.200	89.204
0.02	30.79	305	78	11816	11045	38.741	141.603	93.475
0.03	27.13	137	69	17661	17389	128.912	252.014	98.460
0.05	19.55	243	121	29386	28824	120.930	238.215	98.088
0.1	12.00	426	240	58615	57904	137.594	241.267	98.787
0.2	8.10	1217	530	116845	114126	96.011	215.332	97.673
0.3	6.71	1653	718	175547	171916	106.199	239.437	97.932
0.5	4.91	2593	999	292384	286383	112.759	286.670	97.948
1	2.85	5004	1635	585251	572791	116.957	350.331	97.871

NTUA LTCP Q-band 2-year average, Data Availability: 93.38 %														
Start Date								1st July 2017						
End Date								30th June 2019						
Attenuation threshold [dB]	Accumulate Fading Time [sec]													
	1	10	30	60	120	180	300	600	900	1200	1500	1800	2400	3600
	Normalized Probability of exceedance [%]													
1	100.000	95.777	92.783	90.255	86.938	84.672	81.272	74.920	69.040	63.702	59.546	54.913	48.725	38.682
3	100.000	97.742	95.904	94.052	91.039	88.255	83.434	74.224	65.563	56.701	51.069	46.152	36.846	21.836
5	100.000	97.981	95.970	93.688	89.217	86.037	79.268	65.683	55.432	45.745	41.430	36.791	28.921	14.602
10	100.000	98.017	95.541	92.113	87.396	83.043	75.405	53.302	42.140	32.730	30.863	26.606	6.469	0.000
15	100.000	98.791	96.861	93.827	89.430	83.725	72.777	60.285	47.137	32.272	25.997	10.371	5.569	0.000
20	100.000	98.100	95.910	91.088	85.580	81.886	76.675	54.436	37.855	29.707	7.065	7.065	0.000	0.000
25	100.000	98.254	96.303	93.138	89.602	86.612	78.948	53.632	31.125	9.520	9.520	9.520	0.000	0.000

Probability of exceedance [%]	Corresponding Attenuation A [dB]	Accumulate Fading Time [sec]												
		1	10	30	60	120	180	300	600	900	1200	1500	1800	2400	3600
		Normalized Probability of exceedance [%]													
0.001	34.16	100.000	0.000	0.000	0.000	0.000	0.000	0.000	0.000	0.000	0.000	0.000	0.000	0.000	0.000
0.002	33.76	100.000	4.407	0.000	0.000	0.000	0.000	0.000	0.000	0.000	0.000	0.000	0.000	0.000	0.000
0.003	33.49	100.000	45.418	0.000	0.000	0.000	0.000	0.000	0.000	0.000	0.000	0.000	0.000	0.000	0.000
0.005	33.07	100.000	58.739	36.915	27.985	27.985	21.012	0.000	0.000	0.000	0.000	0.000	0.000	0.000	0.000
0.01	32.30	100.000	89.204	84.580	74.956	60.288	54.248	39.358	14.845	0.000	0.000	0.000	0.000	0.000	0.000
0.02	30.79	100.000	93.475	89.362	84.597	78.639	70.709	54.579	34.140	15.462	15.462	15.462	15.462	0.000	0.000
0.03	27.13	100.000	98.460	96.784	93.698	89.072	85.601	76.462	49.861	28.804	10.577	10.577	10.577	0.000	0.000
0.05	19.55	100.000	98.088	96.454	92.163	86.218	82.475	75.219	55.019	36.623	28.718	6.813	6.813	0.000	0.000
0.1	12.00	100.000	98.787	96.329	94.077	88.953	81.993	73.239	58.400	45.784	36.921	36.921	31.548	8.471	0.000
0.2	8.10	100.000	97.673	94.892	91.134	85.911	80.971	70.416	55.054	42.123	31.840	29.662	28.288	12.038	3.191
0.3	6.71	100.000	97.932	95.588	92.619	87.460	83.211	74.590	57.304	44.655	30.679	27.622	23.104	14.645	2.259
0.5	4.91	100.000	97.948	95.841	93.639	89.255	86.110	79.526	65.574	55.037	45.995	41.015	35.955	28.279	14.305
1	2.85	100.000	97.871	96.000	93.974	91.489	88.758	83.835	74.840	67.552	58.721	52.377	47.149	37.523	23.164

NTUA LTCP Q-band 2-year average, Data Availability: 93.38 %																			
Start Date														1st July 2017					
End Date														30th June 2019					
Attenuation threshold [dB]	Inter-Fade Duration [sec]																		
	1	2	3	5	10	20	30	50	100	200	300	500	1000	2000					
	Normalized Probability of exceedance [%]																		
1	100.000	60.865	45.013	31.192	20.255	14.023	11.729	9.583	7.385	5.772	4.975	4.131	3.109	2.356					
3	100.000	58.262	42.862	29.813	20.738	15.764	13.572	11.539	9.449	7.825	6.985	6.178	4.952	3.952					
5	100.000	63.329	48.689	35.813	26.443	20.339	17.954	15.498	12.494	10.229	9.180	7.964	6.795	5.842					
10	100.000	67.507	57.226	47.236	38.894	33.366	29.680	25.315	21.726	19.108	18.138	15.810	13.579	11.251					
15	100.000	67.538	55.991	47.495	38.344	32.680	30.065	27.887	25.490	22.876	21.351	20.479	18.954	16.993					
20	100.000	67.473	55.376	46.237	35.215	29.839	27.688	24.194	22.043	19.355	18.011	16.667	15.860	15.054					
25	100.000	59.004	47.893	37.931	31.801	26.820	24.904	22.989	20.307	18.391	17.625	17.241	16.092	15.709					

Attenuation threshold [dB]	Inter-Fade Duration [sec]																		
	3000	5000	10000	20000	30000	50000	100000	200000	300000	500000	1000000	2000000	3000000	5000000	10000000				
	Normalized Probability of exceedance [%]																		
1	2.017	1.596	1.181	0.881	0.738	0.574	0.312	0.183	0.111	0.052	0.012	0.000	0.000	0.000	0.000				
3	3.509	2.839	2.362	1.908	1.670	1.420	1.056	0.738	0.579	0.352	0.170	0.034	0.000	0.000	0.000				
5	5.412	4.506	3.600	2.957	2.670	2.241	1.788	1.288	1.049	0.763	0.358	0.095	0.000	0.000	0.000				
10	10.572	9.408	8.050	6.984	6.208	5.529	4.462	3.395	2.813	2.231	1.455	0.485	0.291	0.097	0.000				
15	16.558	14.379	13.290	12.200	11.111	10.022	8.932	6.536	5.664	4.575	3.268	1.525	0.654	0.218	0.000				
20	14.516	12.634	12.097	11.290	10.484	9.409	8.602	7.258	6.183	5.108	4.032	1.882	0.806	0.269	0.000				
25	15.326	13.793	13.027	12.261	11.494	10.345	9.579	8.429	7.663	6.513	4.981	2.299	1.149	0.383	0.000				

NTUA LTCP Q-band 2-year average, Data Availability: 93.38 %																				
Start Date													1st July 2017							
End Date													30th June 2019							
Probability of exceedance [%]	Corresponding Attenuation A [dB]	Inter-Fade Duration [sec]																		
		1	2	3	5	10	20	30	50	100	200	300	500	1000	2000					
		Normalized Probability of exceedance [%]																		
0.001	34.16	100.000	89.130	86.957	69.565	47.826	21.739	15.217	10.870	6.522	4.348	4.348	0.000	0.000	0.000					
0.002	33.76	100.000	63.636	41.364	24.091	12.273	5.909	5.455	3.182	1.818	1.364	0.909	0.909	0.455	0.455					
0.003	33.49	100.000	62.155	39.227	27.901	16.851	9.945	6.354	4.696	2.762	2.210	1.657	1.657	1.657	1.657					
0.005	33.07	100.000	56.628	34.206	20.949	7.365	3.928	2.946	2.291	1.637	1.309	1.146	1.146	1.146	1.146					
0.01	32.30	100.000	72.124	56.195	39.823	21.829	11.947	9.145	5.900	3.982	3.245	2.802	2.655	2.507	2.360					
0.02	30.79	100.000	51.146	36.155	21.340	13.404	9.700	8.466	7.055	6.173	5.467	5.291	5.115	4.938	4.762					
0.03	27.13	100.000	65.789	52.632	42.982	32.018	28.070	26.316	22.368	19.737	17.982	17.982	17.544	17.105	16.667					
0.05	19.55	100.000	69.075	56.069	50.289	40.173	33.526	31.214	28.324	23.988	21.387	19.364	18.786	17.630	16.763					
0.1	12.00	100.000	71.115	56.986	48.823	40.031	33.752	31.083	28.100	25.275	21.664	20.879	19.309	17.268	15.228					
0.2	8.10	100.000	66.895	54.435	42.608	33.949	27.033	24.129	21.489	17.476	14.784	13.200	11.352	9.187	8.025					
0.3	6.71	100.000	63.374	50.131	39.057	29.517	24.355	21.287	18.706	15.638	12.869	11.336	10.288	8.530	7.557					
0.5	4.91	100.000	60.696	46.381	34.746	25.653	19.721	17.430	14.934	12.368	10.192	9.139	7.948	6.803	5.795					
1	2.85	100.000	58.123	43.056	30.552	20.859	15.951	13.876	12.005	9.886	8.140	7.176	6.348	5.056	4.002					

Probability of exceedance [%]	Corresponding Attenuation A [dB]	Inter-Fade Duration [sec]																		
		3000	5000	10000	20000	30000	50000	100000	200000	300000	500000	1000000	2000000	3000000	5000000	10000000				
		Normalized Probability of exceedance [%]																		
0.001	34.16	0.000	0.000	0.000	0.000	0.000	0.000	0.000	0.000	0.000	0.000	0.000	0.000	0.000	0.000	0.000				
0.002	33.76	0.455	0.455	0.455	0.455	0.455	0.455	0.455	0.455	0.455	0.455	0.000	0.000	0.000	0.000	0.000				
0.003	33.49	1.657	1.381	1.381	1.381	1.381	1.381	1.381	1.105	1.105	1.105	0.829	0.552	0.552	0.276	0.000				
0.005	33.07	1.146	0.982	0.982	0.982	0.982	0.818	0.818	0.655	0.655	0.655	0.491	0.327	0.327	0.164	0.000				
0.01	32.30	2.360	2.065	2.065	2.065	1.917	1.770	1.622	1.475	1.180	0.885	0.737	0.590	0.590	0.147	0.000				
0.02	30.79	4.762	4.233	4.056	4.056	3.880	3.704	3.351	3.175	2.822	2.293	1.940	0.882	0.353	0.000	0.000				
0.03	27.13	16.667	15.351	14.474	13.596	12.719	11.842	10.965	10.088	8.772	7.456	5.702	2.632	1.316	0.439	0.000				
0.05	19.55	16.185	14.162	13.584	12.717	11.850	10.694	9.827	7.803	6.647	5.491	4.335	2.023	0.867	0.289	0.000				
0.1	12.00	14.286	12.716	11.774	10.204	9.262	8.320	6.750	5.024	4.553	3.768	2.355	0.785	0.471	0.157	0.000				
0.2	8.10	7.603	6.653	5.597	4.857	4.118	3.590	2.851	2.270	2.006	1.584	0.845	0.317	0.106	0.053	0.000				
0.3	6.71	6.921	6.023	4.863	4.003	3.517	2.955	2.319	1.684	1.496	1.160	0.599	0.224	0.037	0.000	0.000				
0.5	4.91	5.245	4.375	3.481	2.909	2.565	2.153	1.741	1.237	1.008	0.733	0.344	0.092	0.000	0.000	0.000				
1	2.85	3.537	2.891	2.392	1.916	1.678	1.440	1.077	0.760	0.578	0.351	0.159	0.034	0.000	0.000	0.000				

NTUA LTCP Q-band 2-year average, Data Availability: 93.38 %		
Start Date	1st July 2017	
End Date	30th June 2019	
Attenuation threshold [dB]	Total number of inter-fades	Total duration of inter-fades [sec]
1	40404	56679302
3	8805	5659208
5	4194	51187122
10	1031	46701750
15	459	46607521
20	372	43860675
25	261	41747900

Probability of exceedance [%]	Corresponding Attenuation A [dB]	Total number of inter-fades	Total duration of inter-fades [sec]
0.001	34.16	46	19425728
0.002	33.76	220	19425686
0.003	33.49	362	27055858
0.005	33.07	611	27054438
0.01	32.30	678	37121126
0.02	30.79	567	38371710
0.03	27.13	228	41750121
0.05	19.55	346	43859568
0.1	12.00	637	46592082
0.2	8.10	1894	51350328
0.3	6.71	2673	51296383
0.5	4.91	4366	51179194
1	2.85	8821	56562512

NTUA Campus BADR5 Ku-band 3-year average, Data Availability: 96.49 %																	
Start Date								1st July 2017									
End Date								30th June 2020									
Attenuation threshold [dB]	Absolute Fade Slope [dB/sec]																Number of fade slope samples
	0.001	0.002	0.003	0.005	0.01	0.02	0.03	0.05	0.1	0.2	0.3	0.5	1	2	3	5	
	Probability of exceedance [%]																
1	67.079	56.422	49.846	40.817	27.839	15.722	9.954	4.801	0.983	0.076	0.017	0.000	0.000	0.000	0.000	0.000	191040
3	81.299	72.664	66.882	59.006	47.654	33.294	23.252	12.726	2.822	0.272	0.052	0.000	0.000	0.000	0.000	0.000	52271
5	83.330	74.896	68.614	60.692	51.092	39.640	29.960	17.598	4.426	0.480	0.047	0.000	0.000	0.000	0.000	0.000	27697
10	96.791	93.954	91.786	88.161	80.541	66.459	53.402	34.893	10.339	1.307	0.000	0.000	0.000	0.000	0.000	0.000	6732
15	93.971	88.981	85.897	81.670	75.191	64.796	55.994	37.942	13.825	3.084	0.000	0.000	0.000	0.000	0.000	0.000	2886
20	89.598	80.974	76.037	69.783	62.739	51.876	45.425	33.641	12.837	3.950	3.950	0.000	0.000	0.000	0.000	0.000	1519
25	83.156	68.763	61.087	50.640	39.232	24.414	16.631	9.382	6.397	6.397	6.397	0.000	0.000	0.000	0.000	0.000	938

Prob. of exceedance [%]	Corr. Attenuation A [dB]	Absolute Fade Slope [dB/sec]																Number of fade slope samples
		0.001	0.002	0.003	0.005	0.01	0.02	0.03	0.05	0.1	0.2	0.3	0.5	1	2	3	5	
		Probability of exceedance [%]																
0.001	25.17	82.777	68.461	60.603	50.054	38.428	22.390	15.285	8.719	6.459	6.459	6.459	0.000	0.000	0.000	0.000	0.000	929
0.002	18.52	91.104	83.635	79.352	73.696	66.337	54.970	46.568	33.443	14.882	3.295	3.295	0.000	0.000	0.000	0.000	0.000	1821
0.003	15.46	93.420	88.067	84.796	79.591	72.937	62.342	53.383	37.286	13.680	3.086	0.186	0.000	0.000	0.000	0.000	0.000	2690
0.005	12.25	95.719	92.145	89.607	86.055	80.340	68.822	57.635	38.063	11.628	2.405	0.000	0.000	0.000	0.000	0.000	0.000	4532
0.01	8.35	96.673	93.798	91.473	87.639	78.980	64.614	51.482	33.018	9.662	1.201	0.000	0.000	0.000	0.000	0.000	0.000	9077
0.02	6.16	89.363	81.902	76.143	68.758	60.021	47.917	36.744	22.319	6.219	0.695	0.033	0.000	0.000	0.000	0.000	0.000	18267
0.03	5.01	83.518	75.066	68.787	60.840	51.157	39.785	30.077	17.677	4.446	0.483	0.047	0.000	0.000	0.000	0.000	0.000	27533
0.05	3.37	82.446	73.746	67.769	59.785	48.426	34.822	24.791	13.823	3.131	0.310	0.055	0.000	0.000	0.000	0.000	0.000	45540
0.1	1.80	81.664	72.649	66.203	57.192	42.831	27.171	18.065	8.980	1.905	0.162	0.036	0.000	0.000	0.000	0.000	0.000	89700
0.2	1.08	68.245	58.240	51.899	42.951	29.710	16.954	10.759	5.211	1.071	0.083	0.018	0.000	0.000	0.000	0.000	0.000	173716
0.3	0.80	63.877	51.623	44.265	34.968	22.924	12.586	7.785	3.710	0.748	0.057	0.013	0.000	0.000	0.000	0.000	0.000	253366
0.5	0.55	61.109	46.344	37.750	27.545	16.670	8.771	5.332	2.513	0.500	0.038	0.008	0.000	0.000	0.000	0.000	0.000	383747
1	0.38	53.689	37.550	28.738	19.375	10.889	5.526	3.324	1.552	0.307	0.023	0.005	0.000	0.000	0.000	0.000	0.000	626414

NTUA Campus BADR5 Ku-band 3-year average, Data Availability: 96.49 %												
Start Date	1st July 2017											
End Date	30th June 2020											
	Fade Slope [dB/sec]											
Attenuation threshold [dB]	< 0.5	-0.5 to -0.45	-0.45 to -0.4	-0.4 to -0.35	-0.35 to -0.3	-0.3 to -0.25	-0.25 to -0.2	-0.2 to -0.15	-0.15 to -0.1	-0.1 to -0.05	-0.05 to 0.0
	Probability of exceedance [%]											
1	0.000	0.000	0.000	0.000	0.000	0.000	0.034	0.089	0.330	1.958	46.866
3	0.000	0.000	0.000	0.000	0.000	0.000	0.124	0.272	0.995	5.163	41.486
5	0.000	0.000	0.000	0.000	0.000	0.000	0.235	0.448	1.585	6.665	40.474
10	0.000	0.000	0.000	0.000	0.000	0.000	0.698	1.679	2.778	11.676	34.641
15	0.000	0.000	0.000	0.000	0.000	1.040	0.866	2.114	3.049	11.781	30.561
20	0.000	1.975	0.000	0.000	0.000	0.000	0.000	0.066	4.806	7.966	33.772
25	0.000	3.198	0.000	0.000	0.000	0.000	0.000	0.000	0.000	0.320	46.375

	Fade Slope [dB/sec]										
Attenuation threshold [dB]	0.0 to 0.05	0.05 to 0.1	0.1 to 0.15	0.15 to 0.2	0.2 to 0.25	0.25 to 0.3	0.3 to 0.35	0.35 to 0.4	0.4 to 0.45	0.45 to 0.5	> 0.5
	Probability of exceedance [%]										
1	48.333	1.860	0.407	0.081	0.017	0.008	0.017	0.000	0.000	0.000	0.000
3	45.788	4.741	1.029	0.254	0.063	0.033	0.052	0.000	0.000	0.000	0.000
5	41.929	6.506	1.495	0.419	0.123	0.076	0.047	0.000	0.000	0.000	0.000
10	30.466	12.879	2.911	1.664	0.505	0.104	0.000	0.000	0.000	0.000	0.000
15	31.497	12.335	3.534	2.044	0.139	1.040	0.000	0.000	0.000	0.000	0.000
20	32.587	12.837	4.016	0.000	0.000	0.000	0.856	1.119	0.000	0.000	0.000
25	44.243	2.665	0.000	0.000	0.000	0.000	0.000	0.000	2.665	0.533	0.000

NTUA Campus BADR5 Ku-band 3-year average, Data Availability: 96.49 %														
Start Date									1st July 2017					
End Date									30th June 2020					
Attenuation threshold [dB]	Fade Duration [sec]													
	1	10	30	60	120	180	300	600	900	1200	1500	1800	2400	3600
	Normalized Probability of exceedance [%]													
1	100.000	17.433	8.051	5.390	3.588	2.762	1.785	0.825	0.472	0.253	0.168	0.168	0.118	0.084
3	100.000	33.711	21.258	14.843	9.182	6.164	4.151	2.264	1.006	0.503	0.503	0.503	0.377	0.252
5	100.000	29.821	16.250	10.179	6.071	5.536	3.929	1.964	0.893	0.179	0.179	0.179	0.179	0.179
10	100.000	53.763	31.183	24.731	19.355	12.903	7.527	2.151	0.000	0.000	0.000	0.000	0.000	0.000
15	100.000	43.182	27.273	22.727	15.909	9.091	6.818	2.273	0.000	0.000	0.000	0.000	0.000	0.000
20	100.000	32.258	22.581	19.355	9.677	6.452	6.452	3.226	0.000	0.000	0.000	0.000	0.000	0.000
25	100.000	26.667	26.667	26.667	13.333	13.333	6.667	0.000	0.000	0.000	0.000	0.000	0.000	0.000

Probability of exceedance [%]	Corresponding Attenuation A [dB]	Fade Duration [sec]												
		1	10	30	60	120	180	300	600	900	1200	1500	1800	2400	3600
		Normalized Probability of exceedance [%]													
0.001	25.17	100.000	26.667	26.667	26.667	13.333	13.333	6.667	0.000	0.000	0.000	0.000	0.000	0.000	0.000
0.002	18.52	100.000	31.250	28.125	25.000	12.500	6.250	6.250	3.125	0.000	0.000	0.000	0.000	0.000	0.000
0.003	15.46	100.000	33.333	26.190	23.810	14.286	9.524	7.143	2.381	0.000	0.000	0.000	0.000	0.000	0.000
0.005	12.25	100.000	36.986	23.288	19.178	17.808	12.329	5.479	1.370	0.000	0.000	0.000	0.000	0.000	0.000
0.01	8.35	100.000	44.286	27.857	19.286	12.857	11.429	7.143	2.857	0.714	0.000	0.000	0.000	0.000	0.000
0.02	6.16	100.000	38.554	21.687	12.349	8.735	6.928	5.422	2.711	0.904	0.301	0.000	0.000	0.000	0.000
0.03	5.01	100.000	28.671	15.385	9.965	5.944	5.420	3.846	1.923	0.874	0.175	0.175	0.175	0.175	0.175
0.05	3.37	100.000	42.000	25.500	15.833	10.000	7.000	5.167	3.000	1.333	0.833	0.333	0.333	0.333	0.333
0.1	1.80	100.000	31.072	19.403	12.687	8.345	5.767	3.392	1.628	1.085	0.543	0.475	0.339	0.271	0.204
0.2	1.08	100.000	17.748	8.803	6.044	3.848	2.961	2.035	0.907	0.524	0.302	0.222	0.222	0.141	0.121
0.3	0.80	100.000	18.169	8.111	4.928	2.916	2.054	1.288	0.649	0.341	0.202	0.128	0.117	0.064	0.053
0.5	0.55	100.000	12.252	5.125	3.094	1.916	1.461	0.891	0.431	0.297	0.206	0.129	0.101	0.062	0.029
1	0.38	100.000	8.452	2.591	1.541	0.923	0.678	0.452	0.214	0.137	0.102	0.074	0.059	0.044	0.018

NTUA Campus BADR5 Ku-band 3-year average, Data Availability: 96.49 %							
Start Date				1st July 2017			
End Date				30th June 2020			
Attenuation threshold [dB]	**Total number of fades > 1.0 sec**	**Total number of fades > 10.0 sec**	**Total fading time > 1.0 sec (ITU Total Outage time)**	**Total fading time > 10.0 sec (ITU Total unavailable time)**	**Mean Duration of fade events > 1.0 sec**	**Mean Duration of fade events > 10.0 sec**	**Unavailable to Outage Time Ratio[%]**
1	5937	1035	189814	172303	31.971	166.476	90.775
3	795	268	51930	49799	65.321	185.817	95.896
5	560	167	27503	25956	49.113	155.425	94.375
10	93	50	6699	6533	72.032	130.660	97.522
15	44	19	2893	2789	65.750	146.789	96.405
20	31	10	1494	1424	48.194	142.400	95.315
25	15	4	932	890	62.133	222.500	95.494

Probability of exceedance [%]	**Corresponding Attenuation A [dB]**	**Total number of fades > 1.0 sec**	**Total number of fades > 10.0 sec**	**Total fading time > 1.0 sec (ITU Total Outage time)**	**Total fading time > 10.0 sec (ITU Total unavailable time)**	**Mean Duration of fade events > 1.0 sec**	**Mean Duration of fade events > 10.0 sec**	**Unavailable to Outage Time Ratio[%]**
0.001	25.17	15	4	921	883	61.400	220.750	95.874
0.002	18.52	32	10	1800	1709	56.250	170.900	94.944
0.003	15.46	42	14	2696	2578	64.190	184.143	95.623
0.005	12.25	73	27	4512	4345	61.808	160.926	96.299
0.01	8.35	140	62	9054	8762	64.671	141.323	96.775
0.02	6.16	332	128	18237	17402	54.931	135.953	95.421
0.03	5.01	572	164	27307	25768	47.740	157.122	94.364
0.05	3.37	600	252	45211	43901	75.352	174.210	97.102
0.1	1.80	1474	458	88974	85162	60.362	185.943	95.716
0.2	1.08	4964	881	172750	158419	34.801	179.817	91.704
0.3	0.80	9395	1707	253374	226205	26.969	132.516	89.277
0.5	0.55	20878	2558	395211	333114	18.930	130.224	84.288
1	0.38	59699	5046	674099	492881	11.292	97.678	73.117

NTUA Campus BADR5 Ku-band 3-year average, Data Availability: 96.49 %														
Start Date								1st July 2017						
End Date								30th June 2020						
Attenuation threshold [dB]	Accumulate Fading Time [sec]													
	1	10	30	60	120	180	300	600	900	1200	1500	1800	2400	3600
	Normalized Probability of exceedance [%]													
1	100.000	90.775	85.814	82.306	77.561	73.750	66.671	54.119	46.467	39.688	36.227	36.227	33.190	30.134
3	100.000	95.896	92.297	87.992	80.778	74.219	67.244	54.371	39.526	31.539	31.539	31.539	27.325	21.234
5	100.000	94.375	89.667	84.565	77.130	75.410	67.869	50.620	35.116	19.478	19.478	19.478	19.478	19.478
10	100.000	97.522	91.581	88.103	82.714	68.025	52.232	22.854	0.000	0.000	0.000	0.000	0.000	0.000
15	100.000	96.405	92.361	89.284	79.882	64.501	56.170	26.547	0.000	0.000	0.000	0.000	0.000	0.000
20	100.000	95.315	92.570	90.495	73.494	65.328	65.328	43.641	0.000	0.000	0.000	0.000	0.000	0.000
25	100.000	95.494	95.494	95.494	80.687	80.687	57.725	0.000	0.000	0.000	0.000	0.000	0.000	0.000

Probability of exceedance [%]	Corresponding Attenuation A [dB]	Accumulate Fading Time [sec]												
		1	10	30	60	120	180	300	600	900	1200	1500	1800	2400	3600
		Normalized Probability of exceedance [%]													
0.001	25.17	100.000	95.874	95.874	95.874	81.325	81.325	58.089	0.000	0.000	0.000	0.000	0.000	0.000	0.000
0.002	18.52	100.000	94.944	94.056	91.167	73.056	56.667	56.667	37.722	0.000	0.000	0.000	0.000	0.000	0.000
0.003	15.46	100.000	95.623	93.101	91.432	79.043	68.212	59.829	28.375	0.000	0.000	0.000	0.000	0.000	0.000
0.005	12.25	100.000	96.299	92.575	90.381	87.810	74.867	50.244	18.484	0.000	0.000	0.000	0.000	0.000	0.000
0.01	8.35	100.000	96.775	92.158	86.592	79.026	75.403	61.233	32.660	10.482	0.000	0.000	0.000	0.000	0.000
0.02	6.16	100.000	95.421	89.790	82.190	76.301	71.689	65.208	42.381	18.901	7.978	0.000	0.000	0.000	0.000
0.03	5.01	100.000	94.364	89.607	84.945	77.588	75.856	68.261	50.888	35.299	19.548	19.548	19.548	19.548	19.548
0.05	3.37	100.000	97.102	93.203	87.430	80.870	75.059	69.629	57.086	39.935	33.162	24.091	24.091	24.091	24.091
0.1	1.80	100.000	95.716	92.316	87.331	81.014	74.774	65.710	53.359	47.189	37.773	36.404	32.748	30.586	26.890
0.2	1.08	100.000	91.704	87.346	83.986	78.759	74.886	68.735	55.191	47.509	41.050	37.975	37.975	33.262	31.681
0.3	0.80	100.000	89.277	82.907	77.871	71.460	66.644	59.899	49.634	41.218	35.948	32.201	31.515	27.348	26.196
0.5	0.55	100.000	84.288	77.920	73.428	68.213	64.719	57.737	47.439	42.411	37.424	32.044	29.652	25.354	20.242
1	0.38	100.000	73.117	64.647	60.757	56.155	52.981	48.318	39.238	34.315	30.975	27.554	25.395	22.635	16.153

NTUA Campus BADR5 Ku-band 3-year average, Data Availability: 96.49 %																		
Start Date														1st July 2017				
End Date														30th June 2020				
Attenuation threshold [dB]	Inter-Fade Duration [sec]																	
	1	2	3	5	10	20	30	50	100	200	300	500	1000	2000	3000	5000	10000	20000
	Normalized Probability of exceedance [%]																	
1	100.000	70.515	56.232	42.996	31.701	24.266	21.402	18.398	14.797	11.734	10.249	8.407	6.506	5.012	4.373	3.660	3.062	2.498
3	100.000	66.242	53.981	41.959	33.201	27.309	24.841	22.611	19.188	16.322	14.889	13.854	12.500	10.908	10.669	10.510	9.634	8.997
5	100.000	58.323	45.749	36.048	29.581	24.311	21.198	19.042	17.605	16.048	14.611	13.533	12.455	11.497	11.497	11.138	10.898	10.539
10	100.000	75.168	64.430	55.705	41.611	34.899	30.201	28.188	26.174	24.832	23.490	22.148	22.148	21.477	21.477	20.805	20.805	20.805
15	100.000	74.286	62.857	54.286	44.286	32.857	28.571	25.714	22.857	20.000	20.000	20.000	20.000	20.000	20.000	20.000	20.000	20.000
20	100.000	64.583	47.917	37.500	22.917	16.667	16.667	14.583	14.583	14.583	12.500	12.500	12.500	12.500	12.500	12.500	12.500	20.000
25	100.000	47.368	21.053	15.789	10.526	10.526	10.526	10.526	10.526	5.263	5.263	5.263	5.263	5.263	5.263	5.263	5.263	5.263

Attenuation threshold [dB]	Inter-Fade Duration [sec]																	
	3000	5000	10000	20000	30000	50000	100000	200000	300000	500000	1000000	2000000	3000000	5000000	10000000	20000000	30000000	50000000
	Normalized Probability of exceedance [%]																	
1	4.373	3.660	3.062	2.498	2.299	2.108	1.560	1.062	0.755	0.456	0.133	0.017	0.000	0.000	0.000	0.000	0.000	0.000
3	10.669	10.510	9.634	8.997	8.758	8.201	7.006	6.051	4.459	3.503	2.468	1.035	0.637	0.000	0.000	0.000	0.000	0.000
5	11.497	11.138	10.898	10.539	10.299	9.940	8.383	7.545	5.629	4.790	3.114	1.437	1.078	0.240	0.000	0.000	0.000	0.000
10	21.477	20.805	20.805	20.805	20.805	20.134	18.121	18.121	16.107	13.423	10.067	5.369	3.356	0.671	0.000	0.000	0.000	0.000
15	20.000	20.000	20.000	20.000	20.000	18.571	15.714	15.714	15.714	14.286	11.429	5.714	4.286	2.857	0.000	0.000	0.000	0.000
20	12.500	12.500	12.500	12.500	12.500	12.500	8.333	8.333	8.333	8.333	8.333	4.167	4.167	4.167	0.000	0.000	0.000	0.000
25	5.263	5.263	5.263	5.263	5.263	5.263	5.263	5.263	5.263	5.263	5.263	5.263	5.263	5.263	0.000	0.000	0.000	0.000

NTUA Campus BADR5 Ku-band 3-year average, Data Availability: 96.49 %															
Start Date		1st July 2017													
End Date		30th June 2020													
Probability of exceedance [%]	Corresponding Attenuation A [dB]	Inter-Fade Duration [sec]													
		1	2	3	5	10	20	30	50	100	200	300	500	1000	2000
		Normalized Probability of exceedance [%]													
0.001	25.17	100.000	47.368	26.316	15.789	10.526	10.526	10.526	10.526	10.526	5.263	5.263	5.263	5.263	5.263
0.002	18.52	100.000	64.444	48.889	37.778	22.222	22.222	22.222	22.222	22.222	20.000	17.778	17.778	17.778	17.778
0.003	15.46	100.000	73.770	59.016	45.902	39.344	34.426	32.787	31.148	22.951	19.672	19.672	19.672	19.672	19.672
0.005	12.25	100.000	72.642	64.151	52.830	42.453	36.792	35.849	33.019	29.245	25.472	24.528	22.642	22.642	22.642
0.01	8.35	100.000	70.370	61.574	50.463	41.204	37.037	31.944	30.093	26.389	25.463	24.074	21.759	21.296	20.370
0.02	6.16	100.000	66.352	55.766	42.911	34.216	28.355	26.087	23.251	20.416	19.093	17.202	16.068	15.123	14.745
0.03	5.01	100.000	60.369	45.046	34.562	28.226	23.387	20.392	18.318	17.051	15.438	14.055	13.018	11.982	11.060
0.05	3.37	100.000	67.243	55.443	43.947	34.690	30.112	27.263	25.636	22.584	19.430	17.497	16.480	14.751	13.021
0.1	1.80	100.000	68.778	54.590	43.247	33.156	26.669	23.369	20.713	18.096	15.781	14.643	13.126	11.267	9.901
0.2	1.08	100.000	69.689	55.466	42.579	31.567	24.638	21.862	18.448	14.953	12.025	10.718	8.895	6.929	5.491
0.3	0.80	100.000	70.824	57.638	45.728	34.494	26.867	23.528	19.991	15.996	12.193	10.262	8.209	6.097	4.539
0.5	0.55	100.000	76.649	64.415	52.119	39.859	30.806	26.560	21.907	16.677	12.120	9.816	7.424	5.112	3.554
1	0.38	100.000	78.124	65.976	52.616	38.466	28.212	23.516	18.662	13.259	9.034	7.121	5.133	3.336	2.203

Probability of exceedance [%]	Corresponding Attenuation A [dB]	Inter-Fade Duration [sec]													
		3000	5000	10000	20000	30000	50000	100000	200000	300000	500000	1000000	2000000	3000000	5000000	10000000
		Normalized Probability of exceedance [%]														
0.001	25.17	5.263	5.263	5.263	5.263	5.263	5.263	5.263	5.263	5.263	5.263	5.263	5.263	5.263	5.263	0.000
0.002	18.52	17.778	17.778	17.778	17.778	17.778	17.778	13.333	13.333	13.333	13.333	11.111	6.667	6.667	4.444	0.000
0.003	15.46	19.672	19.672	19.672	19.672	19.672	18.033	14.754	14.754	14.754	14.754	11.475	8.197	6.557	3.279	0.000
0.005	12.25	22.642	22.642	22.642	22.642	22.642	21.698	19.811	19.811	17.925	16.981	13.208	6.604	4.717	0.943	0.000
0.01	8.35	20.370	19.907	19.907	18.981	18.981	18.519	16.667	15.741	13.426	9.722	6.481	2.778	2.315	0.463	0.000
0.02	6.16	14.556	13.989	13.800	13.233	13.043	12.665	10.964	10.208	8.507	6.994	4.537	2.079	1.512	0.567	0.000
0.03	5.01	11.060	10.714	10.484	10.138	9.908	9.562	8.065	7.258	5.415	4.608	2.995	1.382	1.037	0.230	0.000
0.05	3.37	12.920	12.716	11.902	11.089	10.885	10.275	8.850	7.528	5.595	4.578	3.154	1.322	0.814	0.000	0.000
0.1	1.80	9.219	8.763	7.436	6.829	6.411	5.728	4.742	3.604	2.618	2.049	1.062	0.341	0.152	0.000	0.000
0.2	1.08	4.792	4.174	3.414	2.796	2.563	2.340	1.742	1.195	0.861	0.577	0.213	0.020	0.000	0.000	0.000
0.3	0.80	3.904	3.216	2.592	2.139	1.968	1.739	1.093	0.741	0.512	0.267	0.027	0.005	0.000	0.000	0.000
0.5	0.55	2.934	2.358	1.770	1.425	1.284	1.110	0.444	0.225	0.122	0.036	0.004	0.000	0.000	0.000	0.000
1	0.38	1.776	1.327	0.896	0.678	0.586	0.453	0.098	0.026	0.008	0.001	0.000	0.000	0.000	0.000	0.000

NTUA Campus BADR5 Ku-band 3-year average, Data Availability: 96.49 %		
Start Date		1st July 2017
End Date		30th June 2020
Attenuation threshold [dB]	**Total number of inter-fades**	**Total duration of inter-fades [sec]**
1	12050	90584166
3	1256	88269033
5	835	80288027
10	149	71052540
15	70	61380209
20	48	57187551
25	19	35249201

Probability of exceedance [%]	**Corresponding Attenuation A [dB]**	**Total number of inter-fades**	**Total duration of inter-fades [sec]**
0.001	25.17	19	35249212
0.002	18.52	45	60593917
0.003	15.46	61	61380378
0.005	12.25	106	67631111
0.01	8.35	216	71050172
0.02	6.16	529	80297292
0.03	5.01	868	80288202
0.05	3.37	983	88275803
0.1	1.80	2636	89861794
0.2	1.08	9871	90602360
0.3	0.80	18748	91042105
0.5	0.55	46657	90892085
1	0.38	141220	90557713

NTUA Campus KaSAT Ka-band 2-year average, Data Availability: 96.15 %																	
Start Date								1st July 2018									
End Date								30th June 2020									
Attenuation threshold [dB]	**Absolute Fade Slope [dB/sec]**																**Number of fade slope samples**
	0.001	**0.002**	**0.003**	**0.005**	**0.01**	**0.02**	**0.03**	**0.05**	**0.1**	**0.2**	**0.3**	**0.5**	**1**	**2**	**3**	**5**	
	Probability of exceedance [%]																
1	74.606	55.537	42.179	25.560	9.905	3.662	2.109	0.950	0.199	0.003	0.000	0.000	0.000	0.000	0.000	0.000	1043136
3	84.411	71.290	60.903	47.463	31.093	18.212	11.853	5.620	1.230	0.021	0.000	0.000	0.000	0.000	0.000	0.000	153992
5	84.933	72.063	62.983	52.797	40.124	27.102	18.986	10.318	2.509	0.030	0.000	0.000	0.000	0.000	0.000	0.000	65970
10	84.859	71.775	64.272	56.931	48.245	36.053	27.439	14.496	2.030	0.336	0.000	0.000	0.000	0.000	0.000	0.000	17832
15	74.658	52.882	41.401	31.765	22.620	12.301	5.831	1.014	0.683	0.683	0.205	0.000	0.000	0.000	0.000	0.000	8780
20	nan	nan	nan	nan	nan	nan	nan	nan	nan	nan	nan	nan	nan	nan	nan	nan	0
25	nan	nan	nan	nan	nan	nan	nan	nan	nan	nan	nan	nan	nan	nan	nan	nan	0

Prob. of exceedance [%]	**Corr. Attenuation A [dB]**	**Absolute Fade Slope [dB/sec]**																**Number of fade slope samples**
		0.001	**0.002**	**0.003**	**0.005**	**0.01**	**0.02**	**0.03**	**0.05**	**0.1**	**0.2**	**0.3**	**0.5**	**1**	**2**	**3**	**5**	
		Probability of exceedance [%]																
0.001	19.52	nan	nan	nan	nan	nan	nan	nan	nan	nan	nan	nan	nan	nan	nan	nan	nan	0
0.002	19.07	46.118	15.294	14.118	14.118	14.118	14.118	14.118	14.118	14.118	14.118	14.118	0.000	0.000	0.000	0.000	0.000	425
0.003	18.73	48.153	24.692	16.749	7.266	3.695	3.695	3.695	3.695	3.695	3.695	3.695	0.000	0.000	0.000	0.000	0.000	1624
0.005	18.14	60.942	35.758	24.255	12.336	3.589	1.922	1.922	1.922	1.922	1.922	1.922	0.000	0.000	0.000	0.000	0.000	3121
0.01	16.80	70.112	45.514	31.705	19.796	9.898	3.618	0.974	0.974	0.974	0.974	0.487	0.000	0.000	0.000	0.000	0.000	6163
0.02	12.72	78.803	61.039	51.471	43.017	34.963	24.439	17.747	7.323	0.499	0.499	0.017	0.000	0.000	0.000	0.000	0.000	12030
0.03	9.85	85.080	72.138	64.807	57.554	49.088	36.593	27.746	14.821	2.194	0.331	0.000	0.000	0.000	0.000	0.000	0.000	18143
0.05	7.19	87.846	77.303	70.515	62.986	52.898	39.056	29.172	16.924	3.813	0.055	0.000	0.000	0.000	0.000	0.000	0.000	29035
0.1	5.33	84.065	70.707	61.367	51.321	39.485	26.956	19.130	10.584	2.615	0.000	0.000	0.000	0.000	0.000	0.000	0.000	61186
0.2	3.46	85.436	72.937	63.082	50.698	35.414	22.058	14.711	7.102	1.574	0.028	0.000	0.000	0.000	0.000	0.000	0.000	116687
0.3	2.81	84.208	70.628	59.586	45.288	28.811	16.385	10.574	5.012	1.086	0.019	0.000	0.000	0.000	0.000	0.000	0.000	176035
0.5	2.18	80.689	65.380	53.780	38.592	21.712	10.998	6.861	3.258	0.688	0.011	0.000	0.000	0.000	0.000	0.000	0.000	289325
1	1.49	77.358	59.787	47.115	31.145	14.514	6.373	3.803	1.747	0.367	0.006	0.000	0.000	0.000	0.000	0.000	0.000	560488

NTUA Campus KaSAT Ka-band 2-year average, Data Availability: 96.15 %												
Start Date	1st July 2018											
End Date	30th June 2020											
	Fade Slope [dB/sec]											
Attenuation threshold [dB]	< 0.5	-0.5 to -0.45	-0.45 to -0.4	-0.4 to -0.35	-0.35 to -0.3	-0.3 to -0.25	-0.25 to -0.2	-0.2 to -0.15	-0.15 to -0.1	-0.1 to -0.05	-0.05 to 0.0
	Probability of exceedance [%]											
1	0.000	0.000	0.000	0.000	0.000	0.000	0.002	0.026	0.065	0.373	51.502
3	0.000	0.000	0.000	0.000	0.000	0.000	0.014	0.168	0.400	2.214	47.947
5	0.000	0.000	0.000	0.000	0.000	0.000	0.012	0.262	0.852	4.087	45.669
10	0.000	0.000	0.000	0.000	0.000	0.000	0.168	0.000	0.791	6.247	46.046
15	0.000	0.000	0.000	0.000	0.000	0.342	0.000	0.000	0.000	0.228	50.900
20	nan	nan	nan	nan	nan	nan	nan	nan	nan	nan	nan
25	nan	nan	nan	nan	nan	nan	nan	nan	nan	nan	nan

	Fade Slope [dB/sec]										
Attenuation threshold [dB]	0.0 to 0.05	0.05 to 0.1	0.1 to 0.15	0.15 to 0.2	0.2 to 0.25	0.25 to 0.3	0.3 to 0.35	0.35 to 0.4	0.4 to 0.45	0.45 to 0.5	> 0.5
	Probability of exceedance [%]										
1	47.548	0.377	0.089	0.015	0.001	0.000	0.000	0.000	0.000	0.000	0.000
3	46.433	2.177	0.542	0.099	0.008	0.000	0.000	0.000	0.000	0.000	0.000
5	44.012	3.723	1.149	0.215	0.018	0.000	0.000	0.000	0.000	0.000	0.000
10	39.457	6.219	0.903	0.000	0.067	0.101	0.000	0.000	0.000	0.000	0.000
15	48.087	0.103	0.000	0.000	0.000	0.137	0.205	0.000	0.000	0.000	0.000
20	nan	nan	nan	nan	nan	nan	nan	nan	nan	nan	nan
25	nan	nan	nan	nan	nan	nan	nan	nan	nan	nan	nan

NTUA Campus KaSAT Ka-band 2-year average, Data Availability: 96.15 %														
Start Date									1st July 2018					
End Date									30th June 2020					
Attenuation threshold [dB]	Fade Duration [sec]													
	1	10	30	60	120	180	300	600	900	1200	1500	1800	2400	3600
	Normalized Probability of exceedance [%]													
1	100.000	15.761	5.566	3.088	1.653	1.125	0.727	0.400	0.300	0.225	0.181	0.142	0.110	0.063
3	100.000	19.071	8.714	5.571	3.762	3.143	2.000	1.048	0.667	0.452	0.333	0.238	0.119	0.071
5	100.000	31.350	19.908	13.272	9.153	6.865	4.577	2.746	1.259	0.686	0.572	0.458	0.458	0.458
10	100.000	39.583	30.208	22.917	15.625	11.458	9.375	2.604	1.042	1.042	0.521	0.521	0.521	0.000
15	100.000	25.000	19.531	16.406	10.156	8.594	5.469	2.344	0.781	0.781	0.781	0.781	0.781	0.000
20	nan	nan	nan	nan	nan	nan	nan	nan	nan	nan	nan	nan	nan	nan
25	nan	nan	nan	nan	nan	nan	nan	nan	nan	nan	nan	nan	nan	nan

Probability of exceedance [%]	Corresponding Attenuation A [dB]	Fade Duration [sec]													
		1	10	30	60	120	180	300	600	900	1200	1500	1800	2400	3600
		Normalized Probability of exceedance [%]													
0.001	19.52	100.000	0.000	0.000	0.000	0.000	0.000	0.000	0.000	0.000	0.000	0.000	0.000	0.000	0.000
0.002	19.07	100.000	0.000	0.000	0.000	0.000	0.000	0.000	0.000	0.000	0.000	0.000	0.000	0.000	0.000
0.003	18.73	100.000	8.678	0.826	0.413	0.413	0.413	0.000	0.000	0.000	0.000	0.000	0.000	0.000	0.000
0.005	18.14	100.000	14.286	7.143	4.082	2.041	1.531	1.531	0.000	0.000	0.000	0.000	0.000	0.000	0.000
0.01	16.80	100.000	18.657	7.090	3.731	1.866	1.866	1.119	1.119	0.373	0.373	0.373	0.000	0.000	0.000
0.02	12.72	100.000	24.691	14.815	10.700	7.407	5.761	4.527	2.058	0.412	0.412	0.412	0.412	0.412	0.000
0.03	9.85	100.000	33.488	25.581	20.465	14.419	10.698	8.837	2.326	0.930	0.930	0.465	0.465	0.465	0.000
0.05	7.19	100.000	29.424	18.107	12.963	8.642	6.996	4.527	2.058	1.235	0.617	0.412	0.412	0.206	0.206
0.1	5.33	100.000	29.245	17.715	11.845	7.862	5.870	3.878	1.992	0.839	0.524	0.419	0.419	0.419	0.419
0.2	3.46	100.000	20.314	10.826	7.689	5.509	3.787	2.487	1.415	0.689	0.536	0.268	0.191	0.077	0.077
0.3	2.81	100.000	20.552	9.336	5.822	3.779	2.840	1.879	1.021	0.654	0.429	0.286	0.245	0.102	0.061
0.5	2.18	100.000	18.400	8.069	5.115	3.380	2.507	1.791	0.951	0.649	0.436	0.347	0.302	0.145	0.045
1	1.49	100.000	17.477	6.738	4.171	2.507	1.837	1.236	0.636	0.457	0.328	0.253	0.223	0.164	0.104

NTUA Campus KaSAT Ka-band 2-year average, Data Availability: 96.15 %							
Start Date				1st July 2018			
End Date				30th June 2020			
Attenuation threshold [dB]	**Total number of fades > 1.0 sec**	**Total number of fades > 10.0 sec**	**Total fading time > 1.0 sec (ITU Total Outage time)**	**Total fading time > 10.0 sec (ITU Total unavailable time)**	**Mean Duration of fade events > 1.0 sec**	**Mean Duration of fade events > 10.0 sec**	**Unavailable to Outage Time Ratio[%]**
1	52016	8198	1027475	871127	19.753	106.261	84.783
3	4200	801	150787	138591	35.902	173.022	91.912
5	874	274	65573	63333	75.026	231.142	96.584
10	192	76	17648	17236	91.917	226.789	97.665
15	128	32	8732	8414	68.219	262.938	96.358
20	0	0	0	0	nan	nan	nan
25	0	0	0	0	nan	nan	nan

Probability of exceedance [%]	**Corresponding Attenuation A [dB]**	**Total number of fades > 1.0 sec**	**Total number of fades > 10.0 sec**	**Total fading time > 1.0 sec (ITU Total Outage time)**	**Total fading time > 10.0 sec (ITU Total unavailable time)**	**Mean Duration of fade events > 1.0 sec**	**Mean Duration of fade events > 10.0 sec**	**Unavailable to Outage Time Ratio[%]**
0.001	19.52	2	0	4	0	2.000		0.000
0.002	19.07	115	0	347	0	3.017		0.000
0.003	18.73	242	21	1291	528	5.335	25.143	40.899
0.005	18.14	196	28	2936	2301	14.980	82.179	78.372
0.01	16.80	268	50	5898	5084	22.007	101.680	86.199
0.02	12.72	243	60	11837	11149	48.712	185.817	94.188
0.03	9.85	215	72	17952	17463	83.498	242.542	97.276
0.05	7.19	486	143	28557	27274	58.759	190.727	95.507
0.1	5.33	954	279	60266	57801	63.172	207.172	95.910
0.2	3.46	2614	531	114824	107210	43.927	201.902	93.369
0.3	2.81	4895	1006	172259	158057	35.191	157.114	91.755
0.5	2.18	8935	1644	283737	257251	31.756	156.479	90.665
1	1.49	20141	3520	550249	490180	27.320	139.256	89.083

NTUA Campus KaSAT Ka-band 2-year average, Data Availability: 96.15 %														
Start Date								1st July 2018						
End Date								30th June 2020						
Attenuation threshold [dB]	Accumulate Fading Time [sec]													
	1	10	30	60	120	180	300	600	900	1200	1500	1800	2400	3600
	Normalized Probability of exceedance [%]													
1	100.000	84.783	75.999	70.651	64.373	60.571	55.937	49.039	45.370	41.516	38.542	35.417	32.049	25.415
3	100.000	91.912	87.047	83.282	78.981	76.425	68.910	57.634	49.696	43.743	39.219	34.675	27.931	24.138
5	100.000	96.584	93.926	90.156	85.314	80.721	73.779	62.998	49.185	41.648	39.772	37.162	37.162	37.162
10	100.000	97.665	95.915	92.787	85.352	78.745	73.515	40.701	26.791	26.791	19.402	19.402	19.402	0.000
15	100.000	96.358	94.606	92.636	83.898	80.692	68.484	48.557	31.058	31.058	31.058	31.058	31.058	0.000
20	nan	nan	nan	nan	nan	nan	nan	nan	nan	nan	nan	nan	nan	nan
25	nan	nan	nan	nan	nan	nan	nan	nan	nan	nan	nan	nan	nan	nan

Probability of exceedance [%]	Corresponding Attenuation A [dB]	Accumulate Fading Time [sec]												
		1	10	30	60	120	180	300	600	900	1200	1500	1800	2400	3600
		Normalized Probability of exceedance [%]													
0.001	19.52	100.000	0.000	0.000	0.000	0.000	0.000	0.000	0.000	0.000	0.000	0.000	0.000	0.000	0.000
0.002	19.07	100.000	0.000	0.000	0.000	0.000	0.000	0.000	0.000	0.000	0.000	0.000	0.000	0.000	0.000
0.003	18.73	100.000	40.899	16.499	14.020	14.020	14.020	0.000	0.000	0.000	0.000	0.000	0.000	0.000	0.000
0.005	18.14	100.000	78.372	70.334	61.921	47.514	41.621	41.621	0.000	0.000	0.000	0.000	0.000	0.000	0.000
0.01	16.80	100.000	86.199	77.162	70.905	63.564	63.564	55.409	55.409	28.942	28.942	28.942	0.000	0.000	0.000
0.02	12.72	100.000	94.188	89.981	86.500	81.119	76.675	70.888	49.768	24.592	24.592	24.592	24.592	24.592	0.000
0.03	9.85	100.000	97.276	95.577	93.093	86.481	80.102	74.922	40.302	26.615	26.615	19.112	19.112	19.112	0.000
0.05	7.19	100.000	95.507	91.960	88.185	81.756	77.263	67.490	46.363	36.737	25.668	20.920	20.920	12.848	12.848
0.1	5.33	100.000	95.910	92.687	88.737	83.107	78.465	71.274	57.181	44.559	39.518	37.489	37.489	37.489	37.489
0.2	3.46	100.000	93.369	89.667	86.559	82.357	76.633	69.587	59.516	46.868	43.079	35.209	32.341	27.057	27.057
0.3	2.81	100.000	91.755	86.215	82.078	77.156	73.288	66.857	56.588	48.919	42.538	36.926	35.023	26.665	23.681
0.5	2.18	100.000	90.665	85.045	81.044	76.437	72.399	67.197	56.067	48.782	41.875	38.199	35.987	25.938	17.290
1	1.49	100.000	89.083	82.331	78.293	73.068	69.502	64.258	55.133	50.330	45.446	41.684	39.875	35.165	28.756

NTUA Campus KaSAT Ka-band 2-year average, Data Availability: 96.15 %																		
Start Date																		1st July 2018
End Date																		30th June 2020
Attenuation threshold [dB]	Inter-Fade Duration [sec]																	
	1	2	3	5	10	20	30	50	100	200	300	500	1000	2000				
	Normalized Probability of exceedance [%]																	
1	100.000	61.441	45.450	31.101	19.223	12.475	10.252	8.415	5.690	3.988	3.215	2.384	1.614	1.115				
3	100.000	56.518	39.632	25.157	13.904	8.663	7.225	5.787	4.373	3.304	2.959	2.507	2.163	1.747				
5	100.000	60.146	44.424	30.530	20.049	14.869	12.066	10.481	8.105	6.764	6.033	5.363	4.692	4.144				
10	100.000	64.110	50.685	39.452	24.932	19.726	17.808	15.616	13.973	12.329	11.507	10.137	8.219	8.219				
15	100.000	61.240	46.512	31.783	21.318	15.504	13.953	13.178	12.016	10.465	9.690	9.302	8.140	7.752				
20	nan	nan	nan	nan	nan	nan	nan	nan	nan	nan	nan	nan	nan	nan				
25	nan	nan	nan	nan	nan	nan	nan	nan	nan	nan	nan	nan	nan	nan				

Attenuation threshold [dB]	Inter-Fade Duration [sec]																	
	3000	5000	10000	20000	30000	50000	100000	200000	300000	500000	1000000	2000000	3000000	5000000	10000000			
	Normalized Probability of exceedance [%]																	
1	0.905	0.730	0.538	0.376	0.272	0.193	0.107	0.054	0.032	0.017	0.004	0.001	0.000	0.000	0.000			
3	1.557	1.438	1.224	1.058	0.986	0.915	0.772	0.594	0.523	0.392	0.202	0.083	0.036	0.012	0.000			
5	3.778	3.534	3.352	2.864	2.742	2.742	2.255	2.194	1.889	1.463	1.097	0.548	0.427	0.122	0.000			
10	7.123	6.575	6.575	5.753	5.479	5.479	4.932	4.932	4.658	3.562	3.014	1.918	1.096	0.274	0.000			
15	6.977	6.977	6.589	6.202	5.814	5.814	5.039	5.039	5.039	4.264	3.876	2.326	1.938	1.163	0.000			
20	nan	nan	nan	nan	nan	nan	nan	nan	nan	nan	nan	nan	nan	nan	nan			
25	nan	nan	nan	nan	nan	nan	nan	nan	nan	nan	nan	nan	nan	nan	nan			

NTUA Campus KaSAT Ka-band 2-year average, Data Availability: 96.15 %																						
Start Date														1st July 2018								
End Date														30th June 2020								
Probability of exceedance [%]	Corresponding Attenuation A [dB]	Inter-Fade Duration [sec]																				
		1	2	3	5	10	20	30	50	100	200	300	500	1000	2000							
		Normalized Probability of exceedance [%]																				
0.001	19.52	100.000	92.500	87.500	75.000	47.500	25.000	22.500	15.000	5.000	0.000	0.000	0.000	0.000	0.000							
0.002	19.07	100.000	67.188	48.125	31.250	17.813	7.188	3.125	0.938	0.000	0.000	0.000	0.000	0.000	0.000							
0.003	18.73	100.000	49.789	30.591	12.658	6.118	3.165	2.532	0.844	0.422	0.422	0.211	0.211	0.211	0.211							
0.005	18.14	100.000	44.324	26.757	11.892	4.324	2.973	2.973	2.162	1.622	1.351	1.351	1.351	1.351	1.351							
0.01	16.80	100.000	50.000	33.582	19.590	9.328	4.291	3.545	2.985	2.612	2.425	2.239	2.239	1.866	1.866							
0.02	12.72	100.000	51.481	36.902	24.146	17.084	13.212	12.301	11.390	10.023	8.656	8.200	7.289	6.378	5.695							
0.03	9.85	100.000	60.358	48.082	33.504	22.762	19.437	18.159	15.345	13.555	11.765	10.997	9.719	7.928	7.928							
0.05	7.19	100.000	61.900	45.446	31.832	22.821	17.336	15.377	13.026	10.284	8.815	7.542	6.562	5.583	4.995							
0.1	5.33	100.000	56.062	38.794	26.138	16.322	12.241	10.467	8.752	7.215	5.973	5.322	4.790	4.199	3.607							
0.2	3.46	100.000	56.915	41.123	26.813	15.676	10.771	9.021	7.271	5.347	4.328	3.789	3.347	2.827	2.308							
0.3	2.81	100.000	55.718	38.453	24.680	14.535	9.457	7.744	6.305	4.581	3.544	3.078	2.676	2.190	1.830							
0.5	2.18	100.000	57.941	41.252	27.033	15.274	9.475	7.413	5.722	4.085	2.963	2.438	2.040	1.647	1.410							
1	1.49	100.000	58.747	42.718	28.229	17.052	11.201	9.210	7.605	5.233	3.695	3.037	2.389	1.748	1.383							

Probability of exceedance [%]	Corresponding Attenuation A [dB]	Inter-Fade Duration [sec]																				
		3000	5000	10000	20000	30000	50000	100000	200000	300000	500000	1000000	2000000	3000000	5000000	10000000						
		Normalized Probability of exceedance [%]																				
0.001	19.52	0.000	0.000	0.000	0.000	0.000	0.000	0.000	0.000	0.000	0.000	0.000	0.000	0.000	0.000	0.000						
0.002	19.07	0.000	0.000	0.000	0.000	0.000	0.000	0.000	0.000	0.000	0.000	0.000	0.000	0.000	0.000	0.000						
0.003	18.73	0.211	0.211	0.211	0.211	0.211	0.211	0.000	0.000	0.000	0.000	0.000	0.000	0.000	0.000	0.000						
0.005	18.14	1.351	1.351	1.351	1.081	1.081	1.081	0.811	0.811	0.811	0.811	0.541	0.270	0.270	0.270	0.000						
0.01	16.80	1.679	1.679	1.679	1.493	1.493	1.493	1.119	1.119	1.119	1.119	0.933	0.560	0.560	0.373	0.000						
0.02	12.72	5.467	5.239	5.011	4.556	4.328	4.328	3.872	3.872	3.645	2.733	2.278	1.367	1.139	0.456	0.000						
0.03	9.85	6.905	6.394	6.394	5.371	5.115	5.115	4.604	4.604	4.348	3.325	2.813	1.790	1.023	0.256	0.000						
0.05	7.19	4.407	4.114	3.918	3.428	3.232	3.232	2.840	2.840	2.547	2.057	1.567	1.175	0.784	0.196	0.000						
0.1	5.33	3.430	3.193	3.075	2.661	2.543	2.543	2.129	2.070	1.774	1.419	1.064	0.532	0.414	0.118	0.000						
0.2	3.46	2.097	1.943	1.693	1.462	1.346	1.269	1.096	0.962	0.827	0.596	0.365	0.154	0.058	0.019	0.000						
0.3	2.81	1.629	1.492	1.301	1.132	1.058	0.963	0.751	0.571	0.487	0.328	0.180	0.063	0.032	0.011	0.000						
0.5	2.18	1.260	1.106	0.956	0.802	0.730	0.652	0.486	0.332	0.260	0.166	0.094	0.028	0.011	0.000	0.000						
1	1.49	1.202	0.999	0.796	0.648	0.546	0.409	0.239	0.162	0.114	0.070	0.027	0.010	0.002	0.000	0.000						

NTUA Campus KaSAT Ka-band 2-year average, Data Availability: 96.15 %			
Start Date		1st July 2018	
End Date		30th June 2020	
Attenuation threshold [dB]	**Total number of inter-fades**	**Total duration of inter-fades [sec]**	
1	112328	59564600	
3	8415	58611174	
5	1641	57065848	
10	365	46856277	
15	258	46864921	
20	0	0	
25	0	0	

Probability of exceedance [%]	**Corresponding Attenuation A [dB]**	**Total number of inter-fades**	**Total duration of inter-fades [sec]**
0.001	19.52	40	1020
0.002	19.07	320	1931
0.003	18.73	474	26873134
0.005	18.14	370	27468745
0.01	16.80	536	40542851
0.02	12.72	439	46861823
0.03	9.85	391	46855982
0.05	7.19	1021	57102838
0.1	5.33	1691	57071151
0.2	3.46	5199	58648660
0.3	2.81	9453	58746968
0.5	2.18	18089	59080488
1	1.49	41355	60063482

Appendix - 4
Site Diversity Statistics

NTUA Ka-band 4-year average, Concurrent Availability: 92.92 %						
Start Date			1st July 2016			
End Date			30th June 2020			
Location			**Data Availability [%]**		**P (A>0.1 dB) [%]**	
Campus			95.70		32.308	
LTCP			96.39		29.683	
Joint Balanced			92.92		14.762	
Joint Independent			-		14.161	
Attenuation Correlation Coefficient			0.0723			
Exceedance Probability [%]	**Attenuation Campus [dB]**	**Attenuation LTCP [dB]**	**Joint Balanced [dB]**	**Joint Independent [dB]**	**Site Diversity Gain [dB] Master: Campus**	**Site Diversity Gain [dB] Master: LTCP**
50	0.009	0.011	-0.072	-0.073	0.081	0.084
30	0.112	0.099	-0.008	-0.009	0.120	0.107
20	0.162	0.142	0.059	0.056	0.103	0.082
10	0.267	0.184	0.137	0.131	0.130	0.047
5	0.419	0.261	0.175	0.169	0.244	0.086
3	0.605	0.359	0.190	0.184	0.415	0.169
2	0.842	0.434	0.198	0.191	0.644	0.236
1	1.447	0.740	0.341	0.198	1.107	0.400
0.5	2.244	1.258	0.558	0.283	1.686	0.700
0.3	2.856	1.755	0.838	0.344	2.019	0.917
0.2	3.407	2.263	1.101	0.374	2.306	1.162
0.1	4.620	3.417	1.563	0.432	3.057	1.854
0.05	7.351	5.472	2.046	0.568	5.305	3.426
0.03	10.345	8.262	2.377	0.683	7.967	5.885
0.02	13.120	10.585	2.643	0.787	10.477	7.943
0.01	20.145	15.193	3.117	1.037	17.028	12.076
0.005	28.360	20.755	3.761	1.350	24.598	16.993
0.003	34.421	23.733	4.309	1.603	30.112	19.424
0.002	36.503	27.528	4.937	1.837	31.566	22.591
0.001	38.270	32.592	6.680	2.256	31.590	25.912

NTUA Ka-band 4-year average, Rain Concurrent Availability: 85.76 %							
Start Date					1st July 2016		
End Date					30th June 2020		
Location					**Data Availability [%]**	**P (A>0.1 dB) [%]**	
Campus					95.70	31.931	
LTCP					96.39	29.701	
Joint Balanced					85.76	14.620	
Joint Independent					-	14.053	
P (Rain Rate > 0.25 mm/h) [%]					0.34		
Attenuation Correlation Coefficient					0.1316		
Rain Rate Correlation Coefficient					0.0886		
Exceedance Probability [%]	**Attenuation Campus [dB]**	**Attenuation LTCP [dB]**	**Rain Rate [mm/h]**	**Joint Balanced [dB]**	**Joint Independent [dB]**	**Site Diversity Gain [dB] Master: Campus**	**Site Diversity Gain [dB] Master: LTCP**
50	0.007	0.011	0.000	-0.073	-0.074	0.080	0.084
30	0.110	0.099	0.000	-0.009	-0.009	0.118	0.107
20	0.160	0.142	0.000	0.058	0.055	0.102	0.084
10	0.257	0.184	0.000	0.136	0.131	0.121	0.048
5	0.398	0.261	0.000	0.174	0.168	0.224	0.087
3	0.583	0.356	0.000	0.190	0.183	0.394	0.167
2	0.788	0.415	0.000	0.197	0.191	0.591	0.218
1	1.359	0.703	0.000	0.331	0.198	1.028	0.372
0.5	2.154	1.198	0.000	0.530	0.278	1.624	0.668
0.3	2.752	1.698	0.646	0.791	0.340	1.960	0.907
0.2	3.280	2.196	1.382	1.046	0.370	2.234	1.150
0.1	4.348	3.351	2.771	1.506	0.405	2.842	1.845
0.05	6.743	5.378	4.236	1.986	0.552	4.757	3.392
0.03	9.506	8.181	5.236	2.341	0.637	7.165	5.840
0.02	12.120	10.572	6.216	2.600	0.756	9.519	7.971
0.01	19.015	15.293	7.985	3.087	0.980	15.928	12.206
0.005	26.940	20.967	10.672	3.763	1.282	23.177	17.204
0.003	32.203	23.937	13.194	4.351	1.540	27.852	19.586
0.002	35.370	27.788	15.395	5.035	1.760	30.336	22.754
0.001	38.112	33.071	22.296	6.914	2.175	31.198	26.157

NTUA Q-band 2-year average, Concurrent Availability: 91.20 %						
Start Date			1st July 2017			
End Date			30th June 2019			
Location			**Data Availability [%]**		**P (A>0.1 dB) [%]**	
Campus			95.33		33.727	
LTCP			93.38		32.676	
Joint Balanced			91.20		17.446	
Joint Independent			-		16.039	
Attenuation Correlation Coefficient			0.2456			
Exceedance Probability [%]	**Attenuation Campus [dB]**	**Attenuation LTCP [dB]**	**Joint Balanced [dB]**	**Joint Independent [dB]**	**Site Diversity Gain [dB] Master: Campus**	**Site Diversity Gain [dB] Master: LTCP**
50	0.025	0.024	-0.059	-0.061	0.084	0.083
30	0.117	0.112	0.010	0.004	0.107	0.102
20	0.162	0.155	0.082	0.073	0.080	0.073
10	0.257	0.198	0.152	0.141	0.104	0.045
5	0.518	0.384	0.187	0.174	0.330	0.196
3	1.099	0.712	0.225	0.187	0.874	0.487
2	1.998	1.264	0.371	0.194	1.627	0.893
1	4.023	2.868	1.002	0.224	3.022	1.866
0.5	6.498	4.924	2.149	0.345	4.349	2.775
0.3	8.800	6.740	3.100	0.393	5.700	3.640
0.2	11.017	8.117	3.945	0.513	7.072	4.172
0.1	16.837	12.072	5.611	0.797	11.226	6.461
0.05	26.250	19.837	7.242	1.353	19.008	12.595
0.03	30.912	27.627	8.372	1.908	22.540	19.255
0.02	32.036	30.965	9.406	2.430	22.630	21.560
0.01	32.379	32.161	11.304	3.412	21.075	20.857
0.005	32.573	32.952	14.137	4.467	18.436	18.816
0.003	32.695	33.248	21.767	5.312	10.929	11.481
0.002	32.767	33.425	28.408	6.077	4.359	5.017
0.001	32.897	33.681	31.667	7.394	1.230	2.015

NTUA Q-band 2-year average, Rain Concurrent Availability: 83.07 %							
Start Date					1st July 2017		
End Date					30th June 2019		
Location					**Data Availability [%]**	**P (A>0.1 dB) [%]**	
Campus					95.33	33.367	
LTCP					93.38	32.493	
Joint Balanced					83.07	17.316	
Joint Independent					-	15.965	
P (Rain Rate > 0.25 mm/h) [%]					0.348		
Attenuation Correlation Coefficient					0.2418		
Rain Rate Correlation Coefficient					0.1012		
Exceedance Probability [%]	**Attenuation Campus [dB]**	**Attenuation LTCP [dB]**	**Rain Rate [mm/h]**	**Joint Balanced [dB]**	**Joint Independent [dB]**	**Site Diversity Gain [dB] Master: Campus**	**Site Diversity Gain [dB] Master: LTCP**
50	0.024	0.023	0.000	-0.059	-0.061	0.084	0.083
30	0.115	0.111	0.000	0.010	0.004	0.106	0.101
20	0.160	0.154	0.000	0.081	0.073	0.079	0.073
10	0.234	0.196	0.000	0.151	0.140	0.082	0.045
5	0.455	0.372	0.000	0.186	0.173	0.269	0.186
3	0.953	0.639	0.000	0.200	0.187	0.753	0.439
2	1.772	1.145	0.000	0.351	0.193	1.420	0.794
1	3.681	2.639	0.000	0.909	0.200	2.773	1.730
0.5	5.926	4.645	0.000	1.953	0.331	3.973	2.692
0.3	8.113	6.423	0.674	2.837	0.383	5.276	3.586
0.2	10.168	7.854	1.423	3.571	0.460	6.598	4.284
0.1	15.681	12.042	2.792	5.057	0.723	10.624	6.984
0.05	24.668	20.177	4.504	6.687	1.200	17.981	13.490
0.03	30.655	28.387	5.417	7.868	1.712	22.787	20.519
0.02	32.034	31.202	6.428	9.059	2.196	22.975	22.143
0.01	32.394	32.244	8.123	11.216	3.153	21.178	21.028
0.005	32.586	33.018	12.225	14.732	4.154	17.854	18.286
0.003	32.711	33.294	14.652	23.831	4.947	8.880	9.463
0.002	32.778	33.467	17.767	29.506	5.647	3.272	3.961
0.001	32.912	33.710	26.351	31.727	6.985	1.185	1.983

Appendix - 5
Time Diversity Statistics

NTUA Campus Ka-band 4-year average, Data Availability: 95.70 %														
Start Date	1st July 2016													
End Date	30th June 2020													
Exceedance Probability [%]	Attenuation [dB] at time delay													
	0 s	1 s	5 s	10 s	1 m	3 m	5 m	10 m	30 m	1 h	3 h	6 h	12 h	18 h
100	nan	nan	nan	nan	nan	nan	nan	nan	nan	nan	nan	nan	nan	nan
99	-0.530	-0.558	-0.563	-0.566	-0.575	-0.578	-0.579	-0.581	-0.585	-0.587	-0.587	-0.588	-0.588	-0.588
95	-0.314	-0.349	-0.357	-0.360	-0.370	-0.374	-0.374	-0.376	-0.380	-0.381	-0.382	-0.382	-0.383	-0.383
90	-0.194	-0.236	-0.251	-0.256	-0.275	-0.282	-0.283	-0.286	-0.292	-0.295	-0.296	-0.297	-0.298	-0.298
80	-0.143	-0.163	-0.168	-0.169	-0.176	-0.179	-0.179	-0.181	-0.183	-0.184	-0.184	-0.185	-0.185	-0.185
70	-0.092	-0.119	-0.125	-0.127	-0.136	-0.140	-0.141	-0.143	-0.147	-0.148	-0.148	-0.148	-0.149	-0.149
60	-0.041	-0.076	-0.083	-0.086	-0.097	-0.102	-0.103	-0.106	-0.111	-0.112	-0.112	-0.113	-0.113	-0.113
50	0.009	-0.033	-0.042	-0.045	-0.058	-0.064	-0.065	-0.069	-0.075	-0.077	-0.077	-0.077	-0.078	-0.078
30	0.112	0.077	0.065	0.061	0.037	0.022	0.019	0.010	-0.004	-0.007	-0.006	-0.007	-0.008	-0.008
20	0.163	0.138	0.130	0.127	0.109	0.099	0.096	0.089	0.075	0.068	0.068	0.066	0.063	0.063
10	0.271	0.199	0.195	0.192	0.181	0.174	0.172	0.167	0.158	0.152	0.150	0.148	0.145	0.144
5	0.429	0.385	0.374	0.367	0.324	0.292	0.281	0.252	0.198	0.194	0.190	0.188	0.186	0.184
3	0.623	0.581	0.568	0.559	0.498	0.446	0.422	0.388	0.342	0.307	0.266	0.242	0.219	0.200
2	0.862	0.811	0.794	0.785	0.726	0.667	0.632	0.575	0.463	0.390	0.351	0.329	0.310	0.294
1	1.481	1.437	1.420	1.408	1.343	1.254	1.189	1.086	0.860	0.710	0.531	0.459	0.402	0.387
0.5	2.291	2.249	2.228	2.212	2.126	2.010	1.937	1.795	1.493	1.244	0.823	0.671	0.585	0.546
0.3	2.898	2.854	2.830	2.810	2.700	2.552	2.456	2.287	1.973	1.747	1.175	0.896	0.765	0.682
0.2	3.428	3.382	3.356	3.335	3.184	2.991	2.873	2.674	2.303	2.075	1.511	1.129	0.944	0.816
0.1	4.579	4.524	4.475	4.426	4.160	3.842	3.643	3.334	2.853	2.569	2.054	1.600	1.320	1.163
0.05	7.239	7.158	7.065	6.974	6.330	5.435	4.935	4.228	3.401	3.035	2.485	2.116	1.782	1.587
0.03	10.198	10.102	9.976	9.859	8.957	7.658	6.754	5.526	3.941	3.371	2.772	2.499	2.129	1.927
0.02	12.956	12.843	12.689	12.517	11.361	9.810	8.560	6.890	4.672	3.710	3.004	2.762	2.359	2.129
0.01	19.878	19.731	19.477	19.190	17.635	14.299	12.632	9.833	6.815	4.425	3.326	3.220	2.707	2.400
0.005	28.050	27.847	27.602	27.334	25.664	22.178	19.294	13.474	9.249	5.733	3.601	3.728	3.000	2.686
0.003	34.038	33.787	33.577	33.334	30.967	26.432	24.319	17.311	11.332	6.683	3.943	4.249	3.289	2.947
0.002	36.427	36.272	36.231	36.186	35.510	30.863	26.583	21.896	12.852	7.374	4.541	4.914	3.620	3.175
0.001	38.253	38.112	38.099	38.089	38.011	37.634	32.767	25.391	15.257	8.550	5.762	6.313	4.230	3.770

NTUA Campus Ka-band 4-year average, Concurrent Availability: 95.70 %													
Start Date	1st July 2016												
End Date	30th June 2020												
Exceedance Probability [%]	Time Diversity Gain [dB] at time delay												
	1 s	5 s	10 s	1 m	3 m	5 m	10 m	30 m	1 h	3 h	6 h	12 h	18 h
100	nan	nan	nan	nan	nan	nan	nan	nan	nan	nan	nan	nan	nan
99	0.028	0.033	0.036	0.045	0.048	0.049	0.051	0.055	0.057	0.058	0.058	0.058	0.058
95	0.035	0.043	0.046	0.056	0.060	0.060	0.062	0.065	0.067	0.068	0.068	0.069	0.069
90	0.042	0.056	0.061	0.081	0.087	0.088	0.092	0.097	0.100	0.101	0.102	0.103	0.104
80	0.020	0.025	0.027	0.033	0.036	0.037	0.038	0.040	0.041	0.042	0.042	0.042	0.042
70	0.028	0.034	0.036	0.045	0.049	0.049	0.051	0.055	0.057	0.057	0.057	0.058	0.058
60	0.035	0.042	0.045	0.056	0.061	0.062	0.065	0.070	0.072	0.071	0.072	0.073	0.072
50	0.043	0.051	0.054	0.067	0.074	0.075	0.078	0.084	0.087	0.086	0.087	0.088	0.088
30	0.036	0.047	0.051	0.075	0.090	0.093	0.102	0.116	0.119	0.118	0.119	0.120	0.120
20	0.024	0.032	0.036	0.053	0.064	0.066	0.073	0.088	0.095	0.095	0.096	0.099	0.099
10	0.072	0.076	0.079	0.090	0.097	0.099	0.104	0.113	0.118	0.121	0.123	0.126	0.127
5	0.045	0.056	0.062	0.106	0.137	0.148	0.177	0.231	0.235	0.239	0.242	0.244	0.245
3	0.042	0.055	0.063	0.125	0.177	0.200	0.234	0.281	0.315	0.357	0.381	0.404	0.423
2	0.052	0.069	0.077	0.136	0.195	0.231	0.287	0.400	0.472	0.512	0.533	0.552	0.568
1	0.044	0.061	0.073	0.139	0.227	0.292	0.395	0.621	0.771	0.950	1.022	1.079	1.094
0.5	0.043	0.063	0.079	0.165	0.281	0.355	0.496	0.799	1.048	1.469	1.620	1.707	1.746
0.3	0.044	0.069	0.088	0.198	0.346	0.442	0.611	0.925	1.151	1.723	2.002	2.133	2.217
0.2	0.046	0.072	0.093	0.245	0.437	0.555	0.754	1.126	1.353	1.917	2.299	2.484	2.612
0.1	0.055	0.104	0.153	0.419	0.737	0.936	1.245	1.726	2.010	2.525	2.979	3.259	3.416
0.05	0.081	0.174	0.266	0.909	1.804	2.304	3.012	3.838	4.204	4.754	5.123	5.457	5.652
0.03	0.096	0.222	0.339	1.241	2.540	3.444	4.672	6.257	6.827	7.426	7.699	8.069	8.271
0.02	0.113	0.267	0.439	1.596	3.146	4.397	6.066	8.285	9.246	9.952	10.194	10.597	10.828
0.01	0.147	0.401	0.688	2.243	5.579	7.247	10.045	13.064	15.453	16.552	16.658	17.171	17.479
0.005	0.203	0.449	0.716	2.386	5.872	8.756	14.576	18.801	22.317	24.449	24.322	25.050	25.364
0.003	0.251	0.461	0.704	3.071	7.606	9.719	16.727	22.706	27.355	30.095	29.788	30.749	31.091
0.002	0.155	0.196	0.241	0.917	5.563	9.844	14.530	23.575	29.053	31.885	31.513	32.807	33.251
0.001	0.141	0.154	0.164	0.243	0.619	5.486	12.863	22.996	29.703	32.491	31.940	34.023	34.483

NTUA LTCP Ka-band 4-year average, Data Availability: 96.39 %														
Start Date								1st July 2016						
End Date								30th June 2020						
Exceedance Probability [%]	Attenuation [dB] at time delay													
	0 s	1 s	5 s	10 s	1 m	3 m	5 m	10 m	30 m	1 h	3 h	6 h	12 h	18 h
100	nan	nan	nan	nan	nan	nan	nan	nan	nan	nan	nan	nan	nan	nan
99	-0.342	-0.373	-0.375	-0.376	-0.379	-0.380	-0.380	-0.381	-0.382	-0.382	-0.383	-0.384	-0.384	-0.384
95	-0.190	-0.197	-0.198	-0.198	-0.199	-0.199	-0.199	-0.199	-0.200	-0.200	-0.205	-0.206	-0.208	-0.207
90	-0.167	-0.179	-0.180	-0.181	-0.182	-0.183	-0.183	-0.183	-0.184	-0.185	-0.185	-0.185	-0.185	-0.185
80	-0.121	-0.143	-0.146	-0.146	-0.148	-0.150	-0.150	-0.151	-0.153	-0.154	-0.155	-0.155	-0.155	-0.155
70	-0.077	-0.108	-0.111	-0.112	-0.114	-0.117	-0.118	-0.119	-0.122	-0.124	-0.125	-0.124	-0.125	-0.125
60	-0.032	-0.072	-0.077	-0.078	-0.081	-0.085	-0.085	-0.087	-0.091	-0.093	-0.095	-0.094	-0.095	-0.095
50	0.012	-0.037	-0.043	-0.044	-0.048	-0.052	-0.053	-0.056	-0.060	-0.064	-0.066	-0.065	-0.066	-0.065
30	0.099	0.054	0.044	0.042	0.033	0.024	0.021	0.015	0.001	-0.004	-0.007	-0.006	-0.007	-0.006
20	0.142	0.111	0.105	0.103	0.097	0.090	0.088	0.084	0.074	0.065	0.058	0.061	0.058	0.060
10	0.185	0.168	0.164	0.163	0.159	0.155	0.154	0.151	0.145	0.140	0.134	0.135	0.133	0.133
5	0.266	0.196	0.194	0.193	0.190	0.187	0.186	0.184	0.180	0.177	0.172	0.171	0.170	0.170
3	0.362	0.301	0.286	0.279	0.242	0.201	0.199	0.198	0.194	0.192	0.187	0.186	0.185	0.185
2	0.440	0.381	0.373	0.369	0.347	0.321	0.308	0.285	0.228	0.199	0.194	0.193	0.192	0.192
1	0.739	0.691	0.675	0.665	0.599	0.552	0.519	0.458	0.378	0.343	0.256	0.209	0.199	0.199
0.5	1.242	1.196	1.181	1.170	1.092	0.983	0.926	0.815	0.628	0.513	0.367	0.334	0.315	0.300
0.3	1.736	1.696	1.675	1.656	1.546	1.398	1.309	1.156	0.899	0.721	0.465	0.382	0.368	0.354
0.2	2.236	2.193	2.171	2.150	1.993	1.780	1.650	1.457	1.137	0.925	0.589	0.448	0.395	0.381
0.1	3.368	3.320	3.283	3.241	2.982	2.641	2.401	2.085	1.563	1.316	0.882	0.663	0.569	0.473
0.05	5.341	5.275	5.206	5.133	4.632	3.945	3.492	2.915	2.102	1.699	1.194	0.962	0.838	0.599
0.03	8.073	7.986	7.888	7.776	6.954	5.772	4.872	3.788	2.545	2.053	1.441	1.201	1.149	0.757
0.02	10.379	10.283	10.140	9.983	9.013	7.611	6.518	4.749	2.931	2.365	1.619	1.416	1.417	0.889
0.01	14.937	14.819	14.645	14.449	12.887	10.932	9.395	7.090	3.620	2.935	2.000	1.747	1.819	1.170
0.005	20.546	20.390	20.161	19.949	17.936	14.668	12.796	9.484	4.517	3.550	2.470	2.110	2.256	1.576
0.003	23.376	23.175	22.888	22.652	21.158	17.509	15.085	11.741	5.654	4.086	3.049	2.391	2.622	1.993
0.002	27.251	27.028	26.758	26.448	23.385	19.543	16.948	13.723	7.216	4.650	3.639	2.629	2.955	2.238
0.001	32.171	31.860	31.517	31.164	28.207	23.167	20.027	17.050	8.604	6.686	4.606	3.067	3.322	2.684

NTUA LTCP Ka-band 4-year average, Data Availability: 96.39 %													
Start Date	1st July 2016												
End Date	30th June 2020												
Exceedance Probability [%]	Time Diversity Gain [dB] at time delay												
	1 s	5 s	10 s	1 m	3 m	5 m	10 m	30 m	1 h	3 h	6 h	12 h	18 h
100	nan	nan	nan	nan	nan	nan	nan	nan	nan	nan	nan	nan	nan
99	0.030	0.033	0.034	0.036	0.038	0.038	0.038	0.039	0.040	0.041	0.041	0.042	0.041
95	0.008	0.008	0.008	0.009	0.010	0.010	0.010	0.010	0.010	0.016	0.017	0.019	0.017
90	0.012	0.014	0.014	0.015	0.016	0.016	0.017	0.017	0.018	0.019	0.018	0.019	0.019
80	0.022	0.024	0.025	0.027	0.028	0.029	0.029	0.031	0.033	0.034	0.033	0.034	0.033
70	0.031	0.034	0.035	0.038	0.040	0.041	0.042	0.045	0.047	0.048	0.048	0.048	0.048
60	0.040	0.045	0.045	0.049	0.052	0.053	0.055	0.058	0.061	0.063	0.062	0.063	0.062
50	0.049	0.055	0.056	0.060	0.064	0.065	0.067	0.072	0.075	0.077	0.076	0.077	0.077
30	0.045	0.055	0.057	0.066	0.075	0.078	0.084	0.098	0.103	0.106	0.105	0.106	0.105
20	0.031	0.037	0.039	0.045	0.052	0.054	0.058	0.068	0.077	0.084	0.081	0.084	0.083
10	0.017	0.020	0.021	0.025	0.030	0.031	0.034	0.040	0.045	0.050	0.050	0.052	0.051
5	0.070	0.072	0.073	0.076	0.079	0.080	0.082	0.086	0.089	0.094	0.095	0.096	0.096
3	0.060	0.076	0.083	0.120	0.161	0.162	0.164	0.167	0.170	0.175	0.176	0.177	0.177
2	0.059	0.067	0.071	0.093	0.119	0.131	0.155	0.212	0.241	0.245	0.247	0.248	0.248
1	0.048	0.064	0.074	0.140	0.188	0.220	0.281	0.362	0.396	0.483	0.530	0.540	0.540
0.5	0.046	0.060	0.072	0.150	0.258	0.316	0.427	0.614	0.729	0.874	0.908	0.927	0.942
0.3	0.040	0.061	0.080	0.190	0.338	0.427	0.580	0.837	1.016	1.271	1.354	1.368	1.382
0.2	0.043	0.065	0.087	0.244	0.456	0.587	0.779	1.100	1.312	1.648	1.788	1.842	1.856
0.1	0.048	0.085	0.127	0.386	0.727	0.967	1.283	1.805	2.052	2.486	2.704	2.799	2.895
0.05	0.066	0.135	0.207	0.709	1.395	1.849	2.426	3.239	3.642	4.147	4.378	4.502	4.742
0.03	0.087	0.185	0.297	1.118	2.301	3.201	4.284	5.528	6.019	6.632	6.871	6.924	7.315
0.02	0.095	0.239	0.396	1.366	2.768	3.860	5.630	7.448	8.013	8.760	8.963	8.962	9.490
0.01	0.117	0.291	0.488	2.050	4.004	5.542	7.846	11.317	12.002	12.937	13.190	13.117	13.767
0.005	0.156	0.385	0.597	2.610	5.878	7.750	11.062	16.029	16.996	18.076	18.436	18.290	18.970
0.003	0.202	0.488	0.724	2.219	5.867	8.292	11.636	17.723	19.290	20.328	20.985	20.754	21.383
0.002	0.224	0.493	0.803	3.866	7.708	10.303	13.528	20.035	22.601	23.612	24.623	24.296	25.013
0.001	0.311	0.654	1.007	3.964	9.004	12.144	15.122	23.568	25.485	27.566	29.105	28.850	29.488

NTUA Campus Q-band 2-year average, Data Availability: 95.33 %														
Start Date								1st July 2017						
End Date								30th June 2019						
Exceedance Probability [%]	Attenuation [dB] at time delay													
	0 s	1 s	5 s	10 s	1 m	3 m	5 m	10 m	30 m	1 h	3 h	6 h	12 h	18 h
100	nan	nan	nan	nan	nan	nan	nan	nan	nan	nan	nan	nan	nan	nan
99	-0.372	-0.388	-0.390	-0.391	-0.394	-0.396	-0.397	-0.399	-0.408	-0.414	-0.415	-0.418	-0.417	-0.419
95	-0.194	-0.218	-0.227	-0.229	-0.241	-0.252	-0.255	-0.260	-0.270	-0.273	-0.274	-0.275	-0.276	-0.276
90	-0.169	-0.182	-0.183	-0.184	-0.185	-0.187	-0.188	-0.189	-0.191	-0.191	-0.191	-0.191	-0.192	-0.192
80	-0.120	-0.142	-0.145	-0.145	-0.148	-0.152	-0.152	-0.154	-0.157	-0.158	-0.158	-0.158	-0.159	-0.159
70	-0.071	-0.103	-0.107	-0.107	-0.112	-0.116	-0.117	-0.120	-0.124	-0.125	-0.125	-0.126	-0.126	-0.126
60	-0.023	-0.065	-0.069	-0.070	-0.075	-0.081	-0.083	-0.085	-0.091	-0.092	-0.092	-0.093	-0.094	-0.093
50	0.025	-0.026	-0.032	-0.033	-0.039	-0.046	-0.048	-0.052	-0.059	-0.060	-0.060	-0.061	-0.061	-0.061
30	0.117	0.078	0.071	0.070	0.059	0.045	0.041	0.033	0.014	0.009	0.011	0.007	0.005	0.006
20	0.162	0.137	0.132	0.131	0.124	0.114	0.111	0.104	0.089	0.085	0.083	0.079	0.077	0.077
10	0.258	0.195	0.193	0.192	0.187	0.181	0.179	0.174	0.164	0.159	0.154	0.150	0.147	0.147
5	0.516	0.452	0.435	0.427	0.390	0.366	0.350	0.314	0.202	0.195	0.190	0.185	0.182	0.182
3	1.080	1.023	1.007	0.997	0.939	0.849	0.786	0.690	0.447	0.350	0.261	0.199	0.196	0.196
2	1.954	1.902	1.885	1.872	1.772	1.629	1.532	1.343	0.903	0.611	0.381	0.311	0.268	0.250
1	3.962	3.909	3.883	3.858	3.680	3.425	3.238	2.919	2.248	1.738	0.980	0.571	0.455	0.390
0.5	6.406	6.344	6.301	6.256	5.945	5.494	5.187	4.708	3.751	3.144	2.077	1.322	0.918	0.736
0.3	8.675	8.602	8.541	8.479	8.065	7.451	7.060	6.362	5.041	4.306	2.999	2.168	1.577	1.222
0.2	10.841	10.753	10.666	10.578	10.000	9.189	8.655	7.831	6.384	5.373	3.790	2.968	2.226	1.715
0.1	16.395	16.249	16.100	15.944	14.831	13.548	12.580	10.899	8.731	7.523	5.227	4.416	3.434	2.804
0.05	25.693	25.489	25.286	25.030	23.336	20.389	18.886	16.070	12.269	9.998	6.785	6.243	4.973	3.696
0.03	30.671	30.462	30.400	30.296	29.128	27.363	25.127	20.745	15.662	12.195	7.707	8.078	6.358	4.227
0.02	32.003	31.867	31.861	31.852	31.726	30.881	29.141	25.776	18.823	14.034	8.229	10.107	7.405	4.598
0.01	32.364	32.215	32.212	32.211	32.184	32.118	32.046	31.719	26.157	16.778	9.100	13.569	9.662	5.591
0.005	32.564	32.397	32.395	32.392	32.382	32.348	32.310	32.225	31.684	21.268	10.118	17.783	11.659	6.429
0.003	32.685	32.514	32.515	32.512	32.499	32.463	32.421	32.365	32.033	24.896	10.955	22.829	12.761	6.961
0.002	32.760	32.572	32.575	32.573	32.562	32.537	32.507	32.455	32.180	27.045	12.450	25.760	13.606	7.251
0.001	32.889	32.693	32.699	32.694	32.677	32.630	32.591	32.564	32.350	28.281	15.284	29.292	14.648	8.112

NTUA Campus Q-band 2-year average, Data Availability: 95.33 %													
Start Date	1st July 2017												
End Date	30th June 2019												
Exceedance Probability [%]	Time Diversity Gain [dB] at time delay												
	1 s	5 s	10 s	1 m	3 m	5 m	10 m	30 m	1 h	3 h	6 h	12 h	18 h
100	nan	nan	nan	nan	nan	nan	nan	nan	nan	nan	nan	nan	nan
99	0.017	0.019	0.019	0.022	0.025	0.026	0.027	0.036	0.042	0.044	0.046	0.045	0.048
95	0.024	0.032	0.034	0.047	0.058	0.061	0.066	0.076	0.079	0.080	0.081	0.081	0.082
90	0.013	0.014	0.014	0.016	0.018	0.019	0.020	0.021	0.022	0.022	0.022	0.022	0.022
80	0.023	0.025	0.025	0.029	0.032	0.033	0.034	0.037	0.038	0.038	0.039	0.039	0.039
70	0.032	0.036	0.036	0.041	0.045	0.046	0.049	0.053	0.054	0.054	0.055	0.055	0.055
60	0.042	0.046	0.047	0.053	0.059	0.060	0.063	0.069	0.070	0.070	0.070	0.071	0.071
50	0.051	0.056	0.057	0.064	0.071	0.073	0.076	0.083	0.085	0.084	0.085	0.086	0.086
30	0.039	0.046	0.047	0.058	0.072	0.076	0.084	0.103	0.108	0.106	0.110	0.112	0.111
20	0.025	0.030	0.031	0.039	0.049	0.052	0.058	0.073	0.078	0.079	0.083	0.086	0.085
10	0.063	0.066	0.067	0.071	0.077	0.079	0.084	0.095	0.100	0.104	0.108	0.111	0.111
5	0.064	0.081	0.090	0.126	0.151	0.167	0.202	0.315	0.321	0.327	0.331	0.334	0.335
3	0.057	0.073	0.083	0.141	0.232	0.294	0.391	0.633	0.730	0.819	0.882	0.884	0.885
2	0.052	0.069	0.082	0.181	0.325	0.422	0.611	1.051	1.343	1.573	1.642	1.686	1.704
1	0.054	0.079	0.104	0.282	0.537	0.724	1.043	1.714	2.225	2.982	3.391	3.507	3.572
0.5	0.062	0.105	0.150	0.461	0.912	1.219	1.698	2.654	3.262	4.329	5.084	5.488	5.670
0.3	0.073	0.134	0.196	0.610	1.224	1.616	2.313	3.634	4.370	5.676	6.507	7.098	7.453
0.2	0.088	0.175	0.263	0.841	1.652	2.186	3.010	4.457	5.469	7.051	7.873	8.615	9.126
0.1	0.146	0.294	0.450	1.564	2.847	3.815	5.496	7.664	8.872	11.168	11.979	12.960	13.590
0.05	0.204	0.407	0.663	2.357	5.304	6.806	9.623	13.424	15.695	18.908	19.450	20.720	21.997
0.03	0.209	0.271	0.375	1.543	3.309	5.544	9.927	15.009	18.476	22.965	22.594	24.313	26.444
0.02	0.136	0.142	0.151	0.277	1.122	2.861	6.226	13.180	17.968	23.773	21.895	24.597	27.405
0.01	0.149	0.153	0.153	0.180	0.246	0.318	0.645	6.208	15.586	23.264	18.795	22.702	26.773
0.005	0.167	0.169	0.172	0.183	0.216	0.254	0.339	0.880	11.297	22.446	14.782	20.905	26.135
0.003	0.172	0.171	0.174	0.187	0.222	0.265	0.320	0.652	7.789	21.731	9.857	19.924	25.724
0.002	0.188	0.185	0.187	0.198	0.223	0.254	0.305	0.580	5.716	20.311	7.001	19.154	25.509
0.001	0.196	0.190	0.195	0.211	0.259	0.298	0.324	0.539	4.608	17.605	3.597	18.241	24.777

NTUA LTCP Q-band 2-year average, Data Availability: 93.38 %														
Start Date								1st July 2017						
End Date								30th June 2019						
Exceedance Probability [%]	Attenuation [dB] at time delay													
	0 s	1 s	5 s	10 s	1 m	3 m	5 m	10 m	30 m	1 h	3 h	6 h	12 h	18 h
100	nan	nan	nan	nan	nan	nan	nan	nan	nan	nan	nan	nan	nan	nan
99	-0.368	-0.385	-0.386	-0.387	-0.390	-0.395	-0.398	-0.399	-0.408	-0.411	-0.423	-0.429	-0.427	-0.429
95	-0.192	-0.199	-0.199	-0.199	-0.206	-0.224	-0.233	-0.238	-0.246	-0.249	-0.254	-0.258	-0.260	-0.258
90	-0.167	-0.179	-0.180	-0.181	-0.182	-0.184	-0.185	-0.186	-0.188	-0.188	-0.188	-0.189	-0.189	-0.189
80	-0.118	-0.141	-0.143	-0.143	-0.146	-0.149	-0.151	-0.152	-0.155	-0.156	-0.156	-0.156	-0.157	-0.156
70	-0.070	-0.103	-0.106	-0.107	-0.110	-0.114	-0.116	-0.118	-0.122	-0.124	-0.123	-0.124	-0.125	-0.124
60	-0.022	-0.065	-0.069	-0.070	-0.075	-0.080	-0.082	-0.085	-0.090	-0.093	-0.091	-0.092	-0.093	-0.092
50	0.024	-0.028	-0.033	-0.034	-0.039	-0.045	-0.048	-0.051	-0.058	-0.061	-0.059	-0.060	-0.062	-0.060
30	0.112	0.072	0.065	0.064	0.055	0.044	0.039	0.031	0.014	0.001	0.009	0.008	0.001	0.006
20	0.155	0.129	0.125	0.124	0.117	0.109	0.105	0.099	0.086	0.076	0.079	0.077	0.072	0.075
10	0.198	0.185	0.183	0.182	0.178	0.173	0.170	0.166	0.157	0.150	0.148	0.146	0.142	0.143
5	0.384	0.348	0.339	0.335	0.306	0.266	0.237	0.199	0.191	0.186	0.182	0.180	0.176	0.176
3	0.713	0.662	0.647	0.636	0.578	0.517	0.470	0.393	0.302	0.212	0.196	0.193	0.190	0.189
2	1.258	1.211	1.196	1.185	1.103	0.985	0.912	0.771	0.502	0.368	0.268	0.200	0.197	0.196
1	2.851	2.807	2.786	2.763	2.590	2.353	2.181	1.883	1.323	0.962	0.519	0.383	0.328	0.292
0.5	4.910	4.861	4.825	4.788	4.529	4.140	3.875	3.445	2.511	1.921	1.114	0.769	0.553	0.416
0.3	6.711	6.658	6.607	6.557	6.210	5.722	5.350	4.778	3.568	2.748	1.689	1.176	0.862	0.655
0.2	8.095	8.032	7.966	7.897	7.476	6.954	6.553	5.957	4.542	3.463	2.236	1.529	1.171	0.937
0.1	11.991	11.903	11.781	11.656	10.756	9.490	8.652	7.653	6.276	4.848	3.290	2.348	1.802	1.680
0.05	19.569	19.425	19.231	19.034	17.384	15.068	13.244	10.349	7.493	6.282	4.205	3.355	2.848	3.062
0.03	27.229	26.964	26.712	26.444	24.425	21.293	18.873	14.623	8.486	7.148	4.988	4.127	3.734	3.957
0.02	30.884	30.711	30.663	30.589	29.947	27.246	23.907	18.353	9.817	7.753	5.585	4.774	4.295	4.725
0.01	32.139	31.969	31.952	31.945	31.801	31.472	30.931	24.579	12.330	9.265	6.531	5.764	5.555	5.950
0.005	32.935	32.803	32.788	32.769	32.611	32.283	32.025	31.127	15.318	11.273	7.520	6.984	7.820	7.127
0.003	33.236	33.084	33.076	33.066	32.974	32.857	32.751	31.802	18.103	12.831	8.406	8.165	9.824	7.861
0.002	33.414	33.260	33.252	33.241	33.162	33.059	33.015	32.066	20.016	14.425	10.084	9.336	11.569	8.405
0.001	33.674	33.514	33.511	33.508	33.427	33.334	33.323	32.875	23.780	17.668	15.774	10.464	15.725	9.520

NTUA LTCP Q-band 2-year average, Data Availability: 93.38 %													
Start Date							1st July 2017						
End Date							30th June 2019						
Exceedance Probability [%]	**Time Diversity Gain [dB] at time delay**												
	1 s	**5 s**	**10 s**	**1 m**	**3 m**	**5 m**	**10 m**	**30 m**	**1 h**	**3 h**	**6 h**	**12 h**	**18 h**
100	nan	nan	nan	nan	nan	nan	nan	nan	nan	nan	nan	nan	nan
99	0.017	0.018	0.019	0.023	0.027	0.030	0.031	0.040	0.044	0.055	0.061	0.059	0.061
95	0.007	0.007	0.007	0.014	0.032	0.041	0.046	0.054	0.057	0.062	0.066	0.068	0.066
90	0.012	0.013	0.013	0.015	0.017	0.018	0.019	0.020	0.021	0.021	0.022	0.022	0.022
80	0.023	0.025	0.025	0.028	0.031	0.032	0.034	0.036	0.038	0.038	0.038	0.039	0.038
70	0.033	0.036	0.037	0.040	0.045	0.046	0.048	0.052	0.055	0.054	0.054	0.055	0.054
60	0.044	0.048	0.048	0.053	0.058	0.060	0.063	0.068	0.071	0.069	0.070	0.072	0.070
50	0.052	0.057	0.058	0.063	0.070	0.072	0.075	0.082	0.086	0.083	0.084	0.086	0.084
30	0.040	0.047	0.048	0.057	0.068	0.073	0.081	0.098	0.111	0.103	0.104	0.111	0.106
20	0.026	0.031	0.032	0.038	0.046	0.050	0.056	0.069	0.079	0.076	0.078	0.083	0.080
10	0.013	0.015	0.016	0.020	0.025	0.028	0.032	0.042	0.048	0.050	0.052	0.056	0.055
5	0.036	0.045	0.049	0.078	0.119	0.147	0.185	0.193	0.198	0.202	0.205	0.208	0.208
3	0.051	0.066	0.077	0.135	0.196	0.243	0.320	0.410	0.501	0.517	0.520	0.523	0.524
2	0.047	0.062	0.073	0.156	0.273	0.346	0.487	0.756	0.891	0.990	1.059	1.061	1.062
1	0.044	0.065	0.087	0.261	0.497	0.669	0.968	1.527	1.889	2.332	2.467	2.522	2.559
0.5	0.049	0.085	0.122	0.381	0.769	1.035	1.464	2.398	2.988	3.796	4.141	4.357	4.493
0.3	0.053	0.104	0.154	0.501	0.989	1.361	1.933	3.143	3.963	5.022	5.535	5.849	6.056
0.2	0.063	0.129	0.198	0.620	1.142	1.542	2.138	3.553	4.632	5.860	6.566	6.925	7.158
0.1	0.088	0.209	0.335	1.235	2.501	3.339	4.338	5.715	7.142	8.701	9.643	10.189	10.311
0.05	0.145	0.339	0.535	2.186	4.501	6.325	9.221	12.076	13.288	15.365	16.214	16.722	16.507
0.03	0.266	0.518	0.785	2.804	5.937	8.356	12.606	18.744	20.082	22.241	23.102	23.495	23.273
0.02	0.173	0.221	0.295	0.937	3.638	6.977	12.531	21.067	23.131	25.299	26.110	26.588	26.159
0.01	0.171	0.188	0.195	0.339	0.667	1.208	7.560	19.810	22.874	25.609	26.375	26.584	26.190
0.005	0.132	0.147	0.166	0.324	0.652	0.910	1.808	17.617	21.662	25.414	25.950	25.115	25.808
0.003	0.152	0.160	0.170	0.262	0.379	0.484	1.434	15.132	20.404	24.830	25.070	23.411	25.375
0.002	0.154	0.161	0.173	0.252	0.354	0.398	1.347	13.398	18.988	23.330	24.078	21.845	25.009
0.001	0.159	0.162	0.165	0.246	0.340	0.350	0.799	9.893	16.006	17.899	23.209	17.949	24.154

NTUA Campus BADR5 Ku-band 3-year average, Data Availability: 96.49 %														
Start Date								1st July 2017						
End Date								30th June 2020						
Exceedance Probability [%]	Attenuation [dB] at time delay													
	0 s	1 s	5 s	10 s	1 m	3 m	5 m	10 m	30 m	1 h	3 h	6 h	12 h	18 h
100	nan	nan	nan	nan	nan	nan	nan	nan	nan	nan	nan	nan	nan	nan
99	-0.300	-0.333	-0.338	-0.339	-0.340	-0.342	-0.344	-0.346	-0.352	-0.356	-0.360	-0.361	-0.362	-0.362
95	-0.186	-0.191	-0.192	-0.192	-0.192	-0.192	-0.193	-0.193	-0.194	-0.195	-0.196	-0.196	-0.196	-0.196
90	-0.165	-0.173	-0.175	-0.175	-0.175	-0.176	-0.176	-0.177	-0.179	-0.181	-0.181	-0.181	-0.181	-0.181
80	-0.122	-0.138	-0.141	-0.141	-0.142	-0.143	-0.144	-0.145	-0.149	-0.152	-0.153	-0.152	-0.152	-0.153
70	-0.079	-0.103	-0.107	-0.107	-0.109	-0.110	-0.111	-0.113	-0.119	-0.123	-0.124	-0.124	-0.123	-0.124
60	-0.037	-0.069	-0.074	-0.074	-0.076	-0.078	-0.079	-0.082	-0.090	-0.095	-0.096	-0.095	-0.095	-0.095
50	0.005	-0.034	-0.040	-0.041	-0.043	-0.045	-0.047	-0.050	-0.061	-0.067	-0.068	-0.067	-0.066	-0.067
30	0.089	0.053	0.044	0.043	0.039	0.035	0.032	0.023	-0.002	-0.011	-0.012	-0.011	-0.010	-0.011
20	0.131	0.107	0.100	0.099	0.097	0.094	0.091	0.086	0.066	0.048	0.045	0.048	0.050	0.047
10	0.172	0.159	0.156	0.155	0.154	0.152	0.150	0.147	0.137	0.127	0.124	0.125	0.126	0.125
5	0.192	0.185	0.183	0.183	0.182	0.180	0.180	0.178	0.172	0.166	0.164	0.164	0.164	0.163
3	0.205	0.196	0.194	0.194	0.193	0.192	0.191	0.190	0.185	0.182	0.179	0.179	0.179	0.178
2	0.293	0.224	0.200	0.199	0.198	0.198	0.197	0.196	0.192	0.190	0.187	0.187	0.186	0.186
1	0.379	0.352	0.338	0.334	0.321	0.306	0.293	0.266	0.199	0.197	0.195	0.194	0.194	0.193
0.5	0.548	0.497	0.467	0.456	0.414	0.393	0.387	0.372	0.325	0.267	0.199	0.198	0.197	0.197
0.3	0.780	0.737	0.714	0.704	0.647	0.583	0.555	0.495	0.387	0.352	0.220	0.199	0.199	0.199
0.2	1.067	1.007	0.987	0.978	0.920	0.832	0.777	0.681	0.516	0.394	0.303	0.236	0.200	0.199
0.1	1.782	1.738	1.706	1.677	1.541	1.390	1.322	1.185	0.939	0.727	0.385	0.359	0.297	0.246
0.05	3.367	3.303	3.237	3.179	2.825	2.466	2.240	1.860	1.446	1.256	0.587	0.490	0.386	0.337
0.03	5.023	4.958	4.892	4.831	4.370	3.707	3.366	2.773	2.035	1.530	0.954	0.599	0.620	0.373
0.02	6.186	6.095	6.007	5.924	5.370	5.020	4.738	3.777	2.682	1.874	1.222	0.736	1.218	0.391
0.01	8.345	8.209	8.052	7.889	7.062	6.508	6.234	5.307	4.148	2.716	1.480	0.933	1.707	0.506
0.005	12.231	12.087	11.916	11.738	10.553	8.675	7.154	6.368	5.285	3.721	1.675	1.186	2.131	0.630
0.003	15.428	15.261	15.038	14.839	13.586	10.765	9.245	6.650	6.177	4.486	1.767	1.393	2.620	0.743
0.002	18.511	18.341	18.160	18.025	16.143	12.654	10.936	7.092	6.369	5.184	1.841	1.568	2.733	0.799
0.001	25.378	25.061	24.916	24.637	21.806	17.730	14.439	8.440	6.626	5.843	1.982	1.889	3.029	0.931

NTUA Campus BADR5 Ku-band 3-year average, Data Availability: 96.49 %													
Start Date							1st July 2017						
End Date							30th June 2020						
Exceedance Probability [%]	**Time Diversity Gain [dB] at time delay**												
	1 s	**5 s**	**10 s**	**1 m**	**3 m**	**5 m**	**10 m**	**30 m**	**1 h**	**3 h**	**6 h**	**12 h**	**18 h**
100	nan	nan	nan	nan	nan	nan	nan	nan	nan	nan	nan	nan	nan
99	0.033	0.038	0.039	0.041	0.042	0.044	0.046	0.052	0.056	0.060	0.061	0.062	0.062
95	0.005	0.006	0.006	0.006	0.006	0.007	0.007	0.008	0.009	0.009	0.010	0.010	0.010
90	0.009	0.010	0.010	0.011	0.011	0.012	0.013	0.015	0.016	0.017	0.017	0.017	0.017
80	0.017	0.019	0.019	0.020	0.021	0.022	0.023	0.028	0.030	0.031	0.031	0.030	0.031
70	0.024	0.028	0.028	0.030	0.031	0.032	0.034	0.040	0.044	0.045	0.045	0.044	0.045
60	0.032	0.036	0.037	0.039	0.040	0.042	0.045	0.053	0.058	0.059	0.058	0.058	0.058
50	0.039	0.045	0.046	0.048	0.050	0.052	0.055	0.065	0.071	0.073	0.072	0.071	0.072
30	0.036	0.045	0.046	0.050	0.054	0.057	0.066	0.091	0.100	0.101	0.100	0.099	0.100
20	0.024	0.030	0.031	0.034	0.037	0.039	0.045	0.065	0.082	0.086	0.083	0.081	0.084
10	0.012	0.016	0.017	0.018	0.020	0.021	0.024	0.035	0.044	0.047	0.046	0.045	0.047
5	0.007	0.009	0.009	0.010	0.012	0.012	0.014	0.021	0.026	0.028	0.028	0.028	0.029
3	0.009	0.011	0.011	0.012	0.013	0.014	0.015	0.020	0.023	0.026	0.026	0.026	0.027
2	0.069	0.093	0.094	0.094	0.095	0.096	0.097	0.100	0.103	0.106	0.106	0.107	0.107
1	0.027	0.041	0.045	0.058	0.073	0.086	0.113	0.180	0.182	0.184	0.185	0.185	0.186
0.5	0.051	0.081	0.092	0.134	0.155	0.162	0.176	0.223	0.282	0.350	0.350	0.351	0.351
0.3	0.043	0.066	0.076	0.133	0.197	0.225	0.285	0.394	0.428	0.561	0.581	0.581	0.581
0.2	0.060	0.080	0.089	0.147	0.235	0.290	0.386	0.551	0.673	0.764	0.831	0.867	0.868
0.1	0.044	0.077	0.105	0.242	0.393	0.460	0.598	0.843	1.056	1.398	1.423	1.485	1.536
0.05	0.064	0.129	0.188	0.542	0.901	1.126	1.507	1.921	2.111	2.779	2.877	2.981	3.029
0.03	0.065	0.131	0.192	0.653	1.316	1.657	2.250	2.988	3.494	4.069	4.424	4.403	4.650
0.02	0.091	0.179	0.263	0.816	1.166	1.448	2.409	3.504	4.312	4.964	5.450	4.968	5.795
0.01	0.136	0.293	0.457	1.283	1.838	2.111	3.039	4.197	5.629	6.865	7.413	6.639	7.839
0.005	0.143	0.315	0.493	1.678	3.556	5.076	5.862	6.946	8.510	10.555	11.044	10.100	11.601
0.003	0.166	0.390	0.589	1.842	4.663	6.183	8.777	9.250	10.942	13.660	14.035	12.807	14.684
0.002	0.171	0.352	0.487	2.368	5.857	7.575	11.419	12.143	13.327	16.671	16.943	15.779	17.713
0.001	0.317	0.462	0.741	3.572	7.648	10.939	16.938	18.752	19.535	23.396	23.489	22.349	24.447

NTUA Campus KaSAT Ka-band 2-year average, Data Availability: 96.15 %														
Start Date									1st July 2018					
End Date									30th June 2020					
Exceedance Probability [%]	Attenuation [dB] at time delay													
	0 s	1 s	5 s	10 s	1 m	3 m	5 m	10 m	30 m	1 h	3 h	6 h	12 h	18 h
100	nan	nan	nan	nan	nan	nan	nan	nan	nan	nan	nan	nan	nan	nan
99	-0.783	-0.831	-0.840	-0.846	-0.877	-0.888	-0.890	-0.900	-0.921	-0.937	-0.956	-0.959	-0.958	-0.959
95	-0.413	-0.473	-0.480	-0.484	-0.506	-0.513	-0.515	-0.521	-0.533	-0.544	-0.561	-0.565	-0.560	-0.563
90	-0.303	-0.343	-0.347	-0.349	-0.362	-0.366	-0.367	-0.370	-0.377	-0.384	-0.395	-0.399	-0.394	-0.397
80	-0.172	-0.195	-0.198	-0.199	-0.219	-0.226	-0.227	-0.233	-0.244	-0.255	-0.277	-0.284	-0.276	-0.281
70	-0.115	-0.146	-0.149	-0.150	-0.159	-0.162	-0.162	-0.165	-0.170	-0.175	-0.186	-0.190	-0.185	-0.188
60	-0.058	-0.097	-0.100	-0.102	-0.112	-0.116	-0.116	-0.119	-0.125	-0.131	-0.144	-0.149	-0.142	-0.147
50	-0.003	-0.048	-0.052	-0.054	-0.066	-0.070	-0.070	-0.073	-0.080	-0.087	-0.102	-0.109	-0.100	-0.105
30	0.120	0.075	0.069	0.065	0.046	0.038	0.038	0.031	0.015	-0.001	-0.020	-0.029	-0.017	-0.024
20	0.180	0.149	0.144	0.141	0.125	0.119	0.118	0.112	0.100	0.086	0.049	0.028	0.056	0.041
10	0.345	0.288	0.276	0.268	0.216	0.198	0.197	0.193	0.183	0.173	0.148	0.134	0.150	0.141
5	0.545	0.484	0.469	0.459	0.394	0.380	0.376	0.363	0.331	0.294	0.196	0.185	0.196	0.189
3	0.744	0.678	0.662	0.650	0.585	0.559	0.551	0.524	0.456	0.391	0.305	0.245	0.300	0.266
2	0.947	0.880	0.863	0.850	0.781	0.747	0.732	0.689	0.588	0.525	0.370	0.324	0.363	0.337
1	1.441	1.372	1.359	1.349	1.275	1.202	1.170	1.097	0.925	0.777	0.527	0.411	0.493	0.426
0.5	2.146	2.076	2.061	2.051	1.976	1.890	1.830	1.717	1.422	1.173	0.717	0.573	0.607	0.567
0.3	2.771	2.696	2.681	2.667	2.568	2.439	2.357	2.213	1.942	1.611	0.902	0.715	0.740	0.672
0.2	3.397	3.318	3.297	3.280	3.148	2.962	2.843	2.649	2.297	2.028	1.110	0.837	0.814	0.761
0.1	5.346	5.244	5.202	5.164	4.819	4.383	4.091	3.715	3.056	2.761	1.638	1.136	0.987	0.938
0.05	7.089	6.973	6.949	6.917	6.712	6.410	6.188	5.661	4.835	3.982	2.294	1.582	1.185	1.151
0.03	9.812	9.646	9.550	9.440	8.528	7.384	6.949	6.566	6.071	5.686	3.712	2.242	1.372	1.345
0.02	12.668	12.475	12.388	12.300	11.499	9.542	8.383	6.976	6.545	6.160	5.487	3.217	1.580	1.528
0.01	16.828	16.679	16.666	16.646	16.423	14.640	12.886	9.558	7.220	6.714	6.228	4.108	2.199	1.855
0.005	18.164	18.006	17.996	17.987	17.903	17.634	16.993	13.615	8.939	7.266	6.600	5.441	2.418	2.199
0.003	18.638	18.497	18.491	18.491	18.462	18.409	18.344	18.037	11.772	7.620	6.753	5.983	2.548	2.450
0.002	18.829	18.687	18.682	18.681	18.660	18.618	18.588	18.509	13.988	7.929	6.846	6.266	2.639	2.589
0.001	19.052	18.894	18.887	18.885	18.871	18.809	18.776	18.742	18.233	11.251	6.966	6.534	2.970	2.792

NTUA Campus KaSAT Ka-band 2-year average, Data Availability: 96.15 %														
Start Date									1st July 2018					
End Date									30th June 2020					
Exceedance Probability [%]	Time Diversity Gain [dB] at time delay													
	1 s	5 s	10 s	1 m	3 m	5 m	10 m	30 m	1 h	3 h	6 h	12 h	18 h	
100	nan	nan	nan	nan	nan	nan	nan	nan	nan	nan	nan	nan	nan	
99	0.048	0.058	0.063	0.094	0.105	0.108	0.117	0.138	0.154	0.173	0.176	0.175	0.176	
95	0.059	0.067	0.071	0.093	0.100	0.101	0.107	0.120	0.131	0.148	0.152	0.147	0.150	
90	0.039	0.044	0.046	0.059	0.063	0.064	0.067	0.074	0.081	0.092	0.096	0.091	0.094	
80	0.023	0.025	0.027	0.047	0.054	0.054	0.060	0.072	0.083	0.105	0.112	0.103	0.109	
70	0.031	0.034	0.035	0.044	0.047	0.047	0.050	0.055	0.060	0.071	0.075	0.070	0.073	
60	0.038	0.042	0.044	0.054	0.057	0.057	0.060	0.066	0.073	0.085	0.091	0.084	0.088	
50	0.045	0.050	0.052	0.063	0.067	0.067	0.071	0.078	0.085	0.100	0.106	0.098	0.103	
30	0.045	0.051	0.054	0.074	0.082	0.082	0.089	0.105	0.121	0.140	0.149	0.137	0.144	
20	0.031	0.036	0.039	0.055	0.061	0.062	0.068	0.080	0.094	0.131	0.152	0.124	0.139	
10	0.057	0.069	0.076	0.128	0.147	0.148	0.152	0.161	0.171	0.197	0.211	0.195	0.204	
5	0.061	0.076	0.087	0.151	0.166	0.169	0.182	0.214	0.251	0.349	0.360	0.349	0.356	
3	0.066	0.082	0.094	0.159	0.185	0.193	0.220	0.288	0.353	0.439	0.499	0.444	0.478	
2	0.068	0.084	0.097	0.166	0.200	0.216	0.258	0.360	0.423	0.577	0.623	0.584	0.611	
1	0.070	0.083	0.093	0.167	0.240	0.271	0.344	0.516	0.664	0.914	1.030	0.949	1.015	
0.5	0.070	0.084	0.095	0.170	0.256	0.316	0.429	0.723	0.972	1.429	1.573	1.539	1.579	
0.3	0.075	0.090	0.104	0.203	0.332	0.414	0.557	0.829	1.159	1.868	2.055	2.031	2.099	
0.2	0.080	0.100	0.118	0.249	0.435	0.555	0.749	1.100	1.369	2.287	2.560	2.584	2.637	
0.1	0.103	0.144	0.182	0.528	0.963	1.255	1.631	2.290	2.585	3.708	4.210	4.359	4.409	
0.05	0.117	0.141	0.172	0.377	0.679	0.902	1.429	2.254	3.107	4.795	5.508	5.905	5.939	
0.03	0.166	0.262	0.371	1.284	2.427	2.863	3.245	3.741	4.126	6.100	7.570	8.440	8.467	
0.02	0.194	0.280	0.368	1.169	3.126	4.285	5.692	6.123	6.508	7.181	9.451	11.089	11.141	
0.01	0.149	0.163	0.183	0.405	2.189	3.942	7.270	9.608	10.114	10.600	12.721	14.630	14.974	
0.005	0.158	0.169	0.178	0.261	0.531	1.171	4.550	9.226	10.899	11.565	12.723	15.747	15.965	
0.003	0.140	0.147	0.147	0.176	0.228	0.294	0.600	6.866	11.017	11.884	12.655	16.089	16.188	
0.002	0.141	0.147	0.148	0.169	0.211	0.241	0.320	4.841	10.900	11.983	12.563	16.189	16.239	
0.001	0.158	0.165	0.167	0.181	0.243	0.276	0.310	0.819	7.801	12.086	12.518	16.082	16.260	

Appendix - 6
Orbital Diversity Statistics

NTUA Campus Ka-band 2-year average, Concurrent Availability: 94.04 %							
Start Date	1st July 2018						
End Date	30th June 2020						
Satellite	Data Availability [%]	P (A>0.1 dB) [%]					
ALPHASAT 19.701 GHz Vertical Pol	95.31	35.663					
KaSAT 19.680 GHz Horizontal Pol	96.15	33.271					
Joint Balanced	94.04	20.638					
Joint Independent	-	14.993					
Attenuation Correlation Coefficient	0.7138						
Exceedance Probability [%]	Attenuation ALPHASAT [dB]	Attenuation KaSAT [dB]	Joint Balanced [dB]	Joint Independent [dB]	Site Diversity Gain [dB] Master: ALPHASAT	Site Diversity Gain [dB] Master: KaSAT	
50	0.024	-0.003	-0.072	-0.090	0.096	0.069	
30	0.130	0.120	0.023	-0.012	0.107	0.097	
20	0.182	0.180	0.105	0.058	0.076	0.075	
10	0.352	0.345	0.186	0.141	0.166	0.159	
5	0.575	0.546	0.344	0.182	0.231	0.202	
3	0.805	0.743	0.483	0.198	0.322	0.260	
2	1.065	0.943	0.603	0.269	0.462	0.340	
1	1.689	1.413	0.978	0.362	0.711	0.434	
0.5	2.428	2.094	1.591	0.444	0.837	0.503	
0.3	3.008	2.719	2.131	0.544	0.876	0.588	
0.2	3.518	3.349	2.655	0.593	0.863	0.694	
0.1	4.627	5.300	3.679	0.759	0.947	1.620	
0.05	7.457	7.007	5.548	0.942	1.909	1.459	
0.03	10.912	9.439	8.108	1.101	2.804	1.331	
0.02	13.765	12.421	10.942	1.238	2.823	1.479	
0.01	22.324	16.868	16.138	1.544	6.186	0.730	
0.005	32.160	18.197	18.116	1.900	14.044	0.081	
0.003	36.264	18.650	18.639	2.167	17.625	0.011	
0.002	38.057	18.838	18.832	2.389	19.226	0.007	
0.001	38.374	19.058	19.053	2.802	19.321	0.006	

NTUA Campus Ka-band 2-year average, Rain Concurrent Availability: 79.82 %		
Start Date	1st July 2018	
End Date	30th June 2020	
Location	**Data Availability [%]**	**P (A>0.1 dB) [%]**
Campus	95.31	35.402
LTCP	96.15	32.958
Joint Balanced	79.82	20.509
Joint Independent	-	14.823
P (Rain Rate > 0.25 mm/h) [%]	1.436	
Attenuation Correlation Coefficient	0.7018	

Exceedance Probability [%]	Attenuation Campus [dB]	Attenuation LTCP [dB]	Rain Rate [mm/h]	Joint Balanced [dB]	Joint Independent [dB]	Site Diversity Gain [dB] Master: Campus	Site Diversity Gain [dB] Master: LTCP
50	0.022	-0.003	0.000	-0.071	-0.090	0.094	0.068
30	0.128	0.118	0.000	0.021	-0.012	0.107	0.096
20	0.181	0.177	0.000	0.104	0.057	0.076	0.073
10	0.349	0.339	0.000	0.185	0.140	0.163	0.154
5	0.565	0.541	0.000	0.340	0.181	0.224	0.201
3	0.779	0.734	0.000	0.473	0.197	0.306	0.261
2	0.997	0.918	0.000	0.589	0.261	0.409	0.329
1	1.570	1.323	1.554	0.908	0.358	0.663	0.415
0.5	2.302	1.896	3.444	1.425	0.434	0.877	0.471
0.3	2.838	2.444	4.977	1.917	0.538	0.922	0.527
0.2	3.296	2.982	6.429	2.361	0.588	0.936	0.621
0.1	4.146	4.569	10.048	3.279	0.745	0.867	1.290
0.05	6.212	6.682	17.128	4.522	0.910	1.690	2.160
0.03	8.857	7.701	25.283	6.751	1.039	2.106	0.950
0.02	11.895	10.393	33.806	9.280	1.169	2.614	1.113
0.01	19.733	14.825	49.356	13.518	1.424	6.215	1.307
0.005	28.495	18.372	68.928	18.348	1.749	10.146	0.024
0.003	34.629	18.734	85.393	18.726	1.997	15.903	0.008
0.002	36.991	18.900	98.531	18.894	2.203	18.096	0.006
0.001	38.285	19.102	108.266	19.097	2.593	19.188	0.004

Appendix - 7
Frequency Scaling Statistics

NTUA Campus Ka-band - Q-band Instantaneous Frequency Scaling													
Start Date			1st July 2016										
End Date			30th June 2020										
Concurrent Data Availability			94.41 %										
Ka-band attenuation [dB]	Q-band Attenuation [dB]												
	Mean value	Std value	Percentile										
			1st	10th	20th	30th	40th	50th	60th	70th	80th	90th	99th
(1.0, 1.2]	3.46	1.81	0.54	0.96	1.65	2.39	2.89	3.46	3.99	4.53	4.98	5.73	8.00
(1.2, 1.4]	3.90	2.07	0.57	1.06	1.78	2.52	3.30	3.94	4.61	5.09	5.64	6.58	8.99
(1.4, 1.6]	4.30	2.31	0.57	1.17	1.88	2.77	3.63	4.31	5.02	5.59	6.28	7.36	9.67
(1.6, 1.8]	4.80	2.55	0.57	1.32	2.12	3.09	4.11	4.81	5.68	6.34	7.02	8.15	10.32
(1.8, 2.0]	5.11	2.70	0.62	1.49	2.39	3.21	4.21	5.12	6.09	6.75	7.53	8.68	10.87
(2.0, 2.2]	5.29	3.07	0.60	1.30	2.09	3.10	4.09	5.11	6.26	7.25	8.22	9.47	12.15
(2.2, 2.4]	5.63	3.20	0.64	1.57	2.45	3.27	4.28	5.53	6.62	7.64	8.61	9.92	13.02
(2.4, 2.6]	5.82	3.38	0.59	1.72	2.57	3.37	4.15	5.48	6.75	7.83	9.03	10.45	14.19
(2.6, 2.8]	6.37	3.67	0.59	1.60	2.63	3.62	4.86	6.58	7.53	8.66	9.78	11.17	14.75
(2.8, 3.0]	6.94	3.82	0.87	1.76	2.99	4.17	5.78	7.01	8.18	9.25	10.55	11.95	15.01
(3.0, 3.2]	7.82	3.86	0.84	2.45	3.67	5.71	6.89	8.10	9.07	10.04	11.35	12.74	15.75
(3.2, 3.4]	8.36	4.38	0.64	2.08	3.24	6.03	7.36	8.78	9.98	11.23	12.39	13.83	17.12
(3.4, 3.6]	8.94	4.51	1.29	2.57	3.39	6.52	8.00	9.80	10.79	11.98	13.15	14.49	17.59
(3.6, 3.8]	10.30	4.15	1.80	3.71	6.61	8.12	9.61	10.84	12.01	13.07	13.99	15.30	18.23
(3.8, 4.0]	11.07	4.45	2.16	4.03	7.47	8.96	10.31	11.48	12.92	14.02	15.01	16.31	21.18
(4.0, 4.2]	11.46	4.78	2.21	3.98	6.72	9.49	10.78	11.92	13.74	14.59	15.35	16.81	22.35
(4.2, 4.4]	12.68	4.19	3.88	7.23	9.65	10.82	11.58	12.48	14.22	15.10	16.11	17.65	23.21
(4.4, 4.6]	13.57	3.88	2.17	9.18	10.55	11.58	12.68	13.57	14.94	15.69	16.54	18.42	22.55
(4.6, 4.8]	14.19	3.46	8.07	9.82	10.89	11.85	13.08	13.98	15.10	16.25	17.01	18.44	23.89
(4.8, 5.0]	15.37	3.72	8.66	10.34	11.74	13.15	14.32	15.43	16.60	17.39	18.34	20.00	24.32
(5.0, 5.2]	16.55	3.76	8.28	11.59	12.80	14.57	15.78	17.10	17.54	18.49	19.54	20.80	26.54
(5.2, 5.4]	16.94	3.73	9.78	11.53	13.20	14.92	16.35	17.55	18.01	19.01	19.92	21.15	26.43
(5.4, 5.6]	17.81	4.11	10.19	11.60	13.82	15.84	17.25	18.21	19.10	19.98	21.17	22.66	27.01
(5.6, 5.8]	19.03	3.98	11.19	13.29	15.67	17.07	18.08	18.92	19.95	21.30	22.75	24.03	27.54
(5.8, 6.0]	20.11	4.45	11.42	14.87	16.50	17.69	18.74	19.40	20.54	22.07	24.12	26.22	32.39
(6.0, 6.2]	20.08	4.12	11.71	14.78	16.67	18.32	19.33	19.72	20.40	21.80	23.45	26.28	30.15
(6.2, 6.4]	21.09	4.15	11.81	15.92	17.89	19.15	20.07	20.56	21.47	22.46	24.23	27.26	31.11
(6.4, 6.6]	21.82	4.37	12.08	16.62	18.25	19.52	20.69	21.29	22.51	23.77	25.46	28.55	31.45
(6.6, 6.8]	21.82	4.16	12.31	17.04	18.76	20.00	20.68	21.46	22.28	23.24	24.75	27.67	30.92
(6.8, 7.0]	22.63	4.40	12.52	17.26	18.98	20.70	21.54	22.29	23.40	24.64	25.74	28.73	32.41
(7.0, 7.2]	23.49	4.50	12.96	18.46	19.86	21.09	22.09	23.16	23.89	25.11	27.66	30.81	32.68
(7.2, 7.4]	23.99	4.43	13.15	18.61	20.54	21.86	22.73	23.93	25.01	26.17	28.31	30.65	32.02
(7.4, 7.6]	24.29	4.58	12.52	18.06	20.04	21.70	23.22	24.74	25.58	26.93	28.30	30.74	32.19
(7.6, 7.8]	24.86	4.61	12.55	18.92	21.43	22.61	23.86	25.55	26.63	27.64	28.96	30.74	32.15
(7.8, 8.0]	25.11	4.70	12.82	18.06	21.57	23.15	24.35	26.00	26.80	27.87	29.38	31.21	32.15
(8.0, 8.2]	25.13	4.60	12.95	18.70	21.07	23.21	24.52	25.88	26.62	27.96	29.01	30.75	32.29
(8.2, 8.4]	25.81	4.62	12.93	19.93	22.63	24.09	25.18	26.16	27.46	29.03	29.92	31.92	32.32
(8.4, 8.6]	26.29	4.31	14.77	20.05	22.94	24.47	25.92	27.15	27.85	29.25	30.21	31.64	32.35
(8.6, 8.8]	26.96	4.30	14.98	20.14	23.67	25.65	27.28	28.25	29.14	29.73	30.64	31.46	32.39
(8.8, 9.0]	26.70	4.39	15.24	20.35	23.35	24.42	26.15	27.87	29.03	29.95	30.63	31.69	32.24
(9.0, 9.2]	27.15	4.35	16.13	19.94	23.88	25.91	26.85	28.19	29.33	30.18	31.04	31.98	32.22
(9.2, 9.4]	27.32	4.06	16.54	21.09	23.75	26.16	27.31	28.35	29.22	30.09	30.55	32.02	32.28
(9.4, 9.6]	27.74	3.94	16.84	21.97	23.88	26.22	27.56	29.08	29.87	30.49	31.06	32.08	32.29
(9.6, 9.8]	28.26	3.93	17.08	22.24	24.87	27.15	28.45	29.65	30.11	30.71	31.92	32.16	32.33
(9.8, 10.0]	28.38	3.94	17.95	22.89	24.26	26.49	28.48	29.93	30.66	31.70	32.06	32.19	32.37
(10.0, 10.2]	28.07	3.93	17.92	22.51	23.93	26.02	28.05	29.78	30.42	30.80	31.95	32.13	32.34
(10.2, 10.4]	28.43	3.86	18.08	23.14	24.18	26.36	29.07	30.32	30.58	30.93	31.96	32.18	32.40
(10.4, 10.6]	28.96	3.84	17.72	22.58	26.18	28.29	29.63	30.56	31.00	31.90	32.14	32.22	32.38
(10.6, 10.8]	29.12	3.55	18.97	23.88	25.93	28.32	29.74	30.60	31.39	31.90	31.98	32.16	32.37
(10.8, 11.0]	28.75	3.73	18.97	23.46	25.32	26.11	28.34	30.58	31.58	31.83	31.98	32.15	32.48
(11.0, 11.2]	28.85	3.52	19.25	24.01	25.73	26.31	28.31	30.50	31.49	31.73	32.04	32.15	32.55
(11.2, 11.4]	29.66	3.30	19.47	25.14	26.30	28.77	30.52	31.37	31.83	32.06	32.17	32.19	32.58
(11.4, 11.6]	29.18	3.43	19.48	25.00	26.13	27.90	28.88	30.49	31.06	31.82	32.09	32.31	32.58
(11.6, 11.8]	29.66	3.06	21.15	25.63	26.72	28.55	30.26	30.72	31.71	31.96	32.16	32.34	32.58
(11.8, 12.0]	30.15	2.88	21.63	26.17	27.47	30.06	30.66	31.68	31.97	32.17	32.33	32.47	32.60
(12.0, 12.2]	29.98	2.68	22.02	26.23	27.08	28.67	30.41	30.82	31.93	32.03	32.21	32.35	32.57
(12.2, 12.4]	30.34	2.58	22.27	26.30	28.34	30.36	30.90	31.14	32.01	32.10	32.23	32.40	32.64
(12.4, 12.6]	30.39	2.66	22.42	26.32	28.54	30.53	30.89	31.65	32.02	32.10	32.21	32.36	32.65
(12.6, 12.8]	30.66	2.53	22.82	26.24	29.31	30.79	31.35	32.01	32.08	32.13	32.27	32.38	33.09
(12.8, 13.0]	30.52	2.58	22.99	26.34	27.99	30.60	31.08	31.81	32.05	32.13	32.17	32.29	33.19
(13.0, 13.2]	30.27	2.59	23.23	26.34	27.79	30.24	31.00	31.34	32.03	32.07	32.18	32.28	32.45
(13.2, 13.4]	30.51	2.52	23.38	26.38	28.36	30.81	31.08	31.64	32.03	32.12	32.25	32.31	32.53
(13.4, 13.6]	30.86	2.36	23.55	26.41	30.13	30.80	31.72	31.98	32.12	32.22	32.32	32.38	32.42
(13.6, 13.8]	30.23	2.50	23.79	26.41	27.06	29.89	30.52	31.53	31.90	32.08	32.23	32.33	32.42
(13.8, 14.0]	30.44	2.36	21.16	26.39	29.79	30.18	30.53	31.07	31.91	32.09	32.22	32.36	32.53
(14.0, 14.2]	30.43	2.42	22.69	26.80	27.80	29.90	30.75	31.87	32.03	32.09	32.17	32.32	32.50
(14.2, 14.4]	30.41	2.23	24.65	27.43	28.13	29.76	30.62	31.61	31.93	32.05	32.11	32.23	32.48
(14.4, 14.6]	30.71	2.18	25.17	26.41	29.38	30.57	31.37	31.93	32.03	32.06	32.12	32.22	32.49
(14.6, 14.8]	30.85	2.21	22.99	27.00	30.05	30.93	31.88	32.01	32.05	32.11	32.17	32.26	32.53
(14.8, 15.0]	30.96	2.05	23.92	27.65	30.28	30.97	31.89	31.98	32.03	32.13	32.19	32.28	32.49

NTUA Campus Ka-band - Q-band Instantaneous Frequency Scaling													
Start Date			1st July 2016										
End Date			30th June 2020										
Concurrent Data Availability			94.41 %										
Ka-band attenuation [dB]	Instantaneous Frequency Scaling Factor												
	Mean value	Std value	Percentile										
			1st	10th	20th	30th	40th	50th	60th	70th	80th	90th	99th
(1.0, 1.2]	3.16	1.64	0.49	0.87	1.49	2.19	2.66	3.15	3.65	4.10	4.54	5.23	7.36
(1.2, 1.4]	3.01	1.59	0.44	0.83	1.38	1.97	2.55	3.05	3.55	3.92	4.36	5.05	6.93
(1.4, 1.6]	2.88	1.54	0.38	0.78	1.26	1.83	2.42	2.89	3.37	3.75	4.19	4.94	6.40
(1.6, 1.8]	2.83	1.50	0.34	0.78	1.26	1.83	2.41	2.82	3.36	3.72	4.13	4.81	6.06
(1.8, 2.0]	2.70	1.42	0.33	0.79	1.26	1.69	2.20	2.70	3.20	3.58	3.96	4.56	5.75
(2.0, 2.2]	2.52	1.46	0.29	0.62	1.00	1.48	1.94	2.44	2.99	3.44	3.92	4.51	5.68
(2.2, 2.4]	2.45	1.39	0.27	0.68	1.07	1.43	1.87	2.41	2.87	3.33	3.74	4.32	5.65
(2.4, 2.6]	2.33	1.35	0.24	0.70	1.03	1.34	1.66	2.21	2.69	3.15	3.62	4.16	5.62
(2.6, 2.8]	2.36	1.36	0.22	0.59	0.97	1.34	1.81	2.44	2.79	3.21	3.64	4.14	5.43
(2.8, 3.0]	2.40	1.32	0.31	0.61	1.02	1.44	1.99	2.42	2.82	3.17	3.64	4.13	5.20
(3.0, 3.2]	2.53	1.24	0.27	0.79	1.20	1.84	2.22	2.63	2.93	3.24	3.66	4.12	5.09
(3.2, 3.4]	2.54	1.33	0.19	0.63	1.00	1.85	2.23	2.68	3.03	3.40	3.76	4.19	5.17
(3.4, 3.6]	2.56	1.29	0.37	0.74	0.97	1.86	2.29	2.81	3.09	3.42	3.76	4.14	5.03
(3.6, 3.8]	2.78	1.12	0.49	1.00	1.80	2.19	2.58	2.92	3.25	3.55	3.79	4.14	4.92
(3.8, 4.0]	2.84	1.14	0.56	1.03	1.92	2.30	2.64	2.95	3.32	3.59	3.85	4.16	5.40
(4.0, 4.2]	2.80	1.17	0.54	0.97	1.62	2.33	2.62	2.90	3.35	3.56	3.75	4.10	5.49
(4.2, 4.4]	2.95	0.98	0.91	1.71	2.25	2.51	2.70	2.91	3.30	3.51	3.76	4.12	5.43
(4.4, 4.6]	3.02	0.86	0.49	2.04	2.35	2.59	2.81	3.02	3.33	3.49	3.68	4.10	5.05
(4.6, 4.8]	3.02	0.74	1.72	2.10	2.32	2.52	2.79	2.98	3.21	3.46	3.62	3.91	5.14
(4.8, 5.0]	3.14	0.75	1.77	2.12	2.41	2.69	2.93	3.16	3.38	3.55	3.74	4.05	4.94
(5.0, 5.2]	3.25	0.74	1.63	2.28	2.52	2.87	3.11	3.35	3.45	3.63	3.81	4.08	5.23
(5.2, 5.4]	3.20	0.70	1.86	2.18	2.50	2.82	3.09	3.31	3.39	3.59	3.77	3.99	5.00
(5.4, 5.6]	3.24	0.74	1.88	2.11	2.52	2.88	3.14	3.32	3.47	3.62	3.85	4.10	4.86
(5.6, 5.8]	3.34	0.70	1.98	2.35	2.74	3.01	3.19	3.33	3.50	3.74	3.99	4.21	4.83
(5.8, 6.0]	3.41	0.75	1.92	2.51	2.81	3.00	3.18	3.28	3.49	3.77	4.12	4.42	5.49
(6.0, 6.2]	3.29	0.67	1.93	2.45	2.71	2.99	3.17	3.23	3.34	3.58	3.82	4.30	4.95
(6.2, 6.4]	3.35	0.66	1.86	2.53	2.85	3.05	3.19	3.27	3.40	3.57	3.85	4.32	4.92
(6.4, 6.6]	3.36	0.67	1.86	2.55	2.80	3.00	3.19	3.27	3.50	3.66	3.92	4.41	4.88
(6.6, 6.8]	3.26	0.62	1.84	2.55	2.80	2.99	3.09	3.20	3.32	3.47	3.70	4.14	4.62
(6.8, 7.0]	3.28	0.64	1.83	2.48	2.76	3.00	3.12	3.24	3.38	3.58	3.73	4.17	4.66
(7.0, 7.2]	3.31	0.63	1.84	2.61	2.78	2.97	3.11	3.27	3.36	3.53	3.89	4.33	4.58
(7.2, 7.4]	3.29	0.61	1.79	2.56	2.80	3.01	3.13	3.28	3.44	3.60	3.87	4.19	4.40
(7.4, 7.6]	3.24	0.61	1.66	2.42	2.65	2.89	3.11	3.31	3.42	3.59	3.78	4.10	4.29
(7.6, 7.8]	3.23	0.60	1.63	2.48	2.79	2.94	3.10	3.32	3.45	3.59	3.75	4.00	4.19
(7.8, 8.0]	3.18	0.60	1.62	2.28	2.75	2.92	3.08	3.30	3.38	3.53	3.72	3.96	4.09
(8.0, 8.2]	3.10	0.57	1.59	2.32	2.61	2.87	3.03	3.19	3.29	3.46	3.57	3.81	4.00
(8.2, 8.4]	3.11	0.56	1.57	2.39	2.71	2.92	3.04	3.15	3.31	3.50	3.60	3.83	3.92
(8.4, 8.6]	3.09	0.51	1.76	2.35	2.70	2.86	3.05	3.19	3.28	3.42	3.55	3.73	3.83
(8.6, 8.8]	3.10	0.49	1.71	2.30	2.71	2.95	3.14	3.25	3.35	3.42	3.51	3.60	3.74
(8.8, 9.0]	3.00	0.49	1.72	2.29	2.62	2.74	2.94	3.12	3.26	3.37	3.44	3.56	3.64
(9.0, 9.2]	2.98	0.48	1.78	2.20	2.65	2.84	2.96	3.10	3.22	3.32	3.41	3.51	3.56
(9.2, 9.4]	2.94	0.44	1.78	2.26	2.57	2.79	2.92	3.05	3.14	3.24	3.29	3.43	3.48
(9.4, 9.6]	2.92	0.41	1.78	2.31	2.50	2.76	2.91	3.07	3.14	3.21	3.27	3.37	3.42
(9.6, 9.8]	2.91	0.40	1.77	2.28	2.56	2.80	2.94	3.05	3.11	3.17	3.28	3.31	3.35
(9.8, 10.0]	2.87	0.40	1.81	2.30	2.44	2.68	2.87	3.03	3.09	3.20	3.24	3.27	3.29
(10.0, 10.2]	2.78	0.39	1.77	2.23	2.38	2.57	2.77	2.95	3.01	3.06	3.16	3.19	3.21
(10.2, 10.4]	2.76	0.37	1.76	2.26	2.34	2.57	2.83	2.94	2.96	3.01	3.09	3.12	3.15
(10.4, 10.6]	2.76	0.36	1.68	2.16	2.48	2.68	2.82	2.91	2.95	3.02	3.05	3.07	3.09
(10.6, 10.8]	2.72	0.33	1.77	2.22	2.41	2.65	2.78	2.86	2.93	2.98	2.99	3.00	3.04
(10.8, 11.0]	2.64	0.34	1.74	2.16	2.32	2.41	2.60	2.80	2.89	2.91	2.94	2.95	2.99
(11.0, 11.2]	2.60	0.32	1.74	2.17	2.32	2.37	2.55	2.74	2.84	2.85	2.88	2.90	2.94
(11.2, 11.4]	2.63	0.29	1.73	2.22	2.32	2.55	2.70	2.77	2.82	2.84	2.85	2.86	2.89
(11.4, 11.6]	2.54	0.30	1.69	2.18	2.28	2.41	2.52	2.65	2.71	2.77	2.79	2.81	2.84
(11.6, 11.8]	2.54	0.26	1.81	2.19	2.29	2.43	2.59	2.62	2.70	2.73	2.75	2.77	2.79
(11.8, 12.0]	2.53	0.24	1.82	2.19	2.31	2.52	2.58	2.66	2.68	2.70	2.72	2.73	2.75
(12.0, 12.2]	2.48	0.22	1.82	2.17	2.24	2.36	2.51	2.55	2.64	2.65	2.66	2.68	2.71
(12.2, 12.4]	2.47	0.21	1.81	2.15	2.30	2.47	2.51	2.54	2.60	2.61	2.63	2.64	2.66
(12.4, 12.6]	2.43	0.21	1.80	2.11	2.29	2.44	2.47	2.53	2.56	2.57	2.58	2.59	2.62
(12.6, 12.8]	2.41	0.20	1.80	2.06	2.32	2.42	2.48	2.52	2.53	2.54	2.55	2.56	2.59
(12.8, 13.0]	2.37	0.20	1.78	2.04	2.17	2.37	2.41	2.46	2.48	2.49	2.50	2.51	2.59
(13.0, 13.2]	2.31	0.20	1.77	2.01	2.12	2.31	2.36	2.39	2.44	2.45	2.46	2.47	2.49
(13.2, 13.4]	2.29	0.19	1.76	1.99	2.14	2.32	2.34	2.38	2.40	2.41	2.42	2.43	2.45
(13.4, 13.6]	2.28	0.17	1.74	1.97	2.23	2.29	2.35	2.37	2.38	2.38	2.39	2.40	2.41
(13.6, 13.8]	2.21	0.18	1.74	1.92	1.97	2.17	2.23	2.30	2.33	2.34	2.35	2.36	2.38
(13.8, 14.0]	2.19	0.17	1.52	1.91	2.14	2.17	2.19	2.24	2.29	2.31	2.32	2.33	2.35
(14.0, 14.2]	2.16	0.17	1.61	1.90	1.98	2.13	2.19	2.26	2.27	2.28	2.29	2.29	2.31
(14.2, 14.4]	2.13	0.16	1.73	1.92	1.96	2.08	2.14	2.21	2.23	2.24	2.25	2.26	2.28
(14.4, 14.6]	2.12	0.15	1.75	1.83	2.03	2.11	2.17	2.20	2.20	2.21	2.22	2.23	2.25
(14.6, 14.8]	2.10	0.15	1.56	1.84	2.04	2.10	2.16	2.17	2.18	2.19	2.19	2.20	2.22
(14.8, 15.0]	2.08	0.14	1.60	1.86	2.03	2.08	2.13	2.14	2.15	2.16	2.16	2.17	2.18

NTUA Campus Ka-band - Q-band Instantaneous Frequency Scaling				
Start Date			1st July 2016	
End Date			30th June 2020	
Concurrent Data Availability			94.41 %	
Exceedance Probability [%]	Attenuation Ka [dB]	Attenuation Q [dB]	Equiprobable Ratio Attenuation Q [dB] / Attenuation Ka [dB]	IFSF Q-band Attenuation [dB] / Ka-band Attenuation [dB], A_{Ka} > 1.0 dB (1.29 % of concurrent data)
50	0.012	0.028	2.231	2.779
30	0.097	0.114	1.174	3.600
20	0.139	0.157	1.128	4.010
10	0.180	0.199	1.103	4.620
5	0.221	0.487	2.201	5.174
3	0.393	1.081	2.753	5.530
2	0.697	1.971	2.828	5.787
1	1.399	3.988	2.850	6.276
0.5	2.218	6.451	2.908	6.955
0.3	2.792	8.717	3.122	7.380
0.2	3.376	10.885	3.224	7.693
0.1	4.835	16.490	3.410	8.194
0.05	8.052	25.851	3.210	8.688
0.03	11.666	30.659	2.628	9.089
0.02	15.111	32.062	2.122	9.370
0.01	23.610	32.356	1.370	9.775
0.005	30.528	32.499	1.065	10.170
0.003	36.579	32.554	0.890	10.361
0.002	38.151	32.581	0.854	10.515
0.001	38.330	32.688	0.853	10.743

NTUA LCP Ka-band - Q-band Instantaneous Frequency Scaling, 2-year average													
Start Date			1st July 2016										
End Date			30th June 2020										
Concurrent Data Availability			92.48 %										
Ka-band attenuation [dB]	Q-band Attenuation [dB]												
	Mean value	Std value	Percentile										
			1st	10th	20th	30th	40th	50th	60th	70th	80th	90th	99th
(1.0, 1.2]	4.13	2.06	0.58	1.32	2.04	2.77	3.45	4.12	4.79	5.39	6.12	6.90	8.61
(1.2, 1.4]	4.41	2.22	0.60	1.34	2.15	2.97	3.66	4.43	5.18	5.89	6.54	7.33	8.88
(1.4, 1.6]	5.14	2.39	0.63	1.71	2.71	3.69	4.45	5.33	6.11	6.75	7.35	8.13	9.93
(1.6, 1.8]	5.83	2.40	0.74	2.45	3.65	4.51	5.43	6.10	6.70	7.29	7.82	8.70	11.06
(1.8, 2.0]	6.67	2.57	0.74	3.24	4.51	5.57	6.30	6.97	7.54	8.11	8.80	9.73	11.93
(2.0, 2.2]	7.24	2.77	0.93	3.35	5.12	6.06	7.02	7.59	8.14	8.68	9.52	10.46	13.15
(2.2, 2.4]	7.64	3.05	0.85	2.60	5.53	6.42	7.21	7.87	8.55	9.24	10.10	11.28	14.23
(2.4, 2.6]	8.37	3.20	0.98	4.15	5.95	6.91	7.71	8.58	9.38	10.20	10.96	12.11	16.09
(2.6, 2.8]	8.87	3.75	1.31	3.05	5.80	6.93	8.05	9.23	9.93	10.92	12.01	13.47	18.24
(2.8, 3.0]	9.50	3.87	1.70	4.01	6.30	7.44	8.52	9.76	10.48	11.47	12.48	14.19	19.91
(3.0, 3.2]	10.27	4.16	1.88	4.85	6.75	7.80	8.66	10.34	11.36	12.66	14.02	15.51	19.84
(3.2, 3.4]	10.75	4.35	2.24	5.31	6.88	7.92	9.18	10.97	11.97	13.20	14.55	16.21	21.07
(3.4, 3.6]	11.54	4.61	2.71	5.19	6.84	8.45	10.65	12.15	13.22	14.55	15.77	17.08	20.93
(3.6, 3.8]	12.16	4.54	2.93	5.88	7.58	9.74	11.55	12.71	13.77	14.99	16.06	17.74	20.99
(3.8, 4.0]	12.78	4.83	3.15	5.39	7.71	10.07	12.67	13.95	14.85	15.83	17.08	18.30	21.27
(4.0, 4.2]	12.69	5.26	3.57	5.28	6.61	8.90	11.91	13.76	14.94	16.15	17.63	19.39	22.06
(4.2, 4.4]	14.31	5.18	3.78	6.59	8.80	11.84	13.89	15.03	16.24	17.56	18.96	20.70	23.48
(4.4, 4.6]	14.56	4.68	4.16	8.19	10.05	11.25	13.94	15.01	16.30	17.57	18.77	20.54	23.63
(4.6, 4.8]	15.44	4.80	4.47	8.62	10.36	12.86	14.83	16.21	17.40	18.37	19.78	21.10	24.07
(4.8, 5.0]	16.13	4.89	4.55	8.71	10.88	14.54	15.64	16.96	17.88	18.99	20.47	22.07	25.32
(5.0, 5.2]	16.87	4.94	4.90	9.32	11.93	15.26	16.32	17.45	18.82	19.82	21.22	22.76	25.64
(5.2, 5.4]	18.73	4.44	9.07	10.88	15.88	17.00	18.12	19.60	20.56	21.30	22.08	24.07	26.48
(5.4, 5.6]	19.47	4.14	10.45	13.00	16.34	17.71	18.71	19.97	20.70	21.55	22.91	25.08	26.81
(5.6, 5.8]	20.58	4.73	10.94	13.08	17.01	18.04	19.41	20.91	21.96	23.59	25.04	27.06	29.01
(5.8, 6.0]	21.02	4.30	11.47	15.01	17.62	18.91	19.98	21.42	22.25	23.00	24.72	26.70	29.14
(6.0, 6.2]	21.05	4.09	11.71	15.80	18.21	18.97	19.96	21.32	21.98	22.99	24.70	26.58	29.32
(6.2, 6.4]	22.22	4.07	11.78	17.40	19.17	20.27	21.70	22.43	23.44	24.15	25.88	27.68	29.65
(6.4, 6.6]	22.41	4.24	11.69	16.17	19.10	21.08	22.40	22.91	23.64	24.21	25.02	28.22	29.99
(6.6, 6.8]	21.89	4.86	11.91	14.16	18.41	19.65	20.50	21.51	22.89	24.59	26.49	28.56	30.41
(6.8, 7.0]	22.55	4.94	11.76	16.42	18.58	19.84	20.90	21.87	23.56	25.12	27.20	29.61	32.34
(7.0, 7.2]	23.34	5.39	11.71	14.41	18.67	20.61	22.10	23.62	25.30	26.96	28.79	30.09	32.73
(7.2, 7.4]	23.86	5.56	11.86	14.69	19.47	21.14	22.95	24.28	25.83	27.67	29.59	30.64	33.10
(7.4, 7.6]	24.75	5.47	11.85	15.58	20.40	22.19	23.70	25.69	27.05	28.48	29.84	31.47	33.23
(7.6, 7.8]	25.50	4.99	11.81	18.08	21.82	23.43	24.35	26.04	27.52	29.21	30.00	30.75	33.17
(7.8, 8.0]	26.07	4.82	11.85	20.34	22.35	23.84	24.81	26.35	27.56	29.86	30.64	31.57	33.12
(8.0, 8.2]	26.34	4.73	11.90	20.20	22.82	24.40	25.72	27.33	28.01	29.79	30.48	31.47	33.23
(8.2, 8.4]	26.89	5.08	11.90	20.95	22.46	24.67	26.53	28.21	29.82	30.21	31.42	32.80	33.31
(8.4, 8.6]	26.76	4.25	13.43	21.45	23.07	24.64	25.85	27.49	28.79	29.80	30.54	31.76	33.22
(8.6, 8.8]	27.37	4.27	17.64	20.79	23.90	25.34	27.36	28.50	29.77	30.28	31.09	31.88	33.37
(8.8, 9.0]	27.95	3.95	15.45	22.30	24.45	26.09	27.81	29.09	29.98	30.83	31.64	32.06	33.11
(9.0, 9.2]	28.75	4.13	14.07	22.50	25.11	27.72	29.22	29.98	30.82	31.68	32.05	32.82	33.53
(9.2, 9.4]	29.54	3.32	19.59	24.20	26.81	29.25	29.73	30.50	31.20	31.84	32.19	32.58	33.53
(9.4, 9.6]	29.85	3.21	20.94	24.49	27.27	29.19	29.99	30.99	31.42	32.02	32.48	33.14	33.51
(9.6, 9.8]	29.54	3.20	21.47	24.81	25.72	28.77	30.11	30.45	31.54	31.92	32.07	32.56	33.41
(9.8, 10.0]	30.23	3.07	22.42	25.55	26.68	29.59	30.16	31.16	31.88	32.08	32.56	33.51	33.95
(10.0, 10.2]	29.32	3.13	22.83	23.93	26.21	28.23	29.22	30.10	30.53	31.59	32.07	32.80	33.83
(10.2, 10.4]	29.93	2.73	22.14	25.62	28.34	29.12	30.08	30.16	31.04	31.92	32.22	32.75	33.78
(10.4, 10.6]	30.47	2.46	23.09	26.08	29.39	30.14	30.30	30.70	31.70	32.10	32.18	32.85	33.80
(10.6, 10.8]	30.45	2.44	23.54	26.15	29.76	30.13	30.34	30.57	31.41	31.91	32.39	33.09	33.86
(10.8, 11.0]	30.18	2.66	24.01	25.87	27.26	29.87	30.14	30.37	31.24	31.79	32.42	33.25	33.88
(11.0, 11.2]	29.91	2.85	24.13	25.71	26.48	28.28	29.87	30.53	31.24	32.05	32.76	33.34	33.84
(11.2, 11.4]	30.02	2.68	24.73	25.75	26.84	28.82	30.37	30.50	31.01	32.06	32.37	33.17	33.87
(11.4, 11.6]	29.51	3.03	24.34	25.69	26.02	26.99	28.83	30.03	30.63	31.87	32.64	33.45	33.90
(11.6, 11.8]	29.30	3.88	22.21	22.89	24.40	27.23	29.53	30.59	31.83	32.20	32.92	33.23	33.91
(11.8, 12.0]	30.76	2.37	26.33	26.82	27.85	30.44	30.64	31.14	31.92	32.12	32.91	33.68	33.90
(12.0, 12.2]	31.05	2.45	25.36	26.98	28.64	30.49	30.82	31.42	32.14	32.82	33.45	33.77	33.91
(12.2, 12.4]	31.04	2.15	25.52	27.57	29.87	30.50	30.62	31.02	31.61	32.22	33.16	33.73	33.92
(12.4, 12.6]	31.18	1.93	26.08	28.65	30.30	30.45	30.75	31.00	31.48	32.36	33.23	33.80	34.22
(12.6, 12.8]	31.01	1.90	26.30	28.03	29.62	30.49	30.76	31.19	31.52	31.93	32.92	33.23	33.88
(12.8, 13.0]	31.08	1.86	26.88	28.48	29.14	30.31	30.86	31.48	31.76	32.44	32.78	33.15	33.87
(13.0, 13.2]	31.40	1.59	27.57	28.63	29.73	30.72	31.47	31.85	32.32	32.49	32.83	33.07	33.83
(13.2, 13.4]	31.50	1.30	27.92	29.99	30.55	30.69	31.26	31.68	32.09	32.36	32.74	32.93	33.83
(13.4, 13.6]	31.55	1.35	28.26	29.79	30.51	30.91	31.25	31.69	32.14	32.47	32.86	32.97	33.83
(13.6, 13.8]	31.78	1.35	28.74	29.58	30.60	31.14	31.69	32.03	32.42	32.84	32.89	33.07	33.83
(13.8, 14.0]	31.77	1.32	28.96	29.84	30.69	31.04	31.65	31.80	32.33	32.77	33.06	33.08	33.83
(14.0, 14.2]	31.28	1.48	29.10	29.34	29.76	30.28	30.95	31.13	31.70	32.31	32.90	33.07	33.83
(14.2, 14.4]	31.65	1.33	29.35	29.50	30.98	31.09	31.18	31.66	31.76	32.58	33.04	33.40	33.84
(14.4, 14.6]	32.22	1.17	29.25	31.01	31.21	31.73	31.87	32.19	32.91	33.06	33.43	33.47	33.49
(14.6, 14.8]	32.14	1.16	29.64	30.78	31.18	31.76	31.82	32.15	32.72	33.04	33.40	33.46	33.84
(14.8, 15.0]	31.97	1.07	29.75	30.16	31.21	31.79	31.88	31.90	31.98	32.83	32.98	33.21	33.77

NTUA LCP Ka-band - Q-band Instantaneous Frequency Scaling, 2-year average													
Start Date			1st July 2016										
End Date			30th June 2020										
Concurrent Data Availability			92.48 %										
Ka-band attenuation [dB]	Instantaneous Frequency Scaling Factor												
	Mean value	Std value	Percentile										
			1st	10th	20th	30th	40th	50th	60th	70th	80th	90th	99th
(1.0, 1.2]	3.78	1.90	0.53	1.20	1.86	2.54	3.18	3.75	4.38	4.93	5.59	6.31	7.92
(1.2, 1.4]	3.41	1.72	0.46	1.04	1.65	2.30	2.82	3.45	4.01	4.53	5.04	5.66	6.85
(1.4, 1.6]	3.43	1.59	0.42	1.15	1.81	2.47	2.98	3.56	4.07	4.51	4.89	5.42	6.54
(1.6, 1.8]	3.44	1.41	0.44	1.46	2.14	2.64	3.22	3.60	3.94	4.27	4.62	5.13	6.53
(1.8, 2.0]	3.52	1.35	0.40	1.71	2.39	2.93	3.33	3.66	3.97	4.26	4.65	5.14	6.41
(2.0, 2.2]	3.46	1.32	0.45	1.63	2.46	2.89	3.34	3.64	3.88	4.15	4.52	4.99	6.23
(2.2, 2.4]	3.33	1.33	0.37	1.13	2.43	2.80	3.15	3.43	3.73	4.02	4.39	4.89	6.18
(2.4, 2.6]	3.36	1.28	0.40	1.66	2.37	2.78	3.11	3.45	3.75	4.08	4.40	4.84	6.47
(2.6, 2.8]	3.29	1.39	0.49	1.15	2.16	2.59	3.00	3.42	3.68	4.04	4.44	5.00	6.73
(2.8, 3.0]	3.28	1.34	0.60	1.38	2.19	2.56	2.96	3.37	3.63	3.97	4.32	4.88	6.90
(3.0, 3.2]	3.31	1.34	0.61	1.55	2.18	2.54	2.79	3.35	3.67	4.09	4.51	5.00	6.37
(3.2, 3.4]	3.26	1.32	0.67	1.59	2.08	2.41	2.78	3.34	3.63	4.02	4.41	4.92	6.29
(3.4, 3.6]	3.30	1.32	0.78	1.47	1.95	2.41	3.04	3.46	3.76	4.14	4.50	4.90	6.03
(3.6, 3.8]	3.29	1.23	0.80	1.55	2.07	2.65	3.14	3.42	3.73	4.05	4.32	4.75	5.65
(3.8, 4.0]	3.28	1.24	0.81	1.36	1.98	2.61	3.25	3.59	3.81	4.05	4.38	4.68	5.48
(4.0, 4.2]	3.10	1.28	0.87	1.29	1.61	2.16	2.88	3.37	3.64	3.93	4.30	4.73	5.40
(4.2, 4.4]	3.33	1.20	0.88	1.53	2.04	2.73	3.24	3.50	3.78	4.08	4.42	4.78	5.40
(4.4, 4.6]	3.24	1.04	0.93	1.81	2.22	2.49	3.12	3.34	3.62	3.90	4.17	4.57	5.27
(4.6, 4.8]	3.29	1.02	0.96	1.82	2.23	2.75	3.17	3.47	3.68	3.91	4.18	4.49	5.14
(4.8, 5.0]	3.30	1.00	0.92	1.78	2.21	2.96	3.21	3.46	3.65	3.89	4.21	4.50	5.13
(5.0, 5.2]	3.31	0.97	0.97	1.84	2.36	2.99	3.20	3.44	3.70	3.88	4.16	4.49	5.01
(5.2, 5.4]	3.53	0.84	1.72	2.04	3.02	3.21	3.41	3.71	3.87	4.02	4.18	4.54	5.02
(5.4, 5.6]	3.54	0.76	1.90	2.38	2.96	3.22	3.40	3.63	3.76	3.93	4.17	4.58	4.89
(5.6, 5.8]	3.61	0.83	1.92	2.30	2.98	3.17	3.43	3.66	3.83	4.13	4.41	4.71	5.10
(5.8, 6.0]	3.57	0.73	1.95	2.55	2.99	3.22	3.40	3.63	3.78	3.92	4.21	4.50	4.90
(6.0, 6.2]	3.45	0.67	1.92	2.56	2.98	3.10	3.29	3.50	3.60	3.76	4.05	4.37	4.81
(6.2, 6.4]	3.53	0.64	1.86	2.79	3.03	3.22	3.42	3.57	3.71	3.80	4.12	4.38	4.70
(6.4, 6.6]	3.45	0.65	1.79	2.49	2.94	3.24	3.45	3.53	3.63	3.71	3.86	4.33	4.62
(6.6, 6.8]	3.27	0.72	1.78	2.13	2.74	2.95	3.06	3.21	3.43	3.67	3.97	4.26	4.53
(6.8, 7.0]	3.27	0.72	1.69	2.39	2.69	2.90	3.03	3.17	3.41	3.65	3.95	4.29	4.69
(7.0, 7.2]	3.29	0.76	1.64	2.02	2.62	2.91	3.11	3.33	3.56	3.80	4.05	4.25	4.61
(7.2, 7.4]	3.27	0.76	1.62	2.02	2.67	2.91	3.15	3.32	3.54	3.79	4.05	4.21	4.53
(7.4, 7.6]	3.30	0.73	1.58	2.09	2.70	2.96	3.18	3.43	3.60	3.78	3.99	4.19	4.41
(7.6, 7.8]	3.31	0.65	1.54	2.36	2.84	3.04	3.18	3.38	3.60	3.80	3.89	3.98	4.29
(7.8, 8.0]	3.30	0.61	1.51	2.57	2.83	3.02	3.14	3.32	3.48	3.77	3.88	4.00	4.23
(8.0, 8.2]	3.25	0.58	1.47	2.49	2.82	3.03	3.17	3.38	3.45	3.67	3.77	3.88	4.12
(8.2, 8.4]	3.24	0.61	1.42	2.51	2.72	2.97	3.19	3.40	3.57	3.64	3.78	3.96	4.04
(8.4, 8.6]	3.15	0.50	1.58	2.53	2.71	2.90	3.03	3.21	3.37	3.49	3.60	3.74	3.91
(8.6, 8.8]	3.15	0.49	2.03	2.40	2.75	2.92	3.13	3.28	3.41	3.48	3.58	3.66	3.86
(8.8, 9.0]	3.14	0.44	1.74	2.50	2.76	2.94	3.13	3.27	3.37	3.46	3.54	3.60	3.72
(9.0, 9.2]	3.16	0.45	1.55	2.48	2.78	3.05	3.20	3.29	3.39	3.49	3.52	3.58	3.69
(9.2, 9.4]	3.18	0.36	2.11	2.59	2.88	3.14	3.20	3.30	3.35	3.43	3.47	3.49	3.60
(9.4, 9.6]	3.14	0.34	2.22	2.58	2.86	3.09	3.15	3.27	3.31	3.37	3.42	3.47	3.52
(9.6, 9.8]	3.05	0.33	2.23	2.56	2.64	2.96	3.09	3.14	3.25	3.28	3.31	3.36	3.46
(9.8, 10.0]	3.05	0.31	2.27	2.57	2.68	2.98	3.05	3.15	3.22	3.25	3.30	3.39	3.41
(10.0, 10.2]	2.91	0.31	2.27	2.39	2.59	2.82	2.91	2.98	3.02	3.12	3.18	3.25	3.36
(10.2, 10.4]	2.90	0.26	2.16	2.49	2.75	2.82	2.90	2.94	3.01	3.09	3.13	3.18	3.28
(10.4, 10.6]	2.90	0.24	2.19	2.50	2.80	2.87	2.89	2.93	3.01	3.06	3.09	3.14	3.23
(10.6, 10.8]	2.85	0.23	2.20	2.44	2.77	2.81	2.83	2.86	2.93	2.98	3.03	3.09	3.17
(10.8, 11.0]	2.77	0.25	2.21	2.37	2.50	2.74	2.77	2.79	2.87	2.92	2.98	3.05	3.13
(11.0, 11.2]	2.69	0.26	2.17	2.32	2.39	2.54	2.70	2.74	2.81	2.88	2.95	3.00	3.05
(11.2, 11.4]	2.66	0.24	2.19	2.28	2.37	2.55	2.68	2.70	2.74	2.83	2.88	2.94	3.00
(11.4, 11.6]	2.56	0.26	2.10	2.24	2.26	2.36	2.51	2.61	2.67	2.77	2.83	2.90	2.94
(11.6, 11.8]	2.50	0.33	1.89	1.95	2.10	2.34	2.53	2.61	2.71	2.75	2.81	2.85	2.91
(11.8, 12.0]	2.59	0.20	2.22	2.26	2.34	2.55	2.58	2.62	2.68	2.71	2.77	2.83	2.86
(12.0, 12.2]	2.56	0.20	2.09	2.23	2.35	2.51	2.54	2.60	2.65	2.72	2.76	2.79	2.82
(12.2, 12.4]	2.52	0.18	2.08	2.24	2.44	2.48	2.50	2.52	2.57	2.63	2.69	2.74	2.77
(12.4, 12.6]	2.49	0.15	2.08	2.29	2.41	2.43	2.45	2.48	2.51	2.58	2.66	2.70	2.73
(12.6, 12.8]	2.44	0.15	2.08	2.21	2.33	2.40	2.42	2.45	2.48	2.51	2.59	2.62	2.67
(12.8, 13.0]	2.41	0.14	2.08	2.20	2.25	2.35	2.39	2.44	2.46	2.52	2.54	2.57	2.63
(13.0, 13.2]	2.40	0.12	2.10	2.19	2.27	2.35	2.39	2.43	2.47	2.48	2.51	2.52	2.58
(13.2, 13.4]	2.37	0.10	2.10	2.25	2.29	2.31	2.35	2.39	2.41	2.44	2.46	2.48	2.54
(13.4, 13.6]	2.34	0.10	2.09	2.21	2.26	2.29	2.32	2.35	2.39	2.41	2.43	2.45	2.51
(13.6, 13.8]	2.32	0.10	2.10	2.17	2.24	2.28	2.32	2.34	2.37	2.39	2.40	2.41	2.47
(13.8, 14.0]	2.29	0.10	2.09	2.15	2.21	2.24	2.27	2.30	2.34	2.36	2.37	2.39	2.44
(14.0, 14.2]	2.22	0.10	2.06	2.09	2.12	2.15	2.19	2.21	2.25	2.30	2.33	2.36	2.40
(14.2, 14.4]	2.21	0.09	2.05	2.07	2.16	2.17	2.18	2.21	2.23	2.28	2.31	2.34	2.38
(14.4, 14.6]	2.22	0.08	2.01	2.14	2.16	2.18	2.19	2.22	2.26	2.29	2.30	2.32	2.32
(14.6, 14.8]	2.19	0.08	2.01	2.09	2.12	2.15	2.17	2.18	2.23	2.25	2.27	2.28	2.30
(14.8, 15.0]	2.15	0.07	1.99	2.02	2.09	2.13	2.14	2.14	2.15	2.20	2.21	2.23	2.27

NTUA LTCP Ka-band - Q-band Instantaneous Frequency Scaling				
Start Date				1st July 2016
End Date				30th June 2020
Concurrent Data Availability				92.48 %
Exceedance Probability [%]	**Attenuation Ka [dB]**	**Attenuation Q [dB]**	**Equiprobable Ratio Attenuation Q [dB] / Attenuation Ka [dB]**	**IFSF Q-band Attenuation [dB] / Ka-band Attenuation [dB], A_{Ka} > 1.0 dB (0.62 % of concurrent data)**
50	0.010	0.030	2.928	3.450
30	0.092	0.111	1.207	4.263
20	0.133	0.151	1.142	4.722
10	0.173	0.191	1.108	5.397
5	0.193	0.360	1.871	5.967
3	0.217	0.688	3.163	6.353
2	0.352	1.252	3.553	6.604
1	0.709	2.863	4.037	7.017
0.5	1.229	4.937	4.019	7.481
0.3	1.747	6.743	3.860	7.798
0.2	2.239	8.121	3.627	7.995
0.1	3.350	12.073	3.604	8.326
0.05	5.270	19.719	3.741	8.574
0.03	8.285	27.414	3.309	8.861
0.02	11.096	30.882	2.783	9.010
0.01	16.593	32.096	1.934	9.190
0.005	22.289	32.958	1.479	9.575
0.003	26.503	33.186	1.252	9.948
0.002	29.730	33.407	1.124	10.040
0.001	33.688	33.598	0.997	10.120

NTUA Campus Ku-band - Ka-band Instantaneous Frequency Scaling													
Start Date			1st July 2017										
End Date			30th June 2020										
Concurrent Data Availability			94.16 %										
Ku-band attenuation [dB]	Ka-band Attenuation [dB]												
	Mean value	Std value	Percentile										
			1st	10th	20th	30th	40th	50th	60th	70th	80th	90th	99th
(1.0, 1.2]	3.97	1.66	1.20	1.98	2.49	2.96	3.46	3.85	4.24	4.68	5.26	6.17	8.85
(1.2, 1.4]	4.33	1.71	1.39	2.12	2.68	3.35	3.81	4.30	4.73	5.18	5.71	6.50	8.96
(1.4, 1.6]	4.64	2.01	1.52	2.03	2.56	3.41	4.05	4.57	5.09	5.64	6.28	7.27	10.00
(1.6, 1.8]	5.18	2.50	1.77	2.28	2.53	3.07	4.34	4.99	5.64	6.42	7.43	8.70	11.81
(1.8, 2.0]	5.95	2.34	2.09	2.88	3.69	4.55	5.16	5.82	6.46	7.09	7.87	9.08	12.31
(2.0, 2.2]	6.27	2.53	2.27	3.03	3.86	4.52	5.29	6.23	6.96	7.77	8.43	9.46	12.68
(2.2, 2.4]	6.77	2.75	2.41	3.39	4.04	4.63	5.75	6.82	7.56	8.26	9.01	10.46	13.33
(2.4, 2.6]	7.77	3.23	2.61	3.97	4.70	5.49	6.61	7.60	8.51	9.14	10.27	12.23	17.01
(2.6, 2.8]	7.98	3.02	2.83	4.10	5.06	5.96	6.85	7.87	8.80	9.55	10.50	12.03	14.84
(2.8, 3.0]	8.81	3.11	3.16	4.72	5.68	6.68	8.07	8.82	9.71	10.51	11.57	12.91	15.21
(3.0, 3.2]	8.91	3.27	3.25	4.85	5.72	6.25	7.88	9.05	9.97	10.72	11.50	13.29	18.01
(3.2, 3.4]	9.06	3.44	3.46	4.63	5.49	6.46	7.71	9.30	10.22	11.19	12.18	13.78	16.33
(3.4, 3.6]	10.35	3.14	3.60	6.10	7.37	8.44	9.88	10.79	11.58	12.18	12.71	14.36	16.83
(3.6, 3.8]	10.73	3.75	3.75	5.40	7.42	8.85	9.88	10.64	11.73	12.73	13.59	15.30	20.18
(3.8, 4.0]	10.56	4.26	4.08	4.56	6.88	7.94	9.21	10.01	11.19	12.93	14.16	16.17	20.80
(4.0, 4.2]	11.62	4.14	4.33	6.32	7.85	9.23	10.35	11.46	12.43	13.45	14.87	17.16	22.98
(4.2, 4.4]	11.87	4.33	4.60	6.56	8.28	9.44	10.38	11.05	12.37	13.80	15.15	17.85	24.33
(4.4, 4.6]	12.46	4.25	4.83	6.93	8.62	10.10	11.07	12.08	13.19	14.49	15.99	17.90	24.28
(4.6, 4.8]	12.83	4.59	4.81	6.90	8.69	10.06	11.30	12.26	13.59	14.91	16.65	19.30	24.34
(4.8, 5.0]	14.28	4.54	5.37	8.49	10.68	11.68	12.25	13.41	15.54	17.08	19.14	20.75	24.09
(5.0, 5.2]	14.09	4.69	5.54	7.80	10.57	11.40	12.69	13.33	14.93	16.44	18.39	20.35	25.50
(5.2, 5.4]	14.92	5.58	5.84	7.90	10.04	11.25	12.64	13.93	16.34	17.94	19.82	23.63	26.71
(5.4, 5.6]	15.99	5.23	6.26	8.91	11.18	12.93	14.45	15.75	17.70	18.82	19.67	23.60	27.22
(5.6, 5.8]	15.90	4.80	6.36	8.98	11.20	13.26	14.78	16.96	17.66	18.47	19.33	21.30	27.51
(5.8, 6.0]	16.95	4.49	7.00	10.91	13.00	14.76	16.99	17.63	18.06	18.85	20.54	22.18	27.91
(6.0, 6.2]	16.35	5.34	6.67	9.18	11.83	13.04	14.54	16.10	17.81	18.75	20.15	22.95	31.63
(6.2, 6.4]	17.22	5.11	6.46	9.47	12.58	14.69	15.91	17.67	18.47	20.33	22.41	24.07	27.88
(6.4, 6.6]	18.79	5.69	6.61	10.36	13.10	15.70	18.38	19.44	20.81	22.81	24.81	25.55	28.56
(6.6, 6.8]	19.03	5.50	8.62	11.35	12.97	15.55	17.22	19.71	20.96	22.70	25.01	25.70	29.23
(6.8, 7.0]	19.87	5.48	8.28	11.89	13.68	17.06	19.20	20.34	21.95	24.44	25.52	25.97	29.40
(7.0, 7.2]	21.08	5.86	8.15	11.52	14.57	17.60	20.43	23.35	25.63	25.95	26.13	26.57	29.92
(7.2, 7.4]	21.00	5.59	8.28	13.10	14.94	17.45	20.31	21.61	25.15	25.62	26.04	26.66	30.75
(7.4, 7.6]	19.86	5.44	8.75	12.47	14.56	16.06	18.36	20.66	21.56	23.28	25.71	26.84	31.22
(7.6, 7.8]	20.17	5.91	9.13	11.78	14.72	15.65	18.79	20.65	22.36	24.69	26.09	27.71	31.77
(7.8, 8.0]	20.40	5.79	9.57	11.64	15.03	15.67	19.41	20.99	22.74	23.80	25.72	27.52	32.39
(8.0, 8.2]	20.57	5.64	9.77	13.11	15.75	17.14	18.14	19.61	22.47	24.74	25.87	27.82	32.14
(8.2, 8.4]	20.07	5.91	9.99	12.99	15.02	15.83	17.07	18.87	21.67	23.68	26.08	28.10	33.31
(8.4, 8.6]	20.75	6.24	10.06	12.60	14.93	16.56	18.16	21.09	22.88	24.61	27.41	28.46	33.85
(8.6, 8.8]	21.22	6.05	10.44	12.87	15.19	17.24	18.87	21.88	23.23	25.02	27.74	28.75	32.78
(8.8, 9.0]	23.97	5.67	10.98	15.60	18.88	21.51	23.32	24.63	26.78	28.43	28.98	29.50	34.52
(9.0, 9.2]	23.60	6.27	11.22	13.49	17.00	20.83	22.68	24.81	27.32	28.33	28.75	30.50	34.22
(9.2, 9.4]	23.36	6.65	11.91	14.27	16.82	19.07	20.20	24.42	25.91	28.25	30.69	31.61	35.53
(9.4, 9.6]	21.28	7.45	10.23	10.52	13.20	15.98	20.16	20.36	23.75	26.32	27.44	31.98	36.43
(9.6, 9.8]	22.38	7.83	10.45	11.58	12.97	16.02	20.44	23.04	26.51	28.61	29.68	32.35	37.09
(9.8, 10.0]	23.62	7.68	10.92	12.84	14.50	17.70	21.62	24.80	26.88	29.21	30.26	33.19	38.03
(10.0, 10.2]	25.51	7.87	11.23	14.17	19.67	21.08	22.81	25.63	27.35	30.41	32.88	38.48	38.80
(10.2, 10.4]	23.60	6.70	10.82	13.19	18.53	21.16	21.54	23.18	26.75	28.60	29.67	30.89	38.45
(10.4, 10.6]	24.73	7.03	10.74	13.44	19.79	21.25	23.62	26.74	28.31	30.36	30.72	31.18	38.34
(10.6, 10.8]	26.24	5.50	11.13	19.59	21.75	24.67	27.05	27.71	28.16	28.98	30.68	31.37	36.93
(10.8, 11.0]	24.61	6.73	11.79	13.34	19.07	20.96	24.14	27.43	28.07	29.40	30.11	31.52	36.68
(11.0, 11.2]	25.13	5.91	14.17	18.41	19.31	21.13	23.05	26.68	27.68	28.92	31.11	31.98	37.25
(11.2, 11.4]	26.60	5.75	14.30	16.24	21.97	24.04	25.76	27.66	28.33	30.63	32.04	32.37	37.27
(11.4, 11.6]	25.70	5.90	12.56	16.56	21.73	22.57	24.63	25.82	28.05	29.93	31.20	32.28	37.23
(11.6, 11.8]	26.44	6.32	12.59	17.40	21.89	22.77	24.46	27.71	29.02	31.64	32.46	32.69	37.56
(11.8, 12.0]	27.62	6.25	13.26	18.59	22.38	23.64	26.34	29.02	31.13	32.41	33.77	33.96	37.16
(12.0, 12.2]	28.63	5.66	16.21	20.48	22.78	25.30	27.76	30.16	31.40	32.01	33.78	34.80	38.08
(12.2, 12.4]	30.57	5.25	18.35	22.57	25.50	27.61	30.78	32.19	33.05	33.53	34.45	37.41	38.28
(12.4, 12.6]	27.01	5.78	17.60	20.72	22.15	22.61	23.37	25.87	27.88	31.12	33.32	34.42	38.31
(12.6, 12.8]	28.04	5.66	18.26	19.80	22.65	24.87	26.42	28.05	29.48	31.59	34.01	35.53	38.27
(12.8, 13.0]	31.08	4.84	19.31	25.90	27.06	28.94	29.50	30.29	32.41	34.43	36.17	36.36	38.24
(13.0, 13.2]	31.37	5.01	19.30	26.00	27.32	29.22	30.38	31.18	33.18	34.93	36.06	38.16	38.24
(13.2, 13.4]	31.39	5.20	19.20	24.71	27.24	28.31	30.24	32.48	34.13	35.54	36.04	38.13	38.24
(13.4, 13.6]	31.59	4.84	19.49	25.16	27.58	29.12	30.97	32.75	34.16	34.70	35.83	36.13	38.22
(13.6, 13.8]	31.24	4.49	19.72	26.80	28.02	28.53	29.53	31.60	33.82	34.59	34.86	36.17	38.22
(13.8, 14.0]	31.55	4.86	19.76	22.43	28.60	29.07	31.76	33.57	34.39	34.67	35.30	36.24	38.22
(14.0, 14.2]	33.26	3.77	19.93	29.14	31.14	32.69	33.29	34.56	34.73	35.19	36.14	36.40	38.21
(14.2, 14.4]	32.97	4.73	20.75	24.85	27.84	32.39	34.62	34.85	35.78	36.13	36.31	36.45	38.22
(14.4, 14.6]	33.19	4.33	20.40	25.63	30.05	32.44	34.69	34.76	34.86	35.16	36.12	38.16	38.21
(14.6, 14.8]	32.49	4.32	20.01	25.10	28.31	32.20	32.75	34.81	34.90	34.93	34.96	36.27	38.25
(14.8, 15.0]	32.05	4.59	20.08	25.03	25.61	31.78	32.83	34.13	34.76	34.85	34.96	36.57	38.25

NTUA Campus Ku-band - Ka-band Instantaneous Frequency Scaling													
Start Date			1st July 2017										
End Date			30th June 2020										
Concurrent Data Availability			94.16 %										
Ku-band attenuation [dB]	Instantaneous Frequency Scaling Factor												
	Mean value	Std value	Percentile										
			1st	10th	20th	30th	40th	50th	60th	70th	80th	90th	99th
(1.0, 1.2]	3.65	1.52	1.11	1.81	2.27	2.75	3.16	3.55	3.89	4.28	4.83	5.69	7.96
(1.2, 1.4]	3.35	1.33	1.07	1.64	2.07	2.59	2.92	3.31	3.65	4.01	4.40	5.06	6.86
(1.4, 1.6]	3.10	1.33	1.03	1.34	1.70	2.31	2.73	3.07	3.39	3.75	4.20	4.80	6.64
(1.6, 1.8]	3.06	1.47	1.08	1.37	1.50	1.80	2.57	2.95	3.32	3.81	4.37	5.10	6.93
(1.8, 2.0]	3.14	1.24	1.12	1.51	1.93	2.40	2.72	3.06	3.39	3.73	4.17	4.81	6.44
(2.0, 2.2]	2.99	1.21	1.08	1.46	1.83	2.16	2.51	2.97	3.33	3.70	4.01	4.55	6.09
(2.2, 2.4]	2.95	1.19	1.06	1.46	1.78	2.03	2.51	2.96	3.32	3.57	3.92	4.54	5.79
(2.4, 2.6]	3.11	1.29	1.05	1.60	1.89	2.21	2.65	3.04	3.41	3.66	4.10	4.88	6.69
(2.6, 2.8]	2.96	1.12	1.06	1.51	1.87	2.20	2.57	2.96	3.27	3.55	3.88	4.45	5.46
(2.8, 3.0]	3.04	1.07	1.09	1.61	1.93	2.31	2.76	3.03	3.34	3.61	4.00	4.47	5.23
(3.0, 3.2]	2.88	1.06	1.05	1.58	1.83	2.00	2.53	2.90	3.23	3.47	3.72	4.31	5.85
(3.2, 3.4]	2.74	1.04	1.05	1.40	1.67	1.96	2.33	2.81	3.07	3.36	3.68	4.18	4.93
(3.4, 3.6]	2.96	0.90	1.03	1.74	2.12	2.40	2.83	3.08	3.32	3.48	3.64	4.10	4.83
(3.6, 3.8]	2.90	1.01	1.02	1.48	2.00	2.40	2.67	2.88	3.17	3.45	3.70	4.14	5.39
(3.8, 4.0]	2.71	1.09	1.04	1.18	1.76	2.05	2.36	2.57	2.89	3.32	3.63	4.15	5.44
(4.0, 4.2]	2.83	1.01	1.06	1.54	1.90	2.25	2.52	2.80	3.05	3.29	3.62	4.18	5.50
(4.2, 4.4]	2.77	1.01	1.07	1.52	1.93	2.21	2.41	2.58	2.90	3.22	3.54	4.13	5.66
(4.4, 4.6]	2.77	0.94	1.07	1.54	1.90	2.25	2.47	2.68	2.92	3.24	3.55	4.00	5.35
(4.6, 4.8]	2.73	0.97	1.02	1.48	1.86	2.15	2.40	2.61	2.90	3.16	3.53	4.06	5.21
(4.8, 5.0]	2.91	0.92	1.09	1.73	2.16	2.39	2.51	2.73	3.17	3.48	3.90	4.24	4.92
(5.0, 5.2]	2.76	0.92	1.08	1.53	2.07	2.23	2.49	2.62	2.94	3.24	3.60	3.99	5.02
(5.2, 5.4]	2.82	1.05	1.11	1.51	1.89	2.13	2.40	2.63	3.09	3.36	3.77	4.50	5.09
(5.4, 5.6]	2.91	0.95	1.14	1.62	2.03	2.35	2.63	2.87	3.22	3.41	3.57	4.33	4.92
(5.6, 5.8]	2.79	0.84	1.12	1.59	1.96	2.32	2.60	2.94	3.08	3.23	3.39	3.72	4.86
(5.8, 6.0]	2.88	0.76	1.18	1.84	2.22	2.51	2.87	2.99	3.07	3.18	3.51	3.78	4.76
(6.0, 6.2]	2.68	0.88	1.09	1.50	1.94	2.12	2.38	2.66	2.92	3.06	3.30	3.75	5.17
(6.2, 6.4]	2.73	0.81	1.02	1.50	2.00	2.34	2.53	2.81	2.94	3.22	3.54	3.79	4.41
(6.4, 6.6]	2.89	0.87	1.03	1.60	2.01	2.41	2.83	2.99	3.21	3.51	3.80	3.91	4.36
(6.6, 6.8]	2.84	0.82	1.29	1.70	1.94	2.31	2.57	2.96	3.13	3.40	3.74	3.85	4.39
(6.8, 7.0]	2.88	0.79	1.20	1.72	1.98	2.47	2.78	2.95	3.19	3.55	3.71	3.75	4.24
(7.0, 7.2]	2.97	0.82	1.16	1.63	2.06	2.47	2.87	3.28	3.59	3.64	3.70	3.72	4.21
(7.2, 7.4]	2.88	0.77	1.14	1.78	2.04	2.40	2.78	2.96	3.44	3.54	3.59	3.67	4.19
(7.4, 7.6]	2.65	0.73	1.16	1.65	1.94	2.14	2.44	2.76	2.88	3.09	3.44	3.58	4.16
(7.6, 7.8]	2.62	0.77	1.19	1.54	1.91	2.03	2.44	2.69	2.91	3.19	3.38	3.60	4.13
(7.8, 8.0]	2.58	0.73	1.21	1.47	1.90	1.99	2.46	2.64	2.88	3.01	3.27	3.49	4.11
(8.0, 8.2]	2.54	0.70	1.20	1.62	1.94	2.10	2.25	2.43	2.77	3.04	3.20	3.44	3.99
(8.2, 8.4]	2.42	0.71	1.21	1.55	1.81	1.92	2.06	2.28	2.61	2.85	3.14	3.37	4.01
(8.4, 8.6]	2.44	0.73	1.18	1.49	1.75	1.95	2.14	2.47	2.68	2.89	3.23	3.35	3.97
(8.6, 8.8]	2.44	0.69	1.21	1.47	1.76	1.99	2.17	2.50	2.66	2.87	3.20	3.32	3.78
(8.8, 9.0]	2.70	0.64	1.23	1.75	2.11	2.42	2.63	2.76	3.02	3.20	3.25	3.34	3.88
(9.0, 9.2]	2.59	0.69	1.24	1.49	1.87	2.29	2.49	2.73	2.99	3.09	3.17	3.34	3.77
(9.2, 9.4]	2.51	0.72	1.28	1.54	1.80	2.06	2.16	2.63	2.78	3.04	3.32	3.40	3.84
(9.4, 9.6]	2.24	0.78	1.08	1.10	1.39	1.68	2.12	2.13	2.51	2.77	2.89	3.37	3.84
(9.6, 9.8]	2.31	0.81	1.09	1.21	1.33	1.66	2.11	2.37	2.74	2.95	3.07	3.33	3.83
(9.8, 10.0]	2.39	0.77	1.11	1.30	1.46	1.78	2.19	2.51	2.72	2.94	3.06	3.33	3.82
(10.0, 10.2]	2.53	0.78	1.12	1.41	1.94	2.10	2.26	2.55	2.71	3.01	3.28	3.81	3.86
(10.2, 10.4]	2.29	0.65	1.05	1.29	1.79	2.05	2.10	2.27	2.61	2.77	2.88	3.00	3.73
(10.4, 10.6]	2.36	0.67	1.02	1.29	1.88	2.02	2.25	2.52	2.70	2.88	2.94	2.97	3.64
(10.6, 10.8]	2.45	0.51	1.04	1.84	2.03	2.30	2.54	2.60	2.65	2.72	2.87	2.94	3.45
(10.8, 11.0]	2.26	0.62	1.09	1.22	1.74	1.92	2.23	2.50	2.58	2.69	2.75	2.89	3.38
(11.0, 11.2]	2.26	0.53	1.28	1.66	1.74	1.90	2.06	2.41	2.49	2.61	2.80	2.87	3.36
(11.2, 11.4]	2.36	0.51	1.26	1.44	1.95	2.14	2.28	2.45	2.51	2.71	2.85	2.87	3.30
(11.4, 11.6]	2.24	0.51	1.10	1.43	1.89	1.96	2.14	2.24	2.43	2.61	2.71	2.80	3.24
(11.6, 11.8]	2.26	0.54	1.08	1.49	1.87	1.95	2.08	2.37	2.49	2.72	2.78	2.79	3.21
(11.8, 12.0]	2.32	0.52	1.12	1.56	1.88	1.99	2.22	2.44	2.62	2.72	2.84	2.85	3.12
(12.0, 12.2]	2.37	0.47	1.34	1.68	1.88	2.09	2.29	2.50	2.59	2.65	2.79	2.89	3.13
(12.2, 12.4]	2.48	0.43	1.49	1.83	2.08	2.26	2.48	2.62	2.68	2.73	2.79	3.05	3.09
(12.4, 12.6]	2.16	0.46	1.40	1.67	1.76	1.80	1.87	2.08	2.23	2.48	2.68	2.75	3.08
(12.6, 12.8]	2.21	0.45	1.45	1.57	1.79	1.97	2.08	2.21	2.33	2.49	2.68	2.80	3.03
(12.8, 13.0]	2.41	0.37	1.50	2.01	2.11	2.25	2.29	2.33	2.52	2.68	2.81	2.83	2.97
(13.0, 13.2]	2.40	0.38	1.48	1.98	2.08	2.22	2.32	2.39	2.53	2.67	2.76	2.90	2.94
(13.2, 13.4]	2.36	0.39	1.45	1.86	2.04	2.14	2.28	2.44	2.56	2.67	2.71	2.85	2.88
(13.4, 13.6]	2.34	0.36	1.45	1.86	2.04	2.16	2.30	2.43	2.53	2.56	2.65	2.68	2.84
(13.6, 13.8]	2.28	0.33	1.45	1.96	2.04	2.09	2.15	2.30	2.47	2.51	2.55	2.64	2.80
(13.8, 14.0]	2.27	0.35	1.42	1.62	2.07	2.10	2.29	2.42	2.47	2.50	2.54	2.61	2.75
(14.0, 14.2]	2.36	0.27	1.41	2.07	2.21	2.31	2.37	2.45	2.46	2.49	2.56	2.59	2.72
(14.2, 14.4]	2.30	0.33	1.45	1.75	1.95	2.26	2.42	2.44	2.51	2.52	2.53	2.55	2.69
(14.4, 14.6]	2.29	0.30	1.41	1.77	2.07	2.24	2.39	2.40	2.40	2.44	2.50	2.62	2.65
(14.6, 14.8]	2.21	0.30	1.36	1.70	1.93	2.19	2.23	2.36	2.37	2.38	2.39	2.47	2.60
(14.8, 15.0]	2.15	0.31	1.35	1.68	1.72	2.13	2.20	2.29	2.33	2.34	2.36	2.46	2.57

NTUA Campus Ku-band - Ka-band Instantaneous Frequency Scaling				
Start Date				1st July 2017
End Date				30th June 2020
Concurrent Data Availability				94.16 %
Exceedance Probability [%]	**Attenuation Ku [dB]**	**Attenuation Ka [dB]**	**Equiprobable Ratio Attenuation Ka [dB] / Attenuation Ku [dB]**	**IFSF Ka-band Attenuation [dB] / Ku-band Attenuation [dB], A_{Ku} > 1.0 dB (0.13 % of concurrent data)**
50	0.006	0.018	2.949	2.973
30	0.089	0.113	1.274	3.668
20	0.129	0.159	1.234	4.107
10	0.169	0.242	1.431	4.768
5	0.189	0.447	2.362	5.408
3	0.197	0.669	3.391	5.831
2	0.238	0.920	3.862	6.142
1	0.356	1.555	4.372	6.711
0.5	0.494	2.358	4.773	7.271
0.3	0.735	2.936	3.998	7.657
0.2	1.002	3.456	3.450	8.415
0.1	1.734	4.607	2.657	9.292
0.05	3.223	7.399	2.296	9.986
0.03	4.851	10.571	2.179	10.384
0.02	5.888	13.584	2.307	10.753
0.01	7.599	21.422	2.819	11.122
0.005	11.851	29.570	2.495	11.367
0.003	15.068	34.998	2.323	11.560
0.002	18.432	36.618	1.987	11.747
0.001	25.802	38.253	1.483	11.973

NTUA Campus Ku-band - Q-band Instantaneous Frequency Scaling													
Start Date			1st July 2017										
End Date			30th June 2019										
Concurrent Data Availability			93.26 %										
Ku-band attenuation [dB]	Q-band Attenuation [dB]												
	Mean value	Std value	Percentile										
			1st	10th	20th	30th	40th	50th	60th	70th	80th	90th	99th
(1.0, 1.2]	11.48	6.74	1.18	1.86	4.96	6.92	9.47	11.24	13.23	15.26	17.39	20.35	28.23
(1.2, 1.4]	13.93	7.12	1.67	4.21	6.63	9.74	11.45	13.79	16.36	18.31	20.06	23.44	30.38
(1.4, 1.6]	13.71	8.22	2.04	3.80	5.24	6.76	9.93	12.79	15.89	18.97	21.54	25.94	32.02
(1.6, 1.8]	15.36	9.15	2.11	5.20	6.62	7.53	8.78	14.25	18.10	21.11	25.18	29.62	32.22
(1.8, 2.0]	19.18	8.56	3.29	7.74	10.12	13.47	16.67	19.35	21.79	24.77	28.47	31.46	32.52
(2.0, 2.2]	19.61	8.68	3.34	7.85	10.87	13.22	16.70	20.03	23.13	26.16	28.93	31.17	32.57
(2.2, 2.4]	19.81	9.24	2.59	6.83	10.57	12.58	16.12	20.43	24.24	27.53	30.14	31.83	32.40
(2.4, 2.6]	19.75	9.94	2.69	5.89	9.71	11.72	15.83	20.89	24.70	28.37	30.66	32.05	32.37
(2.6, 2.8]	17.56	10.84	2.75	3.52	4.76	9.01	12.71	17.05	21.80	27.35	30.44	32.04	32.43
(2.8, 3.0]	22.29	9.40	3.13	8.32	12.28	15.93	20.00	24.96	28.88	30.67	31.98	32.20	32.46
(3.0, 3.2]	22.35	9.13	4.97	8.75	11.83	15.87	20.50	23.47	28.08	30.67	32.00	32.19	32.52
(3.2, 3.4]	22.52	9.14	5.20	8.16	12.11	17.59	21.45	23.74	28.12	30.67	31.98	32.18	32.47
(3.4, 3.6]	21.35	10.40	4.09	6.24	8.40	12.44	19.90	24.24	29.62	30.99	32.00	32.19	32.54
(3.6, 3.8]	22.77	9.31	3.82	7.15	13.78	17.08	20.40	25.91	29.82	31.17	32.06	32.25	32.55
(3.8, 4.0]	23.76	8.09	4.14	12.21	17.08	19.34	20.53	26.28	28.20	31.03	32.04	32.18	32.52
(4.0, 4.2]	19.16	10.42	4.44	5.44	7.77	8.27	15.36	20.95	26.03	27.59	31.10	32.14	32.51
(4.2, 4.4]	22.60	9.35	4.26	7.75	9.38	17.60	22.02	26.27	27.76	30.83	32.02	32.28	32.52
(4.4, 4.6]	26.61	6.94	8.00	15.39	21.25	24.69	27.82	29.55	30.94	32.05	32.19	32.31	32.54
(4.6, 4.8]	26.16	7.05	5.89	12.87	21.26	24.37	26.17	28.25	30.73	31.95	32.10	32.21	32.54
(4.8, 5.0]	27.97	6.52	5.58	18.73	24.84	26.41	29.95	31.64	32.06	32.17	32.28	32.40	32.55
(5.0, 5.2]	26.60	8.45	5.24	10.79	22.59	26.35	28.86	31.30	31.97	32.10	32.29	32.44	32.60
(5.2, 5.4]	22.96	9.68	5.39	9.05	10.81	13.42	23.29	27.45	30.57	32.01	32.31	32.49	32.58
(5.4, 5.6]	22.55	9.83	6.71	8.97	10.23	12.02	23.00	26.34	28.78	32.09	32.30	32.46	32.59
(5.6, 5.8]	23.31	9.94	7.23	8.11	9.69	14.07	25.29	27.65	30.66	32.18	32.33	32.45	32.63
(5.8, 6.0]	28.34	7.31	8.06	13.03	26.27	27.78	31.96	32.18	32.28	32.32	32.39	32.46	32.68
(6.0, 6.2]	20.23	11.09	6.24	6.62	7.34	8.12	12.54	25.52	27.75	31.15	32.15	32.44	32.61
(6.2, 6.4]	22.98	10.59	6.31	7.91	8.41	12.33	24.57	27.99	31.89	32.20	32.44	32.59	32.65
(6.4, 6.6]	22.22	10.77	6.49	6.89	9.19	10.92	20.24	27.55	31.99	32.21	32.36	32.55	32.60
(6.6, 6.8]	22.73	10.83	6.74	6.94	7.07	11.10	25.10	27.85	32.00	32.24	32.35	32.51	32.59
(6.8, 7.0]	24.05	10.66	6.87	7.02	7.46	20.75	26.59	31.39	32.15	32.36	32.50	32.54	32.60
(7.0, 7.2]	25.44	9.85	7.62	8.10	8.77	24.81	28.77	32.09	32.43	32.50	32.52	32.55	32.62
(7.2, 7.4]	27.03	8.84	8.39	9.09	18.97	27.80	31.84	32.14	32.43	32.48	32.54	32.58	32.66
(7.4, 7.6]	27.68	7.49	9.66	12.72	23.12	27.71	30.98	31.94	32.06	32.35	32.46	32.52	32.60
(7.6, 7.8]	28.68	5.79	9.61	19.70	27.56	28.68	29.01	31.96	32.23	32.35	32.45	32.51	32.59
(7.8, 8.0]	28.78	5.60	10.80	19.66	27.65	28.69	29.20	31.98	32.03	32.29	32.42	32.52	32.59
(8.0, 8.2]	28.53	6.50	9.29	18.12	27.11	28.70	31.91	32.12	32.27	32.41	32.43	32.55	32.60
(8.2, 8.4]	28.91	5.97	9.76	19.22	27.64	28.89	31.33	31.95	32.20	32.29	32.45	32.55	32.62
(8.4, 8.6]	29.61	4.70	12.37	23.62	27.70	28.82	31.89	31.98	32.23	32.37	32.44	32.56	32.62
(8.6, 8.8]	30.21	3.72	15.82	24.97	28.03	28.83	31.89	32.18	32.23	32.41	32.47	32.58	32.72
(8.8, 9.0]	30.80	3.61	16.02	27.69	28.95	31.95	32.20	32.28	32.39	32.43	32.49	32.60	32.73
(9.0, 9.2]	30.11	4.42	16.34	23.53	28.75	30.19	32.29	32.37	32.40	32.41	32.43	32.55	32.74
(9.2, 9.4]	30.33	3.28	17.10	26.92	28.42	29.70	30.22	31.92	32.30	32.42	32.55	32.61	32.74
(9.4, 9.6]	28.93	4.00	17.37	23.67	24.16	27.56	28.76	30.21	31.99	32.08	32.30	32.51	32.74
(9.6, 9.8]	29.36	3.70	17.70	24.23	25.53	27.55	28.84	31.92	32.24	32.26	32.36	32.54	32.74
(9.8, 10.0]	29.86	3.53	17.90	25.57	27.39	28.62	30.57	31.99	32.26	32.33	32.46	32.54	32.73
(10.0, 10.2]	30.60	3.12	18.18	27.26	28.78	30.23	31.94	32.19	32.31	32.47	32.49	32.60	32.98
(10.2, 10.4]	30.37	3.28	18.55	27.08	27.85	28.80	31.36	32.15	32.31	32.49	32.51	32.96	33.00
(10.4, 10.6]	30.61	3.00	19.39	26.97	28.41	29.48	32.14	32.17	32.20	32.36	32.49	32.74	32.99
(10.6, 10.8]	30.71	3.35	19.36	27.56	27.70	32.04	32.18	32.23	32.40	32.40	32.45	32.72	32.97
(10.8, 11.0]	29.56	4.00	19.48	22.85	24.87	27.67	31.36	32.20	32.30	32.41	32.43	32.46	32.94
(11.0, 11.2]	30.61	2.75	21.54	26.48	27.67	29.62	32.01	32.23	32.25	32.40	32.43	32.51	32.91
(11.2, 11.4]	30.57	2.73	20.45	27.56	27.67	28.79	31.79	32.24	32.26	32.30	32.39	32.60	32.89
(11.4, 11.6]	30.63	2.73	21.12	27.14	28.55	29.50	31.77	32.16	32.29	32.37	32.50	32.58	32.88
(11.6, 11.8]	30.52	2.89	21.80	26.00	27.65	30.51	31.91	32.02	32.25	32.27	32.32	32.43	32.86
(11.8, 12.0]	30.48	2.87	22.86	25.82	27.62	29.30	31.92	32.03	32.27	32.36	32.39	32.46	32.86
(12.0, 12.2]	30.93	2.59	23.74	27.56	28.71	31.99	32.13	32.30	32.32	32.36	32.41	32.52	32.85
(12.2, 12.4]	30.29	2.79	24.54	25.76	27.53	27.57	31.91	32.14	32.31	32.37	32.40	32.80	32.92
(12.4, 12.6]	31.05	2.49	25.20	27.53	28.73	31.89	32.01	32.18	32.40	32.60	32.96	33.04	33.07
(12.6, 12.8]	31.28	1.75	27.54	28.74	28.77	31.91	31.95	32.01	32.23	32.38	32.52	32.55	32.87
(12.8, 13.0]	31.24	1.80	27.56	28.77	28.78	30.22	32.15	32.32	32.37	32.51	32.52	32.54	32.98
(13.0, 13.2]	31.67	1.60	27.57	28.79	31.99	32.08	32.28	32.33	32.38	32.50	32.51	32.56	33.12
(13.2, 13.4]	31.42	1.85	27.57	27.68	28.80	32.01	32.22	32.33	32.36	32.49	32.51	32.79	33.19
(13.4, 13.6]	31.72	1.59	27.59	28.78	31.99	32.05	32.25	32.34	32.47	32.49	32.55	32.90	33.20
(13.6, 13.8]	31.52	1.79	27.59	27.72	29.56	32.05	32.25	32.34	32.46	32.48	32.51	32.67	33.18
(13.8, 14.0]	31.67	1.52	27.62	28.72	31.99	32.02	32.03	32.07	32.28	32.34	32.45	32.56	33.13
(14.0, 14.2]	31.86	1.29	27.70	28.82	32.02	32.05	32.26	32.28	32.30	32.34	32.44	32.55	33.04
(14.2, 14.4]	32.01	1.41	27.61	28.82	32.02	32.06	32.30	32.38	32.47	32.93	32.95	32.96	33.00
(14.4, 14.6]	31.88	1.41	27.71	28.81	32.02	32.02	32.18	32.36	32.38	32.45	32.84	32.95	33.01
(14.6, 14.8]	31.68	1.70	27.67	28.67	29.85	32.05	32.24	32.44	32.50	32.79	32.87	32.92	33.02
(14.8, 15.0]	31.75	1.67	27.68	28.68	30.96	32.05	32.31	32.47	32.67	32.80	32.84	32.89	33.02

NTUA Campus Ku-band - Q-band Instantaneous Frequency Scaling													
Start Date			1st July 2017										
End Date			30th June 2019										
Concurrent Data Availability			93.26 %										
Ku-band attenuation [dB]	Instantaneous Frequency Scaling Factor												
	Mean value	Std value	Percentile										
			1st	10th	20th	30th	40th	50th	60th	70th	80th	90th	99th
(1.0, 1.2]	10.54	6.15	1.09	1.73	4.53	6.42	8.71	10.26	12.14	14.04	15.80	18.75	25.76
(1.2, 1.4]	10.77	5.51	1.30	3.23	5.18	7.58	8.88	10.75	12.61	14.17	15.65	18.10	23.09
(1.4, 1.6]	9.15	5.46	1.38	2.48	3.48	4.47	6.73	8.61	10.58	12.65	14.37	17.33	20.63
(1.6, 1.8]	9.07	5.38	1.27	3.10	3.98	4.47	5.10	8.32	10.65	12.40	14.91	17.39	19.41
(1.8, 2.0]	10.13	4.53	1.77	4.16	5.30	7.07	8.76	10.24	11.53	13.07	15.08	16.47	17.61
(2.0, 2.2]	9.36	4.15	1.54	3.68	5.19	6.26	7.90	9.57	11.00	12.51	13.85	14.77	15.97
(2.2, 2.4]	8.63	4.01	1.15	3.01	4.56	5.50	7.09	8.92	10.57	11.98	12.96	13.64	14.48
(2.4, 2.6]	7.91	3.99	1.05	2.38	3.83	4.74	6.33	8.37	9.97	11.36	12.25	12.74	13.33
(2.6, 2.8]	6.52	4.02	1.04	1.31	1.79	3.40	4.64	6.26	8.10	10.13	11.31	11.76	12.31
(2.8, 3.0]	7.69	3.25	1.08	2.96	4.22	5.45	6.82	8.60	10.05	10.56	10.88	11.17	11.44
(3.0, 3.2]	7.22	2.96	1.60	2.78	3.85	5.19	6.55	7.67	9.13	9.93	10.22	10.47	10.71
(3.2, 3.4]	6.83	2.77	1.58	2.53	3.70	5.40	6.54	7.26	8.49	9.28	9.58	9.79	10.05
(3.4, 3.6]	6.11	2.98	1.16	1.79	2.40	3.50	5.68	6.86	8.39	8.87	9.11	9.27	9.47
(3.6, 3.8]	6.16	2.53	1.03	1.93	3.72	4.64	5.48	6.98	8.00	8.47	8.63	8.77	8.97
(3.8, 4.0]	6.10	2.07	1.07	3.12	4.42	4.97	5.31	6.68	7.31	7.95	8.16	8.32	8.48
(4.0, 4.2]	4.67	2.54	1.10	1.31	1.90	2.01	3.81	5.13	6.27	6.68	7.62	7.83	8.04
(4.2, 4.4]	5.26	2.17	1.01	1.80	2.19	4.11	5.12	6.10	6.39	7.18	7.40	7.53	7.67
(4.4, 4.6]	5.91	1.55	1.77	3.46	4.72	5.47	6.13	6.61	6.89	7.07	7.15	7.24	7.34
(4.6, 4.8]	5.57	1.50	1.24	2.75	4.54	5.21	5.54	6.05	6.58	6.73	6.81	6.91	7.00
(4.8, 5.0]	5.71	1.33	1.15	3.84	5.07	5.44	6.13	6.43	6.49	6.56	6.61	6.65	6.73
(5.0, 5.2]	5.22	1.66	1.03	2.09	4.43	5.21	5.60	6.15	6.24	6.29	6.33	6.38	6.47
(5.2, 5.4]	4.33	1.83	1.02	1.70	2.02	2.54	4.39	5.13	5.74	6.00	6.08	6.15	6.24
(5.4, 5.6]	4.10	1.79	1.23	1.63	1.88	2.20	4.15	4.83	5.18	5.80	5.86	5.93	6.00
(5.6, 5.8]	4.09	1.74	1.26	1.43	1.70	2.47	4.45	4.82	5.39	5.61	5.65	5.70	5.78
(5.8, 6.0]	4.81	1.25	1.38	2.20	4.46	4.75	5.38	5.43	5.47	5.49	5.52	5.55	5.60
(6.0, 6.2]	3.32	1.82	1.02	1.09	1.20	1.33	2.04	4.18	4.56	5.10	5.26	5.32	5.40
(6.2, 6.4]	3.65	1.68	1.02	1.26	1.33	1.96	3.90	4.47	5.06	5.10	5.13	5.16	5.23
(6.4, 6.6]	3.42	1.66	1.01	1.05	1.39	1.66	3.12	4.24	4.89	4.94	4.97	5.01	5.08
(6.6, 6.8]	3.40	1.62	1.01	1.03	1.06	1.68	3.75	4.17	4.75	4.80	4.83	4.87	4.93
(6.8, 7.0]	3.49	1.54	1.01	1.03	1.07	3.01	3.86	4.52	4.65	4.67	4.70	4.73	4.77
(7.0, 7.2]	3.58	1.38	1.08	1.14	1.22	3.46	4.05	4.50	4.53	4.55	4.57	4.60	4.64
(7.2, 7.4]	3.71	1.21	1.16	1.25	2.60	3.83	4.33	4.40	4.43	4.46	4.49	4.51	4.53
(7.4, 7.6]	3.69	1.00	1.30	1.70	3.11	3.73	4.17	4.25	4.28	4.30	4.33	4.37	4.39
(7.6, 7.8]	3.72	0.75	1.24	2.55	3.56	3.71	3.80	4.14	4.17	4.19	4.21	4.23	4.27
(7.8, 8.0]	3.64	0.71	1.35	2.48	3.48	3.62	3.71	4.03	4.06	4.08	4.10	4.13	4.16
(8.0, 8.2]	3.52	0.80	1.14	2.24	3.32	3.53	3.91	3.95	3.97	3.99	4.01	4.03	4.06
(8.2, 8.4]	3.48	0.72	1.18	2.34	3.33	3.47	3.78	3.84	3.87	3.89	3.91	3.93	3.96
(8.4, 8.6]	3.48	0.55	1.46	2.77	3.27	3.37	3.74	3.77	3.78	3.80	3.82	3.84	3.87
(8.6, 8.8]	3.47	0.43	1.82	2.87	3.24	3.33	3.66	3.69	3.71	3.72	3.73	3.75	3.78
(8.8, 9.0]	3.46	0.41	1.79	3.11	3.28	3.59	3.61	3.62	3.63	3.65	3.66	3.69	3.70
(9.0, 9.2]	3.31	0.49	1.80	2.60	3.14	3.32	3.53	3.54	3.55	3.56	3.58	3.59	3.61
(9.2, 9.4]	3.26	0.35	1.83	2.88	3.07	3.20	3.28	3.44	3.47	3.49	3.50	3.52	3.54
(9.4, 9.6]	3.04	0.42	1.82	2.49	2.54	2.89	3.01	3.19	3.35	3.38	3.40	3.43	3.46
(9.6, 9.8]	3.03	0.38	1.82	2.52	2.65	2.83	2.97	3.28	3.31	3.33	3.34	3.36	3.39
(9.8, 10.0]	3.02	0.35	1.82	2.59	2.76	2.88	3.09	3.23	3.25	3.26	3.28	3.29	3.32
(10.0, 10.2]	3.03	0.31	1.81	2.71	2.83	2.99	3.15	3.18	3.20	3.22	3.23	3.24	3.26
(10.2, 10.4]	2.95	0.32	1.80	2.64	2.70	2.81	3.03	3.12	3.14	3.15	3.17	3.20	3.23
(10.4, 10.6]	2.92	0.29	1.86	2.59	2.72	2.81	3.04	3.06	3.07	3.09	3.10	3.12	3.16
(10.6, 10.8]	2.87	0.31	1.82	2.57	2.61	2.98	3.00	3.01	3.02	3.03	3.05	3.06	3.10
(10.8, 11.0]	2.71	0.37	1.78	2.10	2.27	2.54	2.88	2.95	2.96	2.97	2.98	2.99	3.03
(11.0, 11.2]	2.76	0.25	1.94	2.38	2.49	2.69	2.88	2.90	2.91	2.92	2.93	2.94	2.98
(11.2, 11.4]	2.71	0.24	1.81	2.44	2.47	2.55	2.80	2.85	2.86	2.86	2.87	2.88	2.92
(11.4, 11.6]	2.66	0.24	1.84	2.36	2.47	2.56	2.76	2.79	2.81	2.82	2.83	2.84	2.87
(11.6, 11.8]	2.61	0.25	1.87	2.23	2.38	2.61	2.72	2.74	2.75	2.76	2.77	2.78	2.82
(11.8, 12.0]	2.56	0.24	1.93	2.18	2.32	2.47	2.68	2.69	2.70	2.71	2.72	2.74	2.78
(12.0, 12.2]	2.56	0.21	1.97	2.27	2.36	2.63	2.66	2.67	2.67	2.68	2.68	2.70	2.73
(12.2, 12.4]	2.46	0.23	2.01	2.09	2.23	2.25	2.58	2.61	2.62	2.63	2.64	2.65	2.68
(12.4, 12.6]	2.48	0.20	2.03	2.20	2.29	2.53	2.56	2.58	2.59	2.61	2.62	2.64	2.66
(12.6, 12.8]	2.46	0.14	2.16	2.25	2.27	2.51	2.52	2.53	2.54	2.55	2.56	2.57	2.59
(12.8, 13.0]	2.42	0.14	2.14	2.23	2.24	2.34	2.49	2.49	2.51	2.52	2.53	2.53	2.56
(13.0, 13.2]	2.42	0.12	2.11	2.19	2.43	2.45	2.46	2.47	2.48	2.48	2.49	2.50	2.53
(13.2, 13.4]	2.36	0.14	2.06	2.09	2.17	2.40	2.42	2.43	2.43	2.44	2.45	2.46	2.50
(13.4, 13.6]	2.35	0.12	2.04	2.13	2.35	2.38	2.39	2.39	2.40	2.41	2.42	2.43	2.46
(13.6, 13.8]	2.30	0.13	2.00	2.03	2.16	2.34	2.35	2.36	2.36	2.37	2.38	2.39	2.43
(13.8, 14.0]	2.28	0.11	1.99	2.07	2.29	2.30	2.31	2.32	2.32	2.33	2.34	2.35	2.39
(14.0, 14.2]	2.26	0.09	1.97	2.05	2.27	2.28	2.28	2.29	2.29	2.30	2.30	2.32	2.35
(14.2, 14.4]	2.24	0.10	1.94	2.02	2.23	2.25	2.25	2.27	2.27	2.29	2.31	2.32	2.32
(14.4, 14.6]	2.20	0.10	1.90	1.99	2.21	2.21	2.22	2.22	2.23	2.24	2.26	2.27	2.29
(14.6, 14.8]	2.16	0.12	1.88	1.95	2.04	2.18	2.19	2.20	2.21	2.23	2.23	2.24	2.25
(14.8, 15.0]	2.13	0.11	1.86	1.93	2.08	2.16	2.17	2.18	2.20	2.20	2.21	2.21	2.22

NTUA Campus Ku-band - Q-band Instantaneous Frequency Scaling				
Start Date				1st July 2017
End Date				30th June 2019
Concurrent Data Availability				93.26 %
Exceedance Probability [%]	**Attenuation Ku [dB]**	**Attenuation Q [dB]**	**Equiprobable Ratio Attenuation Q [dB] / Attenuation Ku [dB]**	**IFSF Q-band Attenuation [dB] / Ku-band Attenuation [dB], A_{Ku} > 1.0 dB (0.16 % of concurrent data)**
50	0.008	0.027	3.653	7.022
30	0.090	0.114	1.260	10.667
20	0.131	0.156	1.193	12.780
10	0.171	0.198	1.157	15.422
5	0.191	0.468	2.445	17.609
3	0.199	1.030	5.169	18.894
2	0.281	1.910	6.809	19.721
1	0.375	3.955	10.532	21.466
0.5	0.568	6.456	11.374	23.484
0.3	0.895	8.731	9.758	24.551
0.2	1.238	10.910	8.816	25.490
0.1	2.187	16.591	7.585	26.927
0.05	3.947	25.995	6.585	28.745
0.03	5.325	30.710	5.768	29.674
0.02	6.426	32.068	4.990	30.233
0.01	8.403	32.360	3.851	30.519
0.005	12.389	32.501	2.623	30.929
0.003	16.651	32.555	1.955	31.417
0.002	20.345	32.582	1.601	31.512
0.001	27.039	32.691	1.209	31.812